Vol. 105 March 1, 1979
Complete in one issue

ISSN 0003-2670

# ANALYTICA CHIMICA ACTA

International journal devoted to all branches of analytical chemistry



ELSEVIER SCIENTIFIC PUBLISHING COMPANY

# ANALYTICA CHIMICA ACTA

*International journal devoted to all branches of analytical chemistry*
*Revue internationale consacrée à tous les domaines de la chimie analytique*
*Internationale Zeitschrift für alle Gebiete der analytischen Chemie*

**PUBLICATION SCHEDULE FOR 1979** (incorporating the section on Computer Techniques and Optimization).

| | J | F | M | A | M | J | J | A | S | O | N | D |
|---|---|---|---|---|---|---|---|---|---|---|---|---|
| Analytica Chimica Acta | 104/1 | 104/2 | 105 | 106/1 | 106/2 | 107 | 108 | 109/1 | 109/2 | 110/1 | 110/2 | 111 |
| Section on Computer Techniques and Optimization | | | 112/1 | | | 112/2 | | | 112/3 | | | 112/4 |

**Scope.** *Analytica Chimica Acta* publishes original papers, short communications, and reviews dealing with every aspect of modern chemical analysis, both fundamental and applied. The section on *Computer Techniques and Optimization* is devoted to new developments in chemical analysis by the application of computer techniques and by interdisciplinary approaches, including statistics, systems theory and operation research. The section deals with the following topics: Computerized acquisition, processing and evaluation of data. Computerized methods for the interpretation of analytical data including chemometrics, cluster analysis, and pattern recognition. Storage and retrieval systems. Optimization procedures and their application. Automated analysis for industrial processes and quality control. Organizational problems.

**Submission of Papers.** Manuscripts (three copies) should be submitted to:
for *Analytica Chimica Acta:* Dr. A. M. G. Macdonald, Department of Chemistry, The University, P.O. Box 363, Birmingham B15 2TT, England;
for the section on *Computer Techniques and Optimization:* Dr. J. T. Clerc, Universität Bern, Pharmazeutisches Institut, Sahlistrasse 10, CH-3012 Bern, Switzerland.

**Information for Authors.** Papers in English, French and German are published. There are no page charges. Manuscripts should conform in layout and style to the papers published in this Volume. Authors should consult Vol. 102, p. 253 for detailed information. Reprints of this information are available from the Editors or from: Elsevier Editorial Services Ltd., Mayfield House, 256 Banbury Road, Oxford OX2 7DE (Great Britain).

**Reprints.** Fifty reprints will be supplied free of charge. Additional reprints (minimum 100) can be ordered. An order form containing price quotations will be sent to the authors together with the proofs of their article.

**Advertisements.** Advertisement rates are available from the publisher.

**Subscriptions.** Subscriptions should be sent to: Elsevier Scientific Publishing Company, P.O. Box 211, 1000 AE Amsterdam, The Netherlands. The section on *Computer Techniques and Optimization* can be subscribed to separately.

**Publication.** *Analytica Chimica Acta* (including the section on *Computer Techniques and Optimization*) appears in 9 volumes in 1979. The subscription for 1979 (Vols. 104–112) is Dfl. 1179.00 plus Dfl. 135.00 (postage) (Total approx. U.S. $641.00). The subscription for the *Computer Techniques and Optimization* section only (Vol. 112) is Dfl. 131.00 plus Dfl. 15.00 (postage) (Total approx. U.S. $71.20). Journals are sent automatically by air mail to the U.S.A. and Canada at no extra cost and to Japan, Australia and New Zealand for a small additional postal charge. All earlier volumes (Vols. 1–95) except Vols. 23 and 28 are available at Dfl. 144.00 (U.S. $70.20), plus Dfl. 10.00 (U.S. $4.90) postage and handling, per volume.

Claims for issues not received should be made within three months of publication of the issue, otherwise they cannot be honoured free of charge.

Customers in the U.S.A. and Canada who wish to obtain additional bibliographic information on this and other Elsevier journals should contact Elsevier/North Holland Inc., Journal Information Center, 52, Vanderbilt Avenue, New York, NY 10017. Tel: (212) 867-9040.

# Chromatographie liquide à hautes performances

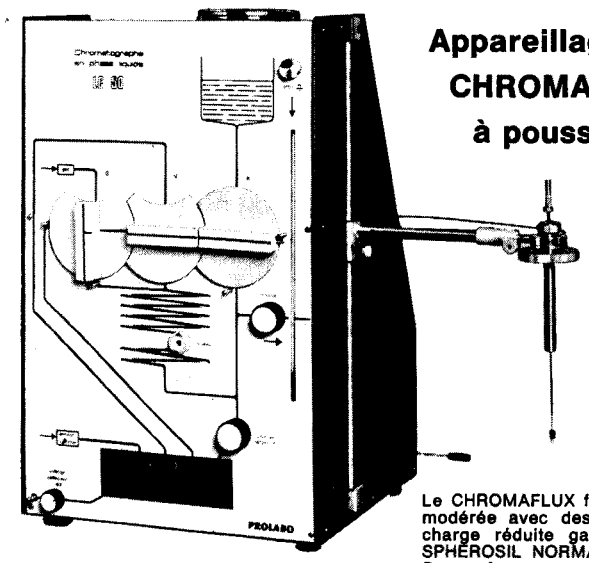


## Appareillage PROLABO CHROMAFLUX LC 50 à poussée de gaz

Le CHROMAFLUX fonctionne sous pression modérée avec des colonnes à perte de charge réduite garnies par exemple de SPHÉROSIL NORMATOM XOA 600 ou 800. Ses performances sont de tout premier plan.

**Emploi facile :**
- Mise au courant immédiate d'une personne non initiée.
- Manipulations simples, sans aucun "tour de main" spécial.
- Ensemble cohérent, mis en œuvre en quelques minutes, raccordable à tout détecteur.

**Entretien simplifié :**
- Colonnes sans raccords spéciaux en bout, se démontant sans outil.
- Circuit en tubes normalisés de 1,6 mm (1/16"). Colonnes de Ø 6,3 mm (1/4").
- Volumes morts très réduits par construction.
- Flancs démontables pour un accès facile aux organes internes.

**Sécurité :**
- Pression modérée, ne dépassant pas 25 bar.
- Sécurité positive au niveau des vannes, liées mécaniquement pour empêcher toute fausse manœuvre.
- Réservoir récupérateur de solvant avec tube de respiration.

**Commodité :**
- Visualisation des circuits en façade.
- Niveau de solvant, réservoir de récupération et débitmètre.
- Réservoir de solvant suffisant pour 1 jour de travail.
- Aiguille d'injection guidée pour injecter dans des conditions bien reproductibles.

**Economie :**
- Prix modéré de l'installation.
- Entretien peu coûteux.
- Faible consommation de solvant.
- Faible consommation de gaz, juste ce qu'il faut pour dégazer lors des remplissages.

### SPHÉROSIL NORMATOM®

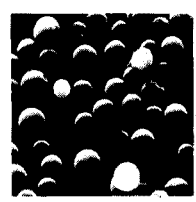

Matériaux de remplissage de colonnes constitués de microbilles de silice calibrées, à surface spécifique élevée (600 $m^2/g$ pour le SPHEROSIL NORMATOM ® XOA 600 et 800 $m^2/g$ pour le XOA 800).

En garnissant de SPHEROSIL NORMATOM ® les colonnes de tout appareil de chromatographie liquide, on obtient des performances exceptionnelles, moyennant une pression motrice modérée.

**PROLABO**

**12, rue Pelée - 75011 PARIS**
**Téléphone : (1) 355.44.88**
**Télex : PRLAB X 680 566 F**

rhône-poulenc

# Association Theory

## The Phases of Matter and Their Transformations

by ROBERT GINELL, *The City University of New York, Brooklyn College, New York, U. S. A.*

## Studies in Physical and Theoretical Chemistry, 1

1978 xiv + 224 pages US $43.00/Dfl. 97.00 ISBN 0-444-41753-2

This book is the first on its subject and should have an illuminating effect on scientific thinking in many fields. It provides a systematic treatment of the theory of association which extends the present quantitative understanding of the nature of matter and its transformations.

The relationship of this theory to thermodynamics yields significant results. A new definition of entropy is provided as well as calculations based on this concept that give valuable insights into the nature of phase transformations. New methods of calculating internal pressure free of assumptions and approximations are given. An equation for the exact calculation of the thickness of the surface film of liquids is presented. The covolume of liquids and some solids is evaluated. Although many tables, diagrams, and data are presented, the emphasis is on understanding what solids and liquids are and how they transform into each other and into gases.

The book will be of particular value to physicists and chemists. It will also be of great interest to biologists, geologists and engineers, and to scientists in general.



ELSEVIER

P.O. Box 211,
1000 AE Amsterdam
The Netherlands

52 Vanderbilt Ave
New York, N.Y. 10017

*The Dutch guilder price is definitive. US $ prices are subject to exchange rate fluctuations.*

8111

ANALYTICA CHIMICA ACTA
VOL. 105 (1979)

# ANALYTICA CHIMICA ACTA

International journal devoted to all branches of analytical chemistry




ELSEVIER SCIENTIFIC PUBLISHING COMPANY

*Anal. Chim. Acta,* Vol. 105 (1979)

Printed in The Netherlands

*Analytica Chimica Acta*, 105 (1979) 1—7


# INVESTIGATIONS OF THE CHEMICAL HOMOGENEITY OF SOLIDS

K. DANZER

*Sektion Chemie und Werkstofftechnik, Technische Hochschule Karl-Marx-Stadt (D.D.R.)*

K. DOERFFEL

*Sektion Chemie, Technische Hochschule "Carl Schorlemmer", Leuna-Merseburg (D.D.R.)*

H. EHRHARDT and M. GEISSLER

*VEB Mansfeld Kombinat "Wilhelm Pieck", Forschungsinstitut für NE-Metalle, Freiberg/Sa. (D.D.R.)*

G. EHRLICH*

*Zentralinstitut für Festkörperphysik und Werkstofforschung der Akademie der Wissenschaften der D.D.R., Dresden (D.D.R.)*

P. GADOW

*Amt für Standardisierung, Meßwesen und Warenprüfung der D.D.R., Berlin (D.D.R.)*

(Received 4th September 1978)

SUMMARY

Chemical homogeneity is a relative property of solid-state materials; it depends not only on their ultimate purposes, but also on the parameters of the analytical procedure applied in the investigation. These features are often given inadequate attention in the characterization of solid materials. A statistical model for representative sampling is used here as the starting point to derive relationships which demonstrate quantitatively the increasing rigour of the homogeneity test with increasing spatial resolution and precision of the analytical procedure. It is also shown that chemical homogeneity can be confirmed at a calculated risk, when the tests do not show the material to be significantly inhomogeneous and when maximum permissible deviations in concentration can be given for a practical application.

Solids are defined as chemically homogeneous if the differences in the composition of definite regions distributed regularly over the whole sample volume do not exceed previously established limits. The sizes of the regions selected and the permissible deviations in the concentrations depend on the effect of the elemental distribution on relevant properties of the solid. Often the analyst is faced with the problem of estimating the homogeneity of a solid sample by analyzing several sub-samples. In the following paragraphs, the assumptions, possibilities and limitations of such "analytical homogeneity tests" will be discussed from a general point of view. For this discussion, it is assumed that the inhomogeneities are distributed stochastically (randomly) throughout the sample to be investigated.

## MODELS FOR CHEMICAL HOMOGENEITY

Inhomogeneities in the chemical composition of a solid sample with respect to a particular element cannot be detected if the standard deviation, $\sigma$, of the concentration of this element determined in different sub-samples, does not exceed significantly the standard deviation $\sigma_A$, which represents the precision of the analytical procedure applied [1]. The distribution of the component sought must then be regarded as homogeneous with respect to the analytical procedure, i.e. the analytical result of any sub-sample does not deviate significantly from the mean result of the whole sample.

These relationships correspond exactly to the sampling conditions for representative samples in bulk analysis. Therefore the formulae derived for sampling, and especially for estimating the sampling error $\sigma_P$, are valid also for investigations of analytical homogeneity of solids. In the latter case, the sampling error $\sigma_P$ is replaced by the standard deviation of the results $\sigma_I$, which is caused by sample inhomogeneity. Thus the equation derived by Wilson [2] to describe the relation between the properties of the sample and the sampling error in a binary mixture AB can be written as

$$(\sigma_I/x)^2 = [(c_A - x)(x - c_B)/x^2]\,[\rho_A\,\rho_B/\bar{\rho}^2]\,[\bar{V}/V_P]$$

where $x$ is the mean concentration of the element to be determined in the sample; $c_A$ and $c_B$ are the concentrations of this element in the constituents A and B, respectively; $\rho_A$ and $\rho_B$ are the densities of constituents A and B, respectively; $\bar{\rho}$ is the mean density of the sample material; $\bar{V}$ is the mean volume of homogeneous regions; and $V_P$ is the volume of the sub-sample, e.g. an excitation volume.

For $\rho_A = \rho_B = \bar{\rho}$, eqn. (1) becomes

$$(\sigma_I/x)^2 = [(c_A - x)(x - c_B)/x^2]\,[\bar{V}/V_P] \qquad (2)$$

Consequently, the relative standard deviation of the analytical results caused by sample inhomogeneity, $(\sigma_I/x)^2$, increases with decreasing concentration $x$ and sub-sample volume $V_P$ and with the increase of the difference $c_A - c_B$.

The overall standard deviation estimated by analysis of several sub-samples, $\sigma$, is caused by sample inhomogeneity, $\sigma_I$, as well as by the statistical errors of the analytical method applied, $\sigma_A$. According to the law of error propagation this can be written as

$$(\sigma/x)^2 = (\sigma_I/x)^2 + (\sigma_A/x)^2 = [(c_A - x)(x - c_B)/x^2]\,[\bar{V}/V_P] + (\sigma_A/x)^2 \qquad (3)$$

The material is considered to be chemically homogeneous if

$$(\sigma_I/x)^2 = [(c_A - x)(x - c_B)/x^2]\,[\bar{V}/V_P] \ll (\sigma_A/x)^2 \approx \sigma^2/x \qquad (4)$$

and inhomogeneous if

$$(\sigma/x)^2 > (\sigma_A/x)^2 \qquad (4a)$$

Thus, for a given concentration $x$ and a given sub-sample volume $V_P$, proof of homogeneity will be the stronger, the smaller is the statistical error of the

analytical procedure $\sigma_A$. Conversely, the rigour of the test increases with decreasing $V_P$ for given values of $x$ and $\sigma_A$.

Clearly, chemical homogeneity is a strictly relative property of solid-state samples not only with regard to their ultimate application as materials, but also with respect to the method of investigation. Consequently, for investigations of chemical homogeneity of solids, the essential information — from a practical point of view — which must be given to the analyst is: (a) the volume $\bar{V}$ of sample regions within which inhomogeneity is irrelevant, and (b) the permissible deviation between the concentrations in the constituents of regions A and B, $c_A$ and $c_B$. The analytical problem is then to select a procedure which fulfils the conditions $V_P \leqslant \bar{V}$ and $\sigma_A \leqslant \sigma_I$ where $\sigma_I$ has to be calculated from eqn. (2) for given $x$, $c_A$, $c_B$, $\bar{V}_I$ and $V_P$. For an optimal choice of procedure, it is desirable to make as quantitative an estimate as possible of the increasing rigour of the test with the decrease of the quotients $\sigma_A/\sigma_I$ and $V_P/\bar{V}$.

## STATISTICAL PRINCIPLES OF CHEMICAL HOMOGENEITY TESTS

From eqns. (4) and (4a), the investigation of chemical homogeneity has to be based on testing the null hypothesis $H_0 : \sigma^2 = \sigma_A^2$ (homogeneity) against the alternative hypothesis $H_1 : \sigma^2 > \sigma_A^2$ (inhomogeneity). In practice, a finite number of measurements provides only a value of the overall standard deviation, $s$, as an estimate of $\sigma$, and the null hypothesis must be checked by the Fisher test ($F$-test) [3]. Accordingly, $H_0$ must be rejected and inhomogeneity of the chemical composition of the sample must be accepted if

$$F = (s/s_A)^2 = [(s/x)^2]/[(s_A/x)^2] > F(\bar{P}; f; f_A) \qquad (5)$$

where $f$ and $f_A$ are the degrees of freedom of $s$ and $s_A$, respectively, and $\bar{P}$ is the one-sided probability (confidence level) [3]. (The $F$-test is carried out for investigations of homogeneity in this way, so that the overall standard deviation $s$ is placed in the numerator, and the error of the analytical ure procedure $s_A$ in the denominator of the quotient.)

Often instead of $\bar{P}$, the significance level $\alpha$ ($= 1 - P$) is given; $\alpha$ represents the probability of making a first-kind error, i.e. rejecting the null hypothesis $H_0$ when it is in fact true.

Equation (5) combined with eqn. (3) makes it possible to estimate, in a more quantitative fashion, the increasing rigour of the proof of homogeneity with increasing precision and spatial resolution of the analytical procedure. The increasing rigour is expressed by an increasing $\bar{P}$ value or a decreasing risk of a first-kind error ($\alpha$). Figure 1 shows the dependence of $\alpha$ on the relative error of the analytical method, $s_A/x$. Figure 2 demonstrates the dependence of $\alpha$ on the relative sub-sample volume $V_P/\bar{V}$.

Statistical tests can, in principle, reject null hypotheses only on a preselected level of significance. Non-rejection must not be confused with acceptance, for it does not deliver any verdict on the real identity of the two measured values

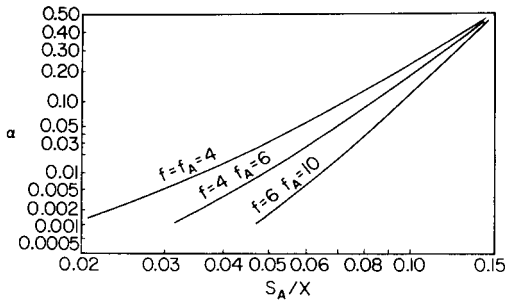


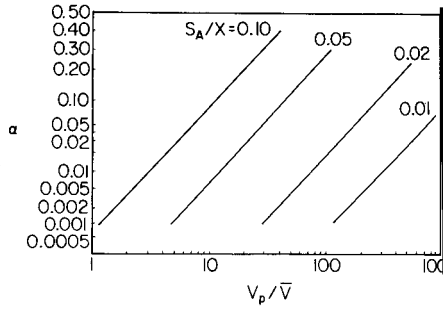


Fig. 1. Dependence of the probability of an erroneous statement of inhomogeneity, i.e. the risk of first-kind error $\alpha$, on the relative error of the analytical procedure $s_A/x$, for different degrees of freedom $f$ and $f_A$ (relative total error $s/x = 0.15$).

Fig. 2. Dependence of the probability of an erroneous statement of inhomogeneity, i.e. the risk of first-kind error $\alpha$, on the relative sub-sample volume $V_P/\bar{V}$, for different relative analytical errors $s_A/x$ (concentrations: $x = 0.5$; $c_A = 1$; $c_B = 0$; degrees of freedom: $f = 4$ and $f_A = 6$).

to be compared. Nevertheless, in the present case, the information gained by the test when the null hypothesis has not been rejected, may be increased by taking into account the maximum permissible relative deviations of concentration, $s^*/x$, which follow from practical, non-statistical considerations but taking into account eqn. (3). Then a specified alternative hypothesis $H_1' : \sigma^2 = (s^*)^2$ can be formulated, for which the risk of error is $\beta$, which represents the probability of non-rejection of the null hypothesis when it is in fact false (second-kind error) [4—6]. Here $\beta$ is a quantitative statistical measure of the correctness of the statement "homogeneous", in so far as concentration deviations up to $s^*/x$ may be neglected from a practical point of view; therefore solids showing such deviations may be characterized as "homogeneous" practically.

The performance of statistical tests including consideration of the second-kind error has been described in detail elsewhere [7—9]. For practical investigations of homogeneity, it is first necessary to prove, by the $F$-test in its well-known form, whether or not there is a significant difference between $(s/x)^2$ and $(s_A/x)^2$. If the difference is not significant, i.e. if the null hypothesis is not rejected, then instead of $F$ a new test criterion $\phi^2$ must be formed by replacing $s/x$ by $s^*/x$ in eqn. (5):

$$\phi^2 = (s^*/s_A)^2 = [(s^*/x)^2]/[(s_A/x)^2] \qquad (6)$$

$\phi^2$ can be obtained as a function of $\alpha$, $\beta$ and the degrees of freedom $f$ and $f_A$ (in general, $f_1$ and $f_2$) from tables or nomograms (e.g. [4, 10]). As an example, Table 1 shows some values of $\phi^2$ for $\alpha = \beta = 0.05$ and different degrees of freedom.

The chemical homogeneity of an investigated solid can be guaranteed on

TABLE 1

Some values of the function $\phi^2$ ($\alpha$, $\beta$, $f_1$, $f_2$) for $\alpha = \beta = 0.05$ [8]

| $f_1$ | $f_2$ | $\phi^2$ | $f_1$ | $f_2$ | $\phi^2$ | $f_1$ | $f_2$ | $\phi^2$ |
|---|---|---|---|---|---|---|---|---|
| 4 | 6 | 8.29 | 6 | 6 | 7.95 | 8 | 6 | 7.73 |
| | 8 | 6.76 | | 8 | 6.30 | | 8 | 6.00 |
| | 10 | 6.05 | | 10 | 5.48 | | 10 | 5.15 |
| | 12 | 5.52 | | 12 | 4.93 | | 12 | 4.62 |

the levels of significance $\alpha$ and $\beta$, within the limits given by the permissible deviations of concentration $s^*/x$, if

$$(s^*/s_A)^2 = \phi^2 \geqslant \phi^2\ (\alpha, \beta, f, f_A) \tag{7}$$

or

$$\beta[\phi^2 = (s^*/s_A)^2; \alpha; f; f_A] \leqslant \beta_{\text{presumed}} \tag{7a}$$

The decrease in the risk $\beta$ of making a second-kind error with increasing total error $s^*/x$ for different analytical errors $s_A/x$ and for given values of $\alpha$, $f$ and $f_A$, is represented graphically in Fig. 3.

*Application to a steel sample*

As an example of the application of the above principles, the distribution of chromium in steel is considered. The surface of a chromium steel showing particles of chromium carbide had to be investigated with respect to the homogeneous distribution of chromium. Deviations in the concentration of chromium up to 15% (relative) within sample areas of 1 mm$^2$ were permissible. The steel was analyzed by x-ray fluorescence spectrometry. For a primary beam diameter of 1 mm, the excited sample area amounted to almost 1 mm$^2$.

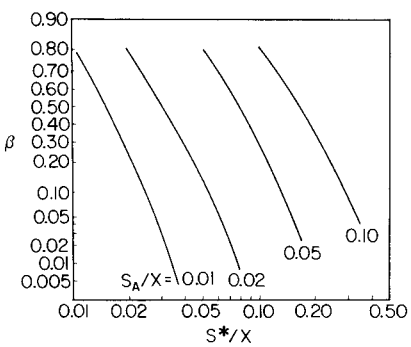


Fig. 3. Dependence of the probability of an erroneous statement of homogeneity, i.e. the risk of second-kind error $\beta$, on the maximum permissible relative deviations of concentration $s^*/x$, for different analytical errors $s_A/x$ (risk of error $\alpha = 0.05$; degrees of freedom $f = 4$ and $f_A = 6$).

In this case, the depth of excitation can be neglected in comparison to the excited surface area, hence it is necessary to consider only the sub-sample areas rather than the sub-sample volumes.

*Analytical results (% w/w).* Single determinations from 5 different sub-samples ($f = 4$) gave the results: 14.39, 11.79, 12.33, 11.87, 13.44; thus $\bar{x} = 12.79$; $s = 1.140$; $s/\bar{x} = 0.089$.
Replicate (7) determinations of the same sub-sample ($f_A = 6$) gave the results 12.24, 12.89, 13.01, 12.37, 12.24, 12.88, 13.64; thus
$\bar{x} = 12.75$; $s_A = 0.510$; $s_A/\bar{x} = 0.040$

F-*test.* $F = (0.089/0.040)^2 \approx (1.140/0.510)^2 = 4.99 < F(\alpha = 0.05; f = 4; f_A = 6) = 6.16$. Hence chemical inhomogeneity cannot be guaranteed at the significance level $\alpha = 0.05$ ($\bar{P} = 0.95$). This shows that the extended $F$-test with $s^*/x = 0.15$ makes it possible to assess homogeneity at the levels of significance $\alpha = \beta = 0.05$.

*Extended* F-*test with the criterion* $\phi^2$. $\phi^2 = (0.15/0.04)^2 = 14.06 > \phi^2 (\alpha = \beta = 0.05; f = 4; f_A = 6) = 8.29$. Thus, despite the chromium carbide particles, the steel must be considered as chemically homogeneous with respect to chromium, if relative deviations in the chromium concentration up to 15% within surface areas of 1-mm$^2$ can be tolerated for the particular application. The correctness of this statement is restricted by a risk of 5% both with respect to the non-confirmation of inhomogeneity and with regard to confirmation of homogeneity within the limits specified.

## CONCLUSIONS

Chemical homogeneity is, on the one hand, a relative property of a solid which depends on the ultimate purpose of the material, and on the other hand, is defined by the spatial resolution and precision of the analytical procedure applied for investigation. This forces the analyst to select a procedure according to the demands on the material specified by the customer. The choice of method can be made objective by estimating the increasing rigour of the examination with decreasing sub-sample volume and decreasing statistical error of the analytical procedure, with the help of the Fisher test. The equations concerning these relationships also allow the number of repeat determinations (degrees of freedom) to be optimized, thus increasing the rigour and reliability of the tests.

Because of the unavoidable connection of investigations of homogeneity with practical problems, it is usually desirable to convert the primary measured units (e.g. absorbances, counts, voltages, etc.) to concentrations by means of an analytical function. In principle, the tests themselves could equally well be carried out with the original values.

The information gained by an investigation of homogeneity in which inhomogeneity cannot be guaranteed, may be increased by taking into account the maximum deviations in concentration that can be tolerated practically.

It is possible to perform an extended $F$-test (with a specified alternative hypothesis), which allows a limited guarantee of homogeneity (within the practically tolerable limits) at a calculated risk.

Statements on the chemical homogeneity or inhomogeneity of solids without data on the spatial resolution and precision of the analytical procedure used are worthless.

The authors thank Professor Dr. J. Barthel, Dresden, for valuable remarks.

REFERENCES

1 H. Malissa, Fresenius Z. Anal. Chem., 273 (1973) 449.
2 A. D. Wilson, Analyst, 89 (1964) 18.
3 K. Doerffel, Statistik in der analytischen Chemie, Deutscher Verlag für Grundstoffindustrie, Leipzig, 1966, p. 123.
4 W. J. Dixon and F. J. Massey, Introduction to Statistical Analysis, 2nd edn., McGraw-Hill, New York, 1957, p. 524.
5 L. Sachs, Statistische Auswertemethoden, 2nd edn., Springer, Berlin, 1969, p. 116.
6 E. Weber, Grundriß der Biologischen Statistik, 7th edn., Gustav Fischer, Jena, 1972, p. 173.
7 D. Winne, Arzneimittel-Forschung, 13 (1963) 1001.
8 M. J. Maurice and K. Buijs, Fresenius Z. Anal. Chem., 244 (1969) 18.
9 G. Ehrlich, Chem. Anal. (Warszawa), in press.
10 D. B. Owen, Handbook of Statistical Tables, Pergamon Press, London, 1962, p. 88.

*Analytica Chimica Acta*, 105 (1979) 9—23


# REDUCTION OF NITRIC OXIDE, NITROUS ACID AND NITROGEN DIOXIDE AT PLATINUM ELECTRODES IN ACIDIC SOLUTIONS: Review and new voltammetric results

BOB G. SNIDER[‡] and DENNIS C. JOHNSON*

*Department of Chemistry, Iowa State University, Ames, Iowa 50011 (U.S.A.)*

(Received 9th October 1978)

SUMMARY

The literature concerning the chemical and electrochemical reactions of nitric oxide, nitrous acid and nitrogen dioxide in aqueous solutions is reviewed briefly, with emphasis on electrochemical reductions at platinum electrodes in acidic solutions. The voltammetric behavior of NO and $NO_2$ at a Pt electrode in perchloric acid is virtually identical to that for $HNO_2$ and this is explained on the basis of a common electroactive precursor concluded to be $NO^+$. Three cathodic waves are obtained for acidic solutions of NO, $HNO_2$ and $NO_2$. The first two waves correspond to reduction of $NO^+$ to NO and $N_2O_3$ to NO, respectively. The presence of $N_2O_3$ results from decomposition of the parent compounds. The presence of $Br^-$ or $Cl^-$ in acidic solutions of the title compounds promotes the voltammetric reductions at lower $H^+$ concentrations. This probably results from formation of electroactive nitrosyl halides.

The complexity of the chemistry and electrochemistry of nitrogen results partly from the fact that stable compounds have been found for nitrogen in oxidation states from −3 to +5. Adding to the complexity is the fact that reaction products often cannot be predicted solely on the basis of thermodynamic considerations [1]. The electrochemical reactions of the oxides of nitrogen(II, III, IV) have been studied quite extensively in acidic solutions and have been proposed as the basis for sensitive electroanalytical determinations of various nitrogen oxides as air pollutants following their dissolution and electrochemical reactions of NO, $HNO_2$ and $NO_2$ in acidic solutions.

## CHEMISTRY OF NO, $HNO_2$ AND $NO_2$

Unlike other compounds with an odd number of electrons, such as $NO_2$, NO is colorless, chemically inactive, and does not dimerize in the gas phase. An explanation for the lack of dimerization is the absence of an increase in the bond order resulting from dimerization. Despite the absence of dimerization

---

[‡]Present address: The Upjohn Company, Kalamazoo, Michigan 49001 (U.S.A.).

in the gas phase, the dimer has been proposed as an intermediate in chemical [2] and electrochemical reactions [3] in aqueous solutions. In a later section the formation of $(NO)_2$ adsorbed at the electrode surface is invoked to explain the voltammetric data for electrochemical reduction of NO in solutions of perchloric acid. Disproportionation of NO occurs in concentrated acid solutions according to reaction 1.

$$4NO + 2H^+ \rightleftharpoons 2NO^+ + N_2O \; ; K = 2 \times 10^{50} \qquad (1)$$

Despite a large value for the equilibrium constant, the reaction is slow in approaching equilibrium [4].

Oxides of nitrogen(III) can exist in a variety of ionic and molecular forms in acidic solutions depending on the acid concentration and activities of anions present in the solutions. Nitrite ion ($NO_2^-$), nitrous acid ($HNO_2$), nitrosonium ion ($NO^+$), nitrous acidium ion ($H_2NO_2^+$), nitrosyl compounds (NOX, where X represents the associated anion) and dinitrogen trioxide ($N_2O_3$) are the species of nitrogen(III) commonly known in aqueous solution. The chemical reactions which interrelate the formation of these compounds are shown below.

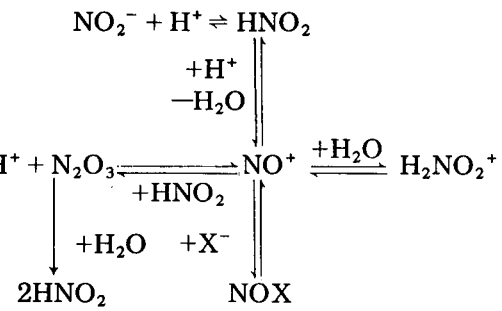


(2)

The $H_2NO_2^+$ ion does not exist in significant concentrations at equilibrium [5] but has been proposed as an intermediate product in chemical reactions [6]. The fraction of the total nitrogen(III) in a solution prepared as 1 mM $HNO_2$ which exists as $N_2O_3$ is also very small. Hence, the predominant species in perchloric acid solutions of $HNO_2$ are $HNO_2$ and $NO^+$.

The equilibrium constant describing the interconversion of $HNO_2$ and $NO^+$ is

$$HNO_2 + H^+ \rightleftharpoons NO^+ + H_2O \; ; K = [NO^+][H_2O]/[HNO_2][H^+] = 2 \times 10^{-7} \qquad (3)$$

The formation of $NO^+$ is promoted by high concentrations of a strong acid for which the activity of water is much less than unity and the activity of $H^+$ is much larger than the molar concentration of the acid. Figure 1 contains plots of the activity of $H_2O$ and $H^+$ in perchloric acid solution as a function of the molar concentration of acid. Also shown is the fraction of total nitrogen(III) converted to $NO^+$, $X_{NO^+}$, at equilibrium as calculated from eqn. (3) for a solution prepared as 1 mM $HNO_2$. The numerical value of $X_{NO^+}$ is 0.5 in 7.5 M $HClO_4$ and the conversion to $NO^+$ is quantitative for perchloric acid concentrations greater than 9 M [5, 7—9]. The predominant factor for promoting

the conversion of $HNO_2$ to $NO^+$ is the dramatic increase in $H^+$ activity by approximately two orders of magnitude for increasing perchloric acid concentrations in the range 7—8 M [10, 11]. The existence of $NO^+$ in solutions of high acid concentration has been confirmed by u.v.—visible and Raman spectroscopy [5, 8, 9].

Nitrous acid is a weak acid with $pK_a = 3.3$. However, $HNO_2$ can also be regarded as the hydroxylated form of $NO^+$ (NOOH). Other nucleophiles can, in effect, replace $OH^-$ from NOOH to give nitrosyl compounds of the type NOX with the equilibrium constant defined by

$$HONO + HX \rightleftharpoons NOX + H_2O \; ; K = [NOX][H_2O]/[HNO_2][HX] \qquad (4)$$

High HX activity and low $H_2O$ activity promote the formation of NOX. Calculated and experimental values of $K$ in eqn. (4) were given by Turney and Wright [12] and are listed in Table 1. The formation of $NOClO_4$ is negligible for intermediate concentrations of $HClO_4$ as indicated by a low value of $K$, and $X_{NO^+} \gg X_{NOClO_4}$. Also shown in Fig. 1 for later consideration is the fraction of nitrogen(III) found to exist as NOCl as a function of HCl concentration for a solution prepared as 1 mM $HNO_2$ [12]. The value of $X_{NOCl}$ is 0.5 for 5 M HCl.

Solutions of $HNO_2$ can decompose according to

$$3HNO_2 \rightleftharpoons HNO_3 + 2NO + H_2O \qquad (5)$$

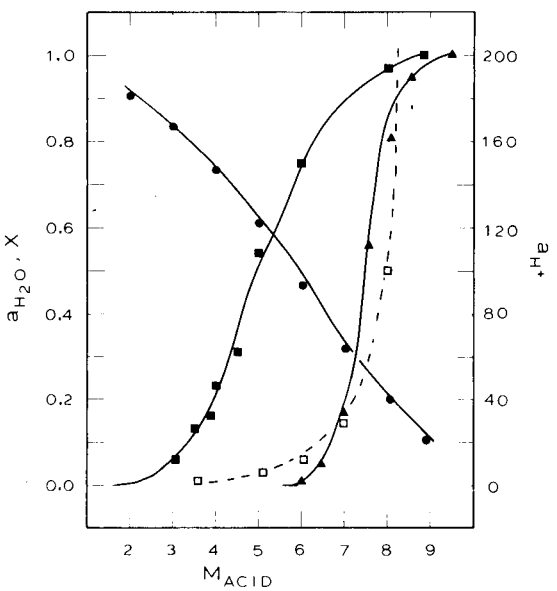


Fig. 1. Correlation of various parameters with acid concentration in aqueous solutions. (•) $a_{H_2O}$ in $HClO_4$; (□) $a_{H^+}$ in $HClO_4$; (▲) $X_{NO^+}$ in $HClO_4$; (■) $X_{NOCl}$ in HCl.

TABLE 1

Value of the equilibrium constants for reaction 4 [12]

| $X^-$ | NOX | $K$ (calc.) | $K$ (exp.) |
|---|---|---|---|
| $ClO_4^-$ | $NOClO_4$ | $7 \times 10^{-5}$ | $2 \times 10^{-7}$ |
| $HSO_4^-$ | $NOHSO_4$ | $9 \times 10^{-6}$ | $3 \times 10^{-5}$ |
| $NO_3^-$ | $N_2O_4$ | $4 \times 10^{-5}$ | $3 \times 10^{-3}$ |
| $Cl^-$ | NOCl | $6 \times 10^{-4}$ | $1 \times 10^{-3}$ |
| $Br^-$ | NOBr | $9 \times 10^{-2}$ | $5 \times 10^{-2}$ |
| $NO_2^-$ | $N_2O_3$ | 18 | — |

and the rate has been reported to depend on solution agitation [13, 14]. The decomposition is not first order in $HNO_2$ and is most prominent at high $HNO_2$ concentration. Kobayaski et al. [13] proposed that the decomposition in quiescent solutions is controlled by the rate of diffusion of $HNO_2$ to the liquid—gas interface. The rate of decomposition in acidic solutions is at a maximum for acid concentrations of about 7 M [5, 14, 15]. At this acidity, $NO^+$ exists at a significant concentration and Bayliss and Watts [14] have proposed a mechanism for the decomposition of $HNO_2$ by reaction 5 which is based on formation of $NO^+$.

The chemical species produced upon dissolution of $NO_2$ in perchloric acid solutions depends upon the acid concentration. The production of $HNO_2$ and $HNO_3$ occurs in dilute acidic solutions (<6 M) by the disproportionation of $NO_2$ [16, 17] as described by

$$2NO_2 + H_2O \rightleftharpoons HNO_2 + HNO_3 \; ; K = 8.5 \times 10^8 \qquad (6)$$

Because of the large value of $K$, the conversion of $NO_2$ to $HNO_2$ and $HNO_3$ can be expected to be virtually quantitative. If a large concentration of $HNO_2$ is produced, significant decomposition of the $HNO_2$ will occur according to reaction 5 with the net reaction $3NO_2 + H_2O \rightleftharpoons 2HNO_3 + NO$.

The predominant nitrogen(III) species in perchloric acid solutions greater than 7 M, is $NO^+$. Hence, the reaction associated with dissolution of $NO_2$ changes from reaction 6 to reaction 7 in concentrated acid solutions [11, 17].

$$2NO_2 + H^+ \rightleftharpoons NO^+ + HNO_3 \; ; K = 2.5 \times 10^{-5} \text{ (for } HClO_4) \qquad (7)$$

## ELECTROCHEMISTRY OF NO, $HNO_2$ AND $NO_2$

This review is restricted to voltammetry at platinum electrodes in acidic solutions. Topol et al. [18] investigated the electrochemistry of NO, $HNO_2$, $NO_2$ and $HNO_3$ at a Pt electrode in concentrated sulfuric acid. They proposed that the nitronium ion ($NO_2^+$) is formed according to the reactions

$$HNO_3 + 2H_2SO_4 \rightleftharpoons NO_2^+ + H_3O^+ + 2HSO_4^- \qquad (8)$$

$$2NO_2 + 3H_2SO_4 \rightleftharpoons NO_2^+ + NO^+ + 3HSO_4^- + H_3O^+ \qquad (9)$$

for solutions of $HNO_3$ and $NO_2$. The dissolutions of $HNO_2$ and NO in concentrated sulfuric acid were proposed to result in production of $NO^+$:

$$HNO_2 + 2H_2SO_4 \rightleftharpoons NO^+ + H_3O^+ + 2HSO_4^- \quad (10)$$

$$2NO + 5H_2SO_4 \rightleftharpoons 2NO^+ + SO_2 + 2H_3O^+ + 4HSO_4^- \quad (11)$$

The electrochemistry of $NO_2^+$ and $NO^+$ produced by reactions 8—11 was studied by Topol et al. by linear-sweep cyclic voltammetry at a stationary electrode [18]. The authors concluded that $NO_2^+$ is reduced in two steps during the negative potential sweep:

$$NO_2^+ + 3H^+ + 2e \rightleftharpoons NO^+ + H_3O^+ \quad (12)$$

$$NO^+ + e \rightleftharpoons NO \quad (13)$$

A single anodic peak was obtained during the subsequent positive potential sweep which was concluded to correspond to reaction 13 going to the left. The authors state that a mechanism for reaction 12 might involve reduction of $NO_2^+$ to $NO_2$ with subsequent disproportionation to $NO_2^+$ and $NO^+$. Because the NO produced by electroreduction of $NO^+$ can react with sulfuric acid by reaction 11, the electrocatalytic reduction of sulfuric acid is possible. This reduction was not observed, however, and the rate of reaction 11 was concluded by Topol et al. to be very slow relative to the rate of the electrode reaction [18]. Production of $NO^+$ from NO in sulfuric acid by reaction 1 was also recognized by Topal et al.

Schmid and Lobeck [19] investigated the reduction of $HNO_2$ in the presence of $HNO_3$ at a Pt electrode in 1—7 M $H_2SO_4$. One anodic wave corresponding to a 2-e process was observed, and $HNO_3$ was concluded to be the product. Three cathodic waves were observed and, based on their relative wave heights, were calculated to correspond to 1-, 2- and 4-e processes. The products of the cathodic processes were concluded to be NO, $N_2O$ and $NH_2OH$, respectively.

Savodnik et al. [20] investigated the reduction of NO at a Pt electrode in 3.0 N $H_2SO_4$. Two reduction waves and two oxidation waves were observed. Based on evidence obtained by gas chromatography, NO was concluded to be quantitatively reduced to $N_2O$ by the reaction $2NO + 2H^+ + 2e \rightleftharpoons N_2O + H_2O$. The second reduction wave was concluded to correspond to the formation of $NH_2OH$ by the reaction $NO + 3H^+ + 3e \rightleftharpoons NH_2OH$.

Heckner and Schmid [21] studied the reduction of $HNO_2$ at a Pt electrode in 2—9 M $HClO_4$. Nitrosonium ion ($NO^+$) was concluded to be the electroactive species formed by a prior chemical reaction (reaction 3). The electrode current for 2—5 M $HClO_4$ was kinetically limited, whereas the current for 6—9 M $HClO_4$ was diffusion-controlled. The effect of decomposition of the $HNO_2$ on the observed electrochemistry was discussed.

Dutta and Landolt [22] investigated the electrochemistry of $HNO_2$, NO and $N_2O$ at a Pt electrode in 4.0 M $H_2SO_4$. Two waves for the oxidation of NO were observed, and the products were concluded to be $HNO_2$ and $NO_2$. Two reduction waves were observed for NO and three reduction waves were observed

for $HNO_2$. The two waves for the reduction of NO were reported to correspond with the second and third waves for the reduction of $HNO_2$. The authors also concluded that NO is an intermediate product of the reduction of $HNO_2$ to $NH_2OH$.

Garcia et al. [23] studied the reduction of $NO^+$ produced by reaction 3 in concentrated sulfuric acid. Nitrosonium ion was reported to be reversibly reduced to NO.

Heckner [16] investigated the reduction of $HNO_2$ in the presence of $HNO_3$ at a Pt electrode in perchloric acid. The studies were performed for the purpose of explaining the observation that the presence of $HNO_2$ is essential for the dissolution of metals in $HNO_3$. The author concluded that $NO^+$ derived from $HNO_2$ is the active oxidant.

Gadde and Bruckenstein [24] studied the reduction of $HNO_2$ at a Pt electrode in 0.10 M $HClO_4$. A porous electrode was used which allowed gaseous products of electrochemical reactions to pass into a mass spectrometer for analysis. An oxidation wave at $E > 0.80$ V vs. SCE and a reduction wave at $E < 0.30$ V were observed. A detectable amount of NO was produced by reduction of $HNO_2$ at $E = 0.50$ V. Nitrous oxide was produced with a high current efficiency for $0.40\ V > E > 0.30$ V. The production of a mixture of $NH_2OH$ (60.7%), $N_2O$ (18.8%) and $NH_3$ (21.6%) was observed at $E = -0.20$ V. The presence of $N_2O$ in the mixture of products was explained on the basis of the reaction $NH_2OH + HNO_2 \rightleftharpoons N_2O + 2H_2O$. The production of $NH_3$ was described, schematically, as $4N(-I) \rightleftharpoons N_2O + 2NH_3$. The authors hesitated to specify the nature of the N(—I) species although nitrogen in $NH_2OH$ has that oxidation state.

Janssen et al. [25] studied the reduction of NO at a Pt electrode in 4.0 M $H_2SO_4$. Reduction of NO to $N_2O$ occurred with 100% current efficiency for the first of the two cathodic waves observed. Products for the second wave were identified as $N_2O$, $NH_2OH$ and $NH_3$. The current efficiency for the formation of $NH_2OH$ and $NH_3$ reached peak values of 70% and 20% for $E$ on the limiting plateau of the second wave. The data on current efficiency and other information from the literature were used by Janssen et al. to propose the following mechanisms.

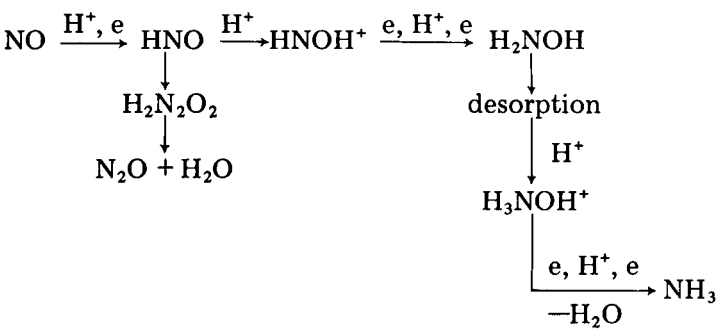


(14)

The observed current efficiencies agree quite well with the results reported by Gadde and Bruckenstein [24] for 0.1 M $HClO_4$ in spite of differences in the reactions proposed.

Barendrecht and van der Plas [26] investigated the reduction of $HNO_2$ in 7.5 M $H_2SO_4$ at a Pt ring-disk electrode. Three reduction waves were observed and attributed to the reactions $NO^+ + e \rightleftharpoons NO$, $2NO + 2H^+ + 2e$ ($\rightleftharpoons 2HNO$) $\rightarrow N_2O + H_2O$, and $HNO + 3H^+ + 2e \rightleftharpoons NH_3OH^+$. The HNO was proposed as an intermediate product in the second reaction because $N_2O$ is a very stable compound, and solutions of $N_2O$ were not reduced.

Disagreement exists in the literature concerning the nature of the electroactive species in acidic solutions of NO. Janssen et al. [25], Savodnik et al. [20], and Dutta and Landolt [22] apparently assumed that NO reacts directly at the electrode. Topol et al. [18] proposed that $NO^+$ is the electroactive species in solutions of NO. There is virtual consensus that $NO^+$ is the electroactive species in the electrochemical reduction of $HNO_2$. The research reported here was initiated to explain the similarities observed in the voltammetric data for NO, $HNO_2$ and $NO_2$ in perchloric acid solutions of intermediate acid concentration, and the changes observed when halide ions are added to the solutions. The results are consistent with the conclusions that $NO^+$ is the electroactive species for acidic solutions of NO, $HNO_2$ and $NO_2$.

## EXPERIMENTAL

### *Instrumentation*

Rotating disk electrodes (RDE) and rotators were from Pine Instrument Co. of Grove City, PA. A tubular electrode (5.0 mm by 1.0 mm i.d.), constructed in the Chemistry Shop of Iowa State University, was used in a flow analyzer with a design [28] inspired by Seymour et al. [27].

The potentiostat was an RDE-3 model (Pine Instrument Co.). The reference electrode was a miniature calomel electrode (Beckman Instruments); the saturated KCl solution in the reference electrode was replaced with a saturated NaCl solution to prevent formation of insoluble $KClO_4$ in the fiber junction when working in $HClO_4$ media. The potential of the reference electrode, $E_{ref}$, was +0.234 V vs. the normal hydrogen electrode. All values of electrode potential reported here are given with respect to $E_{ref}$. The auxiliary electrode was a small coil of Pt wire.

### *Reagents*

Solutions of supporting electrolyte were prepared from reagent-grade acids (Fisher Scientific Co.). Water was demineralized after distillation. Reagent-grade $NaNO_2$ (J. T. Baker Co.) was dried at 90°C for 4 h and then stored in a desiccator. Solutions of $HNO_2$ were prepared when aliquots of standard solutions of $NaNO_2$ were added to the acidic media.

The $NO_2$ was obtained from Matheson Gas Products. Because of the large quantities of NO used, NO was chemically generated [29]. Nitric oxide is

evolved when $H_2SO_4$ is added to a mixture of $KNO_2$ and KI: $KNO_2 + KI + 2H^+ \rightleftharpoons NO + 1/2I_2 + 2K^+ + H_2O$. Current-potential curves for solutions of NO prepared in this manner were indistinguishable from curves for commercial solutions of NO (Matheson Gas Products).

Solutions of NO and $NO_2$ were prepared with an apparatus (Fig. 2) which consisted of an inverted 100-ml volumetric flask containing electrolyte solution and sealed by a Teflon plug into which two Teflon tubes (0.031-in. i.d.) were inserted. A micrometer syringe of 2.0-ml capacity was used to deliver the desired gas into the volumetric flask through tube D. Tube E functioned as a vent to release simultaneously a volume of liquid equal to that of the gas injected. After the gas was delivered into the volumetric flask, valve B was closed, the syringe detached and the flask was shaken while in the inverted position to dissolve the gas into the electrolyte solution. The solution was then diluted to volume and mixed.

The volumes of NO and $NO_2$ required to produce solutions at a given concentration were calculated from the ideal gas law. Injection of 1.8 ml of pure NO into 100 ml of liquid produced a solution $7.36 \times 10^{-4}$ M in NO. The situation is more complicated for $NO_2$ because $NO_2$ dimerizes in the gas phase with an equilibrium constant equal to 8.8 $atm^{-1}$ [1]. The partial pressures of the two species were calculated to be $P_{NO_2} = 0.284$ and $P_{N_2O_4} = 0.715$. A liter of a gas mixture of $NO_2$ and $N_2O_4$ was calculated to be equivalent to 1.72 l of pure $NO_2$.

*Procedures*

Data determined as a function of acid concentration were obtained by diluting the acid in the electrolysis cell with water containing the same concentration of analyte as the solution in the electrolysis cell. For electrochemical

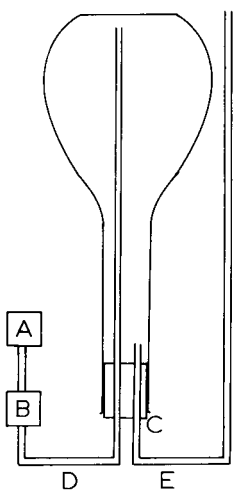


Fig. 2. Diagram of apparatus for preparation of NO and $NO_2$ solutions. (A) micrometer syringe; (B) on-off valve; (C) Teflon plug; (D, E) Teflon tubing, 0.031-in. i.d.

studies of dissolved NO with the RDE, the solution in the electrolysis cell was maintained saturated with respect to NO. The temperature of the electrolysis cell was maintained at 22 ± 2°C for all studies. To minimize variability in results because of decomposition of $HNO_2$ over a long period of time, the data were taken for each concentration exactly 5 min after dilution.

At the start of each series of experiments, the surface of the RDE was polished with 1-$\mu$m Buehler AB polishing alumina on microcloth with water as a lubricant. After polishing, the residual alumina was removed from the electrode surface by wiping with a wet cotton swab, and the electrode surface was rinsed with distilled water.

## RESULTS AND DISCUSSION

### *Voltammetry at Pt electrodes in $HClO_4$*

Current—potential ($i$—$E$) curves were obtained at a Pt tubular electrode for NO, $NaNO_2$ and $NO_2$ dissolved at approximately equal concentrations in 6.0 M $HClO_4$ (Fig. 3). Three cathodic waves were obtained for each of the three solutions and the values of $E_{1/2}$ are tabulated in Table 2. The reversibility of the waves was tested on the basis of the simple criterion for reversibility: $E_{1/3} - E_{2/3} = 0.0356/n$. Values of $E_{1/2}$ for the first cathodic wave were virtually identical for the three solutions and the wave corresponds to a reversible 1 — e reduction. Wave R-II was irreversible with virtually identical values of $E_{1/2}$ for the three solutions. The height of wave R-II relative to wave R-I was variable and is

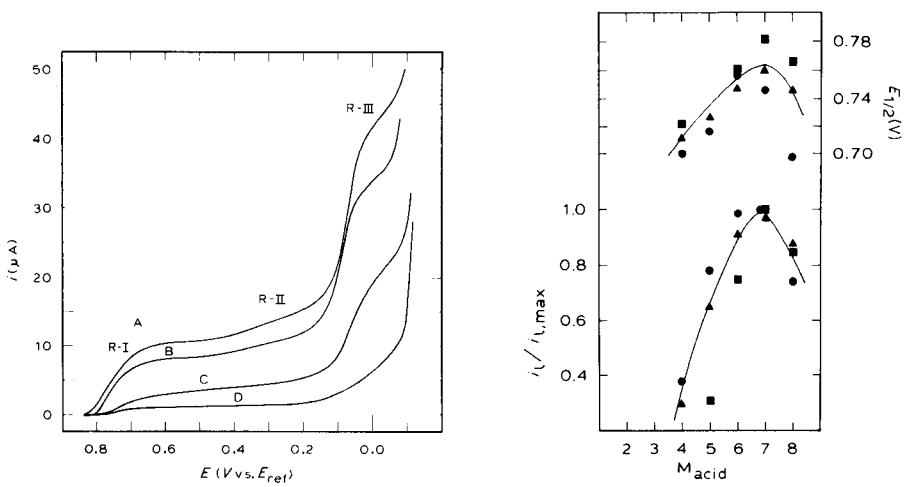


Fig. 3. Current—potential curves for NO, $HNO_2$ and $NO_2$ at a tubular Pt electrode. Potential scan, 1.0 V $min^{-1}$; fluid flow, 0.80 ml $min^{-1}$. (A) $5 \times 10^{-4}$ M $HNO_2$; (B) $5 \times 10^{-4}$ M NO; (C) $5 \times 10^{-4}$ M $NO_2$; (D) blank.

Fig. 4. $i_l/i_{l,max}$ and $E_{1/2}$ of wave R-I for NO, $HNO_2$ and $NO_2$ in $HClO_4$ solutions. (•) $2 \times 10^{-3}$ M NO; $i_{l,max} = 205$ $\mu$A; (▲) $5 \times 10^{-4}$ M $HNO_2$; $i_{l,max} = 65$ $\mu$A; (■) $5 \times 10^{-4}$ M $NO_2$; $i_{l,max} = 15$ $\mu$A.

TABLE 2

$E_{1/2}$ (V vs. $E_{ref}$) for three cathodic waves for NO, $HNO_2$ and $NO_2$ in 6.0 M $HClO_4$

| Compound | R-I | R-II | R-III |
|---|---|---|---|
| NO | 0.760 | 0.32 | 0.10 |
| $HNO_2$ | 0.750 | 0.32 | 0.10 |
| $NO_2$ | 0.756 | 0.32 | 0.10 |
| | reversible | irreversible | irreversible |

discussed in a later section. The values of $E_{1/2}$ for wave R-III were virtually identical. The limiting current for wave R-III was approximately four times that of wave R-I in each of the three solutions, which would seem to indicate that the cathodic waves correspond to 4- and 1-e processes, respectively.

The similarity of the $i$—$E$ curves for the solutions of NO, $HNO_2$ and $NO_2$ is concluded to result because of a common indentity for the electroactive precursor in the three solutions. This species is concluded to be $NO^+$ which is produced from NO, $HNO_2$ and $NO_2$ in concentrated perchloric acid according to eqns. (1), (3) and (7), respectively. The observation in Fig. 3 that the limiting current for 0.5 mM solutions of NO and $NO_2$ is smaller than that for 0.5 mM $HNO_2$ is expected on the basis of eqns. (1) and (3); only half the NO or $NO_2$ is converted to $NO^+$. Wave R—I, then, corresponds to reduction of $NO^+$ to NO at the electrode surface.

The homogeneous conversion of dissolved NO to $NO^+$ by eqn. (1) is reported to be very slow [4, 11]. That does not seem to support the above conclusion unless the conversion occurs on the electrode surface by an electrocatalytic mechanism. A possible mechanism for the disproportionation reaction involving adsorbed dimers of NO is as follows.

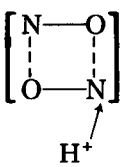


$$\text{adsorbed} \rightarrow NO^+ + [HNO]_{\text{adsorbed}} \; ; \; 2[HNO]_{\text{adsorbed}} \rightarrow N_2O + H_2O \qquad (15)$$

The conclusion that reduction of NO requires a prior heterogeneous reaction at the Pt surface is supported by the observation that a reduction wave for NO is not obtained at gold electrodes even though reversible reduction waves are obtained for $HNO_2$ and $NO_2$ [30, 31].

Experimental results were obtained which are consistent with the conclusion that wave R-II corresponds to the reduction of $N_2O_3$. The concentration of $N_2O_3$ is negligible in solutions of $HNO_2$ with an analytical concentration less than 1.0 mM. However, when sufficient $NaNO_2$ was added to 6.0 M $HClO_4$ so that spontaneous and rapid decomposition of $HNO_2$ was observed with production of gaseous NO and $NO_2$, the solution turned blue corresponding to the presence of $N_2O_3$ [1]. The limiting current for wave R-II in that solution

was approximately equal to the limiting current for wave R-I. The height of wave R-II relative to wave R-I was also observed to increase for 0.5 mM solutions of $HNO_2$ which were allowed to remain in the electrolytic cell for a long period of time to permit decomposition. The decomposition of $HNO_2$ to produce $N_2O_3$, as determined by observation of wave R-II, was accelerated significantly by gentle warming of the solution to 60°C. In that experiment, the solution was cooled back to ambient temperature before the $i$—$E$ curve was recorded.

*Variation of perchloric acid concentration*

The voltammetric behavior of N(II, III, IV) in perchloric acid solutions is a function of the acid concentration. Changes in $E_{1/2}$ and limiting current ($i_l$) as a result of changes in solution conditions can sometimes be used to deduce information regarding the nature of electrode reactions. Wave R-II is irreversible and values of $i_l$ for wave R-III cannot be determined accurately because of the high background currents resulting from the reduction of $H^+$. Consequently, $i_l$ was measured only for wave R-I as a function of the acid concentration.

The limiting current at a rotating disk electrode for a given concentration of the electroactive species is a function of the viscosity of the solution [32]. So that values of $i_l$ measured under conditions resulting in extreme changes of viscosity could be easily compared, the observed values of $i_l$ were recalculated to correspond to a solution with the viscosity of pure water. Values of $i_l$, divided by the maximum limiting current obtained in each study, $i_{l,max}$, are given in Fig. 4 as a function of perchloric acid concentration for NO, $HNO_2$ and $NO_2$ in solution. Values of $E_{1/2}$ for wave R-I obtained for NO, $HNO_2$ and $NO_2$ are also shown as a function of acid concentration.

The great similarity in the trends for the parameters plotted in Fig. 4 for NO, $HNO_2$ and $NO_2$ is consistent with the present conclusion of a single electroactive species ($NO^+$) for the three cases. The values of $i_l/i_{l,max}$ for all three nitrogen compounds increase rapidly with increasing acid concentration in the range 4—7 M $HClO_4$. This corresponds approximately to the range of perchloric acid concentrations in which $X_{NO^+}$ becomes significant (Fig. 1). The enhancement of $i_l$ for the first reduction wave resulting from increased perchloric acid activity is concluded to result from promotion of chemical reactions producing $NO^+$ prior to the electrode reduction as summarized in the following scheme.

$$\begin{array}{l} 2NO \overset{+H^+}{\rightleftharpoons} NO^+ + 1/2N_2O + 1/2H_2O \\ \qquad\qquad \downarrow{\scriptstyle +e^-} \\ \qquad\qquad NO \end{array}$$

$$HNO_2 \overset{+H^+}{\rightleftharpoons} H_2NO_2^+ \overset{-H_2O}{\rightleftharpoons} NO^+ \overset{+e^-}{\rightleftharpoons} NO \qquad (16)$$

$$\begin{array}{l} 2NO_2 \overset{+H_2O}{\rightleftharpoons} HNO_2 + NO_3^- + H^+ \\ \qquad\qquad \downarrow{\scriptstyle +H^+,\ -H_2O} \\ \qquad\qquad NO^+ \overset{+e^-}{\rightleftharpoons} NO \end{array}$$

*Reduction in acidic halide solutions*

The presence of halide ions in acidic solutions of NO, $HNO_2$ and $NO_2$ enhanced the appearance of wave R-I at lower acid concentration. Values of $i_l/i_{l,max}$ and $E_{1/2}$ of wave R-I are plotted in Fig. 5 for hydrochloric acid solutions. The values of $i_l/i_{l,max}$ for NO, $HNO_2$ and $NO_2$ increase rapidly for acid concentration increasing in the range 2—4 M. This is the concentration range in which $X_{NOCl}$ increases significantly (Fig. 1). The fact that the concentration of the nitrosyl compound increases rapidly at lower acidities in hydrochloric acid than in perchloric acid reflects the larger formation constant for NOCl in comparison to $NOClO_4$ (see Table 1). It can be concluded that the nitrosyl halide salts are electroactive at the Pt electrode. The value of $i_l/i_{l,max}$ for NO decreases at the higher hydrochloric acid concentrations (see below).

Recognition of the large value of the formation constant for NOBr, in comparison with that for NOCl, leads to the prediction that addition of bromide ions to solutions of NO, $HNO_2$ and $NO_2$ in perchloric acid should enhance the values of $i_l/i_{l,max}$ for wave R-I at lower halide concentrations. This prediction was verified; values of $i_l/i_{l,max}$ obtained for 4 M $HClO_4$ containing 0.05 M bromide are more than double the values for 4 M $HClO_4$ without bromide (Fig. 6).

Values of $i_{l,max}$ for wave R-I obtained at the rotating Pt disk electrode are given in Table 3. Plots of $i_{l,max}$ vs. $\omega^{1/2}$ were virtually linear with zero intercepts

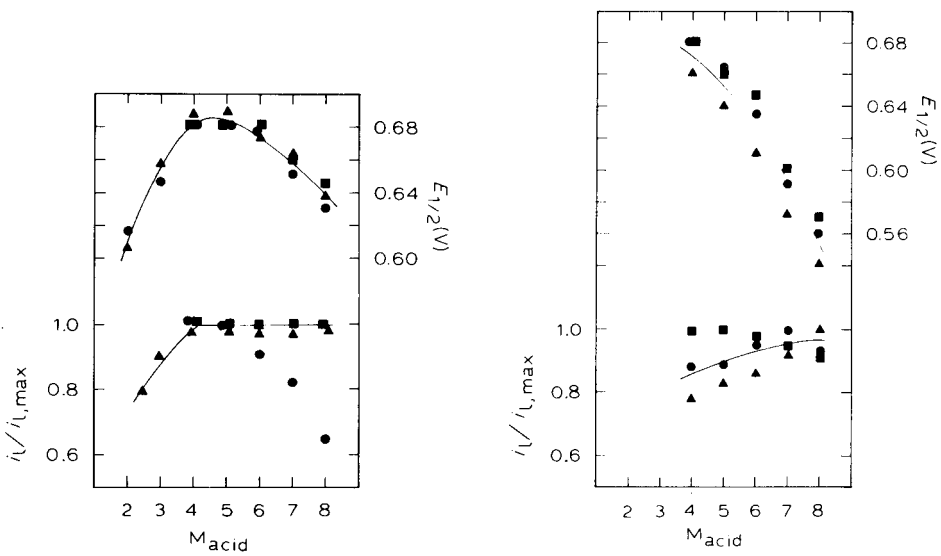


Fig. 5. $i_l/i_{l,max}$ and $E_{1/2}$ of wave R-I for NO, $HNO_2$ and $NO_2$ in HCl solutions. (•) $2 \times 10^{-3}$ M NO; $i_{l,max}$ = 133 μA; (▲) $5 \times 10^{-4}$ M $HNO_2$; $i_{l,max}$ = 56 μA; (■) $5 \times 10^{-4}$ M $NO_2$; $i_{l,max}$ = 21 μA

Fig. 6. $i_l/i_{l,max}$ and $E_{1/2}$ of wave R-I for NO, $HNO_2$ and $NO_2$ in $HClO_4$ solutions containing 0.05 M $Br^-$. (•) $2 \times 10^{-3}$ M NO; $i_{l,max}$ = 175 μA; (▲) $5 \times 10^{-4}$ M $HNO_2$; $i_{l,max}$ = 56 μA; (■) $5 \times 10^{-4}$ M $NO_2$; $i_{l,max}$ = 47 μA.

TABLE 3

$i_{l,max}$ for wave R-I at a rotating Pt disk electrode

| Supporting electrolyte | $i_{l,max}$ ($\mu$A) | | |
|---|---|---|---|
| | $2 \times 10^{-3}$ M NO | $5 \times 10^{-4}$ M $HNO_2$ | $5 \times 10^{-4}$ M $NO_2$ |
| $HClO_4$ | 205 | 65 | 15 |
| $HClO_4$ + 0.05 M $Br^-$ | 175 | 56 | 47 |
| HCl | 133 | 56 | 21 |

for $\omega < 670$ rad $s^{-1}$ (6400 rev $min^{-1}$). Linearity of $i_l - \omega^{1/2}$ plots is diagnostic evidence that the electrode reactions are controlled by mass-transport rather than kinetic processes. A dramatic decrease in $i_{l,max}$ is evident for NO in solutions containing concentrated halide ion. The reduction of NO was concluded above to occur by a mechanism requiring adsorption of NO (see scheme 15). Bromide and chloride ions are strongly adsorbed, in the order $Br^- > Cl^-$, and would be expected to interfere with the adsorption of NO.

Changes in the values of $E_{1/2}$ as a function of acid concentration are also shown in Figs. 4—6 for NO, $HNO_2$ and $NO_2$. The trends for $E_{1/2}$ parallel those for $i_l/i_{l,max}$, which is consistent with the conclusions above. The $E_{1/2}$ values are larger in perchloric acid than in hydrochloric acid solutions and larger in HCl solutions than in $HClO_4$ containing 0.05 M bromide. This is consistent with the fact that the nitrosyl compounds are increasingly stable in the order $ClO_4^- < Cl^- < Br^-$.

*Cyclic voltammetry at a stationary Pt-disk electrode*

Current—potential curves are shown in Fig. 7 for NO, $HNO_2$ and $NO_2$ obtained by cyclic voltammetry at the Pt-disk electrode, under stationary conditions, in 3 M HCl. The $i$—$E$ curves for the three compounds are virtually

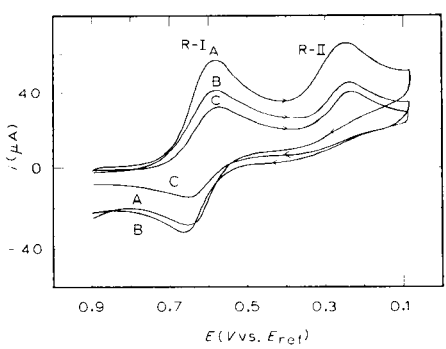


Fig. 7. Current—potential curves for NO, $HNO_2$ and $NO_2$ at a stationary Pt-disk electrode in 3.0 M HCl. Potential scan, 5.0 V $min^{-1}$; first cyclic sweep shown starting at 0.9 V. (A) $5 \times 10^{-4}$ M NO;(B) $5 \times 10^{-4}$ M $HNO_2$; (C) $5 \times 10^{-4}$ M $NO_2$.

identical with regard to number of peaks observed and the peak potentials. The cathodic peaks are labelled to correspond with the cathodic waves obtained for 6.0 M $HClO_4$ at the rotating electrode (Fig. 3). The electrode potential was not scanned sufficiently negative in this experiment to permit observation of a peak corresponding to wave R-III. Whereas two cathodic peaks were observed during the negative potential sweep, only a single anodic peak was obtained on the positive sweep. It can be concluded that the anodic peak corresponds to the oxidation of NO to $NO^+$ and, furthermore, that the reduction product of both waves R-I and R-II is NO. Wave R-II was concluded above to result from $N_2O_3$; the reduction process for R-II is $N_2O_3 + 2H^+ + 2e \rightleftharpoons 2NO + H_2O$.

*Conclusions*

Chemical and electrochemical evidence is consistent with the conclusion that the electroactive precursor is $NO^+$ for the first reduction wave obtained at Pt electrodes for NO, HNO and $NO_2$ in perchloric acid solutions. The $NO^+$ precursor for NO solutions is produced by a heterogeneous process involving adsorbed NO. The $NO^+$ ion has been previously proposed as the electroactive species for several solutions of nitrogen oxides [16, 18, 19, 21—23, 26].

The second reduction wave observed for NO, $HNO_2$ and $NO_2$ in perchloric acid solutions is concluded to correspond to the reduction of $N_2O_3$ present in the solution from decomposition of the parent compounds. This conclusion is in disagreement with many authors [19, 21, 22, 26] who consider that the second wave corresponds to reduction of the NO produced by the first wave. The product of the reductions of $NO^+$ and $N_2O_3$ is considered to be NO. Coulometric evidence supporting this conclusion will be given in a subsequent paper [33].

The presence of bromide or chloride in acidic solutions of the nitrogen compounds enhances the electrode reductions at low $H^+$ concentration by promoting the formation of electroactive nitrosyl halide compounds.

Support of this research by the National Science Foundation through grants GP 40535X and CHE 76-17826 is acknowledged with gratitude.

REFERENCES

1 W. L. Jolly, Inorganic Chemistry of Nitrogen, W. A. Benjamin, Inc., New York, 1964, p. vii.
2 W. L. Jolly, Inorganic Chemistry of Nitrogen, W. A. Benjamin, Inc., New York, 1964, pp. 75—80.
3 J. Masek, Fresenius Z. Anal. Chem., 224 (1967) 99.
4 L. E. Topol, K. B. Oldham and R. G. Alder, J. Inorg. Nucl. Chem., 30 (1968) 2977.
5 N. S. Bayliss, R. Dingle, D. W. Watts and R. J. Wilkie, Aust. J. Chem., 16 (1963) 933.
6 G. Stedman, J. Chem. Soc., (1959) 2949.
7 C. A. Bunton and G. Stedman, J. Chem. Soc., (1958) 2440.
8 W. R. Angus and A. H. Leckie, Proc. Roy. Soc. Lond., (1950) 2576.
9 D. J. Millen, J. Chem. Soc., (1950) 2600.

10 R. A. Robinson and R. H. Stokes, Electrolyte Solutions, Academic Press, 1955, pp. 491 and 504.
11 J. F. Bunnett, J. Am. Chem. Soc., 83 (1961) 4956.
12 T. A. Turney and G. A. Wright, Chem. Rev., 59 (1959) 497.
13 H. Kobayaski, N. Nobutsune, K. Hara, T. Niki and F. Kitano, Nippon Kagaku Kaishi, 3 (1976) 383.
14 N. S. Bayliss and D. W. Watts, Aust. J. Chem., 16 (1963) 927.
15 T. A. Turney and G. A. Wright, J. Chem. Soc., (1958) 2415.
16 H. N. Heckner, J. Electroanal. Chem., 44 (1973) 9.
17 R. C Weast (Ed.), Handbook of Chemistry and Physics, 5th edn., Chemical Rubber Co., Cleveland, Ohio, 1969, p. D-112.
18 L. E. Topol, R. A. Osteryoung and J. H. Christie, J. Electrochem. Soc., 112 (1965) 861.
19 G. Schmid and M. A. Lobeck, Ber. Bunsenges. Phys. Chem., 73 (1969) 189.
20 N. N. Savodnik, V. A. Sheplin and Ts. I. Zalkind, Sov. Electrochem., 7 (1971) 408.
21 H. N. Heckner and G. Schmid, Electrochim. Acta, 16 (1971) 131.
22 D. Dutta and D. Landolt, J. Electrochem. Soc., 119 (1972) 1320.
23 C. T. Garcia, A. J. Calandra and A. J. Arvia, Electrochim. Acta, 17 (1972) 2184.
24 R. G. Gadde and S. Bruckenstein, J. Electroanal. Chem., 50 (1974) 163.
25 L. J. J. Janssen, M. M. J. Pieterse and E. Barendrecht, Electrochim. Acta, 22 (1977) 27.
26 E. Barendrecht and J. F. van der Plas, Rec. Trav. Chem. Pays-Bas, 96 (1977) 133.
27 M. D. Seymour, J. P. Sickafoose and J. S. Fritz, Anal. Chem., 43 (1971) 1734.
28 D. C. Johnson and J. H. Larochelle, Talanta, 20 (1973) 959.
29 H. L. Johnston and W. F. Giauque, J. Am. Chem. Soc., 51 (1929) 3196.
30 J. M. Sedlak and K. F. Blurton, J. Electrochem. Soc., 123 (1976) 1476.
31 C. T. Garcia, A. J. Calandra and A. J. Arvia, Electrochim. Acta, 17 (1972) 2184.
32 V. G. Levich, Physicochemical Hydrodynamics, Prentice-Hall, Englewood Cliffs, New Jersey, 1962.
33 B. G. Snider and D. C. Johnson, Anal. Chim. Acta, 105 (1979) 25.

*Analytica Chimica Acta*, 105 (1979) 25—31


# COULOMETRIC STUDIES OF THE REDUCTION OF NITRIC OXIDE, NITROUS ACID AND NITROGEN DIOXIDE IN ACIDIC HALIDE MEDIA WITH A PLATINUM FLOW-THROUGH ELECTRODE

BOB G. SNIDER[‡] and DENNIS C. JOHNSON*

*Department of Chemistry, Iowa State University, Ames, Iowa, 50011 (U.S.A.)*

(Received 9th October 1978)

SUMMARY

The apparent values of $n$ for the reduction of NO, $HNO_2$ and $NO_2$ in acidic halide solutions of intermediate concentration have been determined coulometrically. The value of $n_{app}$ for $HNO_2$ is 1.0 in HCl solutions for intermediate flow rates at potential values in the range of the first two cathodic waves observed in voltammetric data. The value of $n_{app}$ exceeds 1.0 at low flow rate. The values of $n_{app}$ for reductions of NO in 5 M HCl and $NO_2$ in 3.0 M $HClO_4$ containing 0.1 M bromide are 0.5. These results are explained on the basis of chemical reactions coupled to the electrode processes.

The electrochemical reactions of NO, $HNO_2$ and $NO_2$ at platinum electrodes in acidic media have already been reviewed [1]. Three cathodic waves are observed for acidic solutions of each compound (Fig. 3 of ref. [1]). There is widespread agreement that the electroactive species in solutions of $HNO_2$ is $NO^+$ but there is some hesitancy about the identity of an electroactive precursor in solutions of NO and $NO_2$. Voltammetric data [1] support the conclusion that the electroactive species for acidic solutions of NO and $NO_2$ is also $NO^+$; nitrosonium ion is produced at high acidities. The presence of halide ions in the acid solutions enhances the voltammetric response of NO, $HNO_2$ and $NO_2$ at lower acid concentration [1]. This enhancement was concluded to result from formation of electroactive, slightly dissociated, nitrosyl salts, e.g., NOCl in HCl. Here, further evidence is presented in support of these conclusions for hydrochloric acid and for perchloric acid solutions containing bromide; the evidence was obtained by controlled-potential electrolysis with a platinum flow-through electrode of large area.

Applications of exhaustive electrolysis at controlled potential for the study of electrode reactions have been adequately reviewed by Bard and Santhanam [2]. The apparent number of equivalents per mole of analyte is calculated from the integral of the current—time curve:

$$n_{app} = \int i dt / FN \qquad (1)$$

---

[‡]Present address: The Upjohn Co., Kalamazoo, Michigan 49001 (U.S.A.).

where $n_{app}$ = apparent number of equivalents per mole of analyte; $i$ = electrode current ($A$); $t$ = time (s); $F$ = the Faraday constant (96,487); $N$ = number of moles of analyte.

The value of $n_{app}$ may be affected by chemical reactions coupled to the electrode reaction and, in many cases, non-integral values of $n_{app}$ are obtained. Hence, voltammetric and coulometric data should be considered together in establishing the stoichiometry of electrode reactions [2—4]. Even a very slow coupled chemical reaction involving the electroactive precursor can dramatically affect the value of $n_{app}$ for an electrolysis requiring a long time for completion. Consider e.g., the following general reaction scheme: (1) A + $ne$ → B (electrode reaction); (2) A + B → P (coupled chemical reaction); (3) 2A + $ne$ → P (net electrochemical reaction). If the rate of the second reaction is fa relative to electrolysis, then $n_{app} \rightarrow 0.5n$. Conversely, for a chemical reaction which is slow relative to electrolysis, $n_{app} \rightarrow n$.

The conventional procedure for exhaustive electrolysis involves placement of a large electrode in a rapidly stirred solution of rather large volume, e.g., 10—100 $cm^3$. The time required for complete electrolysis is a function of the cell constant but typically exceeds several minutes. The obvious goal of controlled potential electrolysis for the evaluation of $n$ is complete electrolysis in a minimum of time. This goal can be easily accomplished with coulometric flow-through electrodes designed with maximum internal surface area and minimal interstitial volume for continuous flow analysis [5]. Such electrodes can be operated with an electrolytic efficiency of 100% over a wide range of fluid flow rates, $v_f$. Variation of $n_{app}$ with $v_f$ is indicative of the existence of a coupled chemical reaction occurring at a rate comparable to the rate of electrolysis within the electrode. Depending on the design of the coulometric flow-through electrode, the time required for complete electrolysis of solution in the interstitial volume may be of the order of seconds and even for moderately rapid coupled chemical reactions, $n_{app} = n$.

## EXPERIMENTAL

The platinum rotating disk electrode (RDE) and MSR rotator were from Pine Instrument Co. of Grove City, PA. The coulometric flow-through electro has been previously described (electrode C, ref. [6]). This electrode was prepared from a Pt tubular electrode (2.8 mm i.d. × 1.5 cm) packed with small chips of 30-gauge Pt wire. The electrode was originally reported to operate with an efficiency of 100.0 ± 0.13% for $1.1 \leqslant v_f \leqslant 2.1$ $cm^3$ $min^{-1}$. The interstitial volume of the packed electrode, $V_i$, was determined to be 0.01—0.02 cn For $v_f = 1.0$ $cm^3$ $min^{-1}$, the average residence time of fluid in the electrode ($V_i/v_f$) is estimated to be 0.6—1.2 s. An unpacked Pt tubular electrode (1.0 mr i.d. × 5.0 mm) [6] was used to investigate the analytical application of the electrochemical reduction of $HNO_2$. The efficiency of this electrode was less than 5%. The design of the continuous flow analyzer for forced-flow liquid chromatography has been described previously [6].

A RDE-3 potentiostat (Pine Instrument Co.) was used for potential control;

current—time ($i$—$t$) curves were recorded on a Model SR-255B strip-chart recorder (Heath-Schlumberger Co.). The $i$—$t$ curves were integrated with a Kueffel and Esser planimeter. The calomel reference electrode (Beckman Instrument Co.) had the usual saturated KCl filling solution replaced by a saturated solution of NaCl [1]. The potential of the reference electrode, $E_{ref}$, was 0.234 V vs. NHE.

Solutions of nitrogen compounds were prepared in triply distilled water as described previously [1]. Samples were injected, in the analyzer, into a stream of water which was subsequently mixed with an acid stream prior to passage through the flow-through electrode.

## RESULTS AND DISCUSSION

### *$HNO_2$ in HCl*

The current—potential ($i$—$E$) curve for $HNO_2$ in 5.0 M HCl obtained at a Pt RDE is given in Fig. 1, which also shows the residual curve and the $i$—$E$ curve for an air-saturated solution of 5.0 M HCl. The curves were recorded

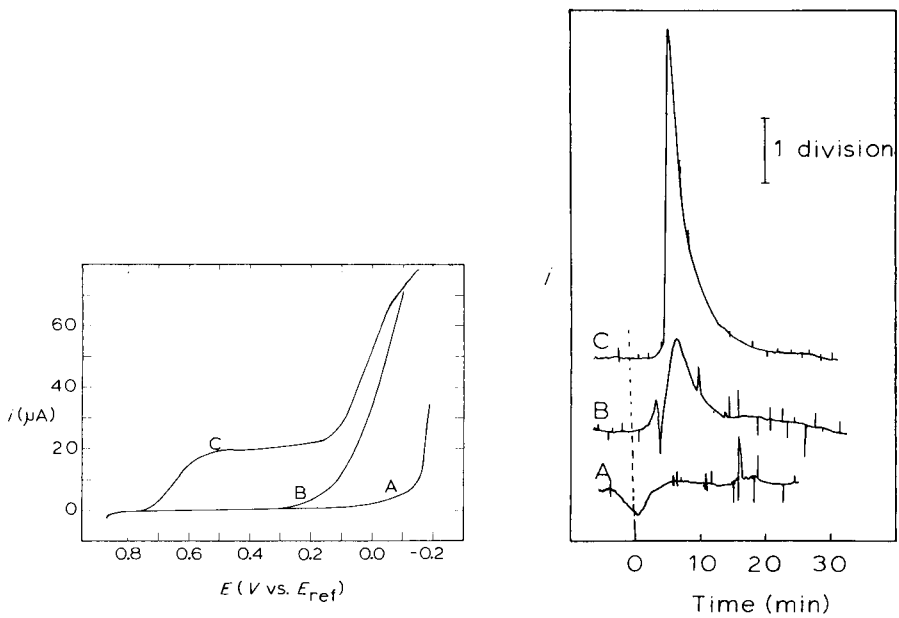


Fig. 1. $i$—$E$ curves at a Pt RDE for $O_2$ and $HNO_2$ in 3.0 M HCl. Electrode area = 0.458 $cm^2$; rotation speed = 900 rev $min^{-1}$; potential scan = 0.5 V $min^{-1}$. (A) Residual curve in deaerated electrolyte; (B) electrolyte saturated with air; (C) deaerated electrolyte containing 1.0 × $10^{-4}$ M $HNO_2$.

Fig. 2. Response of Pt tubular electrode for nitrite $v_f$ = 1.0 $cm^3$ $min^{-1}$; $E$ = 0.40 V; $V_s$ = 0.800 $cm^3$. (A) injection of $H_2O$ (0.1 nA/division); (B) injection of 0.5 ng $NO_2^-$ (0.1 nA/division); (C) injection of 5.0 ng $NO_2^-$ (0.2 nA/division).

during the sweep from positive to negative. Three reduction waves are observed for $HNO_2$ in this media. Only the first reduction wave is clearly defined and accurate values of limiting current and half-wave potential are not obtainable for wave 2 (0.3 V) and wave 3 (0.1 V). The existence of the second reduction wave at 0.3 V was more evident in voltammetric data obtained for a stationary disk electrode (Fig. 7 [1]).

The value of $n_{app}$ was calculated by eqn. (1) from data obtained with the coulometric flow-through electrode for the first reduction wave of $HNO_2$ in hydrochloric acid solutions. Results are given in Table 1 as a function of the acid concentration in the combined streams (sample + reagent) passing through the electrode. The electrode potential was 0.500 V vs. $E_{ref}$ and corresponds to the limiting-current plateau of the first cathodic wave for $HNO_2$. The value of $n_{app}$ increased with increasing acid concentration to a value of 1.0 for $\geqslant$ 5 M HCl. The limiting current measured for $HNO_2$ at $E$ = 0.500 V vs. $E_{ref}$, for a Pt RDE, is at a maximum value for $\geqslant$ 4 M HCl [1]. These results are consistent with the following reaction sequence wherein $HNO_2$ is converted to the electroactive precursor NOCl in solutions of high HCl activity: (1) $HNO_2 + HCl \rightarrow H_2O + NOCl$ (preceding chemical reaction); (2) $NOCl + e \rightarrow NO + Cl^-$ (electrode reaction); (3) $HNO_2 + HCl + e \rightarrow H_2O + NO + Cl^-$ (net electrochemical reaction with 1 equivalent per mole of $HNO_2$).

Values of $n_{app}$ were determined for the reduction of $HNO_2$ in 5 M HCl as a function of electrode potential (Table 2). The value of $n_{app}$ for 5 M HCl is almost 1.0 throughout the potential range 0.5—0.1 V vs. $E_{ref}$ corresponding to waves 1 and 2 observed voltammetrically with the Pt RDE (see Fig. 1). This result is in agreement with the earlier conclusion [1] that wave 2 does not result from the direct, successive reduction of the product of wave 1. The value of $n_{app}$ for reduction of $HNO_2$ in 5 M HCl was also determined at 0.50 V as a function of flow rate $v_f$. The results (Table 3) show that $n_{app}$ is about 1.0 at intermediate flow rates tested (0.5—1.0 $cm^3\ min^{-1}$) but increases with decreasing flow rate for lower flow rates. These results are consistent with a

TABLE 1

Values of $n_{app}$ for reduction of $HNO_2$ as a function of HCl concentration ($E$ = 0.500 V vs. $E_{ref}$; $v_f$ = 1.0 $cm^3\ min^{-1}$; 5.00 × $10^{-4}$ M $HNO_2$; $V_s$ = 0.197 $cm^3$ (sample volume injected)

| HCl (M) | 2.0 | 3.0 | 4.0 | 5.0 | 6.0 | 7.0 |
|---|---|---|---|---|---|---|
| $n_{app}$ | 0.45 | 0.74 | 0.91 | 0.96 | 1.01 | 1.05 |

TABLE 2

Values of $n_{app}$ for reduction of 5.00 × $10^{-4}$ M $HNO_2$ in 5 M HCl as a function of $E$ (V vs. $E_{ref}$) (Flow rate and electrode as in Table 1)

| $E$ | 0.700 | 0.600 | 0.500 | 0.400 | 0.300 | 0.200 | 0.100 | 0.000 | −0.100 | −0.200 |
|---|---|---|---|---|---|---|---|---|---|---|
| $n_{app}$ | 0.07 | 0.66 | 0.91 | 0.91 | 0.94 | 0.97 | 0.95 | 1.31 | 1.91 | 1.98 |

TABLE 3

Values of $n_{app}$ for reduction of $5.00 \times 10^{-4}$ M $HNO_2$ in 5.0 M HCl as a function of $v_f$ (in $cm^3\ min^{-1}$)
($E$ = +0.500 V vs. $E_{ref}$; $V_s$ = 0.197 $cm^3$)

| $v_f$ | 1.0 | 0.75 | 0.50 | 0.40 | 0.30 | 0.25 |
|---|---|---|---|---|---|---|
| $n_{app}$ | 1.01 | 1.01 | 1.03 | 1.20 | 1.35 | 1.55 |

reaction scheme wherein the NO produced from $HNO_2$ by the net electrochemical reaction mentioned in the preceding paragraph undergoes slow disproportionation by the coupled chemical reaction: $4NO + 2HCl \rightleftharpoons 2NOCl + N_2O$. The net electrochemical reaction (2 equivalents per mole $HNO_2$) is then $2HNO_2 + 4HCl + 4e \rightleftharpoons N_2O + 3H_2O + 4Cl^-$.

Excessive dispersion of the sample occurs in the electrolyte stream at $v_f < 0.25\ cm^3\ min^{-1}$ with the result that the $i$—$t$ peaks are very broad and flat. Accurate integration of such peaks was impossible with the equipment available and sufficiently meaningful data could not be obtained at very low $v_f$ to determine if the limiting value of $n_{app}$ was indeed 2.0 for $v_f \rightarrow 0$.

The value of $n_{app}$ determined for reduction of $HNO_2$ in 5 M HCl was 2.0 at a potential in the region of the limiting current plateau for wave 3 (see Table 2). This result is consistent with the reactions proposed by Gadde and Bruckenstein [7]: $HNO_2 + 4H^+ + 4e \rightleftharpoons NH_2OH + H_2O$ (electrode reaction); $NH_2OH + HNO_2 \rightleftharpoons N_2O + 2H_2O$ (coupled chemical reaction); $2HNO_2 + 4H^+ + 4e \rightleftharpoons N_2O + 3H_2O$ (net electrochemical reaction with 2 equivalents per mole $HNO_2$). The ratio of wave heights for waves 3 and 1, obtained at a Pt RDE for $HNO_2$ in 5 M HCl, could not be determined precisely but definitely exceeds a value of 3 for 900 rev $min^{-1}$ (see Fig. 1). The residence time of reaction products at the surface of the RDE electrode under typical operating conditions is much less than the residence time for the coulometric flow-through electrode.

*NO in HCl and $NO_2$ in bromide-containing $HClO_4$*

Coulometric results for NO and $NO_2$ suffered from a general lack of precision because of problems related to preparation of the solutions. Values of $n_{app}$ for replicate analyses of solutions of NO in 5.0 M HCl and for $NO_2$ in 3.0 M $HClO_4$ containing 0.1 M bromide are given in Table 4. The results for both gases are consistent with earlier conclusions [1] that the electroactive species in acidic solutions of the gases containing halides is the product of chemical reactions preceding the electron transfer. Thus for NO in hydrochloric acid solutions, the chemical reaction is

$$4NO + 2HCl \rightleftharpoons 2NOCl + N_2O + H_2O$$

and the net electrochemical reaction (0.5 equivalent per mole of NO) is

$$4NO + 2HCl + 2e \rightleftharpoons 2NO + N_2O + H_2O + 2Cl$$

TABLE 4

Values of $n_{app}$ for NO in 5.0 M HCl and for $NO_2$ in 3.0 M $HClO_4$ + 0.1 M $Br^-$ ($E$ = 0.400 V vs. $E_{ref}$; $v_f$ = 1.0 $cm^3$ $min^{-1}$; $V_s$ = 0.197 $cm^3$)

| NO content (M) | $n_{app}$ | $NO_2$ content (M) | $n_{app}$ |
|---|---|---|---|
| $4.1 \times 10^{-4}$ | 0.52, 0.45 | $5 \times 10^{-4}$ | 0.45, 0.52 |
| $2.0 \times 10^{-4}$ | 0.42, 0.60 | | 0.41, 0.48 |
| | Av. 0.49 | | Av. 0.46 |

For $NO_2$ in bromide-containing perchloric acid solutions, the preceding chemical reaction is

$$2NO_2 + HBr \rightleftharpoons NOBr + NO_3^- + H^+$$

and the net electrochemical reaction (0.5 equivalent per mole $NO_2$) is

$$2NO_2 + e \rightleftharpoons NO + NO_3^-$$

*Determination of nitrite*

The results of these studies on the electrochemical response of $HNO_2$ in hydrochloric acid solutions form the basis of a determination of nitrite in prepared water samples. The motivation for this study was the development of an indirect analytical procedure for nitrosamines based on photolytic decomposition to nitrite in neutral or alkaline solutions followed by amperometric determination of the nitrite produced. A stream of 9.0 M HCl was mixed with the sample stream in the continuous flow analyzer to produce a resultant stream containing 4.5 M HCl which passed through the Pt tubular electrode. An electrode potential of 0.40 V vs. $E_{ref}$ was chosen for detection of nitrous acid. At this potential, reduction of NOCl occurs at a rate limited by mass transport. Dissolved oxygen is electro-inactive in this medium at this potential. Data are given in Table 5 for the calibration of the flow analyzer with the Pt

TABLE 5

Calibration of Pt tubular detector for determination of $NO_2^-$ in 4.5 M HCl ($E$ = 0.40 V vs. $E_{ref}$; $v_f$ = 1.0 $cm^3$ $min^{-1}$; $V_s$ = 0.800 $cm^3$)

| log [$NO_2^-$] (M) | log ($V_s$[$NO_2^-$]) (mol) | log $\int i dt/F$ (mol) | Electrolytic recovery (%) |
|---|---|---|---|
| −8.0 | −11.09 | −12.42 | 4.67 |
| −7.0 | −10.09 | −11.47 | 4.17 |
| −6.0 | −9.09 | −10.47 | 4.16 |
| −5.0 | −8.09 | −9.44 | 4.46 |
| −4.0 | −7.09 | −8.45 | 4.36 |
| −3.0 | −6.09 | −7.40 | 4.81 |
| | | Av. = | 4.43 |
| | | Std. dev. = | 0.26 |

tubular electrode as the detector. Standard solutions were $NaNO_2$ in triply-distilled water. The volume of the sample loop on the sample-injection value, $V_s$, was 0.800 $cm^3$ for this study. The calibration was linear over the concentration range $10^{-8}$—$10^{-3}$ M $NaNO_2$. Solutions prepared with $NaNO_2$ concentrations greater than $10^{-3}$ M were observed to decompose rapidly to gaseous products when mixed with acid. The products are probably NO and $NO_2$. The presence of gas bubbles in the flow analyzer leads to erratic results by disrupting the liminar fluid dynamics and calibration for solutions of concentration greater than $10^{-3}$ M was not attempted.

Typical response of the tubular detector is shown in Fig. 2 for injections of $1.4 \times 10^{-8}$ M and $1.4 \times 10^{-7}$ M $NO_2^-$. These concentrations correspond to 0.5 ng and 5.0 ng $NO_2^-$, respectively, in the 0.800-$cm^3$ sample. The detection peak for injection of pure water is also shown in Fig. 2. The exact source of electrical noise observed at high current sensitivity, such as used for Fig. 2, is not known but is probably related to hydrodynamic phenomena. A current spike is always instantaneously produced when the sample-injection valve is manipulated. Noise of an equivalent magnitude can also be generated by tapping the flexible Teflon tubing of the flow analyzer with a pencil.

*Conclusions*

The electrochemical reductions of NO, $HNO_2$ and $NO_2$ in 5 M HCl and 3.0 M $HClO_4$ containing 0.1 M $Br^-$ occur by mechanisms involving formation of nitrosyl halides as the electroactive compound. A linear calibration curve is obtained for $NO_2$ in 4.5 M HCl over a concentration range of five decades. The numerical value of $n_{app}$ for $HNO_2$ in HCl, determined by a coulometric electrode, is 1.0 for $0.5 \leqslant v_f \leqslant 1.0$ $cm^3$ $min^{-1}$. However, $n_{app}$ increases above 1.0 for $v_f < 0.5$ $cm^3$ $min^{-1}$. Hence, electroanalytical procedures for determining nitrite in these acid solutions must be calibrated with the identical hydrodynamic conditions used for the analysis.

Support of this research by the National Science Foundation through grants GP 40535X and CHE 76-17826 is acknowledged with gratitude.

REFERENCES

1 B. G. Snider and D. C. Johnson, Anal. Chim. Acta, 105 (1979) 9.
2 A. J. Bard and K. S. V. Santhanam, in A. J. Bard (Ed.), Electroanalytical Chemistry, Marcel Dekker, New York, vol. 4, 1970.
3 D. H. Geske and A. J. Bard, J. Phys. Chem., 63 (1959) 1057.
4 L. Meites and S. A. Moros, Anal. Chem., 31 (1959) 23.
5 T. Fujinaga and S. Kihara, C.R.C. Critical Reviews in Analytical Chemistry, 6 (1977) 223.
6 D. C. Johnson and J. H. Larochelle, Talanta, 20 (1973) 959.
7 R. G. Gadde and S. Bruckenstein, J. Electroanal. Chem., 50 (1974) 163.

*Analytica Chimica Acta*, 105 (1979) 33—41


# POTENTIOMETRIC STRIPPING ANALYSIS FOR MERCURY

DANIEL JAGNER

*Department of Analytical Chemistry, University of Göteborg and Chalmers University of Technology, S-41296 Göteborg (Sweden)*

(Received 25th September 1978)

## SUMMARY

In potentiometric stripping analysis for mercury, elemental mercury is deposited on a glassy carbon electrode surface by means of potentiostatic reduction. It is then oxidized by potassium permanganate added to the sample prior to analysis and the "redox titration curve" thus obtained is recorded on a high-input impedance recorder. Deaeration of the sample is unnecessary. The analytical range is $5 \times 10^{-9}$—$10^{-3}$ M mercury(II), the times needed for potentiostatic accumulation ranging from 64 min at $10^{-8}$ M to 1 min at concentrations above $10^{-6}$ M. The chemistry of the stripping process is discussed and an automatic instrument for potentiometric stripping analysis is described.

Potentiometric stripping analysis [1, 2] is based on pre-concentration of the metal analyte by means of potentiostatic reduction and amalgamation (plating) on a glassy carbon electrode. After pre-concentration the potentiostatic circuitry is disconnected and the amalgamated metals are titrated consecutively either by mercury(II) ions, added to the sample before analysis, or by the dissolved oxygen present in the sample. The redox potential of the glassy carbon electrode is recorded on a high-impedance $x$—$t$ recorder or on a pH meter [3], the time elapsing between two consecutive equivalence points being taken as the analytical signal for the element oxidized. Since mercury has been added to the sample prior to analysis in the previous applications of potentiometric stripping analysis, the technique has hitherto not been suitable for the determination of mercury.

A procedure for potentiometric stripping determination of mercury with potassium permanganate as oxidant in non-deaerated samples is described in this paper.

## EXPERIMENTAL

### *Instrumentation*

The Potentiometric Stripping Analyzer (Radiometer, Prototype) can be programmed to give plating potentials between —2 and 0 V vs. SCE and plating times between 1 and 64 min. Two seconds before stripping is initiated, i.e. the potentiostat is disconnected, the paper feed of the recorder (Radiometer

REC 61) is started automatically and subsequently terminated after a given fraction of the plating time. The Analyzer can be operated in a repetitive mode whereby a new plating/stripping cycle is initiated automatically after the first stripping curve has been recorded.

The electrochemical cell was a modified titration assembly (Radiometer TTA 60). Three different titration vessels, ranging from 2 to 50 ml, either of glass or disposable polyethylene, were used as sample vessels. Stirring was achieved by means of a constant-rate mechanical Teflon stirrer.

The glassy carbon working electrode (Radiometer F 3500) had a total surface area of 8 $mm^2$ and was pressure-fitted into a Teflon rod with an outer diameter of 7 mm. No glue of any kind was used in the electrode. A saturated calomel electrode (Radiometer K 4040) was used as reference and a platinum foil (Radiometer P 1042) as counter electrode. The reference electrode was tested for mercury(I) leakage; none was detected for at least three weeks.

*Chemicals*

All chemicals used, except mercury(II) nitrate, were of Suprapur grade.

*Procedure*

To 20—50 ml of sample solution, 2—5 ml of a standard solution containing 2.5 M sodium chloride, 0.25 M sodium acetate, acetic acid and copper(II) (2 mg $l^{-1}$), is added. Potassium permanganate is added to a total concentration of about $0.08 \times 10^{-3}$ M. If the sample consumes permanganate, more permanganate is added until the sample has a clearly visible pink colour.

The glassy carbon electrode is polished for 5—10 s with diamond paste and washed with acetone. The sample is inserted in the analyzer and the stirrer started. The redox potential, as measured on the recorder, should be in the region of 0.4—0.7 V vs. SCE. If the potential is below 0.4 V, more potassium permanganate is added until the optimum redox range is reached.

The Analyzer is adjusted to a plating potential of —0.70 V vs. SCE and plating is started. After about 10 s, the potentiostat is disconnected by using the Reset function of the instrument. The potential is allowed to drop to the base-line region of 0.4—0.8 V vs. SCE. This normally takes less than 2 s. This short plating/stripping cycle is repeated once. The plating time is adjusted to the value to be used during analysis and plating is started. The stripping curve is evaluated as shown below. The mercury(II) concentration is determined by standard addition, or from a calibration curve, or by the use of an internal standard, e.g. the copper(II) added.

## RESULTS AND DISCUSSION

*Effect of copper(II)*

When present in concentrations below $10^{-5}$ M, mercury(II) is difficult to plate onto a glassy carbon electrode. Copper(II) is, however, readily plated onto a polished glassy carbon surface. Once a small amount of copper has

been plated onto the electrode surface, mercury is easily deposited on the copper film. This is demonstrated by curves (a) and (b) of Fig. 1. Stripping curve (a) was recorded after plating for 8 min at —0.70 V vs. SCE in a sample containing $5 \times 10^{-7}$ M mercury(II), 0.25 M chloride, and $0.08 \times 10^{-3}$ M potassium permanganate, buffered at pH 4.7 with acetate buffer. Curve (b) was recorded under the same experimental conditions after the addition of copper(II) corresponding to 200 $\mu g\ l^{-1}$ to the sample. As can be seen from Fig. 1, the mercury signal is hardly discernible without the addition of copper(II) which increases the sensitivity by almost two orders of magnitude.

The stripping plateau for copper in Fig. 1 shows a slight potential increase during stripping. This is probably due to a difference between the kinetics of the stripping of copper and of amalgamated copper. The copper stripping plateaux are, however, reproducible and almost independent of the concentration of mercury in the sample. A copper concentration of 200 $\mu g\ l^{-1}$ proved to be suitable for the deposition of mercury on a glassy carbon electrode. For mercury(II) concentrations below $10^{-7}$ M, where plating times of 4 min or more must be used, the copper(II) concentration can, however, be decreased to 50 $\mu g\ l^{-1}$.

To initiate the deposition of copper on a freshly polished glassy carbon surface, it may be necessary to apply the plating potential, e.g. —0.70 V vs. SCE, for a couple of seconds followed by a stripping before the analytical procedure is started. Unless copper has been deposited, no mercury will be deposited during the first seconds of plating. Once sensitized by one or two short plating/stripping cycles, the deposition of mercury will start immediately after the plating potential has been applied.

*Choice of oxidant and pH*

The oxidant to be used for potentiometric stripping analysis of mercury must be strong enough to oxidize mercury to mercury(II). Dissolved oxygen, for example, is not sufficiently strong an oxidant. Two obvious choices are permanganate and dichromate. Cerium(IV) is less suitable, because strong acidification of the samples with sulfuric acid would be necessary.

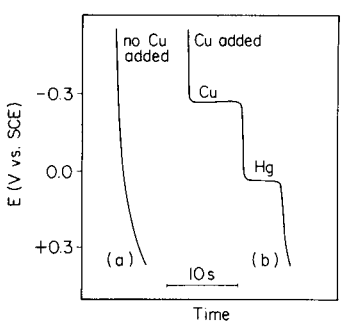


Fig. 1. Effect of the addition of copper(II) on the mercury stripping signal. Both curves were recorded after plating for 8 min in a sample containing $5 \times 10^{-7}$ M mercury(II) and $0.08 \times 10^{-3}$ M potassium permanganate.

Permanganate and dichromate were tested in a series of experiments at different pH values. Curve (a) of Fig. 2 shows the stripping curve recorded, after plating for 4 min at 0.7 V vs. SCE, in a sample containing $2 \times 10^{-6}$ M mercury(II), copper(II) (200 $\mu g\ l^{-1}$), 0.025 M chloride, and $0.08 \times 10^{-3}$ M permanganate, buffered at pH 2 with hydrochloric acid. Curve (b) of Fig. 2 shows the stripping curve under the same experimental conditions except that the sample was buffered at pH 4.7 with 0.025 M sodium acetate—acetic acid. For curve (c) permanganate was replaced by $0.012 \times 10^{-3}$ M dichromate and the sample was acidified with 0.1 M hydrochloric acid.

Figure 2 shows that both permanganate and dichromate can be used as oxidants for mercury stripping. For dichromate, however, the samples must be made more acidic than for permanganate; this may be a disadvantage under certain circumstances. Furthermore, permanganate has a much stronger colour than dichromate and it is therefore easier to see if the oxidant has been consumed by species present in the sample. Figure 2 also shows that the optimum pH range for permanganate is 3—6. As sodium acetate can be obtained commercially in a very high degree of purity this would seem to be the most suitable buffer.

*Analytical concentration range*

The analytical range for mercury determinations by means of potentiometric stripping analysis was investigated in samples containing 0.25 M sodium chloride, and 200 $\mu g$ Cu $l^{-1}$, buffered with acetate to pH 4.7. The mercury(II) concentration varied between $10^{-8}$ M and $10^{-4.3}$ M (approximately 2—10000 $\mu g\ l^{-1}$). The samples were plated at —0.7 V vs. SCE for 32 min ($10^{-8}$ and $2 \times 10^{-8}$ M), 16 min ($10^{-7}$ M), 4 min ($10^{-6}$ and $10^{-5}$ M), or 1 min (above $10^{-5}$ M). The analytical signals, normalized for the different plating times, are shown in Fig. 3, and the stripping curve recorded for the $10^{-7}$ M mercury(II) sample is shown in Fig. 4. Figure 3 shows that potentiometric stripping analysis can be used for the determination of mercury(II) over the whole range investigated. The range can in fact be increased up to $10^{-2.3}$ M mercury(II); these results

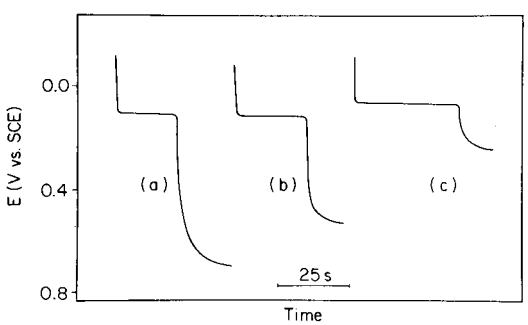


**Fig. 2. Potentiometric stripping curves obtained by using $0.08 \times 10^{-3}$ M permanganate as oxidant at pH 2 (curve a) and at pH 4.7 (curve b); or $0.012 \times 10^{-3}$ M dichromate as oxidant at pH 1 (curve c). Sample concentration of mercury(II) is $2 \times 10^{-6}$ M and plating time is 4 min.**

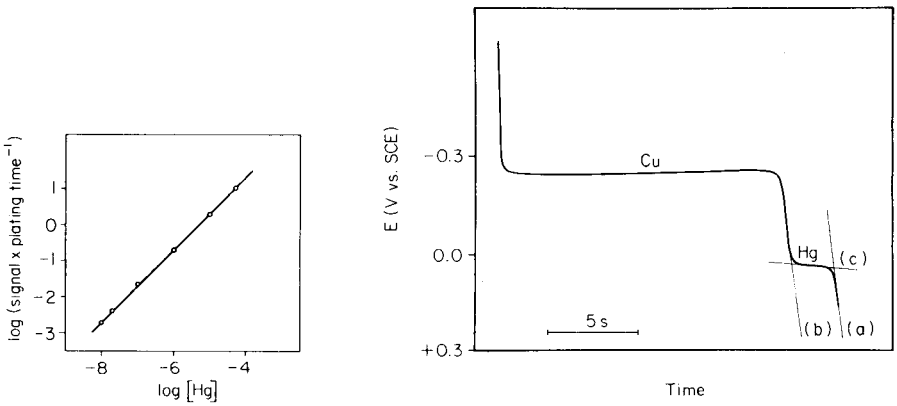


Fig. 3. Analytical concentration range for the potentiometric stripping determination of mercury.

Fig. 4. Potentiometric stripping curve recorded after plating for 16 min at —0.7 V vs. SCE in a sample containing $10^{-7}$ M mercury(II). The time lapse between the intersection of line (c) with the parallel lines (a) and (b) comprises the analytical signal.

are not shown in Fig. 3 because they required much higher total buffer concentrations owing to the acidity of the mercury(II) stock solution.

*Evaluation of the stripping signal*

The evaluation of the stripping signal is illustrated on the mercury plateau of Fig. 4. Line (a) is drawn through the stripping curve after the mercury plateau; line (b) is drawn parallel to line (a) through the stripping curve before the mercury plateau. Line (c) is drawn through the stripping curve at the half-stripping potential. The time distance between the intersection of line (c) with lines (a) and (b) is taken to be the analytical signal for mercury.

*The stripping process: memory effects*

Acidic potassium permanganate readily oxidizes mercury to mercury(II). The primary redox process recorded during stripping in chloride media might consequently be either the one-electron process $2Hg(s) + 2Cl^- \rightarrow Hg_2Cl_2(s) + 2e^-$, or the two-electron process $Hg(s) + nCl^- \rightarrow HgCl_n^{2-n} + 2e^-$ ($n = 1$—$4$), depending on the kinetics of the oxidation processes and on the kinetics of the formation of mercury(II) chloride complexes. If formation of calomel is the primary process, this will be followed by oxidation of mercury(I) to mercury(II):

$$Hg_2Cl_2(s) + (2n - 2)Cl^- \rightarrow 2HgCl_n^{2-n} + 2e^- \qquad (n = 2\text{—}4)$$

In order to determine the primary oxidation process, three samples, containing $5 \times 10^{-7}$ M mercury(II), 200 $\mu$g Cu $l^{-1}$, $0.08 \times 10^{-3}$ M potassium permanganate and different concentrations of chloride ions, were plated at —0.7 V vs. SCE

for 4 min. The ionic strength was kept constant at 1.00 M with sodium perchlorate. The composition of the samples are specified in Table 1 and the different stripping curves are shown as (a)-(c) in Fig. 5. Also specified in Table 1 are the theoretical half-stripping potentials ($E_{1/2}$) for 1-e and 2-e processes. In the calculations of the $E_{1/2}$ values for the 2-e process the stability constants for the mercury(II)—chloride system were chosen as [4]:

$\log \beta_1 = 6.72$, $\log \beta_2 = 13.23$, $\log \beta_3 = 14.2$ and $\log \beta_4 = 15.3$.

As can be seen from Table 1, the $E_{1/2}$ values found agree satisfactorily with the assumption that formation of calomel is the primary stripping process. The difference between the calculated and experimental values for $E_{1/2}$ vs. SCE are mostly due to the difference between the activity factors for chloride at 1 M ionic strength and inside the calomel electrode.

Further evidence for the formation of calomel on the glassy carbon electrode surface is provided by the memory effects shown in Fig. 6. For this, a sample having the same composition as sample A of Table 1 was plated for 4 min at —0.70 V and the stripping curve was recorded (curve a); 5 s after the recording of the mercury stripping plateau, the potentiostat was switched on at —0.70 V vs. SCE and a new stripping curve was recorded immediately (curve b). This stripping curve shows a memory effect for mercury from the previous plating/stripping cycle. Copper shows no such memory effect. The same

TABLE 1

Effect of chloride ion concentration on the half-stripping potential ($E_{1/2}$) for mercury at ionic strength 1.

| Sample | $[H^+]$ (M) | $[Cl^-]$ (M) | $E_{1/2}$ vs. SCE (mV) | | | |
|---|---|---|---|---|---|---|
| | | | Found | Theor. for 1-e process | Theor. for 2-e process | Assuming formation of $HgCl_n$ |
| A | 0.01 | 0.01 | 142 | 150 | — | |
| B | 0.01 | 0.1 | 83 | 91 | 59 | 72 |
| C | 0.01 | 0.5 | 32 | 49 | 42 | 72.5 |

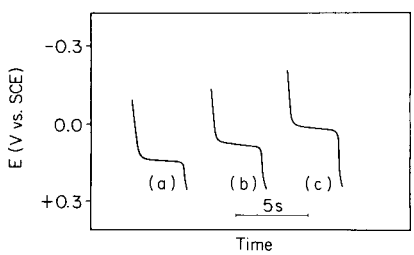


Fig. 5. Potentiometric stripping curves for mercury recorded in 0.01 M chloride; (a) 0.1 M chloride (b) and 0.5 M chloride (c) at 1.00 M ionic strength. Plating was done for 4 min at —0.7 V vs. SCE in samples containing $5 \times 10^{-7}$ M mercury(II).

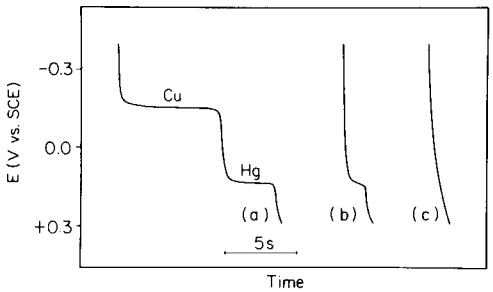


Fig. 6. Memory effects in potentiometric stripping analysis for mercury. Curve (a) was recorded after 4 min of plating at —0.7 V vs. SCE in a sample containing $5 \times 10^{-7}$ M mercury(II) and 0.01 M chloride. Curve (b) was recorded 5 s after the completion of the mercury stripping in curve (a) without any plating; curve (c) was recorded 20 s after the completion of mercury stripping in curve (a).

experiment was repeated with the difference that a time lapse of 20 s was allowed between the recording of the mercury stripping plateau and the re-activation of the potentiostat. The stripping curve registered (curve c) showed no mercury memory effect. The memory effect is probably due to the presence of calomel on the electrode surface when the reducing potential is applied. Some of this calomel is rapidly reduced to mercury thus giving rise to a new mercury stripping plateau. Further experiments showed that increasing the chloride concentration above approximately 0.1 M resulted in very rapid dissolution of calomel, and memory effects were then not encountered. In potentiometric stripping analysis for mercury it is thus advantageous to add chloride ions to the sample so that the memory effect is eliminated.

*Detection limit*

The detection limits in potentiometric stripping analysis cannot be defined uniquely because they depend inversely on the plating time (cf. Fig. 3). Plating times exceeding 1 h are, however, seldom required. The detection limit with plating for 64 min can be estimated from, for example, Fig. 4, for which $10^{-7}$ M mercury(II) was plated for 16 min. Assuming that a signal of 0.1 s is the detection limit on the recorder track, the detection limit can be estimated as approximately $5 \times 10^{-9}$ M. In fact, plating times up to 4 h can be exploited. For longer plating times, depletion of permanganate seriously affects the stripping curves.

*Accuracy and precision*

The accuracy was tested by means of calibration plots in the concentration range $5 \times 10^{-9}$—$10^{-4}$ M (cf. Fig. 3). The reproducibility of the mercury signal on repetitive plating/stripping in the same sample was estimated from 20 consecutive plating/stripping sequences in a sample containing 0.25 M chloride, 200 $\mu$g Cu $l^{-1}$, $0.08 \times 10^{-3}$ M potassium permanganate and $10^{-7}$ M mercury(II),

buffered at pH 4.7 with acetate. Plating was done for 16 min at −0.7 V vs. SCE. The relative standard deviation was 6.5% for the mercury signal and 3.6% for the ratio between the copper and mercury signals. The copper-to-mercury signal ratio has a better reproducibility because it is not affected by variations in stirring or by slight losses of permanganate even during plating for 5 h. Copper is, however, oxidized both by permanganate and by dissolved oxygen. In a separate experiment, with a sample of the same composition, the sample was deaerated with nitrogen prior to repetitive plating/stripping. The relative standard deviation of the mercury signal was unaffected but the relative standard deviation of the copper-to-mercury ratio decreased to 2.7%. Copper can thus be used as internal standard, the best results in this case being obtained in deaerated samples.

*Organic mercury compounds*

Organic mercury compounds decompose in the acidic permanganate medium used in potentiometric stripping analysis for mercury(II). This was confirmed by a calibration curve, in the $10^{-7}$—$10^{-6}$ M range, prepared with methylmercury chloride. This calibration curve did not differ significantly from a calibration curve prepared with mercury(II) nitrate.

*Interferences*

There are two kinds of interference which may affect the potentiometric stripping signals in the determination of mercury(II). Elements which can be deposited on the glassy carbon surface and which have the same oxidation potential as mercury will interfere with the mercury stripping signal. The only element likely to fulfil these requirements is silver; indeed, silver ions were found to interfere with the mercury signal. To determine mercury in the presence of silver, or silver in the presence of mercury, the medium must be modified to give a greater difference between the oxidation potentials of silver and mercury. Work towards this end is in progress.

The second type of interference is due to the presence of oxidizable species in the sample. Such species will consume potassium permanganate. For such samples it is advisable to allow a time lapse of ca. 1 h between the addition of permanganate and the commencement of the analysis. During this period, the concentration of free permanganate will normally be stabilized; if necessary more permanganate can be added.

Both these sources of interference can be eliminated by means of the tin(II) reduction method frequently used in the atomic absorption determination of mercury. Preliminary experiments indicate that this method is very easily adapted to potentiometric stripping analysis for mercury. The mercury vapor can be collected directly in the buffered potassium permanganate solution used for potentiometric stripping analysis. Details of this procedure will be given elsewhere [5].

Potentiometric stripping analysis can be carried out with very simple instrumentation and without sample deaeration. When timing circuits are used,

as in the instrument used here, most of the analysis can be done unattended. It is possible to control the chemistry of the stripping process in potentiometric stripping analysis more easily than in anodic stripping voltammetry, and the method yields good accuracy and precision without any loss of sensitivity.

REFERENCES

1 D. Jagner and A. Graneli, Anal. Chim. Acta, 83 (1976) 19.
2 D. Jagner and K. Årén, Anal. Chim. Acta, 100 (1978) 375.
3 D. Jagner, Anal. Chem., 52 (1979) 1924.
4 Critical Stability Constants, Plenum Press, New York, 1976.
5 D. Jagner and K. Årén, to be published.

*Analytica Chimica Acta*, 105 (1979) 43—52


# POTENTIOMETRIC DETERMINATION OF GLUCOSE BY ENZYMATIC OXIDATION IN A FLOW SYSTEM

LO GORTON* and KHAN M. BHATTI**

*Department of Analytical Chemistry, University of Lund, POB 740, S-220 07 Lund (Sweden)*

(Received 18th July 1978)

SUMMARY

A potentiometric determination is described for glucose based on oxidation by 1,4-benzoquinone with immobilized glucose oxidase as catalyst in an enzyme reactor. The electrode is preceded by an analytical dialysis unit to remove proteins. The ratio of quinone to hydroquinone was measured with a flow-through gold electrode. Another gold electrode preceded the enzyme reactor to correct for serum components (e.g. ascorbic acid) which can also reduce quinone. The operating range is 0.04—10 $\times 10^{-3}$ M $\beta$-D-glucose. The dialysis proceeds with a linear dependence on glucose concentration, and the dialysis ratio can be adjusted by changing the buffer flow rate.

Because of the importance of glucose determinations in body fluids, many methods have been studied in recent years. Glucose can be oxidized to gluconic acid, with glucose oxidase as a selective catalyst. The co-enzyme flavine adenine dinucleotide (FAD) is simultaneously reduced to $FADH_2$, but can be reoxidized by oxygen: $FADH_2 + O_2 \rightarrow FAD + H_2O_2$. This reaction has been used as the basis for a number of methods for determining glucose. The consumption of oxygen can be monitored amperometrically or with an oxygen electrode [1]. The hydrogen peroxide can be determined electrochemically either by oxidation at a platinum electrode [2] or by a catalytic decomposition to oxygen and water on the surface of an oxygen electrode [3]. The above-mentioned reaction can also be coupled to other catalytic reactions. Molybdenum(VI) [4] or peroxidase [5] can catalyze the oxidation by hydrogen peroxide of iodide to iodine. The iodine or iodide can be monitored electrochemically. Peroxidase can also catalyze the oxidation of hexacyanoferrate(II) by hydrogen peroxide [6]. There are disadvantages with all these methods, hence various improvements have been described, and have been reviewed recently [7].

Williams et al. [8] described an amperometric method in which 1,4-benzoquinone (Q) oxidized the co-enzyme: $FADH_2 + Q \rightarrow FAD + QH_2$. The hydroquinone ($QH_2$) produced was monitored amperometrically at a platinum electrode. A background current was produced by plasma components which

**Permanent address: Physical Research Division P.C.S.I.R., Karachi Laboratories, University Road, Karachi (Pakistan).

reduced Q to $QH_2$. Thus a differential measurement was required. Two indicator electrodes were used, one covered with immobilized glucose oxidaze and the other without enzyme. The difference in current between these two indicator electrodes was a linear function of the glucose concentration.

This report concerns a study of a potentiometric method based on oxidation with 1,4-benzoquinone. The concentration ratio $[Q]/[QH_2]$ is monitored with a gold electrode in a flow system. The enzyme is immobilized on glass and contained in a small reactor. The advantages expected when the present investigation was planned were the following. The reactor concept allows quantitative conversion of β-D-glucose to gluconic acid, in contrast to the membrane used by earlier workers. A potentiometric detection system should be less affected by flow rate and temperature. An independent test of a new analytical dialyzer was also included in the investigation.

## THEORY

The overall reaction in the enzyme reactor is:

$$\beta\text{-D-glucose} + Q + H_2O \rightarrow \text{gluconic acid} + QH_2 \qquad (1)$$

The response reaction of the redox electrode at constant pH and ionic strength obeys the Nernst law. Originally the amounts of quinone and hydroquinone present are $[Q]_{init}$ and $[QH_2]_{init}$. Hence the response of a redox electrode placed after an enzyme reactor will be

$$E = E' + \frac{RT}{2F} \ln \left\{ \frac{[Q]_{init} - 0.635\ [\text{D-glucose}]}{[QH_2]_{init} + 0.635\ [\text{D-glucose}]} \right\} \qquad (2)$$

The factor 0.635 represents the fraction of β-D-glucose in the D-glucose solution. Only the β-form is enzymatically active with glucose oxidase [9].

Various species common in body fluids may reduce 1,4-benzoquinone to hydroquinone. This will alter the original ratio $[Q]_{init}/[QH_2]_{init}$. The actual concentrations of quinone and hydroquinone before the enzymatic reaction can be written

$$[Q]_{act} = [Q]_{init} - \Sigma[I_j] \text{ and } [QH_2]_{act} = [QH_2]_{init} + \Sigma[I_j] \qquad (3)$$

where $I$ is an interferent, which for simplicity is supposed to react with the quinone to yield an equal concentration of hydroquinone. An electrode placed before the enzyme reactor will therefore have the potential

$$E = E' + (RT/2F) \ln [Q]_{act}/[QH_2]_{act} \qquad (4)$$

The potential of the redox electrode placed after the glucose oxidase reactor will then be

$$E = E' + \frac{RT}{2F} \ln \left\{ \frac{[Q]_{act} - 0.635\ [\text{D-glucose}]}{[QH_2]_{act} + 0.635\ [\text{D-glucose}]} \right\} \qquad (5)$$

$[Q]_{act}$ and $[QH_2]_{act}$ can be evaluated from eqns. (3) and (4). When these values are put into eqn. (5), the concentration of D-glucose can be found.

This potentiometric method was shown to be suitable for use with a dialysis step to remove proteins, which would otherwise interfere severely. The dialyzer used consists of a tubular dialysis membrane concentrically mounted in a glass tube. Solute species diffuse from the sample solution (outer tubing, concentration $C_s \times 10^{-3}$ M) into the buffer (inner tubing, flow rate $f$ ml $min^{-1}$), where the concentration ($C_e \times 10^{-3}$ M) will be measured by the electrodes after a short time. The pressure in the inner tubing is higher owing to its smaller diameter. This has the effect that the only force driving glucose from the outer tube to the inner tube is the concentration gradient. This difference in pressure also prevents large molecules (e.g. proteins) from clogging the membrane. In the outer tubing the sample solution flows rapidly enough to keep the concentration of diffusing species essentially constant. Back-diffusion is negligible because $C_s$ is much larger than $C_e$.

Thus the total flux $F$ (mol $s^{-1}$) through the dialysis membrane can be expressed by $F = AD\,(C_s - C_e)/l$, where $A$ is the membrane area, $l$ its thickness and $D$ the diffusion coefficient of glucose. The solute diffusing into the buffer is transported to the detector. When a steady state is achieved, $F = f_e C_e$. For $C_s \gg C_e$, these two equations give

$$C_e = ADC_s/lf_e = kC_s \qquad (6)$$

Equation (6) shows that there is a linear relationship between $C_e$ and $C_s$. The constants can be compounded to a new constant, $k$, different for each solute.

If the electrodes are placed in a buffer solution after the dialyser, eqns. (3)—(5) will remain valid if $\Sigma[I_j]$ is replaced by $\Sigma k_j[I_j]$ and the factor 0.635 in eqn. (5) is replaced by 0.635 $k$(glucose).

## EXPERIMENTAL

Glucose oxidase from *Aspergillus niger* (EC.1.1.3.4) (Serva 22741, 150 mg protein) was immobilized on CPG-10 controlled-pore glass (Corning Glass Works; pore size 654 Å, 80—120 mesh) with glutaraldehyde [10]. The enzyme-treated glass was filled into a PVC reactor tube (i.d. 3.0 mm, length 43 mm, volume 300 $\mu$l) with connectors for 0.5-mm i.d. Teflon tubes. Silver frits (1/8 in. diameter, 0.015-mm holes; Reeve Angel Cert. No. LA 200) were placed at both ends of the reactor to keep the enzyme within the PVC tube.

The enzyme, both soluble [11] and immobilized [12], is active in a broad pH range (4—7) with maximum activity at pH 5.5. As the enzymatic reaction yields gluconic acid, and the enzyme is immobilized on porous glass beads, there will be a slight decrease in the pH in the enzyme environment, compared to the bulk solution. Hence the buffer pH chosen was 6.0. The ionic strength of the buffer was increased with sodium sulphate to decrease the electrokinetic potential.

The buffer solution (0.1 M phosphate buffer, pH 6.0 which was 0.1 M in $Na_2SO_4$, and contained various amounts of quinone) was pumped with an Ismatec MP13 GJ-4 peristaltic pump. The flow rate through the enzyme reactor

was varied between 0.6 and 3.0 ml $min^{-1}$. The samples, which contained glucose and buffer, were introduced into the stream with a rotary sample valve (Altex, model 202). The flow which contained either buffer or buffer with glucose passed through the enzyme reactor and through the tubular gold electrode (Fig. 1). This electrode (Fig. 2) was made from a solid gold rod (o.d. 9 mm, length 20 mm); the electrode part of this rod was a drilled hole (i.d. 0.8 mm, length 6 mm). To insert the electrode into the flow stream, screw fittings were made to suit the connectors of Altex or Chromatronix couplings for Teflon tubing. The reference electrode (Radiometer K 401 calomel electrode), was placed as a piston in a syringe cylinder, the tip of which was pressed down into a PVC block made to fit a luer connection. Alternatively, for determining glucose in solutions containing interferents reacting with benzoquinone, another flow-through gold electrode was inserted in front of the enzyme reactor (Fig. 2). The electrodes were connected to a twin differential high-impedance amplifier (Fig. 3) with a common connection to the solution via a flow-through stainless steel ground electrode (Fig. 2). There was some electrical noise from the pump

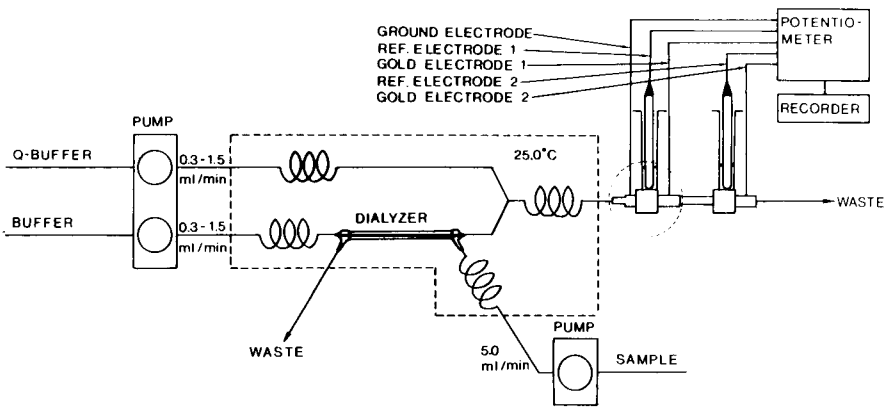


Fig. 1. Diagram of the flow system, the dialyzer, and the enzyme reactor electrode arrangement. The encircled part of the figure is magnified in Fig. 2.

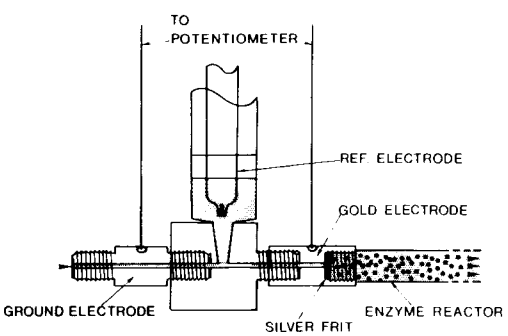


Fig. 2. Diagram of the pre-electrode system and the enzyme reactor.

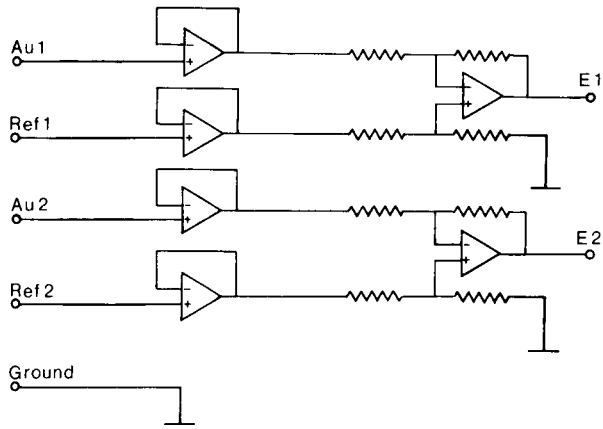


Fig. 3. Circuit for measurement of the differential potentials $E1$ and $E2$, where Au1 and Ref1 represent the pre-electrode system and Au2 and Ref2 represent the electrode system after the enzyme reactor. The high-impedance amplifier and the differential amplifier used are 1035-02 Teledyne Philbrick and AD504M Analog Devices, respectively.

when the electrodes were connected to a single-ended pH meter like the Radiometer PHM64, but this was eliminated by the differential arrangement. A fast-response recorder (Philips PM 8202) was used.

The dialyzer used was a flow-through hollow-fibre micro-dialyzer (AB GAMBRO, POB 10015, S-220 10 Lund; Swedish patent 396819). When not in use it was stored in a refrigerator and soaked with glycerine to prevent bacterial growth. All solutions were thermostated with a Julabo Paratherm U2 electronic thermostat.

1,4-Benzoquinone (Riedel-de-Haën) was recrystallized twice from cyclohexane (p.a.) and dried in a vacuum with paraffin oil for 24 h. It was stored in the dark. A stock solution of D-glucose in pH 6.0 phosphate buffer with $Na_2SO_4$ was prepared. It was 1.575 M in D-glucose, which is 1.000 M in β-D-glucose [9] with 0.02% w/v sodium azide as a preservative. The solution was kept for at least 24 h at room temperature to come to mutarotation equilibrium. All solutions were deaerated and kept in the dark.

## RESULTS

### *Behaviour of the enzyme reactor*

An attempt was made to determine the kinetic constants of the immobilized glucose oxidase in a microreactor. Because of the very rapid reaction, only approximate values could be obtained with the technique used [13]. The Michaelis–Menten constant for the sequential reactions (with quinone) was found to be about $10^{-2}$ M for 0.05 M quinone at a flow of 8 ml $min^{-1}$. The constant increased when the flow rate was decreased. $V_{max}$ was such that with the reactor described above, 99.99% (for both [Q]) of the β-D-glucose should be

converted in flows of 2.5 ml $min^{-1}$ at actual quinone concentrations of 0.05 and 0.005 M, respectively.

To test the quinone/hydroquinone system, solutions of hydroquinone of known concentrations were rapidly mixed with a solution of buffered 0.005 M quinone in a vessel with gold and reference electrodes; 90% of the total response was obtained after 0.7 s and 99% after 5.8 s. The response time thus seemed to be of the same magnitude as the expected mixing time in the vessel. The potentials obtained were very close to the calculated ones, and when plotted against the logarithm of the quinone/hydroquinone concentration ratio the slope and the intercept of the curves were 29.4 mV/decade and 110 mV, respectively. The gold electrode was also tested in a flow system, where different solutions of varying concentrations of hydroquinone were introduced into a buffered quinone solution. The same results as above were obtained.

The next step was to insert the enzyme reactor into the flow system and to introduce glucose solutions of different strengths. A series of samples with various amounts of glucose was prepared and run in a buffer with an initial quinone concentration of 0.05 M and no initial hydroquinone. The quinone concentration must be higher than the concentration of β-D-glucose in the sample. The expression within the brackets in eqn. (2) was computed, because the glucose concentrations in the samples were known. The observed electrode

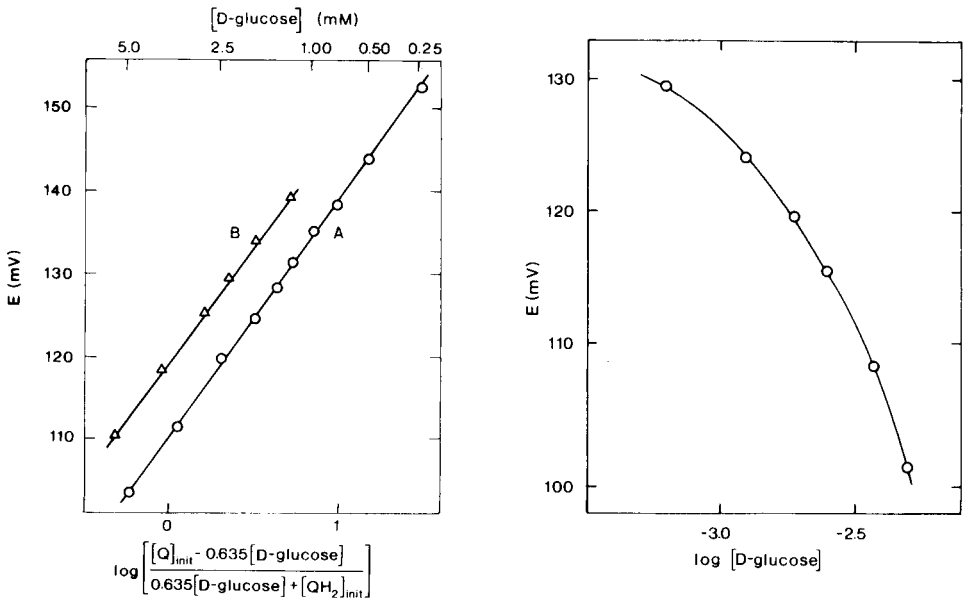


Fig. 4. Calibration curves for D-glucose. Curve A, $[Q]_{init}$ = 0.05 M, $[QH_2]_{init}$ = 0; curve B, $[Q]_{init}$ = 0.005 M, $[QH_2]_{init}$ = 0.0005 M, displaced by 10 mV upwards for clarity.

Fig. 5. Plot of the potential as a function of the logarithm of the D-glucose concentration: the results are those of curve B in Fig. 4.

potentials were plotted versus the logarithm of the calculated expression. The result is shown in Fig. 4, together with the result from another series of measurements made for different quinone and hydroquinone concentrations. The slopes of the curves are 28.8 and 28.2 mV/decade for 0.05 M and 0.005 M quinones respectively, which is close to the Nernstian slope for $n = 2$ (29.0 mV/decade at 19°C). The intercepts, $E'$, were 110.4 and 109.4 mV, respectively, which are close to the expected value (109.8 mV). The linearity is very good as shown by correlation coefficients of $r = 0.9999$ for both plots.

The results in Fig. 4 show that reaction (1) proceeds quantitatively and that eqn. (2) holds in the flow system. A calibration curve drawn in the usual manner (i.e. $E$ vs. log [D-glucose]) will be curved, as shown in Fig. 5. The working range covers a concentration interval well below the normal glucose level in serum. The lowest concentration of β-D-glucose which gave a potential in agreement with eqn. (2) was $0.04 \times 10^{-3}$ M. The reason may be that the potentiometric detection system does not operate properly at this level or that there is some residual hydroquinone in the quinone.

*Dialysis experiments*

Dialysis experiments were carried out as follows. To test eqn. (6), $C_s$ was varied between $1.25 \times 10^{-3}$ M and $50 \times 10^{-3}$ M β-D-glucose, which corresponds approximately to $2.0—80 \times 10^{-3}$ M D-glucose. The flow rate ($f_e$) in the inner tubing was varied between 0.38 and 1.23 ml $min^{-1}$. The flow rate in the outer tubing (the sample solution) had no influence on the $k$(glucose) value if it was greater than 4.7 ml $min^{-1}$. In all the dialysis experiments, the initial concentration of quinone was 0.025 M after mixing (Fig. 1). No hydroquinone was added.

Table 1 shows that the amount of β-D-glucose dialyzed is a linear function of the sample concentration. The experimental values in Table 1 are the mean values of four different runs. The correlation coefficients show that the linearity is good. The intercepts of the lines fall close to zero as expected. The dialysis factor ($k$) increases for small values of the concentration $C_s$. This calls for recalibration of the dialyzer when accurate results are needed at these levels.

To ensure that the dialyzer excluded proteins, an albumin solution (6.9 g of Bovine Albumin/100 ml, Sigma No. A-6003) was dialyzed and the dialysate was examined spectrometrically at 280 nm. Less than 0.01% (the detection limit) of the protein was dialyzed.

One of the commonest interferents with glucose determinations in body fluids is ascorbic acid. The reaction between quinone and ascorbic acid was studied spectrophotometrically. It was found that the reaction was complete within the mixing time. Table 2 shows the results when ascorbic acid and β-D-glucose were present in the outer stream of the dialyzer. The dialyzed amount of β-D-glucose is the same linear function of the sample concentration even when ascorbic acid is present.

In comparing the four different $k$(glucose) values obtained in the experiments in Tables 1 and 2, it would be expected from eqn. (6) that $k$(glucose)

TABLE 1

Results from dialysis experiments of β-D-glucose at two different flow rates

| Outer tubing | Inner tubing | | | |
|---|---|---|---|---|
| Flow rate 5.0 ml $min^{-1}$ | Flow rate 0.615 ml $min^{-1}$ | | Flow rate 1.23 ml $min^{-1}$ | |
| [β-D-G] (mM) | [β-D-G]dialyzed (mM) | $k$(glucose) | [β-D-G]dialyzed (mM) | $k$(glucose) |
| 1.25 | 0.097 | 0.0776 | 0.049 | 0.0392 |
| 2.5 | 0.190 | 0.0760 | 0.096 | 0.0384 |
| 5.0 | 0.376 | 0.0752 | 0.187 | 0.0374 |
| 10.0 | 0.748 | 0.0748 | 0.380 | 0.0380 |
| 15.0 | 1.123 | 0.0749 | 0.576 | 0.0384 |
| 20.0 | 1.492 | 0.0746 | 0.761 | 0.0381 |
| 25.0 | 1.860 | 0.0744 | 0.954 | 0.0382 |
| 30.0 | 2.223 | 0.0741 | 1.154 | 0.0385 |
| 35.0 | 2.612 | 0.0746 | 1.339 | 0.0383 |
| 40.0 | 2.984 | 0.0746 | 1.537 | 0.0384 |
| 45.0 | 3.347 | 0.0744 | 1.725 | 0.0383 |
| 50.0 | 3.717 | 0.0743 | 1.918 | 0.0384 |
| | $r$ = 0.9999[a] $b$ = 0.0743 $a$ = 0.0047 mM | | $r$ = 0.9999 $b$ = 0.0384 $a$ = −0.002 mM | |

[a] $r$ = correlation coefficient, $a$ = intercept, $b$ = mean $k$(glucose).

× flow rate would be a constant. Table 3 shows that this was the case even when ascorbic acid was present. Thus the behaviour of the dialysis is in good agreement with theory.

Finally, a reference serum (Technicon SMA Reference Serum 2/S GPT) was dialyzed which contained $12.4 \times 10^{-3}$ M D-glucose as determined enzymatically with two methods by the manufacturer. Three standard additions of D-glucose were made and the results are shown in Table 4.

## DISCUSSION

The new analytical flow-through dialyzer follows the predicted theory, and could become a general tool for measurements of many biological substances. It is well known that when small molecules in biological samples are monitored most analytical detection systems are subject to errors from a number of interferents, especially proteins. These will be easily excluded by the dialyzer. The $k$-value was independent of the outer flow rate when it was above a certain minimum value. Thus $k$ can be adjusted to suit the actual analytical system by varying the inner flow rate. To optimize the sensitivity, the volume after the dialyzer should be minimized to prevent unnecessary sample dilution.

The dependence of the detection system on the flow rate is minimized. The electrokinetic potential was decreased to a negligible value by the high ionic strength. The potentiometric system is inherently very insensitive to

TABLE 2

Dialysis experiment with ascorbic acid added, at two different flow rates[a]

| Outer tubing | | Inner tubing | | | | | | | |
|---|---|---|---|---|---|---|---|---|---|
| Flow rate 5.0 ml min$^{-1}$ | | Flow rate 0.38 ml min$^{-1}$ | | | | Flow rate 0.75 ml min$^{-1}$ | | | |
| [β-D-G] (mM) | [Ascorbic acid] (mM) | $E_1$ (mV) | $E_2$ (mV) | [β-D-G]dialyzed (mM) | $k$(glucose) | $E_1$ (mV) | $E_2$ (mV) | [β-D-G]dialyzed (mM) | $k$(glucose) |
| 5 | 5 | 158.9 | 152.4 | 0.59 | 0.118 | 165.0 | 159.5 | 0.30 | 0.060 |
| 10 | 10 | 153.2 | 145.6 | 1.20 | 0.120 | 160.8 | 153.6 | 0.61 | 0.061 |
| 15 | 15 | 149.8 | 141.5 | 1.82 | 0.121 | 157.8 | 149.7 | 0.92 | 0.061 |
| 20 | 20 | 147.4 | 138.4 | 2.48 | 0.124 | 155.5 | 146.6 | 1.28 | 0.064 |
| 25 | 25 | 145.6 | 136.0 | 3.14 | 0.126 | 153.5 | 144.4 | 1.57 | 0.063 |
| 30 | 30 | 144.1 | 134.2 | 3.69 | 0.123 | 152.0 | 142.5 | 1.88 | 0.063 |
| 35 | 35 | 142.6 | 132.2 | 4.44 | 0.127 | 150.4 | 140.8 | 2.20 | 0.063 |
| 40 | 40 | 141.3 | 130.8 | 4.94 | 0.124 | 149.1 | 139.3 | 2.49 | 0.062 |
| | | $r$ = 0.9996 | | | $b$ = 0.126 | $r$ = 0.9998 | | | $b$ = 0.063 |
| | | $a$ = −0.048 mM | | | | $a$ = −0.011 mM | | | |

[a] $r$, $a$, $b$ as in Table 1.

TABLE 3

Dialysis parameters[a]

| Flow rate (ml min$^{-1}$) | $k$(glucose) | $k_{gl}f_e$ (ml min$^{-1}$) |
|---|---|---|
| 0.375 | 0.126 | 0.0473 |
| 0.615 | 0.0743 | 0.0457 |
| 0.750 | 0.063 | 0.0472 |
| 1.23 | 0.0384 | 0.0472 |
| $r$ = 0.9993; $a$ = −0.0011 mM; $b$ = 0.047 ml min$^{-1}$ | | |

[a] $r$, $a$ as in Table 1, $b$ = mean $k$(glucose) $f_e$; $f_e$ = flow rate.

fluctuations in flow rate, but responds comparatively quickly to changes in glucose concentration. Even though the results in this report were calculated from the two potentials with a simple calculator, a minicomputer with a short program would very rapidly evaluate the D-glucose concentration.

With the arrangement described it is of the utmost importance that the electrodes in the two detectors used give the same potential for the same kind of solution. When investigated, the calomel electrodes differed by 0.3 mV and the gold electrodes, made from the same gold rod, differed at most by 0.2 mV. Both electrodes were calibrated at the same time with solutions of different concentrations of quinone and hydroquinone. They responded equally, giving the same slopes and intercepts of their calibration curves. These values were necessary for the calculations. An advantage with this electrode arrangement is that the quinone content could always be checked by using the pre-electrode (potential $E_1$). Another kind of arrangement would be to split the flow before the enzyme reactor. At one moment the flow would go through the enzyme

TABLE 4

Analysis of a reference serum

| Volume of β-D-glucose added[a] (μl) | Total [β-D-glucose] (× $10^{-3}$ M) | |
|---|---|---|
| | Calculated | Found |
| — | 7.87 | 7.80 |
| 50.0 | 9.85 | 10.03 |
| 120 | 12.61 | 12.72 |
| 180 | 14.97 | 15.14 |

[a]Volume of 1.00 M β-D-glucose solution added to 25.0 ml of reference serum.

reactor giving the potential $E_2$. Without passing the enzyme reactor the same solution could the next moment pass the electrode to give the potential $E_1$.

The reactor technique results in a quantitative conversion of the substrate. Thus the sensitivity of the method is increased compared to enzyme electrodes with a layer of catalyst surrounding the electrode.

The authors thank Professor Gillis Johansson for valuable discussions concerning this work and AB GAMBRO for the gift of the dialyzer.

REFERENCES

1 S. J. Updike and G. P. Hicks, Nature, 214 (1967) 986.
2 L. C. Clark, Jr., Biotechnol. Bioeng. Symp. 3 (1972) 377.
3 S. J. Updike, M. C. Shults, J. K. Kosovich, I. Treichel and P. M. Treichel, Anal. Chem., 47 (1975) 1457.
4 R. A. Llenado and G. A. Rechnitz, Anal. Chem., 45 (1973) 2165.
5 G. Nagy, L. H. v. Storp and G. G. Guilbault, Anal. Chim. Acta, 66 (1973) 443.
6 W. J. Blaedel and C. L. Olson, U.S. Patent 3,367,849 (1968).
7 G. G. Guilbault, Clinical and Biochemical Analysis, Vol. 4, Handbook of Enzymatic Methods of Analysis, Marcel Dekker, Inc., New York, 1976.
8 D. L. Williams, A. R. Doig, Jr. and A. Korosi, Anal. Chem., 42 (1970) 118.
9 J. Okuda and I. Miwa, Anal. Biochem., 39 (1971) 387.
10 G. Johansson and L. Ögren, Anal. Chim. Acta, 84 (1976) 23.
11 H. J. Bright and M. Appleby, J. Biol. Chem., 244 (1969) 3625.
12 K. B. Ramachandran and D. D. Perlmutter, Biotechnol. Bioeng., 18 (1976) 669.
13 G. Johansson and L. Ögren, in E. Pungor (Ed.), Ion-Selective Electrodes, Akadémiai Kiadó, Budapest, 1977, p. 93.

*Analytica Chimica Acta*, 105 (1979) 53—65


# THE BEHAVIOUR OF COPPER(II)-SELECTIVE ELECTRODES IN CHLORIDE-CONTAINING SOLUTIONS

PIETRO LANZA

*Chemical Institute "G. Ciamician", University of Bologna, 40126 Bologna (Italy)*

(Received 17th May 1978)

SUMMARY

Calibration curves for copper(II) in solutions containing various chloride ion concentrations are examined in detail. The mechanism of the interferences on the behaviour of the copper(II)-selective electrode is discussed. The anomalous slopes observed can be explained by considering the sensitivity of the electrode membrane to the silver ions released from the electrode surface by chemical interaction with the solution. The effects of the formation of silver-chloride complexes and of the changes in the membrane are described.

The nature of the potential of a selective electrode, whether based on a liquid or a solid membrane, is somewhat complex. The theories concerning the various types of selective electrodes have been described in several monographs [1—3] and reviews [4—6]. A general equation for the electrode potential must take into account that the response not only depends on the activity of the electroactive species in the solution, but is also a function of the activities of the components in the sensing membrane. The electrode potential is therefore influenced by any change in the membrane composition that affects the chemical potential of its components. General equations of this type have been proposed by Sato [7] and other authors [8, 9].

In the present paper, some anomalies in the behaviour of copper(II)-selective electrodes based on mixed copper(II) sulphide—silver(I) sulphide membranes in the presence of chloride ions [10—12] are discussed. Some aspects of these unwelcome phenomena are explained by considering the relevant equilibria in the solution contacting the electrode and the membrane—solution interactions.

## EFFECT OF CHLORIDE IONS ON THE RESPONSE OF A CuS—$Ag_2S$ MEMBRANE

In studying the determination of copper in sea water with a copper(II)-selective electrode of the $Ag_2S$—CuS type (Orion model 94-29A), Jasinski et al. [10] found slopes of 50 mV per decade change in copper concentration. This anomalous slope was ascribed to the high chloride concentration and to the electrode material, but no interpretation was put forward. As the slope

was reproducible, even if unexplained theoretically, it was regarded as an empirical parameter relating measured potential to the logarithmic copper(II) activity. In the Orion Instruction Manual [11], interferences are indicated when the concentrations of copper(II) and chloride become so high that solid silver chloride can be formed. This is generally ascribed to the reaction

$$Ag_2S(s) + Cu^{2+} + 2Cl^- \rightleftharpoons CuS(s) + 2AgCl(s) \quad (1)$$

The equilibrium constant, expressed in terms of concentration, is given by $K = 1/[Cu^{2+}][Cl^-]^2 = 6.3 \times 10^5$ (see Appendix) and solid silver chloride can be formed when $[Cu^{2+}][Cl^-]^2$ exceeds $1.6 \times 10^{-6}$. Interferences, however, were observed by Jasinski et al. [10] at concentration ranges where solid silver chloride would not be formed. More recently, Midgley [13] made careful observations on the interference of chloride, and found distinct effects even when the halide concentration was less than that predicted for causing interference by silver chloride formation.

The occurrence of reaction (1) is not itself enough to explain the copper-ion calibration slope being different from the expected value of 29.6 mV per decade. Indeed, if $[Cu^{2+}][Cl^-]^2 < 1.6 \times 10^{-6}$, a film of $Ag_2S$ and CuS cannot form and the above phenomenon should not occur [11, 14]; if $[Cu^{2+}][Cl^-]^2$ exceeds $1.6 \times 10^{-6}$, the solid AgCl phase appears and the system becomes unresponsive. After the equilibrium has been reached, the copper(II) activity should remain constant despite further copper additions, which will simply increase the solid silver chloride at the expense of silver sulphide if enough chloride is present. If the chloride ion activity is constant, the copper(II) activity remains constant, and the calibration slope becomes zero.

Equilibrium (1) can be considered only if solid AgCl is formed, i.e. if enough silver(I) to saturate the solution has been released from the electrode. The solubility of AgCl depends strongly on the chloride concentration, owing to the formation of AgCl (aq), $AgCl_2^-$, $AgCl_3^{2-}$ and $AgCl_4^{3-}$ complexes [15, 16]. The formation curves of these complexes and their distribution as a function of the chloride concentration are shown in Fig. 1. A more general expression of the interaction, therefore, may be:

$$Ag_2S + Cu^{2+} + 2\bar{n}\ Cl^- \rightleftharpoons CuS + 2AgCl_{\bar{n}}^{-\ (\bar{n}-1)} \quad (2)$$

where $\bar{n}$ is the average coordination number at the chloride concentration of the system. The equilibrium constant, expressed in terms of concentration (with the charges of the complex omitted for simplicity), is $K_{(Cl)} = [AgCl_{\bar{n}}]^2/[Cu^{2+}][Cl^-]^{2\bar{n}}$, i.e., a function of the stability constants of the $AgCl_i$ complexes and of their distribution. It can be calculated for given chloride concentrations (see Appendix).

The trend of the calibration curves for $Cu^{2+}$ ions in the presence of known chloride concentrations can also be calculated provided that the interaction is essentially due to reaction [2]. If $C_{Cu^{2+}}$ is the concentration of added $Cu^{2+}$ at a given point of the calibration curve and $x$ is the concentration that reacts, then $K_{(Cl)} = 4x^2/(C_{Cu^{2+}} - x)[Cl^-]^{2\bar{n}}$. The calibration curve is the diagram

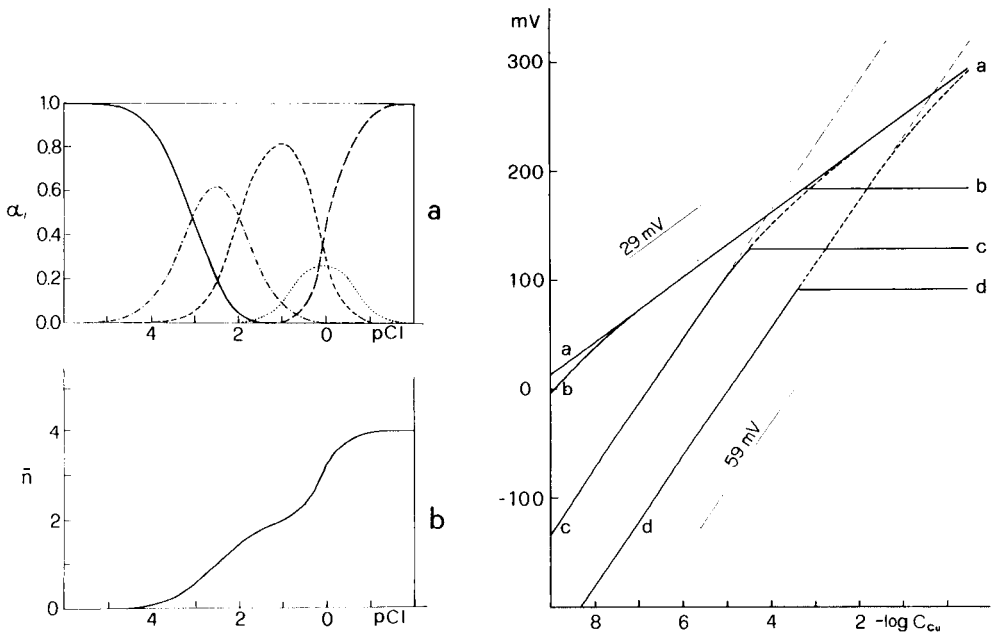


Fig. 1. Distribution curves (a) and formation curve (b) in the silver(I) chloride system. (——) $AgCl_4^{3-}$; (·····) $AgCl_3^{2-}$; (----) $AgCl_2^-$; (·····) AgCl (aq.); (——) AgCl(s).

Fig. 2. Calculated Cu(II) calibration curves at different chloride concentrations: (a) 0 M; (b) 0.1 M; (c) 1.0 M; (d) 3.0 M.

$E$ vs. log $C_{Cu^{2+}}$, where the potential of the selective electrode at 25°C is given by

$$E = E^0_{sel} + 0.0296 \log (C_{Cu^{2+}} - x) \quad (3)$$

$E^0_{sel}$ being the standard potential of the selective electrode, referred to a suitable reference electrode; it accounts for the activity coefficients when the ionic strength is kept constant. Equation (3) shows that for $x \ll C_{Cu^{2+}}$ the calibration curve has the Nernstian slope of 29.6 mV per decade. If $x \approx C_{Cu^{2+}}$, i.e., if the $Cu^{2+}$ added reacts almost quantitatively according to reaction (2), then $[AgCl_{\bar{n}}] = 2x \triangleq 2C_{Cu^{2+}}$ and from the first definition of $K_{(Cl)}$, $[Cu^{2+}] = 4C^2_{Cu^{2+}}/K_{(Cl)}\,[Cl^-]^{2\bar{n}}$. The electrode potential, expressed as a function of the added $Cu^{2+}$ ion, is then given by

$$E = E^{0'}_{sel} + 2 \times 0.0296 \log C_{Cu^{2+}} \quad (4)$$

where

$$E^{0'}_{sel} = E^0_{sel} + 0.0296 \log (4/K_{(Cl)}\,[Cl^-]^{2\bar{n}}) \quad (5)$$

Therefore, the slope is 59.2 mV per decade. Equation (5) shows that the conditional standard potential, $E^{0'}_{sel}$, is a function of the chloride concentration.

Obviously, the $AgCl_{\bar{n}}$ concentration cannot exceed the limits imposed by

the solubility of the silver chloride; therefore, the copper(II) concentration, in the presence of solid AgCl and $Ag_2S$, reaches a maximum value given by

$$[Cu^{2+}] = [AgCl_{\bar{n}}]^2_{sat}/K_{(Cl)}\,[Cl^-]^{2\bar{n}} \qquad (6)$$

where $[AgCl_{\bar{n}}]_{sat} = [Ag^+]_{sat} + [AgCl]_{sat} + [AgCl_2^-]_{sat} + [AgCl_3^{2-}]_{sat} + [AgCl_4^{3-}]_{sa}$ i.e. the total silver concentration in the AgCl-saturated solution. Under these conditions, the calibration slope is zero.

Figure 2 shows calculated calibration curves at various chloride ion concentrations for a selective electrode with a standard potential ($E^0$) of 0.280 V vs. SCE. The curves correspond to the behaviour of an ideal electrode, in equilibrium with the solution, such that it cannot undergo any change in compositior and its standard potential remains constant. The straight lines with a slope of 59.2 mV per decade correspond to the conditions where $x \approx C_{Cu^{2+}} = 1/2\,[AgCl_i$ These lines would connect with the straight lines given by eqn. (3), which correspond to conditions where interferences are not observed ($x \ll C_{Cu^{2+}}$). In practice, this zone is attained only at low chloride concentrations, because, as the dashed lines show, the copper(II) ion concentration is limited by the silver chloride solubility (see eqn. 6). The extrapolated straight lines with a slope of 59.2, extend into a super-saturation zone, but they can be used for graphical calculation of the corresponding conditional standard potential, $E^{0\prime}$, by extrapolating the $E$ value to $-\log C_{Cu^{2+}} = 0$.

The $E^{0\prime}$ values, calculated from eqn. (5), for chloride concentrations of 0.1, 1.0 and 3.0, are 0.536, 0.401 and 0.292, respectively.

## EXPERIMENTAL

The copper-selective electrodes used were the Orion Model 94-29A, the AMEL (Milan) Model 201 and an electrode with a CuS—$Ag_2S$ membrane as prepared by Mascini and Liberti [17]. The Orion electrode is of all-solid construction. The Amel and Mascini electrodes contain an internal electrolyte and an Ag/AgCl inner electrode. The saturated calomel reference electrode used was connected, when necessary, by a $KNO_3$ salt bridge. Potentials were measured with a Tacussel Model ISIS 20000 digital pH meter/millivoltmeter, connected to a Leeds-Northrup Model XL 681A potentiometric recorder.

Silver sulphide was prepared by adding silver nitrate to sodium sulphide [18]

Most of the copper(II) calibration curves were prepared at an ionic strength of 1 M, adjusted with $KNO_3$; in some cases, 3 M KCl solutions were used. The test solutions were prepared by introducing suitable quantities of a standard copper(II) solution into 50-ml volumetric flasks and diluting to the mark with one of the following solutions: (a) 1 M $KNO_3$—$10^{-3}$ M $HNO_3$; (b) 0.1 M KCl—0.9 M $KNO_3$—$10^{-3}$ M $HNO_3$; (c) 1 M KCl—$10^{-3}$ M HCl; or (d) 3 M KCl—$10^{-3}$ M HCl. Lower copper(II) concentrations were prepared by successive 1:10 dilutions with the appropriate solution.

Calibration measurements were usually done by transferring the electrodes sequentially from dilute to more concentrated solutions. All solutions were

kept acidic to avoid hydrolytic effects. Measurements were made under magnetic stirring in a nitrogen atmosphere.

## RESULTS AND DISCUSSION

The behaviour of the electrodes was studied by examining the calibration curves obtained under different experimental conditions, including the presenc of suspensions of AgCl and $Ag_2S$. Electrodes of diverse origin were used, because noteworthy differences in behaviour were expected from the different sorts of membrane.

*Behaviour in solutions containing chloride*

The results of some experiments are shown in Fig. 3, in which the responses of the electrodes in solutions containing 0, 0.1, 1.0 and 3.0 M chloride concentrations are compared. Even with 0.1 M chloride present, there is a clear change in the behaviour of the Orion electrode, and this becomes even clearer in 1.0 M chloride solution for which the potential remains constant in the pCu range 2—5 (Fig. 3C). The Amel and Mascini electrodes in 1.0 M chloride solutions give calibration plots with slopes approaching 59 mV/pCu. In 3 M KCl solutions (Fig. 3D), the responses become very unstable, and reach moderately constant potentials only after a long time.

In order to obtain values comparable between themselves, the series of measurements in 3 M KCl were repeated with regeneration of the electrodes before each measurement; regeneration was done by leaving the electrodes alternately in 1 M $NH_3$ and in copper-free 3 M KCl until constant potentials were reached. The results obtained are reported in Fig. 4. At the lower copper concentrations, the electrodes assume much more negative potentials, which are quite stable and reproducible, and tend to respond to copper(II) with a slope of 59 mV/pCu up to concentrations of about $10^{-3}$ M. Above $10^{-3}$ M Cu(II), the potentials first reach, quite rapidly, values situated approximately on the expected straight line, but then the readings shift slowly towards final apparent equilibrium potentials which are much more positive than those observed for the same copper(II) concentrations in the absence of chlorides. These potential shifts which become faster as the copper(II) concentration increases, are indicated in Fig. 4 by dashed vertical lines; the times necessary to reach an apparent state of equilibrium are indicated beside the vertical lines. The potential variations as functions of time for the Mascini and Orion electrodes are reported in Fig. 5. It seems that electrodes give a fairly rapid response to the copper(II) activity, and then undergo a gradual potential shift because of a slow transformation of the membrane by chemical reaction with the solution. The occurrence of reaction (1) involves a gradual replacement of $Ag_2S$ by AgCl on the electrode surface. To a lesser extent, the phenomenon is also encountered in 1.0 M chloride solutions.

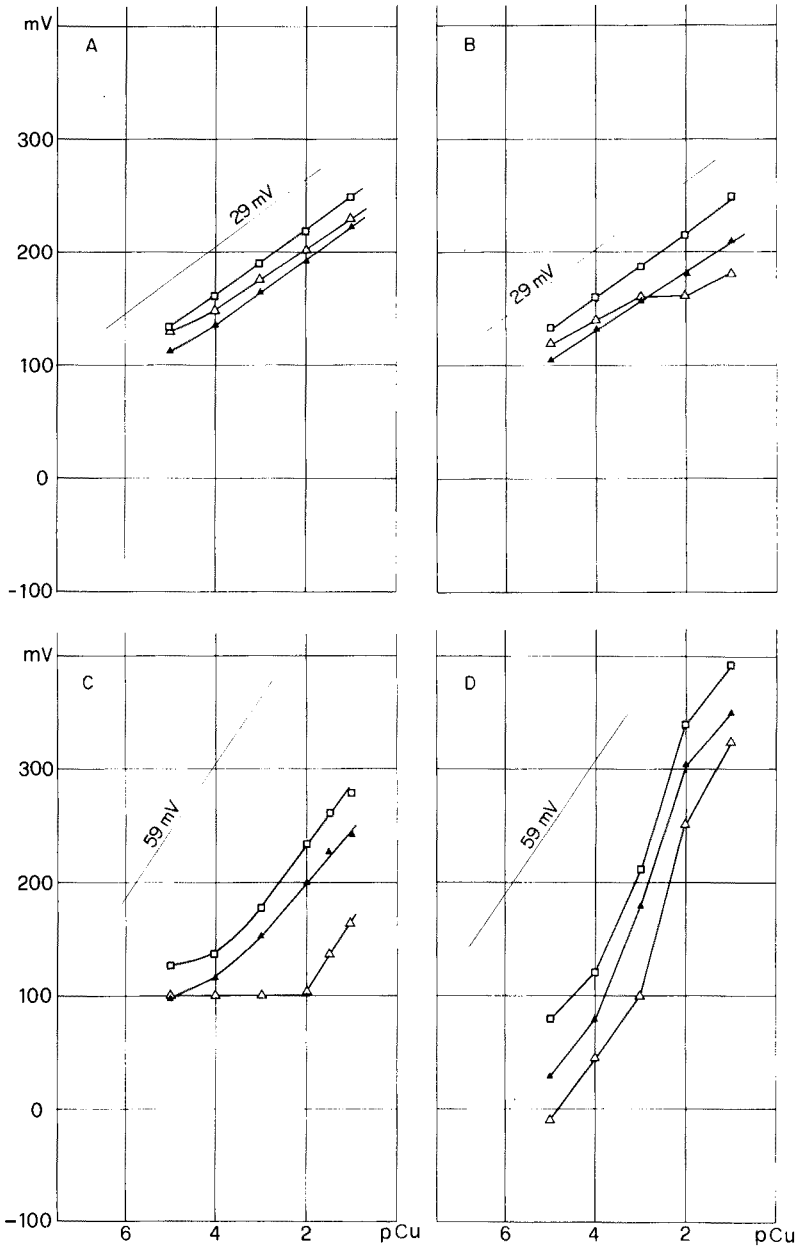


Fig. 3. Copper(II) calibration curves for different electrodes ((□) Mascini; (△) Orion; (▲) Amel) in various media. (A) 1 M $KNO_3$—$10^{-3}$ M $HNO_3$; (B) 0.1 M KCl—0.9 M $KNO_3$—$10^{-3}$ M $HNO_3$; (C) 1 M KCl—$10^{-3}$ M HCl; (D) 3 M KCl—$10^{-3}$ M HCl.

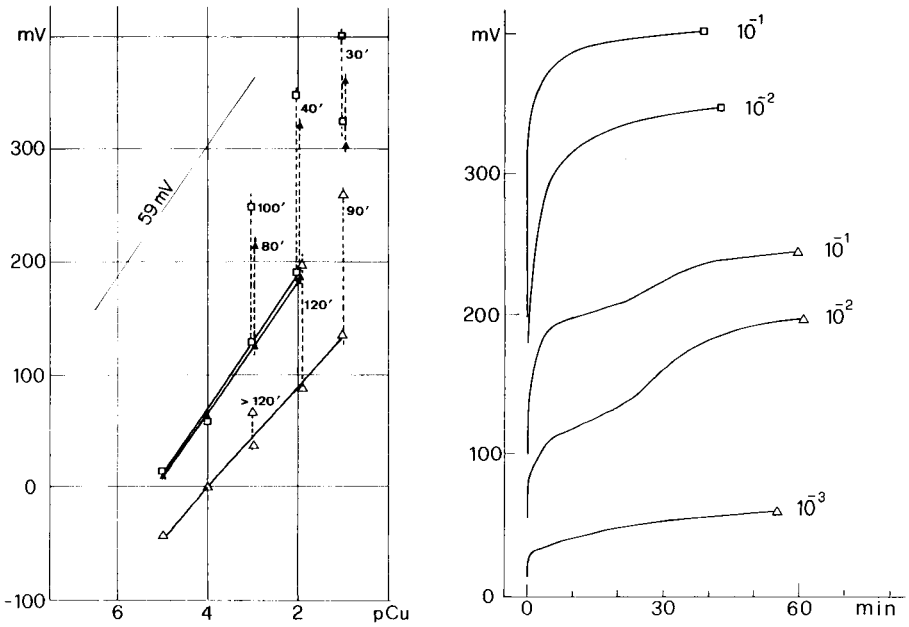


Fig. 4. Copper(II) calibration curves in 3 M KCl—$10^{-3}$ M HCl for the (□) Mascini, (△) Orion and (▲) Amel electrodes, which had been regenerated before each measurement; the vertical lines show the slow potential shifts, and the numbers on each line show the times (in min) needed to reach the higher potentials.

Fig. 5. The trend of potential as a function of time in 3 M KCl—$10^{-3}$ M HCl for different copper(II) concentrations: (□) Mascini; (△) Orion.

*Behaviour in solutions containing chlorides in equilibrium with $Ag_2S$*

The measurements reported in the preceding section were repeated with solutions that had been previously brought to equilibrium with a silver sulphide suspension. This was done to eliminate or weaken the chemical action of the solutions on the electrode membrane. The results obtained in 3 M chloride solution are reported in Fig. 6. The presence of $Ag_2S$ in the 0.1 M and 1.0 M chloride solutions does not cause significant differences. In the 3 M solution, all three electrodes show similar behaviour at low copper(II) concentrations, and the slope is about 60 mV per decade. At pCu less than 3, where the solution does not act on the membrane, a narrow region of the curve shows zero slope. According to theoretical expectations, this would correspond to the appearance of the silver chloride solid phase. In the 0.1 M Cu(II) solution, all three electrodes give large increases of potential that are not foreseeable with solutions already in equilibrium with $Ag_2S$, when only those equilibria are considered that involve the presence of $Ag_2S$, AgCl and CuS in the solutions containing copper(II) and chloride ions. In fact, this trend is not encountered in the calculated curves, which stresses the effect of unexpected chemical

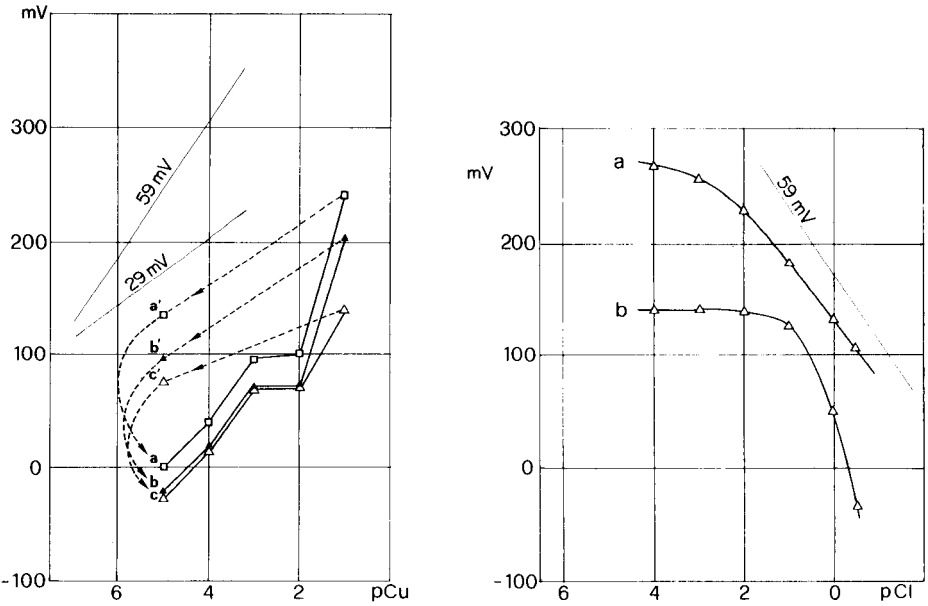


Fig. 6. Calibration curves in 3 M KCl—$10^{-3}$ M HCl in equilibrium with $Ag_2S$: (□) Mascini; (△) Orion; (▲) Amel. For explanation, see text.

Fig. 7. Effect of chloride ion on the Orion electrode response: (a) electrode surface changed; (b) electrode surface renewed.

reactions. The alteration of the membrane which, in practice causes a shift of the standard conditional potential, manifests itself by strongly influencing the subsequent electrode responses.

A very clear example of the effects arising from membrane alteration is illustrated in Fig. 6; the same solutions ($10^{-5}$ M Cu(II) in 3 M KCl) gives entirely different potentials, depending on whether the electrodes have been regenerated (a, b, c) or come directly from the 0.1 M Cu(II) solution (a', b', c').

*Electrode response to chloride*

Electrodes that have remained for a sufficient time in contact with solutions which can alter the membrane composition, i.e. when $[Cu^{2+}][Cl^-]^2 \gg 1.6 \times 10^{-6}$, become reversible to the chloride ion. The behaviour is illustrated in Fig. 7. The appearance of this reversibility was observed by Crombie et al. [12] and was attributed to the alteration caused by AgCl formation on the surface. When the electrodes are regenerated with ammonia solutions, the reversibility for chloride ions disappears. With regard to the sensitivity for chloride, the three electrodes examined behaved in an entirely analogous way.

*Electrode response to silver(I) ions*

According to eqns. (4—6), the electrodes should have a Nernstian response

in the presence of silver(I) ions in solution. It is well known that the silver(I) interferes strongly on the functioning of the copper(II)-selective electrode. Jasinski et al. [10] observed that small silver(I) additions have the same effect as equivalent copper(II) additions. In order to examine more carefully the responses to silver(I) ions, silver(I) was added coulometrically to $10^{-5}$ M copper(II) solutions containing 0.1, 1.0 and 3.0 M chloride. The results obtained are shown in Fig. 8. A definite amount of copper(II) ions ($10^{-5}$ M) was added to the solutions to stabilize the electrode potential. The curves were drawn, rather arbitrarily, on the assumption that the Ag(I) concentration is additive with that equivalent to the initial copper(II), i.e. $-\log C_{Ag^+} = -\log (2 \times 10^{-5} + [Ag^+])$.

The addition of silver(I) to the 0.1 and 1.0 M chloride solutions does not alter the electrode potential significantly. Only at the highest silver(I) concentrations are potential increases observed with the Amel and Mascini electrodes; the phenomenon could perhaps be attributed to membrane alterations. The Orion electrode seems to be particularly indifferent. In a 3 M chloride solution, the silver(I) additions provoke linear increases of the potential with nearly Nernstian slopes for all three electrodes, until constant values are reached for pAg 2—2.5. In Fig. 8, the detached horizontal lines indicate the potential values measured after addition of an excess of silver nitrate, with formation of a definite AgCl precipitate. With 0.1 and 1.0 M KCl solutions, it is obvious that the solution becomes saturated with AgCl from the first addition, so that the electrode potential remains constant. In 3 M chloride solution, an abundant $AgCl_4^{3-}$ complex formation is possible before the saturation point is reached. It is interesting to note that the curves reported follow

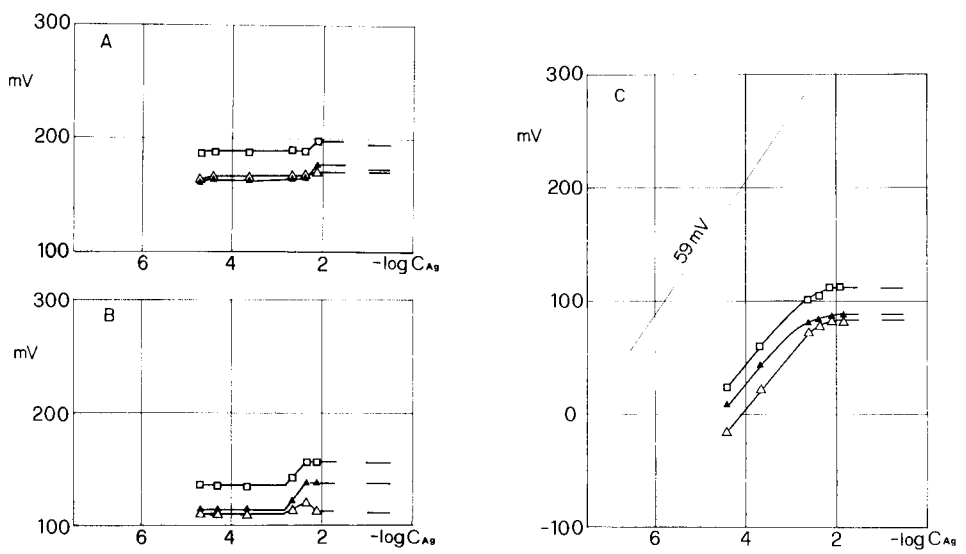


Fig. 8. Effect of silver(I) on the electrode response in (A) 0.1 M KCl, (B) 1.0 M KCl and (c) 3.0 M KCl: (□) Mascini; (△) Orion; (▲) Amel.

the trend of the calculated calibration curves for copper(II) (Fig. 2). In effect, it appears that under the experimental conditions used additions of copper(II) or silver(I) provide almost equivalent responses.

*Behaviour in chloride solutions in equilibrium with solid AgCl*

To examine the response to copper(II) ions in solutions having constant silver(I) activity, various copper(II) concentrations were measured in 3 M KCl solution previously saturated with AgCl. The results are shown in Fig. 9. The initial regions of the curves, with zero slope, are followed by regions of very sharp potential increases. Some other facts, however, can help to explain this unexpected behaviour.

Figure 9 also shows the potential changes of a silver electrode dipped in the same solutions. Although the chloride activity must be considered essentially constant, large potential increases are found with increases in the copper(II) concentration. At $10^{-2}$ and $10^{-1}$ M copper(II) concentrations, measurements are made impossible by the excessive instability of the response. The potentials oscillate over a range of more than 100 mV and readings become very sensitive to stirring; this indicates a strong chemical reaction at the electrode surface. The phenomenon can be explained on the basis of the oxidizing properties of copper(II) in the presence of large amounts of chloride. In fact, the conditional potential of the $Cu^{2+} + e \rightleftharpoons Cu^{+}$ couple assumes the values —0.051 V, 0.205 V and 0.303 V (vs. SCE) at chloride concentrations of 0.0, 1.0 and 3.0 M, respectively. Thus the silver electrode, in concentrated chloride solutions exerts a strong reducing action on the copper(II) present in solution.

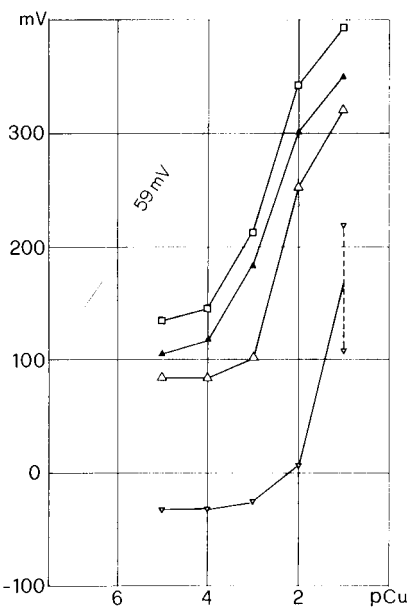


Fig. 9. Calibration curves in 3.0 M KCl saturated with AgCl: (□) Mascini; (△) Orion; (▲) Amel; (▽) silver electrode.

An analogous action, although weaker in effect owing to the less negative potential, is exerted by the copper-selective electrodes. When a 0.1 M copper(II) solution in 3 M KCl is left in contact with $Ag_2S$ for some days, a yellowish-green amorphous precipitate appears slowly and floats on the liquid surface. That this was sulphur was confirmed spectrophotometrically from the characteristic spectrum with maxima at 262 and 225 nm [20] after extraction of the separated and dried powder with n-hexane.

The formation of the sulphur is probably due to the reaction

$$Ag_2S + 2Cu^{2+} + 4Cl^- \rightarrow 2AgCl + 2CuCl + S$$

Reactions of this nature can explain the increases of potential that were constantly encountered in the experiments with more concentrated copper(II) solutions (see, e.g. Fig. 6). A deeper study of the oxidation—reduction equilibria pertaining to copper-selective electrodes would be essential for a more complete interpretation of the interferences.

## CONCLUSIONS

The electrode behaviour can be summarized as follows.

(a) The simultaneous presence of copper(II) and chloride causes the reaction $Ag_2S + 2\bar{n}\,Cl^- + Cu^{2+} \rightarrow CuS + 2AgCl_{\bar{n}}$, and the electrode then responds to the released silver activity with a slope of 59 mV per decade.

(b) If the conditions are such as to produce silver chloride precipitation on the membrane, a constant Cu(II) and Ag(I) activity tends to establish itself at the electrode surface. As a result, within certain limits, successive additions of copper(II) do not alter the electrode potential. The reaction leads to a gradual replacement of $Ag_2S$ by AgCl on the electrode surface, which becomes reversible for chloride ions.

(c) The increase in the redox potential of the Cu(II)/Cu(I) couple in the presence of chlorides can provoke reactions such as $Ag_2S + Cu^{2+} + 4Cl^- \rightarrow 2AgCl + 2CuCl + S$. In practice, every membrane alteration manifests itself by a shift in the standard potential of the electrode. This could explain the fact, easily observable, that calibration curves measured in successive runs or after diverse treatments have constant slopes but do not always coincide.

Overall, it can be concluded that the presence of chloride, even at very low concentrations, provokes interferences that, at the very least, make frequent calibration checks essential. In routine analytical applications, therefore, the use of these electrodes is limited to chloride-free solutions, and preliminary treatments are needed to remove such sources of interference.

The author thanks Prof. M. Mascini and L. Grifone (AMEL, Milan) for kindly supplying the electrodes and Dr. P. L. Buldini for valuable assistance.

## APPENDIX

*Numerical values used in the computations*

| Salt | Solubility product $-\log K_{sp}$ [15] | Complex | Stability constant $\log \beta_i$ [19] |
|---|---|---|---|
| AgCl | 9.8 | AgCl | 3.05 |
| $Ag_2S$ | 49.0 | $AgCl_2^-$ | 5.05 |
| CuS | 35.2 | $AgCl_3^{2-}$ | 5.05 |
| | | $AgCl_4^{3-}$ | 5.29 |

*Equilibrium constants*

The equilibrium constant of the reaction $Ag_2S(s) + Cu^{2+} + 2Cl^- \rightleftharpoons CuS(s) + 2AgCl(s)$ is given by $K = [AgCl]_s^2[CuS]_s/[Ag_2S]_s[Cu^{2+}][Cl^-]^2 = 1/[Cu^{2+}][Cl^-]^2$. At equilibrium with the AgCl, $Ag_2S$ and CuS solid phases, the equation $[Cu^{2+}][S^{2-}]([Ag^+][Cl^-])^2/[Ag^+]^2[S^{2-}] = [Cu^{2+}][Cl^-]^2$ can be written. By substituting the numerical values, one obtains: $[Cu^{2+}][Cl^-]^2 = 1.6 \times 10^{-6}$, therefore $K = 1/[Cu^{2+}][Cl^-]^2 = 6.3 \times 10^5$.

*Calculation of the equilibrium constants of the general equation*

$$Ag_2S(s) + Cu^{2+} + 2\bar{n}Cl^- \rightleftharpoons CuS(s) + 2AgCl_{\bar{n}}^{-(\bar{n}-1)} \quad (1A)$$

The formation of the $AgCl_{\bar{n}}^{-(\bar{n}-1)}$ complex can be considered as the result of the following parallel reactions: $\alpha_1(Ag^+ + Cl^- \rightarrow AgCl_{aq}); \beta_1 = 1.12 \times 10^3$; $\alpha_2(Ag^+ + 2Cl^- \rightarrow AgCl_2^-), \beta_2 = 1.12 \times 10^5$; $\alpha_3(Ag^+ + 3Cl^- \rightarrow AgCl_3^{2-}); \beta_3 = 1.12 \times 10^5$; $\alpha_4(Ag^+ + 4Cl^- \rightarrow AgCl_4^{3-}), \beta_4 = 1.95 \times 10^5$. Coefficients $\alpha_i$ are the fractions of the $AgCl_i$ complexes at equilibrium (see Fig. 1a). As $\Sigma\alpha_i = 1$, the result of these Ag—Cl reactions is $Ag^+ + \bar{n}Cl^- \rightleftharpoons AgCl_{\bar{n}}^{-(n-1)}$, where $\bar{n}$ is the average coordination number (see Fig. 1b). The equilibrium constant can be expressed as

$$K_{\bar{n}} = [Ag/Cl_{\bar{n}}]/[Ag^+][Cl^-]^{\bar{n}} = \beta_1^{\alpha_1}\beta_2^{\alpha_2}\beta_3^{\alpha_3}\beta_4^{\alpha_4} \quad (2A)$$

The $\bar{n}$ and $\alpha_i$ values can be calculated as a function of the chloride concentration (see following Table).

The equilibrium of reaction (1A) can be expressed by the constant $K = [AgCl_{\bar{n}}]^2/[Cu^{2+}][Cl^-]^{2\bar{n}}$, and when this is combined with eqn. (2A), the equation obtained is

$$K = K_{\bar{n}}^2[Ag^+]^2[Cl^-]^{2\bar{n}}/[Cu^{2+}][Cl^-]^{2\bar{n}} = K_{\bar{n}}^2[Ag^+]^2/[Cu^{2+}] \quad (3A)$$

As $[Ag^+]^2/[Cu^{2+}] = K_{sp}(Ag_2S)/K_{sp}(CuS) = 10^{-13.8}$, the required constant is $K = 10^{-13.8}K_{\bar{n}}^2$. The calculated values of $K$ at the relevant chloride concentrations a

| $[Cl^-]$ | $\bar{n}$ | $\alpha_1$ | $\alpha_2$ | $\alpha_3$ | $\alpha_4$ | $K_{\bar{n}}$ | $K$ |
|---|---|---|---|---|---|---|---|
| 0.1 | 2.0 | 0.082 | 0.82 | 0.082 | 0.014 | $7.56 \times 10^4$ | $9.06 \times 10^{-5}$ |
| 1.0 | 3.2 | 0.0026 | 0.26 | 0.26 | 0.46 | $1.44 \times 10^5$ | $3.30 \times 10^{-4}$ |
| 3.0 | 3.7 | — | 0.051 | 0.15 | 0.79 | $1.72 \times 10^5$ | $4.67 \times 10^{-4}$ |

REFERENCES

1 R. A. Durst (Ed.), Ion-selective Electrodes, NBS. Spec. Publ. 314, Washington, 1969.
2 G. J. Moody and J. D. R. Thomas, Selective Ion-sensitive Electrodes, Merrow, Watford, 1971.
3 J. Koryta, Ion-selective Electrodes, Cambridge University Press, 1975.
4 J. Koryta, Anal. Chim. Acta, 61 (1972) 329.
5 J. Koryta, Anal. Chim. Acta, 91 (1977) 1.
6 R. Buck, Anal. Chem., 48 (1976) 23R.
7 M. Sato, Electrochim. Acta, 11 (1966) 361.
8 T. Hepel, M. Hepel and M. Leszko, Analyst, 102 (1977) 132.
9 H. R. Wuhrman, W. E. Morf and W. Simon, Helv. Chim. Acta, 56 (1973) 1011.
10 R. Jasinski, J. Trachtenberg and D. Andrychuk, Anal. Chem., 46 (1974) 364.
11 Orion Research Inc., Cupric Ion Electrode (Mod. 94-29) Instruction Manual (1971).
12 D. J. Crombie, G. J. Moody and J. D. R. Thomas, Talanta, 21 (1974) 1094.
13 D. Midgley, Anal. Chim. Acta, 87 (1976) 19.
14 J. W. Ross, in R. A. Durst (Ed.), Ion-selective Electrodes, ref. 1.
15 L. G. Sillén and A. E. Martell, Stability Constants, Chem. Soc. (London) Spec. Publ. no. 17, 1964.
16 K. H. Lieser, Z. Anorg. Allg. Chem., 292 (1957) 97.
17 M. Mascini and A. Liberti, Anal. Chim. Acta, 53 (1971) 206.
18 G. J. M. Heijne, W. E. Van Der Linden and G. Den Boef, Anal. Chim. Acta, 89 (1977) 287.
19 J. N. Butler, Ionic Equilibrium, Addison-Wesley, New York, 1964.
20 M. J. Maurice, Anal. Chim. Acta, 16 (1957) 572.

*Analytica Chimica Acta*, 105 (1979) 67—75


# SINGLE-POINT TITRATIONS
## Part 4. Determination of Acids and Bases with Flow Injection Analysis*

OVE ÅSTRÖM

*Department of Analytical Chemistry, University of Umeå, S-901 87 Umeå (Sweden)*
(Received 20th July 1978)

SUMMARY

A single-point titrimetric system for acids and bases based on the flow injection principle is reported. The sample (30 μl) is introduced into a water stream with a pneumatic injector; this stream reacts with a linear acidic or basic buffer solution in a merging stream, and the peak height is recorded potentiometrically with a glass electrode in a flowthrough cell. The peak maxima are a linear function of the acid or base concentration in the range 0.01—0.1 M. At a sampling rate of 180 samples per hour, the relative standard deviation is less than 1%. The method can be used at sampling rates as high as 720 samples per hour.

The increasing demand for titrimetric analyses as a result of the growing number of samples in various fields has led to a need for faster methods for analyses. Two main approaches have been used in the development of rapid analytical methods, i.e., either discrete or continuous methods. In the discrete method each sample is treated as a separate unit; it is placed in a separate container and the usual chemical stages such as addition of reagents, dilution and mixing are done in much the same way as manual analyses. The titrants are mostly delivered and measured with motor-driven burettes, pneumatic pipettes [1] or syringes. The equivalence volume is evaluated from the titration curves or by more sophisticated methods such as the second derivative [2], Gran plots or related functions. Discrete analyzers have the advantage of possessing a high degree of precision and a high through-put, while reagent consumptions are only those required for each sample. One of their disadvantages is their relatively complex construction and their high cost compared with continuous analyzers.

Very few papers have dealt with continuous flow titrations. Blaedel and Laessig [3—5] have described a continuous automatic burette-less titrimeter. In their method the sample was pumped at a constant speed with the reagent pumped at a variable speed, and the potential was measured with electrodes after mixing. By preselection of the equivalence-point potential and application of a servocontrol to the reagent pump to maintain the potential at the preselected value, the pump speed became a measure of the concentration of the

*Part 3: Anal. Chim. Acta, 97 (1978) 259.

sample stream. Fleet and Ho [6] reported a gradient titration method where the gradient stream was created similarly to the old liquid-chromatographic technique. After the gradient had mixed with the sample stream, the potential was monitored with an electrode; the elapsed time between the rising and falling parts of the titration curve was then directly proportional to the concentration of the sample. One drawback of these systems is the relatively low sampling frequency, about one sample every 6 min.

Růžička et al. [7] adapted the gradient idea to the flow injection analysis system in a further development of the continuous titrimetric technique. The gradient was created within a continuous unsegmented flowing stream, either in a single or in a double line. The ingenuity of their method is that the concentration gradient is created by the sample in a gradient device consisting of tubes with different bores. The time between the equivalence points for the rising and falling parts of the titration curve is proportional to the logarithm of the sample concentration. The sampling frequency is increased to between 20 and 60 titrations per hour, which is a considerable improvement on earlier methods.

One of the main features of the earlier work in this series [8, 9] has been to minimize the laborious and time-consuming work involved in titrations. A combination of the single-point titration with the flow injection technique is very promising in the pursuit of this goal. The present paper shows that these techniques can be combined for the determination of acids and bases. Relationships between such parameters as flow rate, length of mixing coil, sample volume and reagent composition are discussed so that maximum precision and speed of analysis can be achieved.

## EXPERIMENTAL

### *Apparatus*

A Gilson Minipuls II peristaltic pump (Gilson, France) was used with standard PVC tubes, the desired flow rates being obtained by changing tubes and pump speed. Several other pumps were tested but the Gilson pump was preferred because of low flow pulsation.

An Altex dual-wavelength u.v. detector model 152 (Altex Scientific Inc., USA) was used together with the dual wavelength optical unit equipped with a 20-$\mu$l flow cell (10-mm light path).

A digital differential potentiometer, built in this department, was connected either to a Hewlett-Packard Moseley model 680 recorder or to a Hewlett-Packard model 7030 AM X-Y recorder. Additionally, a peak reading unit, also constructed in this department [10], was connected to the potentiometer. This unit makes it possible to monitor both the peak height and the peak area; it measures the base-line just before the peak rises and then holds the maximum peak value, so that a slow drift in the system can be automatically compensated. The reference electrode was an Orion double-junction electrode with the electrode solutions recommended by Orion. The glass electrode was a

special Ingold glass electrode (Ingold AG, Zürich) with a flat surface area of about 20 $mm^2$.

The manifold (Fig. 1) was made from Teflon tubing (0.50 and 1.5 mm i.d.) and Lego building blocks (Lego, Billund, Denmark). Coils were made by winding appropriate lengths of Teflon tubes on Perspex tubes (15 mm o.d.). Y-shaped connections were also made of Perspex. Connections between different manifold parts were standard liquid chromatography connectors (Altex). The sample, usually 30 $\mu$l, was injected into the flow line of water (flow rate $x$); after mixing with the buffer solution (flow rate $y$), the change in concentration was measured with the glass electrode. The signal from the glass electrode was always monitored on a recorder, while simultaneously the peak height was recorded on the peak module.

The potentiometric flow cell was made of Perspex and was similar to that described by Hansen, Růžička et al. [11, 12] (see Fig. 2). The solution flowed from the tip of a syringe needle tangentially over the glass electrode surface down the cell wall and into the reservoir in which the Orion double-junction electrode was immersed. A needle was used in order to obtain the correct angle and distance to the electrode. By differential pumping, a constant level of liquid was maintained in the reservoir. With this arrangement a very small dead volume — less than 20 $\mu$l — was obtained and the thin liquid layer at the electrode surface was renewed many times per second.

The injection device comprised a standard liquid chromatography inlet slide valve for lower pressure (Altex model 201-06 with two pneumatic actuators). The actuators were driven by air, which was controlled by a magnetic valve, in turn controlled by an electric switch. With this arrangement neither

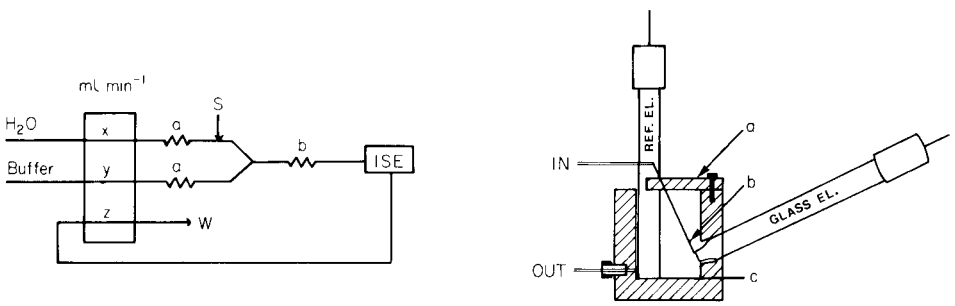


Fig. 1. Confluence manifold used for flow injection analysis of bases and acids. Buffer solution is pumped through line $y$ at a rate of 0.45 ml $min^{-1}$ and water through line $x$ at a rate of 4.5 ml $min^{-1}$. To maintain a constant level of liquid in the flow cell, $z$ is pumped at a rate of 9 ml $min^{-1}$. Coils $a$ are each 60 cm long and the mixing coil $b$ is 300 cm long. The first coils serve as pulse dampers. All teflon tubes have an i.d. of 0.5 mm. S denotes the point of injection; generally a volume of 30 $\mu$l was injected pneumatically.

Fig. 2. Flow-through cell with a glass electrode and reference electrode. The flow enters the cell through the hypodermic needle (b), which is movable in all directions by means of the Perspex piece (a) with a slit in the middle. The reservoir solution in which the reference electrode is submerged is grounded at point (c) to the differential amplifier.

electric switches nor electric cables were near the electrodes, and electrostatic effects were avoided. The sample loop, which consisted of a tube coil, was exchangeable, so that different sample volumes from several ml down to a few μl could be selected. Owing to the high switching speed of the slide valve (a few microseconds) there was no noticeable interruption of the flow, and less disturbance of the dispersion pattern in the flow line was caused than with manual syringe injection.

*Reagents*

Buffer solutions were made as described earlier [8, 9]. Water from a Millipore Super-Q water system was used and all reagents were of analytical-reagent grade. Hydrochloric acid and sodium hydroxide were prepared from Titrisol 0.1 M standard solutions (Merck). Weaker solutions were prepared by successive dilutions.

## RESULTS AND DISCUSSION

*Glass electrode and buffer solutions*

In a previous paper of this series [9], it was shown that when the linear buffer solution used for single-point titrations was diluted, the relationship between concentration and pH still remained linear and could be used analytically, although the original slope was not maintained. Combination of the flow injection technique with the linear buffer solution is thus facilitated. The conditions for dilution of the sample are fulfilled by the arrangement shown in Fig. 1. Compared with ordinary titrations, this technique has the advantage that the glass electrode will be in buffered surroundings during the whole titration cycle. This gives a much more stable potential of the glass electrode, for it is well known that when the buffer capacity diminishes around the equivalence point in an ordinary acid–base titration, the potential becomes rather unstable. The slow response of the glass electrode in poorly buffered solutions has been noted by several authors [13–15]; Wikby and Karlberg [16] pointed out that the buffer capacity was the determining factor for the response time. However, the response times of glass electrodes are very fast [7, 17, 18] compared with the flow injection peak, and are of the order of milliseconds in buffered solutions. Obviously, the rate-determining step in a flow analysis must not be the electrode. That the glass electrode readings are fast and less subject to drift in buffered solution favours the flow injection technique. The rather rapid changes which occur in flow injection do not affect the potential readings because the dispersed sample zone is buffered over its entire length and the glass electrode response is fast. Compared with the method described in the previous papers [8, 9], the method presented here possesses the great advantage that the glass electrode does not need to be calibrated against a known standard buffer solution, so that maintenance and procedure are much easier.

*Manifolds*

For titration of the sample with the linear buffer mixture, a certain degree of mixing is necessary. This is achieved by controlling the dispersion of the injected sample zone, which is effected by choosing suitable pumping speed, sample size and manifold parts.

The confluence system shown in Fig. 1 was preferred to a straight configuration, which would require a long time to achieve the desired mixture of the sample with the buffer. The inevitable large dilution would cause a loss of sensitivity, and the sampling rate would be lower. The confluence configuration has the advantage that when the sample is injected into the water line, the blank value from pure water is not detectable.

During the development work, a continuous slow change occurred in the pumping tubes and was manifested as a decrease in flow rate. Frequent calibration compensated for this decrease in flow provided that the changes in the different tubes were of the same degree. In the final arrangement, the flow rates were controlled as indicated in Fig. 1.

*Ratio of water to buffer solutions*

The rates of the merging flows were investigated to give simultaneously a high sampling rate, a linear range up to at least 0.1 M acid or base, low reagent consumption and a small sample volume. A ratio larger than 10 between the water and buffer flows causes a decrease in the linear range, provided that the sample size and total flow are the same. The same linear range could be achieved only with sample volumes of less than 30 $\mu$l; with the sample injector used, this would be difficult unless tubing of very narrow bore were used, and this would increase the pressure in the system, causing leakage problems at the connections. Analogously, a decrease in the ratio between the water and buffer flows will give an increased linear range, but a decreased sensitivity.

*Flow arrangement and analytical results*

Figure 2 shows the electrode configuration and the flow arrangement. The last part of the flow line consists of a hypodermic needle (b) so that the flow over the glass electrode can be arranged perpendicularly to the sensor. The Perspex piece (a) can swing horizontally around the screw and has a slit in the middle which allows the needle to be moved in all directions. This glass electrode has a larger active surface area than a PVC membrane electrode, so that, to wet the whole surface, the position of the needle is much more critical. If the needle tip is too close to the electrode surface, the sample tends to adhere to the needle giving rise to tailed peaks. A similar effect appears if the drainage from the lower edge of the glass electrode surface is inadequate so that a thick liquid layer builds up instead of a thin one. Unfortunately, if the drainage is too effective, flow pulsations become more noticeable. Hence a good compromise has to be found between stable baseline and tailed peaks. Figure 3 shows two sets of calibration curves for sodium hydroxide. Similar curves were obtained for hydrochloric acid, formic acid, acetic acid and *N*-methyl-

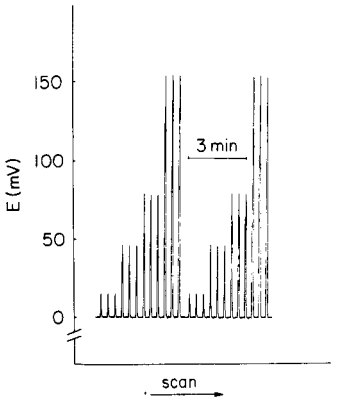


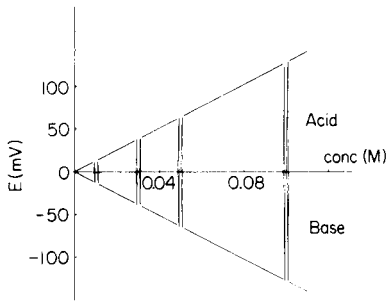


Fig. 3. Two sets of standard sodium hydroxide solutions injected at a rate of 180 samples per hour. From left to right: 0.01, 0.03, 0.05 and 0.10 M. Injected volume 30 $\mu$l. Flow rates as in Fig. 1.

Fig. 4. Calibration plot for 0.01, 0.03, 0.05 and 0.10 M acid and base.

diethanolamine. In the case of bases, the buffer (see Fig. 1) is the acidic buffer solution, and in the case of acids the basic buffer is used [8, 9]. The sampling rate was 180 per hour; as can be seen from Fig. 3 a very stable baseline and good reproducibility were obtained. The sampling rate can easily be doubled and baseline readings can still be made between the samples.

To assess the reproducibility, four different solutions were injected, ten times each; the results (Table 1) show a very high degree of reproducibility and the excellent linear response of the system is apparent from the value (0.9999) of the regression coefficient. Calibration plots for acid and base are shown in Fig. 4.

*Sampling rate*

The possibility of increasing the sampling speed is most easily seen in Fig. 5, which shows two sets of samples, 0.1 M and 0.03 M sodium hydroxide, respectively. The second sample in each set was injected 5 s after the first. As can be seen, the contribution of the first sample to the second one is vanishingly

TABLE 1

Reproducibility of the titration method at four different sample concentrations (regression coefficient 0.9999)

| NaOH sample solution (M) | Mean of peak maxima (mV) | R.s.d. (%) ($n$ = 10) |
|---|---|---|
| 0.0100 | 13.9 | 1.7 |
| 0.0297 | 41.0 | 0.5 |
| 0.0495 | 68.2 | 0.4 |
| 0.0990 | 135.4 | 0.2 |

small. Consequently the sampling rate can be increased to one sample every 5 s, i.e. 720 samples per hour. In this situation, the baseline is not reached between each sample (cf. Fig. 5), but the peak value can still be used for concentration calculations provided that the imaginary base line is steady. Figure 6 shows an authentic run of 0.03 M sodium hydroxide at a speed of 720 samples per hour. Although the baseline is not reached between each sample, successive peaks do not tend to increase, as would have occurred if there had been significant carryover.

*Sample size, dispersion, coil length and flow rate*

The influence of coil length (*b* in Fig. 1) and sample size is shown in Fig. 7. An increasing deflection is attained with increasing sample size and diminishing coil length. When the sample size is increased, the linear range diminishes and the highest attainable peak within the linear range will be around 200 mV. If the sample concentration is increased to 0.1 M for the two highest sample sizes, a saturation level is attained; it is possible to use a 100-$\mu$l sample with a 200-cm coil, but this is very critical and awkward to attain the optimum settings Instead a coil length of 300 cm and a sample size of 30 $\mu$l was chosen: coil lengths of 100 cm and 200 cm give larger peaks, but the 300-cm coil gives much more reproducible peak values.

The sample dispersion is reflected by the plots shown in Fig. 8. It should be noted that although the pumping dial is set at zero, the pump still pumps. In order to check that the results obtained with the glass electrode were due only to dispersion in the system, indicator samples were injected and measured spectrophotometrically. The two different measuring systems gave similar curves, which indicates that the glass electrode is not the limiting factor in the measuring system. The dispersion patterns are in accordance with the results obtained by several authors [19—21]. To prevent the sample from dispersing before the mixing point, the distance between the injector and mixing points is kept as short as possible; later, some mixing is essential, and this can be achieved by increasing the pumping rate and/or the coil length. In

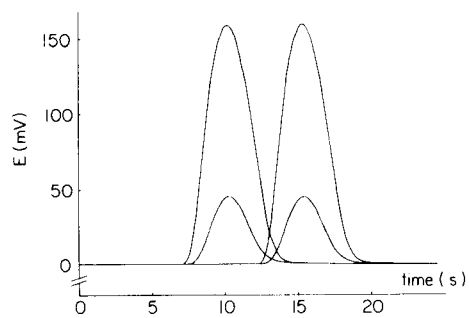


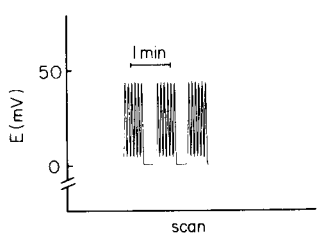


Fig. 5. The influence of one sample on the next for an injection interval of 5 s. Two concentrations, 0.03 and 0.10 M NaOH respectively, are shown.

Fig. 6. Determination of 0.03 M sodium hydroxide at a rate of 720 samples per hour.

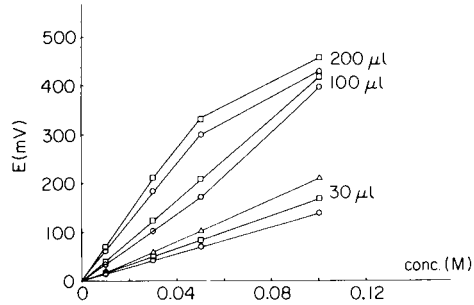


Fig. 7. Influence of sample size, concentration and coil length ($b$) on peak height: (○) 300 cm, (□) 200 cm, (△) 100 cm coil length.

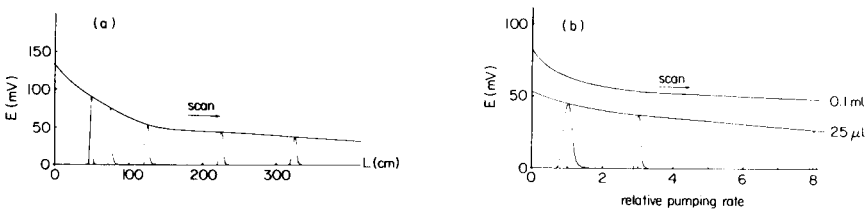


Fig. 8. Influence of different parameters on peak height and dispersion. (a) Effect of length of coil $b$ for 30-μl samples; (b) effect of sample size and pumping rate.

order to obtain good reproducibility, high analysis rate and proper mixing simultaneously, the 300-cm coil was chosen, giving good reproducibility and proper mixing rather than high peak values, whereas the pumping rate was chosen to give high analysis rate, reproducibility and peak height. A pumping rate corresponding to 3 in Fig. 8(b) was chosen and the true values are shown in Fig. 1.

The author thanks Ms. Kerstin Palmgren for skilful help with the experiments and Dr. Michael Sharp for linguistic revision of the manuscript. The gift of the glass electrode from Ingold AG, Zürich, is greatly appreciated.

REFERENCES

1 See, e.g. L. Petersson and F. Ingman, Talanta, 24 (1977) 79, 87.
2 G. M. Hieftje and B. M. Mandarano, Anal. Chem., 44 (1972) 1616.
3 W. J. Blaedel and R. H. Laessig, Anal. Chem., 36 (1964) 1617.
4 W. J. Blaedel and R. H. Laessig, Anal. Chem., 37 (1965) 333, 1255, 1651.
5 W. J. Blaedel and R. H. Laessig, Anal. Chem., 38 (1966) 186.
6 B. Fleet and A. Y. W. Ho, Anal. Chem., 46 (1974) 9.
7 J. Růžička, E. H. Hansen and H. Mosbaeck, Anal. Chim. Acta, 92 (1977) 233.
8 O. Åström, Anal. Chim. Acta, 88 (1977) 17.
9 O. Åström, Anal. Chim. Acta, 97 (1978) 259.
10 E. Lundberg, Appl. Spectrosc., 32 (1978) 276.

11 E. H. Hansen A. K. Ghose and J. Růžička, Analyst, 102 (1977) 705.
12 E. H. Hansen, F. J. Krug, A. K. Ghose and J. Růžička, Analyst, 102 (1977) 714.
13 G. Mattock, pH Measurements and Titration, Heywood, London, 1961.
14 G. A. Perley, Anal. Chem., 21 (1949) 559.
15 M. W. Geerlings, Plant and Process Dynamic Characteristics, Proc. Conf., Cambridge, England, 1956, p. 101.
16 A. Wikby and B. Karlberg, J. Electroanal. Chem., 43 (1973) 325.
17 A. Distèche and M. Dubuisson, Rev. Sci. Instrum., 25 (1954) 86.
18 A. Distèche, Mem. Acad. Belg., Ser. 2, 32 (1960) 1.
19 O. Levenspiel, Chemical Reaction Engineering, 2nd edn., Wiley, New York, 1972.
20 H. Bate, S. Rowlands and J. A. Sirs, J. Appl. Physiol., 34 (1973) 866.
21 D. A. Lane and J. A. Sirs, J. Phys. Sci. Instrum., 7 (1974) 51.

*Analytica Chimica Acta*, 105 (1979) 77—81


# A RUBIDIUM ION-SELECTIVE ELECTRODE FOR THE ASSAY OF POLYENE ANTIBIOTICS

R. F. COSGROVE

*The Squibb Institute for Medical Research, Reeds Lane, Moreton, Wirral, Merseyside L46 1QW (Gt. Britain)*

A. E. BEEZER*

*Department of Chemistry, Chelsea College, London University, Manresa Road, London SW3 6LX (Gt. Britain)*

(Received 5th June 1978)

SUMMARY

The preparation of a rubidium ion-selective electrode is described. The performance characteristics of the electrode are such that it can be used as an alternative to atomic absorption spectrometry in the assay of bulk nystatin, by measuring the rubidium ion efflux from specially prepared yeast cells. The electrode simplifies assay procedures because rubidium(I) can be determined directly in cell suspensions without prior centrifugation; assay time is reduced to 10 min. The sensitivity of the method is 2 units of antibiotic per ml, which is comparable with other physico-chemical methods of bioassay but some 10 times more sensitive than the conventional agar diffusion assay.

In some areas of antibiotic potency determinations, physico-chemical methods of bioassay have replaced the classical microbiological procedures [1]. The polyene antifungal antibiotics cause permeability changes in the cell membrane of susceptible micro-organisms with a resulting efflux of various cell constituents [2—5]. The measurement of one or more of these constituents is suitable for application of some physico-chemical technique. Potassium is said to be the first ion to be released from the cell as a result of membrane damage and has been monitored by the use of ion-selective electrodes [6, 7], and atomic absorption spectrometry [8].

A method of assay for polyene antibiotics has been reported in which yeast cells loaded with rubidium ions were subjected to the antibiotic and the subsequent efflux of rubidium from these cells was measured by atomic absorption spectrometry [9]. The advantages and validity of measuring rubidium, which has a very low level of natural occurrence, over potassium have been previously documented [10]. Atomic absorption spectrometry suffers from two main disadvantages: the necessity of removing the treated cells from the suspension before analysis and the consumption of the sample during analysis. It was felt that a rubidium ion-selective electrode would overcome these disadvantages.

Rubidium-selective electrodes are not available commercially, unlike potassium electrodes. Potassium-selective liquid-membrane electrodes are far more selective than glass electrodes and generally employ the macrocyclic antibiotic valinomycin [11]. The first potassium-selective electrode based on valinomycin was described by Pioda et al. [12] and the similarity in response to both $K^+$ and $Rb^+$ ions was illustrated by Mascini and Pallozzi [13]. In an attempt to assay $Rb^+$ with such an electrode, the internal standard solution of a commercially available liquid membrane potassium electrode was replaced by an appropriate rubidium chloride standard solution and the membrane was also soaked in this solution prior to use. This electrode gave a sufficiently high selectivity coefficient for rubidium over potassium to be used in the $Rb^+$ efflux assay for nystatin.

## EXPERIMENTAL

### *Electrodes and instrumentation*

A Philips 560 K ion-selective electrode was used with a Philips RH 44/21SD/1 double-junction reference electrode with ground-glass sleeve, connected to a Philips digital ion-activity meter (PW 9414/01) linked to a Philips PM 8251 chart recorder (Pye Unicam). The potassium-selective electrode was supplied dry. During its assembly which was otherwise in accordance with the manufacturer's instructions, the internal reference solution used was $10^{-3}$ M RbCl ($I = 10^{-3}$ M) instead of the electrolyte supplied. The assembled electrode was equilibrated in $10^{-3}$ M RbCl for at least 2 h prior to use. The reference electrode was prepared in the normal way with the inner compartment containing saturated KCl solution and the outer compartment 0.1 M $NH_4NO_3$. The activity meter was standardized and used as recommended by the manufacturer. All measurements were made on stirred solutions (magnetic stirrer).

### *Nystatin solutions and inoculum*

Nystatin bulk material (E. R. Squibb & Sons Ltd.) was weighed and dissolved in dimethylformamide (DMF) and diluted with Tris buffer (0.2 M tris(hydroxymethyl)methylamine, adjusted to pH 7.5 with HCl) to the required concentration. The final concentration of DMF in all solutions in contact with the electrode was 0.2%. The method of preparation, storage and recovery of liquid nitrogen-stored inocula of $Rb^+$-loaded *Saccharomyces cerevisiae* (SQ 1600), were as previously described [9].

### *Determinations of electrode sensitivity and selectivity*

Standard solutions of RbCl covering the range $10^{-1}$—$10^{-6}$ M were prepared in deionized water. The potentials for these solutions were measured at 22°C with continuous stirring. Both the separate-solutions and mixed-solutions methods [14] were used to determine the selectivity of the electrode for $Rb^+$ over $K^+$. For the first method, which is based on the equation $(E_2—E_1)/2.303\ RT/F = \log K_{MN}$, the potentials for KCl solutions in the range $10^{-1}$—$10^{-6}$ M were

compared with the potentials for RbCl solutions of similar molarity. For the second method, electrode potentials were determined for KCl solutions of fixed molarity ($10^{-4}$ and $10^{-5}$) mixed with RbCl solutions ranging from $10^{-1}$ to $10^{-9}$ M. Results were calculated as described by Moody and Thomas [14]. Selectivity coefficients for other ions which could interfere, i.e. $Na^+$, $NH_4^+$ and $Mg^{2+}$, were determined by the first method.

*$Rb^+$efflux from cells*

After thawing, 1 ml of cell suspension was added to 50 ml of Tris buffer which had been pre-warmed to 50°C (the pH at 50°C was not measured). Aliquots (0.1 ml) of a nystatin solution at a suitable concentration were added as appropriate. The change in potential was measured either continuously on a chart recorder, or, if several samples were running simultaneously, by transfer of the electrodes from one solution to another, 10 min after the start of each incubation. All solutions were held at 50°C and stirred throughout.

## RESULTS AND DISCUSSION

*Performance of the rubidium-selective electrode*

The electrode exhibits nearly Nernstian behaviour for rubidium concentrations between $10^{-1}$ and $10^{-5}$ M, irrespective of whether Tris or aqueous solutions are used at both 22°C and 50°C (Table 1). The reproducibility of the electrode, defined as the mean deviation of the measured potential when the electrode is transferred three times from a $10^{-3}$ M to a $10^{-2}$ M rubidium chloride solution, was found to be ± 0.3 mV. The response time of the electrode was less than 30 s when the electrode was transferred three times from a $10^{-3}$ M rubidium chloride solution to a $10^{-2}$ M solution.

The selectivity of the electrode for $Rb^+$ over $K^+$, assessed by the separate-solutions method, was found to be $1.6 \times 10^{-1}$; the mixed-solutions method gave the value $2 \times 10^{-1}$ with $10^{-4}$ M $K^+$ and $7 \times 10^{-1}$ with $10^{-5}$ M. Selectivity

TABLE 1

Electrode response for standard solutions of rubidium chloride in Tris buffer and in deionized water measured at 22°C and 50°C

| [RbCl] (M) | Electrode response (mV) | | | |
|---|---|---|---|---|
| | 22°C | | 50°C | |
| | Tris | $H_2O$ | Tris | $H_2O$ |
| $10^{-1}$ | 314 | 299 | 294 | 288 |
| $10^{-2}$ | 255 | 248 | 243 | 233 |
| $10^{-3}$ | 199 | 193 | 187 | 178 |
| $10^{-4}$ | 141 | 135 | 130 | 120 |
| $10^{-5}$ | 90 | 83 | 77 | 67 |
| $10^{-6}$ | 61 | 53 | 47 | 38 |

coefficients for $Na^+$, $NH_4^+$ and $Mg^{2+}$ were calculated to be $2.8 \times 10^{-6}$, $1.1 \times 10^{-2}$ and $6.3 \times 10^{-6}$, respectively; these values are very close to those quoted for these ions for the potassium electrode, from which this electrode was developed ($3 \times 10^{-6}$, $1 \times 10^{-2}$ and $6 \times 10^{-6}$, respectively).

The sensitivity of the electrode for $Rb^+$ over $K^+$ is adequate for its use as an alternative to atomic absorption spectrometry in the assay of polyene antibiotics. There is less than $10^{-5}$ M $K^+$ present in the yeast cell inoculum after growth in rubidium chloride medium, harvesting and storage as described earlier [9].

*The assay system*

The efflux of $Rb^+$ ions from yeast cells subjected to a range of nystatin concentrations was monitored continuously over a 15-min period at 50°C. The combined chart recorder traces from this study are shown in Fig. 1. If the electrode potential (from these traces) after 10-min incubation times is plotted against the logarithm of the nystatin concentration, a straight line is obtained between the concentrations of 8 units $ml^{-1}$ and 2 units $ml^{-1}$. This is the normal form of relationship (log dose vs. response) found in bioassays based on the agar-plate diffusion method [15] and forms the basis of the proposed assay. The alternative method of measuring $Rb^+$ efflux by atomic absorption spectrometry [9], requires a 30-min incubation period at 37°C followed by centrifugation of the suspension before a similar result can be obtained. The incubation period in this method could possibly be shortened by increasing the incubation temperature, but physical problems then arise in the preparation of the system, the incubation, centrifugation and removal of the supernatant liquid. The electrode system does not require centrifugation or separation as observations may be made directly on the cell suspensions at the chosen temperature of the incubation.

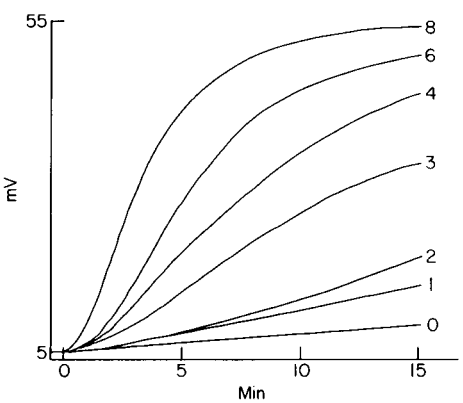


Fig. 1. $Rb^+$ efflux from yeast cells subjected to various concentrations of nystatin at 50°C. The nystatin concentrations (I.U. $ml^{-1}$) are indicated on the curves. The electrode was coupled to a chart recorder for continuous monitoring.

Thus, the use of the electrode is far more convenient and allows shorter incubation times. The sensitivity of the two methods (2 units $ml^{-1}$) is identical and both methods are about ten times more sensitive than the conventional agar diffusion assay.

The reproducibility of the response of the electrode with the cryogenically stored inoculum has remained excellent over the two-month period that the electrode has so far been in use. The membrane of the potassium electrode is said to have a life of 4—6 months, and the $Rb^+$ electrode should last as long. At the end of the useful lifetime of the membrane, replacement is very simple.

In conclusion, the $Rb^+$ electrode described provides a convenient measurement of $Rb^+$ released from yeast cells in the assay of bulk nystatin by the $Rb^+$ efflux method [9]. The extension of its use to the bioassay of formulated pharmaceuticals containing nystatin and other polyenes and also to the assay of clinical specimens is currently being investigated.

The authors thank Dr. J. A. W. Dalziel and Ms. R. Hyla of Chelsea College, London University, for helpful discussions and advice, and Ms. Sandra Baines of E. R. Squibb & Sons Ltd., for technical assistance.

REFERENCES

1 J. W. Lightbown, Proc. Anal. Div. Chem. Soc., 13 (1976) 137.
2 S. C. Kinsky, J. Bacteriol., 82 (1961) 889.
3 J. O. Lampen, P. M. Arnow, Z. Borowska and A. I. Laskin, J. Bacteriol., 84 (1962) 1152.
4 F. Marini, P. Arnow and J. O. Lampen, J. Gen. Microbiol., 24 (1961) 51.
5 D. D. Sutton, P. M. Arnow and J. O. Lampen, Proc. Soc. Exp. Biol. Med., 108 (1961) 170.
6 E. F. Gale, J. Gen. Microbiol., 80 (1974) 451.
7 S. M Hammond, P. A. Lambert and B. N. Kliger, J. Gen. Microbiol., 80 (1974) 325.
8 I. Ndzinge, S. D. Peters and A. H. Thomas, Analyst, 102 (1977) 328.
9 R. F. Cosgrove, J. Appl. Bacteriol., 44 (1978) 199.
10 R. F. Cosgrove and J. E. Fairbrother, Antimicrob. Agents Chemother., 11 (1977) 31.
11 R. P. Buck, Anal. Chem., 46 (1974) 28R.
12 L. A. R. Pioda, V. Stankova and W. Simon, Anal. Lett., 2 (1969) 665.
13 M. Mascini and F. Pallozzi, Anal. Chim. Acta, 73 (1974) 375.
14 G. J. Moody and J. D. R. Thomas, Selective Ion Sensitive Electrodes, Merrow, London, 1971.
15 F. Kavanagh, Analytical Microbiology II, Academic Press, New York and London, 1972.

*Analytica Chimica Acta*, 105 (1979) 83—89


# THE NONAQUEOUS POTENTIOMETRIC DETERMINATION OF COMMERCIAL BENZOPHENONE OXIME (LIX) EXTRACTANTS

D. J. BARKLEY

*Mineral Sciences Laboratories, CANMET, Department of Energy, Mines and Resources, Ottawa K1A 0G1 (Canada)*

(Received 25th July 1978)

SUMMARY

A nonaqueous potentiometric method for the determination of substituted benzophenone oxime reagents (LIX) used as extractants in copper extraction processes is described. t-Butanol is used as the solvent and tetrabutylammonium hydroxide as the titrant. End-points are detected with a glass-modified calomel electrode system; a slow rate of titrant delivery is used near the inflection point. The *syn* and *anti* isomers of LIX reagents (substituted *o*-hydroxybenzophenone oximes) can be differentiated.

LIX extractants, a series of substituted 2-hydroxybenzophenone oximes (General Mills Inc.), are currently being investigated in these Laboratories. The pure extractants are not available; it is important that the composition and stability of the commercial extractants be known for fundamental studies so that the extraction processes can be interpreted and optimized.

The basic molecule from which LIX extractants are derived is 2-hydroxybenzophenone oxime, substituted in the 5-position by an alkyl group; LIX 70 is also substituted in the 3-position by a chlorine atom [1]. LIX 63 is an aliphatic $\alpha$-hydroxyoxime [2]. Table 1 indicates the commercially available extractants of this type. Asymmetrical ketones, such as 2-hydroxybenzophenones, may occur as the *syn* and *anti* isomers. In the *anti* isomer the orientation of the oxime group is such that complex formation with metal ions should be faster [3].

The components in the extractants have been determined spectrophotometrically after separation by extraction and thin-layer chromatography [3], but a more direct and simpler method suitable for use under plant conditions was needed. A procedure generally employed in plants using LIX extractants utilizes the loading capacity of the extractant for copper as a measure of LIX concentration [4]; the copper load is determined by stripping the copper and applying some suitable method. This indirect analysis allows only the *anti* isomer to be determined. A direct determination of both the *syn* and *anti* isomers is to be preferred.

The application of nonaqueous titrimetry to the analysis of these extractants

TABLE 1

Commercial oxime extractants

| Extractant | Structure | Supplier |
|---|---|---|
| LIX 63 | 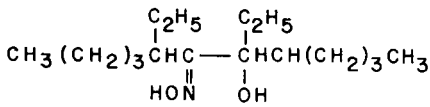 | General Mills |
| LIX 64 | 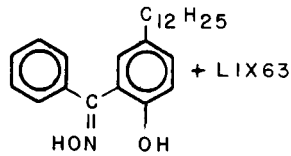 | General Mills |
| LIX 64N | LIX 65N + LIX 63 (~1 vol.%) | General Mills |
| LIX 65N | 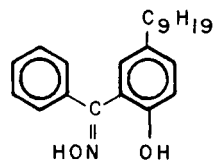 | General Mills |
| LIX 70 | 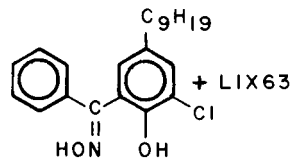 | General Mills |
| LIX 71 | LIX 70 + LIX 65N | General Mills |
| LIX 73 | LIX 70 + LIX 65N + LIX 63 | General Mills |
| P1; P17 ($R_1$ = H or Benzyl) | 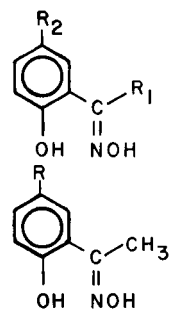 | Acorga |
| SME 529 | | Shell Chemicals |

has been limited because of their very weakly acidic nature [5]. A study was undertaken to ascertain whether or not conditions could be established to titrate commercial oxime extractants in nonaqueous media, and furthermore, if adequate differentiation could be obtained to permit the determination of the isomeric forms. A potentiometric titration procedure is described below and titration curves for the commercially available LIX extractants are shown. Also included are titration curves for another oxime extractant, Shell SME 529.

## EXPERIMENTAL

### *Apparatus*

Potentiometric titration curves were obtained with a Mettler automatic titration system, which consisted of a piston burette with a stepping motor drive (DV11), an electrode potential amplifier (DK10), a rate and end-point control unit (DK11), and a chart recorder (GA13). Titrations were done in a heavy-walled 50-ml beaker with tapered base and a plastic cover which held 2 electrodes and a burette tip. A magnetic stirrer was used. The titrant was dispensed from a 10-ml burette supplied by a 500-ml storage vessel fitted with a guard tube containing Ascarite.

The glass indicator electrode (Fisher No. 13-634-3) was kept in water when not in use to avoid possible dehydration of the glass membrane. It was presoaked in t-butanol for about 2 min before use. The calomel reference electrode (Fisher No. 13-639-51) had a porous ceramic junction, which provided good contact with a slow electrolyte flow. The aqueous potassium chloride in the calomel electrode was replaced with a saturated solution of tetramethylammonium chloride in 2-propanol as recommended by Fritz [6]. This electrode combination gave reproducible titration curves for about 2 h, after which there was a gradual displacement of the curves to higher potentials. The effect was most pronounced in the region of the curve preceding the equivalence point; the overall effect was to compress the curve and decrease the potential break.

### *Reagents*

Preliminary work showed that the LIX extractants could be titrated in acetone, MIBK and pyridine, but that optimal differentiation and reproducibility were obtained in t-butanol. This solvent is obtainable commercially in high purity, and a blank titration of the pure solvent with tetrabutylammonium hydroxide produced a nearly linear change in e.m.f. with constant volume increments of the titrant.

Tetrabutylammonium hydroxide was obtained as a 25% solution in methanol (Eastman Organics or J. T. Baker Chemical Company). An approximately 0.1 M solution was obtained by 10-fold dilution with t-butanol; prepared in this manner the titrant was reasonably stable (the concentration changed by about 3% over three weeks). The titrant was standardized against benzoic acid dissolved in t-butanol.

The purified LIX 65N and LIX 63 samples used were prepared as described by Ashbrook [3]. The samples of oxime extractants analyzed were normal production materials. A 10-ml sample (measured in a 10-ml volumetric flask) was weighed and then diluted to 50 ml with t-butanol. A further dilution of 10 ml to 50 ml was made and aliquots were taken for the determination.

### *Procedure*

A suitable amount of the diluted extractant containing 0.1—0.5 mmol, was

transferred to the titration vessel and diluted to 20 ml with t-butanol, and the vessel was closed by screwing it into the cap bearing the electrodes. Magnetic stirring was begun and the potential monitored. Initial stabilization generally required no more than 1 min, after which the titration was begun. The delivery rate control was set at its minimum (1 ml $min^{-1}$), and the end-point control unit at the automatic slope-fitting position. As a result the titrant was delivered near the inflection point in increments of about 0.005 ml. The solvent blank at the equivalence points was less than 0.02 ml and therefore was neglected.

To remove copper and other metals from a LIX-containing solvent obtained from a solvent extraction process circuit, samples were prepared as follows; approximately 25 ml of sample was shaken in a separatory funnel with an equal volume of 15% (v/v) sulphuric acid for 1 min. The aqueous phase was discarded and the extraction repeated. The organic phase was then shaken with an equal volume of water. This step was repeated three times or until a test of the aqueous phase was neutral. To remove entrained water the organic phase was filtered through a Whatman IPS separating paper. A 10.0-ml aliquot was transferred to a 50-ml volumetric flask and diluted with t-butanol, and a suitable aliquot was used for the determination.

## RESULTS AND DISCUSSION

The six extractants presently available from General Mills, LIX 64, 64N, 65N, 70, 71 and 73 contain two isomers. The *syn* isomer of LIX 65N can be prepared in a pure form from the as-received material [3]. The result of titrating a 0.100-g sample of this isomer is shown in Fig. 1, curve A. There is only one inflection on the curve, and the recovery obtained for the *syn* isomer was 99%. The *syn* isomer can be converted to a mixture of isomers on heating [3]. Curve B, Fig. 1, shows the results obtained by heating a 0.100-g sample at 125°C for 0.5 h, dissolving the melt in t-butanol, and titrating the mixture as described. The first inflection on the curve corresponds to the *syn* isomer

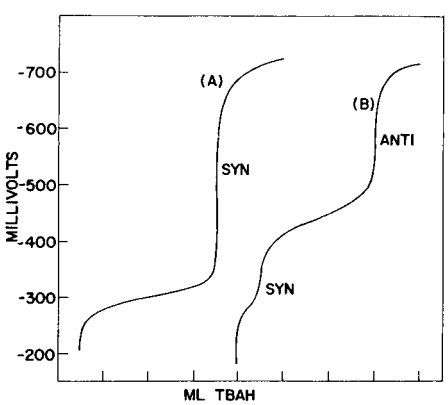


Fig. 1. Differentiation of the isomers of LIX 65N: (A) *syn* isomer; (B) melted *syn* isomer.

concentration and the second represents the *anti* isomer end-point; the results show the *syn* isomer to be the stronger acid. The concentration of isomers was calculated from the titration curve to be 82.3% (w/w) *anti* and 17.7% *syn* isomer.

The extractants LIX 64, 64N, 70 and 73 are reported to contain a small amount of LIX 63, an aliphatic $\alpha$-hydroxyoxime. Titrations of a sample of purified LIX 63 did not give detectable inflection points, nor did titrations of the material as-received. LIX 63 is clearly a much weaker acid than the aromatic *anti* isomer of LIX 65N. Samples of LIX 65N containing up to 5% (v/v) of LIX 63 could be titrated, but above this concentration the end-point for the *anti* isomer was biased. Since the reported concentration of LIX 63 is about 1% in those extractants which contain this reagent [7], the described procedure will be able to determine the *anti* and *syn* isomers of the main constituents.

Figure 2 shows the tiration curves for as-received samples of LIX 64, 64N, 65N, 70, 71 and 73. The concentrations of isomers in the as-received extractants, calculated from their titration curves, are reported in Table 2. The results for LIX 64N and 65N are compared with values obtained by the copper equivalent method [8], which has been used to indicate the "active constituent" or the concentration of *anti* isomer in the extractant.

Similar reagents have been proposed or considered as copper-selective extractants including a substituted *o*-hydroxyacetophenone oxime (Shell Chemical Ltd., SME 529) and substituted salicylaldoximes (Acorga P1 and P17) (see Table 1). Two as-received samples of SME 529 were titrated by the described procedure, with the results shown in Fig. 3. As the initial production batch of Shell SME 529 (sample A) was known to be impure, this would explain the different shapes of the curves obtained for samples A and B; sample B, which was produced at a later date, was a purer product. One inflection point was obtained which would indicate that SME 529 consists of one isomer. The concentration of the extractant was calculated to be 2.08 M

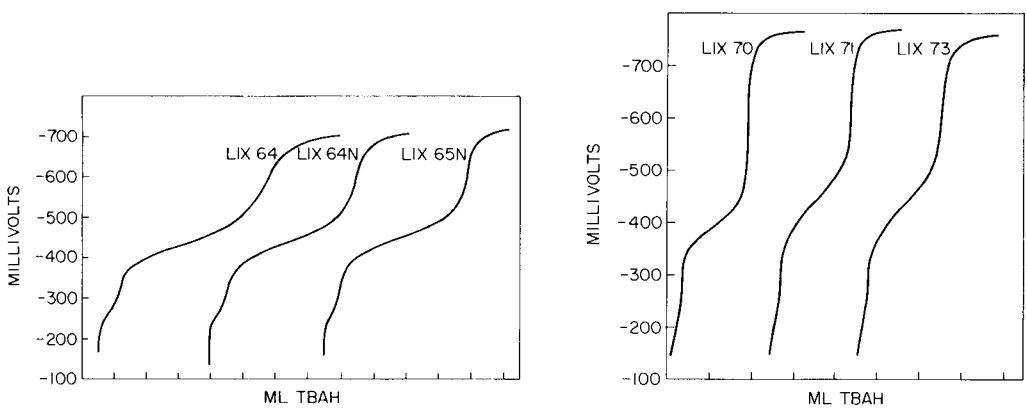


Fig. 2. Titration curves of as-received LIX extractants.

TABLE 2

Concentrations of isomers in as-received LIX extractants

| Extractant | S.g. at 25°C | Conc. of isomer (M) | | Ratio *anti/syn* |
|---|---|---|---|---|
| | | *Anti* | *Syn* | |
| LIX 64 | 0.905 | 1.12 | 0.17 | 6.6 |
| LIX 64N | 0.890 | 0.96[a] | 0.13 | 7.4 |
| LIX 65N | 0.886 | 0.96[a] | 0.13 | 7.4 |
| LIX 70 | 0.909 | 0.82 | 0.15 | 5.5 |
| LIX 71 | 0.895 | 0.83 | 0.12 | 6.9 |
| LIX 73 | 0.895 | 0.87 | 0.15 | 5.8 |

[a]Results obtained by the copper equivalent method were 0.90 for LIX 64N and 0.83 for LIX 65N.

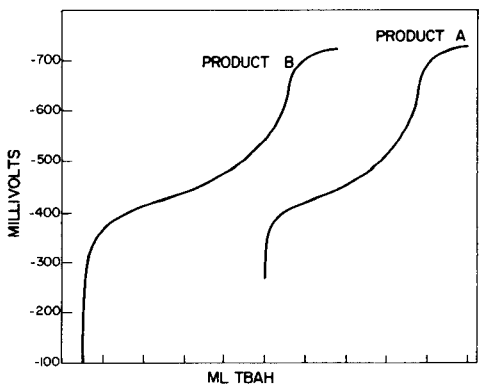


Fig. 3. Titration curves of two samples of as-received Shell SME 529.

in product A and 2.75 M in product B. Acorga P1 and P17 would be expected to titrate similarly to Shell SEM 529.

Oxime extractants in use in extraction operations are diluted with a diluent such as kerosene. The concentration of extractant in a diluent can range from 5% to 50% (v/v). This solvent mixture may also contain a modifier such as 2-ethylhexanol or isodecanol to improve the solvent characteristics. No interference occurred from the concentrations of kerosene or of these alcohols present in the final aliquot taken for the titration. Copper and other metals that may be present in a sample taken from an extraction circuit had to be removed.

The recoveries of LIX 64 and LIX 65N from samples taken from extraction circuits were determined. The samples, which were "loaded" with copper, were stripped of the metal with dilute sulphuric acid as described in the procedure, and aliquots of a diluted sample were taken for the titration. The results of these determinations and a statistical analysis are given in Table 3.

TABLE 3

Determination of LIX 64N and LIX 65N from extraction process solutions

| | LIX 64N (M) | | LIX 65N (M) | |
|---|---|---|---|---|
| | *Syn* | *Anti* | *Syn* | *Anti* |
| Average | 0.026 | 0.217 | 0.023 | 0.216 |
| No. of Determinations | 6.0 | 6.0 | 8.0 | 8.0 |
| Range | 0.002 | 0.002 | 0.002 | 0.005 |
| R.s.d. (%) | ±2.1 | ±0.37 | ±2.8 | ±0.81 |

The proposed method is adaptable for the determination of oxime extractants in process plant operations. Also, the method should be a useful adjunct to other means of isolation and identification of oxime extractants.

The author thanks Dr. A. W. Ashbrook of Eldorado Mining and Refining for supplying samples of purified LIX 65N and LIX 63 and for helpful discussion. The author is indebted to J. A. F. Bouvier for technical assistance.

REFERENCES

1 A. W. Ashbrook, Hydrometallurgy, 1 (1975) 5.
2 F. Habashi, Principles of Extractive Metallurgy, Vol. 11, Gordon and Breach, New York, 1970.
3 A. W. Ashbrook, J. Chromatogr., 105 (1975) 141.
4 A. W. Ashbrook, Talanta, 22 (1975) 334.
5 A. W. Ashbrook, Ext. Metall. Division, Mines Branch (now CANMET) Report EMA 73-22 (1973), Dept. of Energy, Mines and Resources, Ottawa.
6 J. S. Fritz, Acid—Base Titrations in Nonaqueous Solvents, Allyn and Bacon, Boston, 1973.
7 A. W. Ashbrook, Ext. Metall. Division, Mines Branch (now CANMET) Report EMA 73-25 (1973), Dept. of Energy, Mines and Resources, Ottawa.
8 Ashford Metallurgical Laboratory, Charter Consolidated Ltd., Ashford, Kent, U.K., 1975.

*Analytica Chimica Acta*, 105 (1979) 91—97


# DIRECT DETERMINATION OF PENTACHLOROPHENOL BY DIFFERENTIAL PULSE POLAROGRAPHY

ALBERT L. WADE and FRED M. HAWKRIDGE*

*Department of Chemistry, Virginia Commonwealth University, Richmond, Virginia 23284 (U.S.A.)*

HOWARD P. WILLIAMS

*Department of Chemistry, University of Southern Mississippi, Hattiesburg, Mississippi 39401 (U.S.A.)*

(Received 16th August 1978)

SUMMARY

Differential pulse polarography at the dropping mercury electrode and differential pulse voltammetry at the carbon paste electrode are used for direct determinations of pentachlorophenol at concentrations down to 0.27 ppm. PCP is electrochemically reduced in phosphate buffers of pH 8 to produce a concentration-dependent current peak at −0.8 V vs. Ag/AgCl. The procedure requires only 15 min. Cyclic voltammetry at the hanging mercury drop electrode is used to evaluate the electrochemical reaction and to establish the reversibility of the PCP electrode reaction.

Concern over environmental contamination leading to the introduction of highly toxic pentachlorophenol (PCP) into human and animal systems has led to the need for developing more rapid, sensitive and selective methods of analysis. PCP or its sodium salt has been used extensively as a pesticide, molluscicide, fungicide, bactericide, herbicide and defoliant [1]. Municipal water supplies are often processed from streams contaminated with dangerous levels of PCP [2—5]. PCP is lethal to many species of fish in concentrations above 0.2 ppm [6], and produces a wide assortment of clinical symptoms in living organisms [9—13].

Many methods have been developed for determining trace concentrations of PCP based on colorimetric tests, paper and thin-layer chromatography (t.l.c.) spectrophotometry and gas chromatography (g.c.). The earlier methods have been reviewed [1]. Frei-Hausler et al. [14] used a fluorigenic derivative of PCP and t.l.c. to determine sub-microgram concentrations of PCP. Fountaine et al. [3] used an ultraviolet spectrophotometer with a hollow-cathode copper lamp to develop a method for PCP with a detection limit of 2 ppb. Several g.c. methods, most of which depend on electron capture detection, have been developed for PCP and its derivatives with improved detection limits and sensitivities.

Few electrochemical procedures for PCP are available. Mizunoya [20]

converted PCP to chloranil and determined its concentration by polarography. Zemkin et al. [21] used a.c. polarography to determine PCP in photographic gel. In this paper, differential pulse techniques of electrochemical analysis are described for the direct determination of trace amounts of PCP. The nature of the PCP reaction is evaluated by cyclic voltammetry, and bulk controlled-potential electrolysis of PCP is attempted.

## EXPERIMENTAL

### *Equipment*

The Princeton Applied Research Model 174 Polarographic Analyzer used was equipped with a Model 174 Drop Timer and with an MFE 815 X-Y Plotamatic Recorder. A digital voltmeter was used for accurate determination of the voltage applied to the working electrode.

The working electrode was a standard dropping mercury electrode (DME) in differential pulse polarography, and a carbon paste-nujol electrode [22] with a 3-mm i.d. Teflon cup in differential pulse voltammetry. A Princeton Applied Research Model 9323 hanging mercury drop electrode (HMDE) was used as the working electrode for cyclic voltammetry. For controlled-potential electrolysis, the working electrode was a mercury pool contacted by a platinum wire below the mercury surface. The same reference and auxiliary electrodes were used with all these working electrodes. A silver—silver chloride reference electrode containing 1.0 M KCl was constructed in the laboratory; it gave a potential of +0.230 V vs. NHE in a saturated solution of quinhydrone at pH 7 [23]. A platinum wire with platinum gauze attached was used as the auxiliary electrode, which was isolated in a glass tube sealed with porous Vycor for the controlled-potential electrolysis of PCP. Cell electrolyte and phosphate buffer were used in this auxiliary electrode compartment.

The cell consisted of a 30-ml beaker containing a snug-fitting lucite cover with four holes to support the components of the cell assembly. Prepurified nitrogen was passed through a gas scrubber containing distilled water into the cell. All potentials are reported against the aqueous silver—silver chloride reference electrode.

### *Reagents*

Only analytical reagent-grade chemicals were used; further purification was not done. The purity of the PCP (Eastman Chemical Co., lot F2C; m.p. 187—188.5°C) was checked. The infrared spectrum from 4000—700 $cm^{-1}$ was identical with the Aldrich Spectrum for 99+% pure PCP [24], and no impurities were identified by electron-impact mass spectrometry (ionizing current, 70 eV), t.l.c. (see below) or gas chromatography on a 7% SP-1000-Chromosorb G-HP column (6 ft. × 8 mm) with flame-ionization detection.

Stock solutions of PCP ($1 \times 10^{-3}$ M) were prepared daily in the buffer system under investigation. Incremental additions of this stock solution were made to the sample cell by a 25-$\mu$l Eppendorf pipette for the analyses.

A 50:50 mixture of monosodium and disodium hydrogen phosphate was prepared at the indicated buffer strengths for all the electrochemical procedures. A 0.01 M concentration of this mixture was used in differential pulse polarography and cyclic voltammetry, a 0.1 M concentration in differential pulse voltammetry, and a 0.5 M concentration in controlled potential electrolysis. Sodium hydroxide was used to adjust the pH of these solutions as required, and NaCl at concentrations corresponding to the buffer strength was added as a further electrolyte.

*Procedures*

*Differential pulse polarography.* The following operating conditions were selected for differential pulse polarography (d.p.p.) at the DME: 2-mV $s^{-1}$ scan rate, 1.5-V scan range, 25-mV pulse modulation amplitude, minimum current range and 1-s drop time.

A 25-ml aliquot of phosphate buffer was transferred to the cell, the electrode assembly was inserted, and the solution was outgassed for 10 min with nitrogen which was then passed over the surface of the solution. The current—voltage profile was then recorded over the range of interest. Subsequently, successive 25-$\mu$l aliquots of PCP stock solution were injected into this buffer, each new addition raising the PCP concentration of the solution by $1 \times 10^{-6}$ M. A d.p. polarogram was recorded after each addition, nitrogen being bubbled through for a few seconds before the recording. Each polarographic scan was completed in 5 min.

*Differential pulse voltammetry.* For differential pulse voltammetry (d.p.v.) at the carbon paste electrode, the operating conditions and procedure were the same as for d.p.p. at the DME. The voltammograms were developed with a 1.0-s pulse rate. After each analysis, the carbon paste at the end of the electrode was replaced.

*Cyclic voltammetry.* In cyclic voltammetry at the HMDE, the ranges of settings on the polarographic analyzer were as follows: scan rate, 50—500 mV $s^{-1}$; pulse modulation amplitude, 25 mV; d.c. mode; full scale current sensitivities, 1—5 $\mu$A. The PCP solution was transferred to the electrochemical cell and outgassed for 10 min before the scan. Techniques used included scanning different sections of the complete cyclic range independently, scanning at different rates and at different current sensitivities, and beginning the scans at different points on the reduction and oxidation cycles.

*Controlled-potential electrolysis.* For bulk electrolysis, the PCP solution was transferred to the electrolysis cell, a mercury pool was added, the electrode assembly and a small magnetic stirrer were inserted, and a fixed potential of —1.1 V versus Ag/AgCl was applied to the working electrode. The cell solution was outgassed with prepurified nitrogen and stirred magnetically throughout the 72-h period of electrolysis. After electrolysis, the cell products were isolated from the buffer and electrolyte by acidifying with phosphoric acid, and extracting into ether. This material was used for the subsequent investigation of electrolysis products.

*Thin-layer chromatography.* In the t.l.c. procedure for pure and electrolyzed PCP, the materials were spotted on pre-coated silica-gel glass plates (20 × 20 cm Brinkmann Instruments). The solvent systems used were n-hexane [25], chloroform [26], chloroform—acetic acid (100:1) [8], benzene—ethyl acetate (10:1) and acetone—1 M NaOH (94:6) [27]. The chlorinated phenols on the thin-layer plates were detected with a silver nitrate reagent (0.05% w/v) in (1 + 9) 2-phenoxyethanol-acetone solution [27] and a copper sulfate—pyridine reagent [28] in each solvent system. An unknown compound, located in the chloroform solvent system, was isolated on a preparative thin-layer plate and extracted into ether. Infrared analysis was made on this material with the beam-condensing unit before and after purification from a Florisil column.

## RESULTS AND DISCUSSION

The d.p.p. study of PCP at the dropping mercury electrode showed that PCP is electrochemically reduced at a peak potential of ca. —0.8 V versus Ag/AgCl, and that direct determinations are possible for PCP concentrations down to 0.27 ppm. Zemkin et al. [21] have previously reported a.c. polarographic peaks at —0.85 V (vs. SCE) for much higher concentrations of PCP in photographic gelatin.

Concentration-dependent polarograms were obtained for $1-10 \times 10^{-6}$ M PCP in phosphate buffer solutions of pH 7—11. Figure 1 shows the well-defined peaks obtained for 1.1—2.7 ppm PCP at pH 9. The effects of pH on the reduction behavior of PCP are shown in Fig. 2. Excellent concentration-dependent linearity was found at each of these pH conditions with correlation coefficients of 0.98 or better for most of the data (Table 1). In general, as the pH of the buffer was raised, the sensitivity of the measurements increased over this pH range. The only exception was found at pH 8, which yielded a greater sensitivity for PCP than was found in either the pH 9 or 10 buffers. Consequently, the pH 8 phosphate buffer system was selected for developing the electrochemical method for PCP.

Variability in current sensitivity from 2.16 to 4.40 nA per ppm PCP was found in the pH range 7—11. This type of behavior suggests that ion-pairing may be involved; it seems reasonable to expect a difference in the diffusion coefficients of the undissociated phenol, the ion-paired phenol and the phenoxide ion, which would be reflected in the PCP behavior at different pH conditions. The cyclic voltammetry scans were the same for different pH conditions, indicating that the number of electrons in the reaction remains constant. The variation in the current response of PCP as a function of pH could alternatively be due to the participation of protons or hydroxide ions in the electrode reaction. PCP was electrochemically inactive below pH 6.5.

Studies of the redox properties of PCP at the carbon paste electrode were made with differential pulse voltammetry (d.p.v.). Such a system would give versatility to a differential pulse method for PCP in situations where the DME would be inconvenient to use, e.g. in a flowing system. The d.p.v. technique

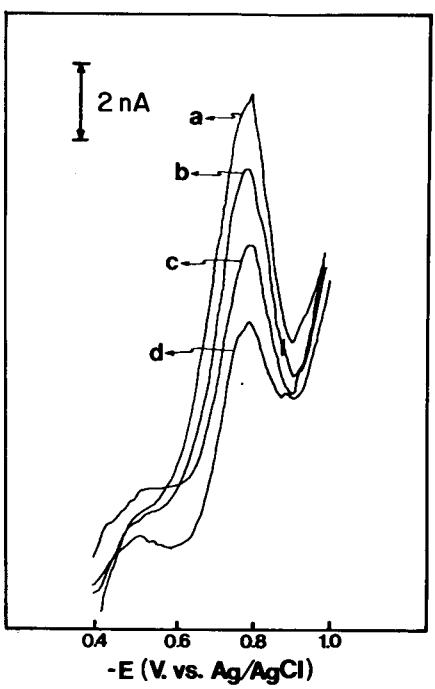


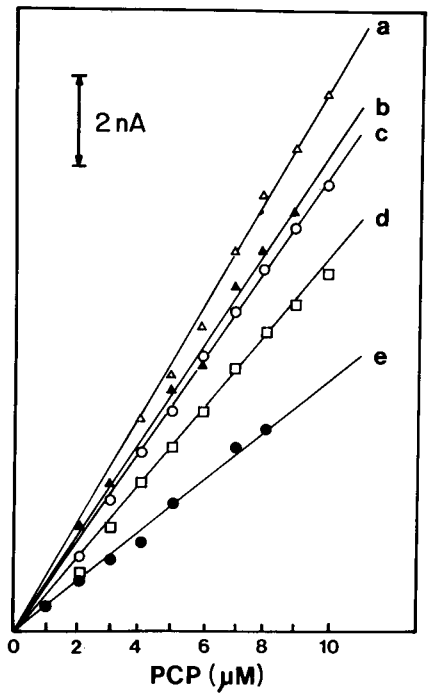


Fig. 1. Differential pulse polarograms of PCP at the DME in 0.01 M phosphate buffer pH 9.0: (a) 10 μM (b) 8 μM (c) 6 μM (d) 4 μM.

Fig. 2. The effects of pH on differential pulse polarograms of PCP in 0.01 M phosphate buffer at the DME. pH: (a) 11 (b) 8 (c) 10 (d) 9 and (e) 7.

TABLE 1

Data from the study of pentachlorophenol at the DME in 0.01 M phosphate buffer

| PCP used ($\times 10^{-6}$ M) | Current (nA) produced at | | | | |
|---|---|---|---|---|---|
| | pH 7 | pH 8 | pH 9 | pH 10 | pH 11 |
| 1 | 0.5 | 1.1 | — | 0.6 | 0.7 |
| 2 | 1.0 | 2.3 | 1.2 | 1.6 | 1.7 |
| 3 | 1.5 | 3.2 | 2.2 | 2.8 | 2.7 |
| 4 | 1.9 | 4.0 | 3.2 | 3.9 | 4.6 |
| 5 | 2.7 | 5.3 | 4.0 | 4.8 | 5.5 |
| 6 | 4.0 | 5.8 | 4.8 | 6.0 | 6.6 |
| 7 | 4.0 | 7.5 | 5.7 | 7.0 | 8.2 |
| 8 | 4.4 | 8.3 | 6.5 | 8.0 | 9.5 |
| 9 | — | 9.0 | 7.1 | 8.8 | 10.5 |
| 10 | — | — | 7.8 | 9.7 | 11.7 |
| $r^a$ | 0.983 | 0.997 | 0.864 | 0.999 | 0.999 |

[a]Correlation coefficient.

can be used for the direct determination of PCP down to 0.27 ppm in a pH 8 phosphate buffer system. Concentration-dependent voltammograms were obtained for $1—5 \times 10^{-6}$ M (0.27—1.33 ppm) of PCP in a 0.1 M phosphate buffer system. Figure 3 shows the well-defined peaks that were obtained.

Cyclic voltammetry was used for qualitative evaluation of the type of electrochemical reaction occurring and to study the reversibility of the PCP reaction. Figure 4 shows the region of interest in the cyclic voltammogram that was obtained at two scan rates on PCP at the HMDE. During the cathodic potential scan, a sharp and highly symmetrical peak was produced at —0.4 V and a broad peak appeared at ca. —0.8 V versus Ag/AgCl. Both of these peaks were coupled with their respective oxidation peaks during the anodic scan. The reduction peak at —0.4 V was separated from its oxidation peak by 25 mV and exhibited the typical adsorption—desorption behavior of a non-faradaic peak with its symmetrical shape about the peak potential and its decrease in prominence as the scan rate was increased [29]. The concentration-dependent peak of interest was at —0.8 V, and it exhibited behavior typical of a faradaic electron-transfer reaction. Neither of the current peaks for PCP was affected by starting the voltage scans at different points in the cycle.

Controlled-potential electrolysis was used to investigate the reduction products of PCP. At least two reports have indicated that PCP preferentially undergoes reductive dechlorination at the positions *ortho* and *para* to the phenol group [30, 31]. No reduction products of PCP could be detected by

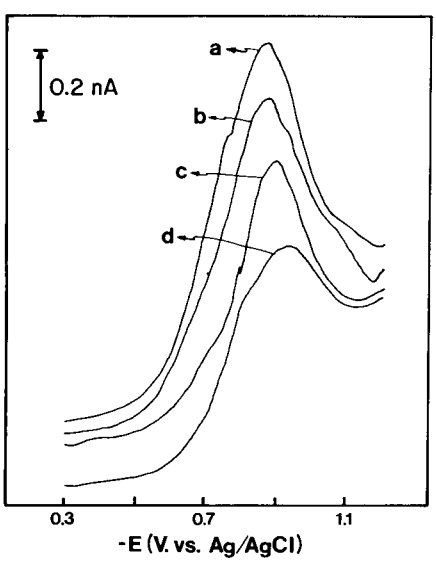


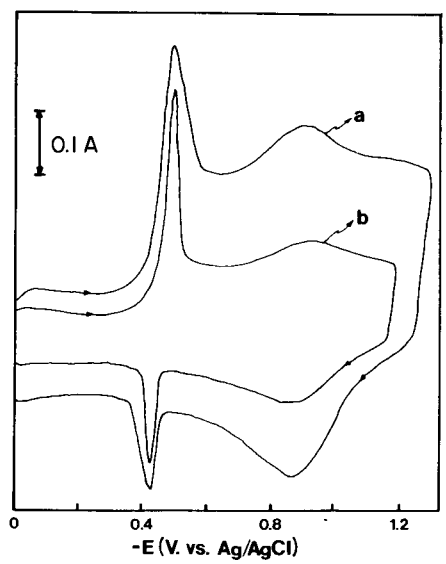


Fig. 3. Differential pulse voltammograms of PCP at the carbon paste electrode in 0.1 M phosphate buffer pH 8.0: (a) 5 $\mu$M (b) 4 $\mu$M (c) 2 $\mu$M and (d) 1 $\mu$M.

Fig. 4. Cyclic voltammograms of $0.5 \times 10^{-3}$ M PCP in 0.01 M phosphate buffer pH 10.0. Scan rate: (a) 0.5, (b) 0.2 V $s^{-1}$.

gas, infrared or thin-layer chromatographic techniques in the present work. This investigation did not elucidate the nature of the PCP reduction product(s). The surface of the mercury pool may have been passivated even with constant agitation, which prevented significant reduction of PCP.

REFERENCES


1 A. Bevenue and H. Beckman, Residue Rev., 19 (1967) 83.
2 J. E. Fountaine, P. B. Joshipura and P. N. Keliher, Water Res., 10 (1976) 185.
3 J. E. Fountaine, P. B. Joshipura, P. N. Keliher and J. D. Johnson, Anal. Chem., 47 (1975) 157.
4 J. E. Fountaine, P. B. Joshipura, P. N. Keliher and J. D. Johnson, Anal Chem., 46 (1974) 62.
5 D. R. Buhler, M. E. Rasmusson and H. S. Nakaue, Environ. Sci. Technol., 7 (1973) 929.
6 C. J. Goodnight, Ind. Eng. Chem., 34 (1942) 868.
7 E. C. Weinbach, Biochemistry, 43 (1957) 393.
8 J. Saarikoski and K. Kaila, Bull. Environ. Contam. Toxicol., 17 (1977) 40.
9 D. Gordon, Med. J. Aust., 43 (1956) 485.
10 H. Bergner, P. Constantinidis and J. H. Martin, Can. Med. Assoc. J., 92 (1965) 448.
11 J. B. Chapman and P. Robson, Lancet, 1 (1965) 1266.
12 A. M. Robson, J. M. Kissane, N. H. Elvick and L. Pundavela, J. Pediatr., 75 (1969) 309.
13 P. Smejtek, K. Hsu and W. H. Perman, Biophys. J., 16 (1976) 319.
14 M. Frei-Hausler, R. W. Frei and O. Hutzinger, J. Chromatogr., 84 (1973) 214.
15 A. S. Y. Chau and J. A. Coburn, J. Assoc. Off. Anal. Chem., 57 (1974) 389.
16 H. van Langeveld, J. Assoc. Off. Anal. Chem., 58 (1975) 19.
17 E. C. Villanueva, R. W. Jennings, V. W. Burse and R. D. Kimbrough, J. Agric. Food Chem., 23 (1975) 1089.
18 C. D. Chriswell, R. C. Chang and J. S. Fritz, Anal. Chem., 47 (1975) 1325.
19 W. Krijgsman and C. G. van de Kamp, J. Chromatogr., 131 (1977) 412.
20 Y. Mizunoya, Bunseki Kagaku, 11 (1962) 393: CA 59: 6999j.
21 E. A. Zemkin, V. M. Gorokhovskii, N. A. Kalinovskaya, G. L. Kogan and V. M. Cherepnev, Zh. Nauchn. Prikl. Fotogr. Kinematogr., 20 (1975) 44.
22 R. N. Adams, Electrochemistry at Solid Electrodes, M. Dekker, New York, 1969, pp. 280—283.
23 R. Hill, Modern Methods of Plant Analysis, Vol. 1, Springer-Verlag, New York (1956) 393.
24 The Aldrich Library of Infrared Spectra, 2nd edn.
25 H. J. Petrowitz, Fresenius Z. Anal. Chem., 230 (1967) 250.
26 R. Deters, Chem.-Ztg., 86 (1962) 388: CA 57: 14229a.
27 M. G. Zigler and W. F. Phillips, Environ. Sci. Technol., 1 (1967) 65.
28 J. R. Davies and S. T. Thuraisingham, J. Chromatogr., 35 (1968) 43.
29 E. Jacobsen and T. Rojahn, Anal. Chim. Acta, 61 (1972) 320.
30 A. Ide, Y. Niki, F. Sakamoto, I. Watanabe and H. Watanabe, Agric. Biol. Chem., 36 (1972) 1937.
31 K. Wedemeyer, W. Kiel and W. Evertz, German Patent Number 1,470,929 (April 1977).

*Analytica Chimica Acta*, 105 (1979) 99—107


# VOLTAMMETRIC DETERMINATION OF IRON(II) AND IRON(III) IN STANDARD ROCKS AND OTHER MATERIALS

W. MICHAEL MOORE*

*The Standard Oil Company (Ohio), 4440 Warrensville Center Road, Cleveland, Ohio 44128 (U.S.A.)*

(Received 24th July 1978)

SUMMARY

Voltammetry at a rotating platinum electrode in concentrated electrolyte solutions containing HCl and LiCl is described for simultaneous determinations of iron(II) and iron(III) in a variety of materials. Applications of the method to some U.S. Geological Survey standard rocks, a Georgian clay, and an iron-containing multiple vitamin tablet are described. For materials which can be dissolved without altering the original iron(II)/iron(III) ratio, this method enables the two valence states to be determined rapidly and simultaneously. The technique is precise (r.s.d. ≈ 2%) and relatively free from interference, and requires only a recording d.c. polarograph.

Since iron is the second most abundant metal in the earth's crust and is probably the most important industrial element [1], it has had a wide and varied analytical history. For many iron determinations, it is not important to know if the iron was originally present in the divalent or trivalent state. However, certain samples require differentiation and determination of both iron(II) and iron(III). Simultaneous determinations have been performed on a variety of materials, which include rocks [2, 3], minerals [3, 4], soils [5], iron ores [6], glasses [7], slags [8], and biological systems [9].

The distribution of iron(II) and iron(III) in silicate minerals has remained of active interest in geochemistry [10]. The recent trend in analytical geochemistry has been toward the use of rapid solid-state methods. Semiquantitative determinations of iron(II) and iron(III) have been reported with Mössbauer [11, 12] and electron microprobe [13] methods. The speciation of iron has remained almost exclusively a chemical problem, however, with the most precise data having been obtained by titrimetric procedures [10, 14—16].

Any instrumental technique which makes possible simultaneous independent determinations of iron(II) and iron(III) has obvious advantages over titrimetric and other chemical methods employing several time-consuming chemical steps and generally determining one of the iron species via a difference measurement.

*Present address: Sprague Electric Company, Research and Development Center, North Adams, Massachusetts 01247 (U.S.A.).

Pulse polarographic methods have seldom been used for simultaneous determinations of iron(II) and iron(III). Morris and Faulkner [17] recently outlined the difficulties encountered when normal pulse voltammetry is applied to electrochemically poised systems such as the Fe(III)/Fe(II) redox couple. Parry and Anderson [18] successfully employed a pulse polarographic method for determinations of iron(II) and iron(III) in process streams; however, their technique was based on the use of a supporting electrolyte (sodium pyrophosphate) in which the Fe(III)/Fe(II) couple exhibits the proper degree of irreversibility to permit simultaneous determinations. This method would not be generally suitable for the determination of iron oxidation states in complex mixtures.

In contrast to pulse polarographic techniques, direct current polarographic methods are well suited to simultaneous determinations of iron(II) and iron(III). Bien and Goldberg [4] determined Fe(II) and Fe(III) in decomposed refractory minerals by a d.c. polarographic technique in citrate medium. More recently, Beyer et al. [19] employed a polarographic procedure to determine iron(II) and iron(III) in rock standards from the U. S. Geological Survey. These workers decomposed rocks in a boiling mixture of hydrofluoric and sulfuric acids and obtained polarograms in concentrated oxalate solutions. The Fe(II)/Fe(III) ratio was obtained by conventional d.c. polarography while a.c. polarography was employed to determine the total iron content accurately.

The problem of measuring the distribution of iron oxidation states in some molybdate-containing solids arose in this laboratory. Polarography in oxalate solution was considered as an analytical possibility, but molybdenum(VI) undergoes a two-step reduction commencing near 0.0 V (vs. SCE) at a dropping mercury electrode which obscures the diffusion currents from the iron(II) and iron(III) oxalate complexes; the half-wave potential for the Fe(III)/Fe(II) redox couple occurs near −0.15 V vs. Ag/AgCl in oxalate solution [19]. In contrast, the half-wave potential for the Fe(III)/Fe(II) system is +0.3 to +0.4 V(vs. SCE) at a rotating platinum electrode (RPE) in HCl, which renders voltammetric determinations of iron(II) and iron(III) possible in the presence of a large excess of molybdenum(VI).

Although there are early descriptions of the voltammetric behavior of iron at platinum electrodes [20—22], this method has seldom been employed to determine iron(II) and iron(III) in geological, or other real-life samples. The goal of this study was to develop a voltammetric technique applicable to simultaneous determination which is accurate, relatively free from interference, and easily implemented.

## EXPERIMENTAL

### *Apparatus*

*Instrumentation.* A Princeton Applied Research Corporation (PAR) Model 170 Electrochemistry System was employed in the d.c. mode for recording

most voltammograms. For some determinations an equivalent system comprising a Bioanalytical Systems Model DCV-4 Voltammeter and Hewlett-Packard Model 7015A $X$—$Y$ Recorder was utilized.

*Cells.* Either standard (K0060) or water-jacketed (K0064) PAR polarographic cell bottoms were employed with a PAR cell top (K0066).

*Electrodes.* A hook-type rotating platinum electrode (EA 222) and synchronous rotator (EA 682) were used (Brinkmann Instruments); the rotator was operated at 900 r.p.m.

As described by Adams [23], electrode pretreatment is an important consideration in solid-electrode voltammetry. Platinization of the working electrode resulted in considerable improvement in the voltammograms obtained for iron-containing solutions. The platinum electrode was platinized by placing it in concentrated chromic acid solution for 5—10 min at ambient temperature, followed by cathodization at —0.1 V vs. SCE for 30 min. Figure 1 compares voltammograms obtained using rotating platinum electrodes with smooth and platinized surfaces.

The reference electrode was a saturated calomel electrode (SCE) and a platinum wire served as the auxiliary electrode. Both of these electrodes can be placed directly into the solution being analyzed.

*Chemicals*

Reagent-grade lithium chloride and hydrochloric acid were dissolved in deionized, doubly-distilled water to prepare electrolyte solutions.

Standardized solutions of iron(III) and iron(II) were prepared in dilute hydrochloric acid and used for calibration purposes. Purified iron wire (99.9%) was accurately weighed and dissolved in concentrated hydrochloric acid, and the resulting solution was boiled with dilute hydrogen peroxide and made up to volume to yield 0.101 M iron(III) solution. Iron(II) sulfate solution (0.0995 M) in dilute hydrochloric acid was standardized by titration in phosphoric acid medium with potassium dichromate titrant and diphenylamine as an indicator [24].

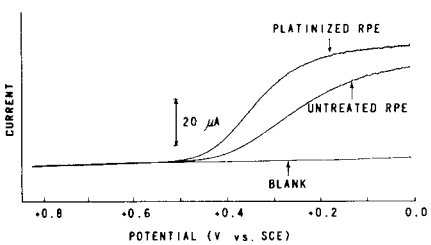


Fig. 1. Voltammograms for $0.5 \times 10^{-3}$ M Fe(III) in 1 M HCl—3 M LiCl solution obtained with platinized and untreated (smooth) rotating platinum electrodes. The potential scan rate was 10 mV $s^{-1}$.

*General voltammetric procedure*

After the electrode pretreatment procedure, place 10.00 ml of electrolyte solution into a cell properly fitted with electrodes. Electrolyte solutions are concentrated mixtures of HCl and LiCl; the exact electrolyte composition is variable and depends on the nature of sample being examined. Apply the initial potential (generally —0.1 V vs. SCE) to the rotating platinum electrode (RPE) and purge the solution with humidified argon while the resulting catnodic current decays to near zero. Then blanket the solution with argon (or nitrogen) and scan the applied potential in a positive direction at a rate of 10 mV $s^{-1}$ to record a background voltammogram. Record sample voltammograms in a similar fashion. If high-precision results are desired, record the voltammograms at 25 ± 0.1°C.

*Procedure for determination of iron(II) and iron(III) in standard rocks*

Place the rock samples in an oven at 120°C for 2 h and cool in a desiccator. Weigh a sample (about 250 mg) of the rock accurately and place in a platinum crucible. Place the crucible into a nitrogen-filled glove bag, add 5.0 ml of (1 + 1) sulfuric acid and 2.5 ml of 48% hydrofluoric acid, and place the crucible, with lid, on a hot plate for 10—12 min. The temperature of the hot plate should be sufficient to boil the solution, and vapors should be observed. After cooling to room temperature, remove the crucible from the glove bag and transfer the contents to a 50-ml volumetric flask. Wash the crucible several times with 0.1 M HCl and dilute to the mark with 0.1 M HCl.

Add a 5-ml aliquot of the dissolved rock solution to a thermostatted polarographic cell and deaerate for 5 min. Then add a 5.0-ml portion of a solution which is 4 M in HCl and 12 M in LiCl, and continue degassing for an additional 5 min to dissipate the heat of mixing. Next, start the synchronous rotator and apply a potential of —0.1 V vs. SCE to the RPE for 2 min to establish a constant current. Scan the potential at 10 mV $s^{-1}$ to +0.7 V to record the sample voltammogram. Measure the limiting currents for Fe(III) and Fe(II) at 0.0 and 0.6 V, respectively.

To record a background voltammogram, transfer 10.00 ml of a solution consisting of 1 M $H_2SO_4$, 2 M HCl, and 6 M LiCl to a clean polarographic cell and scan the applied potential from —0.1 to +0.7 V. Measure the background current at 0.0 and +0.6 V, and make the appropriate corrections in the limiting currents for the sample. Calibrate the system by adding aliquots of the iron(II) and iron(III) standards to the blank solution; perform a potential scan after each addition. Limiting currents for iron standards are measured at 0.0 V for iron(III) and +0.6 V for iron(II); each is corrected by subtracting the appropriate blank current.

## RESULTS AND DISCUSSION

*Electrolyte selection*

For successful performance of this voltammetric technique, the supporting electrolyte must meet two important criteria: (1) the Fe(III)/Fe(II) redox

couple must be well-behaved (not necessarily reversible); and (2) both oxidation states must exhibit reasonable chemical stability in the electrolyte medium.

The Fe(III)/Fe(II) couple exhibits marked irreversibility at the RPE in moderate concentrations (0.1—1.0 M) of the common mineral acids. The voltammetric behavior of iron was better in hydrochloric acid than in the other acids examined, and higher concentrations were therefore tested as the electrolyte. Reversible behavior for iron was achieved only in concentrated (12 M) HCl ($E_{1/2}$ = +0.190 V vs. SCE), but iron(II) was spontaneously oxidized in this medium. Electrochemical reversibility was also achieved in an electrolyte solution containing 4 M HCl and 12 M LiCl ($E_{1/2}$ = +0.287 V vs. SCE), and iron(II) was stable toward oxidation in this medium in the absence of oxygen (Fig. 2).

The chemical stability of the Fe(III)/Fe(II) system is greater in HCl—LiCl electrolytes which give some degree of electrochemical irreversibility. This point was illustrated by determinations of iron(II) and iron(III) in some solids, from which iron could be extracted by shaking with hydrochloric acid. When iron was extracted with an air-saturated solution consisting of 1 M HCl and 3 M LiCl, there was no iron(II) oxidation. When similar extractions were done with appreciably more concentrated HCl—LiCl electrolytes, however, iron(II) was oxidized by the dissolved oxygen present. The electrolytes employed for voltammetric experiments generally contained 1—2 M HCl and 3—6 M LiCl; the Fe(III)/Fe(II) couple was not strictly reversible in these systems, but voltammograms were still quite good and satisfactory chemical stability resulted.

*Calibration*

The diffusion currents were proportional to the concentrations of iron(II) and iron(III) in solution over reasonable ranges. When a potential scan rate of 10 mV $s^{-1}$ was employed with the RPE, the magnitudes of the limiting currents for iron(II) and iron(III) were strictly independent of each other.

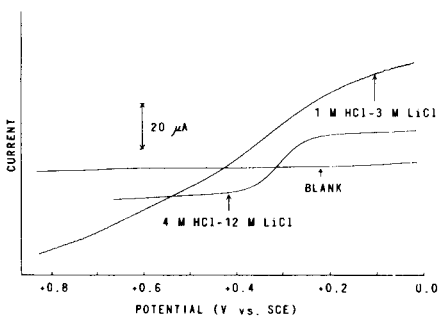


Fig. 2. Voltammograms obtained in separate solutions consisting of 1 M HCl—3 M LiCl and 4 M HCl—12 M LiCl, respectively. In each case, both Fe(II) and Fe(III) were 0.5 × $10^{-3}$ M and an untreated RPE was employed.

Excellent correlation coefficients resulted from linear regression analyses of limiting-current data for iron(II) and iron(III). For three typical calibrations with iron(II) and iron(III) standards for the approximate ranges $2.5 \times 10^{-4}$ M—$5.0 \times 10^{-3}$ M for both iron(II) and iron(III), respectively, the average correlation coefficients were 0.999956 for iron(II) and 0.999918 for iron(III). In addition, the slopes of the iron(II) and iron(III) calibration lines were almost equal; the iron(II) calibration slope was the larger, usually by about 2%.

*Results for standard rocks*

Powdered samples of U.S.G.S. standard rocks were analyzed for iron(II) and iron(III) by the procedure given in the Experimental section. Results of these determinations, along with published averages, are shown in Table 1. In general, the voltammetric results compared well with the published data. However, while the voltammetric values for iron(II) varied in a random fashion with respect to published averages, all the iron(III) values were slightly low. This discrepancy probably resulted from the complexation of iron(III) in solution by residual fluoride not volatilized during the rock decomposition step. Slightly improved results should be possible through more efficient removal of fluoride.

Typical voltammograms obtained for rock standards are shown in Fig. 3.

*Precision and sensitivity*

The results for U.S.G.S. standard rocks (Table 1) were obtained from five separate determinations; the relative standard deviations ranged between 0.5 and 2.6%. To examine the precision possible with the basic voltammetric method (minus sample preparation), replicate measurements of $1.0 \times 10^{-3}$M iron(III) were done. In each case, a blank was scanned, followed by a 50-$\mu$l addition of standard to 5.0 ml of electrolyte. The average blank-corrected limiting current for five trials was 66.5 $\mu$A and the standard deviation was 1.31 $\mu$A (r.s.d. 2.0%). Thus, if any relative standard deviation significantly larger than 2% is obtained, difficulties with preliminary chemical steps should be suspected.

TABLE 1

Weight percentages of iron(II) and iron(III) in U.S.G.S. standard rocks by voltammetry

| U.S.G.S. standard (Split/position) | Voltammetric results (±s.d.; n = 5) | | Published averages[a] | |
|---|---|---|---|---|
| | Fe(II) | Fe(III) | Fe(II) | Fe(III) |
| GSP-1 (84/18) | 1.82 ± 0.034 | 1.16 ± 0.018 | 1.80 | 1.24 |
| AGV-1 (78/28) | 1.65 ± 0.010 | 3.04 ± 0.078 | 1.59 | 3.15 |
| G-2 (17/14) | 1.04 ± 0.006 | 0.71 ± 0.010 | 1.13 | 0.76 |

[a]Taken from reference [19].

Since the method is based on d.c. voltammetry, the sensitivity is not excellent. The uncertainty in measuring and correcting limiting currents for background was generally about 1 $\mu$A. To obtain a reasonable signal/noise ratio, a minimum limiting current of about 10 $\mu$A should be obtained. With a platinized RPE in 1 M HCl—3 M LiCl electrolyte, a concentration of about $10^{-4}$ M iron(II) or iron(III) was generally needed to attain this level.

*Miscellaneous applications*

The present method was employed to examine the distribution of iron oxidation states in a multiple vitamin tablet containing iron, and in a Georgian clay sample.

One tablet was pulverized and the iron extracted by shaking for 2 h with a 25-ml portion of 0.1 M HCl; a 1.0-ml aliquot of this solution was added to 9.0 ml of 4 M HCl—12 M LiCl supporting electrolyte, and a voltammogram obtained. A concentrated electrolyte solution was required to obtain workable voltammograms with the vitamin extract, possibly because competition existed for complexation of iron between chloride ion and one or more components in the tablet.

A voltammogram obtained with the vitamin extract is shown in Fig. 4; obviously the iron in the tablet was almost entirely present as iron(II). The stated content was 18 mg of ferrous iron (as fumarate) per tablet. The limiting current obtained for iron(II) was initially near that expected for 18 mg of iron, but exact determinations were not attempted because the limiting current plateau decreased slightly on successive scans. It seems probable that some component of the complex sample adsorbed on the RPE, resulting in a decrease in effective electrode surface area. The problem was not studied further.

The iron(II) and iron(III) contents of a sample of Georgian clay were determined. The procedure was similar to that outlined for iron determinations in standard rocks, except that 75 mg of sample was employed. Duplicate determinations gave averages of 7.1% Fe(III) and 0.35% Fe(II) in the clay sample (Fig. 5). A large proportion of iron(III) was, of course, expected. The total iron in this specimen was found to be 8.0% by x-ray fluorescence analysis of the solid material; this result is in fairly good agreement with the total amount of iron (7.45%) determined by voltammetry.

*Interference*

The relatively successful determinations of iron(II) and iron(III) in such complex mixtures as soil, rocks, and a vitamin tablet suggest that the technique is not subject to much interference.

Interference can be chemical or electrochemical in nature. Unless proper care is taken, oxygen can interfere by oxidizing iron(II). Any substances which react at the platinum electrode at potentials more positive than 0.0 V vs. SCE will interfere. Fortunately, most metal cations are reduced at potentials which are significantly more negative than that of the Fe(III)/Fe(II) redox system and do not, therefore, interfere with this determination of iron(II) and

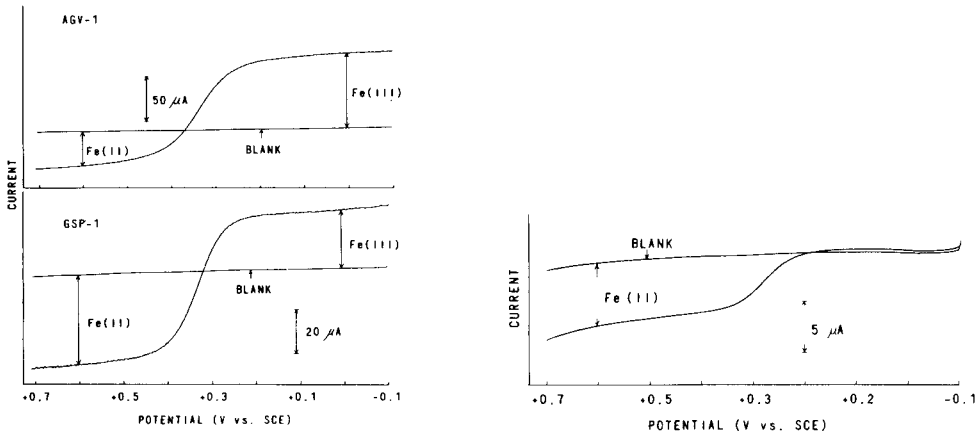


Fig. 3. Typical voltammograms obtained with dissolved rock standards. The supporting electrolyte was 2 M HCl—6 M LiCl.

Fig. 4. Voltammograms obtained for an iron-containing multiple vitamin tablet in a 4 M HCl—12 M LiCl electrolyte solution.

iron(III). No attempt is made here to enumerate all the possible interferences; however, an example is included of how a chemical interference was overcome by an adjustment of electrolyte concentration.

Determinations of iron(II) and iron(III) in solutions containing excess of molybdenum(VI) were required. In an electrolyte solution comprising 4 M HCl and 12 M LiCl, iron(II) is rapidly oxidized by molybdenum(VI). This was established when the addition of aliquots of standard iron(II) solution to the polarographic cell produced increasingly large limiting currents from iron(III). However, when the concentration of supporting electrolyte was reduced to 1 M HCl and 3 M LiCl, repeated voltammograms showed that iron(II was no longer oxidized by molybdenum(VI) and simultaneous determinations of the oxidation states of iron became feasible.

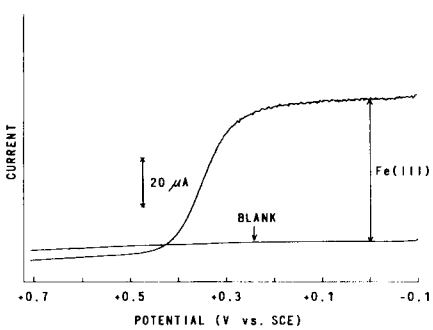


Fig. 5. Voltammograms obtained with a decomposed Georgian clay sample in a 2 M HCl—6 M LiCl electrolyte.

The extreme dependence of the chemical reaction between molybdenum(VI) and iron(II) upon the concentrations of HCl and LiCl may appear perplexing. However, Rao and Sagi [25] reported similar behavior for this redox reaction in phosphoric acid. The Fe(III)/Fe(II) couple has a higher formal potential than the Mo(VI)/Mo(V) couple in phosphoric acid solutions up to a concentration of 5.8 M, beyond which it is lower. When the phosphoric acid concentration is greater than 11.0 M, the difference in formal potentials is sufficiently great to enable molybdenum(VI) to oxidize iron(II) rapidly. A similar reversal in the magnitudes of the redox potentials for the Fe(III)/Fe(II) and Mo(VI)/Mo(V) couples probably occurs in solutions containing HCl and LiCl, resulting in the observed chemical behavior.

*Conclusion*

The results reported above suggest that this voltammetric method should be applicable to determinations of iron(II) and iron(III) in a wide variety of materials. Naturally, sample preparation must be such that the original distribution of oxidation states is not appreciably altered prior to the voltammetric determination. If this can be done, the method is fast and relatively free from interference.

REFERENCES


1 W. E. Harris and B. Kratochvil, Chemical Separations and Measurements, Saunders, Philadelphia, 1974, p. 77.
2 D. Whitehead and S. A. Malik, Anal. Chem., 47 (1975) 554.
3 C. V. Clemency and A. F. Hagner, Anal. Chem., 33 (1961) 888.
4 G. S. Bien and E. D. Goldberg, Anal. Chem., 28 (1956) 97.
5 C. G. Dodd and D. J. Kaup, Clay Miner. Bull., 5 (1963) 290.
6 Y. Okura, Bunseki Kagaku, 9 (1960) 845.
7 U. Abed, Anal. Chim. Acta, 47 (1969) 495.
8 R. L. Altman, Anal. Chim. Acta, 63 (1973) 129.
9 R. L. Chaney, J. C. Brown, and L. O. Tiffin, Plant Physiol., 50 (1972) 208.
10 E. Kiss, Anal. Chim. Acta, 89 (1977) 303.
11 R. K. Puri, Indian J. Pure Appl. Phys., 10 (1972) 841.
12 T. Yoshioka, Y. Goshi, and H. Kohno, Anal. Chem., 40 (1968) 603.
13 A. L. Albee and A. A. Chodos, Am. Mineral., 55 (1970) 491.
14 L. E. Reichen and J. J. Fahey, U.S. Geol. Surv. Bull., No. 1144-B (1962).
15 H. N. S. Schafer, Analyst, 91 (1966) 755.
16 R. Meyrowitz, Anal. Chem., 42 (1970) 1110.
17 J. L. Morris, Jr. and L. R. Faulkner, Anal. Chem., 49 (1977) 489.
18 E. P. Parry and D. R. Anderson, Anal. Chem., 45 (1973) 458.
19 M. E. Beyer, A. M. Bond, and R. J. W. McLaughlin, Anal. Chem., 47 (1975) 479.
20 H. A Laitinen and I. M. Kolthoff, J. Phys. Chem., 45 (1941) 1061.
21 H. A. Laitinen and I. M. Kolthoff, J. Phys. Chem., 45 (1941) 1079.
22 I. M. Kolthoff and E. R. Nightingale, Jr., Anal. Chim. Acta, 17 (1957) 329.
23 R. N. Adams, Electrochemistry at Solid Electrodes, Dekker, New York, 1969, pp. 206.
24 L. M. Melnick, in I. M. Kolthoff and P. J. Elving (Eds.), Treatise on Analytical Chemistry, Part II, Vol. 2, Interscience, New York, 1962, pp. 293.
25 G. G. Rao and S. R. Sagi, Talanta, 10 (1962) 169.

*Analytica Chimica Acta*, 105 (1979) 109—117


# AN ELECTROCHEMICAL DETECTOR WITH A DROPPING MERCURY ELECTRODE FOR HIGH-PERFORMANCE LIQUID CHROMATOGRAPHY

L. MICHEL and A. ZATKA

*Analytical Laboratories, Sandoz Ltd., Basle (Switzerland)*

(Received 17th July 1978)

SUMMARY

The electrochemical flow-through cell described has an active volume of less than 1 μl, and incorporates a dropping mercury electrode with drop times of about 0.05 s. Its performance as a detector for high-performance liquid chromatography is assessed for *p*-nitrophenol and nitrobenzene. The detection limits are 4—5 ng; the relative standard deviation of the peak height is better than 5% for the range 5—150 ng. The dependence of the response on flow rate, mercury pressure and drop time is described.

Electrochemical cells have long been examined as detectors in liquid chromatography because of their inherent sensitivity, simple construction, low cost and easily controlled selectivity. Drake [1] was the first to describe a polarographic cell as a detector for chromatographic effluents. Much work has been done by Kemula and his coworkers in the field of chromatopolarography, as they called this combination of methods [2, 3]. Various authors [4—7] have tried to construct polarographic cells for monitoring high-performance liquid chromatographic (h.p.l.c.) effluents. In newer reviews, the dropping mercury electrode (DME) is dismissed as an "awkward device, trying the patience of chromatographers" [8], and other electrode materials, particularly carbon paste [9] and glassy carbon [10] have been preferred. Glassy carbon has certainly some advantages; however, the DME remains unrivalled in its cathodic range and constantly renewed surface, which eliminates all problems arising from surface passivation at high concentrations.

The main reason for abandoning the DME lies in the dropping process, which causes high noise levels, and does not allow a reduction in cell volume corresponding to the needs of modern h.p.l.c. [11]. The rapidly dropping horizontal capillary [12] has not been mentioned in connection with h.p.l.c. Hartmann and Budan [13] as well as Mairanovskii et al. [14] found that a solid body (glass filament or spatula) situated against the capillary orifice of the DME causes a remarkable reduction in the drop time. This innovation has received little attention, being overshadowed by the development of pulse techniques. However, combination of the horizontal Smoler capillary [15] with a solid body makes it possible to construct a polarographic cell with a

very short drop time and a very small working volume. The design and performance of this cell are described below.

## EXPERIMENTAL

### *Preliminary tests*

The fundamental properties of the horizontal capillary in contact with a glass rod were studied by using a titration vessel (Karl Fischer vessel, Metrohm EA 965) with a side neck, through which the capillary was introduced via a rubber stopper. A glass rod (spatula) was held in one of the necks of the plastic lid (Metrohm EA 874). The curves were recorded on a Polarecord (Metrohm E 261 R).

The drop time of the capillary in the flow-through cell was measured by recording $i/t$ curves at constant potential on the Electrochemical System PAR 170 (Princeton Applied Research) with a fast time base (100 ms/in.). Though the recorder system is too slow to draw the wave form correctly, the number of waves per second can easily be measured.

### *The flow-through cell*

The cell, shown schematically in Fig. 1, is made of acrylic plastic (Plexiglas). The polarographic capillary (1; 4 mm o.d.; Metrohm EA 671) passes horizontally through bolt (2). The effluent from the chromatographic column is introduced via a metal capillary (3; 1.3 mm o.d.) held by a standard plastic fitting (4) (Altex), and flows downwards through the vertical channel. Against the DME, and in the same axis, is mounted a piston (5) with a slightly convex, highly polished surface. This piston moves in bolt (6) and its distance from the capillary orifice is regulated by adjusting a fine screw (7). The mercury capillary, the solution inlet tube and the piston are sealed by rubber O-rings (8, 9 and 10). Just below the DME is drilled a slightly inclined side-channel (11), into which the salt bridge of the anode is introduced (Ag/AgCl reference electrode with a plastic bridge and glass frit diaphragm; Metrohm EA 428).

Transparent acrylic resin is a very convenient material for experiments where the function of the DME must be visually controlled; however, it is

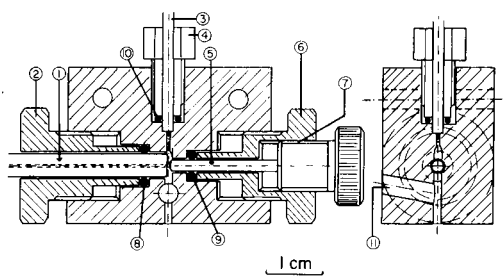


Fig. 1. The flow-through cell with piston.

attacked by many of the nonaqueous solvents used in h.p.l.c. An identical cell was therefore made from PTFE (Teflon). With a small sacrifice of noise because of the impossibility of ideal adjustment, a much wider field of application resulted.

Another version of the cell is shown in Fig. 2. The cell body is again made of PTFE, but instead of a piston, a round glass plate (1) is used. This is sealed by an O-ring (2), and held in place by a metallic ring (3). The effluent channel consists simply of a groove in the surface opposite the glass plate. As the position of the glass plate is fixed, the capillary must be moved to adjust the distance from the plate. A fine motion in the direction of the axis without turning the capillary is achieved by a screw mechanism (4). The inlet tube and the auxiliary electrode are the same as in the preceding case. The performances of these cells are almost identical; because of the materials used, the second cell is also useful for nonaqueous solutions.

*The electrical circuit*

A simple d.c. measurement at constant potential usually gives the best results [8, 16]. The detector works on the limiting current plateau and the half-wave potentials are not used for identification, so that precise potential control is unnecessary, and the simple circuit shown in Fig. 3 is quite satisfactory. On the potentiometer R1, the desired voltage is adjusted and checked with voltmeter V. The cell current is measured as a voltage on resistance R2, and recorded on a potentiometric recorder (Philips PM 8100). The chain R3—R4 serves to suppress the background current so that the maximum sensitivity of the recorder (1 mV full scale) can be used. A capacitor C is used to damp current oscillations, and shielded leads are used.

*The chromatographic system*

The chromatographic system consisted of a Haskel pump (Model 26 920,

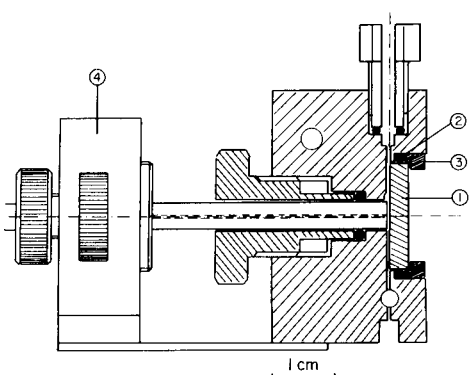


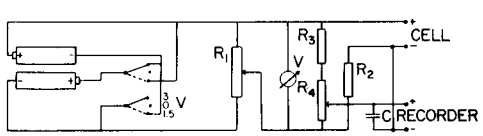


Fig. 2. The flow-through cell with plate.

Fig. 3. The measuring circuit. $R_1 = 50\ K\Omega$, $R_2 = 20\ K\Omega$, $R_3 = 0.5\ M\Omega$, $R_4 = 10\ K\Omega$, $C = 20\ \mu F$.

pressure amplification 1:23) driven by cylinder nitrogen, a Chromatronix injection system with a 20-$\mu$l loop, and a stainless steel column (4 mm i.d., 10 cm long) filled with Nucleosil C18 (10 $\mu$m). A Nucleosil C18 precolumn of the same size was used to remove impurities from the solvent stream. The Haskel pump was later replaced by an Altex pump, Model 110, equipped with a Pye-Unicam damping unit. A Perkin-Elmer u.v. detector (Model 087-306; 254 nm) was used in some experiments prior to the polarographic detector.

*Deaeration system*

As oxygen is reduced at the mercury electrode, it must be removed from the eluant. Two deaeration systems were used. With the Haskel pump, bubbling with pure nitrogen was used; the eluant was first filtered through a glass frit (G2); through the same filter plate, nitrogen (99.999%) presaturated with the solution in a wash bottle, was then introduced for 1 h. Vacuum was then applied for 10 min and the solution was transferred to the pump reservoir by gentle nitrogen pressure. A slow stream of nitrogen was kept flowing over the surface of the solution in the reservoir. The whole system was built of glass with ground ball joints.

With the Altex pump, deaeration was done by boiling. The metallic inlet tubing of the pump with filter was introduced through the central neck into a three-neck round-bottom flask and sealed with a rubber stopper. One of the side necks was equipped with a reflux cooler, and the other with a thermometer. This system is much simpler; there are no solvent losses and vacuum application is unnecessary. The boiling liquid can be pumped directly, as it cools sufficiently in the inlet line (30 cm) before entering the pump.

The injected samples were deaerated directly in the syringe, as described below.

*Chemicals*

For the preliminary tests, a $4 \times 10^{-4}$ M solution of $Cd^{2+}$ in aqueous 0.1 M KCl was used. For the chromatographic tests, the eluant was Britton—Robinson universal buffer solution of pH 3.8 diluted with methanol (1:1). The final apparent pH was 4.5. *p*-Nitrophenol and nitrobenzene (analytical grade; Merck) were used as test substances. The stock solutions contained 0.14 mg of *p*-nitrophenol and 0.16 mg of nitrobenzene per ml. From these solutions, 1—50-$\mu$l aliquots were measured with a Terumo microsyringe and diluted in a 1-ml glass syringe, in which they were mixed and deaerated by a gentle stream of nitrogen, introduced through a long injection needle. This 1-ml syringe was then used for repeated injections into the 20-$\mu$l loop of the injection system.

For the determination of the upper limit of the dynamic range, more concentrated solutions (10 mg $ml^{-1}$) were used.

## RESULTS AND DISCUSSION

*Horizontal capillary with rod*

The functioning of the horizontal capillary in combination with the piston

or plate was tested with the cadmium solution. Curves obtained with the classical vertical position of the capillary, the freely dropping horizontal capillary and the horizontal capillary with the glass piston or plate were compared for two different capillaries. The results are shown in Table 1. With the glass rod, the current oscillations are essentially invisible even at zero damping of the Polarecord. The curves are identical whether a slow (5.5 mV $s^{-1}$) or fast (33.3 mV $s^{-1}$) scan rate was used. Even the classical RC-derivative circuit may be used with fast scan rates and without damping; a peak of 218 mm (1.09 $\mu$A) with visible oscillations less than 1 mm (5 nA) was obtained under the conditions of test no. 7 with this equipment.

*The flow-through cell as detector for h.p.l.c.*

In the h.p.l.c. system described, a series of 30 chromatograms with varying quantities of *p*-nitrophenol (2.9—144 ng) and nitrobenzene (3.2—160 ng) was run at a flow rate of 0.3 ml $min^{-1}$. The peak heights were measured and evaluated by regression analysis. The results are shown in Table 2. With higher quantities (0.23—4.6 $\mu$g) at correspondingly reduced sensitivity, the standard deviation decreased to 1.6% and the linear correlation coefficient was 0.999. The quantities injected were then increased until the limit of the linear range was reached (final line, Table 2).

The long term drift (8-h test) was found to be 30 $\mu$V $h^{-1}$, i.e. 1.5 $\mu$A $h^{-1}$. This is caused predominantly by variations in the oxygen content of the eluant.

*Influence of eluant flow rate*

This effect was studied by two methods. Direct injection into the detector was first used, the volume injected being so large (1—2 ml) that a signal plateau resulted. The influence of peak-enlarging effects of the chromatographic system was thus eliminated, and only the effect of the flow rate on the electrochemical yield was measured (Fig. 4).

TABLE 1

Comparison of the performance of two capillaries in vertical and horizontal positions without and with rod or plate
($4 \times 10^{-4}$ M $Cd^{2+}$ in 0.1 M KCl deaerated by nitrogen)

| Test No. | Capillary[a] | Rod | Drop time (s) | Signal (mm) | Oscillations (mm) | Damping | Signal/Noise |
|---|---|---|---|---|---|---|---|
| 1 | 1 V | no | 1.77 | 87 | 10 | 5 | 8.7 |
| 2 | 2 V | no | 2.08 | 116.5 | 22 | 5 | 5.3 |
| 3 | 1 H | no | 0.7 | 66 | 5 | 5 | 13.2 |
| 4 | 2 H | no | 0.54 | 93 | 2.2 | 5 | 42.3 |
| 5 | 1 H | yes | 0.1 | 32 | 0.8 | 4 | 40 |
| 6 | 1 H | yes | 0.07 | 32 | 0.2[b] | 0 | 160 |
| 7 | 2 H | yes | 0.06 | 51 | 0.2[b] | 0 | 255 |

[a]V and H indicate the vertical and horizontal positions of the capillaries.
[b]Line width.

TABLE 2

Characteristics of the polarographic detector determined by chromatographic analysis for *p*-nitrophenol and nitrobenzene
(Peak heights as a function of concentration)

| Parameter | *p*-Nitrophenol | Nitrobenzene |
|---|---|---|
| Sensitivity (mV $\mu g^{-1}$) | 2.29 | 2.31 |
| Detection limit (ng) | 4.4 | 4.4 |
| Detector noise ($\mu V$) | 5 | 5 |
| Linear correlation coefficient | 0.9985 | 0.9986 |
| Standard deviation (%) (5—150 ng) | 4.1 | 4.5 |
| Upper limit of linear range (ng) | 8000 | 24000 |

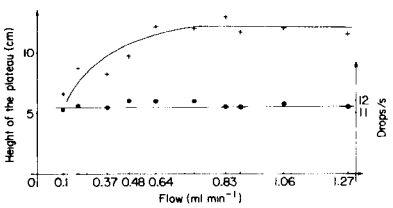


Fig. 4. The influence of flow-rate on the electrochemical signal (without chromatographic system) for an injected volume of 1.8 ml: (+) height of the plateau; (•) mercury drop rate.

Measurements were then made with the chromatographic system with the u.v. and electrochemical detectors in series. Various eluant flow rates were used for injections (20 $\mu$l) of 4.6 $\mu$g of *p*-nitrophenol and the u.v. and polarographic signals were recorded simultaneously on a two-channel recorder (Fig. 5). The ratios of the u.v. and electrochemical signals (peak heights and peak areas) were calculated and plotted against the flow rate (Fig. 6). In this way, the variations in the peak heights or areas caused by the chromatographic systems alone were eliminated. In Fig. 4 a decrease in signal is observed at flow rates below about 0.6 ml $min^{-1}$. Figures 4 and 6 show a plateau above these flow rates. The scatter of the signals increases with the flow rate. These results indicate that optimum conditions are reached at a flow rate of 0.5—0.6 ml $min^{-1}$.

*Influence of mercury pressure and drop time*

A single solution containing both test substances (86 ng of *p*-nitrophenol and 96 ng of nitrobenzene) was injected at various mercury column heights. The background current was compensated and read as voltage on the dial of the 14-turn potentiometer R4. The results are shown in Fig. 7. The background signal is with good confidence ($r$ = 0.998) proportional to the column height, showing that the background current is mostly the charging current of the mercury electrode. Its noise is lower than $\pm 5$ $\mu$V.

For *p*-nitrophenol, the exponent of $h$ was calculated to be 0.503, which

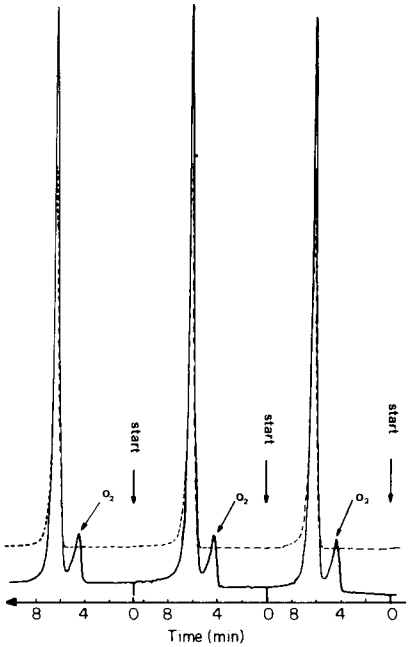


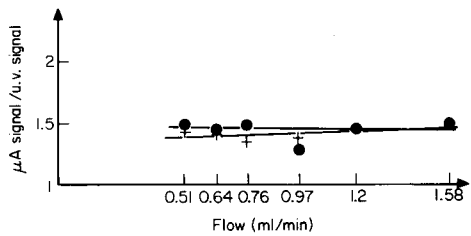


Fig. 5. U.v. and electrochemical detection of 4.6 μg of *p*-nitrophenol after h.p.l.c. (——) Electrochemical detection (10 mV full scale); (-----) U.v. detection at 254 nm (0.1 absorbance units full scale). (The samples were not deoxygenated before injection.)

Fig. 6. Influence of the flow rate on the electrochemical signal and comparison with the u.v. signal after h.p.l.c. (+) Ratio of areas of the electrochemical and u.v. peaks; (•) ratio of heights of the electrochemical and u.v. peaks.

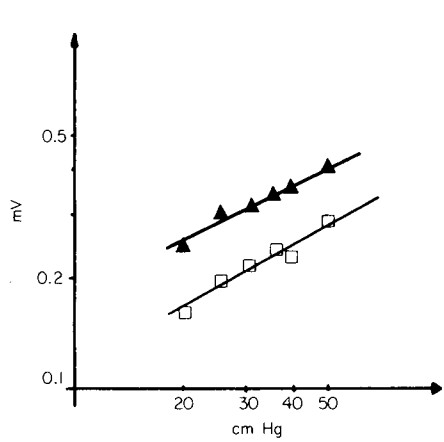


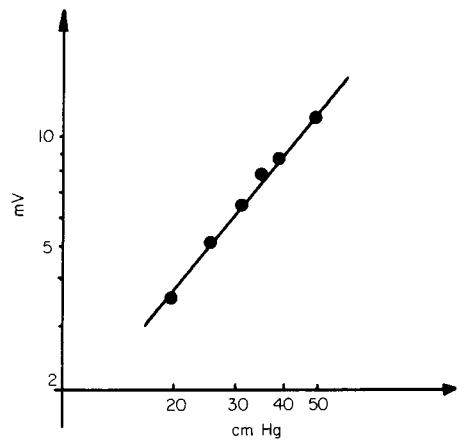


Fig. 7. The peak currents and the background current in relation to the mercury column height. (•) Background current; (▲) *p*-nitrophenol; (□) nitrobenzene.

corresponds very closely to the theoretical value for the diffusion-controlled process at a freely dropping electrode (0.500). For nitrobenzene a slightly higher value (0.575) was found. These results indicate that even under the circumstances of the chromatographic system, it is a diffusion process that controls the transport to the electrode surface.

The drop time at constant column height can be altered by varying the distance between the capillary orifice and the piston. Precise optical measurements of this distance were impossible because of optical imperfections of the system, and the drop time was measured by recording *i/t* curves as described under Experimental. Two solutions containing both components (*p*-nitrophenol and nitrobenzene) at different concentrations were used. The background current was compensated to a steady level and its magnitude read on the potentiometer dial. The results are shown in Fig. 8. The peak currents increase with drop time while the background current decreases. It is the increasing base-line noise which sets limits to the use of longer drop times. The best compromise between sensitivity and base-line noise is reached at drop times of about 0.05—0.06 s, which corresponds to a distance between the piston and the capillary orifice of approximately 70 $\mu$m, as estimated by microscopic observation. The active cell volume is then about 0.3 $\mu$l. The rinse volume is of course greater, but experiments with u.v. and electrochemical detectors in series have shown no enlargement of the peak even at the maximum drop time used, i.e. about 0.1 s, so that the rinse volume of the electrochemical cell is notably smaller than that of the preceding u.v. cell.

*Conclusion*

The polarographic cell should be suitable as an h.p.l.c. detector for all

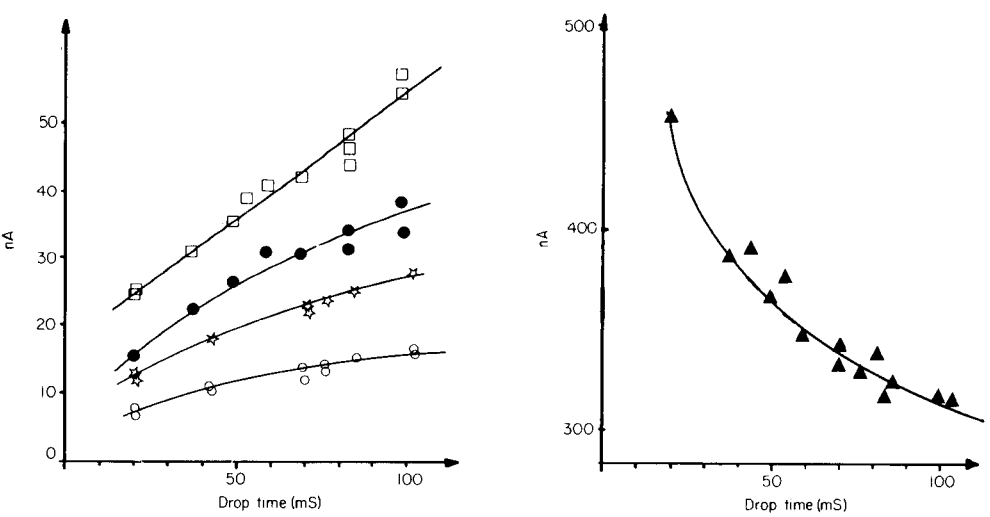


Fig. 8. The peak currents and background current in relation to the drop time. (○) 159 ng of nitrobenzene; (☆) 144 ng of *p*-nitrophenol; (●) 255 ng of nitrobenzene; (□) 230 ng of *p*-nitrophenol; (▲) background current.

substances reducible at the mercury electrode. The sensitivity, which depends on the number of electrons involved in the electrode reaction and the elution system used, can be defined only for a particular system in the same way as for u.v. detectors. The construction is very simple, and the costs are considerably lower than those of other h.p.l.c. detectors. Operation and maintenance of the cell are very easy and do not require special electrochemical knowledge.

The very small cell volume makes it particularly interesting for use with short columns and for miniaturized h.p.l.c. systems.

REFERENCES

1 B. Drake, Acta Chem. Scand., 4 (1950) 554.
2 W. Kemula, Roczniki Chem., 26 (1952) 281.
3 W. Kemula, Pure Appl. Chem., 25 (1971) 763.
4 J. G. Koen, J. F. K. Huber, H. Poppe and G. den Boef, J. Chromatogr. Sci., 8 (1970) 192.
5 R. Stillman and T. S. Ma, Mikrochim. Acta, 32 (1973) 49.
6 B. Fleet and G. G. Little, J. Chromatogr. Sci., 12 (1974) 747.
7 T. Wasa and S. Musha, Bull. Chem. Soc. Jpn., 48 (1975) 2176.
8 P. T. Kissinger, Anal. Chem., 49 (1977) 447A.
9 L. J. Felice, W. P. King and P. T. Kissinger, J. Agric. Food Chem., 24 (1976) 380.
10 J. Lankelma and H. Poppe, J. Chromatogr., 125 (1976) 375.
11 G. Schomburg, Fresenius Z. Anal. Chem., 277 (1975) 275.
12 E. Scarano, M. G. Bonicelli and M. Forina, Anal. Chem., 42 (1970) 1470.
13 H. Hartmann and G. Budan, Chem. Ztg., 74 (1950) 606.
14 S. G. Mairanovskii, N. V. Barashkova and Yu. B. Vol'kenshtein, Elektrokhimiya, 1 (1965) 72.
15 I. Smoler, Collect. Czech. Chem. Commun., 19 (1954) 238.
16 D. G. Schwartzfager, Anal. Chem., 48 (1976) 2189.

*Analytica Chimica Acta*, 105 (1979) 119—128


# ANALYSIS FOR POLYNUCLEAR AROMATIC HYDROCARBONS IN WORKING ATMOSPHERES BY COMPUTERIZED GAS CHROMATOGRAPHY-MASS SPECTROMETRY†

ALF BJØRSETH*

*Central Institute for Industrial Research, Blindern, Oslo 3 (Norway)*

GÖRAN EKLUND

*Department of Analytical Chemistry, University of Gothenburg, Fack, S-402 20 Göteborg (Sweden)*

(Received 6th July 1978)

SUMMARY

Polynuclear aromatic hydrocarbons in particulate matter from working atmospheres have been analyzed by a glass capillary gas chromatography—mass spectrometer—computer system which has high separation efficiency and is capable of separating and identifying these complex mixtures. More than one hundred polynuclear aromatic hydrocarbons have been identified in samples from a coke plant and an aluminum smelter, including both pure polycyclic aromatic hydrocarbons and compounds where a CH-group is substituted with the hetero atoms oxygen, nitrogen, or sulfur. The occurrence of polynuclear aromatic hydrocarbons in working atmospheres is compared to that in ambient air and emissions from other sources.

Polynuclear aromatic hydrocarbons (PNA) are prevalent environmental contaminants [1], and are suspected to be human carcinogens [2]. They are present in tar, pitch and oils or are formed by imperfect combustion of carbonaceous materials, e.g. wood, coal, oil [1]. Exposure to such PNA-containing materials as soots, tars and oils may cause occupational cancer [3].

There are several reasons why a complete characterization of the PNA in a sample requires an analytical system with high resolution and sensitivity. The formation of PNA usually takes place by a large number of high-temperature reactions; the resulting mixture of PNA is complex. Furthermore, the carcinogenic activity of a particular compound depends on its structure. Molecular shape, size, electronic and steric factors all seem to be important. For example, the addition of alkyl substituents at different positions in the ring of certain polycyclic aromatic hydrocarbons (PAH) can have an activating or deactivating influence [4, 5]. Similarly, the substitu-

†This work is part of a joint Norwegian project on "Polycyclic aromatic hydrocarbons in the work environment" between the Institute of Occupational Health, The Engineering Research Foundation at the Technical University of Norway, and the Central Institute for Industrial Research.

tion of a CH-group with a hetero atom may increase or decrease the carcinogenic activity of a particular compound [6, 7]. These considerations indicate that complete information on the individual compounds must be included in studies concerning PNA in the working atmosphere in order to evaluate the potential occupational hazard.

PAH have previously been studied in great detail in ambient air [8], automobile exhaust gases [9] and oil-based domestic heating ovens [10]. In these cases the technique of gas chromatography/mass spectrometry (g.c.-m.s.) has been utilized. Less is known about PAH in working atmospheres. The methods used for analyzing PNA in the working environment include determination of Benzene-Soluble Matter, g.c. and u.v. spectroscopic methods, and the selective detection of benzo(a)-pyrene (BaP) [11—13]. However, most of the methods used for monitoring PAH in working atmospheres give limited information about the complex composition of the PAH fraction.

Recently, glass-capillary gas chromatography (g.c.$^2$) has been used in the determination of PAH in working atmospheres [14, 15]. These studies demonstrated the multiplicity of the components present in working atmospheres in aluminum and coke plants. Many of the compounds have not yet been identified, mainly because of a lack of analytical tools for the identification of minor components in the complex mixtures.

Glass-capillary gas chromatographs coupled with computerized mass spectrometers compose a sophisticated analytical system. The g.c.$^2$-m.s.-computer system provides both quantitative and qualitative data as well as the capacity to store and retrieve the large amounts of information generated in each experiment. Recently, a study of PAH in the soot of an aluminum electrolysis furnace was published, in which about 40 PAH compounds were separated and identified by g.c.-m.s. [16]. Lao et al. [17] have also identified a large number of PNA's in air containing coal tar volatiles. The aim of the present study was, by means of a g.c.$^2$-m.s.-computer system, to identify PNA appearing in trace quantities in working atmospheres. This paper presents the results from an aluminum smelter and a coke plant.

## EXPERIMENTAL

### *Sampling and clean-up*

Air filter samples were collected by pulling ca. 1 $m^3$ of air through glass fibre filters by means of a pump with a capacity of about 1 $m^3$ $h^{-1}$. The filters were extracted in a Soxhlet apparatus with cyclohexane. The extracts were cleaned by liquid—liquid extraction and subsequent back-extraction into cyclohexane by the addition of water. The extracts were than concentrated to 0.5—1 ml in a modified Vigreux apparatus. A complete description of the sampling and clean-up methods is given elsewhere [18].

### *Gas chromatography*

The gas chromatographic analysis was performed on a Carlo Erba Fractovap

2101 equipped with a glass capillary column, splitless injector, and f.i.d. The chromatographic conditions were: glass capillary column, 50 m × 0.34 mm i.d., coated with SE-54 (H. and G. Jaeggi, 9043 Trogen, Switzerland); carrier gas, hydrogen at ca. 3 ml $min^{-1}$ at ambient temperature; injector and detector temperature, 275°C; initial column temperature, 115°C; programmed temperature rate, 3°C $min^{-1}$; final temperature, 260°C. The techniques for handling, cleaning, and mounting the glass capillary column have been described [19].

The cyclohexane extract (ca. 2 $\mu$l) was injected by the splitless injection technique [20]. The chromatographic peaks were displayed on an Omniscribe (Houston instruments) recorder. The peaks in the chromatograms were identified by comparing the retention times with those of a standard [18].

*G.c.-m.s.-computer system*

The g.c.-m.s.-computer system is a combination of a Carlo Erba Fractovap 2101 gas chromatograph and a Varian-MAT 112 mass spectrometer with a Spectro system 100 MS computer. The gas chromatographic conditions were as described above, with the exception that helium was used as carrier gas at ca. 2 ml $min^{-1}$ at ambient temperature. Details concerning the g.c.-m.s. system are reported elsewhere [21].

Mass spectra were recorded in the mass range *m/e* 50—500 at a scan rate of 1 s per decade, with automatic repetitive scanning. There was a programmed delay of 0.5 s after each scan and a spectrum was recorded approximately every 1.5 s. The spectra were stored on a magnetic disk.

The following experimental conditions were chosen: ionization energy, 70 eV; emission current, 1.5 mA; acceleration voltage, 800 V; multiplier voltage, 2 kV; ion source temperature, 260°C; interface temperature, 300°C; resolution, 700. The total ion current (TIC) from a second ion source with an ionization energy of 20 eV was used as the signal for the gas chromatographic trace.

## RESULTS

Gas chromatograms of the PNA fractions of particulates in an aluminum smelter and a coke plant are shown in Figs. 1 and 2. This system is characterized by high resolution and sensitivity and is capable of separating critical isomers, e.g. benzo(a)pyrene from benzo(e)pyrene and benz(a)anthracene from chrysene [18].

Identification was achieved in the g.c.$^2$-m.s. analysis. In the course of each analysis more than 2500 mass spectra were recorded and stored on a magnetic disk. Figures 3 and 4 show typical traces of TIC for an aluminum and a coke plant, respectively. The mass spectra were compared with those of a standard mass spectra library [22, 23]. The compounds identified are listed in Table 1; the identification has in several cases been confirmed by comparing the g.c. retention times with those of a prepared PAH standard. More than 100 com-

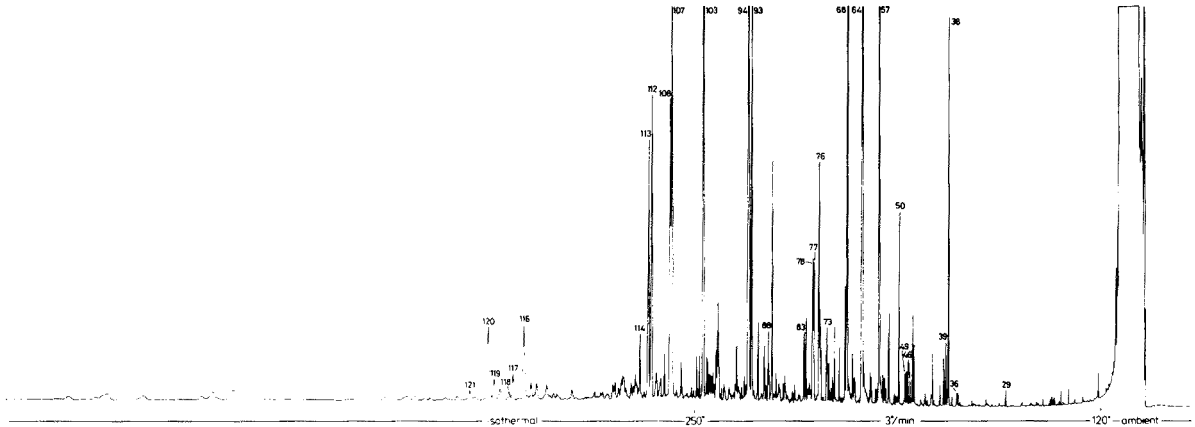


Fig. 1. Gas chromatogram of PAH in particulate matter from the working atmosphere in an aluminum smelting plant; peak identity given in Table 1.

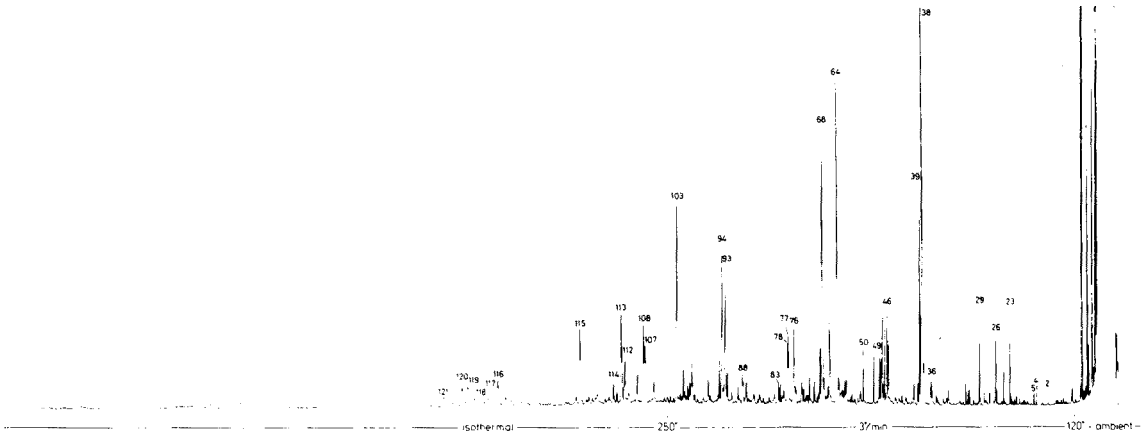


Fig. 2. Gas chromatogram of PAH in particulate matter from the working atmosphere in a coke plant; peak identity given in Table 1.

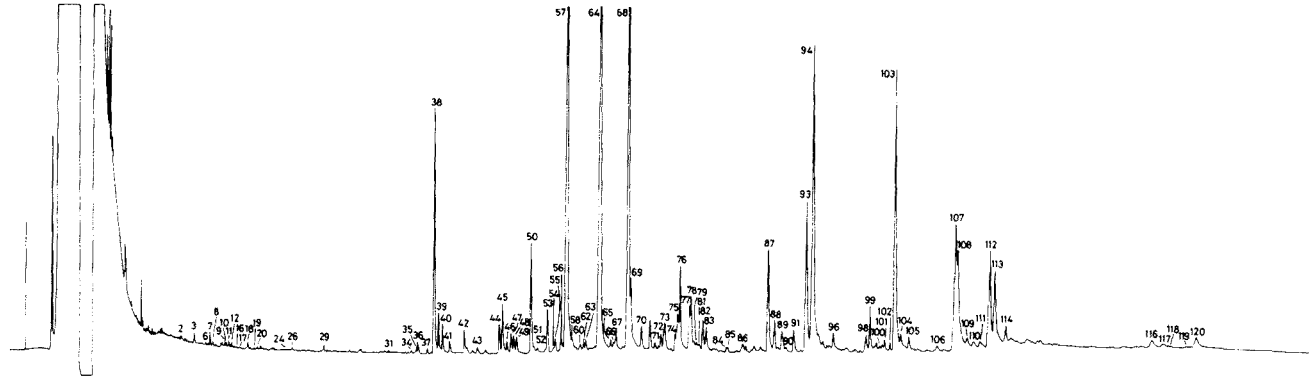

Fig. 3. Total ion-current trace of a g.c.-m.s. analysis of PAH in particulates from the working atmosphere in an aluminum smelting plant; peak identity given in Table 1.

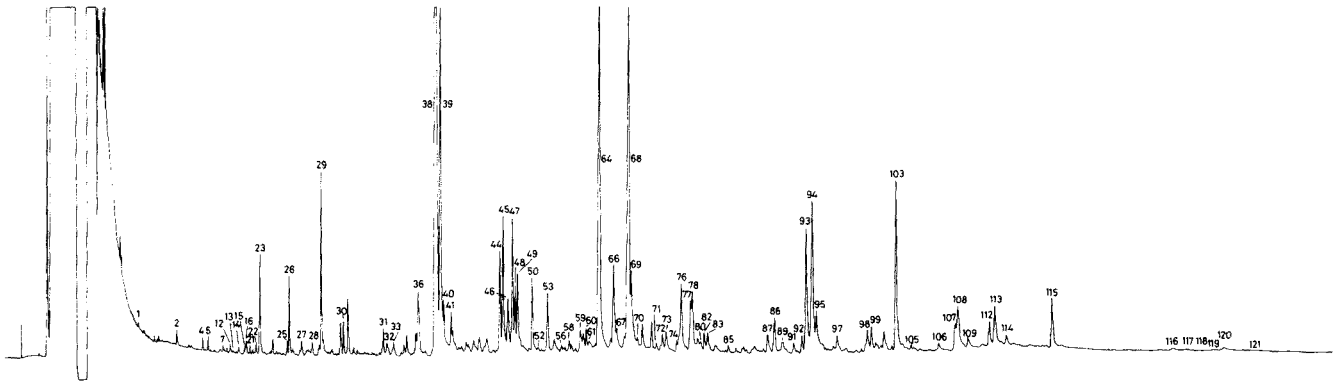

Fig. 4. Total ion-current trace of a g.c.-m.s. analysis of PAH in particulates from the working atmosphere in a coke plant; peak identity given in Table 1.

TABLE 1

PNA identified in particulate matter from working atmospheres

| Peak number | Compound | Identification | | | |
|---|---|---|---|---|---|
| | | Coke plant | | Aluminum plant | |
| | | G.c.-m.s. | G.c. | G.c.-m.s. | G.c. |
| 1 | Propylbenzene | + | | | |
| 2 | Naphthalene | + | + | + | + |
| 3 | Quinoline | | | + | |
| 4 | 2-Methylnaphthalene | + | + | | |
| 5 | 1-Methylnaphthalene | + | + | | |
| 6 | MW = 142 | | | + | |
| 7 | Methylquinoline | + | | + | |
| 8 | Methylquinoline | | | + | |
| 9 | Methylquinoline | | | + | |
| 10 | Methylquinoline | | | + | |
| 11 | Methylquinoline | | | + | |
| 12 | Biphenyl | + | + | + | + |
| 13 | Methylquinoline | + | | | |
| 14 | Dimethylnaphthalene | + | | | |
| 15 | Dimethylnaphthalene | + | | | |
| 16 | Dimethylquinoline | + | | + | |
| 17 | Dimethylquinoline | | | + | |
| 18 | Dimethylquinoline | | | + | |
| 19 | Dimethylquinoline | | | + | |
| 20 | Dimethylquinoline | | | + | |
| 21 | Acenaphthene | + | + | + | |
| 22 | Dimethylquinoline | + | | | |
| 23 | Acenaphthylene | + | + | | |
| 24 | Dimethylquinoline | | | + | |
| 25 | Naphthylnitrile | + | | | |
| 26 | Dibenzofuran | + | + | + | + |
| 27 | Naphthylnitrile | + | | | |
| 28 | Methylacenaphthylene | + | | | |
| 29 | Fluorene | + | + | + | + |
| 30 | Methylacenaphthylene | + | | | |
| 31 | 9-Methylfluorene | + | + | + | + |
| 32 | 2-Methylfluorene | + | + | | |
| 33 | 1-Methylfluorene | + | + | | |
| 34 | Fluorenone | | + | + | + |
| 35 | Methylbenzothiophene | | | + | |
| 36 | Dibenzothiophene | + | + | + | + |
| 37 | Methyldibenzofuran | | | + | |
| 38 | Phenanthrene | + | + | + | + |
| 39 | Anthracene | + | + | + | + |
| 40 | Benzoquinoline | + | | + | |
| 41 | Acridine | + | + | + | + |
| 42 | Cyclopenta(def)phenanthrene | | | + | |
| 43 | Methyldibenzothiophene | | | + | |
| 44 | Methylanthracene/Methylphenanthrene | + | | + | |
| 45 | Methylanthracene/Methylphenanthrene | + | | + | |

TABLE 1 (continued)

| Peak number | Compound | Identification | | | |
|---|---|---|---|---|---|
| | | Coke plant | | Aluminum plant | |
| | | G.c.-m.s. | G.c. | G.c.-m.s. | G.c. |
| 46 | 2-Methylanthracene | + | + | + | + |
| 47 | 4,5-Methylenephenanthrene | + | | + | |
| 48 | Methylanthracene/Methylphenanthrene | + | | + | |
| 49 | 1-Methylphenanthrene | + | + | + | + |
| 50 | Carbazole | + | + | + | + |
| 51 | Methylbenzoquinoline? | | | + | |
| 52 | Methylbenzoquinoline? | + | | + | |
| 53 | MW = 204 | + | | + | |
| 54 | MW = 206 | | | + | |
| 55 | Dimethylnaphthothiophene | | | + | |
| 56 | Methylcarbazole | + | | + | + |
| 57 | 3,6-Dimethylphenanthrene (IS)[a] | | | + | + |
| 58 | Dimethylphenanthrene | + | | + | |
| 59 | MW = 209 | + | | | |
| 60 | Dimethylphenanthrene/Methylcarbazole | + | | + | |
| 61 | Dimethylphenanthrene/Methylcarbazole | + | | | |
| 62 | Methylcarbazole | | | + | |
| 63 | Methylcarbazole | | | + | |
| 64 | Fluoranthene | + | + | + | + |
| 65 | Benzylnaphthalene | | | + | |
| 66 | Benz(e)acenaphthylene | + | | + | |
| 67 | Benzo(def)dibenzothiophene | + | | + | |
| 68 | Pyrene | + | + | + | + |
| 69 | Ethylmethylenephenanthrene | + | | + | |
| 70 | Ethylmethylenephenanthrene | + | | + | |
| 71 | MW = 203 | + | | + | |
| 72 | Dihydrobenzofluorene | + | | + | |
| 73 | Methylpyrene | + | + | + | + |
| 74 | Methylpyrene | + | | + | |
| 75 | Methylpyrene | | | + | |
| 76 | Benzo(a)fluorene | + | + | + | + |
| 77 | Benzo(b)fluorene | + | + | + | + |
| 78 | 4-Methylpyrene | + | + | + | + |
| 79 | Mn = 232 | | | + | |
| 80 | Benzocarbazole | + | | | |
| 81 | Methylpyrene | | | + | |
| 82 | Methylpyrene | + | | + | |
| 83 | 1-Methylpyrene | + | | + | |
| 84 | Fluorenenitrile | | | + | |
| 85 | Mn = 244 | + | | + | |
| 86 | Styrylnaphthalene | | | + | |
| 87 | Benzothionaphthene | + | | + | |
| 88 | Benzo(c)phenanthrene | + | + | + | + |
| 89 | Benzophenanthridine | + | | + | |
| 90 | Benzodibenzothiophene | | | + | |
| 91 | Benzo(a)dibenzothiophene | + | | + | |
| 92 | Benzo(ghi)fluoranthene | + | | | |
| 93 | Benz(a)anthracene | + | + | + | + |

TABLE 1 (continued)

| Peak number | Compound | Identification | | | |
|---|---|---|---|---|---|
| | | Coke plant | | Aluminum plant | |
| | | G.c.-m.s. | G.c. | G.c.-m.s. | G.c. |
| 94 | Chrysene, triphenylene | + | + | + | + |
| 95 | MW = 227 | + | | | |
| 96 | Methylbenz(a)anthracene/Methylchrysene | | | + | |
| 97 | Benzanthrone | + | | | |
| 98 | Methylbenz(a)anthracene/Methylchrysene | + | | + | |
| 99 | Benzocarbazole | + | | + | |
| 100 | MW = 240 | | | + | |
| 101 | Methylchrysene | | | + | |
| 102 | Benzocarbazole | | | + | |
| 103 | β,β-Binaphthyl (IS) | + | + | + | + |
| 104 | Binaphthyl | | | + | |
| 105 | Benzocarbazole | + | | + | |
| 106 | Ethylchrysene/dimethylchrysene | + | | + | |
| 107 | Benzo(b)fluoranthene | + | + | + | + |
| 108 | Benzo(j+k)fluoranthene | + | + | + | + |
| 109 | Benzofluoranthene | + | | + | |
| 110 | MW = 258 | | | + | |
| 111 | MW = 258 | | | + | |
| 112 | Benzo(e)pyrene | + | + | + | + |
| 113 | Benzo(a)pyrene | + | + | + | + |
| 114 | Perylene | + | + | + | + |
| 115 | *m,m'*-Tetraphenylene (IS) | + | + | | |
| 116 | *o*-Phenylenepyrene | + | + | + | + |
| 117 | Dibenz(a,h)anthracene/Dibenz(a,c)anthracene | + | + | + | + |
| 118 | Dibenzanthracene | + | | + | |
| 119 | Benzo(b)chrysene | + | | + | |
| 120 | Benzo(ghi)perylene | + | + | + | + |
| 121 | Anthanthrene | + | + | + | + |

[a]IS = internal standard.

pounds were identified in the working atmospheres of an aluminum plant and a coke plant. About 30 of these, including all the main compounds, have previously been reported from g.c.[2] analysis. Information about the presence of the remaining compounds in working atmospheres is scarce.

As shown in Table 1, the majority of the compounds identified are parent PAH or their methyl, dimethyl, and/or their ethyl derivatives. Most of the alkyl derivatives of PAH appear as a large number of isomers, and a complete identification can only be reached by combining data for g.c.-m.s. and g.c.[2] retention times.

A number of PNA containing N, O or S were also identified. Mass spectra of some PNA compounds were observed in both working atmospheres studied in this work, and might therefore be regarded as typical in industrial processes involving coke, coal or tar. Mass spectra of the PNA compounds are not given as they have already been reported [22, 23].

## DISCUSSION

Glass capillary g.c.-m.s. is a valuable tool in characterizing the PNA content of complex samples. The important feature of the instrument described here is that the separation efficiency achieved by the glass capillary column is retained by the direct inlet to the ion source. This permits a base line separation of benzo(e)pyrene (BeP) from benzo(a)pyrene (BaP), benz(a)-anthracene from chrysene/triphenylene, phenanthrene from anthracene, and partial separation of benzo(b)fluoranthene from benzo(k)fluoranthene. It is noteworthy, however, that even with the high resolution possessed by this system, several overlapping peaks may occur and this may, in turn, preclude quantitative analysis.

The g.c.$^2$-m.s. system has a very high sensitivity with the ability to obtain good mass spectra at the 1-ng level. This results in the identification of PNA components present at less than 0.5 ppm in the final extract. It has been shown that the addition of alkyl substituents to PNA may change the biological activity from that of the parent compound [2, 4, 5]. It is therefore of great importance to be able to analyse the samples as completely as possible in order to evaluate possible occupational hazards.

Besides the pure hydrocarbons, a number of PNA containing heteroatoms have been identified. Those containing nitrogen include quinoline, benzoquinoline, acridine, phenanthridine, carbazole, benzocarbazole, benzophenanthridine, and alkyl derivatives of these compounds. Of special interest is naphthylnitrile, identified in the working atmosphere of the coke plant. To the best of our knowledge, this compound has not been identified previously in environmental samples, but the analogous fluorene carbonitrile has been determined in urban ambient air [8] and in the working atmosphere of the aluminum smelter. The samples also contain a number of sulfur-containing compounds including dibenzothiophene, benzothiophene, and their methyl derivatives. These findings are in accordance with recent studies of sulfur-containing PNA in carbon blacks obtained from sulfur-containing petroleum feedstocks [24]. The samples also contain several oxygenated PNA, including dibenzofuran, methoxyfluorene, phenylbenzaldehyde and benzanthrone (7H-benz(d,e)anthracene-7-one). The latter compound is of particular environmental interest as it is also found in urban air [25] and in oxygenated fractions of air extracts that seem to be carcinogenic [26].

As revealed by Figs. 1 and 2, the gas chromatographic profiles are similar for the working atmosphere in the coke plant and aluminum smelter. This is in accordance with earlier observations that the PAH profile, composed of the main PAH compounds, tends to be constant under stable operational conditions, and similar for coke plants and aluminum smelters [14, 15]. It is also reasonable to assume that this might be the case for components present in medium and minor quantities, although the latter are more susceptible to random variations and contamination.

The authors are indebted to Dr. B. Josefsson for valuable discussions and to Mr. B. Olufsen for skilful technical assistance. Financial support to A.B. from the Royal Norwegian Council for Scientific and Industrial Research under contract B. 1551.4879, and to G.E. from Knut and Alice Wallenberg's Foundation, is gratefully acknowledged.

REFERENCES

1 Particulate Polycyclic Organic Matter, National Academy of Science, Washington D.C., 1972.
2 A. Dipple in C. E. Searle (Ed.), Chemical Carcinogens, ACS Monograph 173, Am. Chem. Soc., Washington D.C., 1976, p. 245.
3 M. D. Kipling in C. E. Searle (Ed.), Chemical Carcinogens, ACS Monograph 173, Am. Chem. Soc., Washington D.C., 1976, p. 315.
4 R. Schoental, in E. Clar (Ed.), Polycyclic Hydrocarbons, Academic Press, London, 1964, p. 133.
5 D. Hoffmann, W. E. Bondinell and E. L. Wynder, Science, 183 (1974) 215.
6 B. D. Tilak, Tetrahedron, 9 (1960) 76.
7 E. Campaigne, D. R. Knapp, E. S. Neiss and T. R. Bosin, Adv. Drug Res., 5 (1970) 1.
8 R. C. Lao, R. S. Thomas, H. Oja and L. Dubois, Anal. Chem., 45 (1973) 908.
9 G. Grimmer, H. Böhnke and A. Glaser, Erdöl und Kohle-Petrochemie, 30 (1977) 411.
10 A. Herlan and J. Mayer, Zbl. Bakt. Hyg., I Abt. Orig. B., 165 (1977) 192.
11 K. A. Schulte, D. J. Larsen, R. W. Hornung and J. V. Crable, HEW Publication No (NIOSH) 74-105, National Institute for Occupational Safety and Health, Cincinatti, Ohio 45202, 1974.
12 T. D. Searl, F. J. Cassidy, W. H. King and R. A. Brown, Anal. Chem., 42 (1970) 954.
13 H. Boden, J. Chromatogr. Sci., 14 (1976) 391.
14 A. Bjørseth, O. Bjørseth and P. E. Fjeldstad, Scand. J. Work, Environ. Health, in press.
15 A. Bjørseth, O. Bjørseth and P. E. Fjeldstad, Scand. J. Work, Environ. Health, in press.
16 H. Tausch and G. Stelik, Chromatographia, 10 (1977) 350.
17 R. C. Lao, R. S. Thomas and J. L. Monkman, J. Chromatogr., 112 (1975) 681.
18 A. Bjørseth, Anal. Chim. Acta, 94 (1977) 21.
19 K. Grob and H. Jaeggi, Chromatographia, 5 (1972) 382.
20 K. Grob and G. Grob, J. Chrom. Sci., 7 (1969) 584.
21 G. Eklund, B. Josefsson and A. Bjørseth, J. Chromatogr., 150 (1977) 161.
22 E. Stenhagen, S. Abrahamson and F. W. McLafferty (Eds.), Registry of Mass Spectral Data, Wiley-Interscience, New York, 1974.
23 A. Cornu and R. Massot, Compilation of Mass Spectral Data, Volume 1 and 2, Heyden, London, 1975.
24 M. L. Lee and R. A. Hites, Anal. Chem., 48 (1976) 1890.
25 E. Sawicki, Arch. Environ. Health, 14 (1967) 46.
26 S. S. Epstein, Arch. Environ. Health, 10 (1965) 233.

*Analytica Chimica Acta*, 105 (1979) 129—137


# MASS-ANALYZED ION KINETIC ENERGY SPECTRA OF THE $[M + 1]^+$ IONS OF ALIPHATIC ESTERS PRODUCED BY CHEMICAL IONIZATION

J. RONALD HASS*, DONALD J. HARVAN and MAURICE M. BURSEY

*Environmental Biology and Chemistry Branch, National Institute of Environmental Health Sciences, P.O. Box 12233, Research Triangle Park, North Carolina 27709 (U.S.A.)*

(Received 22nd June 1978)

## SUMMARY

To test the similarity of chemical ionization (CI) spectra of esters to the collision-induced decomposition mass-analyzed ion kinetic energy (CID-MIKE) spectra of protonated esters, the CID-MIKE spectra of the $[M + 1]^+$ ions of nineteen aliphatic esters were studied. The major fragments produced in the two kinds of experiment are similar, but there are significant differences in the ions of high mass, which would reduce the usefulness of library searches of CI spectra to identify MIKE spectra of $[M + 1]^+$ ions.

The advent of analytical applications of mass-analyzed ion kinetic energy spectrometry [1, 2] has been complicated by the observation [3] that collision-induced decomposition mass-analyzed ion kinetic energy (CID-MIKE) spectra of the molecular ions are, in general, not sufficiently similar to the electron-impact (EI) mass spectra of the same molecules to allow identification by comparison to mass spectra in library collections. Since chemical ionization (CI) spectra are characterized by fewer peaks, a study was designed to see how much analogy there is between the ion kinetic energy spectra of $[M + 1]^+$ ions produced from typical compounds and the chemical ionization spectra of these compounds produced in the usual fashion with methane. Esters were among the first classes of compounds to be studied by chemical ionization mass spectrometry [3], and the study of the MIKE spectra of protonated esters has a certain historical symmetry.

## EXPERIMENTAL

Most of the esters were either commercial samples or synthesized by mixing equimolar amounts of alcohol and acid chloride and passing the reaction mixture through alumina. The t-butyl pivalate was prepared by further addition of a stoichiometric amount of pyridine to the mixed alcohol and acid chloride and filtering off the pyridinium chloride before passing through alumina. Hexadecyl acetate and octadecyl acetate were prepared from the alcohol and 2:1 pyridine—acetic anhydride.

A VG Micromass ZAB/2F mass spectrometer equipped with a collision cell and MIKES scan unit was used to obtain MIKE spectra. The ion source was operated at 210°C with Linde 99.97% methane admitted to give a reading of $8 \times 10^{-5}$ torr on the source ionization gauge, which corresponds to ca. 0.3 torr in the source. Under these conditions, the ratio *m/z* 29: *m/z* 27 was ca. 15:1. At measured source pressures of $10^{-6}$ torr, several of the heavier esters showed $[M + 1]^+$ peaks 20—30 times more intense than M without the addition of methane. Since MIKE spectra are independent of energy content, these ions were used in place of $[M + 1]^+$ ions generated from $CH_5^+$. The emission current was 1 mA and the electron energy was 150 eV. Samples were introduced through an all-glass heated inlet system. For collision-induced fragmentation, the collision cell was operated at an analyzer ionization gauge reading of 6—$8 \times 10^{-7}$ torr. The actual cell pressure was then ca. $10^{-3}$ torr and the main beam intensity was reduced to ca. 50% of its initial value. Nitrogen was used as collision gas. The MIKE spectra were scanned at 100 ms/eV.

## RESULTS

Tables 1 and 2 present the CID-MIKE spectra of several categories of small aliphatic esters. The results suggest that there are simple trends which make these spectra useful for structural identification. Among the acetates only those with an R group larger than methyl (Table 1) show hydrogen rearrangement ions:

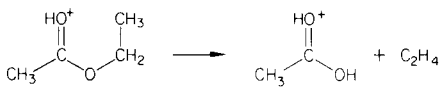


(1)

The methyl ester molecular ion does not produce $CH_3CO_2H_2^+$; this is consistent with the CI spectra of methyl esters contrasted with those of other kinds of esters [3]. Instead, it produces substantial amounts of *m/z* 43 (acetyl ion), *m/z* 15 (methyl ion), *m/z* 29 and 31 ($HCO^+$ and $CH_3O^+$), *m/z* 45, and ions with *m/z* ratios M and M − 1. Finding the last ion suggests that not all [M − 1] ion production in chemical ionization is by hydride ion abstraction from neutral molecules.

The minor reactions of the other three small acetate esters can be discussed simultaneously. The diminution of the acetyl ion intensity with increasing molecular weight is quite abrupt, *m/z* 43 in the isopropyl ester being due mostly to $C_3H_7^+$ (compare the intense $C_4H_9^+$ ion in the t-butyl ester). The ethyl ester really has no other significant peaks; in the isopropyl and t-butyl esters, the more numerous peaks of notable intensity are hydrocarbon ions and all can be associated with the increasingly large, branched alkyl group of the alcohol moiety. The $CH_3CO_2H_2^+$ ion is much less abundant than the $C_4H_9^+$ ion, which, together with other hydrocarbon ions derived from it, accounts for more than 90% of the fragment-ion current in the CID-MIKE spectrum.

The acetates set trends for the behavior of the $[M + 1]^+$ ions of the other small esters (Table 1). In the methyl esters, the acyl ion continues to be

TABLE 1

MIKE spectra of $[M + 1]^+$ ions of aliphatic esters

| | Methyl | Ethyl | Isopropyl | t-Butyl | | Methyl | Ethyl | Isopropyl | t-Butyl |
|---|---|---|---|---|---|---|---|---|---|
| *Acetate* | | | | | *Propionate* | | | | |
| 13 | 5 | | | | 14 | 4 | | | |
| 14 | 12 | | | | 15 | 10 | | | |
| 15 | 30 | | | 7 | 26 | 12 | | | |
| 27 | | | 1 | 12 | 27 | 23 | 4 | 1 | 2 |
| 29 | 22 | 1 | | 19 | 29 | 41 | 8 | 2 | 4 |
| 31 | 18 | | | | 31 | 14 | 1 | | |
| 39 | | | 1 | 6 | 39 | 7 | | 1 | 2 |
| 41 | 10 | | 2 | 7 | 40 | 4 | | | |
| 42 | | 1 | 2 | | 41 | 6 | | 2 | 3 |
| 43 | 100 | 2 | 11 | 8 | 42 | 8 | | 1 | |
| 45 | 26 | 1 | 2 | 4 | 43 | 16 | 1 | 5 | 1 |
| 56 | | | | 7 | 45 | 28 | 4 | 1 | 2 |
| 57 | | | | 100 | 53 | 4 | | | 1 |
| 59 | 10 | | | | 55 | 18 | 2 | 1 | 2 |
| 60 | | 1 | 3 | | 57 | 100 | 12 | 3 | 100 |
| 61 | | 100 | 100 | 11 | 59 | 15 | | 1 | 2 |
| 62 | | | 2 | | 60 | | | 1 | |
| 73 | 50 | | | | 73 | | 4 | 1 | |
| 74 | 14 | | | | 74 | | 8 | 3 | 3 |
| 75 | m.b.[a] | | 1 | | 75 | | 100 | 100 | 13 |
| 77 | | | 1 | | 77 | | 4 | 1 | |
| 88 | | 1 | | | 87 | 17 | | | |
| 89 | | m.b. | | | 88 | 14 | | | |
| 101 | | | 1 | | 89 | m.b. | | 1 | |
| 102 | | | 1 | | 91 | | | 1 | 1 |
| 103 | | | m.b. | | 101 | | 8 | | |
| 115 | | | | 2 | 102 | | 15 | 1 | |
| 117 | | | | m.b. | 103 | | m.b. | | |
| | | | | | 115 | | | 4 | |
| *Isobutyrate* | | | | | 116 | | | 1 | |
| 15 | 15 | | | 2 | 117 | | | m.b. | |
| 27 | 26 | 1 | 1 | 2 | 130 | | | | 1 |
| 29 | 13 | 2 | 1 | 3 | 131 | | | | m.b. |
| 31 | 10 | | | 2 | | | | | |
| 39 | 19 | 1 | | 3 | *Pivalate* | | | | |
| 41 | 21 | 1 | 2 | | 15 | 8 | | | |
| 43 | 100 | 7 | 8 | 6 | 27 | 8 | 3 | 1 | |
| 45 | 25 | 4 | 1 | 6 | 29 | 10 | 6 | 1 | 1 |
| 53 | 6 | | | 2 | 31 | 3 | 1 | | |
| 55 | 21 | 1 | 1 | | 33 | 3 | | | |
| 56 | | | | 5 | 39 | 13 | 3 | 1 | 1 |
| 57 | 18 | 1 | 1 | 83 | 41 | 21 | 4 | 2 | 2 |
| 59 | 13 | | | | 43 | 13 | 3 | 4 | 1 |
| 60 | | | | 2 | 45 | 13 | 2 | 1 | |
| 69 | 6 | | | | 53 | | 1 | | |
| 71 | 81 | 8 | 3 | 3 | 55 | 5 | 2 | 1 | |
| 73 | | 6 | 3 | | 57 | 36 | 15 | 3 | 13 |

TABLE 1 (continued)

| | Methyl | Ethyl | Isopropyl | t-Butyl | | Methyl | Ethyl | Isopropyl | t-Butyl |
|---|---|---|---|---|---|---|---|---|---|
| *Isobutyrate (continued)* | | | | | *Pivalate (continued)* | | | | |
| 74 | 19 | 1 | 1 | 3 | 59 | 13 | 3 | 1 | |
| 75 | 19 | | | | 69 | 8 | 1 | 1 | |
| 85 | 6 | | | | 71 | 8 | 2 | 1 | |
| 87 | 59 | 1 | | | 73 | 5 | 2 | 1 | |
| 88 | 88 | 5 | 3 | | 74 | 5 | | | |
| 89 | | 100 | 100 | 100 | 75 | | 1 | | |
| 101 | 6 | 1 | | | 76 | | 1 | | |
| 102 | 12 | 1 | | | 85 | 100 | 16 | 6 | 2 |
| 103 | m.b. | | | 3 | 87 | 8 | 4 | 3 | 1 |
| 116 | | 1 | | | 88 | | 3 | | 1 |
| 117 | | m.b. | | | 89 | | 1 | | |
| 131 | | | m.b. | | 101 | 33 | 1 | | |
| 145 | | | | m.b. | 102 | 36 | | | 1 |
| | | | | | 103 | | 100 | 100 | 100 |
| | | | | | 115 | 5 | 3 | | |
| | | | | | 116 | 5 | 3 | | |
| | | | | | 117 | m.b. | | | |
| | | | | | 129 | | 1 | 1 | |
| | | | | | 131 | | m.b. | | |
| | | | | | 145 | | | m.b. | |
| | | | | | 159 | | | | m.b. |

[a]Main beam.

TABLE 2

MIKE spectra of propyl butyrate $[M + 1]^+$ ions: $Pr_1OOC(=O)—Pr_2$

| | 1 = *n* 2 = *n* | 1 = *n* 2 = *i* | 1 = *i* 2 = *n* | 1 = *i* 2 = *i* |
|---|---|---|---|---|
| 27 | 3 | 1 | 1 | 1 |
| 29 | 1 | | 1 | |
| 39 | 2 | 1 | 1 | 1 |
| 41 | 5 | 2 | 2 | 2 |
| 43 | 16 | 9 | 6 | 8 |
| 55 | 1 | | 1 | 1 |
| 57 | 1 | 1 | 1 | 1 |
| 60 | 4 | | 3 | |
| 71 | 6 | 6 | 2 | 3 |
| 73 | 3 | 1 | 2 | 3 |
| 74 | 2 | | 1 | 1 |
| 87 | 2 | 1 | | |
| 88 | 6 | 2 | 3 | 3 |
| 89 | 100 | 100 | 100 | 100 |
| 102 | 1 | | 1 | |
| 130 | 2 | 2 | 1 | |
| 131 | m.b. | m.b. | m.b. | m.b. |

important; and other ions of low mass whose formation is concordant with the above interpretation of methyl acetate are found. In methyl isobutyrate and pivalate, losses of 15 and 16 mass units become important, no doubt relating to branching in the acyl group, and the alkyl group derived from the acyl portion is now sufficiently stable to appear as a notable peak. Spectra of the remaining ethyl and isopropyl esters are dominated by the $RCO_2H_2^+$ ion, as before, but fragments formed from the decomposition of the alkyl group derived from the acyl portion are now more important. The domination of the spectra of the t-butyl esters by *m/z* 57 decreases with increasing size and branching of the acyl group, in spite of the stability of the t-butyl ion. The heavier t-butyl esters are again dominated by the acyl ion.

The least expected feature of the spectra is the reduction in relative intensity of minor fragments as branching increases. Thus, the principal fragment (base peak in Table 1) in ethyl, isopropyl and t-butyl acetate accounts for 93%, 78%, and 55% of the fragment-ion current, respectively. In the propionates, the values for the ethyl, isopropyl, and t-butyl esters are 58%, 76%, and 73%; in the isobutyrates, 70%, 80%, and 44%; and in the pivalates, 56%, 78%, and 82%. Although at first more fragmentation routes are available to the heavier ion on collision, eventually the number of degrees of freedom in the ion becomes so great that the collisional excitation is dispersed among many modes and only a few kinds of cleavage occur. This has both advantages and disadvantages for structural analysis of $[M + 1]^+$ ions. While it would be easy to spot a few characteristic details of a heavy $[M + 1]^+$ ion structure, one would be reluctant to spend much time pondering a peak of a few percent relative intensity which could in fact be a key to the structure.

For example, in Table 2, the spectra of the $[M + 1]^+$ ions of all the isomers of propyl butyrate are seen to be fairly similar. It would be difficult to establish the degree of branching in an unknown isomer, although the gross structural organization would be clear from the base peak corresponding to $RCO_2H_2^+$ in each case. The *m/z* 71 ion, $RCO^+$, is of course twice as abundant in the n-propyl esters as in the isopropyl esters, and the *m/z* 60 ion is much more significant for n-butyrates than isobutyrates. If the composition of this ion is related to the n-propyl group, then a number of attractive mechanisms can be written for its formation, including

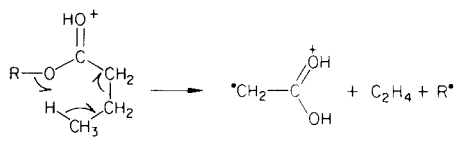


(2)

but the driving force for formation of this odd-electron ion from an even-electron precursor is not clear.

Typical $[M + 1]^+$ MIKE spectra of fatty acid methyl esters and long-chain alcohol acetates are presented in Table 3. The acetates have quite simple spectra. The alkyl ion from the alcohol dominates the spectrum. The $C_nH_{2n+1}$ and $C_nH_{2n-1}$ series account for most of the peaks. The envelope of the alkyl

TABLE 3

MIKE spectra of long-chain fatty ester $[M + 1]^+$ ions

| | Methyl 12-methyl-tetradecanoate | Methyl hexa-decanoate | Methyl octa-decanoate | Hexadecyl acetate | Octadecyl acetate |
|---|---|---|---|---|---|
| 27 | | | 3 | | |
| 29 | 8 | 1 | 5 | | |
| 41 | 23 | 8 | 22 | 4 | |
| 43 | 47 | 20 | 40 | 5 | 2 |
| 55 | 39 | 22 | 40 | 4 | 3 |
| 57 | 52 | 24 | 40 | 9 | 5 |
| 59 | 16 | 10 | 20 | | |
| 61 | | | | 5 | 3 |
| 69 | 25 | 20 | 31 | 3 | 3 |
| 71 | 17 | 15 | 23 | 7 | 4 |
| 74 | 34 | 34 | 44 | | |
| 83 | 19 | 18 | 24 | 3 | 3 |
| 85 | | | | 6 | 4 |
| 87 | 100 | 100 | 100 | | |
| 97 | 15 | 16 | 97 | 2 | 2 |
| 99 | | | | 3 | 2 |
| 101 | 8 | 8 | 11 | | |
| 103 | 7 | 6 | 6 | | |
| 111 | 7 | 7 | 10 | | |
| 113 | | | | 2 | 2 |
| 115 | 4 | 3 | 6 | | |
| 117 | 5 | | | | |
| 122 | | | | 2[a] | |
| 125 | 5 | 3 | 5 | | |
| 127 | | | | 2 | 2 |
| 129 | 7 | 5 | 8 | | |
| 135 | 3 | | 3 | | |
| 137 | | | | | 2[a] |
| 139 | 3 | 3 | 4 | | |
| 141 | | | | 3 | 2 |
| 143 | 15 | 16 | 16 | | |
| 153 | 3 | 2 | 3 | | |
| 155 | | | | 3 | 2 |
| 157 | 5 | 4 | 3 | | |
| 163 | | 2 | 4 | | |
| 169 | | | | 2 | 2 |
| 171 | 4 | 6 | 2 | | |
| 183 | | | | 2 | 2 |
| 185 | 5 | 6 | 5 | | |
| 197 | | | | | 2 |
| 199 | 16 | 7 | 6 | | |
| 213 | 14 | 5 | 4 | | |
| 225 | 9 | | | 100 | |
| 227 | 6 | 18 | 3 | | |
| 239 | | 15 | | | |
| 241 | | 6 | 4 | | |
| 242 | 3 | | | | |

TABLE 3 (continued)

| | Methyl 12-methyl-tetradecanoate | Methyl hexa-decanoate | Methyl octa-decanoate | Hexadecyl acetate | Octadecyl acetate |
|---|---|---|---|---|---|
| 253 | | | | | 100 |
| 254 | | | 10 | | |
| 255 | | | 7 | | |
| 256 | | 5 | | | |
| 257 | m.b. | | | | |
| 271 | | m.b. | | | |
| 284 | | | 4 | | |
| 285 | | | | m.b. | |
| 299 | | | m.b. | | |
| 313 | | | | | m.b. |

[a]Doubly charged ion.

ion series is quite similar to that observed for the MIKE spectrum of the alkyl ion from the acetate, namely, $m/z$ 225 or 253, at the high mass end of the scan. At the low mass end, the peaks in the $[M + 1]^+$ ion MIKE spectrum are higher than in the alkyl ion MIKE spectrum; consequently, the production of these ions to some extent passes through a different intermediate than the alkyl ion. The small amount of $m/z$ 61 produced is consistent with the trend noted in Table 1. Two peaks are seen at $m/z$ 122 and $m/z$ 137; their sharpness suggests their formation in a charge-stripping process:

$$M^+ + N_2 \rightarrow M^{2+} + N_2 + e \qquad (3)$$

The methyl esters of fatty acids have $[M + 1]^+$ ion MIKE spectra which have the $C_nH_{2n+1}^+$ and $C_nH_{2n-1}^+$ series dominant at the low mass end and the $(CH_2)_nCOOCH_3^+$ series dominant at the high end. The most intense peak in the spectra is $CH_2CH_2COOCH_3^+$, which would be formed through a six-membered transition state with the loss of an alkane:

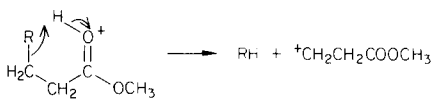


(4)

Both the importance of this peak and the occurrence of so many other $(CH_2)_nCOOCH_3^+$ ions, which also would be formed by alkane loss through larger rings, tend to support the contention [4] that alkane losses are generally more important mass spectral fragmentation routes than formerly supposed. The acyl ions are observed, as expected, and the even-electron ions at $m/z$ 74 ($CH_2{=}C(OH)OCH_3^{\cdot+}$) and M + 1—15 are observed. The peaks at 103, 135, and 163 must involve hydrogen rearrangements whose driving forces are not yet understood. Possibly because the fraction of ion current carried by ions still retaining hydrocarbon chains is greater in the long-chain esters, spectral differences arising from structural differences are less subtle. The presence of

branching in methyl 12-methyl-tetradecanoate would be inferred from the increased relative abundance of $m/z$ 57, 199, and 213, for example.

*Comparison with CI spectra of esters*

The CI spectra may contain peaks resulting from either ion—molecule reactions ($[M + 1]^+$, $[M + 29]^+$, ester interchange peaks (3), etc.) or fragmentation reactions ($R^+$, $RCO^+$, $RCO_2H^+$, etc.) whereas the CID-MIKE spectra are necessarily restricted to peaks corresponding to fragmentation reactions of the mass-selected ion. Ion—molecule reaction peaks other than $[M + 1]^+$ rarely account for more than 3% of the total sample ion current, but fragmentation reaction peaks often contribute greater than 12% to the sample ion current. Thus, if the principal mechanisms for formation of ions with $m/z$ less than the $[M + 1]^+$ ion in the CI spectra involve initial formation of an excited $[M + 1]^+$ ion followed by fragmentation of this species, then the CID-MIKE spectrum of the $[M + 1]^+$ ion should qualitatively resemble the CI spectra of the esters. Otherwise, there should be no particular relationship between the two types of spectra.

Fragment-ion current is carried primarily by $R^+$, $RCO^+$, and $RCO_2H_2^+$ in both types of spectra. The latter are formed by the most exothermic processes from M + 1, with $\Delta H$ as negative as $-40$ kcal $mol^{-1}$ [3]. Formation of $R^+$ from $ROH_2^+$ is almost as favorable. Further fragmentation of $R^+$ by loss of H or $H_2$ is roughly equally minor in both sets of spectra. In contrast, peaks at masses equal to M and M $-$ 1 are much more prominent in the CI spectra than in the MIKE spectra, often being 20% as high as the $[M + 1]^+$ peak in the former but of trivial intensity in the latter. Thus, while there is evidence, particularly for very small molecules, that the $[M - 1]^+$ ion is formed in part from the $[M + 1]^+$ ion, most such ions come from hydride abstraction from the neutral molecule and, as previously postulated, are not at all associated with the $[M + 1]^+$ ion. The $ROH_2^+$ peak is more prominent in both kinds of spectra of small methyl esters but for other esters is even less significant on MIKE than CI spectra, often being undetected in the former. Current from various ion series in the MIKE spectra of the long-chain esters is substantial; but their CI spectra are dominated by the $[M + 1]^+$ and $[M - 1]^+$ peaks, and the ion series are much less important.

Thus, to insure the highest chance of assigning the MIKE spectrum of the $[M + 1]^+$ ion of an aliphatic ester, the comparison algorithm should not place emphasis on the high-mass end of the CI spectrum to which it is compared.

## CONCLUSIONS

The following conclusions can be drawn about MIKE spectra of $[M + 1]^+$ ions of aliphatic esters. First, it is simple to identify the mass of the acyl group because the spectra contain appropriate peaks, which in the case of isopropyl and particularly ethyl esters dominate the spectrum. Because the ion current is overwhelmingly carried by $RCO_2H_2^+$ in the latter case, the monitoring

method of choice for identification of a carboxylic acid would be through the *ethyl* ester derivative for mass separation-mass spectrometry (m.s.-m.s.) [2] or for g.c.-MIKE spectrometry [5], although quantitative formation of ethyl esters with ethanol is more difficult. Secondly, the ethyl ester also avoids most complications arising from ester interchange peaks in methane CI spectra with which the MIKE spectra would be compared. Thirdly, the fragmentation patterns are those to be expected on the basis of decomposition of even-electron ions. Fourthly, differences between linear and branched alkyl portions of small isomeric esters are not sufficient, in the cases selected to avoid special situations, to distinguish the isomers without resorting to minor peaks. In long-chain esters branching can be detected, however. Finally, libraries of CI spectra of esters may be useful for identification of MIKE spectra of $[M + 1]^+$ ions if the comparison downgrades the substantial differences at the high-mass end of the spectrum.

REFERENCES

1 R. W. Condrat and R. G. Cooks, Anal. Chem., 50 (1978) 81A.
2 F. W. McLafferty and F. M. Bockhoff, Anal. Chem., 50 (1978) 69.
3 M. S. B. Munson and F. H. Field, J. Am. Chem. Soc., 88 (1966) 4337.
4 J. F. Litton, T. L. Kruger and R. G. Cooks, J. Am. Chem. Soc., 98 (1976) 2011.
5 D. J. Harvan, J. R. Hass and D. J. S. Birch, presented at the 26th Annual Conference on Mass Spectrometry and Allied Topics, St. Louis, Missouri, May 1978.

*Analytica Chimica Acta*, 105 (1979) 139—146


# THE DETERMINATION OF PENTOBARBITAL AND OTHER BARBITURATES IN BLOOD PLASMA BY GAS—LIQUID CHROMATOGRAPHY WITH ON-COLUMN AND PRE-COLUMN BUTYLATION

A. HULSHOFF*, O. A. G. J. VAN DER HOUWEN and D. M. BARENDS

*Pharmaceutical Laboratory, University of Utrecht, Catharijnesingel 60, Utrecht (The Netherlands)*

H. B. KOSTENBAUDER

*College of Pharmacy, University of Kentucky, Lexington, KY 40506 (U.S.A.)*

(Received 14th August 1978)

## SUMMARY

Two g.l.c. methods for the determination of pentobarbital and other barbiturates are reported. In the first method the plasma samples are extracted with toluene; the toluene layer is back-extracted with a small volume of a tetrabutylammonium hydroxide solution of which an aliquot is injected into the gas chromatograph. This method is simple and rapid, and sensitive enough for monitoring pentobarbital plasma concentrations in the therapeutic range. A number of barbiturates are not well extracted from toluene by tetrabutylammonium hydroxide because of ion-pair partitioning. The extraction efficiency of barbiturates from toluene is much improved by back-extraction of the toluene layer with a tetramethylammonium hydroxide solution; clean chromatograms are obtained from blank plasma when the toluene layer is back-extracted, instead of evaporated, prior to derivative formation. This modification is introduced in the second method; an aliquot of the tetramethylammonium hydroxide layer is subjected to a pre-column butylation procedure which converts the barbiturates completely without any decomposition in the injection port; the sensitivity is at least as good as that of the on-column technique.

Barbiturates are often converted to derivatives before passage through a gas chromatographic column. In a much-used on-column flash methylating method [1—3], the drug is extracted from the plasma with toluene and back-extracted with a small volume of a methanolic solution of trimethylphenylammonium hydroxide (TMPAH) or tetramethylammonium hydroxide (TMAH), of which an aliquot is injected into the gas chromatograph. The compound is methylated in the injection port at high temperatures. The simplicity of the method is attractive. Its main disadvantages are: the formation of decomposition products at the high temperatures in strongly alkaline medium during the methylation process; the re-methylation of drugs that are biologically de-methylated, resulting in the same end-product for the parent compound and the metabolite; and the possibility of a reduction in column life caused by multiple injections of strongly alkaline solutions.

Butylation of the compounds eliminates the problem of the formation of

the same end-product from different compounds. However, on-column flash butylation [4, 5] with tetrabutylammonium hydroxide (TBAH) also gives rise to the formation of more than one product during conversion. This can be overcome by the alkylation of the compounds before injection into the gas chromatograph, as described by Greeley [6] and by IJdenberg [7]. In this paper, determinations of pentobarbital in plasma by an on-column flash butylation technique and by a pre-column butylation technique based on Greeley's method [6] are described. The extraction of other barbiturates in both procedures is also investigated.

## EXPERIMENTAL

### *Apparatus*

A Varian-Aerograph Model 2700 gas chromatograph equipped with flame ionization detectors was used for the on-column butylation experiments. The glass column (180 cm × 6 mm o.d.) was packed with 3% OV 17 on 100—120-mesh Gas-Chrom Q (Applied Science Labs., State College, Pa.), conditioned overnight at 250°C (40 ml $min^{-1}$ nitrogen flow), and silylated at 250°C by injecting five 10-$\mu$l portions of Silyl 8 (Pierce, Rockford, Ill., U.S.A.). The operating conditions were: injection port temperature, 325°C; column tempera ture, 215°C; detector temperature, 260°C; carrier gas (nitrogen) flow-rate, 40 ml $min^{-1}$; hydrogen flow-rate, 40 ml $min^{-1}$; air flow-rate, 350 ml $min^{-1}$.

A Packard-Becker Model 419 gas chromatograph equipped with flame ionization detectors was used for the pre-column butylation experiments. The glass column (150 cm × 2 mm i.d.) was packed with 3% OV 17 on 100—120-mesh Chromosorb WHP (Chrompack, Middelbury, The Netherlands), and conditioned overnight at 250°C (20 ml $min^{-1}$ nitrogen flow). The operating conditions were: injection port temperature, 230°C; column temperature, 195°C; detector temperature, 230°C; carrier gas (nitrogen) flow-rate, 20 ml $min^{-1}$; hydrogen flow-rate, 25 ml $min^{-1}$; air flow-rate, 250 ml $min^{-1}$. Peak areas were obtained with the chromatographic Data Analyser System IV B (Spectra Physics, Santa-Clara, CA). Ultraviolet absorption of barbiturate solutions was measured with a Unicam SP 500 spectrophotometer with matched 1-cm cells.

### *Reagents and materials*

Commercial pentobarbital, secobarbital, heptobarbital, phenobarbital, mephobarbital and hexobarbital were used without purification. TBAH (1 M in methanol) was obtained from Eastman-Kodak, TMAH (20% in methanol) and 1-iodobutane from Aldrich Chemicals, and dioctyl sodium sulfosuccinate (DOSS) from Merck. Other solvents and reagents were of analytical grade.

### *Procedure A. Determination of pentobarbital in plasma with on-column butylation*

Prepare an internal standard solution (8 $\mu$g $ml^{-1}$) of mephobarbital in

toluene, containing 1% (v/v) of methanol. Prepare the TBAH solution by mixing equal volumes of the methanolic 1 M solution and water. Add 1 ml of 1 M hydrochloric acid and 5.00 ml of the internal standard solution to 1.00 ml of plasma in a centrifuge tube and shake for 15 s with a vortex-type mixer. Centrifuge for 3 min at 2500 G, transfer the toluene layer to a centrifuge tube, and shake for 1 min with 50 $\mu$l of TBAH solution. After centrifugation for 1 min at 2500 G, inject 2.5 $\mu$l of the TBAH layer slowly (5 s) into the gas chromatograph.

*Procedure B. Determination of pentobarbital and mephobarbital in plasma with pre-column butylation*

Prepare an internal standard solution (10 $\mu$g ml$^{-1}$) of heptobarbital in toluene containing 1% (v/v) of methanol. Add 0.1 ml of 4 M hydrochloric acid and 3.00 ml of the internal standard solution to 1.00 ml of plasma in a centrifuge tube. Shake for 30 s (vortex-type mixer), centrifuge for 3 min at 2500 G, transfer the toluene layer to a centrifuge tube, and shake for 1 min with 25 $\mu$l of 20% TMAH in methanol. Centrifuge for 2 min at 2500 G, and transfer 10 $\mu$l of the TMAH layer to a glass capillary tube (5 cm × 3 mm i.d.); add 35 $\mu$l of N,N-dimethylacetamide (DMA) and 10 $\mu$l of 1-iodobutane. Mix the contents of the tube; after 5 min, centrifuge for 1 min at 2500 G. Inject 2—4 $\mu$l of the clear supernatant solution into the gas chromatograph.

*Procedure C. Extraction of barbiturates from water with toluene*

Prepare separate solutions (40 $\mu$g ml$^{-1}$) of pentobarbital, secobarbital, heptobarbital, phenobarbital, mephobarbital and hexobarbital in water. Add 3.00 ml of 1 M hydrochloric acid to 10.00 ml of the barbiturate solution and shake for 1 min with 30.0 ml of toluene containing 1% (v/v) of methanol. Centrifuge for 5 min at 2500 G, and mix 5.00 ml of the clear aqueous phase with 1.15 ml of 1 M sodium hydroxide and 3.85 ml of 0.05 M borax solution (pH 10). Measure the absorbance of the resulting solution at 240 nm against a blank solution prepared by treating 10 ml of water in the same manner. Prepare standard solutions by adding, to 5.00 ml of a mixture of 3.00 ml of 1 M hydrochloric acid and 10.00 ml of barbiturate solution, 1.15 ml of 1 M sodium hydroxide and 3.85 ml of 0.05 M borax solution (pH 10). Measure the absorbance at 240 nm.

*Procedure D. Extraction of barbiturates from toluene with TMAH*

Prepare barbiturate standard I by dissolving pentobarbital, hexobarbital and phenobarbital in DMA (3 mg ml$^{-1}$ for each compound). Prepare barbiturate standard II by dissolving secobarbital, mephobarbital and heptobarbital in DMA (3 mg ml$^{-1}$ for each compound).

For barbiturate solution I, dissolve 30 mg of each of pentobarbital, hexobarbital and phenobarbital in 250 ml of toluene. For barbiturate solution II, dissolve 30 mg of each of secobarbital, mephobarbital and heptobarbital in 250 ml of toluene.

Internal standard solution I contains 1 mg $ml^{-1}$ of heptobarbital in toluene; internal standard solution II contains 1 mg $ml^{-1}$ of phenobarbital in toluene.

Shake 5.00 ml of barbiturate solution I (vortex-type mixer) for 1 min in a centrifuge tube with 100 $\mu$l of 20% TMAH in methanol. Centrifuge for 3 min at 2500 G, and transfer 5.0 $\mu$l of the TMAH layer to a glass capillary tube (5 cm × 3 mm i.d.) Add 30 $\mu$l of internal standard solution I and 10 $\mu$l of DMA. Mix, add 10 $\mu$l of 1-iodobutane, mix, and after 5 min centrifuge for 1 min at 2500 G. Inject 1—2 $\mu$l of the clear supernatant solution into the gas chromatograph.

Mix 10.0 $\mu$l of barbiturate standard I in a glass capillary tube with 30 $\mu$l of internal standard solution I and 5 $\mu$l of 20% TMAH in methanol. Add 10 $\mu$l of 1-iodobutane, mix, and after 5 min centrifuge for 1 min at 2500 G. Inject 1—2 $\mu$l of the clear supernatant solution into the gas chromatograph. Follow the same procedure with barbiturate solution II, internal standard solution II, and barbiturate standard II.

*Procedure E. Extraction of barbiturates from toluene by TBAH*

*Method E1.* Follow procedure D, but use a mixture of equal volumes of 1 M TBAH in methanol and water instead of the TMAH solution (centrifugation after the addition of 1-iodobutane is not necessary).

*Method E2.* For each of the six barbiturates investigated, prepare a solution by dissolving 30 mg of the compound in 250 ml of toluene. Shake 50.0 ml of barbiturate solution with 1.00 ml of the TBAH solution in methanol/water described above for 1 min. Filter the toluene layer through phase-separating paper (Whatman 1PS). Evaporate 40.0 ml of the clear toluene solution under reduced pressure. Dissolve the residue in 5 ml of a 3 M sodium acetate—acetic acid buffer solution (pH 2.8) and add 10 ml of water, 45 ml of chloroform, and 5 drops of a solution of methyl yellow in ethanol (0.05%). Shake well, and titrate with 0.005 M DOSS solution, shaking the mixture after each addition, until the yellow colour of the chloroform layer changes to orange. Prepare and titrate blank solutions by treating 50-ml portions of toluene in the same manner.

## RESULTS AND DISCUSSION

The determination of pentobarbital in plasma with on-column flash butylation described (Procedure A), is analogous to MacGee's method [1] with TMAH replaced by TBAH. The TBAH solution in methanol had to be diluted with water to reduce its miscibility with toluene. Slow injection of the TBAH layer produced higher peaks, in agreement with MacGee's findings [8]. Typical chromatograms obtained with blank plasma and with plasma to which pentobarbital and mephobarbital were added, are shown in Fig. 1. Both barbiturates give rise to a major peak and at least one minor peak, as reported previously[5].

A calibration plot was constructed by applying the proposed procedure to

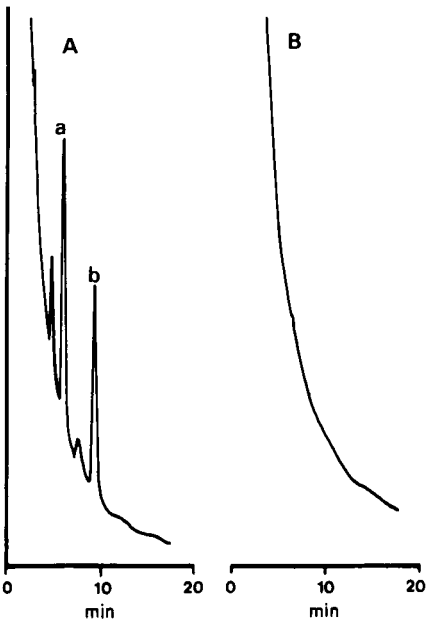


Fig. 1. On-column flash butylation. Chromatogram B was obtained from an extract of blank plasma, and chromatogram A from an extract of blank plasma spiked with pentobarbital (a) and mephobarbital (b). For chromatographic conditions and extraction procedure, see Procedure (A).

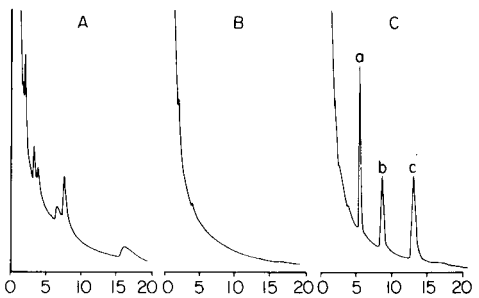


Fig. 2. Pre-column butylation. Chromatogram A was obtained by injection of the butylated residue of the toluene extract of blank plasma; chromatogram B from blank plasma; chromatogram C from blank plasma spiked with pentobarbital (a), mephobarbital (b), and heptobarbital (c). For chromatographic conditions and extraction procedure, see Procedure B.

plasma samples (1.0 ml) spiked with 0.5—15 $\mu$g of pentobarbital. Following chromatography, the heights of the peaks corresponding to the butylated products of pentobarbital and mephobarbital (Fig. 1, peak a and peak b, respectively) were measured and the peak-height ratios were plotted against the concentration of pentobarbital in the sample. The results are summarized in Table 1. The calibration plot was a straight line through the origin. The sensitivity of the method is sufficient for monitoring pentobarbital plasma concentrations in the therapeutic range. The absolute recoveries of pentobarbital and mephobarbital were determined by comparing the peak areas following this procedure with the peak areas obtained by injection of an aliquot of a solution of pentobarbital and mephobarbital in the TBAH solution. No correction was made for the volume change of the TBAH layer after extraction. The (apparent) absolute recoveries were 51% for pentobarbital ($n$ = 10, c.v. = 8%) and 20% for mephobarbital ($n$ = 10, c.v. = 11%). In order to determine the cause of these rather poor recoveries, the efficiency of the

TABLE 1

On-column flash butylation. Peak-height ratios of pentobarbital to mephobarbital (internal standard), and coefficients of variation (c.v.), obtained with plasma samples (1 ml) containing 0.5—15 $\mu g\ ml^{-1}$ of pentobarbital

| Concentration ($\mu g\ ml^{-1}$) | p.h.r.[a] | p.h.r./concentration | c.v. (%) |
|---|---|---|---|
| 0.5 | 0.065 | 0.130 | 16 |
| 2.5 | 0.338 | 0.135 | 5.5 |
| 5 | 0.649 | 0.130 | 3.1 |
| 7.5 | 1.007 | 0.134 | 3.6 |
| 10 | 1.358 | 0.136 | 2.7 |
| 15 | 2.051 | 0.137 | 3.8 |

[a]p.h.r. = Peak-height ratio. Each ratio is the mean value of 6 determinations.

extraction procedure was investigated for pentobarbital, mephobarbital and four other barbiturates. The percentage of barbiturate extracted from acidified water with toluene, containing 1% of methanol, was calculated from the u.v. absorbances of barbiturate solutions before and after extraction (Procedure C). Of the six barbiturates, only heptobarbital (23%) is poorly extracted: phenobarbital was extracted to the extent of 60% and the others at >85%. The extraction of heptobarbital was much improved with diethyl ether—toluene mixtures (results not shown).

The extraction of barbiturates from toluene with a small volume of TBAH solution was investigated by a gas chromatographic technique (Procedure E, method 1). Following chromatography, the percentage of the extracted drug was calculated from the resulting peak-area ratios (barbiturate/internal standard). A correction was made for the 10% reduction in volume of the TBAH layer with extraction. The results (Table 2) indicate that the rather poor recoveries from plasma of pentobarbital and mephobarbital, obtained with the extraction procedure preliminary to the on-column flash butylation,

TABLE 2

Extraction of barbiturates from toluene with solutions of TBAH and of TMAH

| Compound | Extraction with TBAH (%) | | Extraction with TMAH (%) |
|---|---|---|---|
| | Determined by titration[a] | Determined by g.l.c.[a] | |
| Pentobarbital | 59 | 52 | 94 |
| Secobarbital | 43 | 38 | 96 |
| Heptobarbital | 97 | 85 | 93 |
| Phenobarbital | 98 | 93 | 93 |
| Mephobarbital | 24 | 19 | 87 |
| Hexobarbital | 28 | 25 | 77 |

[a]Each result is the mean of 4 pairs of determinations.

are caused by the back-extraction step of the compounds from toluene with TBAH. Borg and Schill [9] found that barbiturates can be extracted into chloroform, in their monovalent anionic form, as ion-pairs, from aqueous alkaline solutions. The influence of ion-pair partitioning on the extraction efficiency of the barbiturates in the toluene—TBAH system was investigated (Procedure E, method 2) by titration of the $TBA^+$ ions in the toluene layer after extraction by a modification of an earlier procedure [10, 11]. The results correspond well with those of the gas chromatographic technique (Table 2), indicating that, after extraction, the barbiturates remain in the toluene mainly as ion-pairs with $TBA^+$ as the counter-ion. Borg and Schill [9] concluded that ion-pairs were not formed with the divalent anions of the barbiturates. In strongly alkaline solutions, the second dissociation equilibrium of the non-*N*-methylated barbiturates therefore influences the extraction of the monovalent barbiturate anion with $TBA^+$, resulting in an optimum pH for the extraction of the barbiturate from alkaline solutions. An optimum pH for the extraction (as ion-pairs) of *N*-methylated barbiturates (e.g. hexobarbital and mephobarbital) does not exist; ion pairs of these compounds are equally well extracted from strongly alkaline solutions, and this may explain the poor extraction of these compounds from toluene with the TBAH solution.

The extraction of the barbiturates from toluene can be much improved by the use of a methanolic TMAH solution instead of TBAH, as shown by the results in Table 2 (Procedure D; a correction was made for the 25% reduction in volume of the TMAH layer with extraction.)

With Greeley's pre-column butylation method [6] the barbiturates are almost completely converted to one product. The excess of TMAH in the reaction mixture is removed by the addition of an excess of 1-iodobutane, yielding 1-butanol and TMA-iodide (precipitate). The resulting solution is therefore practically neutral. An obvious procedure for the determination of barbiturates in plasma with the use of pre-column butylation involves extraction of the plasma with toluene, evaporation of the organic solvent instead of back-extraction, and butylation of the residue. A typical chromatogram of blank plasma, treated in this manner, is shown in Fig. 2A. A number of potentially interfering peaks in the chromatogram can be eliminated by extraction of the compounds from the toluene layer with TBAH solution (Fig. 1) or with TMAH solution (Fig. 2). A procedure for the determination of pentobarbital and mephobarbital in plasma was based on Greeley's pre-column butylation method [6] following extraction of the compounds and internal standard from acidified plasma with toluene, and back-extraction of the toluene layer with methanolic TMAH solution (Procedure B).

A typical chromatogram is shown in Fig. 2C. A calibration plot was constructed from plasma samples spiked with pentobarbital and mephobarbital ($0.5—10\ \mu g\ ml^{-1}$) by plotting the peak-height ratios for pentobarbital/internal standard and mephobarbital/internal standard against the pentobarbital and mephobarbital concentrations, respectively. The results are summarized in Table 3. For both compounds the calibration was a straight line through the

TABLE 3

Pre-column butylation. Peak-height ratios of pentobarbital to heptobarbital (internal standard), and of mephobarbital to heptobarbital, and coefficients of variation (c.v.), obtained with plasma samples (1 ml) containing 0.5—10 $\mu g\ ml^{-1}$ of pentobarbital and mephobarbital

| Concentration ($\mu g\ ml^{-1}$) | Pentobarbital | | | Mephobarbital | | |
|---|---|---|---|---|---|---|
| | p.h.r.[a] | p.h.r./concentration | c.v. (%) | p.h.r.[a] | p.h.r./concentration | c.v. (%) |
| 0.5 | 0.186 | 0.372 | 7.4 | 0.084 | 0.168 | 7.8 |
| 2.5 | 0.973 | 0.389 | 5.2 | 0.415 | 0.166 | 3.1 |
| 5 | 1.908 | 0.382 | 4.2 | 0.828 | 0.166 | 3.5 |
| 7.5 | 2.872 | 0.383 | 3.6 | 1.256 | 0.167 | 3.6 |
| 10 | 3.677 | 0.377 | 4.6 | 1.677 | 0.168 | 4.1 |

[a]p.h.r. = Peak-height ratio. Each ratio is the mean value of 6 determinations.

origin. The precision at a concentration of 0.5 $\mu g\ ml^{-1}$, which is about the lowest measurable pentobarbital plasma level with the on-column flash butylation technique, is still fairly good because of the better extraction efficiency and the much smaller solvent peak.

The determination of barbiturates in plasma by the pre-column butylation procedure, compared with the on-column technique, involves more manipulations and the time needed for the analysis of 10 samples is about 20 min longer. However, decomposition of the products during the butylation procedure does not occur; the lower injection port temperature, and the injection of solutions from which the excess of quaternary ammonium base has been removed, may prolong the column life.

REFERENCES

1 J. MacGee, Anal. Chem., 42 (1970) 421.
2 E. B. Solow and J. B. Green, Neurology, 22 (1972) 540.
3 R. J. Perchalski and B. J. Wilder, in C. E. Pippenger, J. K. Penry and H. Kutt (Eds.), Antiepileptic Drugs: Quantitative Analysis and Interpretation, Raven Press, New York, 1978, p. 75.
4 M. Kowblansky, B. M. Scheinthal, G. D. Cravello and L. Chafetz, J. Chromatogr., 76 (1973) 467.
5 W. D. Hooper, D. K. Dubetz, M. J. Eadie and J. H. Tyrer, J. Chromatogr., 110 (1975) 206.
6 R. H. Greeley, Clin. Chem. N.Y., 20 (1974) 192.
7 F. N. IJdenberg, Pharm. Weekbl., 110 (1975) 21.
8 J. MacGee, Clin. Chem. N.Y., 17 (1971) 587.
9 K. O. Borg and G. Schill, Acta Pharm. Suec., 5 (1968) 323.
10 G. N. Thomis and A. Z. Kotionis, Anal. Chim. Acta, 14 (1956) 11.
11 Anon., Pharm. Weekbl., 104 (1969) 1247.

*Analytica Chimica Acta*, 105 (1979) 147—152


# THE DEGRADATION OF ACIDIC POLYSACCHARIDES DURING STRUCTURAL ANALYSIS INVOLVING PERMETHYLATION†

D. M. W. ANDERSON* and A. STEFANI

*Department of Chemistry, The University, Edinburgh EH9 3JJ (Gt. Britain)*

(Received 23rd September 1978)

SUMMARY

The extent of the degradation of gum exudates from *Acacia* and *Combretum* spp. in different methylation procedures has been studied. Methylation of *C. nigricans* gum with the sodium hydride—iodomethane—dimethyl sulphoxide system caused losses of rhamnose and galacturonic acid that did not occur with two other systems. In a study of the extent of the degradation suffered by the gums from *Acacia seyal* and *Combretum nigricans* during methylation with the Haworth method, partially methylated products, isolated at intervals during the reaction, were analysed: *C. nigricans* gum suffered much more rapid and extensive degradation than *A. seyal* gum; this degradation must be taken into account in structural analyses of gums of the *Combretum* genus.

In the structural analysis of complex polysaccharides, procedures involving attempted permethylation of the natural product, methanolysis, and analysis of the subsequent complex mixture of *O*-methyl sugars are widely used. Of the many methylation methods proposed, those of Purdie and Irvine [2], Haworth [3], Kuhn et al. [4, 5] and Hakomori [6] are the most frequently used; efforts to improve their efficiency [7] and to devise new procedures [8, 9] continue. An ideal system, giving complete methylation in high yield, in few stages, with minimal degradation of the starting material, has yet to be devised. For some polysaccharides, the Hakomori method [6] gives high yields in few stages but it gives selective cleavage of labile rhamnose groups in some acidic polysaccharides [10]; the possibility of other forms of degradation has been discussed [11].

Prior to undertaking the extensive analyses involved in a structural study of a complex polysaccharide, preliminary experiments to assess the lability of the polysaccharide in different methylation systems are desirable [10]; all too frequently, structural studies are based on the product from only one attempted methylation and steps are not taken to assess the extent and/or nature of the degradation that inevitably results from the use of sequential treatments, involving drastic reaction conditions, in attempts to secure a satisfactorily high methoxyl content regardless of other considerations.

†Part 52 of the Series "Studies of Uronic Acid Materials". For part 51, see [1].

This paper reports experiments undertaken to assess the lability during methylation of *Combretum nigricans* gum, which was shown in other preliminary experiments to have some unusual structural features and interesting industrial properties [12].

## EXPERIMENTAL

### *Origin of gum samples*

Gum from *Combretum nigricans* Lepr. ex Guill. et Perr. var. Eliottii (Engl. & Diels) Aubrèv. was collected by Mr. Oseni, Western Region Department of Forestry, Ibadan, Nigeria. Gum from *Acacia seyal* Del. var. *seyal* was collected at Umm Ruaba Forest Reserve by Mr. A. G. Seif-el-Din, Gum Research Officer to the Republic of the Sudan.

### *Analytical methods*

Standard methods of analysis for the determination of nitrogen, methoxyl, intrinsic viscosity and weight-average molecular weight, and chromatographic conditions for the separation of methylated sugars after methanolysis, were as described previously [13].

### *Methylations of* Combretum nigricans *gum*

These were conducted in a three-necked 500-ml Pyrex flask containing a magnetic stirrer bar and placed in an ice-bath; nitrogen was introduced via a rubber septum in one neck, a condenser was fitted to the middle neck, and the remaining neck was stoppered except when additions of reagents were made.

In the Haworth methylation [3], the gum (2.4 g), dissolved in 50 ml of water, was placed in the 3-necked flask; sodium hydroxide (30% w/v, 56.8 ml) and dimethyl sulphate (40.7 ml) were added dropwise, and the mixture was stirred gently for 24 h. The contents of the flask were adjusted to pH 7 (sodium hydroxide) and dialysed against running tap water for 24 h. The dialysed solution was returned to the flask, sodium hydroxide (30% w/v, 92.2 ml) and dimethyl sulphate (66.1 ml) were added dropwise, and the mixture was stirred gently for 24 h. After adjustment to pH 7 (sodium hydroxide) the solution was dialysed for 4 d, and then freeze-dried. Yield, 73% (product A, Table 1). Found: methoxyl, 35%; $(\alpha)_D = -51°$.

In the Hakomori methylation [6], the gum (1.0 g), dissolved in freshly distilled dimethyl sulphoxide (100 ml), was placed in the 3-necked flask. Sodium hydride (2 g) was added in ca. 0.1-g portions during 1 h, with gentle stirring, and iodomethane (10 ml) was added dropwise over 2 h. The stirring was continued for 24 h. A further 3 additions of sodium hydride (each of 1 g) and of iodomethane (each of 5 ml) were made similarly on 3 successive days. The mixture was then dialysed for 3 d against running tap-water and freeze-dried. Yield, 82% (Product B, Table 1). Found: methoxyl, 30%; $(\alpha)_D = -53°$.

TABLE 1

Proportions of methanolysis products obtained from *C. nigricans* gum methylated by three different systems

| *O*-methyl sugars | Methylated product | | |
|---|---|---|---|
| | A Haworth method | B Hakomori method | C NaOH -DMSO -DMS |
| 2,3,4-Tri-*O*-methyl-L-rhamnose | 2.2 | 0 | 4.4 |
| 3,4-Di-*O*-methyl-L-rhamnose | 9.8 | 10.0 | 9.9 |
| 3-*O*-Methyl-L-rhamnose | 2.4 | 3.4 | 2.4 |
| 2,3,5-Tri-*O*-methyl-L-arabinose | 14.5 | 17.8 | 18.8 |
| 2,3,4-Tri-*O*-methyl-L-arabinose | 0.2 | 0.6 | 0.5 |
| 3,5-Di-*O*-methyl-L-arabinose | 1.3 | 0.8 | 1.3 |
| 2,5-Di-*O*-methyl-L-arabinose | 1.3 | 0.3 | 1.3 |
| 2,4-Di-*O*-methyl-L-arabinose | 22.3 | 18.5 | 17.9 |
| 2,3,4,6-Tetra-*O*-methyl-D-galactose | 22.2 | 11.7 | 11.5 |
| 2,3,6-Tri-*O*-methyl-D-galactose | 6.0 | 13.9 | 8.7 |
| 2,3,4-Tri-*O*-methyl-D-galactose | 3.2 | 8.7 | 6.5 |
| 2,3,4-Tri-*O*-methyl-D-glucuronic acid[a] | 11.0 | 13.8 | 13.7 |
| 2,3,4-Tri-*O*-methyl-D-galacturonic acid[a] | 1.2 | 0.3 | 1.0 |
| 2,3-Di-*O*-methyl-D-galacturonic acid[a] | 2.3 | 0 | 1.9 |

[a]As methyl ester methyl glycoside.

In a methylation with sodium hydroxide—dimethyl sulphoxide—dimethyl sulphate [14], the gum (1.0 g), dissolved in freshly distilled dimethyl sulphoxide (100 ml), was placed in the 3-necked flask. Sodium hydroxide pellets (17.6 g) were added in small portions during 1 h, with adequate cooling. Dimethyl sulphate (42.3 ml) was then added, dropwise, during 0.5 h, and the mixture was stirred gently for 24 h. Sufficient water was added to dissolve a small residue of sodium hydroxide, which was then neutralized carefully (sulphuric acid). The solution was dialysed against running tap-water for 4 d, and then freeze-dried. Yield, 64% (Product C, Table 1). Found: methoxyl, 29%; $(\alpha)_D = -44°$.

*Analysis of methylated products A, B & C*

The methylated products A, B and C were methanolysed and the resulting mixtures of methylated sugars were examined by g.l.c. under standardized conditions [13]. The results (Table 1) indicate that extensive loss of chain-terminal rhamnose groups (determined, after methylation, as 2,3,4-tri-*O*-methyl-L-rhamnose) and of galacturonic acid (determined as 2,3-di- and 2,3,4-tri-*O*-methyl-D-galacturonic acid) took place in the Hakomori methylation (Product B), which is therefore unsatisfactory chemically for this gum. It was decided to assess the extent of the physical degradation of *C. nigricans* gum caused during a Haworth methylation, and to compare the results with

those given by a gum, of closely similar initial molecular weight, belonging to a more widely studied botanical group. *Acacia seyal* gum was chosen for this purpose.

*Haworth methylation of* Combretum nigricans *gum*

The gum (30.0 g) was added to water (900 ml); sodium hydroxide (100 ml, 30% w/v) was added to disperse the gel and give complete dissolution of the gum. The solution was filtered (muslin, followed by Whatman No. 1 paper). The methylation was carried out on 600 ml of the resulting solution under nitrogen at room temperature. The remainder of the solution was freeze-dried to give a reference sample of the unmethylated gum, for which analytical data are shown (sample C.N.) in Table 2.

To the gum solution (600 ml), dimethyl sulphate (23 ml) and sodium hydroxide (25 ml, 30% w/v) were added dropwise with gentle stirring during 3 h. At this stage a portion (ca. 100 **ml)** of the solution was removed, dialysed for 4 d and freeze-dried (yield, 2.3 g; sample Me 1, Table 2). To the residual bulk solution, further additions of dimethyl sulphate (17 ml) and sodium hydroxide (17 ml) were made dropwise over 3 h, after which a second portion (100 ml, Me 2) was removed and treated as above (yield, 2.5 g). The residual mixture was stirred gently overnight, then a third addition of dimethyl sulphate (20 ml) and sodium hydroxide (20 ml) was made dropwise over 3 h, after which a third portion (100 ml, Me 3) was removed, dialysed, freeze-dried etc., as described previously. This procedure was repeated a further 3 times, i.e. after further intervals of 3, 27 and 30 h. Six samples of gum of progressively increasing methoxyl content (Me 1—Me 6) were thus obtained after reaction for 3, 6, 27, 30, 51 and 54 h. Total yield of methylated products, 13.1 g. Analytical data for C.N. and Me 1—6 are given in Table 2.

*Haworth methylation of* Acacia seyal *gum*

The entire procedure described for *C. nigricans* gum was repeated for a sample of *Acacia seyal* gum, so that a reference sample of the unmethylated gum (A.S.) and 6 samples of gum (Me 1—6) corresponding to different stages of methylation were obtained. Total yield of methylated products, 15.0 g.

TABLE 2

Data[a] for partially methylated samples of *Combretum nigricans* gum (solubilized form)

| | C.N. | Me 1 | Me 2 | Me 3 | Me 4 | Me 5 | Me 6 |
|---|---|---|---|---|---|---|---|
| Period of methylation (h) | 0 | 3 | 6 | 27 | 30 | 51 | 54 |
| Nitrogen (%) | 0.10 | 0.03 | 0 | 0 | 0 | 0 | 0 |
| Specific rotation $(\alpha)_D$ in water (degrees) | −45 | −53 | −54 | −61 | −63 | −64 | −65 |
| Methoxyl (%) | 0.54 | 7.6 | 14.0 | 22.0 | 29.0 | 32.0 | 38.5 |
| Intrinsic viscosity, $\eta$ (ml $g^{-1}$) | 54 | 45 | 43 | 36 | 20 | 11 | 8 |
| Molecular weight, $\bar{M}_W$ ($\times 10^5$) | 9.6 | 2.9 | 2.8 | 2.6 | 2.2 | 1.7 | 1.6 |

[a]All data corrected to a dry-weight basis.

Analytical data for A.S. and Me 1—6 are given in Table 3. A portion of the dialysate from fraction Me 3 was concentrated (rotary evaporator, 30°C) to a syrup and examined by paper chromatography: a complex mixture of methylated sugars was present, for which spots giving $R_G$ 0.51 and $R_G$ 0.73, corresponding to di-*O*-methyl- and tri-*O*-methylgalactoses, were the most prominent.

## DISCUSSION

In the comparative methylations of *Combretum nigricans* gum, the Hakomori method gave the highest yield (82%) but selective elimination of chain-terminal rhamnose units and also of galacturonic acid occurred (Table 1). This has been explained [10] in terms of a β-elimination at C-4 of the uronic acid groups; *C. nigricans* gum therefore behaves similarly to some *Acacia* gums under Hakomori's conditions [6], which cannot be recommended for this type of polysaccharide. Whether this will be a useful generalization within the *Combretum* group must await further investigation: there is already evidence [12] that the *Combretum* genus, complex both botanically and chemically, gives at least two different structural types of gum polysaccharide; in only one of these do some of the rhamnose and uronic acid residues appear to occupy chain-terminal positions which are susceptible to the β-elimination reaction. There is no doubt that base-catalysed reactions occur at greatly increased rates in dimethyl sulphoxide, in which the strongly basic methylsulphinyl carbanion is readily formed [15], and that the Hakomori system is much more strongly alkaline in reaction [16] than a well-conducted Haworth methylation.

In view of the indications that, of the three methylation systems examined, the Haworth method appeared to give the best compromise available in terms of yield, methoxyl content, and freedom from selective elimination reactions, it was decided to test the stability of the *C. nigricans* gum molecule under the Haworth methylation conditions, which have been used the most extensively in gum structural analyses to date. Consideration of the data given in Tables 2 and 3 shows that although *A. seyal* gum quickly undergoes a decrease

TABLE 3

Data[a] for partially methylated samples of *Acacia seyal* gum

| | A.S. | Me 1 | Me 2 | Me 3 | Me 4 | Me 5 | Me 6 |
|---|---|---|---|---|---|---|---|
| Period of methylation (h) | 0 | 3 | 6 | 27 | 30 | 51 | 54 |
| Nitrogen (%) | 0.07 | 0 | 0 | 0 | 0 | 0 | 0 |
| Specific rotation $(\alpha)_D$ in water (degrees) | +57 | +49 | +48 | +46 | +45 | +44 | +42 |
| Methoxyl (%) | 1.5 | 12.1 | 20.4 | 23.4 | 36.2 | 38.8 | 39.0 |
| Intrinsic viscosity, $\eta$ (ml $g^{-1}$) | 12.7 | 14.3 | 14.7 | 14.3 | 13.2 | 11.1 | 11.0 |
| Molecular weight, $\bar{M}_w$ ($\times 10^5$) | 9.4 | 6.6 | 6.7 | 6.2 | 6.2 | 6.0 | 5.9 |

[a]All data corrected to a dry-weight basis.

in molecular weight from $9.4 \times 10^5$ to $6.6 \times 10^5$ within 3 h, during which time the nitrogen content is eliminated (possibly significantly), the molecular weight undergoes little further reduction over 54 h and the intrinsic viscosity decreases slightly. The specific rotation steadily becomes less positive as the methoxyl content increases. With *C. nigricans* gum, the optical rotation steadily becomes more negative as the methoxyl content increases, but the molecular weight suffers a much greater % decrease than *A. seyal* gum within 3 h, and, furthermore, continues to decrease to 16% of its original value after 54 h. In addition, the intrinsic viscosity falls steadily over the 54 h period to ca. 15% of its original value. As with *A. seyal* gum, the major drop in molecular weight corresponds to elimination of the greater part of the original nitrogen content. Additional analytical evidence for the part played by the nitrogen content in terms of the physico-chemical behaviour of gum polysaccharides is difficult to ascertain.

Clearly there is a considerable difference between the stabilities of *C. nigricans* gum and *A. seyal* gum (a typical member of the *Gummiferae* division of the genus *Acacia*) under Haworth methylation conditions. It would appear that, whereas the *Acacia* gums are known to degrade through a process of elimination of labile groupings within the side-chains, with the galactan core of the highly branched molecule remaining intact, *Combretum nigricans* gum may belong to a class in which either a more readily identifiable repeating block structure occurs or labile sugar residues occur more extensively within the core of the gum molecule. To distinguish between these possibilities will require carefully designed analytical studies which must take into account the unusual lability established in this study.

We thank Rowntree-Mackintosh (York) for financial support and Mr. Oseni and Mr. Seif-el-Din for the supply of the gum specimens used.

REFERENCES

1 D. M. W. Anderson and P. C. Bell, Carbohydr. Res., 57 (1977) 215.
2 T. Purdie and J. C. Irvine, J. Chem. Soc., 83 (1903) 1021.
3 W. N. Haworth, J. Chem. Soc., 107 (1915) 8.
4 R. Kuhn, H. Trischmann and I. Löw, Angew. Chem., 67 (1955) 32.
5 K. Wallenfels, G. Bechtler, R. Kuhn, H. Trischmann and H. Egge, Angew. Chem., Int. Edn. Engl., 2 (1963) 515.
6 S. Hakomori, J. Biochem. (Tokyo), 55 (1964) 205.
7 S. Bose and P. L. Soni, Sci. Cult., 40 (1974) 368.
8 J. Arnaps, L. Kenne, B. Lindberg and J. Löngren, Carbohydr. Res., 44 (1975) C5.
9 J. M. Berry and L. D. Hall, Carbohydr. Res., 47 (1976) 307.
10 D. M. W. Anderson, I. C. M. Dea, P. A. Maggs and A. C. Munro, Carbohydr. Res., 5 (1967) 489.
11 H. Bjorndal, C. G. Hellerquist, B. Lindberg and S. Svenson, Angew. Chem., Int. Edn. Engl., 9 (1970) 610.
12 D. M. W. Anderson, Proc. Biochem., 13(7) (1978) 4.
13 D. M. W. Anderson and P. C. Bell, Anal. Chim. Acta, 79 (1975) 185.
14 H. C. Srivastava, S. N. Harshe and P. P. Singh, Tetrahedron Lett., 27 (1963) 1869.
15 E. J. Corby and M. Chaykovsky, J. Am. Chem. Soc., 84 (1962) 866; 87 (1965) 1345.
16 D. Martin, A. Weise and H.-J. Niclas, Angew. Chem., Int. Edn. Engl., 6 (1967) 318.

*Analytica Chimica Acta*, 105 (1979) 153—161


# PERIODATE OXIDATION ANALYSIS OF CARBOHYDRATES
## Part 12. Rapid Determination of Aldehydes in the Oxidation Products of Oligoglycosides by the Dithioacetal Method

SUSUMU HONDA*, YOSHIKO TAKAI and KAZUAKI KAKEHI

*Faculty of Pharmaceutical Sciences, Kinki University, Kowakae, Higashi-osaka (Japan)*

(Received 18th July 1978)

SUMMARY

A rapid and convenient analysis for glycosidic linkages in oligoglycosides was developed by improving the dithioacetal method. A sample (0.1—1 μmol) was oxidized with an aqueous or aqueous methanolic 0.05 M solution of sodium metaperiodate for 3 h at 50°C. An equivalent amount of silver nitrate was added and the mixture was evaporated to dryness. The residue was treated with a 2:1 (v/v) mixture of ethanethiol and trifluoroacetic acid for 10 min at 25°C, and subsequently trimethylsilylated with hexamethyldisilazane and trimethylchlorosilane for 30 min at 50°C. Gas chromatography of the product allowed the simultaneous determination of the conjugated aldehydes in the oxidation product with high reproducibility. The glycosidic linkages in various oligoglycosides were examined by this procedure.

A previous paper [1] reported a convenient method involving mercaptalation and trimethylsilylation for the simultaneous gas chromatographic determination of the conjugated aldehydes in periodate oxidation products, and applied this method to the examination of the glycosidic linkages in carbohydrate materials [2—5]. In applying this procedure to linkage analysis, samples are usually treated with periodate for a long time, below room temperature, to prevent non-specific oxidations which lead to abnormal reduction of periodate. However, as the object of this method is to determine the aldehydes in the products, and concomitant non-specific oxidation does not interfere with this determination, samples may be oxidized at higher temperatures to achieve economy of time. The mode of oxidation of a number of oligoglycosides has been examined at higher temperatures, and a limit of temperature for normal Malaprade oxidation has been obtained. Another problem in periodate oxidation analysis is that the oxidation products should be desalted, either by extraction with solvents [2] or by passage through resin columns [1, 3—5] before being subjected to component analysis. This desalting process is laborious and sometimes causes complete loss of the products, e.g. from ionic glycosides such as glycopeptides and glycoproteins. A procedure for processing the products of oxidation, so as to minimize analysis time, has also been devised.

## EXPERIMENTAL

### *Chemicals*

The reagents were of the highest grade commercially available. Pyridine, dehydrated by heating with barium oxide, was distilled before use. Samples of methyl α-D-xylopyranoside, methyl α-D-glucopyranoside, steroid glycosides and glycoproteins were obtained from Sigma Chemical Co. Methyl glucobiosides were prepared by Königs—Knorr condensation of the corresponding acetobromo sugars with methanol in the presence of silver carbonate [6], followed by deacetylation with methanolic sodium methoxide [7]. Samples of flavonoid and triterpenoid glycosides were gifts from Professor K. Takaishi of this faculty and Professor I. Kitagawa of Osaka University, respectively. The preparation of the authentic specimens of dithioacetal derivatives has been described [1].

### *Apparatus*

Gas chromatography was performed on a Shimadzu 4BMPF instrument equipped with a hydrogen f.i.d. A glass column (0.3 cm i.d., 2 m) packed with 3% OV-1 on Chromosorb W was used and the carrier gas (nitrogen) was regulated at 50 ml $min^{-1}$ throughout the work. In the analysis for glycosidic linkages in oligoglycosides, a gradient of 100 → 250°C (5° $min^{-1}$) was applied each time after injection of a sample. However, the column was maintained at 180°C for other purposes. Peaks were integrated by a Shimadzu Chromatopak E1A integrator. G.c.—m.s. of the compound giving peak 2 was carried out on a Shimadzu LKB 9000B spectrometer. The conditions for the column were the same as described above. The temperature of the ion source was 270°C and the spectrum was obtained at 70 eV.

The p.m.r. spectrum of the compound giving peak 2 was recorded at 60 MHz on a Hitachi R-20B spectrometer. The sample was dissolved in chloroform-*d* and the chemical shifts were referred to tetramethylsilane (internal standard).

### *Temperature dependence of the oxidation of methyl α-D-glucopyranoside with periodate*

A sample of this glycoside (100 μmol) was dissolved in 0.05 M sodium metaperiodate (20.0 ml) and the solution was kept in the dark at the temperature given in Fig. 1. Aliquots (2 ml) were removed at intervals and deionized by passage through a small column of Amberlite CG-120 ($H^+$-form, 0.5 ml) and CG-400 (acetate-form, 0.5 ml), and the column was washed with water (20 ml). The combined eluate and the washing fluid were concentrated and the volume was adjusted to 2.00 ml. Three 200-μl portions were evaporated to dryness, and the aldehydes in each residue were analyzed by the dithioacetal method [1]. The average value of three determinations is plotted in Fig. 1.

*Comparison of the methods of treatment for the products of oxidation*

A sample (10 μmol) of methyl α-D-xylopyranoside or methyl α-D-glucopyranoside was dissolved in 0.05 M sodium metaperiodate (2.00 ml) and the solution was kept for 3 h at 50°C in the dark. The reaction solution was cooled to room temperature and three 200-μl portions were worked up as follows. (a) The first aliquot was deionized by passing it through a column of Amberlite CG-120 ($H^+$-form, 0.5 ml) and CG-400 (acetate-form, 0.5 ml) and the column was washed with water (20 ml). The combined eluate and the washing fluid were evaporated to dryness. (b) A methanolic 1% solution of ethylene glycol (100 μl) was added to the second aliquot, and the mixture was allowed to stand for 15 min in the dark and then evaporated to dryness. (c) Silver nitrate solution (100 μl, 0.1 M) was added to the third aliquot with vigorous shaking, and the mixture was evaporated to dryness. Each resultant residue was subjected to component analysis by a slight modification of the dithioacetal method [1] with a mixture of ethanethiol and trifluoroacetic acid (2:1 v/v) and conducting mercaptalation for 10 min at 25°C.

*Isolation of the compound giving peak 2*

Methyl α-D-glucopyranoside (1 mmol) was dissolved in 0.05 M sodium metaperiodate (200 ml), and the solution was kept for 3 h at 50°C in the dark. A 1% methanolic solution of ethylene glycol (100 ml) was added, and the mixture was allowed to stand for 15 min in the dark and then evaporated to dryness. A mixture (2:1 (v/v); 20 ml) of ethanethiol and trifluoroacetic acid was added to the residue, and the mixture was kept for 10 min at 25°C with constant stirring. Then pyridine (50 ml) was added, the mixture was evaporated to dryness, and the residue was extracted with ether—n-hexane (1:1 (v/v), 30 ml). Evaporation of the solvent left a syrupy residue, which was fractionated on a column (2 cm i.d., 40 cm) of silica gel with the same solvent system. The 80—130-ml eluates were collected and evaporated to dryness to give a syrupy residue, which gave a gas chromatographic peak identical with peak 2.

*Procedure for the analysis of glycosidic linkages in oligoglycosides*

Dissolve a sample of an oligoglycoside (0.1—1 μmol) in an aqueous solution (200 μl) of 0.05 M sodium metaperiodate, and keep the solution for 3 h at 50°C in the dark. For water-insoluble glycosides, e.g. plant glycosides, oxidize a sample in aqueous methanolic solution (1:1 (v/v), 200 μl) of 0.05 M sodium metaperiodate for 3 h at 50°C, and treat the solution in a similar manner. Add an aqueous solution (100 μl) of 0.1 M silver nitrate with vigorous shaking, and evaporate the mixture in vacuo in a desiccator containing sodium hydroxide. Add a mixture (2:1 (v/v), 20 μl) of ethanethiol and trifluoroacetic acid to the residue, dissolve the dialdehyde product as completely as possible by gentle swirling, and keep the mixture for 10 min at 25°C. Then add successively a solution in pyridine (50 μl) of D-xylitol (internal standard, 1 μmol), hexamethyldisilazane (100 μl), and trimethylchlorosilane (50 μl), and keep

the mixture for 30 min at 50°C with occasional shaking. Centrifuge the mixture, and inject a 1-$\mu$l sample of the supernatant into the gas chromatography column. Identify the peaks of diethyldithioacetal derivatives by comparing their retention times with those of authentic specimens. Their molar response factors were recorded previously [1]. The peak of methyl $\beta$-D-glucopyranoside trimethylsilylate appears between the peak of the D-erythrose derivative and that of the hydroxymalonaldehyde derivative with a molar response factor of 0.87 relative to D-xylitol trimethylsilylate.

## RESULTS AND DISCUSSION

Figure 1 shows the reaction courses of periodate oxidation of methyl $\alpha$-D-glucopyranoside at various temperatures, as estimated by the yields of aldehydes in the products. Previous mechanistic studies showed [3] that the $C_3$—$C_4$ bond in this glycoside is first cleaved, and cleavage of the $C_2$—$C_3$ bond follows. The first cleavage results in the formation of dialdehyde **1**,

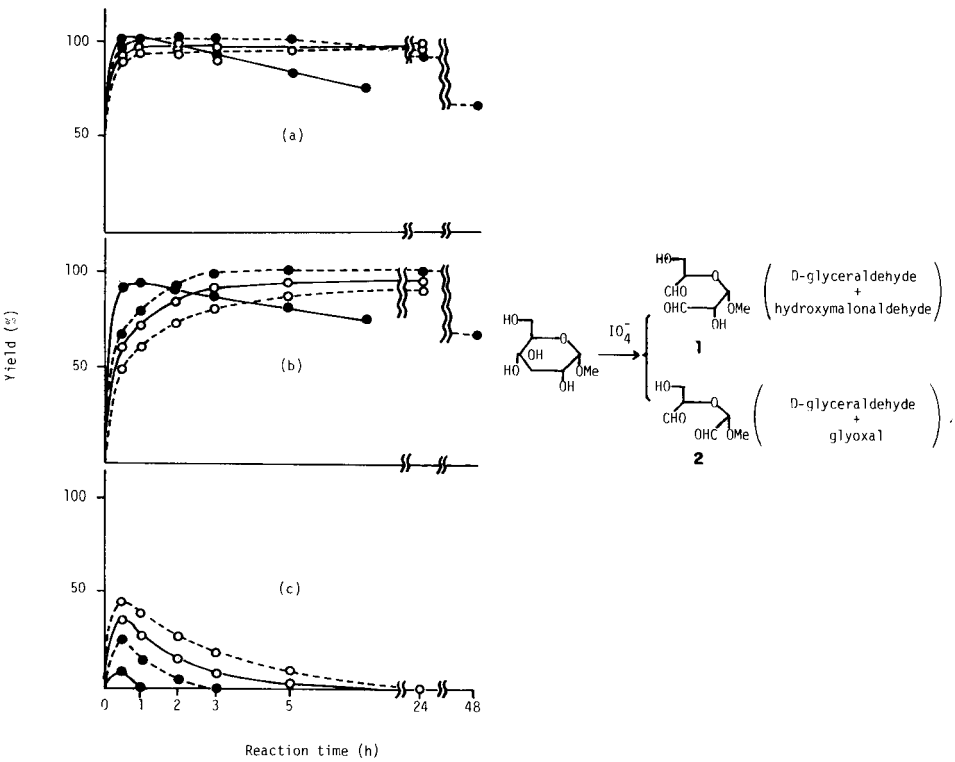


Fig. 1. Temperature dependence of the yields of aldehydes in the oxidation products of methy $\alpha$-D-glucopyranoside. (a) D-Glyceraldehyde, (b) glyoxal, (c) hydroxymalonaldehyde. ○--○, 25°C; ○—○, 37°C; ●--●, 50°C; ●—●, 75°C.

which is further oxidized to give dialdehyde 2. Therefore, a mixture of these two dialdehydes is found at initial stages of the oxidation, but the proportion of dialdehyde 1 continuously decreases, and that of dialdehyde 2 increases, as the reaction proceeds. D-Glyceraldehyde is the component common to these two dialdehydes, but the yields of hydroxymalonaldehyde and glyoxal are indicative of the yields of dialdehydes 1 and 2, respectively. It is observed from Fig. 1 that the yield of hydroxymalonaldehyde, i.e. that of dialdehyde 1, increased rapidly to a maximum after 1 h, but decreased gradually thereafter. Finally hydroxymalonaldehyde disappeared after 24 h at 25°C. The increase in the yield of glyoxal, i.e. that of dialdehyde 2, corresponded to the decrease in that of hydroxymalonaldehyde, and its yield reached almost 100% after 24 h. Elevation of temperature accelerated the reaction rate, so that disappearance of hydroxymalonaldehyde, and completion of the cleavage of both bonds, was observed in a shorter time (3 h at 50°C, 1 h at 75°C). However, considerable amounts of D-glyceraldehyde and glyoxal decomposed after 1 h at a temperature as high as 75°C, presumably from over-oxidation caused by partial hydrolysis. In contrast, appreciable decomposition was not observed during oxidation for 3 h at 50°C. Under these conditions oxidation proceeded completely in Malapradian fashion.

Figure 2(a) shows the gas chromatograms obtained for the products of oxidation for 3 h (50°C) of methyl α-D-xylopyranoside and methyl α-D-glucopyranoside, which were desalted with resins. The two component aldehydes in the product from the former glycoside (glycolaldehyde and glyoxal) were converted quantitatively to the diethyldithioacetal trimethylsilylate and the bis(diethyldithioacetal), observed as peaks 1 and 4, respectively. For the oxidation of the latter glycoside, the glycolaldehyde derivative (peak 1) was replaced by the D-glyceraldehyde derivative (peak 3).

When the dithioacetal method was applied to the products of oxidation, treated with ethylene glycol to stop oxidation but not desalted, the intensity of peak 4 diminished, but a new peak 2 appeared between peaks 1 and 3 (Fig. 2b). The product from methyl α-D-xylopyranoside gave a chromatogram in which both peaks 1 and 4 had small intensities, but peak 2 had larger intensity than that from methyl α-D-glucopyranoside. Both two-carbon aldehydes (glycolaldehyde and glyoxal) seem to give the same derivative. The mass spectrum of the compound of peak 2 gave a molecular ion at *m/e* 210, together with fragments of *m/e* 135 and 149 assignable to $C^+H\langle^{SEt}_{SEt}$ $M^+$ minus SEt, respectively (Fig. 3a). The p.m.r. spectrum of the peak 2 compound, isolated by liquid chromatography, indicated the presence (triplet) of the ethyl group and a methine proton (triplet) at ca. 1.3 and 4.0 ppm, respectively (Fig. 3b). Four methylene protons were also observed at 2.5—3.1 ppm (multiplet). These assignments suggest the structure shown in Fig. 3 for the compound of peak 2. This peak appeared when iodide, iodate, or periodate was mixed with the authentic specimen of dialdehyde 2 and the mixtures were analyzed by the dithioacetal method, but were not detected when salts such as sodium sulfate, sodium chloride, and sodium acetate were mixed with dialdehyde 2.

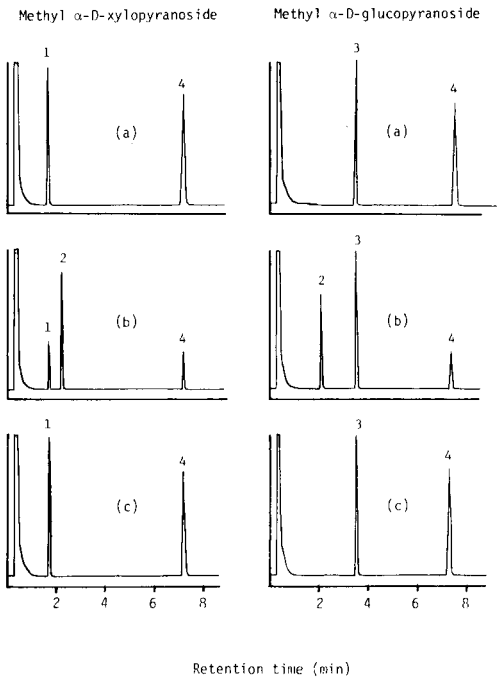


Fig. 2. Analysis of the conjugated aldehydes in the oxidation products of methyl α-D-xylo- and α-D-glucopyranosides by the dithioacetal method. The products of oxidation were (a) deionized, (b) treated with excess of ethylene glycol, and (c) treated with equimolar amounts of silver nitrate, prior to component analysis. Peak assignment: (1) glycolaldehyde diethyldithioacetal trimethylsilylate; (2) the structure of the compound is proposed in Fig. 3; (3) D-glyceraldehyde diethyldithioacetal trimethylsilylate; (4) glyoxal bis(diethyldithioacetal).

The formation of the compound giving peak 2 appears to result from catalytic action of the iodide ion and/or its oxidized species on glyoxal bis(diethyldithioacetal). Therefore, elimination of such ions offers the best way to restore the pattern of the chromatogram in which each aldehyde gives a single peak; removal of other ions seems to be unnecessary. Of the several attempts made to achieve this purpose, the addition of silver nitrate was the most effective and convenient. This treatment precipitated the iodide ion and its oxidized species as their silver salts, which do not interfere with the mercaptalation process because of their low solubility in the reagent. The chromatographic patterns were essentially the same as those for the desalted products (Fig. 2c).

Mercaptalation was carried out previously [1] with a mixture (10:1 (v/v)) of ethanethiol and trifluoroacetic acid, but the acid concentration was increased in the present work to increase the solubility of the oxidized samples and to reduce the analysis time. With a 2:1 (v/v) mixture, mercaptalation was complete in 10 min.

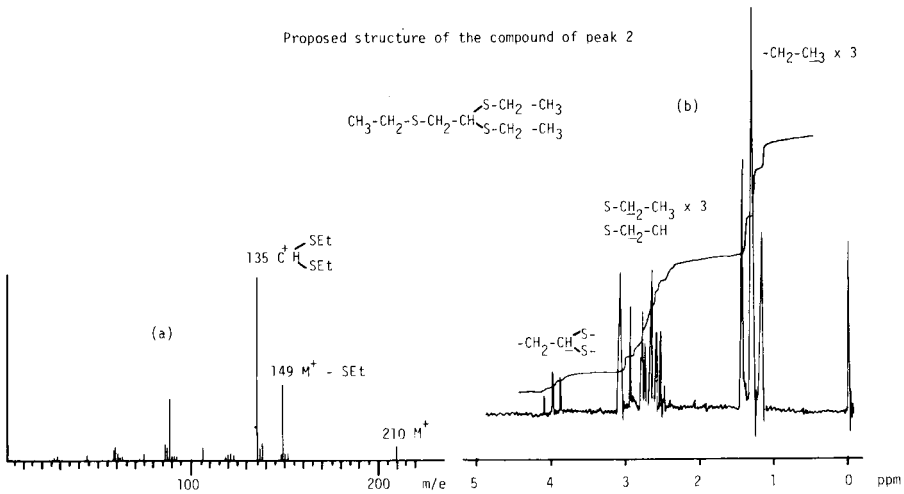


Fig. 3. Mass (a) and p.m.r. (b) spectra of the compound giving peak 2.

TABLE 1

Accuracy and precision of the determination of the conjugated aldehydes in the oxidation products of methyl α-D-glucopyranoside

| Amount of sample added (mol) | No. of detns. | Aldehyde found (mol) | | | | Molar ratio | |
|---|---|---|---|---|---|---|---|
| | | D-Glyceraldehyde | | Glyoxal | | D-Glycer-aldehyde/ glyoxal | C.v. (%) |
| | | Average value | C.v. (%) | Average value | C.v. (%) | | |
| $1.00 \times 10^{-7}$ | 8 | $7.5 \times 10^{-8}$ | 4.0 | $7.2 \times 10^{-8}$ | 3.9 | 1.03 | 3.9 |
| $1.00 \times 10^{-6}$ | 10 | $8.8 \times 10^{-7}$ | 4.2 | $8.8 \times 10^{-7}$ | 4.0 | 1.00 | 2.4 |

On the basis of these results, a standard rapid procedure for the analysis of the glycosidic linkages in oligoglycosides was devised. Table 1 shows the data obtained for the determination of the aldehydes present in oxidation products of methyl α-D-glucopyranoside given by this procedure. The recovery of aldehydes was low, especially when small amounts of sample were used; this is probably caused by adsorption on the surface of the precipitates. However, the molar proportions were not affected by the presence of the precipitates, and the reproducibility of their determination was high.

Table 2 gives the results of the application of this procedure to various kinds of oligoglycosides. The molar proportions of the aldehydes for all the methyl glucobiosides were in good agreement with those reported for the products of oxidation for 24 h at 25°C which were desalted with resins [1]. The data for the plant glycosides were also consistent with those obtained by oxidation for 48 h at 25°C and by ethanol extraction of the products [2].

TABLE 2

Determination of the conjugated aldehydes in the oxidation products of various oligoglycosides[a]

| Glycoside and its structure | Reaction time (h) | Molar proportion of aldehydes | | | | | | |
|---|---|---|---|---|---|---|---|---|
| | | GlycolA | GlycerA | LactA | E | GO | HMA | Other aldehyde |
| Methyl β-sophoroside β-Glc-(1→2)-β-Glc-Me | 3 | 0.00(0) | 2 (2) | 0.00(0) | 0.00(0) | 1.06(1) | 0.88(1) | — |
| Methyl β-laminaribioside β-Glc-(1→3)-β-Glc-Me | 3 | 0.00(0) | 1 (1) | 0.00(0) | 0.00(0) | 1.04(1) | 0.00(0) | Me-Glc 0.97(1) |
| Methyl β-cellobioside β-Glc-(1→4)-β-Glc-Me | 3 | 0.00(0) | 1 (1) | 0.00(0) | 0.95(1) | 2.09(2) | 0.00(0) | — |
| Methyl β-gentiobioside β-Glc-(1→6)-β-Glc-Me | 3 | 0.00(0) | 2 (2) | 0.00(0) | 0.00(0) | 2.06(2) | 0.00(0) | — |
| Rutin α-Rha-(1→6)-β-Glc-quercetin | 3 | 0.00(0) | 1 (1) | 1.06(1) | 0.00(0) | 1.83(2) | 0.28(0) | — |
| | 5 | 0.00(0) | 1 (1) | 1.02(1) | 0.00(0) | 1.92(2) | 0.12(0) | — |
| Naringin α-Rha-(1→2)-β-Glc-naringenin | 3 | 0.00(0) | 1 (1) | 1.00(1) | 0.00(0) | 0.75(1) | 1.25(1) | — |
| | 5 | 0.00(0) | 1 (1) | 1.05(1) | 0.00(0) | 0.90(1) | 1.11(1) | — |
| Robinin α-Rha-(1→6)-β-Gal-kaempferol α-Rha- | 3 | 0.00(0) | 1 (1) | 1.76(2) | 0.00(0) | 2.45(3) | 0.57(0) | — |
| | 5 | 0.00(0) | 1 (1) | 1.86(2) | 0.00(0) | 2.76(3) | 0.26(0) | — |
| Tomatine β-Xyl-(1→3), β-Glc-(1→2) / β-Glc-(1→4)-β-Gal-tomatidine | 3 | 0.96(1) | 1 (1) | 0.00(0) | 0.00(0) | 2.78(3) | 0.00(0) | Glc-Thr |
| Digitonin β-Xyl-(1→3), β-Glc-(1→3)-β-Gal-(1→2) / β-Glc-(1→4)-β-Gal-digitogenin | 3 | 0.95(1) | 1 (1) | 0.00(0) | 0.00(0) | 2.84(3) | 0.00(0) | — |
| Mi-saponin A α-Rha-(1→3)-β-Xyl-(1→4)-α-Rha-(1→2)-α-Ara- protobassic acid β-Glc- | 3 | 0.95(1) | 1 (1) | 0.90(1) | 0.00(0) | 2.81(3) | 1.00(1) | Xyl-DHBA |
| Sakuraso-saponin β-Glc-(1→2), α-Rha-(1→2)-α-Rha-(1→2)-β-Gal-(1→4) / β-GlcUA-protoprimulagenin A | 3 | 0.00(0) | 2 (2) | 1.96(2) | 0.00(0) | 1.88(2) | 1.90(2) | — |
| Ovalbumin (egg) | 3 | 0.00 | 1 | 0.00 | 0.00 | 1.23 | 0.00 | — |
| Bromelain (pineapple stem) | 3 | 0.00 | 1 | 0.00 | 0.38 | 1.64 | 0.00 | — |
| Ribonuclease B (bovine pancreas) | 3 | 0.00 | 1 | 0.00 | 0.00 | 1.27 | 0.00 | — |
| Invertase (yeast) | 3 | 0.00 | 1 | 0.00 | 0.48 | 0.49 | 0.54 | — |

[a]The numbers in parentheses are theoretical values. Ara, L-arabinose; Xyl, D-xylose; Gal, D-galactose; Glc, D-glucose; Rha, L-rhamnose; GlcUA, D-glucuronic acid; GlycolA, glycolaldehyde; GlycerA, D-glyceraldehyde; LactA, L-lactaldehyde; E, D-erythrose; Thr, D-threose; GO, glyoxal; HMA, hydroxymalonaldehyde; DHBA, dihydroxybutyraldehyde.

The difficultly oxidizable glycosides (rutin, naringin, and robinin) were also oxidized for 5 h at 50°C. Under these conditions, the data obtained were closer to the theoretical values. Unlike neutral glycosides, the samples of glycoproteins did not give appreciable amounts of aldehyde derivatives when the products were desalted with resins or extracted with ethanol. Although the data available were not always consistent with the glycosidic linkages reported in the literature because of the low purity of the samples, this improved procedure is also applicable to these ionic, high-molecular-weight glycosides.

The authors are grateful to Dr. T. Adachi (Japan Food Analysis Center) for the measurement of the mass spectrum. This work was supported in part by a Grant-in-Aid for Scientific Research from the Ministry of Education.

REFERENCES

1 S. Honda, Y. Fukuhara and K. Kakehi, Anal. Chem., 50 (1978) 55.
2 S. Honda, T. Takeda and K. Kakehi, Carbohydr. Res., submitted.
3 S. Honda, N. Hamajima and K. Kakehi, Carbohydr. Res., 68 (1979) 77.
4 S. Honda, Y. Ohkaru and K. Kakehi, Anal. Chim. Acta, 98 (1978) 85.
5 S. Honda, K. Kakehi and Y. Kubono, Carbohydr. Res., submitted.
6 W. Königs and E. Knorr, Ber., 34 (1901) 957.
7 G. Zemplèn and A. Kunz, Ber., 56 (1923) 1705.

*Analytica Chimica Acta*, 105 (1979) 163—176


# THE CORRECTION OF INTERFERENCE EFFECTS IN THE DETERMINATION OF THE RARE EARTH ELEMENTS AND HAFNIUM BY SPARK-SOURCE MASS SPECTROMETRY

J. R. BACON and A. M. URE*

*The Macaulay Institute for Soil Research, Craigiebuckler, Aberdeen AB9 2QJ (Gt. Britain)*

(Received 31st July 1978)

SUMMARY

Superpositional interferences from oxide ion species cause significant errors in the spark-source mass spectrometric determination of hafnium and the rare earth elements, when aluminium is used as the conducting matrix for samples such as rocks and soils. A mathematical correction procedure is described in which corrections are made in any particular exposure by using intensity measurements derived from that exposure alone. Its effectiveness is demonstrated for the USGS Standard Rocks BCR-1, AGV-1 and G-2.

Spark-source mass spectrometric (s.s.m.s.) methods for the determination of rare earth element contents in geological materials have been developed [1—7], all of which use graphite electrodes and photographic plate detection. Similar methods have been applied to the analysis of various rock samples [8—22]. There has been confusing evidence over the occurrence of interference effects, but their analytical significance in the determination of the rare earth elements has not been studied in detail. Whereas Morrison and Kashuba [7] found no evidence for the interference of barium oxide on the europium lines, Roaldset [17] considered it necessary to make a correction for this effect. Several workers have reported results for thulium despite the acknowledgement by Taylor and co-workers [4, 11] of possible interference from the carbon matrix which might account for the slightly high results for thulium reported by Graham and Nicholls [19]. A procedure based on ion-exchange chromatography and s.s.m.s. has been described [23—25] and although there was no evidence for the occurrence of barium and rare earth oxide species, there was some evidence for barium fluoride interference, presumably derived from the digestion procedure with hydrofluoric acid.

The s.s.m.s. procedure used in this work for the analysis of rocks and soils with aluminium as conducting powder has been described [26] and the occurrence of oxide interferences on the rare earth lines has been briefly discussed [27].

The theoretical resolution required to separate interfering oxide and halide species from element lines is at least 25,000 [28]. As this is unattainable in

practice, another approach has been adopted in which intensities in any one exposure are corrected for interference by a mathematical procedure using intensity information derived from that exposure alone.

The rare-earth group is self-contained: there are almost no other interferences from elements outside it, as the mass range is considerably higher that that of most other major or minor elements in the sample. Furthermore, most lines in this group have intensities which can be measured accurately on the same exposure, and this is a necessary condition for the application of a correction scheme. Most of the rare earth elements are multi-isotopic with the consequence that their interference effects are spread over several mass units and only a few lines are free from interference. This results in a complex spectrum which, however, facilitates the construction of a correction scheme because the relative isotopic abundances can be used to calculate the intensity of a particular isotope from that of another which is accessible to measurement.

## EXPERIMENTAL

An AEI MS702R spark-source mass spectrometer fitted with a modified automatic gap control system [29], an AEI ion-beam chopper and photographic plate detection system, was employed as already described [26, 27].

Electrodes are made in a PTFE mould by pressing hydraulically mixtures of 1 part of finely ground sample and 1 part of pure (99.999%) aluminium conducting powder containing 125 ppm indium (as oxide) and 100 ppm iridium (as ammonium chloroiridate) as internal standards. The sample electrode is sparked against a counter electrode of dagger-shaped pure aluminium foil, and exposures from $10^{-3}$ to 600 nanocoulombs (nC) are recorded on Ilford Q-2 photoplates. A continuous recording of the optical transmission of each exposure on the developed plate is made with a scanning microphotometer, and the relative intensities of the lines are calculated from an emulsion calibration curve. The intensities are then corrected, if necessary, for superpositional interferences as detailed below. From these corrected intensities of the internal standard lines and the analyte element lines, semiquantitative values for the concentrations of the elements in the sample are calculated by using correction factors for the variation of plate sensitivity with mass and for the ionization potential of the elements relative to that of the indium internal standard.

To obtain quantitative results, the semi-quantitative values are finally standardized by using relative sensitivity coefficients (RSC) which should be unity if these correction factors accurately model the situation, but which in practice lie between 0.5 and 2.0 for most elements [26].

## OCCURRENCE OF INTERFERENCES

The occurrence of interferences on some rare earth element lines in the analysis of standard rock samples was obvious from the failure of the line intensities of the isotopes of, for example, gadolinium to correspond to the

natural isotopic abundances. This is seen in Table 1 where, for five gadolinium isotopes of similar abundance, the measured relative intensities range over more than a factor of 6 from 6.2 to 40.7. If the small effects of coincident Dy isotopes of mass 156, 158 and 160 are neglected, the only source of these enhanced Gd intensities appears to be the oxide ions of La, Ce, Pr and Nd. Furthermore, when the RSC's were determined by analysing standard rock samples, it was observed (Table 2) that the light rare earth elements La, Ce, Pr and Nd had RSC's between 1.28 and 1.58 but those for Eu, Gd, Tb and Yb were considerably greater than 2.0. Only oxide ion interferences appear to offer an explanation of these enhanced values, and this enhancement pattern of the RSC's for the heavier rare earth elements will be shown to be consistent with the magnitude of the interference correction derived on the assumption that oxide ion interference is a major contributor.

The fact that certain oxide ions of barium (BaO) and the rare earth elements (LnO) are produced is demonstrated by the spectra (Figs. 1—3) of synthetic standard samples containing these elements as pure oxides (BaO and $Ln_2O_3$) in a simulated soil base whose composition (Table 3) approximately corresponds to that of a soil derived from an intermediate igneous rock or an average shale. It should be noted that the rare earth oxide ions, LnO, shown in the spectra are different in form from the oxides, $Ln_2O_3$, used to make up the standard samples. Three different standards (1, 2 and 3, Table 4) and appropriate dilutions with soil base, were prepared so that interfering species could

TABLE 1

Evidence for interference on gadolinium isotopes in USGS standard rock BCR-1

| Gd Isotopes | % Abundance [30] | Measured relative intensity | Possible interfering species |
|---|---|---|---|
| 155 | 14.87 | 34.8 | LaO |
| 156 | 20.56 | 40.7 | CeO |
| 157 | 15.70 | 6.6 | PrO |
| 158 | 24.77 | 11.7 | CeO NdO |
| 160 | 21.79 | 6.2 | NdO |

TABLE 2

Relative sensitivity coefficients derived from uncorrected s.s.m.s. analysis of USGS BCR-1 and published contents [24]

| Element | *m/e* | RSC | Element | *m/e* | RSC | Element | *m/e* | RSC |
|---|---|---|---|---|---|---|---|---|
| La | 139 | 1.28 | Eu | 151 | 3.11 | Er | 168 | 1.95 |
| Ce | 140 | 1.58 | Gd | 160 | 3.65 | Tm | 169 | 1.77 |
| Pr | 141 | 1.45 | Tb | 159 | 4.04 | Yb | 171 | 2.58 |
| Nd | 143 | 1.49 | Dy | 163 | 1.75 | Lu | 175 | 1.57 |
| Sm | 147 | 2.17 | Ho | 165 | 1.70 | | | |

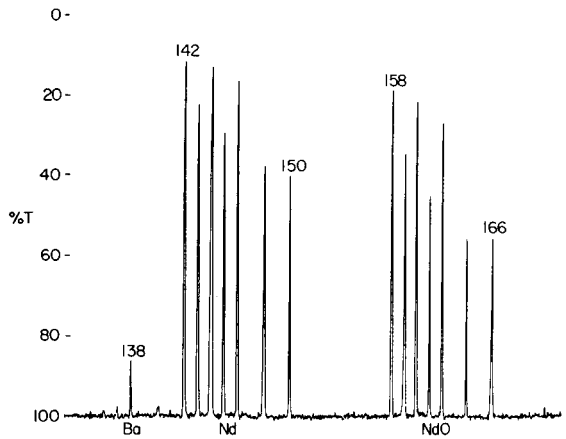


Fig. 1. Rare earth spectrum of soil base with neodymium oxide added (standard 3, Table 4).

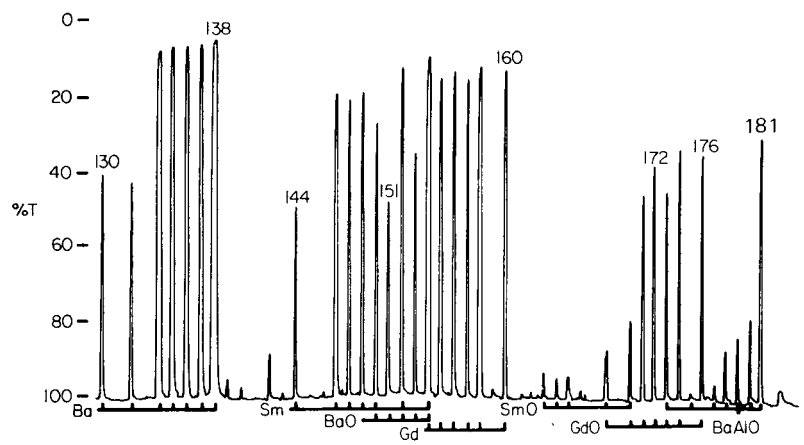


Fig. 2. Rare earth spectrum of soil base with barium, samarium and gadolinium oxides added (standard 2, Table 4).

be segregated from those interfered with. A fourth standard containing barium, all the rare earth elements and hafnium at levels similar to a rock or soil was also prepared.

In the spectrum of soil base alone with no added elements, only a small blank level of barium and traces of La and Ce are detectable. Figure 1 shows the spectrum of soil base with only neodymium oxide added (standard 3, Table 4). The isotope intensity pattern of neodymium is shown clearly with the same pattern being repeated 16 mass units higher, with almost the same intensity, this being the neodymium oxide group. The neodymium oxide lines occur at mass units *m/e* 158, 159, 160, 161, 162, 164 and 166, and it is evident that such lines would interfere severely with gadolinium, terbium and dysprosium isotopes occurring at the same mass units.

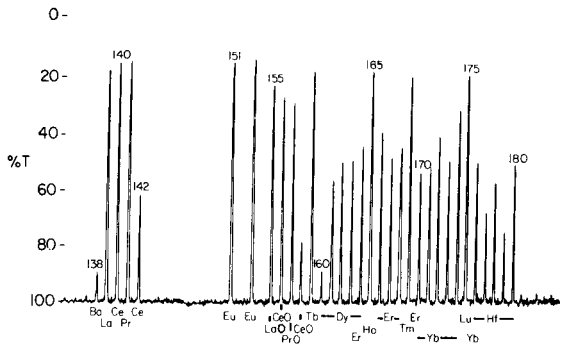


Fig. 3. Rare earth spectrum of soil base with oxides of all the rare earths added except those of neodymium, samarium and gadolinium (standard 1, Table 4).

TABLE 3

Composition of unignited synthetic soil base

| Component | Content (%) | Component | Content (%) | Component | Content (%) |
|---|---|---|---|---|---|
| $SiO_2$ | 62 | $Na_2CO_3$ | 3.5 | MgO | 2 |
| $Al_2O_3$ | 20 | $K_2SO_4$ | 3.5 | $TiO_2$ | 1 |
| $Fe_2O_3$ | 5 | $CaCO_3$ | 3 | | |

TABLE 4

Standards in ignited (1050°C) soil base

| No. | Standard |
|---|---|
| 1 | 1% rare earths (all rare earths except Gd, Sm and Nd) + 1% Hf, Y; and dilutions |
| 2 | 1% Gd, Sm and 10% Ba; and dilutions |
| 3 | 1% Nd; and dilutions |
| 4 | Complete standard; 1000 ppm Ba + 100 ppm Gd, Nd, Sm + 10 ppm other rare earths, Hf and Y |

Figure 2 shows the spectrum of soil base with barium, samarium and gadolinium oxides added; a similar pattern of oxide and an additional series of BaAlO composite oxide lines can be seen. It is noticeable, however, that the intensity of the oxide lines relative to the parent metal lines varies considerably for the different elements. For neodymium, the oxide lines are of similar intensity to the metal lines, for gadolinium about half, and for barium and samarium only a very small fraction. Two of the barium oxide lines occur at $m/e$ 151 and 153; because of the high contents of barium in most soils or rocks, these would interfere considerably with both europium isotopes.

Figure 3 shows the spectrum of soil base with addition of all the rare earth oxides except for neodymium, samarium and gadolinium and with no barium

added. The strong pattern of lanthanum, cerium and praseodymium oxide lines, which would interfere with the gadolinium isotopes, is clearly shown. The heavier rare earth elements form oxide lines less readily, as no lines for the oxides of Ho, Er, Tm, Yb and Lu at *m/e* greater than 180 are detected.

It can be argued that the production of oxide ions of an element reduces the intensity of the parent metal ion and that in consequence a specific correction for this reduced metal ion intensity is required in addition to the normal procedure adopted of standardizing the analysis by the use of RSC's. While these aspects are being further investigated, the experimental evidence to date suggests that, on the contrary, oxide ions are not necessarily produced at the expense of the parent metal ions and it is not anticipated that improvements in analytical precision could be achieved from this type of correction.

In summary, the analysis of the standard rock BCR-1 has provided evidence of interferences on the heavier rare earth elements which can satisfactorily be explained in terms of the superpositional oxide ion interference demonstrated with the synthetic standard samples. It is therefore essential to make a correction for these effects before accurate analysis is possible.

## INTERFERENCE CORRECTION

It is not possible to make a correction, for example, for neodymium oxide interference from a knowledge of the neodymium intensity; the ratio $^{m}Nd/^{m}NdC$ is not constant from one exposure to another [27]. This is demonstrated in Table 5, which lists the mean intensity ratios found in replicate exposures for $^{143}Nd/^{145}Nd$ and $^{144}Nd/^{145}Nd$ together with $^{143}Nd/^{143}Nd^{16}O$ and $^{144}Nd/^{144}Nd^{16}O$. While the neodymium isotope ratios show a precision of 10—14%, the intensity ratio of a neodymium isotope to its oxide has a poor precision of about 70%; moreover, the individual measured values show periodical shifts in the ratio, presumably corresponding to different sparking positions or conditions and different rates of production of oxide and isotope ions.

The interference correction procedures are based on subtraction or elimination by the solution of simultaneous equations of that component of line intensity attributable to the interfering ion. The intensity of the interfering oxide ion line, e.g. $^{m}NdO$, can be predicted from a knowledge of the intensity, in the same exposure, of an oxide ion line of another isotope, $^{n}NdO$, of the same element because the isotopic abundance ratio $^{m}Nd/^{n}Nd = {}^{m}NdO/{}^{n}NdO$ (Table 6).

These findings for oxide molecular ions have been found to be valid both for molecular ions in general and for multiply charged ions. Two conclusions can therefore be drawn. First, the molecular ion ($^{a}MX^{+}$) and multiply charged ion ($^{a}M^{n+}$) intensities have no constant relationship to the singly charged parent element isotope ion ($^{a}M^{+}$) intensity nor to the element (M) content. Therefore, since the ratios $^{a}MX^{+}/^{a}M^{+}$ and $^{a}M^{n+}/^{a}M^{+}$ are not constant in different exposures the intensity of an interfering ion ($^{a}MX^{+}$ or $^{a}M^{n+}$) cannot be calculated from the intensity of $^{a}M^{+}$. Secondly, the extent of oxide ion

TABLE 5

Comparison of replicate measurements of neodymium isotope intensity ratios with ratios of neodymium isotope intensities to the corresponding neodymium oxide ion intensities

| | Relative intensity ratios | | | |
|---|---|---|---|---|
| | $^{143}Nd/^{145}Nd$ | $^{143}Nd/^{143}Nd^{16}O$ | $^{144}Nd/^{145}Nd$ | $^{144}Nd/^{144}Nd^{16}O$ |
| Mean | 1.50 | 3.44 | 2.86 | 4.63 |
| $n$ | 18 | 18 | 12 | 12 |
| R.s.d. (%) | 13.9 | 70.0 | 10.9 | 66.2 |

TABLE 6

Comparison of neodymium isotope abundance ratios from published values [30] with neodymium isotope and neodymium isotope oxide ratios measured by s.s.m.s. in standard sample 3 of Table 4

| Neodymium isotope ratios | $\frac{^{142}Nd}{^{145}Nd}$ | $\frac{^{143}Nd}{^{145}Nd}$ | $\frac{^{144}Nd}{^{145}Nd}$ | $\frac{^{146}Nd}{^{145}Nd}$ | $\frac{^{148}Nd}{^{145}Nd}$ | $\frac{^{150}Nd}{^{145}Nd}$ |
|---|---|---|---|---|---|---|
| Ratio of metal isotope abundances; published values [30] | 3.27 | 1.47 | 2.88 | 2.07 | 0.69 | 0.68 |
| Measured ratio of metal isotope intensities | 3.50 | 1.50 | 2.86 | 2.09 | 0.68 | 0.64 |
| Measured ratio of isotope oxide intensities | 3.29 | 1.57 | 2.89 | 2.08 | 0.69 | 0.68 |

formation has been shown to vary from element to element and the assumption can be made that this is valid for molecular and multiply charged species in general.

Although attempts have been made [31] to correct molecular interferences on the rare earth elements by making precisely those assumptions precluded by these two conclusions, the contribution of an interfering ion to the total measured intensity can only be calculated by using the fact that in any one exposure the intensity ratios $^{a}MX^{+}/^{b}MX^{+}$ and $^{a}M^{n+}/^{b}M^{n+}$ are equal to the isotope abundance ratio $^{a}M/^{b}M$.

The correction scheme is based on the equations in Table 7 which detail the ion species considered to occur at each value of $m/e$. At $m/e$ 144, for example, the measured relative intensity RI 144 equals the sum of the intensities of the neodymium and samarium isotopes $^{144}Nd^{+}$ and $^{144}Sm^{+}$. These equations essentially catalogue the interference effects which the correction procedure takes account of in the analysis of rock and soil samples when aluminium conducting material is used. From them, solutions are found for the contribution of each ion species to the measured line intensity. The solutions given in the scheme in Table 8 are not unique but are the ones found to give the most reproducible results for rocks and soils. They have also been

TABLE 7

Equations defining the relative intensities at the selected values of $m/e$ (e.g. RI 151) in terms of the intensities of the contributing ion species (e.g. $^{151}Eu^+$ and $(^{135}Ba^{16}O)^+$)

| |
|---|
| RI 139 = $^{139}La^+$ |
| RI 140 = $^{140}Ce^+$ |
| RI 141 = $^{141}Pr^+$ |
| RI 143 = $^{143}Nd^+$ |
| RI 144 = $^{144}Nd^+ + ^{144}Sm^+$ |
| RI 145 = $^{145}Nd^+$ |
| RI 147 = $^{147}Sm^+$ |
| RI 149 = $^{149}Sm^+$ |
| RI 151 = $^{151}Eu^+ + (^{135}Ba^{16}O)^+$ |
| RI 153 = $^{153}Eu^+ + (^{137}Ba^{16}O)^+$ |
| RI 159 = $^{159}Tb^+ + (^{143}Nd^{16}O)^+$ |
| RI 160 = $^{160}Dy^+ + ^{160}Gd^+ + (^{144}Nd^{16}O)^+ + (^{144}Sm^{16}O)^+$ |
| RI 161 = $^{161}Dy^+ + (^{145}Nd^{16}O)^+$ |
| RI 163 = $^{163}Dy^+ + (^{147}Sm^{16}O)^+$ |
| RI 165 = $^{165}Ho^+ + (^{149}Sm^{16}O)^+$ |
| RI 167 = $^{167}Er^+ + (^{151}Eu^{16}O)^+$ |
| RI 168 = $^{168}Er^+ + ^{168}Yb^+ + (^{152}Sm^{16}O)^+ + (^{152}Gd^{16}O)^+$ |
| RI 169 = $^{169}Tm^+ + (^{153}Eu^{16}O)^+$ |
| RI 170 = $^{170}Er^+ + ^{170}Yb^+ + (^{154}Sm^{16}O)^+ + (^{154}Gd^{16}O)^+$ |
| RI 171 = $^{171}Yb^+ + (^{155}Gd^{16}O)^+$ |
| RI 172 = $^{172}Yb^+ + (^{156}Gd^{16}O)^+ + (^{156}Dy^{16}O)^+$ |
| RI 173 = $^{173}Yb^+ + (^{157}Gd^{16}O)^+ + (^{130}Ba^{27}Al^{16}O)^+$ |
| RI 174 = $^{174}Yb^+ + ^{174}Hf^+ + (^{158}Gd^{16}O)^+ + (^{158}Dy^{16}O)^+$ |
| RI 175 = $^{175}Lu^+ + (^{132}Ba^{27}Al^{16}O)^+$ |
| RI 176 = $^{176}Lu^+ + ^{176}Yb^+ + ^{176}Hf^+ + (^{160}Gd^{16}O)^+ + (^{160}Dy^{16}O)^+$ |
| RI 177 = $^{177}Hf^+ + (^{161}Dy^{16}O)^+ + (^{134}Ba^{27}Al^{16}O)^+$ |
| RI 178 = $^{178}Hf^+ + (^{162}Dy^{16}O)^+ + (^{135}Ba^{27}Al^{16}O)^+$ |
| RI 179 = $^{179}Hf^+ + (^{163}Dy^{16}O)^+ + (^{136}Ba^{27}Al^{16}O)^+$ |

used successfully for some other types of sample such as plant materials [26] but different equations may be required where other interference effects are identified.

No allowance is made for the interference of $(^{159}Tb^{16}O)^+$, $(^{162}Er^{16}O)^+$, and $(Ba^{16}O_2)^+$ species because their inclusion would make solution difficult or impossible. Their omission does not affect the validity of the scheme, for in practice, in rocks and soils, their contributions are negligible.

*Interference correction scheme*

Examples of the various routes to solutions for intensities of different ion species are given in Table 8. These and similar methods have been used to evolve the correction scheme detailed in Table 9. This is in the form of equations for the intensities of the various ion species, e.g. $^{155}Gd^{16}O$, in terms of measured relative intensities (RI 171) and relative intensity contributions calculated for coincident ion species ($^{171}Yb$). The intensities of these ion species are those required for calculation of element contents directly or for incorporation in

TABLE 8

Examples of different routes to solutions for corrected intensities

(1) For neodymium by subtraction

$$\text{RI } 144 = {}^{144}\text{Nd} + {}^{144}\text{Sm};\ \text{RI } 147 = {}^{147}\text{Sm} = \frac{14.92}{3.03}\,{}^{144}\text{Sm}^{a}$$

$$\therefore {}^{144}\text{Nd} = \text{RI } 144 - 0.203\ (\text{RI } 147)$$

(2) For europium by solution of two simultaneous equations

$$\text{RI } 153 = {}^{153}\text{Eu} + {}^{137}\text{Ba}^{16}\text{O} = \frac{52.21}{47.79}\,({}^{151}\text{Eu}) + \frac{11.41}{6.58}\,({}^{135}\text{Ba}^{16}\text{O}$$

$$\text{RI } 151 = {}^{151}\text{Eu} + {}^{135}\text{Ba}^{16}\text{O}$$

$$\text{Thus } {}^{151}\text{Eu} = 2.703\ (\text{RI } 151) - 1.559\ (\text{RI } 153)$$

(3) For hafnium by solution of three simultaneous equations

$$\text{RI } 177 = {}^{177}\text{Hf} + {}^{161}\text{Dy}^{16}\text{O} + {}^{134}\text{Ba}^{27}\text{Al}^{16}\text{O}$$

$$\text{RI } 178 = {}^{178}\text{Hf} + {}^{162}\text{Dy}^{16}\text{O} + {}^{135}\text{Ba}^{27}\text{Al}^{16}\text{O}$$

$$= \frac{27.14}{18.49}\,({}^{177}\text{Hf}) + \frac{25.46}{18.87}\,({}^{161}\text{Dy}^{16}\text{O}) + \frac{6.58}{2.44}\,({}^{134}\text{Ba}^{27}\text{Al}^{16}\text{O})$$

$$\text{RI } 179 = {}^{179}\text{Hf} + {}^{163}\text{Dy}^{16}\text{O} + {}^{136}\text{Ba}^{27}\text{Al}^{16}\text{O}$$

$$= \frac{13.78}{18.49}\,({}^{177}\text{Hf}) + \frac{24.93}{18.87}\,({}^{161}\text{Dy}^{16}\text{O}) + \frac{7.87}{2.44}\,({}^{134}\text{Ba}^{27}\text{Al}^{16}\text{O})$$

Thus

$${}^{177}\text{Hf} = 1.901\ (\text{RI } 178) - 0.788\ (\text{RI } 177) - 1.345\ (\text{RI } 179) \qquad (a)$$

$${}^{161}\text{Dy}^{16}\text{O} = 1.227\ (\text{RI } 179) + 2.720\ (\text{RI } 177) - 2.476\ (\text{RI } 178) \qquad (b)^{b}$$

$${}^{134}\text{Ba}^{27}\text{Al}^{16}\text{O} = 0.118\ (\text{RI } 179) + 0.575\ (\text{RI } 178) - 0.932\ (\text{RI } 177) \qquad (c)^{b}$$

[a]Ratios such as 14.92/3.03 are isotope abundance ratios [30].
[b]Equations (b) and (c) are required to provide solutions for other corrections — see text.

subsequent equations. For example, in Table 8 (part 3), the solution for $^{177}$Hf (eqn. a) is used directly in the correction scheme (Table 9) for the calculation of corrected $^{177}$Hf intensities from which hafnium contents are found. This corrected $^{177}$Hf intensity is also used in the subsequent equation for $^{171}$Yb in the correction scheme (Table 9). Equations (b) and (c) give solutions for the intensities of $^{161}$Dy$^{16}$O and $^{134}$Ba$^{27}$Al$^{16}$O which are required for subsequent equations in the correction scheme.

The equations are used in the sequence presented so that the intensities of the various ion species can be calculated and their validity assessed before use in subsequent equations. This allows an unreasonable value produced by one equation to be detected before it is incorporated in a subsequent one. A negative value of intensity, for example, calculated in this way can then be treated as zero or an intensity found to be greater than the measured line intensity

TABLE 9

Correction scheme: equations defining the intensities of various ion species (e.g. $(^{155}Gd^{16}O)^+$) in terms of measured relative intensities (RI 171) and relative intensity contributions calculated for coincident ion species ($^{171}Yb^+$)

$^{139}La$ = RI 139
$^{140}Ce$ = RI 140
$^{141}Pr$ = RI 141
$^{143}Nd$ = RI 143
$^{144}Nd$ = (RI 144) − 0.203 (RI 147)
$^{145}Nd$ = RI 145
$^{147}Sm$ = RI 147
$^{149}Sm$ = RI 149
$^{151}Eu$ = 2.703 (RI 151) − 1.559 (RI 153)
$^{177}Hf$ = 1.901 (RI 178) − 0.788 (RI 177) − 1.345 (RI 179)
$^{161}Dy^{16}O$ = 1.227 (RI 179) + 2.720 (RI 177) − 2.476 (RI 178)
$^{134}Ba^{27}Al^{16}O$ = 0.118 (RI 179) + 0.575 (RI 178) − 0.932 (RI 177)
$^{175}Lu$ = RI 175 − 0.0488 ($^{134}Ba^{27}Al^{16}O$)
$^{171}Yb$ = 0.851 (RI 174) + 0.026 (RI 175) − 0.967 (RI 176) + 0.265 ($^{177}Hf$) + 0.115 ($^{161}Dy^{16}O$) − 0.001 ($^{134}Ba^{27}Al^{16}O$)
$^{155}Gd^{16}O$ = RI 171 − $^{171}Yb$
$^{147}Sm^{16}O$ = 1.787 (RI 170) − 0.974 (RI 168) − 0.410 ($^{171}Yb$) − 0.246 ($^{155}Gd^{16}O$)
$^{163}Dy$ = RI 163 − $^{147}Sm^{16}O$
$^{145}Nd^{16}O$ = RI 161 − 0.760 ($^{163}Dy$)
$^{160}Gd$ = RI 160 − 0.0935 ($^{163}Dy$) − 2.881 ($^{145}Nd^{16}O$) − 0.203 ($^{147}Sm^{16}O$)
$^{159}Tb$ = RI 159 − 1.476 ($^{145}Nd^{16}O$)
$^{165}Ho$ = RI 165 − 0.926 ($^{147}Sm^{16}O$)
$^{168}Er$ = RI 168 − 0.0081 ($^{171}Yb$) − 1.799 ($^{147}Sm^{16}O$) − 0.145 ($^{155}Gd^{16}O$)
$^{151}Eu^{16}O$ = RI 167 − 0.866 ($^{168}Er$)
$^{169}Tm$ = RI 169 − 1.092 ($^{151}Eu^{16}O$)

treated as equal to the measured line intensity for the next stage of the calculation.

Any correction applied must use only terms derived from relative intensity measurements taken on the same exposure, as the level of interfering species varies not only from sample to sample but also between different exposures for the same sample, as shown in Table 5.

*Results and verification of the correction procedure*

Europium contents, determined by the procedure described above, for several standard rock samples are compared in Table 10, with recent published contents [24, 25, 32—34]. With the exception of standard rock NIM-S, the agreement with one, and generally both, of the published values quoted is good. In the case of NIM-S the content by the present method appears high and may indicate an incomplete correction of a very large BaO interference on a low europium content. Table 10 also shows that although the magnitude of the interfering BaO contribution (a) is approximately proportional to the barium content (b), the relationship is not sufficiently constant, as shown by the variation in ratio b/a, to enable the magnitude of the interference to be deduced

TABLE 10

Barium oxide interference in the determination of europium in various standard rock samples

| Standard rock | Europium content (ppm) | | | (a) Interfering BaO contribution; ppm equivalent europium | (b) Ba content* (ppm) | b/a |
|---|---|---|---|---|---|---|
| | S.s.m.s. | Ref. [24, 25] | Ref. [32] | | | |
| AGV-1 | 1.2 | 1.8 | 1.5 | 2.1 | 1200 | 560 |
| BCR-1 | 1.9 | 1.95 | 1.7 | 1.3 | 680 | 530 |
| G-2 | 1.3 | 1.7 | 1.4 | 1.5 | 1850 | 1260 |
| NIM-G | 0.32 | 0.39 | 0.4 | 0.19 | 210 | 1100 |
| NIM-L | 1.2 | 1.0 | 1.1 | 0.62 | 450 | 730 |
| NIM-N | 0.28 | 0.67 | 0.3 | 0.05 | 110 | 2200 |
| NIM-P | 0.14 | 0.12 | — | 0.05 | 48 | 960 |
| NIM-S | 0.73 | 0.24 | 0.3 | 2.6 | 2400 | 930 |
| JG-1 | 0.78 | 0.7** | 0.61 | 0.51 | 470** | 920 |
| JB-1 | 0.91 | 1.5** | 1.0 | 1.2 | 470** | 380 |

*Ref. [34]. **Ref. [33].

from a knowledge of the barium content. From this evidence the analytical procedure provides reliable europium contents even when the contribution from the interfering component is almost twice that of the true europium content.

The degree of interference typically encountered in the analysis of U.S. Geological Survey standard rocks BCR-1, AGV-1 and G-2 is illustrated for hafnium and all the rare earth elements for which the correction procedure is applied in Table 11. This shows, for example, that in BCR-1, 40% of the total line intensity at *m/e* 160 in this exposure is due to gadolinium, 29% in AGV-1 and only 12% in G-2. Interferences are seen to be of major proportions for Eu, Gd, Tb and Hf but less important for the other elements.

Analyses for the rare earth elements and hafnium after correction for interference effects as described above are finally standardized by using RSC's derived from analysis of synthetic standard samples (Table 4) which are free of interference effects. The results obtained, after interference corrections have been made and RSC's applied, are given in Table 12 for the analysis of USGS Standard Rocks BCR-1, AGV-1 and G-2 for the rare earths and hafnium. The contents of yttrium for these rock and soil samples are also included so that they can be used in Fig. 4 (see below). The results are compared with published values [24, 32, 34] when available and show generally excellent agreement.

The method has been applied to the analysis of soils and an example is given in Table 12 for a Scottish top-soil sample derived from an andesite parent material. It can be seen that the soil contents are intermediate between those of AGV-1 and G-2 perhaps resembling AGV-1 the more closely. The similarity

TABLE 11

Corrected contents of three USGS standard rocks as percentages of the uncorrected contents

| Element | *m/e* | BCR-1 | AGV-1 | G-2 |
|---|---|---|---|---|
| Nd | 144 | 97 | 98 | 98 |
| Eu | 151 | 50 | 23 | 36 |
| Gd | 160 | 40 | 29 | 12 |
| Tb | 159 | 46 | 40 | 12 |
| Dy | 163 | 97 | 99 | 87 |
| Ho | 165 | 98 | 99 | 81 |
| Er | 168 | 94 | 96 | 86 |
| Tm | 169 | 59 | 94 | 100 |
| Yb | 171 | 74 | 88 | 68 |
| Lu | 175 | 99 | 98 | 94 |
| Hf | 177 | 27 | 13 | 47 |

TABLE 12

Contents (ppm) of USGS Standard Rocks by s.s.m.s. together with published contents [24, 32, 34] and contents (ppm oven dry) of top soil (ignited 450°C) derived from andesite parent material

| Element | BCR-1 | | | AGV-1 | | | G-2 | | | Soil |
|---|---|---|---|---|---|---|---|---|---|---|
| | S.s.m.s. | Ref. [24] | Ref. [32] | S.s.m.s. | Ref. [24] | Ref. [32] | S.s.m.s. | Ref. [24] | Ref. [32] | S.s.m.s. |
| La | 24 | 23.8 | | 30 | 35 | | 98 | 100 | 90 | 44 |
| Ce | 44 | 49 | | 53 | 57 | | 140 | 160 | | 83 |
| Pr | 5.9 | 6.3 | | 6.1 | 6.7 | | 23 | 16.8 | | 6.8 |
| Nd | 27 | 28.7 | 22 | 32 | 37.5 | 27 | 73 | 58.1 | 50 | 22 |
| Sm | 7.3 | 5.8 | 6.3 | 7.2 | 6.8 | 5.9 | 11 | 9.05 | 9.6 | 4.5 |
| Eu | 1.9 | 1.95 | 1.7 | 1.2 | 1.8 | 1.5 | 1.3 | 1.7 | 1.4 | 1.2 |
| Gd | 6.2 | 6.9 | | 8.2 | 5.2 | | 4.1 | 5.8 | | 5.8 |
| Tb | 1.0 | 0.85 | | 0.77 | 0.68 | | 0.52 | 0.47 | | 0.69 |
| Dy | 7.3 | 5.7 | 4.9 | 5.1 | 3.5 | 3.3 | 2.4 | 2.4 | 2.3 | 4.3 |
| Ho | 0.88 | 1.06 | 1.0 | 0.51 | 0.68 | 0.7 | 0.38 | 0.34 | 0.4 | 0.62 |
| Er | 3.4 | 3.0 | 3.5 | 1.7 | 1.8 | 1.9 | 1.4 | 0.93 | 0.93 | 2.1 |
| Tm | 0.46 | 0.43 | 0.44 | 0.33 | 0.3 | 0.23 | 0.13 | 0.12 | | 0.42 |
| Yb | 3.2 | 2.9 | 3.2 | 2.8 | 1.6 | 1.6 | 1.2 | 0.93 | 0.6 | 2.5 |
| Lu | 0.42 | 0.51 | | 0.29 | 0.27 | | 0.17 | 0.14 | 0.15 | 0.36 |
| Hf | 4.1 | 4.5?[a] | | <5 | 5[a] | | 9.5 | 7.5?[a] | | 8.2 |
| Y | 36 | 46[a] | | 7.2 | 12[a] | | 28 | 26[a] | | 31 |

[a]Ref. [34].

between the soil and AGV-1 shown by the graphs (Fig. 4) of the ratios, derived from Table 12, of the rare earth contents to average chondrite contents [35] is confirmation of the andesitic nature of this parent material.

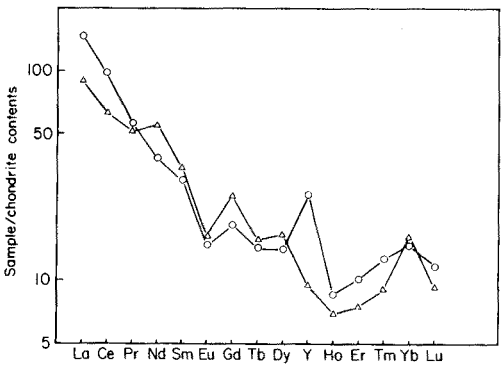


Fig. 4. Ratios of sample contents to average chondrite contents [35] for a soil derived from andesite parent material (○) and for USGS rock AGV-1 (△).

## CONCLUSIONS

The present study has shown that interference effects do occur in the spark-source mass spectrometric determination of hafnium and the rare earth elements. While oxide interferences on the rare earth elements may be less with a carbon matrix than with aluminium they do exist [17, 31] and account must be taken of these and other superpositional interferences.

The correction procedure described here for the rare earth elements is applicable in its general principles to other elements [26]. Such corrections rely on the correct identification of the interfering species and on accurate measurements of intensities. Experience has shown that in some exposures, interferences other than those allowed for in the correction scheme, may occasionally occur or inaccurate intensity measurements be obtained for a variety of reasons. While unreasonable values are usually recognised and rejected during the stepwise procedure described, it is desirable to make multiple exposures for each analysis to eliminate occasional rogue results.

The results obtained show that the overall precision of about ±25% for contents determined from a single exposure is not seriously degraded by the correction procedure while the accuracy is greatly improved. In practice since each analysis is an average of determinations made in at least 4 exposures the precision attained is ±10—15% [26]. The application of this technique to the determination of hafnium and the rare earth elements in standard rock samples will be presented in a subsequent paper.

## REFERENCES

1 R. Brown and W. A. Wolstenholme, Nature, 201 (1964) 598.
2 S. R. Taylor, Nature, 205 (1965) 34.
3 S. R. Taylor, Geochim. Cosmochim. Acta, 29 (1965) 1243.
4 S. R. Taylor, Geochim. Cosmochim. Acta, 35 (1971) 1187.
5 G. D. Nicholls, A. L. Graham, E. Williams and M. Wood, Anal. Chem., 39 (1967) 584.

6 G. D. Nicholls, Proc. Brit. Ceram. Soc., (1970) 85.
7 G. H. Morrison and A. T. Kashuba, Anal. Chem., 41 (1969) 1842.
8 S. R. Taylor, Geochim. Cosmochim. Acta, 30 (1966) 1121.
9 S. R. Taylor and A. J. R. White, Bull. Volcanol., 24 (1966) 177.
10 S. R. Taylor, M. P. Gorton, P. Muir, W. Nance, R. Rudowski and N. Ware, Proc. 4th Lunar Sci. Conf., Houston, Texas, 1973, p. 1445.
11 B. Mason, J. A. Nelen, P. Muir and S. R. Taylor, Meteoritics, 11 (1975) 21.
12 W. B. Nance and S. R. Taylor, Geochim. Cosmochim. Acta, 40 (1976) 1539.
13 A. Peccerillo and S. R. Taylor, Earth Planet. Sci. Lett., 32 (1976) 121.
14 P. C. Rankin, J. Geol. Soc. Jpn., 82 (1976) 215.
15 P. R. Kyle and P. C. Rankin, Geochim. Cosmochim. Acta, 40 (1976) 1497.
16 P. Jakes and J. Gill, Earth Planet. Sci. Lett., 9 (1970) 17.
17 E. Roaldset, Talanta, 17 (1970) 593.
18 E. Roaldset, Geochim. Cosmochim. Acta, 39 (1975) 455.
19 A. L. Graham and G. D. Nicholls, Geochim. Cosmochim. Acta, 33 (1969) 555.
20 G. H. Morrison, J. T. Gerard, A. T. Kashuba, E. V. Gangadharam, A. M. Rothenberg, N. M. Potter and G. B. Miller, Proc. Apollo 11 Lunar Sci. Conf., 2 (1970) 1383.
21 G. H. Morrison, A. T. Kashuba and A. M. Rothenberg, Adv. Mass Spectrom., 5 (1971) 520
22 G. H. Morrison, R. A. Nadkarni, N. M. Potter, A. M. Rothenberg and S. F. Wong, Radiochem. Radioanal. Lett., 11 (1972) 251.
23 A. Strasheim. F. W. E. Strelow and P. F. S. Jackson, XVII Coll. Spect. Int. Florence, Acta, 1 (1973) 306.
24 F. W. E. Strelow and P. F. S. Jackson, Anal. Chem., 46 (1974) 1481.
25 P. F. S. Jackson and F. W. E. Strelow, Chem. Geol., 15 (1975) 303.
26 A. M. Ure and J. R. Bacon, Analyst, 103 (1978) 807.
27 A. M. Ure and J. R. Bacon, Proc. Anal. Div. Chem. Soc., 13 (1976) 124.
28 H. Liebl, Int. Symp. Microchemical Techniques, Davos, Abstracts, (1977) 41.
29 C. W. Magee and W. W. Harrison, Anal. Chem., 45 (1973) 220.
30 A. E. I. Technical Information Sheet No. A2021.
31 S. R. Taylor and M. P. Gorton, Geochim. Cosmochim. Acta, 41 (1977) 1375.
32 J. G. Sen Gupta, Geostandards Newsl., 1 (1977) 149.
33 A. Ando, M. Kurasawa, T. Ohmori and E. Takeda, Geochem. J., 8 (1974) 175.
34 S. Abbey, Geological Survey Paper 74-41, Geol. Survey of Canada, (1975).
35 L. A. Haskin, F. A. Frey, R. A. Schmitt and R. M. Smith, in L. H. Ahrens (Ed.), Physics and Chemistry of the Earth, Volume 7, Pergamon, Oxford, 1966, p. 169.

*Analytica Chimica Acta*, 105 (1979) 177—184


# INSTRUMENTAL DEAD-TIME AND ITS RELATIONSHIP WITH MATRIX CORRECTIONS IN X-RAY FLUORESCENCE ANALYSIS

I. L. THOMAS* and M. T. HAUKKA

*School of Earth Sciences, Department of Geology, University of Melbourne, Parkville, Victoria 3052 (Australia)*

D. H. ANDERSON**

*Department of Mathematics, University of Melbourne, Parkville, Victoria 3052 (Australia)*

(Received 17th April 1978)

SUMMARY

The relationship between instrumental dead-time and the self-absorption coefficients, $\alpha_{ii}$, in x.r.f. matrix correction by means of influence coefficients, is not generally recognized but has important analytical consequences. Systematic errors of the order of 1% (relative) for any analyte result from experimental uncertainties in instrumental dead-time. Such errors are applied unevenly across a given range of concentration because the error depends on the calibration standards and on the instrumental conditions used. Refinement of the instrumental dead-time value and other calibration parameters to conform with influence coefficients determined elsewhere assumes exact knowledge of dead-time of the instrument used originally, and quite similar excitation conditions and spectrometer geometry for the two instruments. Though these qualifications may not be met, adjustment of any of the parameters (dead-time, reference concentration, background concentration, self-absorption and other influence coefficients) can be easily achieved.

The loss of counts arising from the inability of the detection electronic system to resolve pairs of pulses arriving within about 2 $\mu$s of each other, this period being the "dead-time", has been described by numerous authors with reference to x-ray fluorescence spectrometry (x.r.f.). The essential features have been discussed by Hutchison [1], who described a method for determining instrumental dead-time for x.r.f. which was claimed to be accurate to the nearest 0.4 $\mu$s. It can be demonstrated that uncritical reliance on the dead-time determined by this or other methods of similar accuracy, combined with reference standard calibration based on only a few primary standards, can lead to significant systematic errors in the calculation of compositions of unknown samples.

Correction of measured intensities for instrument dead-time need not be performed when changes are made to some of the parameters used in the x.r.f. equation. Such changes are no more difficult to effect than is careful calibration of a reference standard sample for each element determined.

---

**Present address: Mathematics Department, Faculty of Military Studies, The University of N.S.W., Royal Military College, Duntroon, A.C.T. 2600.

DEAD-TIME CORRECTION

Hutchison [1] has presented a relationship for the dead-time, $t$, which is not self-prolonging:

$$I = I^0/(1.0 - t\,I^0) \tag{1}$$

where $t$ is in s, $I$ is the corrected count rate per s, and $I^0$ is the observed count rate.

When concentrations of components $i$ ($C_i$) in a fused disc are calculated, the system of equations represented as

$$C_i = K_i R_i \left(F_i + \sum_{j=1}^{n} \alpha_{ij} C_j\right) \qquad (\text{for } i = 1,...,n) \tag{2}$$

uses the count ratio $R_i = I_{i,S}/I_{i,R}$ corrected for dead-time, where subscript $i$ represents the analyte (emitter element), and subscripts S and R refer to sample (unknown) and reference standard, respectively. $K_i$ is the nominal concentration of component $i$ in the reference standard (assuming that the total matrix effect is 1.0), and the bracketted part is the total matrix effect of the sample for emitter $i$. $F_i$ is the influencing flux constant for emitter $i$; coefficients $\alpha_{ij}$ represent the inter-element influences (primary and secondary beam mass absorption, and enhancement) of each element $j$ on the emitter $i$, and include the "self-absorption" coefficient $\alpha_{ii}$; $C_j$ is the concentration of each component $j = 1,..,i,..,n$.

The true intensity ratio, $R_i$, is given by

$$R_i = [I^0_{i,S}/I^0_{i,R}]\,[(1 - tI^0_{i,R})/(1 - tI^0_{i,S})] \tag{3}$$

Now, $(1 - tI^0_{i,R})$ is constant for a particular reference standard and may be absorbed into the constant $K_i$ in eqns. (2). Therefore, it is possible to define

$$K^0_i = (1 - tI^0_{i,R})\,K_i \tag{4}$$

and substitute expression (3) for $R_i$ in eqn. (2) to obtain

$$C_i = [K^0_i R^0_i/(1 - tI^0_{i,S})]\,[F_i + \sum_{j=1}^{n} \alpha_{ij} C_j] \qquad (\text{for } i = 1,...,n) \tag{5}$$

where $R^0_i = I^0_{i,S}/I^0_{i,R}$ is the observed intensity ratio for constituent $i$. Multiplying both sides of eqn. (5) by $(1 - tI^0_{i,S})$ yields

$$(1 - tI^0_{i,S})\,C_i = K^0_i R^0_i \left(F_i + \sum_{j=1}^{n} \alpha_{ij} C_j\right), \text{ hence}$$

$$C_i = K^0_i R^0_i \left(F_i + \sum_{j=1}^{n} \alpha_{ij} C_j + tI^0_{i,R} C_i/K^0_i\right) \text{ (for } i = 1,...,n) \tag{6}$$

If new coefficients, $\alpha^0_{ij}$, are defined such that

$$\alpha^0_{ij} = \alpha_{ij},\ j \neq i \text{ and } \alpha^0_{ii} = \alpha_{ii} + tI^0_{i,R}/K^0_i \tag{7}$$

then eqn. (6) may be written

$$C_i = K_i^0 R_i^0 \left(F_i + \sum_{j=1}^{n} \alpha_{ij}^0 C_j\right) \qquad (\text{for } i = 1,\ldots,n) \qquad (8)$$

which is precisely the same form as eqn. (2).

Therefore, it is not necessary to correct the intensity measurements for dead-time. If the observed intensities are used to compute the coefficients, $\alpha_{ij}$, then these coefficients will actually be those in eqns. (6) and (8), and the constants $K_i$ will automatically be $K_i^0$. If, however, the coefficients $\alpha_{ij}$ have been calculated by some other laboratory from intensity measurements which have been corrected for dead-time, then it will be necessary to modify the constants $K_i$ and coefficients $\alpha_{ii}$ according to eqns. (3) and (7), respectively.

Suppose that experimental coefficients $\alpha_{ij}$ for a series of emitters $i = 1,\ldots,n$ appropriate to a well-proven fusion method are taken from the literature, and that exact correction of intensities for dead-time is a requisite for their successful use. Further, suppose that the actual dead-time of the instrument used is not precisely known, and a value $t' \neq t$ is used; then, appropriate constants $K_i'$ and coefficients $\alpha_{ii}'$ should apply.

The consequences of using the literature $\alpha_{ii}$ values rather than $\alpha_{ii}'$ are examined below. The constants $K_i$ must always be determined accurately by the user for a particular set of instrumental conditions, regardless of whether instrument dead-time is accurately known or not.

*Uncertainty in dead-time determination*

Hutchison [1] suggests that his method for determination of dead-time is accurate to 0.4 $\mu$s, or ca. ±20%. It can be shown that such a relative uncertainty is more nearly ±10%, which can be explained by the counting errors of his pairs of observations (see Appendix).

Although the relationship between $\alpha_{ii}$, $t$, and $K_i$ is shown from eqns. (4), (6) and (7), the question of the magnitude of the effect of an erroneous dead-time and also the complexity of the relationship in terms of quantitative x.r.f. analysis, require numerical illustration. The example given here pertains to some actual intensity measurements obtained by a low-dilution fusion method [2, 3] for which influence coefficients $\alpha_{ij}$ were shown to give precise and accurate results for a wide range of geological samples. (The influence coefficients used below are unpublished and apply to a rhodium anode x-ray tube for all emitters; see below.) Table 1 shows the uncorrected intensities, $I^0$, the

TABLE 1

Observed and corrected intensities for reference and pure silica samples (cps for Si K$\alpha$)

| | $I^0$ | $I'$ ($t$ = 2.0) | $I'$ ($t$ = 2.4) |
|---|---|---|---|
| Reference (R) | 17507.17 | 18142.41 | 18275.04 |
| Sample (S) | 39798.02 | 40889.07 | 41568.96 |
| Ratio, $R_{Si}$ | — | 2.2537833 | 2.2746307 |

intensities "properly" corrected for dead-time ($I$) by using $t$ = 2.4 $\mu$s and "erroneously" corrected values ($I'$) obtained by using $t'$ = 2.0 $\mu$s, for a sample (S) of pure silica, and a reference standard (R). A measurement procedure identical to Hutchison's but with a different calculation method (see Appendix) showed that the observed dead-time was ca. 2.4 $\mu$s. The $K_i$, $b_i$ values (determined by using a wide range of primary standards), the influence coefficients $\alpha_{i\mathrm{Si}}$, and the $F_{\mathrm{Si}}$ values appropriate to the observed dead-time are given in Table 2. Substitutions in eqn. (2) give $C_{\mathrm{Si}}$ = 100.00%. Now, if the "erroneous" dead-time, 2.0 $\mu$s, is used with pure silica as the only primary standard to determine the reference standard nominal concentration, $K'_{\mathrm{Si}}$, and if all influence coefficients are assumed to be exact, then $C_{\mathrm{Si}} = 100 = K^*_{\mathrm{Si}} \times 1.9811$, so that $K^*_{\mathrm{Si}}$ = 50.478% is needed, i.e. a relative increase of nearly 1% over the reference standard nominal concentration $K_{\mathrm{Si}}$ appropriate for the true dead-time 2.4 $\mu$s.

The magnitude of this difference is certainly significant analytically, but the effect is compounded further by unequal application of the error across a range of analyte concentrations. The problem is that for dead-time $t'$ (2.0 $\mu$s), and reference standard concentration $K'_{\mathrm{Si}}$, there is an appropriate $\alpha'_{\mathrm{SiSi}}$ value which is not the same as $\alpha_{\mathrm{SiSi}}$. The reference standard nominal concentration $K^*_{\mathrm{Si}}$ ($\neq K'_{\mathrm{Si}}$) calculated allows the "literature" self-absorption coefficient $\alpha_{\mathrm{SiSi}}$ to be retained for 100% $SiO_2$ only. Any samples containing less than 100% silica will have a systematic bias in the calculated contents when this calibrated $K^*_{\mathrm{Si}}$ and the erroneous dead-time $t'$ are used. The same argument applies to all other emitters, and will be accentuated when $I_{i,\mathrm{S}}$ is considerably different from $I_{i,\mathrm{R}}$ and count rates are higher than the moderate values shown in Table 1. The extent of the systematic bias depends on the (erroneous) dead-time value used, and on the relative concentrations of primary standard, reference standard and unknown sample for each component.

Thus a large number of primary standards varying widely in all analyte concentrations is absolutely essential for calibration of the reference standard,

TABLE 2

Influence coefficients[a] and calibration constants[b] for different x-ray tubes for a dead-time of 2.4 $\mu$s

| Emitter ($i$) | Tube | $F_i$ | $\alpha_{i\mathrm{Si}}$ | $\alpha_{i\mathrm{Fe}}$ | $\alpha_{i\mathrm{K}}$ | $K_i$ | $b_i$ |
|---|---|---|---|---|---|---|---|
| Si K$\alpha$ | Rh | 0.496 | 0.383 | 0.717 | 0.363 | 50.015 | 0.080 |
| | Cr | 0.531 | 0.308 | 0.745 | 0.322 | 50.150 | 0.155 |
| Fe K$\alpha$ | Rh | 0.276 | 0.571 | 1.192 | 1.998 | 7.440 | 0.060 |
| | Au | 0.271 | 0.578 | 1.112 | 2.033 | 7.450 | 0.011 |

[a] $F_i$ = flux constant; $\alpha_{i\mathrm{Si}}$ = influence coefficient for oxide component $SiO_2$ on emitter $i$.
[b] $K_i$ = Reference standard nominal concentration; $b_i$ = background concentration. The same reference standard and identical primary standards at sample-to-flux (lithium borate) ratio of 1:2 were used in calibration.

especially if the instrumental dead-time is imprecisely known and fairly large. This also suggests that counting rates should be maintained at moderate levels.

## MODIFICATION OF INFLUENCE COEFFICIENTS

The interdependence of $\alpha_{ii}$, $K_i$, and $t$ (the dead-time) allows refinement of the dead-time to be carried out at the time of calibration of the reference standard, if $\alpha_{ii}$ must be kept constant. However, modification of the $\alpha_{ii}$ values should not be prohibited if the dead-time is inexactly known. There is a tendency to regard published influence coefficients as pristine and invariant, and to attach too much significance to measured dead-time values.

That influence coefficients may be validly changed, even though the dead-time is not exactly known, can be demonstrated by considering the effects of changing instrumental conditions. Two types of changes can be considered: excitation source or potential, and instrumental geometry.

Influence coefficients have been reported [2] for a fusion method with a lithium borate flux at a sample-to-flux ratio of 1:2, for which the conditions set for the Siemens SRS-1 sequential spectrometer were maintained. A chromium anode x-ray tube was used for Na, Mg, Al, Si, P, K, Ca and Ti, and a gold tube for Mn and Fe (all K$\alpha$ lines). Later, it was found that a thin-window (0.120 mm) rhodium anode x-ray tube gave considerably better sensitivity for the lighter elements, and was adequate for heavier elements [4], but it was discovered that the influence coefficients previously determined with the chromium and gold tubes were unusable for the range of geological samples of interest here.

Influence coefficients and reference standard nominal concentrations and background values were determined with the same reference standard, dead-time (2.4 $\mu$s), and wide range of primary standards as used earlier [2]. Table 2 compares some of the influence coefficients for Si K$\alpha$ and Fe K$\alpha$, and also presents reference standard nominal concentrations and backgrounds.

For Si K$\alpha$, $K_i$ and $b_i$ are little changed, but the extent of the change in influence coefficients can be gauged from the calculated value of 95.7% $SiO_2$ for the pure silica specimen, when the chromium-tube influence coefficients were used with rhodium-tube Si K$\alpha$ intensities. Similar changes were observed (though not accurately determined) for $\alpha_{TiTi}$ with gold tube compared with the chromium-tube, the latter being particularly sensitive for Ti K$\alpha$. Although self-absorption coefficients, $\alpha_{ii}$, appear to show the greatest change, Table 2 illustrates that all $\alpha_{ij}$ values must be redetermined when the excitation conditions necessary are substantially different from those used for determination of influence coefficients.

An equally important consideration in using $\alpha$-factors supplied by others is instrumental geometry. The relationship between fluorescence intensities, mass absorption coefficients and other parameters such as the geometric factor ($A$) has been given, for example, by Bertin [5]. Because the geometry of x.r.f. instruments varies from one manufacturer to another, the primary beam

absorption as a proportion of the total mass absorption part of Bertin's equation (4.10) will vary with $A$.

Primary beam absorption becomes a large proportion of the total matrix effect for Kα lines of elements heavier than potassium [2]; the proportion probably increases with atomic number. The geometric factor will be important for these elements and therefore experimental influence coefficients, which are some average combination of primary and secondary mass absorption and possibly enhancement effects, may not be directly transferable between instruments of different geometry. It was found here that the dead-time used in calculation had to be changed from 2.4 μs to 3.6 μs when iron was determined by the fusion method of Norrish and Hutton [6], to achieve accurate results for moderate to high $Fe_2O_3$ levels in the rock standards NIM-D, CRPG-Mica Fe, and synthetics with up to 30% $Fe_2O_3$. The Norrish—Hutton α-factors were determined with Philips equipment; the Siemens instrument used here has a different geometric factor.

The increase in primary beam absorption is observed for the $\alpha_{ii}$ and $\alpha_{i,i\pm1}$ coefficients, where $\alpha_{i,i\pm1}$ are absorbers next higher and lower in atomic number than the emitter element $i$ (see Fig. 1 in [2]). This means that mutual changes in $K_i$, $t$, and $\alpha_{ii}$ cannot completely remove the effects of geometrical differences between instruments. However, for silicate rocks where manganese and cobalt are at low concentrations, $K_{Fe}$, $t$, and $\alpha_{FeFe}$ mutually changed by careful calibration would eliminate geometric effects ($i = 26$ is Fe; $i + 1$ is Co; $i - 1$ is Mn).

## DISCUSSION

The number of x-ray spectrometers in service for which the dead-time of the counting system remains significant (i.e., without additional electronics such as pulse pile-up rejection) is probably quite large, and for many the instrument dead-time may be known only with an accuracy of ca. ±20%. Unless a wide range of primary standards varying widely in all analyte concentrations is used in calibration of reference standards, significant bias in calculated results may occur. (Short-cut methods of reference calibration and determination of α-factors as described by Tertian [7] and others appear to be hazardous, particularly if only one standard per element is used as in fundamental parameter method calibration [8]). Published influence coefficients will only be applicable if the value for the instrument dead-time used in correcting measured count rates is exactly matched via calibration with the reference standard concentrations. The reference standard analyte concentrations should be appropriate to the majority of unknown sample compositions, count rates should not be excessively high, and of course low dead-time electronics are to be preferred.

Significant modification of influence coefficients may be necessary if the excitation conditions (source, potential) for analysis are markedly different from those used in the determination of the influence coefficients. Spectro-

meter geometry may also be important for Kα lines of elements of $Z \geqslant 19$ where primary beam absorption becomes dominant for some absorbers, and several influence coefficients for these emitters may require alteration to be effective across the range of commercial x-ray spectrometers.

Modification of self-absorption coefficients and reference standard nominal concentrations would enable observed intensities to be used always in analysis, provided that calibration is done in this way.

Obviously then, some sets of influence coefficients may not be immediately of universal application. However, careful calibration makes it possible to adjust the parameters ($t$, $K_i$, $b_i$, $\alpha_{ii}$, $\alpha_{ij}$, $F_i$) as necessary. Some guidelines for determination of influence coefficients and calibration constants have been presented by Haukka and Thomas [2].

The paucity of published influence coefficients even for relatively simple systems such as silicate rock—borate fluxes with ten or so influencing elements, may be related to the minor problems in transferring influence coefficients between instruments.

## APPENDIX

Hutchison [1] measured count rates on two samples A and B at different generator currents, so that for two currents there are four measurements $a$, $b$, $a_1$, $b_1$. Dead-time is given by

$$t = [a_1 b - a b_1] / [ab\,(a_1 - b_1) - a_1 b_1\,(a - b)] \qquad (9)$$

Assuming count rates (cps) of $a = 40\,000$, $a_1 = 12\,500$, $b = 2\,500$ and $b_1 = 750$, then corresponding counting errors for 100 s counts (square root of counts, recalculated to cps) are $\Delta a = 20.0$, $\Delta a_1 = 11.180$, $\Delta b = 5.0$, $\Delta b_1 = 2.739$. From eqn. (9), $t = 1.518\ \mu$s. The logarithmic form of eqn. (9) is

$$\log t = \log (a_1 b - a b_1) - \log [ab(a_1 - b_1) - a_1 b_1 (a - b)]$$

Now $\mathrm{d}(\log t)/\mathrm{d}t \simeq \Delta \log t / \Delta t = 1/t$, so that $\Delta \log t = \Delta t / t$, which is the relative error in $t$. When partial differentials are used for $a$, $b$, $a_1$, $b_1$ in eqn. (9) the expression for the relative error in $t$ is substituted, then

$$\frac{\Delta t}{t} \leqslant \left|\Delta a \left[\frac{-b_1}{Y} - \frac{b(a_1 - b_1) - a_1 b_1}{Z}\right]\right| + \left|\Delta b \left[\frac{a_1}{Y} - \frac{a_1 b_1 + a(a_1 - b_1)}{Z}\right]\right|$$

$$+ \left|\Delta a_1 \left[\frac{b}{Y} - \frac{ab - b_1(a - b)}{Z}\right]\right| + \left|\Delta b_1 \left[\frac{-a}{Y} - \frac{(-ab) - a_1(a - b)}{Z}\right]\right| \qquad (10)$$

where $\Delta a$, $\Delta b$, .. are actual errors (cps) in $a$, $b$, .., and $Y = (a_1 b - a b_1)$ and $Z = ab(a_1 - b_1) - a_1 b_1 (a - b)$.

Calculation from eqn. (10) with the values given earlier yields $\Delta t/t \leqslant 0.213088$ = 21.3%, i.e. the maximum error in the determined dead-time for $\pm 1\sigma$ counting errors. When $t = 1.518\ \mu$s, $\Delta t_{max} = 0.32\ \mu$s for the data given.

Hutchison estimated accuracy at 0.4 μs for $t = 2.2\ \mu$s, which is of the same order (18% relative) as the maximum error calculated above with count rates

of similar magnitude to those quoted by Hutchison [1]. He gave 21 values of dead-time calculated (to the nearest 0.1 $\mu$s) from all combinations of 7 pairs of data; the average value was 2.19 $\mu$s (s.d., 0.17 $\mu$s, r.s.d., 7.6%). Thus a realistic error for comparison might be 10% relative, or 0.2 $\mu$s rather than 0.4 $\mu$s, provided that all possible combinations of the data are calculated. The maximum deviation is 0.4 $\mu$s.

An alternative method, used in this laboratory for some years, is as follows. Pairs of measurements are obtained exactly as described by Hutchison. Ratios of count rates corrected for dead-time are obtained for each pair of observations, the dead-time being incremented over a chosen range in say 0.1-$\mu$s steps. The standard deviations of the ratios are computed; the set of corrected ratios with the minimum standard deviation corresponds to the "best" dead-time. As the method is indirect, there is no temptation to under-utilize the measured data, and the criterion of minimum variance even encourages the collection of a large number of pairs of measurements. A computer program is used for calculation.

We thank Dr. R. W. LeMaitre, Geology Department, Melbourne University, for the use of his (1971) program for the calculation of instrument dead-time.

REFERENCES

1 C. S. Hutchison, X-Ray Spectrom., 5 (1976) 194.
2 M. T. Haukka and I. L. Thomas, X-Ray Spectrom., 6 (1977) 204.
3 I. L. Thomas and M. T. Haukka, Chem. Geol., 21 (1978) 39.
4 M. T. Haukka, T. C. Hughes and I. L. Thomas, Siemens Rev., XLV (1978) 225.
5 E. P. Bertin, Principles and Practice of X-Ray Spectrometric Analysis, Plenum Press, New York, 2nd edn., 1975, p. 117.
6 K. Norrish and J. T. Hutton, Geochim. Cosmochim. Acta, 33 (1969) 431.
7 R. Tertian, X-Ray Spectrom., 4 (1975) 52.
8 J. W. Criss, L. S. Birks and J. V. Gilfrich, Anal. Chem., 50 (1978) 33.

*Analytica Chimica Acta*, 105 (1979) 185—197


# MULTI-ELEMENT ANALYSIS OF BLOOD FOR TRACE METALS BY NEUTRON ACTIVATION ANALYSIS

NEIL I. WARD and DOUGLAS E. RYAN*

*Trace Analysis Research Centre, Chemistry Department, Dalhousie University, Halifax, N.S. B3H 4J1 (Canada)*

(Received 23rd August 1978)

SUMMARY

Fourteen elements can be rapidly determined in whole blood by the neutron activation analysis procedure described. Three of these (Ag, Cl, Se) are measured after a 10-s irradiation and eleven others (Al, Ba, Br, Ca, Cu, I, Mg, Mn, Mo, Rb, V) are determined by a 180-s irradiation of a 1-$cm^3$ sample of whole blood after destruction of organic matter and removal of sodium by hydrated antimony pentoxide. A further 13 elements (As, Au, Co, Cr, Cs, Fe, Hg, K, Na, Ni, Sb, Sc, Zn) are determined after overnight irradiation in the SLOWPOKE reactor.

The importance of essential elements in body metabolism is receiving increasing recognition, and the toxicity of some elements as well as the beneficial effects of others to humans are well known [1, 2]. The human body continuously assimilates a variety of elements [3]; these elements are closely related to human health and disorders since their deficiency or excess induces physiological changes [4—8]. The concentrations of elements (trace elements in particular) in human tissues and fluids are ordinarily very low, in the $\mu g\ ml^{-1}$ and $\mu g\ l^{-1}$ range, and are normally maintained within very narrow limits. A meaningful understanding of trace element requirements in human metabolism and health depends on the ability to determine the concentrations of trace elements in body tissues and fluids.

Methods that have been used to determine four or more elements in blood include anodic stripping voltammetry [9, 10], atomic absorption and fluorescence spectrometry [11—17], colorimetry and spectrophotometry [18, 19], flame photometry [20], photon-induced x-ray spectrometry [21—25], ion-selective electrodes [26], spark-source mass spectrometry [27—30], and x-ray fluorescence [31—34]. These techniques are not readily adaptable to simultaneous determination of the low concentrations present in whole blood, serum and plasma.

Neutron activation analysis (n.a.a.) has frequently been applied to trace element analysis of body tissues and fluids [35—49]. Most applications deal with the determination of more than 5 or 6 elements by either purely instrumental neutron activation analysis (i.n.a.a.) [35—46] or with the help of radio-

chemical separations [47—50]. De Goeij et al. [39] reported a comparative evaluation of five methods of n.a.a. (destructive and non-destructive), and gave quantitative results for 14 trace elements in 1 $cm^3$ of whole blood. In most applications, a conventional high flux reactor has been used for activation and relatively long-lived isotopes were measured after comparatively long irradiation and decay periods. Behne and Jürgensen [36] determined Br, Cs, Fe, Na, Rb, Se and Zn in human blood serum by irradiation of 300 $\mu$l of serum in ampoules of high silica quartz for 10 days at a flux of $5 \times 10^{13}$ n $cm^{-2}$ $s^{-1}$; the $\gamma$-ray spectra were measured 10 days after irradiation (Br and Na) and after 3 months (Cs, Fe, Rb, Se and Zn). Versieck et al. [45] reported a simultaneous determination method for Fe, Zn, Se, Rb and Cs in serum by i.n.a.a., in which lyophilized samples were irradiated for 12 days at a flux of $10^{13}$ n $cm^{-2}$ $s^{-1}$, followed by counting periods of 6 and 15 h after a 1- and 3-month decay time, respectively. Similarly, Zdankiewicz and Fasching [46] measured 13 elements in whole blood using spotted filter paper disks, by two irradiations for 7 and 35 h with respective decay times of 1 and 3 weeks; counts of 9000-s to 43000-s duration were taken with a decay period of 5 months necessary between the two irradiations.

After activation with thermal neutrons, whole blood (and blood serum), like other biological materials, shows a $\gamma$-spectrum in which $^{24}Na$ is the predominant nuclide; bromine, chlorine and phosphorus ($^{32}P$ bremsstrahlung) also increase background activity. The elimination of sodium without affecting the concentration of other nuclides would in many cases permit the simultaneous determination of many short-lived nuclides, e.g. $^{28}Al$, $^{139}Ba$, $^{80}Br$, $^{49}Ca$, $^{66}Cu$, $^{128}I$, $^{27}Mg$, $^{56}Mn$, $^{101}Mo$, $^{86m}Rb$, $^{52}V$. Sodium has been removed by precipitation as sodium chloride [51] and as a sodium organic salt [52]. The selectivity of these reported procedures, in general, is low and therefore limited in application. The use of ion exchange [53—57], extraction chromatography [58], extraction with butanol-HCl mixtures [59], and electrochemical separations with a glass membrane [60] to remove radiosodium from whole blood, has been reported. Extensive studies have been done by Girardi et al. [61, 62] on radiochemical separation techniques by retention on ionic precipitates, and in particular on hydrated antimony pentoxide (HAP). Although other investigators [55, 63—67] have studied the selectivity of HAP for sodium removal, almost all have used radiochemical separations and, for biological applications, have been limited to long-lived nuclides.

This paper reports on a n.a.a. method with a pre-irradiation HAP separation of sodium after wet ashing of the organic matter in a teflon bomb. The procedure should be applicable to other biological matrices such as urine and body tissues.

## EXPERIMENTAL

### *Instrumentation*

All irradiations were done in the Dalhousie University SLOWPOKE-2

Reactor at a flux of $5 \times 10^{11}$ n $cm^{-2}$ $s^{-1}$. The characteristics, such as flux composition, homogeneity and reproducibility, have been previously reported [68]. Activated samples were counted with a 60-$cm^3$ Canberra Ge(Li) detector (full width at half maximum of 1.88 keV at the 1.332 MeV photopeak of $^{60}Co$, peak-to-Compton ratio of 35:1, and an efficiency of 9.5%) in conjunction with a Tracor Northern TN-11 model 4096-channel pulse-height analyzer.

*Sample preparation and procedure*

The pooled whole blood was provided by the Halifax Infirmary and the pooled blood serum was obtained from the Victoria General Hospital, both of Halifax, Nova Scotia; the samples were stored in 1000-$cm^3$ polyethylene containers at a temperature of less than 6°C. Reported cases of contamination during sample collection, storage and preparation for trace element analysis [69—75] were considered and controlled throughout the sample preparation.

An outline of the procedure followed is shown in Fig. 1. Wet destruction of organic matter was accomplished by adding 2 $cm^3$ of doubly distilled 12 M nitric acid (Fisher Scientific Co. Ltd., A-200) to 2 $cm^3$ of sample in a teflon bomb and heating at 110°C for 12 h. The resulting digested sample solution was taken to dryness under an i.r. lamp (1—2 h) to remove chloride and the residue was redissolved in 1 $cm^3$ of doubly distilled 12 M nitric acid; the solutions were transferred to polyethylene irradiation vials and the vials heat-sealed before storing until irradiation.

Three sets of standard irradiation, decay and counting conditions were selected, permitting the determination of very short-lived, short-lived and long-lived nuclides (Table 1). Prior to digestion, an irradiation for 10 s was carried out to determine very short-lived nuclides. After digestion, a 1:1 volume separation of the sample solution for the HAP separation and long-lived nuclide analysis is necessary.

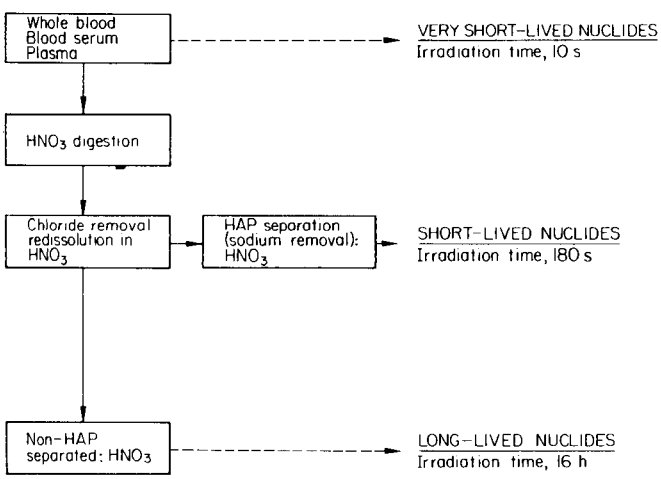


Fig. 1. Procedure outline.

TABLE 1

Irradiation[a] conditions for the neutron activation analysis of whole blood, blood serum and plasma after a pre-irradiation separation step with hydrated antimony pentoxide (HAP)

| | Irradiation time | Decay time | Counting time | Major nuclides measured |
|---|---|---|---|---|
| Very short-lived nuclides[b] | 10 s | 10 s | 60 s | $^{110}$Ag, $^{38}$Cl, $^{77m}$Se |
| Short-lived nuclides | 180 s | 60 s | 600 s | $^{28}$Al, $^{80}$Br, $^{49}$Ca, $^{66}$Cu, $^{128}$I, $^{27}$Mg, $^{86m}$Rb, $^{52}$V |
| | | 660 s | 600 s | $^{139}$Ba, $^{56}$Mn, $^{101}$Tc($^{101}$Mo) |
| Long-lived nuclides[b] | 16 h (overnight) | 3 d | 1800 s | $^{76}$As, $^{198}$Au, $^{51}$Cr, $^{42}$K, $^{122}$Sb |
| | | 6 d | 1800 s | $^{59}$Fe, $^{203}$Hg, $^{24}$Na, $^{46}$Sc, $^{65}$Zn |
| | | 3 w | 3600 s | $^{60}$Co, $^{134}$Cs, $^{58}$Co($^{58}$Ni) |

[a]All samples were irradiated at the Dalhousie University SLOWPOKE-2 Reactor at a flux of $5 \times 10^{11}$ n cm$^{-2}$ s$^{-1}$. [b]Not HAP separated.

Disposable polyethylene columns (7-mm i.d.; Vemor, Italy) with 15-cm$^3$ reservoirs were used in the HAP separation. The columns were prepared by placing a Nuclepore (0.4 $\mu$m) filter at the bottom and filling with HAP (Carlo Erba, Italy) to the 3-cm level (ca. 0.1 g); 5 cm$^3$ of 12 M doubly distilled $HNO_3$ were added to wet and settle the column bed. The exchange was then carried out by adding 1 cm$^3$ of sample solution to the column, followed by 5 successive 1 cm$^3$ volumes of the 12 M $HNO_3$; the total volume eluted was collected into 7.0 cm$^3$ polyethylene vials.

The 12 M $HNO_3$ eluting solution was doubly distilled in a pyrex distillation unit and stored in acid-washed polypropylene containers. Polyethylene containers of sizes 7.0 and 1.5 cm$^3$ (Durham Aircraft Corporation, USA) were used throughout as sample containers and irradiation vials.

Neutron activation analysis was used to check all solutions and irradiation containers for possible contamination.

*Preparation of standards*

Multi-element standards were prepared from Fisher Atomic Absorption standard solutions (1000 $\mu$g ml$^{-1}$) and analytical-grade reagents. To determine the accuracy and precision of the multi-element standards from which the nuclide sensitivities (counts per $\mu$g) were calculated after the standard irradiation schemes already outlined, the National Bureau of Standards Standard Reference Material Bovine Liver (NBS-SRM 1577) was analysed.

## RESULTS AND DISCUSSION

*Effect of activation of whole blood, blood serum and plasma*

The instrumental approach to thermal neutron activation analysis of biological samples is limited to elements with nuclides of very short ($^{20}$F, $t_{\frac{1}{2}}$ = 11.2

$^{77m}$Se, $t_{\frac{1}{2}}$ = 17.5 s), or long ($^{60}$Co, $t_{\frac{1}{2}}$ = 5.26 y; $^{59}$Fe, $t_{\frac{1}{2}}$ = 45 d; $^{65}$Zn, $t_{\frac{1}{2}}$ = 245 d etc.) half-lives because of the high matrix activities of some minor components, especially those of $^{82}$Br ($t_{\frac{1}{2}}$ = 1.48 d), $^{38}$Cl ($t_{\frac{1}{2}}$ = 37 min), $^{24}$Na ($t_{\frac{1}{2}}$ = 15 h) and $^{32}$P ($t_{\frac{1}{2}}$ = 14.3 d; bremsstrahlung radiation). The interference from $^{32}$P as a result of the $^{32}$P(n,$\alpha$)$^{28}$Al reaction is corrected for in the determination of $^{28}$Al. To do rapid multi-element n.a.a. of most biological samples, it is necessary to remove the interference effects so that such short-lived nuclides as $^{28}$Al ($t_{\frac{1}{2}}$ = 2.2 min), $^{66}$Cu ($t_{\frac{1}{2}}$ = 5.1 min), $^{27}$Mg ($t_{\frac{1}{2}}$ = 9.5 min), $^{86m}$Rb ($t_{\frac{1}{2}}$ = 1.04 min), and $^{52}$V ($t_{\frac{1}{2}}$ = 3.8 min) can be measured.

Activation of whole blood at a neutron flux of $5 \times 10^{11}$ n cm$^{-2}$ s$^{-1}$ for 180 s, followed by a 60-s decay, shows a $\gamma$-ray spectrum in which $^{80}$Br, $^{38}$Cl and $^{24}$Na are the predominant nuclides (Fig. 2). Wet destruction of the sample with 12 M nitric acid removes the interference from $^{38}$Cl (Fig. 3). It is therefore necessary to measure $^{38}$Cl under very short-lived nuclide irradiation conditions (10 s).

The elimination of sodium with HAP followed by irradiation for 180 s produces a $\gamma$-ray spectrum (Fig. 4) in which 11 short-lived nuclides can be

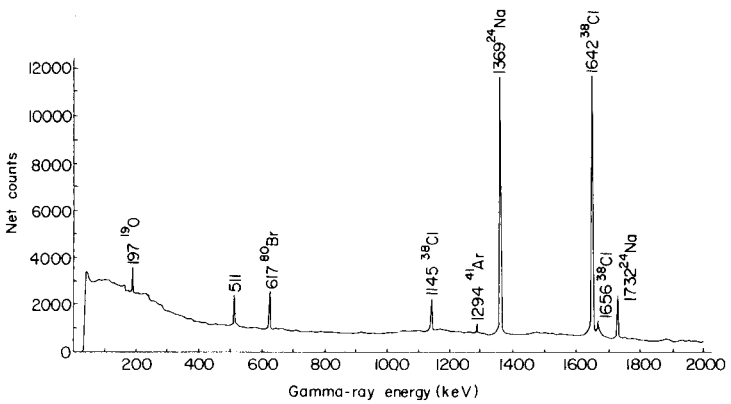


Fig. 2. Pooled whole blood spectrum; 180-s irradiation.

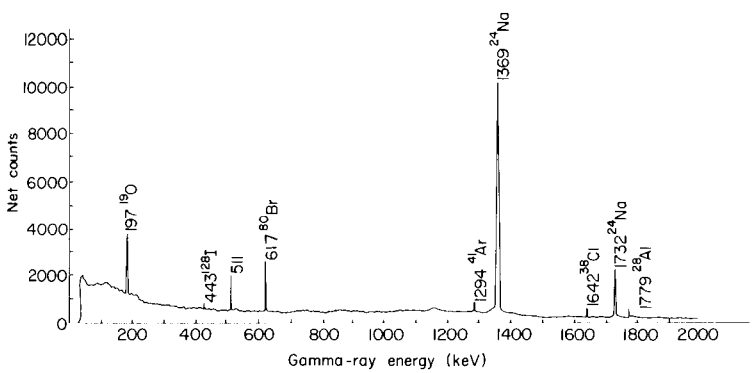


Fig. 3. Nitric acid digested blood spectrum; 180-s irradiation.

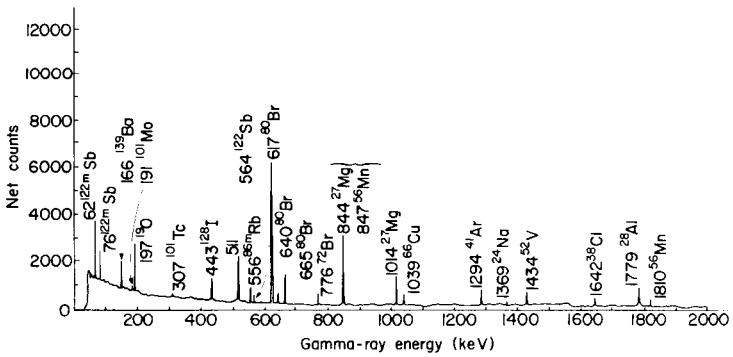


Fig. 4. HAP-separated blood sepctrum; 180-s irradiation.

determined in whole blood. An irradiation time of 180 s produces minimal interference from $^{80}Br$ (which has a very low concentration compared to Cl and Na in whole blood).

Table 2 lists the elements that can be conveniently measured by the n.a.a. scheme involving a pre-irradiation HAP separation step, and the range of very short-lived, short-lived and long-lived nuclides. It should be pointed out that the three sets of irradiation, decay and counting conditions (Table 1) are not optimum for all nuclides in each group (e.g., minimum detection limits, based on half-life alone are obtained for an irradiation time twice $t_{\frac{1}{2}}$) but they enable determination of a number of elements simultaneously with adequate sensitivities.

*Hydrated antimony pentoxide and the retention process*

The selectivity of HAP for sodium has been previously investigated [55, 63–67]. Girardi et al. [61, 62], using HAP in the form of a chromatographic column or in batch equilibrium, showed a retention capacity of the order of 30 mg Na $g^{-1}$ of HAP. Nagy et al. [55] reported studies on the influence of sodium concentration, flow rate and HAP grain size in terms of sorption efficiency.

The retention of different ions by HAP was studied by column experiments with radiotracers (long-lived nuclides) and by chemical separation procedures (short-lived nuclides) for multi-element standards prepared in varying concentrations of doubly distilled nitric acid (2 M, 6 M, 8 M, 10 M , 12 M and 15 M); 1 $cm^3$ of solution was passed through the column and the retention was determined after washing with 10 $cm^3$ of eluting solution. The elements studied (and their valence state) included: $^{110}Ag(I)$, $^{28}Al(III)$, $^{26}As(V)$, $^{198}Au(III)$, $^{139}Ba(II)$, $^{80}Br(I)$, $^{49}Ca(II)$, $^{38}Cl(I)$, $^{60}Co(II)$, $^{51}Cr(III)$, $^{134}Cs(I)$, $^{66}Cu(II)$, $^{59}Fe(III)$ $^{203}Hg(II)$, $^{128}I(I)$, $^{42}K(I)$, $^{27}Mg(II)$, $^{56}Mn(II)$, $^{101}Mo(VI)$, $^{24}Na(I)$, $^{58}Ni(I)$, $^{86m}Rb(I)$ $^{122}Sb(III)$, $^{46}Sc(III)$, $^{77m}Se(VI)$, $^{52}V(V)$, $^{65}Zn(II)$.

Only sodium was quantitatively retained at all concentrations of nitric acid. Optimum selectivity occurred in 12 M $HNO_3$ with silver, arsenic and selenium being the only elements incompletely removed from the HAP. It is therefore

TABLE 2

Elements measured

| Element | Nuclide | γ-ray energy used (keV) | Nuclide half-life | Element | Nuclide | γ-ray energy used (keV) | Nuclide half-life |
|---|---|---|---|---|---|---|---|
| *Very short-lived nuclides* | | | | *Long-lived nuclides* | | | |
| Silver | $^{110}$Ag | 658 | 24.0 s | Arsenic | $^{76}$As | 559 | 26.3 h |
| Selenium | $^{77m}$Se | 161 | 17.5 s | Gold | $^{198}$Au | 412 | 2.7 d |
| *Short-lived nuclides* | | | | Cobalt | $^{60}$Co | 1173 | 5.26 y |
| Aluminium | $^{28}$Al | 1779 | 2.3 min | Chromium | $^{51}$Cr | 320 | 27.8 d |
| Barium | $^{139}$Ba | 166 | 1.38 h | Cesium | $^{134}$Cs | 605 | 2.05 y |
| Bromine | $^{80}$Br | 617 | 18 min | Iron | $^{59}$Fe | 1099 | 45 d |
| Calcium | $^{49}$Ca | 3083 | 8.5 min | Mercury | $^{203}$Hg | 279 | 46.6 d |
| Chlorine | $^{38}$Cl | 1642[a] | 37 min | Potassium | $^{42}$K | 1524 | 12.5 h |
| Copper | $^{66}$Cu | 1039 | 5.1 min | Sodium | $^{24}$Na | 1369 | 15 h |
| Iodine | $^{128}$I | 443 | 25 min | Nickel | $^{58}$Co($^{58}$Ni) | 811 | 71.3 d |
| Magnesium | $^{27}$Mg | 1014[b] | 9.5 min | Antimony | $^{122}$Sb | 564 | 2.8 d |
| Manganese | $^{56}$Mn | 847 | 2.58 h | Scandium | $^{46}$Sc | 1120 | 84 d |
| Molybdenum | $^{101}$Tc | 307 | 15 min | Zinc | $^{65}$Zn | 1115 | 245 d |
| Rubidium | $^{86m}$Rb | 556 | 1.04 min | | | | |
| Vanadium | $^{52}$V | 1434 | 3.8 min | | | | |

[a] $^{38}$Cl is determined in undigested sample (10 s irradiation). [b] $^{27}$Mg at 844 keV suffers from interference by $^{56}$Mn at 847 keV.

necessary for the very short-lived (Ag, Se) and long-lived (As) nuclides to be determined without HAP separation, which fortunately corresponds to irradiation conditions under which $^{24}$Na activity is reduced.

An explanation of the sodium exchange process based on radio-sodium batch equilibrium separations has been reported by Girardi and Sabbioni [61]. Under the conditions used in these experiments the sodium exchange proceeded relatively rapidly at an elution flow rate of 2—3 cm$^3$ min$^{-1}$. The passage of a standard radiotracer solution of $^{56}$Mn and $^{128}$I through a HAP column (Fig. 5) showed that the percentage nuclide eluted as a function of volume eluted (for an eluting solution of doubly distilled 12 M $HNO_3$, at a flow rate of 2 cm$^3$ min$^{-1}$)

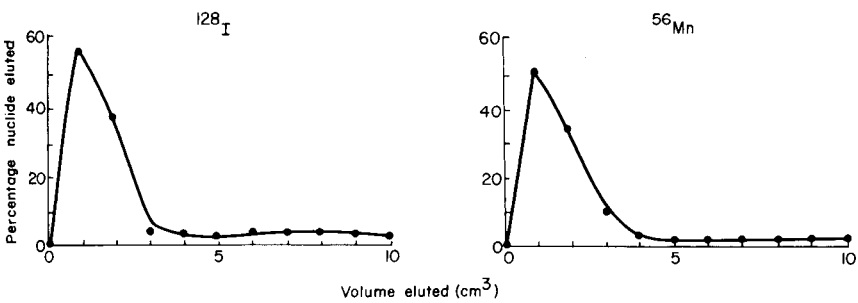


Fig. 5. Elution curves from HAP columns for $^{128}$I (443 keV) and $^{56}$Mn (847 keV).

enables maximum sodium selectivity and complete recovery of the $^{56}Mn$ and $^{128}I$ nuclides with less than 5 $cm^3$ of eluting solution. This pattern is general for all nuclides investigated except Ag, As, Na and Se which are totally or partially retained by the column.

*Accuracy and precision for SRM Bovine Liver*

Information about the accuracy of this n.a.a. method based on the pre-irradiation HAP separation in order to determine short-lived nuclides, was obtained by analysing Bovine Liver (NBS-SRM 1577) under the same irradiation conditions and experimental scheme outlined for whole blood, blood serum and plasma. The elemental content obtained from the average of six determinations of this SRM (Table 3) agrees extremely well with both certified

TABLE 3

Analysis of NBS Bovine Liver (NBS-SRM 1577)

| Element | Nuclide | Elemental content ($\mu g\ g^{-1}$, dry weight basis) | |
|---|---|---|---|
| | | This work | Cert. [a]/uncert. [b] values |
| Silver[c] | $^{110}Ag$ | 0.040 ± 0.008 | (0.186), 0.04 ± 0.006[b] |
| Aluminium | $^{28}Al$ | 23.4 ± 0.6 | 23.6 ± 2 |
| Arsenic[c] | $^{76}As$ | 0.054 ± 0.002 | 0.055 |
| Gold | $^{198}Au$ | 0.0070 ± 0.0008 | 0.006 ± 0.001[b] |
| Barium[c] | $^{139}Ba$ | 0.22 ± 0.02 | — |
| Bromine | $^{80}Br$ | 8.22 ± 0.4 | 8.5 ± 1.0[b] |
| Calcium[c] | $^{49}Ca$ | 125 ± 13 | 124 ± 6 |
| Chlorine | $^{38}Cl$ | 2680 ± 80 | (0.27%), 0.261 ± 0.02% |
| Cobalt[c] | $^{60}Co$ | 0.178 ± 0.005 | (0.18) |
| Chromium[c] | $^{51}Cr$ | 0.21 ± 0.07 | 0.2 |
| Cesium[c] | $^{134}Cs$ | 0.015 ± 0.002 | 0.013 |
| Copper | $^{66}Cu$ | 188 ± 10 | 193 ± 10 |
| Iron | $^{59}Fe$ | 265 ± 11 | 268 ± 8 |
| Mercury[c] | $^{203}Hg$ | 0.017 ± 0.002 | 0.016 ± 0.002 |
| Iodine | $^{128}I$ | 0.20 ± 0.01 | (0.18), 0.22 ± 0.03[b] |
| Potassium | $^{42}K$ | 0.91 ± 0.08% | 0.97 ± 0.06% |
| Magnesium | $^{27}Mg$ | 608 ± 6 | 604 ± 9 |
| Manganese | $^{56}Mn$ | 10.0 ± 0.7 | 10.3 ± 1.0 |
| Molybdenum | $^{101}Tc(^{101}Mo)$ | 3.3 ± 0.2 | 3.2 |
| Sodium | $^{24}Na$ | 0.244 ± 0.016% | 0.243 ± 0.013% |
| Nickel[c] | $^{58}Co(^{58}Ni)$ | 0.20 ± 0.03 | 0.18 ± 0.026 |
| Rubidium | $^{86m}Rb$ | 18.0 ± 0.3 | 18.3 ± 1.0 |
| Antimony | $^{122}Sb$ | 0.026 ± 0.001 | (0.005), 0.016[b] |
| Scandium[c] | $^{46}Sc$ | 0.0011 ± 0.0001 | 0.001 ± 0.0001[b] |
| Selenium | $^{77m}Se$ | 1.09 ± 0.08 | 1.0 ± 0.1 |
| Vanadium | $^{52}V$ | 0.033 ± 0.003 | 0.06 ± 0.005[b] |
| Zinc | $^{65}Zn$ | 129 ± 4 | 130 ± 13 |

[a]Certified NBS values [76]. [b]Uncertified values [77]. [c]250- and 500-mg portions of standard material analysed. All other values based on 100-mg portions.

and uncertified values [76, 77]. Reasonable sensitivity for most elements could be obtained with 100-mg samples of the standard material (NBS recommends 250 mg because of possible inhomogeneity). For $^{110}$Ag, $^{76}$As, $^{139}$Ba, $^{49}$Ca, $^{60}$Co, $^{51}$Cr, $^{134}$Cs, $^{203}$Hg, $^{58}$Ni and $^{46}$Sc, 250—500 mg of sample was necessary for reliable results.

An evaluation of the precision of the analyses is based on the determined elemental content of six different portions of NBS Bovine Liver (Table 3). The standard deviations from the mean elemental content were, except for Au and Ca, less than ± 10%.

*Detection limits and elemental content of human pooled whole blood and blood serum*

The elemental contents of human pooled whole blood (Table 4) and pooled

TABLE 4

Analysis of pooled whole blood: concentrations are given in $\mu$g ml$^{-1}$

| Nuclide | Elemental content | Literature values[b] | Detection[c] limit ($L_D$) |
|---|---|---|---|
| | Mean ± S.D.[a] | | |
| $^{110}$Ag | 0.018 ± 0.002 | 0.001—0.040 | 0.002 |
| $^{28}$Al | 0.402 ± 0.008 | 0.100—2.000 | 0.081 |
| $^{76}$As | 0.018 ± 0.005 | 0.005—0.800 | 0.008 |
| $^{198}$Au | 0.00025 ± 0.00004 | 0.00050 | 0.00002 |
| $^{139}$Ba | 0.24 ± 0.02 | 0.06—0.45 | 0.07 |
| $^{80}$Br | 3.95 ± 0.14 | 1.30—10.00 | 0.12 |
| $^{49}$Ca | 60.0 ± 6.8 | | 7.8 |
| $^{38}$Cl(%) | 0.370 ± 0.008 | 0.360—0.400 | 0.0002 |
| $^{60}$Co | 0.067 ± 0.002 | 0.001—0.200 | 0.008 |
| $^{51}$Cr | 0.028 ± 0.009 | 0.008—0.140 | 0.020 |
| $^{134}$Cs | 0.0022 ± 0.0008 | 0.0020—0.0110 | 0.0018 |
| $^{66}$Cu | 1.24 ± 0.04 | 0.52—2.00 | 0.42 |
| $^{59}$Fe | 485.0 ± 86.0 | 350—525 | 3 |
| $^{203}$Hg | 0.024 ± 0.005 | 0.002—0.085 | 0.010 |
| $^{128}$I | 0.055 ± 0.008 | 0.002—0.100 | 0.011 |
| $^{42}$K(%) | 0.019 ± 0.002 | 0.017—0.021 | 0.0004 |
| $^{27}$Mg | 43.0 ± 1.8 | 24.8—52.0 | 6.0 |
| $^{56}$Mn | 0.069 ± 0.008 | 0.0005—0.240 | 0.030 |
| $^{101}$Tc($^{101}$Mo) | 0.084 ± 0.012 | 0.001—0.160 | 0.080 |
| $^{24}$Na(%) | 0.36 ± 0.02 | 0.35—0.38 | 0.0002 |
| $^{58}$Co($^{58}$Ni) | 0.14 ± 0.02 | 0.02—0.30 | 0.03 |
| $^{86m}$Rb | 2.75 ± 0.08 | 1.20—6.00 | 0.80 |
| $^{122}$Sb | 0.0090 ± 0.0004 | 0.0010—0.0200 | 0.0011 |
| $^{46}$Sc | 0.0086 ± 0.0008 | 0.0020—0.0140 | 0.0003 |
| $^{77m}$Se | 0.092 ± 0.001 | 0.007—0.320 | 0.042 |
| $^{52}$V | 0.0170 ± 0.0005 | 0.0005—0.1500 | 0.0030 |
| $^{65}$Zn | 8.8 ± 0.2 | 3.3—13.7 | 0.5 |

[a]Standard deviation from 10 determinations. [b]References [1, 2, 36, 47, 78]. [c]Concentrations in $\mu$g ml$^{-1}$, based on ref. [79].

TABLE 5

Analysis of pooled blood serum: concentrations are given in $\mu g\ ml^{-1}$

| Nuclide | Elemental content | Literature values[b] | Detection[c] limit ($L_D$) |
|---|---|---|---|
| | Mean ± S.D.[a] | | |
| $^{110}Ag$ | N.D.[d] | 0.0006—0.0020 | 0.002 |
| $^{28}Al$ | 0.170 ± 0.006 | 0.130—0.210 | 0.073 |
| $^{76}As$ | 0.020 ± 0.002 | 0.001—0.050 | 0.008 |
| $^{198}Au$ | 0.000040 ± 0.000006 | 0.000100 | 0.000020 |
| $^{139}Ba$ | 0.20 ± 0.03 | 0.07—0.43 | 0.06 |
| $^{80}Br$ | 2.94 ± 0.05 | 1.80—4.60 | 0.10 |
| $^{49}Ca$ | 97.0 ± 3.2 | 72.0—110.0 | 5.9 |
| $^{38}Cl(\%)$ | 0.350 ± 0.002 | 0.320—0.380 | 0.0003 |
| $^{60}Co$ | 0.014 ± 0.006 | 0.004—0.021 | 0.006 |
| $^{51}Cr$ | N.D. | 0.0028—0.0324 | 0.030 |
| $^{134}Cs$ | 0.0023 ± 0.0004 | 0.0010—0.0032 | 0.0014 |
| $^{66}Cu$ | 1.03 ± 0.01 | 0.05—1.30 | 0.46 |
| $^{59}Fe$ | N.D. | 0.5—1.25 | 2 |
| $^{203}Hg$ | 0.026 ± 0.002 | 0.040 | 0.008 |
| $^{128}I$ | 0.058 ± 0.002 | 0.028—0.064 | 0.010 |
| $^{42}K(\%)$ | 0.0164 ± 0.0007 | 0.0136—0.0207 | 0.0003 |
| $^{27}Mg$ | 20.3 ± 0.3 | 15.0—28.6 | 5.0 |
| $^{56}Mn$ | N.D. | 0.0005—0.0200 | 0.018 |
| $^{101}Tc(^{101}Mo)$ | N.D. | 0.0084—0.0114 | 0.080 |
| $^{24}Na(\%)$ | 0.322 ± 0.002 | 0.311—0.341 | 0.0003 |
| $^{58}Co(^{58}Ni)$ | N.D. | 0.008—0.040 | 0.030 |
| $^{86m}Rb$ | 1.04 ± 0.04 | 0.80—1.70 | 0.65 |
| $^{122}Sb$ | 0.0038 ± 0.0004 | 0.0030—0.0050 | 0.0010 |
| $^{46}Sc$ | 0.0020 ± 0.0002 | 0.0002—0.0060 | 0.0003 |
| $^{77m}Se$ | 0.118 ± 0.006 | 0.060—0.150 | 0.050 |
| $^{52}V$ | 0.0160 ± 0.0003 | 0.0080—0.0240 | 0.0040 |
| $^{65}Zn$ | 1.01 ± 0.04 | 0.68—1.36 | 0.5 |

[a]Standard deviation from 10 determinations. [b]References [1, 2, 36, 47, 78]. [c]Concentrations in $\mu g\ ml^{-1}$, based on ref. [79]. [d]Not determined.

blood serum (Table 5) were determined for 10 replicate samples. Comparison is made with reported literature values [1, 2, 36, 47, 78], and the detection limits ($L_D$), based on Currie's criterion [79] are given.

Eighteen elements can be determined in whole blood with relatively high precision ($< \pm 10\%$ S.D.); Ag, Hg, I, Mo and Ni are determined with $< \pm 20\%$ S.D. and As, Au, Cr and Cs with $< \pm 35\%$. All 27 elements are easily measured above the calculated detection limits. In comparison, only 16 elements can be determined in blood serum with a standard deviation of $< \pm 10\%$; Au, Ba, Ca, Co and Cs are determined with a standard deviation of $< \pm 20\%$. It is also possible to measure $^{140}La$ ($t_{\frac{1}{2}}$ = 40.2 h, at 1596 keV) in both whole blood and blood serum.

Under the experimental conditions (Table 1) used for the multi-element

determination of pooled blood serum, it was not possible to measure Cr, Fe, Mn and Mo, as their elemental levels were below the limits of detection. Increased sensitivity for $^{56}$Mn and $^{101}$Mo($^{101}$Tc) would result after longer irradiation (10—60 min) at a higher thermal neutron flux of $1.0 \times 10^{12}$ n cm$^{-2}$ s$^{-1}$, but a compromise is necessary as an overall increase in background activity, in particular from $^{80}$Br and $^{82}$Br, would reduce significantly the sensitivities for other short-lived nuclides ($^{28}$Al, $^{27}$Mg and $^{52}$V).

The method described permits determination of 23 or more elements in whole blood, blood serum and plasma; 3 irradiation conditions at a flux of $5 \times 10^{11}$ n cm$^{-2}$ s$^{-1}$ are used. Rapid multi-element analysis is thus possible by n.a.a. so that processing of the large number of biological samples necessary in clinical and human disorder studies can be done in a reasonable time rather than necessitating long irradiation and decay periods.

This work was supported by a grant from the National Research Council of Canada.

REFERENCES

1 D. H. K. Lee (Ed.), Metallic Contaminants and Human Health, Academic Press, New York, 1972.
2 E. J. Underwood, Trace Elements in Human and Animal Nutrition, Academic Press, New York, 4th ed., 1977.
3 G. F. Clemente, J. Radioanal. Chem., 32 (1976) 25.
4 L. Ahlstrom, Kem. Tidskr., 89 (1977) 22.
5 I. H. Qureshi and M. N. Cheema, Report NCD-2 (ACG) from INIS Atomindex, 8 (1977) 8.
6 B. Yu. Shpal and E. M. Neiko, Vrach, Delo., 2 (1978) 10.
7 T. R. Copeland, J. H. Christie, R. A. Osteryoung and R. K.. Skogerboe, Anal. Chem., 45 (1973) 2171.
8 M. J. Pinchin and J. Newham, Anal. Chim. Acta, 90 (1977) 91.
9 E. Berman, Appl. Spectrosc., 29 (1975) 1.
10 J. D. Bogden and M. M. Joselow, J. Am. Ind. Hyg. Assoc., 35 (1974) 88.
11 G. D. Christian, Anal. Chem., 41 (1969) 24A.
12 G. L.. Everett, Analyst, 101 (1976) 348.
13 H. Koizumi and K. Yasuda, Anal. Chem., 48 (1976) 1178.
14 H. Metzger and W. Lautenschlaeger, Ger. Forschung. Berghof. G. M. B. H., Patent, 1977.
15 A. Montaser, S. R. Goode and S. R. Crouch, Anal. Chem., 46 (1974) 599.
16 R. A. A. Muzzarelli and R. Rocchetti, Talanta, 22 (1975) 683.
17 R. A. A. Muzzarelli and R. Rocchetti, Talanta, 24 (1977) 77.
18 E. A. Gainullina, T. K.. Aidarov and L. S. Zakharov, Lab. Delo-Cisti, 2 (1973) 83.
19 M. G. Kalinin, Fiziko-Khimicheskie Problemy V Sovermennoi Biologii I Meditsine, Materially Konferentsii, Tyumenskii Gros. Med. Inst., (1970) 136.
20 A. Johansson and L. E. Nilsson, Spectrochim. Acta Part B, 31 (1976) 419.
21 M. Barrette, G. Lamoureux, E. Lebel, R. Lecomte, P.. Paradis and S. Monaro, Nuclear Inst. Methods, 134 (1976) 189.
22 D. N. Breiter and M. L. Roush, Am. J. Phys., 43 (1975) 569.
23 P. S. Ong, P. K. Lund. C. E. Litton and B. A. Mitchell, Advan. X-ray Anal., 16 (1973) 124.
24 R. L. Watson, C. J. McNeal and F. E. Jenson, Advan. X-ray Anal., 18 (1975) 288.
25 R. Woldseth, Semiconductor Detectors in Medicine, (Symposium) Springfield, Va., Conf-730321 (1973) 10.

26 J. Růžička, E. H. Hansen and E. A. Zagatto, Anal. Chim. Acta, 88 (1977) 1.
27 D. F. Ball, M. Barber and P. G. T. Vossen, Biomed. Mass Spect., 1 (1974) 365.
28 R. A. Bingham and P. G. T. Vossen, Lab. Pract., 24 (1975) 233.
29 W. Gooddy, T. R. Williams and D. Nicholas, Brain, 97 (1974) 327.
30 M. L. Jacobs, Health Educ. Welfare (U.S.), 75 (1975) 91.
31 R. Cesareo, Eur. J. Nucl. Med., 1 (1976) 49.
32 R. W. Flint, C. D. Lawson and S. Standil, J. Lab. Clin. Med., 85 (1975) 155.
33 A. Gallmann, A. Guillaume and P. Fintz, J. de Physique, 8 (1973) 21.
34 I. G. Stump, J. Carruthers, J. M. D'Auria, D. A. Applegarth and A. G. F. Davidson, Clin. Biochem., 10 (1977) 127.
35 N. V. Bagdavadze and L. M. Mosulishvili, J. Radioanal Chem., 24 (1975) 65.
36 D. Behne and H. Jürgensen, J. Radioanal. Chem., 42 (1978) 447.
37 R. Cornelis, A. Speecke and J. Hoste, Anal. Chim. Acta, 68 (1973) 1.
38 E. Damsgaard, K. Heydorn, N. A. Larsen and B. Nielsen, Riso Rept. 271 (1973).
39 J. J. M. De Goeij, P. S. Tjioe, C. Pries and J. H. L. Zwiers, Report IRI-133-76-10 (1976) from INIS Atomindex, 8 (1977).
40 K. Fritze and R. Robertson, J. Radioanal. Chem., 1 (1968) 463.
41 K. Kasperek, Proc. Int. Conf. Nucl. Methods Environ. Res. 2nd, 1974, (CONF-740701) 154.
42 J. M. A. Lenihan in J. M. Lenihan and S. J. Thomson (Eds.), Activation Analysis: Principles and Applications, Academic Press, London, 1965, p. 119.
43 G. J. Lutz, R. J. Boreni, R. S. Maddock and J. Wing, Activation Analysis: A Bibliography through 1971, National Bureau of Standards, Washington, D.C., 1972.
44 R. A. Nadkarni and G. H. Morrison, Radiochem. Radioanal. Lett., 24 (1976) 103.
45 J. Versieck, J. Hoste, F. Barbier, H. Michels and J. DeRudder, Clin. Chem., 23 (1977) 1301.
46 D. D. Zdankiewicz and J. L. Fasching, Clin. Chem., 22 (1976) 1361.
47 T. F. Budinger, J. R. Farwell, A. R. Smith and H. Bichsel, Int. J. Appl. Radiat. Isot., 23 (1972) 49.
48 M. C. Haven, G. T. Haven and A. L. Dunn, Anal. Chem., 38 (1966) 141.
49 R. Malvano, U. Rosa and P. Grosso, Int. J. Appl. Radiat. Isot., 18 (1967) 121.
50 P. D'Hondt, P. Lievens, J. Versieck and J. Hoste, Radiochem. Radioanal. Lett., 31 (1977) 231.
51 M. P. Menon and R. E. Wainerdi, Proc. 1965 Intern. Conf. Modern Trends in Activation Analysis, Texas A. and M. University, Texas, U.S.A., 1965, 152.
52 W. Bock-Wertmann, Proc. Intern. Conf. Activation Techniques in the Life Sciences, paper SM-91/24, IAEA (1967).
53 N. Spronk, Trans. Am. Nucl. Soc., 6 (1963) 398.
54 J. A. Buono, J. C. Buono and J. L. Fasching, J. Radioanal. Chem., 36 (1977) 353.
55 L. G. Nagy, C. Török, G. Foti, T. Toth and L. Feuer, J. Radioanal. Chem., 16 (1973) 245.
56 C. W. Tang and C. J. Maletskos, Science, 167 (1970) 52.
57 P. S. Tjioe, J. J. M. De Goeij and J. P. W. Houtman, J. Radioanal. Chem., 37 (1977) 511.
58 Yu. F. Korshunov, L. I. Zhuk, I. I. Orestova, E. S. Gureev and A. A. Kist, Zh. Anal. Khim., 31 (1976) 1962.
59 M. P. Menon and R. E. Wainerdi, Proc. 1965 Intern. Conf. Modern Trends in Activation Analysis, Texas A, and M. University, Texas, U.S.A., 1965, 114.
60 W. J. deWet. J. S. Afr. Chem. Inst., 22 (1969) 168.
61 F. Girardi and E. J. Sabbioni, J. Radioanal. Chem., 1 (1968) 169.
62 F. Girardi, R. Pietra and E. J. Sabbioni, J. Radioanal. Chem., 5 (1970) 147.
63 I. N. Bourrelly, C. C. Leyrergue, N. Deschamps, H. Jaffrezic, B. Vialatte, S. Alexandrov and H. N. Barrandon, Radiochem. Radioanal. Lett., 5 (1970) 43.
64 W. A. Haller, R. H. Filby and L. A. Rancitelli, Nucl. Appl; 6 (1969) 365.
65 R. A. Nadkarni and W. D. Ehmann, Radiochem. Radioanal. Lett., 2 (1969) 161.
66 H. R. Ralston and E. S. Sato, Anal. Chem., 43 (1971) 129.
67 G. Von Török and J. F. Diehl, Radiochim. Acta, 15 (1971) 96.
68 D. E. Ryan, D. C. Stuart and A. Chattopadhyay, Anal. Chim. Acta, 100 (1978) 87.

69 V. D. Anand, J. M. White and H. V. Nino, Clin. Chem., 21 (1975) 295.
70 K. Matamba and D. Behne, Rapp. Rech. - Cent. Reg. Etud. Nucl. Kinshasa, 20 (1974) 124.
71 B. Maziere, A. Gaudry, J. Gros and D. Comar, Radiochem. Radioanal. Lett., 28 (1977) 155.
72 J. W. Mitchell, Anal. Chem., 45 (1973) 492A.
73 A. Taylor and V. Marks, Ann. Clin. Biochem., 10 (1973) 42.
74 E. Z. Helman, D. K. Wallick and J. M. Reingold, Clin. Chem., 17 (1971) 61.
75 N. I. Ward and D. E. Ryan, unpublished data.
76 National Bureau of Standards, Certificate of Analysis, Standard Reference Material 1577, Bovine Liver, Washington, D.C., 1977.
77 A. Chattopadhyay, K. M. Ellis and K. N. DeSilva, Intern. Atom. Energy Agency, Intern. Symp., Nucl. Activ. Techniq. in Life Sci., Vienna, Austria, 1978.
78 E. I. Hamilton, M. J. Minshi and J. J. Cleary, Sci. Total Environ., 1 (1972/3) 341.
79 L. A. Currie, Anal. Chem., 40 (1968) 586.

*Analytica Chimica Acta*, 105 (1979) 199—212


# OPTIMIZATION OF INSTRUMENTAL VARIABLES IN FLAME ATOMIC ABSORPTION SPECTROMETRY

N. W. BOWER[‡] and J. D. INGLE, Jr.*

*Department of Chemistry, Oregon State University, Corvallis, Oregon 97331 (U.S.A.)*

(Received 31st August 1978)

SUMMARY

The optimization of flame atomic absorption instrumental variables such as hollow-cathode lamp current, slit width, slit height, flame type and stoichiometry, burner position, resonance line, and integration time for best precision or signal-to-noise ratio is discussed. Because different types of noise are limiting in different absorbance regions, optimum values of instrumental variables can vary with the absorbance measured.

In previous papers [1, 2] the factors which affect the relative precision of atomic absorption (a.a.s.) measurements were treated theoretically. The theory allows prediction of how the relative standard deviation in absorbance ($\sigma_A/A$) varies with absorbance ($A$) and the relative contribution of different noise sources to the total precision.

The precision characteristics of a representative group of twenty-one elements were determined and compared to theoretical predictions under the normal instrumental conditions recommended by the manufacturer, and in some cases, under conditions different from normal [3—5]. It was shown that agreement between theory and experiment was reasonably good, that different noise sources are important in different absorbance regions, and that dominant noise sources for a given element could be predicted to some extent from the analytical wavelength.

The purpose of this paper is to indicate how the relative contribution of different noise sources and the overall precision of measurement are affected by instrumental conditions. The instrumental variables studied are hollow-cathode lamp current, slit width, slit height, flame type and stoichiometry, burner position, resonance line, and integration time. In addition, the effects of the use of a gas sheath and the chemical interferences in solutions are evaluated. Although all measurements were made on one particular instrument, the results indicate the most critical variables and trends so that other users can efficiently optimize the most important variables on their particular instrument.

[‡]Present Address: Department of Chemistry, The Colorado College, Colorado Springs, CO 80903, U.S.A.

## EXPERIMENTAL

A Varian-Techtron AA-6 spectrometer was used with an external voltmeter and computer (PDP-11/20) to obtain the data as previously described [3—5]. Readout resolution was 0.001% $T$ and was never limiting. Thirty 1-s measurements were taken for every case except where otherwise noted. Calculations of $\sigma_A/A$ and the magnitude of different noise sources were carried out as previously described [3—5].

## RESULTS AND DISCUSSION

Previous work has indicated that a precision plot ($\sigma_A/A$ vs. $A$) for most elements has the general form shown in Fig. 1. Region I covers absorbances from the detection limit to about 0.1 absorbance units (a.u.); in this region signal shot noise, lamp flicker noise, and flame transmission noise usually limit precision. For elements with resonance lines below 250 nm, flame transmission flicker noise is usually the dominant noise source. Region II extends from about 0.1 a.u. up to 1.0 or 1.5 a.u., where region III takes over, and is the region most analytically useful. Region II is dominated by analyte absorption noise in most cases. Here $\sigma_A/A$ is relatively constant and may decrease at higher absorbances if there is negative deviation in the calibration curve. Finally region III is reached when flame background emission noise or analyte emission noise predominates. This region is rarely used analytically but is useful for verifying theories about precision. Analyte emission noise is likely to predominate for resonance lines above 350 nm, and background emission noise will be dominant if the resonance line sits on top of a bandhead in the flame background.

For some elements, e.g. As, Se, V, region III is not observed because large negative deviations prevent high absorbances from being reached. Also for some elements the relative background noise is high because it appears on top of an emission bandhead (e.g. with Mo, Ca) or because the hollow-

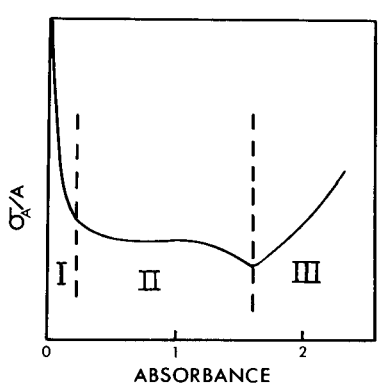


Fig. 1. Hypothetical precision plot demonstrating precision regions.

cathode lamp is of low intensity (e.g. for As, Se, Fe) so that background emission noise is significant or dominant in region II and sometimes even region I.

Because different noise sources generally predominate in the three regions, it is critical to realize that optimal instrumental settings for the best signal-to-noise ratio ($S/N$) or precision will vary depending on the region in which measurements are made. Changing an instrumental variable may affect $\sigma_A/A$ by changing either $A$ or $\sigma_A$ or both, and thus cause measurements to be moved from one region to another. In region I the absolute noise or $\sigma_A$ (which is essentially the blank noise) is relatively constant so that $\sigma_A/A$ can be improved by decreasing $\sigma_A$ or increasing $A$ until measurements are limited by analyte absorption noise or move into region II. In region II, $\sigma_A$ is proportional to $A$ until significant negative deviation occurs in the linear calibration plot, and the precision of determining a concentration ($\sigma_c/c$) does not change unless an instrumental change causes measurements to move into region I or III. In region III, $\sigma_A$ increases with $A$ so that precision can generally be improved only by decreasing the noise or $\sigma_A$.

One more important point is the dependence of the relative magnitude of different noise sources on the product of the absolute lamp radiant power striking the photomultiplier tube (PMT) photocathode and the sensitivity of the PMT photocathodic surface. This product is the photocathodic current ($i_r$) and can be significantly changed by varying the lamp current, the slit width, the slit height, and resonance lines, and to a lesser degree, by the transmission characteristics of the flame. The relative source, flame transmission, and analyte absorption noises are independent of $i_r$ as a first approximation. The relative signal shot noise is proportional to $i_r^{-1/2}$, and the relative analyte or background emission noise is proportional to $i_r^{-1}$ if the absolute value of the emission noise is not changed. Most variables except the lamp current affect the absolute emission noises, and in region III $\sigma_A/A$ is proportional to the ratio of the r.m.s. emission noise to $i_r$.

*Lamp Current*

Higher lamp currents mean higher intensities and less relative signal shot noise and emission noises, but they lead to reduced lamp life and often reduced sensitivities and larger negative deviations in the calibration curve because of increased self-absorption and line broadening in the lamp. If signal shot noise were limiting, increased lamp current would improve precision. However, with the Varian AA-6 for the elements tested, signal shot noise is never a dominant noise source at any absorbance for normally used currents. Decreasing the lamp current to reduce the intensity by a factor of ten from normal would increase the relative signal shot noise by a factor of $10^{1/2}$. For most elements, except selenium and arsenic for which background emission noise is much higher, this change would have little effect on precision at low absorbances.

In region I, increased lamp current could improve precision and detection limits only if the relative source flicker noise ($\xi_1$) was reduced and only to the

TABLE 1

Dependence of sensitivity and lamp flicker factor on lamp current for measurements of zinc, cadmium, sodium and iron
(All measurements were made with 0.2-nm spectral bandpass, 10-mm slit height, 1-s integration time, air/acetylene flame; $m_a$ is the concentration in ppb which yields 99% $T$; the signal shot noise at lowest lamp current equals 14, 13, 7.6, and 17 × $10^{-4}$, respectively, for Zn, Cd, Na, and Fe; $\xi_1$ is the lamp flicker factor which is the relative noise in the lamp signal after subtraction of signal shot noise, dark current noise, and amplifier-readout noise.)

| Lamp current (mA) | $m_a$ | $\xi_1$ (×$10^4$) | $m_a\xi_1$ (×$10^2$) | Lamp current (mA) | $m_a$[a] | $\xi_1$ (×$10^4$) | $m_a\xi_1$ (×$10^2$) |
|---|---|---|---|---|---|---|---|
| *Zinc* | | | | *Cadmium* | | | |
| 2 | 0.12 | 17 | 2.0 | 3 | 11 | 28 | 3.1 |
| 5 | 0.17 | 10 | 1.7 | 7 | 15 | 5.8 | 0.9 |
| 10 | 0.25 | 9.4 | 2.4 | 12 | 22 | 5.1 | 1.1 |
| 15 | 0.34 | 7.7 | 2.6 | | | | |
| *Sodium* | | | | *Iron* | | | |
| 1 | 1.5 | 15 | 0.23 | 2 | 60 | 9.4 | 5.6 |
| 3 | 2.0 | 6.0 | 0.12 | 6 | 62 | 5.6 | 3.5 |
| 6 | 3.0 | 2.6 | 0.08 | 15 | 80 | 2.0 | 1.6 |
| 10 | 6.5 | 2.5 | 0.16 | | | | |

[a]Data from Varian [6].

point that flame transmission noise became dominant [3, 4]. The lamp flicker factor, $\xi_1$, i.e. relative noise from source flicker, varies from about $2 \times 10^{-4}$ to $2 \times 10^{-3}$ for the elements tested for a 1-s integration. $\xi_1$ would be expected to vary with lamp current, because this should affect the dynamic nature of the sputtering of the hollow-cathode surface, as well as the degree of self-absorption. In Table 1, data for a few elements are presented to show the relationship between the lamp current and $\xi_1$. Generally the higher the current, the lower the lamp flicker. It is necessary to balance this reduction in noise gained by a reduced lamp flicker against the probable reduced sensitivity incurred at high lamp currents; hence for best precision in region I one must optimize $\sigma_A/A$ or $\sigma_{rt}/A$, where $\sigma_{rt}$ is the noise in the 100% $T$ signal. In Table 1 the products of the sensitivity and the lamp flicker factor are shown for four elements. This product is proportional to the detection limit, i.e. inversely proportional to the precision at small absorbances. There is usually a minimum somewhere near 6—7 mA for Westinghouse lamps; but for a few elements such as iron this is clearly not the minimum, so that it is necessary to determine the optimum for each element. (Even different lamps for the same element may be different, depending on the cathode sputtering properties and age of the lamp). Because flame transmission noise is about the same size (e.g. Na, Fe) or much greater

(e.g. Zn, Cd) than source flicker noise, changing the lamp current from normal to high values will result in no, or only up to a factor of 2, improvement in precision in region I. Indeed, this may decrease precision for a given concentration if the $m_a$ is significantly degraded.

For work in region II, i.e. with moderate absorbances, the usual analytical region, low to moderate lamp currents will be the best. There, lamp flicker noise is not limiting and the lamp current will not affect the precision or $S/N$ though it will affect which concentrations give the optimum precision of measurement. Lower lamp currents will often reduce the degree of non-linearity of calibration curves and increase lamp life. However, region III, where there will be an increase in $\sigma_A/A$, may start at lower concentrations for lower lamp currents.

In region III, lower lamp signals will decrease the ratio of lamp signal to emission noise and hence decrease the precision. Therefore, higher lamp currents may be advantageous for many elements in region III, but this must be balanced against larger negative deviations from linearity, so that $\sigma_A/A$ or actually $\sigma_c/c$ should be optimized. Data for calcium in Table 2 (spectral bandpass 0.2 nm at 3 and 7 mA) illustrate that increasing the lamp current and reducing the gain by a factor of 5 will improve $\sigma_A/A$ by a factor of 6 at high absorbances where analyte emission noise is limiting as predicted.

A titanium lamp was run at its normal 20 mA current and also at 5 mA to determine the effect on precision at all absorbances [4]. There was little difference in precision because emission noises were never limiting. For the twenty-one elements studied, lamp currents higher than normal would significantly increase precision at moderate absorbances only for calcium in a nitrous oxide—acetylene flame and for arsenic and selenium

TABLE 2

Dependence of the relative standard deviation on slit height, width and lamp current for 100-ppm calcium in a $N_2O$—$C_2H_2$ flame

| Slit height (mm) | Spectral bandpass (nm) | $A$ | $E_e$ [a] | $E$(PMT) (V) | Lamp current (mA) | $\sigma_A/A$ (%) |
|---|---|---|---|---|---|---|
| 10 | 0.2 | 2.44 | —[b] | 287.4 | 7 | 2.5 |
| 4 | 0.2 | 2.43 | 1.78 | 287.4 | 7 | 1.4 |
| 2 | 0.2 | 2.45 | 0.94 | 287.4 | 7 | 0.95 |
| 1 | 0.2 | 2.51 | 0.45 | 287.4 | 7 | 0.44 |
| 2 | 0.5 | 2.18 | —[b] | 336.2 | 4.5 | 2.3 |
| 2 | 0.2 | 2.45 | 0.94 | 287.4 | 7 | 0.82 |
| 2 | 0.2 | 2.50 | —[b] | 357.0 | 3 | 5.0 |
| 2 | 0.1 | 2.94 | 0.89 | 336.2 | 7 | 1.3 |

[a]The analyte emission signal $E_e$ was measured in the emission mode.
[b]Value off scale.

because of the large relative flame or analyte emission noises. This is the basic reason for the common use of more intense electrodeless discharge lamps for the latter two elements; i.e. not because of signal shot noise limitations.

*Slit width*

Increasing the slit width increases the lamp radiant power impingent on the PMT and hence reduces the relative amount of signal shot noise at all absorbances. However, as previously mentioned, signal shot noise is not a dominant noise source in the measurements presented at typical slit widths at any absorbance. Wider slits also increase the background and analyte emission signals, and hence the absolute amount of emission noises. For many elements, increasing the slit width lets through lines other than the desired resonance line from the hollow-cathode lamp, which reduces sensitivity and causes more severe negative deviation. The effect of slit width on source and flame transmission flicker had not been previously studied in detail.

In region I, wider slits would help if the relative amount of source or flame transmission flicker noise were reduced. In Table 3 the dependency of the lamp flicker ($\xi_1$) and flame transmission flicker ($\xi_2$) on the slit width is shown for zinc. Both flicker factors are almost halved at larger slit widths. Wider slits might be expected to provide some improvement, because the wider slits mean that a larger portion of the hollow-cathode image and flame is viewed and spatial inhomogeneities would be averaged out. Any reduction in noise must be balanced against a loss in sensitivity so that $\sigma_A/A$ or $\sigma_{rt}/A$ must be optimized. For most of the elements tested, changing the spectral

TABLE 3

Dependence of the lamp flicker factor ($\xi_1$) and the flame transmission flicker factor ($\xi_2$) on spectral bandpass and slit height at the analytical wavelength for zinc (213 nm)

| Spectral bandpass (nm) | Slitheight (mm) | $\xi_1$ ($\times 10^4$) | $\xi_2$ ($\times 10^3$)[a] | % $T$ |
|---|---|---|---|---|
| 0.1 | 2 | —[b] | 6.3 | 5 |
| 0.2 | 2 | 7.2 | 6.2 | 18 |
| 0.5 | 2 | 9.4 | 2.9 | 47 |
| 1.0 | 2 | 4.8 | 3.1 | 100 |
| 0.5 | 1 | 8.7[c] | 5.3 | 53 |
| 0.5 | 2 | 7.4 | 7.8 | 83 |
| 0.5 | 4 | 3.2 | 8.7 | 98 |
| 0.5 | 10 | 4.1 | 5.7 | 100 |

[a] $\xi_2$ is the flame transmission flicker factor obtained under fuel-rich conditions and is the relative noise in the reference signal after subtraction of lamp noise and flame background emission noise.

[b] Measurement dominated by signal shot noise = $3.0 \times 10^{-4}$ at 0.1 nm.

[c] Signal shot noise at 1 mm = $3.4 \times 10^{-4}$.

bandpass from 0.1 to 1.0 nm reduces the sensitivity by very little except for a few elements (e.g. Ni, Co, Mn).

In region II, where measurements are limited by the analyte absorption flicker, changing the slit width had no measurable effect on the precision and hence this fluctuation must be primarily time-dependent rather than spatially dependent. The main advantages of a narrow slit would be to improve the sensitivity for some elements so that lower concentrations would be moved from region I to region II with improvement in precision and with wider linear calibration ranges.

In region III, halving the slit width will halve the lamp signal and the analyte emission signal, and will reduce the background signal to a quarter of its original value (if the background is a continuum over the spectral bandpass). This will increase the relative analyte emission noise ($\sigma_e/E_r$) and $\sigma_A/A$ by $2^{1/2}$ if the signal is limited by analyte emission shot noise, but will not affect matters if the precision is limited by analyte emission flicker noise. It will also halve the relative background emission noise if the signal is limited by background emission flicker noise but will cause no change if the precision is limited by background emission shot noise. Hence in region III, the slit must be optimized for the lowest $\sigma_A/A$ depending on which noise source is limiting. At the lamp modulation frequency only the white shot noise in either the background or analyte emission signals is usually observed; thus decreasing the slit width will normally result in no change (if flame background noise predominates) or a decrease in the precision (if analyte emission noise predominates). Thus larger than normal slit widths usually will improve precision in region III if analyte emission noise is limiting and if negative deviations from linear calibration plots are not significantly increased.

Comparison of $\sigma_A/A$ at spectral bandpasses of 0.2 and 0.1 nm at 7 mA (Table 2) shows that precision is decreased by a factor of about $2^{1/2}$ by using a smaller slit width as predicted if the signal is limited by analyte emission shot noise. An examination of manganese at different slit widths [4] showed that there was little difference in precision at all absorbances, except that for a spectral bandpass of 0.05 nm, the light levels were reduced to the point that signal shot noise was limiting in region I.

*Slit height*

Slit height has much the same effect as slit width except for the important difference that slit width controls the spectral bandpass as well as the volume of the flame or the area of the lamp image viewed; slit height controls only the latter aspect and can therefore be used solely to reduce the amount of light reaching the PMT.

Table 3 shows the lamp and flame flicker factors for zinc versus the slit height. The lamp flicker does not improve much with slit heights larger than 2—4 mm, while the flame flicker does not seem to depend on the slit height. The amount of light transmitted increases with slit height; but for zinc

hollow-cathode lamps, the image of the cathode surface focused on the slit is only 2—3 mm in diameter, so that little can be gained by increasing the slit height much beyond 2 mm. As happened for the slit width, the flame transmission flicker might be expected to improve with larger slit height, but the data do not support such an hypothesis. However, the 2-mm slit height is about 13 times greater than the width corresponding to a 0.2-nm spectral bandpass, so that flame inhomogeneities may not be significant at this level. The vertically oriented inhomogeneities may also be less important than the horizontal (cross burner) components (see below).

For region I, the slit height should be 2—3 mm or whatever is the diameter of the hollow-cathode image viewed. In region II, little is gained by changing the slit height, except that sensitivity may decrease at large slit heights if the absorption properties of the element are especially dependent on burner height (e.g., for potassium). Finally, in region III, a short slit height would be useful in reducing the contribution from emission noises. Reducing the slit height from 10 to 2 mm has little effect on the lamp signal but can significantly reduce the background or analyte emission signal and noise and thereby improve the precision when limited by emission noise. Table 2 verifies these predictions for calcium.

*Flame Type*

Generally either nitrous oxide—acetylene or air—acetylene flames are used in a.a.s. The former flames are usually preferred for refractory elements and to minimize solute vaporization effects. The type of flame affects the flame transmission flicker noise, analyte emission noise, and background emission noise. The relative flame background and analyte emission noise are greater by factors of 3—12 in the nitrous oxide—acetylene flame (3—5); this degrades precision in region III and decreases the absorbance at which region III is reached. Because of this, much better precision is obtained for calcium in the cooler air—acetylene flame at moderate and high absorbances [3]. As flame transmission noise increases with flame absorbance, the more transparent nitrous oxide—acetylene flame can yield better precision in region I for elements, e.g. arsenic, with resonance lines at wavelengths below 250 nm where the flame absorbs significantly. However, if the hollow-cathode lamp intensity is weak enough that flame background emission noise is significant at low absorbances, e.g. for selenium, the nitrous oxide—acetylene flame will decrease the precision in region I [4]. For elements at wavelengths where the flame does not absorb significantly, there is little difference in flame transmission noise ($\xi_2$).

*Flame stoichiometry*

Flame stoichiometry has the same effect as flame type in that it varies the atomization efficiency, the relative amount of analyte and flame background emission noise which affects primarily region III, and the flame transmission noise ($\xi_2$) for wavelengths below 250 nm which affects precision in region I.

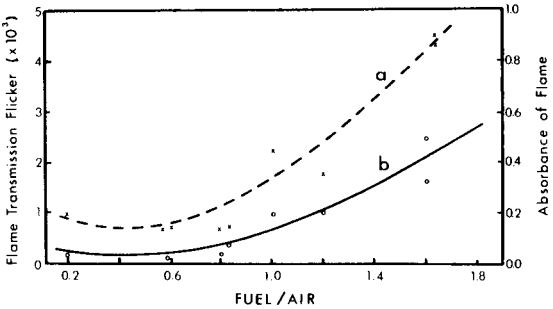


Fig. 2. Dependence of flame absorbance ($A$) and flame transmission flicker noise ($\xi_2$) on flame stoichiometry. Curve (a) (×), $\xi_2$; curve (b) (○), $A$.

The effect of flame stoichiometry on flame transmission noise measured at the Zn wavelength (213.9) with a blank is illustrated in Fig. 2. Clearly, flame transmission noise increases with flame absorbance. In region I, zinc is limited by flame transmission noise, thus a more reducing flame should decrease the precision ($\sigma_A/A$). In general, since flame background emission noise increases with the fuel-to-oxidant ratio, the precision in region III will be worse for a reducing flame and the absorbance at which region III starts may be lowered.

*Burner position*

The burner position is fairly easy to optimize; experimentally, it was found that the maximum $S/N$ occurs at the same burner position as a maximum in the absorbance, at least for optimizations with concentrations from regions I and II. In Figs. 3—5, profiles for the air—acetylene flame are presented for both $A$ and $\sigma_A/A$. Noise profiles agree with those published [7]. These were obtained by measuring the absorbance and its relative standard deviation at a number of different positions with manual relocation of the burner. Concentrations of analyte were selected in each case so that analyte absorption flicker would predominate, except for the 0.5 ppm zinc readings, where flame transmission flicker predominates. The losses in sensitivity or precision are presented as factors of the best signal or precision; thus the 10× line for a precision profile indicates that the precision is 10× worse than at the best position. A 0.2-nm spectral bandpass and 2-mm slit height were used for all measurements.

The absorbance maxima correspond roughly with the precision maxima although the region over which $\sigma_A/A$ is constant is often much larger. Moreover, the different elements do not have the same absorbance or noise profiles; the profile for potassium is best quite near the burner head. The data for zinc (Fig. 3A) indicate that the absorbance profiles vary with concentration, probably because of the higher concentration "loading" the flame to a greater degree. The precision profiles (Fig. 3B) are much more similar, however, indicating that the cases dominated by flame transmission flicker noise and those dominated by analyte absorption noise are not

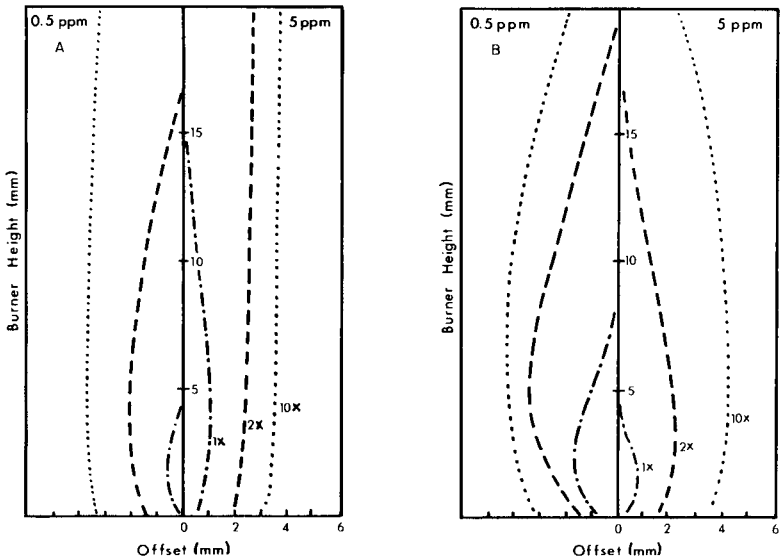


Fig. 3. Absorbance ($A$) and precision ($B$) profile for 0.5 ppm zinc (limited by flame transmission noise) and 5 ppm zinc (limited by analyte absorption flicker noise).

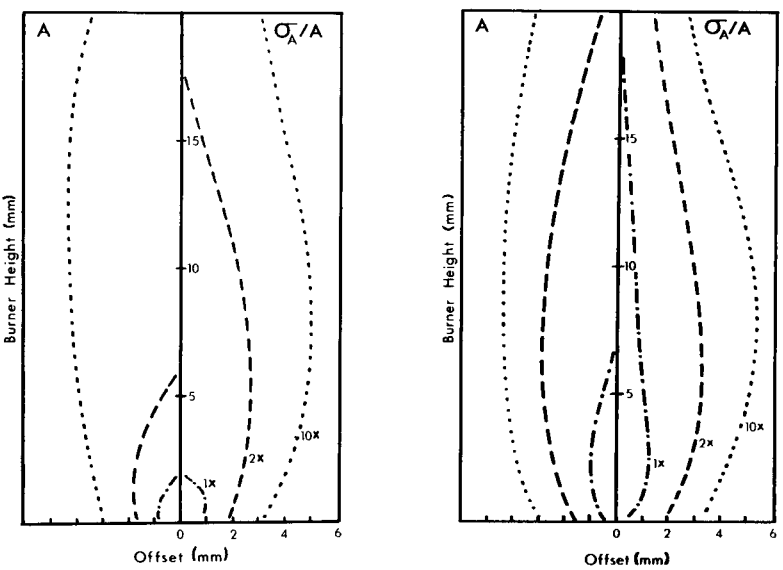


Fig. 4. (left) Absorbance and precision profiles for 2.5 ppm potassium (limited by analyte absorption flicker noise).

Fig. 5. (right) Absorbance and precision profiles for 2.5 ppm copper (limited by analyte absorption flicker noise).

significantly different, which suggests a possible common origin for the two fluctuations, e.g. variable gas rates or hot spots in the flame. At the edges of the flame or at very high burner heights, the turbulence caused by entrained air and by cooling of the flame leads to a decrease in both the precision and the absorbance. In region III, the optimum burner height would be different than in regions I and II only if the emission noise from analyte and background and the analyte absorbance varied differently with burner height.

*Resonance line*

Different resonance lines may be selected, usually to change the sensitivity so that higher concentrations of the analyte can be determined without dilution of the sample, or to avoid some matrix problem such as absorption by NaCl at the normal nickel wavelength (232.0 nm). Since the noises discussed here are generally independent of the actual analyte concentration or the analytical sensitivity, precision plots done at different resonance lines should be quite similar. Significant differences in precision at a given absorbance will occur if the resonance lines are of quite different intensity or quite different in wavelength, so that the relative amount of flame transmission noise, analyte emission noise, or flame background emission noise would be quite different. Previous data for nickel and aluminum run at different wavelengths show that there is little difference in precision characteristics [4].

*Integration time*

The magnitude of all noises would be expected to decrease for longer integration times until the point is reached where drift is significant over the time required to make the measurements to calculate standard deviations. In region I, the improvement in precision would be proportional to the square root of the integration time if signal shot noise is limiting. Since source and flame transmission noise are normally limiting and these tend to be inversely proportional to the frequency, the improvement in precision will be less than the square root of the integration time and will depend on the analyte and on the hollow-cathode lamp. For copper and zinc [3], precision in region I is increased by a factor of 1.5—3 (i.e. $< 10^{1/2}$) when the integration time is increased from 1 s to 10 s.

In region II, analyte absorption noise is limiting; it also tends to be inversely proportional to frequency. Increasing the integration time from 1 to 10 s generally improves the precision by a factor of 2—3. Integration times greater than 10 s do not provide significant improvement, in agreement with earlier reports [8].

The limiting noises in region III, i.e. analyte and flame background emission noise, should be white at the lamp modulation frequency and a $10^{1/2}$ improvement in precision was observed for copper and zinc when integration time was increased from 1 s to 10 s. Noise from the dark current or amplifier-readout system ($\sigma'_{ot}$) would be frequency-dependent but is not limiting under normal conditions.

*Other variables*

An inert gas sheath improves sensitivity for refractory elements [9]. It was felt that a gas sheath might also improve precision in region I by reducing flame transmission noise, flame turbulence, and air entrainment. However, no improvement in precision was observed when a nitrogen gas sheath (Varian sheath attachment for slot burner) was employed and at high nitrogen flow rates, the precision was worse. A gas sheath might improve precision in region III by reducing the flame background signal and noise.

Interferences are normally considered as substances which affect the absorbance of a given concentration of an element. To test if certain interferences might also affect the precision and noise, phosphate was added to calcium solutions in an air—acetylene flame to decrease the absorbance. The precision ($\sigma_A/A$) was found to be the same as that for a less concentrated calcium solution (without phosphate) which gave the same absorbance. Thus the interference affected the absorbance but not the inherent noise characteristics. High concentrations (3—15%) of NaCl and $NaNO_3$ were added to nickel solutions and the absorbances were monitored at the Ni 232.0-nm line. It was expected that molecular absorption by NaCl and $NaNO_3$ [10], which was measured to be 0.01—0.02 a.u., would increase flame transmission noise, but no significant decrease in precision was observed. Likewise, 0.05 (w/v)% of $SiO_2$ and $Al_2O_3$ added to zinc solutions, as examples of refractory particulates, had no effect on precision when absorbances were monitored at the 213.9-nm Zn line.

Analyte absorption flicker noise appears to be independent of most experimental variables (except integration time) but strongly dependent on fluctuations in delivery of the analyte to the flame. For copper, changing the viscosity by adding 3% NaCl or 4% $LiBO_2$, or by using glycerin (viscosity about 100 times greater than water) or acetone (about 1/3 viscosity of water) instead of water did not affect precision in region II. Likewise boiling solutions [11] or addition of 0.1% Triton X-100 had no effect.

## CONCLUSIONS

The data presented indicate that variables should be optimized depending on the absorbance range of interest and that the parameters given in the manufacturers' "cookbooks" do not necessarily provide optimum precision in all absorbance regions. In general, longer integration times up to about 10—20 s will improve precision but only in region III where noise is often white will the improvement be proportional to the square root of the integration time. For any absorbance, it is best to adjust the slit height to the size of the hollow-cathode beam image focused on the entrance slit (ca. 2—4 mm), because a larger slit height will not increase the lamp signal but will increase the analyte emission and background emission signal and noise. In general, the burner position (i.e. the path height) should be adjusted for maximum absorbance although it should be remembered that the height over

which the absorbance and precision are constant may vary with analyte concentration.

To optimize the detection limit and precision at low absorbances (region I), the slit width, lamp current, flame stoichiometry, and type of flame should be adjusted for maximum $S/N$ or lowest $\sigma_A/A$. In general, larger slit widths and lamp currents, and lower fuel-to-oxidant ratios (for resonance lines below 250 nm) will decrease the relative amount of source or flame transmission noise but also the sensitivity or absorbance for a given concentration. Where flame transmission noise is dominant ($\lambda < 250$ nm), a nitrous oxide—acetylene flame will yield less flame transmission noise and better precision than an air—acetylene flame, unless the higher background emission noise of the hotter flame becomes significant compared to other noise sources in region I. Thus for each element and instrument, the optimum parameters must be determined by experimentally determining the magnitude of the variable that yields maximum $S/N$ or minimum $\sigma_A/A$. At moderate absorbances (region II), the manufacturer's typical parameters should yield the best precision, because most experimental variables do not affect analyte absorption noise but only determine the absorbance region over which analyte absorption noise is dominant. In general, lower lamp currents and slit widths are preferred to decrease non-linearity.

Generally, measurements are not made at high absorbances (region III) because of significant non-linearity in calibration curves. In terms of precision it is best to dilute solutions so that measurements are made in region II. However, the precision in region III can be improved by using larger slit widths if analyte emission noise is dominant ($\lambda > 350$ nm) and larger lamp currents if either analyte or flame background emission noise predominates. Increasing the magnitude of either variable can reduce sensitivity or increase negative deviations so that the optimum value must be determined by experimental optimization of the $S/N$ or $\sigma_A/A$. In general, the cooler air—acetylene flame will yield better precision in region III than the nitrous oxide—acetylene flame or than more reducing flames because of lower emission signals and noise. This must be balanced against any loss in atomization efficiency.

It is quite feasible for the user of a modern spectrometer to optimize measurements for the particular instrument, hollow cathode, analyte, and analyte concentration range. With modern microprocessor-based instruments which allow programmed repetitive measurements and which provide readout of the mean, standard deviation and relative standard deviation, plots of $\sigma_A/A$ versus variable setting can be quickly obtained.

This work was partially supported by the NIH Biomedical Sciences Support Grant RR7079.

REFERENCES

1 J. D. Ingle, Jr., Anal. Chem., 46 (1974) 2161.
2 N. W. Bower and J. D. Ingle, Jr., Anal. Chem., 48 (1976) 686.
3 N. W. Bower and J. D. Ingle, Jr., Anal. Chem., 49 (1977) 574.
4 N. W. Bower and J. D. Ingle, Jr., Anal. Chem., in press (Feb.).
5 N. W. Bower, Ph.D. Thesis, Oregon State University, 1978.
6 Varian Hollow-Cathode Lamp Data Book.
7 M. F. Reed and E. D. Rees, Spectroscopy Series I, v. II, International Scientific Communications, Inc., Greens Farms, Conn., 1974, p. 95.
8 F. Fernandez and J. Kerber, Am. Lab., 8 (1976) 49.
9 M. D. Amos, P. A. Bennett, and K. G. Brodie, Reson. Lines, 2 (1970) 3.
10 G. Herzberg, Molecular Spectra and Molecular Structure, Vol. I, Prentice-Hall, New York, 1939, p. 554.
11 W. H. Scheub and C. J. Stromsky, At. Absorpt. Newsl., 6 (1967) 95.

*Analytica Chimica Acta*, 105 (1979) 213—218


# A BOOSTED-OUTPUT SPECTRAL LAMP WITH INTERCHANGEABLE CATHODE FOR ATOMIC FLUORESCENCE SPECTROMETRY

J. V. SULLIVAN

*CSIRO Division of Chemical Physics, P.O. Box 160, Clayton, Victoria 3168 (Australia)*

(Received 23rd August 1978)

SUMMARY

The new type of boosted-output atomic spectral lamp described has a readily-interchangeable cathode that requires only a small quantity of pure material. The direction of argon flow-through is designed to enable the lamp to be used with cathodes of relatively volatile elements such as arsenic and selenium, without the element being deposited on the exit window. The high numerical aperture of the lamp makes it suitable for use in atomic fluorescence spectrometry. Its warm-up time is faster than that of commercially-available electrodeless discharge lamps and its performance in flame atomic fluorescence at least as good. For less-volatile metals the performance is equal to that of earlier types of demountable boosted-output lamp.

The use of a demountable boosted glow-discharge lamp in atomic absorption and fluorescence spectrometry has recently been described [1]. Though this type of lamp may be operated with a wide range of cathode materials, it has proved unsatisfactory for arsenic, selenium and tellurium because these elements are quickly deposited on the exit window, which is thus rendered opaque. This paper describes a new design of boosted-output spectral lamp, with an interchangeable cathode, in which this drawback is overcome.

## EXPERIMENTAL

### *Design of lamp*

Figure 1 shows the general design of the lamp, which consists essentially of two glass tubes placed at right angles to each other (Australian Patent Specification 25601/77). The cathode, A, which screws into the water-cooled block, B, is attached to the lamp by means of an O-ring seal, C. It is cylindrical in shape and may, if desired, be a hollow cathode. Generally, however, a solid cylinder, into the top of which a pellet has been pressed, is used. This pellet is approximately 7 mm in diameter and 5 mm thick. The use of a pellet in a cylinder of inexpensive material such as iron helps to conserve the pure material used in the cathode. The cathode fits snugly into a silica tube, D, which acts as the arrester, confining the sputtering discharge to the front of this cathode by means of the gap, E (ca. 0.1 mm),

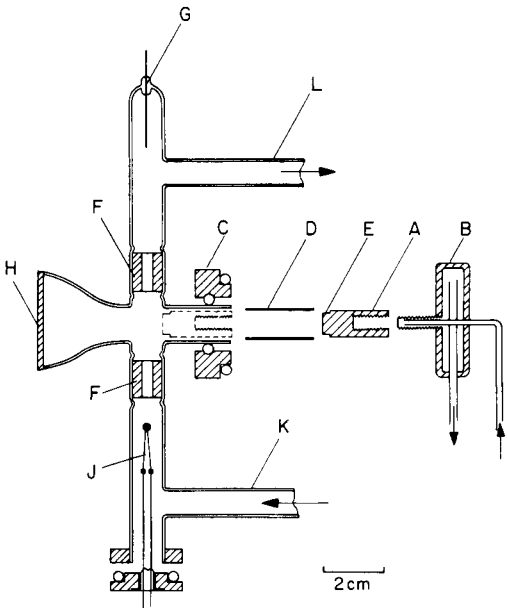


Fig. 1. Schematic diagram of boosted-output lamp with interchangeable cathode.

between the cathode wall and the inner surface of the silica tube. This tube is a close fit in the glass tube surrounding it.

Two silica tubes, F, 15 mm long and with inner and outer diameters of 3 mm and 10 mm respectively, are located in the lamp body. These serve to constrict the booster discharge in the region of the cathode, thus increasing the current density and hence the effective excitation. G is a common anode for the sputtering and booster discharges. A silica window, H, 40 mm in diameter and approximately 40 mm from the cathode surface, may be attached by a suitable sealing compound such as Araldite, though it is advantageous to seal the window to the lamp by means of an O-ring in order to facilitate removal for occasional cleaning.

The cathode of the secondary discharge is the filament, J, which consists of approximately 40 mm of rhenium wire (0.25-mm diameter) with a bead of lanthanum hexaboride fused at the centre [2, 3]. Fusion of the bead to the rhenium wire results in efficient heating of the hexaboride when current (ca. 6 A) is passed through the filament. Lanthanum hexaboride, when heated, is a copious electron emitter and possesses the advantage, in demountable lamps, that it will withstand repeated exposure to air.

The power supply for the lamp incorporates a filament heater (6.3 V, 10 A) and two current-regulated outputs, one delivering 100 mA at 900 V to operate the flow discharge, and the other 750 mA at 120 V to operate the booster discharge. Optional electronic modulation of the outputs at 285 Hz is incorporated in the power supply.

Argon gas, whose pressure (2—3 torr) and flow rate (ca. 0.4 l $min^{-1}$) are

regulated by a gas-control unit [4], enters at K and leaves at L. The flow of gas perpendicular to the line of observation ensures that sputtered vapour is swept from the vicinity of the window, which may thus be positioned close to the region of the cathode. This results in a lamp having high numerical aperture, which is an advantage in atomic fluorescence.

For selenium and arsenic, the pellets consist of silver selenide ($Ag_2Se$) and tin arsenide (SnAs), respectively. These compounds are made by reacting stoichiometric ratios of the appropriate elements in evacuated silica ampoules for several hours at about 800°C. Preliminary results indicate that these compounds form suitable materials for pellets, and when used in a lamp result in intense emission of the resonance lines. For cadmium, lead and antimony, pellets were machined from rods of high-purity material (99.999+%; Materials Research Corporation, Orangeburg, New York).

With none of the elements tried so far has any deposition of vapour on the surface of the window been observed after approximately 100 h of operation.

*Methods of evaluation of lamp performance*

In order to compare the performance of the new lamps with that of the electrodeless-discharge lamps (EDL) commonly used as sources for atomic fluorescence spectrometry, it was necessary to modulate the output of all lamps for compatibility with the synchronous demodulation system of the Varian-Techtron AA-4 amplifier.

Commercial EDL's (Perkin-Elmer Corporation, Norwalk, Conn.) were run from the d.c. power supply provided by the manufacturers, at the recommended, or slightly higher, power levels. Their light output was modulated at 285 Hz by a mechanical chopper locked into the AA-4 amplifier. The output of the new lamps could be modulated either electronically or with the mechanical chopper.

The signal and warm-up characteristics of the lamps were compared by using a Jarrell-Ash 0.5-m grating monochromator and a photomultiplier type R106, the output signal from the amplifier being fed to a Hitachi QPD54 recorder.

Atomic fluorescence measurements were made with the non-dispersive flame fluorescence instrument described by Larkins [5], which had a nitrogen-sheathed air—acetylene flame viewed by a photomultiplier type R166.

## PERFORMANCE OF LAMP

Figure 2 shows the warm-up curves for a demountable arsenic lamp and an arsenic EDL. It can be seen that the output from the demountable lamp reaches 99% of its final value after about 25 min, while that from the EDL takes about 90 min.

Figures 3—7 show recorder traces of non-dispersive atomic fluorescence signals for arsenic, selenium, cadmium, lead and antimony. They were obtained by using the demountable boosted-output lamp, which was run

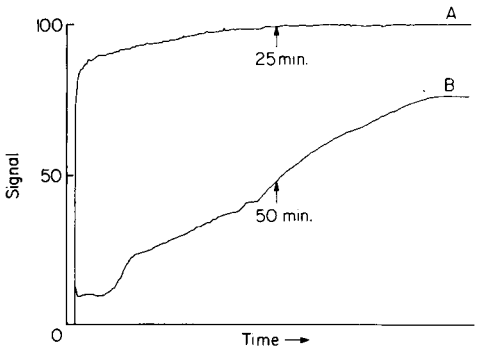


Fig. 2. Warm-up characteristics of (A) boosted-output and (B) electrodeless-discharge arsenic lamps. Wavelength 193.7 nm; spectral bandpass 0.8 nm; photomultiplier dynode voltage 325 V. Boosted-output lamp: glow-discharge current 24 mA d.c.; booster current 500 mA d.c.; mechanical chopping. EDL run at 8 W. Note the two-fold difference in the time scales for curves (A) and (B).

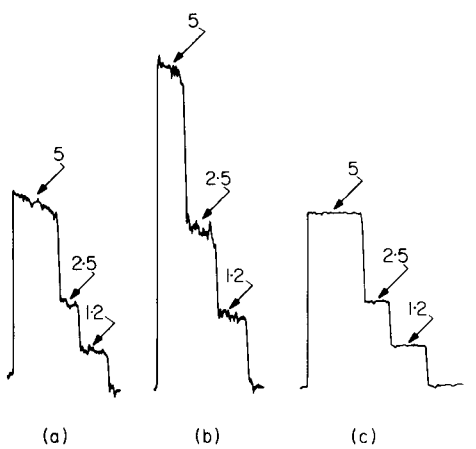


Fig. 3. Non-dispersive atomic fluorescence signals from arsenic. (a) EDL, 12 W, photomultiplier dynode voltage 450 V; (b) EDL, 12 W, photomultiplier dynode voltage 500 V; (c) boosted-output lamp 14 mA/500 mA, electronically modulated, photomultiplier dynode voltage 500 V. The signal from the EDL had not reached a steady value when the measurements were made. The numbers on the traces indicate concentration of arsenic in $\mu g\ ml^{-1}$.

both with electronic modulation and with mechanical chopping of the emitted radiation. The latter allowed a direct comparison with the measurements made with the electrodeless-discharge lamps. It can be seen that in all cases the signal-to-noise ratio of the fluorescence signal is better with the new lamp than with the EDL, even when the radiation is chopped mechanically. When the new lamp is electronically modulated, this advantage is increased.

Table 1 shows the limits of detection in non-dispersive flame atomic

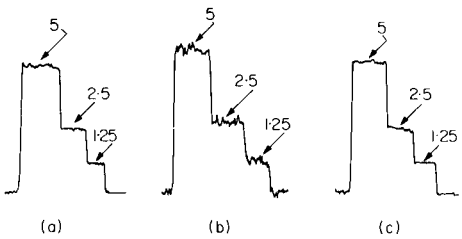


Fig. 4. Non-dispersive atomic fluorescence signals from selenium. (a) Boosted-output lamp, 10 mA/500 mA, both d.c., mechanical chopping; (b) EDL, 9 W; (c) boosted-output lamp, 10 mA/500 mA, electronically modulated. The numbers on the traces indicate concentration of selenium in $\mu g\ ml^{-1}$.

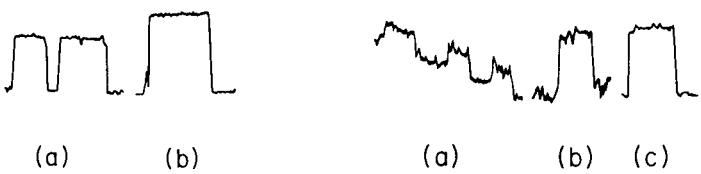


Fig. 5. (left). Non-dispersive atomic fluorescence signals from cadmium (2 ng $ml^{-1}$). (a) EDL, 7.5 W (repeated measurements); (b) boosted-output lamp, 10 mA/500 mA, electronically modulated.

Fig. 6. (right). Non-dispersive atomic fluorescence signals from lead (80 ng $ml^{-1}$). (a) EDL, 10 W (repeated measurements); (b) boosted-output lamp 20 mA/500 mA, both d.c., mechanical chopping. (c) boosted-output lamp 10 mA/500 mA, electronically modulated. The signal from the EDL had not reached a steady value when the measurements were made.

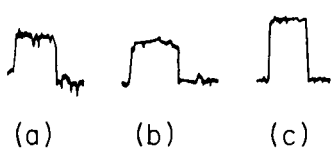


Fig. 7. Non-dispersive atomic fluorescence signals from antimony (100 ng $ml^{-1}$). (a) EDL, 10 W; (b) boosted-output lamp, 13 mA/500 mA, both d.c., mechanical chopping; (c) boosted-output lamp, 10 mA/500 mA, electronically modulated.

fluorescence measured with the new boosted-output lamp (electronically modulated) and the commercially-made EDL's. These figures are compared with those found by Larkins [5] using earlier types of lamp. The limits of detection found with the EDL's for arsenic and selenium should be treated with caution, because the use of a wide-blade chopper for the high-numerical aperture system led to instability in flame separation. This instability was the principal cause of the noise recorded on the traces shown in Figs. 3 and 4, and accounts for the apparent poor limits of detection. The effect of flame instability is less important for the remaining elements because their fluorescence lines are not so strongly absorbed by the flame gases.

TABLE 1

Limits of detection in non-dispersive atomic fluorescence[a]

| Element | Boosted-output lamp (ng $ml^{-1}$) | EDL (ng $ml^{-1}$) | Earlier lamps (Larkins [5]) (ng $ml^{-1}$) |
|---|---|---|---|
| As | 100 | 400 | 6000[b] |
| Se | 150 | 650 | 6000[b] |
| Cd | 0.1 | 0.2 | 0.2[c] |
| Pb | 10 | 50 | 150[d] |
| Sb | 10 | 50 | 40[e] |

[a]The limits of detection follow the very conservative definition used by Larkins [5], viz. the concentration giving a signal equal to twice the peak-to-peak fluctuation when only water or a dilute acid is aspirated. [b]Hollow-cathode lamp source. [c]Metal vapour discharge lamp (Philips). [d]Boosted hollow-cathode lamp of the Sullivan—Walsh type [6]. [e]Boosted hollow-cathode lamp of the Lowe type [7].

## CONCLUSIONS

The new boosted-output spectral lamp has better warm-up characteristics than commercial electrodeless-discharge lamps. Its performance in non-dispersive flame atomic fluorescence is at least as good as theirs for the five relatively volatile elements so far tested. For less-volatile elements it is equal to that of earlier types of demountable boosted-output lamp.

The author is indebted to Dr. J. B. Willis for discussion and advice.

## REFERENCES

1 J. V. Sullivan and J. C. Van Loon, Anal. Chim. Acta, 102 (1978) 25.
2 J. M. Lafferty, J. Appl. Phys., 22 (1951) 299.
3 K. N. Ramachandran, Rev. Sci. Instrum., 46 (1975) 1662.
4 P. L. Larkins, unpublished work.
5 P. L. Larkins, Spectrochim. Acta, Part B, 26 (1971) 477.
6 J. V. Sullivan and A. Walsh, Spectrochim. Acta, 21 (1965) 721.
7 R. M. Lowe, Spectrochim. Acta, Part B, 26 (1971) 201.

*Analytica Chimica Acta*, 105 (1979) 219—231


# THE DETERMINATION OF BERYLLIUM AND MANGANESE IN AEROSOLS BY ATOMIC ABSORPTION SPECTROMETRY WITH ELECTROTHERMAL ATOMIZATION

P. GELADI and F. ADAMS*

*Department of Chemistry, University of Antwerp (U.I.A.), B-2610 Wilrijk (Belgium)*

(Received 20th August 1978)

SUMMARY

The determination of beryllium and manganese in air particulate matter collected on filter material is discussed. Destruction by digestion with nitric and perchloric acids and by low-temperature ashing with dissolution of the ash in a hydrofluoric—nitric acid mixture were tested. The graphite furnace parameters were investigated for different acid solutions. Interferences of some cations and anions that are abundant in aerosol material are described. Accuracy was checked against standard samples. For manganese, the results are compared with those obtained by energy-dispersive x-ray fluorescence.

Increasingly, attention is being paid to the elemental and chemical composition of airborne dusts generated by natural and industrial processes. Because of the small amounts of material collected and the low concentration levels encountered, trace-element techniques such as optical emission spectrometry, x-ray fluorescence spectrometry, instrumental neutron activation analysis and atomic absorption spectrometry (a.a.s.) must be used. This paper describes the flameless a.a.s. procedures that are used in this laboratory for the determination of beryllium and manganese in airborne dusts.

Some forms of beryllium are known to be very toxic. The element is of no use to human metabolism, and the major source of intake is by inhalation, which even in small amounts can produce chronic effects over the whole body. It is not very abundant, but the metal and its alloys are used for many industrial applications. Manganese is very abundant in the earth's crust (12th on the list), and its world production is very large. It is used in the iron and steel industry and in smaller amounts in the chemical industry and dry battery manufacture. It is one of those elements which in small amounts is necessary for human metabolism, but which may be dangerous in larger amounts. The most hazardous source of intake is again by inhalation. Manganese may cause lung inflammation and effects on the central nervous system. The Threshold Limit Value (TLV) for beryllium is 2 $\mu g\ m^{-3}$ average for a 40-h working week, a peak concentration of 25 $\mu g\ m^{-3}$ for a single exposure, and 0.01 $\mu g\ m^{-3}$ for urban air. For manganese, the TLV value is 5 $mg\ m^{-3}$ and the Maximum Allowable Concentration (MAC) (USSR) is 0.3 $\mu g\ m^{-3}$ [1].

In previous papers, determinations of aluminium [2] and of cadmium, copper, iron, lead and zinc [3] in airborne material collected on filter papers have been described; the techniques used were flame and flameless atomic absorption spectrometry. In addition to collection on cellulose (paper) filters as used earlier [2, 3], some other techniques for the collection of airborne dust, mainly collection on polymer substrates, were tested. This demanded the development of other techniques for destruction of the filter and dissolutio of the airborne material. In the development of these destruction methods, it was kept in mind that the resulting solution should allow the determination of all the above-mentioned elements.

Destruction of filter paper was done by the method of the Belgian Institute of Standardization, in which nitric and perchloric acids were used. For the polymer membranes, such as Nuclepore filters and Mylar Spectrofilm, low-temperature ashing was followed by dissolution in a hydrofluoric–nitric acid mixture, with the amounts of acid used adapted to the very small amount of material present.

A special problem is posed by fly-ash material which compared to the usual airborne dust contains very little organic material and a high proportion of oxides and siliceous materials which are not easily dissolved. Therefore a procedure based on hydrofluoric, nitric and perchloric acids was used in this case.

The flameless procedure was chosen because of its sensitivity and the small amounts of sample required. Because of the different existing flameless systems literature information on any typical system is not always readily available, and because of the complexity of the flameless systems compared to the flame, the instrument manuals generally provide far from adequate information on any specific analytical problem. Therefore, furnace program parameters had to be established; especially the ashing and atomization conditions had to be optimized. The results discussed below are directed towards practical purposes, without going too far into theoretical considerations.

Another severe problem which is usually encountered in flameless atomic absorption is the abundance of matrix-specific interferences. Such interferences were investigated for the cations most abundant in average airborne material and for some of the inorganic acids most often used. The results give practical guidelines about the combinations that should be preferred or avoided. In order to test the complete analytical procedure, including decomposition and measurement of the solutions, reference samples of a different nature were analyzed carefully. For the manganese concentrations, the results of atomic absorption and energy-dispersive x-ray fluorescence [4] spectrometry were compared.

## EXPERIMENTAL

### *Apparatus*

A Perkin-Elmer 502 atomic-absorption spectrometer was used, in combination with a PE HGA-74 graphite furnace atomizer. Absorbances were read

as peak height from a Hitachi—Perkin-Elmer 56 strip-chart recorder and from the built-in peak-read device of the spectrometer. The furnace was flushed with argon (l'Air Liquide N46) at a flow rate of 300 ml $min^{-1}$ internally and 900 ml $min^{-1}$ externally. The gas flow could be changed during the atomization stage to increase sensitivity, by means of the stopped (Gas-Stop), reduced (Mini-flow) and continuous flow settings.

Solutions were injected with Eppendorf micropipettes with disposable polypropylene tips. Deuterium background correction was done with a Perkin-Elmer 303-0875 system. The spectral light sources are listed in Table 1, together with their wavelengths and the conventional sensitivities obtainable with the graphite furnace. For beryllium and manganese, the spectral bandwidths of the slit were 0.7 and 0.2 nm, respectively. For all measurements of sensitivity, the gas-stop mode was used in the atomization step. The useful range is here defined as the range between the lowest value that can easily be read in the gas-stop mode and the upper limit of linearity in the continuous gas flow mode. As usual, the volume injected and the gas flow during atomization can be adjusted to adapt the sensitivity as appropriate. The low-temperature ashing apparatus was a Tracerlab LTA-302.

*Reagents*

A standard stock solution of beryllium (1 g $l^{-1}$) was obtained by dissolving 0.5 g of beryllium (Fluka 14201) in the minimum amount of 4.5 M sulfuric acid and diluting to 500 ml. For manganese, Merck Titrisol 9988 ($MnCl_2$) was dissolved in 0.1 M $HNO_3$ to give a 1 g $l^{-1}$ solution.

For investigations of furnace parameters and interferences, the acids and salts used were of analytical-reagent grade. Suprapur-grade acids were used for the destruction of samples to minimize blanks. All dilutions were made with doubly-distilled water from a quartz apparatus. Because of the risk of losses from neutral solutions [5], all dilutions were made in 0.1 M acid and reprepared regularly.

TABLE 1

Characteristics of spectral light sources

| Element | Hollow-cathode lamp | Lamp current (mA) | Wavelength (nm)[a] | Sensitivity (pg)[b] | Useful range (ng) |
|---|---|---|---|---|---|
| Be | PE 303-6013 | 25 | 234.8 | 2 | 0.03—3 |
| Mn | PE 303-6043 | 20 | 279.5 | 5 | 0.05—10 |
| | | | 279.8 | 7 | 0.05—10 |
| | | | 280.1 | 13 | 0.1—25 |
| | | | 403.1 | 73 | 0.5—200 |

[a]The wavelengths most often used are underlined. [b]Defined as the amount of material for which $A$ = 0.0044.

*Sampling procedures*

The aerosol samples were collected on Whatman 41 filter paper, Nuclepore N-040 and N-800 polycarbonate membrane filter and on Mylar Spectrofilm (4 $\mu$m thick). Total dust was collected with a high-volume sampler on paper filters and with a low-volume sampler on Nuclepore membranes. The high-volume sampler was the same as that described by Dams and Heindryckx [6]. The low-volume sampler consisted of a Becker VT 1.5 vacuum pump, a Schleicher—Schüll FP 050/2 (50-mm) filter holder and a Contigea SG 6 gas meter. For the collection of airborne dust in fractions of different particle size, a Battelle impactor [7] was used. The material was collected on Mylar Spectrofilm coated with vaseline and on a Nuclepore N-040 back-up filter.

*Destruction procedures*

Different destruction procedures were selected according to the materials present. For material collected on filter papers, a boiling mixture of nitric and perchloric acid was used. Fly ash was decomposed with a $HF—HNO_3—HClO_4$ mixture in a teflon test tube. The material collected on membrane filters was decomposed by low-temperature ashing and the residue dissolved in a $HF—HNO_3$ mixture.

*$HNO_3—HClO_4$ digestion [8].* About 10 $cm^2$ of aerosol-loaded filter paper was pretreated with 7.5 ml of boiling concentrated nitric acid (65%). Then, 5 ml of perchloric acid (70%) was added, and heating was continued until the solution became clear and colorless. The excess of acid was boiled off and the dry material redissolved in 2.5 ml of concentrated nitric acid and 10 ml of water by gentle heating. The solution obtained was cooled and diluted to 50 ml in a graduated flask. Known amounts of standard and filter blanks were taken through the whole procedure.

*$HF—HNO_3—HClO_4$ digestion.* The sample material (50—100 mg) was weighed into a PTFE test tube, and 1 ml of hydrofluoric acid (48%) was added. After 20 min, 1 ml of nitric acid (65%) and 1 ml of perchloric acid (70%) were added, and the test tubes were slowly heated to 210°C during an hour. The mixture was kept at 210°C for another hour and the excess of acid was then boiled off. The dry residue was dissolved in 1 M nitric acid and diluted to 50 ml. Known amounts of standard and blanks were taken through the whole procedure.

*Low-temperature ashing.* A piece (1—3 $cm^2$) of membrane filter was cut out and put in a teflon cup, which was placed in the low-temperature asher for 2 h at a power of 100 W and an oxygen pressure 100—150 Pa. Afterwards, the cups were transferred to teflon test tubes and 1 ml of hydrofluoric acid (48%) and 0.5 ml of nitric acid (65%) were added. The test tubes were kept at room temperature for 1 h and then gently heated to the boiling point of nitric acid for another hour. The excess of acid was boiled off and the dry residue was dissolved in 2 ml of 0.1 M nitric acid. Blanks were taken through the whole procedure.

The amounts and volumes described above can be varied slightly to correct for excessive or insufficient filter loadings.

*Atomic absorption spectrometry*

The furnace programs used are shown in Table 2 (see below).

## RESULTS AND DISCUSSION

*Furnace programs*

Furnace parameters were established for both elements in different commonly used acid media. Ashing losses were measured as a function of the ashing temperature and atomization yields as a function of the atomization temperature, with all other parameters kept constant, under the conditions giving the highest sensitivity. The results obtained are shown in Fig. 1. They should also be applicable for other wavelengths and gas-flow settings.

For beryllium, the influence of the acids on the atomization yield is very small, so that a common atomization temperature can be chosen for all the acid media mentioned. For manganese, the acid has a larger effect on the atomization yield. Nevertheless, the atomization temperature should be very close to the maximum of 2700°C. The choice of acid has a large effect on the ashing losses for beryllium. For manganese, the behaviour is much the same in

TABLE 2

Furnace program parameters used for the flameless determination of beryllium and manganese in air particulate matter

| Program step | Temperature/time | |
|---|---|---|
| | Be | Mn |
| Drying | 100°C for a time (seconds) twice the injected volume in μl | |
| Ashing | 900°C/20 s | 1200°C/20 s |
| Atomization | 2700°C/10 s | 2600°C/10 s |
| Clean-up | 2700°C/20 s | 2700°C/10 s |

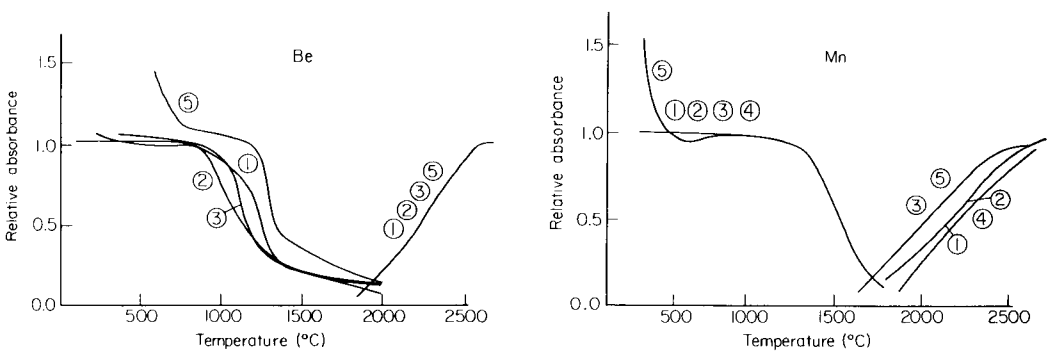


Fig. 1. Ashing and atomization curves for 0.1 N acid solutions: (1) HCl, (2) $HNO_3$; (3) $H_2SO_4$; (4) $HClO_4$; (5) $H_3PO_4$. Be, 20 μl of 10 ppb solution injected. Mn, 20 μl of 20 ppb solution injected.

all cases except for the phosphoric acid medium. The behaviour of phosphoric acid with both metals is very typical and is a good example of what might happen if the ashing step were omitted. In this case, the acid volatilizes during the atomization step and causes light scattering and/or peak shape deformation by co-volatilization of the element to be determined. Although the effect is very pronounced for phosphoric acid, it could occur to a lesser extent for the other acids as well.

In order to investigate the ashing behaviour of the two elements in acid media more thoroughly, ashing losses as a function of ashing time at constant temperatures were measured. Two typical examples are shown in Fig. 2. The maximum temperature above which ashing losses of beryllium started to occur was 900°C for HCl and $HNO_3$, and 1000°C for $H_2SO_4$ and $H_3PO_4$. For manganese the corresponding temperature was 1200°C for all five acids investigated. The actual furnace parameters that were used are given in Table 2. After an acid decomposition, an ashing time of 20 s was considered to be sufficient to remove any acid or organic material left. Because of the atomization kinetics the peak maximum is usually reached 2—5 s after the start, so that an atomization time of 10 s was chosen. Clean-up is done until memory effects disappear, usually after 10 s for manganese and 20 s for beryllium, which is known to be very prone to memory effects [9, 10]. In the literature, ashing temperatures between 1000 and 1500°C have been given for beryllium [11—13] and between 1000 and 1200°C for manganese [14—18], depending largely on the type of furnace used.

*Interferences*

Several possible interferences on the determination of beryllium and manganese were studied. Because acids were used for decomposition of the samples and for the stabilization of dilute solutions, anion interferences were investigated for HCl, $HNO_3$, $H_2SO_4$, $HClO_4$, $H_3PO_4$. The absorbance losses as a function of acid normality are shown in Fig. 3. While the effect is very small for the non-oxidizing acids, it is larger for nitric acid and very large for perchloric acid. For beryllium, no measurements were possible in perchloric acid of more than

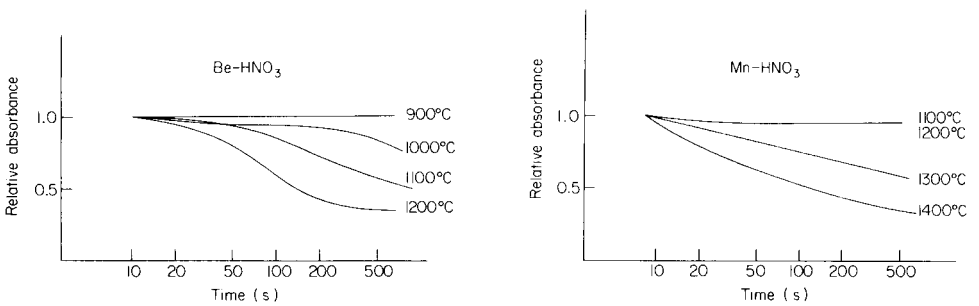


Fig. 2. Ashing losses as a function of ashing time for 10 ppb Be in 0.1 M $HNO_3$ and for 20 ppb Mn in 0.1 M $HNO_3$ at different ashing temperatures; 20 $\mu$l injected.

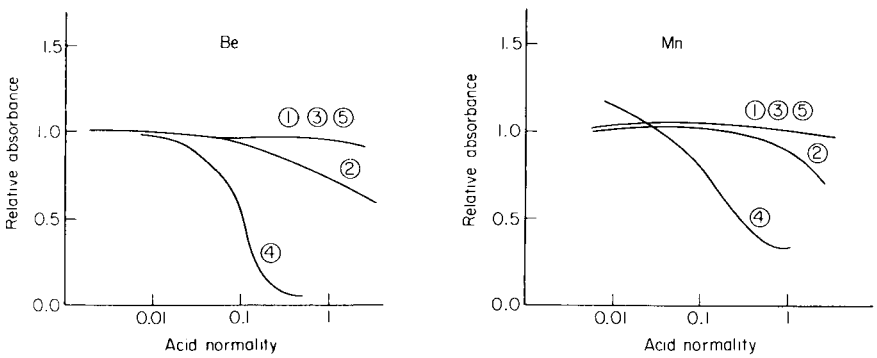


Fig. 3. Interferences of (1) HCl; (2) $HNO_3$; (3) $H_2SO_4$; (4) $HClO_4$; (5) $H_3PO_4$ on 10 ppb Be and 20 ppb Mn; 20 µl injected into the furnace with parameters as described in text.

0.1 M, an effect that was also encountered for Al [2], as could be expected because of the very similar chemical behaviour of both elements [19].

A decreasing effect of nitric acid on the absorbance of manganese is also described by Smeyers-Verbeke et al. [15] and by McArthur [16]. Sighinolfi [11] describes a decreasing effect of nitric acid on Be absorbance. The pronounced effect of perchloric acid on some metals and especially Mn and Al is investigated by Julshamn [14]. His curve for the interference of perchloric acid on Mn is quite similar to ours.

For the study of the interferences of cations, Na, K Mg and Pb were added as nitrate and Ca, Al and Fe as chloride up to concentration ratios considerably exceeding the average aerosol composition. The results are shown in Fig. 4 and take into account the blanks for the reagents added. Because of the expected error of ±5% for flameless determinations, only values outside the 95—105% range were considered as significant. For beryllium, there is interference from 40-fold amounts of lead, 400-fold amounts of calcium and 3000-fold amounts of iron and aluminium. The large positive interference

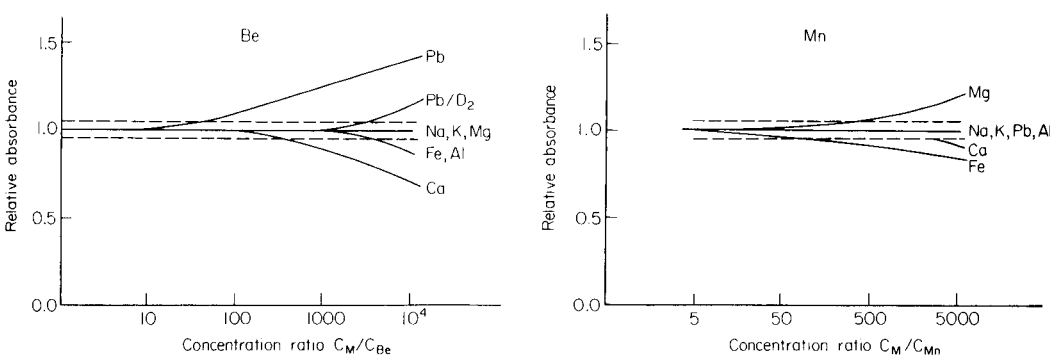


Fig. 4. Interferences of cations on the absorbance of 10 ppb Be and 20 ppb Mn; 20 µl injected with furnace parameters as described in text.

from lead can be avoided by using deuterium correction. Because of the small amounts of beryllium that can be expected in airborne dust, the use of deuterium background correction is advisable for this element. For manganese, interferences from 100-fold amounts of iron, 400-fold amounts of magnesium and 4000-fold amounts of calcium can be expected, but these levels are not usually encountered.

Sighinolfi [11] described similar depressive effects of calcium and iron on the beryllium absorbance. Smeyers-Verbeke et al. [15] reported interferences on manganese for many cations and anions that are usually encountered in biological materials and demonstrated synergic effects for several cations and anions when present together.

*Blanks*

Because of the small amounts of material used in the analysis, the blank values of the reagents are important. To check the water and the acids, 25 ml of material was concentrated by evaporation and the residue was dissolved in 0.1 M nitric acid of previously determined purity. In the evaporation, care was taken to avoid boiling, which could lead to sputtering losses. This was done by heating to slightly below the boiling point and evaporation under infrared irradiation. The net concentrations for the different kinds of reagents are given in Table 3.

The blank values for the different filter materials were also determined. For Whatman 41 cellulose filter the beryllium and manganese concentrations were 0.022 and 0.66 ng $cm^{-2}$, respectively, or about 2.5 and 70 ppb. The manganese concentrations of the Nuclepore filter and the Mylar spectrofilm coated with Apiezon L were below 1 ng $cm^{-2}$; Maenhaut and Zoller [20] gave

TABLE 3

Blank values for the reagents

| Reagent | Grade and source | Element concentration ($\mu g\ l^{-1}$) | |
|---|---|---|---|
| | | Be | Mn |
| Water | Distilled | <0.01 | 0.03 |
| | Double distilled in quartz | <0.01 | 0.01 |
| $HNO_3$ | Analytical, Merck 454 | <0.01 | 1 |
| | Suprapur, Merck 441 | <0.01 | 1 |
| HCl | Analytical, Merck 319 | <0.01 | 0.4 |
| | Suprapur, Merck 318 | <0.01 | 0.5 |
| $HClO_4$ | Analytical, Merck 519 | 0.03 | 1.6 |
| | Suprapur, Merck 518 | <0.01 | 0.5 |
| $H_2SO_4$ | Analytical, Merck 731 | 0.015 | 2.2 |
| | Suprapur, Merck 714 | <0.01 | 0.6 |
| HF | Analytical, Merck 334 | <0.01 | 158 |
| | Suprapur, Merck 335 | <0.01 | 0.1 |
| | Analytical, Baker 9560 | <0.01 | 42 |

a value of 0.16 ng $cm^{-2}$ determined by instrumental neutron activation analysis. For beryllium, so little material was found on the high-volume samplers, that it was not considered necessary to analyze the low-volume samples collected on Nuclepore filter. From the blank concentrations for beryllium and manganese for the filter material and the reagents, blank values (and thus detection limits) were calculated for the destruction procedures (Table 4). However, in practice, it was difficult to reach these theoretical blank values for manganese.

*Analysis of reference samples*

Kodak TEG-50-A gelatin [21], NBS fly-ash SRM 1633 [22] and the Milan aerosol standard [23] were used as reference samples. The method of destruction was selected according to the nature of the material. The results are given in Table 5. Three methods of quantification were used: (a) calibration graph method with the standard composition matching the unknown as closely as possible; (b) comparison of unknown samples with a synthetic standard taken through the whole procedure of decomposition; and (c) the standard addition method. The third method is time-consuming because of the large number of determinations required for the analysis of one unknown sample, but it gives the best results. For beryllium, fairly good results were found for the gelatin, the fly ash and the synthetic standard. Deuterium background correction, which is often said to be necessary to avoid interferences, tended to give less accurate results because of the increased complexity of the instrumentation. For the Milan sample, which is typical of a city aerosol, no beryllium could be detected.

For manganese, fairly good results were obtained for the gelatin and fly-ash samples; with the Milan aerosol standard, standard addition gave the most accurate results. The poorer results for the calibration graph method may have been caused by traces of perchloric acid left in the solution after decomposition of the sample. It was also noticed that precipitates of Mn oxides, e.g. $MnO_2$ could be formed when manganese solutions were treated with strongly oxidizing acids such as the $HNO_3$—$HClO_4$ mixture. These precipitates were usually formed in the test tubes containing the synthetic standard and did not redissolve completely in the 1 M nitric acid.

*Comparison between atomic absorption and x-ray fluorescence*

For manganese, a comparison between atomic absorption and a routine x-ray fluorescence (x.r.f.) procedure [4] was possible. Results obtained by both methods are shown in Table 6 for aerosols on cellulose filters after destruction with $HNO_3$—$HClO_4$ and in Table 7 for samples collected with a low-volume sampler on Nuclepore filters after low-temperature ashing. The results for the paper filters show an average deviation between the two methods of 17%, which agrees well with the similar data for Cu, Fe and Pb [3]. The results in Table 7 indicate that for concentrations lower than about 50 ng $cm^{-2}$, large deviations of up to a factor 2 are possible. For results well above this determination limit, an average deviation of 21% was found, which is very good considering the low concentration of the element in the air (20—40 ng $m^{-3}$).

TABLE 4

Blank values for filtration media and destruction procedures used

| Destruction procedure | | Blank value | | Dimension |
|---|---|---|---|---|
| | | Be | Mn | |
| $HNO_3$—$HClO_4$ | Analytical reagents | <0.1 | 2.5 | ng $cm^{-2}$ |
| | Suprapur reagents | <0.1 | 2.0 | ng $cm^{-2}$ |
| HF—$HNO_3$—$HClO_4$ | Analytical reagents | <5.5 | 1660 | ng $g^{-1}$ |
| | Suprapur reagents | <5.3 | 56 | ng $g^{-1}$ |
| Low-temperature ashing | Analytical reagents | — | 80 | ng $cm^{-2}$ |
| | Suprapur reagents | — | <1.5 | ng $cm^{-2}$ |

TABLE 5

Accuracy tests for beryllium and manganese in some reference materials (Average concentrations ($\mu g\ g^{-1}$) are given with standard deviations and number of determinations in parentheses. Kodak TEG-50-A was analyzed after destruction with $HNO_3$—$HClO_4$ and the other samples after destruction with HF—$HNO_3$—$HClO_4$.)

| Element | Sample | Element found | | | Certified value |
|---|---|---|---|---|---|
| | | Calibration graph | Synthetic standard | Standard addition | |
| Be | Kodak TEG-50-A | 59 ± 5 (7) | — | 50 ± 3 (7) | 55 |
| | NBS fly ash | 12.1 (4)<br>10.1 (4)[a] | 13.2 (4)<br>12.6 (4)[a] | 13.5 (4)<br>— | (12)<br>(12) |
| | Aerosol standard | 0.1 (1) | — | — | — |
| | Synthetic standard | 0.025 (1)<br>0.024 (1)<br>0.020 (1)[a]<br>0.020 (1) | —<br>—<br>—<br>— | 0.027 (1)<br>0.024 (1)<br>—<br>— | 0.025<br>0.025 |
| Mn | Kodak TEG-50-A | 47.7 ± 0.6 (7)[b]<br>49.6 ± 0.2 (7)[c] | 51.6 ± 0.6 (7)[b]<br>55.8 ± 0.2 (7)[c] | —<br>47.2 (1) | 52 ± 7 |
| | NBS fly ash | 546 (1)<br>558 (1)<br>600 (1)<br>580 (1) | | 499 ± 22 (7) | 493 ± 7 |
| | Aerosol standard | 1085 ± 45 (5) | 1553 ± 65 (5) | 1201 ± 180 (10) | 1273 ± 90 (15)[d] |

[a] With $D_2$ correction. [b] At 279.3 nm. [c] At 403.1 nm. [d] Average of results of other laboratories (instrumental neutron activation and atomic absorption).

## *Conclusions*

The furnace parameters established for the flameless determination of beryllium and manganese agree well with other values from the literature, although sometimes different types of furnaces or matrices have been employed. For the destruction of airborne dust and filter collection material, different approaches can be used according to the nature and amount of material present. As far as interferences are concerned, special care should be taken to avoid or eliminate all traces of perchloric acid since these may lead to erroneous

TABLE 6

Comparison of manganese concentrations determined by flameless a.a.s. and by energy-dispersive x.r.f. for industrial aerosols collected on Whatman 41 paper filters in a high-volume sampler after destruction with $HNO_3$—$HClO_4$

| Filter | Concentration (ng cm$^{-2}$) | | Concentration ratio for a.a.s./x.r.f. |
|---|---|---|---|
| | A.a.s. | X.r.f. | |
| D 17 | 62 | 49 | 1.27 |
| D 39 | 1356 | 1721 | 0.79 |
| D 46 | 450 | 533 | 0.84 |
| D 64 | 658 | 586 | 1.12 |
| D 69 | 101 | 131 | 0.77 |
| D 76 | 79 | 89 | 0.89 |
| D 78 | 145 | 193 | 0.75 |
| D 113 | 1549 | 1732 | 0.89 |
| D 147 | 469 | 551 | 0.85 |
| D 149 | 611 | 522 | 1.17 |
| D 151 | 1908 | 1839 | 1.04 |
| Average ratio | | | 0.94 ± 0.19 ($n$ = 11) |

TABLE 7

Comparison of manganese concentrations determined by flameless a.a.s. and by energy-dispersive x.r.f. for aerosols collected on Nuclepore N-040 membrane filters in a low-volume sampler after low-temperature ashing

| Filter | Concentration (ng cm$^{-2}$) | | Concentration ratio for a.a.s./x.r.f.[a] |
|---|---|---|---|
| | A.a.s. | X.r.f. | |
| G 5 A | 30 | 17 | (1.76) |
| B | 35 | 21 | (1.67) |
| G 6 A | 86 | 87 | 0.99 |
| B | 89 | 87 | 1.02 |
| G 7 A | 139 | 129 | 1.08 |
| B | 71 | 57 | 1.25 |
| G 8 A | 81 | 100 | 0.81 |
| B | 47 | 52 | (0.90) |
| G 9 A | 79 | 54 | 1.46 |
| B | 32 | 27 | (1.19) |
| G 10 A | 65 | 50 | 1.30 |
| B | 74 | 48 | 1.54 |
| G 11 A | 69 | 79 | 0.87 |
| B | 52 | 68 | 0.76 |
| Average ratio | | | 1.09 ± 0.29 ($n$ = 11) |

[a]When one or both concentrations in a pair was under 50 ng cm$^{-2}$, the ratio is between parentheses and was not included in the calculation of the average.

results. Other metals are unlikely to interfere with the determination of manganese. For beryllium, the use of deuterium background correction can be recommended in some cases, but care is needed because electronic instability may lead to imprecise results when background correction is used in combination with the transient absorbance signals from the furnace. For the blanks, the only problem encountered originates in the high manganese content of the hydrofluoric acid. The other blank values were so low that accidental contamination should be feared more than regular blank values, especially for the common element manganese.

In the analysis of standards, good agreement with certified values was found for different kinds of standard materials which required different kinds of decomposition procedure. For manganese, the comparison between a.a.s. and x.r.f. shows good agreement when the concentrations are not too low; 20 ng m in the air can be regarded as the limit of determination for reasonably accurate analysis.

The procedures for decomposition of the samples and analysis of the resulting solution by flameless a.a.s. are suitable for manganese and beryllium collected on different kinds of materials such as cellulose filter paper, polycarbonate membrane filters and polyester films that can be used in different types of sampling equipment. Fly-ash samples can also be analyzed. The methods can be used equally well for the determination of aluminium, cadmium, copper, iron and lead for which the flameless determinations have already been described. For zinc there might be a problem with the small amounts of material collected with a low-volume sampler or a cascade impactor. For beryllium, concentrations in a large number of industrial and urban samples, were often below the detection limit of the method even for samples taken with a high volume filter-unit during 24-h periods.

This research was carried out within the framework of the National Research and Development Program on Environment of the Interministerial Commission for Science Policy. The technical assistance of W. Van Mol for sampling and analysis by a.a.s. is gratefully acknowledged. The x.r.f. analyses were done by P. Van Espen.

REFERENCES

1 M. Winell, Ambio, 4 (1975) 34.
2 A. Pilate, P. Geladi and F. Adams, Talanta, 24 (1977) 512.
3 P. Geladi and F. Adams, Anal. Chim. Acta, 96 (1978) 229.
4 P. Van Espen and F. Adams, Anal. Chim. Acta, 75 (1974) 61.
5 E. Gladney and W. Goode, Anal. Lett., 10 (1977) 619.
6 R. Dams and R. Heindryckx, Atmos. Environ., 7 (1973) 319.
7 R. Mitchell and J. Pilcher, Ind. Eng. Chem., 51 (1959) 1039.
8 Belgisch Instituut voor Normalisatie, Document NBN T94-101 (1976).
9 D. Grewal and F. Kearns, At. Absorpt. Newsl., 16 (1977) 131.
10 E. Gladney, At. Absorpt. Newsl., 16 (1977) 42.
11 P. Sighinolfi, At. Absorpt. Newsl., 11 (1972) 96.
12 R. Bettger, A. Ficklin and T. Rees, At. Absorpt. Newsl., 14 (1975) 124.

13 W. Robbins, J. Runnels and R. Merryfield, Anal. Chem., 47 (1975) 2095.
14 K. Julshamn, At. Absorpt. Newsl., 16 (1977) 149.
15 J. Smeyers-Verbeke, Y. Michotte, P. Van den Winkel and D. Massart, Anal. Chem., 48 (1975) 125.
16 J. McArthur, Anal. Chim. Acta, 93 (1977) 77.
17 Y. Thomassen, R. Solberg and J. Hansen, Anal. Chim. Acta, 90 (1977) 279.
18 E. McLaughlin, S. Slavin and D. Manning, Atomic Absorption Application Study nr. 546 (1973), The Perkin-Elmer Corporation, Norwalk, Conn.
19 F. Cotton and G. Wilkinson, Advanced Inorganic Chemistry, Interscience, 1972, p. 207.
20 W. Maenhaut and W. Zoller, Proc. 1976 Int. Conf. Modern Trends in Activation Analysis, 1976, vol. 1, p. 416.
21 D. Anderson, J. Murphy and W. White, Anal. Chim., 48 (1976) 116.
22 J. Ondov, W. Zoller, I. Olmez, N. Arras, G. Gordon, L. Rancitelli, K. Abel, R. Filby, K. Shah and R. Ragiani, Anal. Chim., 47 (1975) 1102.
23 S. Finzi, Euratom Ispra, Document 1183 (1973).

*Analytica Chimica Acta*, 105 (1979) 233—245


# SAMPLING AND ANALYTICAL METHODS FOR THE DETERMINATION OF COPPER, CADMIUM, ZINC, AND NICKEL AT THE NANOGRAM PER LITER LEVEL IN SEA WATER

KENNETH W. BRULAND* and ROBERT P. FRANKS

*Center for Coastal Marine Studies, Division of Natural Sciences, University of California, Santa Cruz, CA 95064 (U.S.A.)*

GEORGE A. KNAUER and JOHN H. MARTIN

*Moss Landing Marine Laboratory, Moss Landing, CA 95039 (U.S.A.)*

(Received 27th June 1978)

SUMMARY

Sea-water samples collected by a variety of clean sampling techniques yielded consistent results for copper, cadmium, zinc, and nickel, which implies that representative, uncontaminated samples were obtained. A dithiocarbamate extraction method coupled with atomic absorption spectrometry and electrothermal atomization is described which is essentially 100% quantitative for each of the four metals studied, has lower blanks and detection limits, and yields better precision than previously published techniques. A more precise and accurate determination of these metals in sea water at their natural ng $l^{-1}$ concentration levels is therefore possible. Samples analyzed by this procedure and by concentration on Chelex-100 showed similar results for cadmium and zinc. Both copper and nickel appeared to be inefficiently removed from sea water by Chelex-100. Comparison of the organic extraction results with other pertinent investigations showed excellent agreement.

One of the most recent comprehensive reviews dealing with trace metals in sea water is that by Brewer [1], but few definitive conclusions could be drawn concerning the distributions and marine geochemistry of individual trace metals. This was presumably the result of the severe problems encountered by investigators in both laboratory analysis and contamination-free sampling of sea water for trace metals at parts-per-trillion (ng $l^{-1}$) concentrations.

In the past three years, however, more consistent results have been presented in several papers; for cadmium, nickel and copper [2], copper [3—7], cadmium [8—10] and nickel [11]. In addition, an oceanographically-consistent zinc profile has recently been reported [12]. This recent research leads to the conclusions that these trace metals are present in sea water at much lower concentration levels than previously believed, and that they appear to have well-defined distributions in the world's oceans.

The first step toward an understanding of the geochemistry of any trace element in sea water is the development of sample collection and analytical procedures that provide accurate, meaningful data. Presented in this paper are

the clean sampling and analytical techniques developed in this laboratory to allow the accurate determinations of cadmium, copper, nickel, and zinc.

In order to validate these procedures, it was necessary to demonstrate that agreement could be obtained by using completely different sampling and concentration techniques. In April 1977, a station in the California Current off Central California (37°05'N, 123°22'W) was occupied in order to perform such an intercomparison for these trace metals. Samples from a vertical profile of 18 depths were collected with two types of deep water samplers. Subsurface samples were collected from a small, inflatable raft. These samples were then analyzed for the four metals by two different extraction—concentration techniques.

## EXPERIMENTAL

### *Collection methods*

Surface samples were collected from a small raft rowed crosswind and more than 200 m away from the research vessel. Acid-cleaned polyethylene bottles (500 and 1000 ml) were submerged off the bow, rinsed and filled with sea water.

Deeper samples were collected by using two different sampling systems. Teflon-coated 30-l PVC ball-valve samplers (General Oceanics, Go-Flo) were modified by replacement of the standard stopcock with a teflon valve. The Go-Flo samplers are designed to enter the water in a closed, sealed position. At a depth of 10 m, a pressure release allows the ball valves to open and the sampler to fill with water. It then free flushes until tripped by a teflon messenger. The sampler was clamped on Dacron-sheathed, plastic Phillystran hydroline 10 m above a polypropylene-enclosed lead weight. The hydroline was led through a stainless steel snatch block-meter wheel to a portable winch with a stainless steel drum. The other sampling system used in this comparative study was the CIT deep-water, common-lead sampler designed and constructed by Schaule and Patterson [13].

Sample handling and processing were done on board ship inside a modular Porta-lab equipped with a positive pressure filtered air supply and specifically designed for trace metal analysis. After collection, the Go-Flo samplers were secured in a rack on the outside of the Porta-lab where the teflon valve was rinsed with ultra-clean water and connected to a length of teflon tubing. This tubing led through the wall of the Porta-lab to a polypropylene ball valve used to control the flow of sea water. In addition, trace metal samples from the CIT sampler were taken by Schaule while collecting samples for lead analysis.

The sea-water samples were preserved after collection by the addition of 4 ml of 6 M quartz-redistilled (Q-) hydrochloric acid per liter.

Because of the potential for contamination, most of the sea-water samples were not filtered. The primary purpose of this study was to compare sampling techniques; this comparison could be performed more easily without the extra processing step of filtration. However, two of the Go-Flo samples were filtered

to determine, (1) the feasibility of, and contamination potential from, the filtering procedure, and (2) the percentage of each metal associated with the particulate phase. The sea water was filtered through pre-cleaned, 142-mm, 0.4-$\mu$m Nucleopore filters contained in teflon filter holders. The Go-Flo samplers were pressurized through a Swagelok fitting at the top of the sampler with filtered, high-purity nitrogen. Dissolved trace metal samples were collected from the filter effluent line.

*Cleaning procedures*

Much of the development of cleaning techniques was prompted by the work of Patterson and Settle [14]. Plastic ware was initially rinsed in acetone, washed with Micro detergent, rinsed with glass-distilled deionized water (dd-water ), soaked for at least one day in hot 3 M (GFS) hydrochloric acid (or for one week in 6 M hydrochloric acid at room temperature), rinsed with dd-water, soaked in 0.5—1 M (GFS) nitric acid for at least three days and rinsed with dd-water. In addition, plastic ware in which samples would be stored or processed was further rinsed with quartz-distilled water (Q-water), soaked in 0.5—1 M Q-nitric acid for at least a week, rinsed with Q-water, and dried in a laminar-flow clean air bench.

The Go-Flo samplers were thoroughly cleaned with Micro detergent, rinsed with deionized water, filled with 1 M (GFS) hydrochloric acid for several days and rinsed with dd-water.

*Solvent extraction*

Two separate concentration techniques were utilized: a solvent extraction technique and a column ion-exchange technique with Chelex-100.

The organic extraction technique was developed as a modification of that presented by Kinrade and Van Loon [15]. The technique involves chelation with ammonium 1-pyrrolidinedithiocarbamate (APDC) and diethylammonium diethyldithiocarbamate (DDDC), a double extraction into chloroform, and back-extraction into nitric acid. Approximately 250 g of acidified sea water was transferred to a 250-ml teflon separatory funnel and buffered to about pH 4 with 2 ml of ammonium acetate (prepared by bubbling purified ammonia through 11 M Q-acetic acid); 1 ml of a solution containing 1% (w/v) each of APDC and DDDC (stabilized in a 1% ammonium hydroxide solution and purified by chloroform extraction) and 8 ml of Q-chloroform were then added, and the mixture was shaken vigorously for 2 min. After 5 min to allow phase separation, the chloroform fraction was drained into a 125-ml teflon separatory funnel, and 4 ml of 7.5 M Q-nitric acid was added to initiate degradation of the dithiocarbamates. An additional 6 ml of Q-chloroform was added to the original sea-water sample for a second extraction of the chelated species, as well as to rinse the solution and the separatory funnel. After phase separation, the chloroform was combined with the first fraction and shaken vigorously for 2 min. The phases were allowed 5 min to separate, after which the chloroform phase was discarded.

The 4-ml acid phase containing the back-extracted metals was then drained into a 10-ml fused quartz beaker, and 2 ml of 7.5 M Q-nitric acid was used to rinse the 125-ml separatory funnel and stem. This rinse was combined with the acid in the quartz beaker. The 6-ml back-extract was evaporated to dryness in a clean-air fume hood, and the residue was further oxidized by 250 $\mu$l or 500 $\mu$l of concentrated Q-nitric acid. The residue in the quartz beaker was redissolved in warm 1 M Q-nitric acid and quantitatively transferred with 250-$\mu$l rinses (ca. 1.25 ml total) to a 1.8-ml polyvial. This solution was subsequently analyzed by flameless atomic absorption spectrometry (f.a.a.s.).

This procedure yields a 200:1 concentration, and at the same time removes the Group I and II elements that can interfere with the f.a.a.s. Because of the high sensitivity of f.a.a.s. for zinc and cadmium, the procedure can often produce samples with zinc and cadmium concentrations too high for direct analysis. When necessary, these samples were diluted (by weight) with 1 M Q-nitric acid to bring the metal concentration into the proper working range. This dilution was seldom necessary for copper or nickel.

The most important criterion in the development of the organic extraction technique was to achieve quantitative yields with a high degree of precision. The dithiocarbamates (APDC and DDDC) were chosen after a study by Kinrade and Van Loon [15] showed that the combination of these chelating reagents worked well for the extraction of a variety of metals over a fairly wide pH range. In addition, APDC and DDDC discriminate extremely well against the major cations in sea water. Chloroform was chosen as the organic solvent since it allowed a double forward extraction with two relatively small volumes of solvent. Ammonium acetate was used because it has a good buffering capacity at the optimum pH for extraction (about pH 4) and because it could be made quite cleanly. It should be noted that acetate ion can form complexes with some metals that may interfere with extractions, but there is no interference for cadmium, copper, zinc, and nickel. This extraction technique developed independently here is similar to that recently described by Danielsson et al. [16]. The major differences are the use of a citrate buffer and Freon TF as the organic solvent by the earlier investigators.

Detailed radiotracer studies for cadmium, copper, and zinc were employed in development of the method. The overall recoveries by the prescribed procedure for sea-water samples spiked with $^{115m}$Cd, $^{64}$Cu, and $^{65}$Zn were 98.9 ± 0.7% ($n$ = 10), 97.9 ± 1.2% ($n$ = 3), and 99.0 ± 0.8% ($n$ = 5), respectively. The first chloroform fraction extracted 90—92% of all three metals. Combined extraction into two batches of chloroform prior to back-extraction was 99.4 ± 0.4% ($n$ = 11) for cadmium, 98.0 ± 1.2% ($n$ = 11) for copper and 99.2 ± 0.7% ($n$ = 5) for zinc. APDC alone extracted 99.2% of the cadmium, 98.5% of the copper, and 100.0% of the zinc, while DDDC alone produced yields of 96.0% for cadmium, 97.5% for copper, and 90.6% for zinc. These studies show that either the APDC/DDDC combination or APDC alone provide nearly 100% quantitative recoveries with relatively small standard deviations. The standard deviations observed were of the same order as would be expected from the tracer $\gamma$-counting error alone.

*Chelex-100 technique*

The Chelex-100 ion-exchange concentration technique [17] was modified somewhat. The resin (sodium form, 100—200 mesh) was cleaned with 6 M (GFS) hydrochloric acid by daily suspension, decantation and addition of fresh acid for one week. It was then rinsed with Q-water and 2 M Q-nitric acid, followed by a final rinse with Q-water. The resin was then changed to the ammonia form and 7.5 ml of resin was loaded into polypropylene disposable columns. The excess of ammonia was rinsed from the columns with about 50 ml of Q-water until the pH dropped below 9. The columns were topped up with 1 cm of Q-water over the resin bed and stored upright in individual plastic bags.

The Chelex concentration step was performed at sea immediately after sample collection. Sea water (4 l) was drawn from the samplers into acid-cleaned polyethylene bottles, and water was pumped through teflon tubing directly into the columns. A multi-channel peristaltic pump, located downstream of the columns, was used to maintain the flow rate at 3.5—4.5 ml $min^{-1}$. The effluent was collected and measured volumetrically. Upon completion of pumping, the columns were capped at both ends, placed in individual polyethylene bags, and frozen for storage. At no time during preparation, processing, or storage was the resin allowed to go dry. After return to the shore lab, the columns were thawed, washed with 50 ml of Q-water to remove excess of salts, and eluted with 30 ml of 2 M Q-nitric acid into small polyethylene bottles. The concentration factor resulting from this technique was approximately 120:1.

Radiotracer studies, with $^{65}Zn$- and $^{115m}Cd$-spiked sea-water samples, showed recoveries of 99 and 100%, respectively, for this concentration procedure. Stable tracer studies also indicated that quantitative yields are obtained for relatively high levels ($\mu g\ l^{-1}$) of copper and nickel. Studies by other investigators support these results [17—19].

In addition to the trace metals of interest, large amounts of calcium and magnesium are also retained on the Chelex resin and eluted with the acid. This sample matrix can markedly suppress the absorbance signal during f.a.a.s. The amounts of these interfering salts were found to be constant from column to column, and a matching matrix of precleaned alkali metal and alkaline earth salts was used in the preparation of the f.a.a.s. standards (Ca, 1800 ppm; Mg, 1700 ppm; Na, 150 ppm; and K, 20 ppm). The instrumental sensitivity for standards prepared in this manner was identical to that for stable spikes concentrated from Chelex-treated, metal-free sea water.

*Flameless atomic absorption analysis (f.a.a.s.)*

Cadmium, copper, nickel, and zinc in the extracted samples were determined by f.a.a.s. A Varian AA-6 spectrometer with a model 90 carbon rod atomizer (CRA-90) and a BC-6 hydrogen continuum automatic background corrector, and a Perkin-Elmer 603 spectrometer with a Model 2100 graphite furnace (HGA-2100) and deuterium-arc background corrector were used. Hollow-cathode lamps were used as light sources. In general, manufacturer-recommended

procedures were followed, except that relatively higher temperatures for shorter durations were utilized during atomization. In addition, with the Varian CRA-90, P-10 gas (90% argon, 10% methane) was mixed with the nitrogen flow (flow ratio 1:6) during the ashing and atomization steps. The use of P-10 gas prolonged the life of the pyrolytic coating of the carbon rods and increased precision.

*Blanks, detection limits and precision*

The blanks and detection limits for the two concentration techniques are presented in Table 1. Blanks were determined by extracting previously-processed sea water and/or Q-water. The solvent extraction blanks were below the instrumental detection limits for cadmium and nickel. The zinc blank was small compared to sea-water values other than for surface water, and the copper blank, while significant, was uniform with a standard deviation of only 4 ng $l^{-1}$. The detection limits for copper and zinc are based on 2.5 times the standard deviation of the blanks, while those for cadmium and nickel are governed by the instrumental detection limits. The blanks for the Chelex concentration technique are set primarily by the instrumental detection limits for the concentrated sample.

The precision of the solvent extraction technique, expressed as a pooled relative standard deviation (RSD) for replicate samples, is 5.3%, 6.3%, and 3.8% for copper, nickel, and cadmium, respectively. Excluding samples containing less than 50 ng $l^{-1}$, the pooled RSD for zinc is 4.5%. The lack of sufficient replicates for the Chelex technique precluded an estimate of its precision.

## RESULTS AND DISCUSSION

The results of the comparison study are presented in Table 2. Technically, the data presented for unfiltered samples should be called "acid-soluble" or "labile". The solvent extraction results are equivalent to the dissolved fraction plus the particulate and colloidal metal leached into solution during acidification of the samples for storage. This technique should closely approximate

TABLE 1

Blanks and detection limits
(All values in ng $l^{-1}$)

| Element | Solvent extraction | | Chelex-100 | |
|---|---|---|---|---|
| | Blank | Detection limit | Blank | Detection limit |
| Cu | 23 ± 4 | 10 | 4 | 6 |
| Cd | <0.2 | 0.2 | <0.6 | 0.6 |
| Zn | 2 ± 1 | 2 | 5 | 15 |
| Ni | <8 | 10 | 40 ± 2 | 15 |

TABLE 2

Results of comparison study
(All values in ng $l^{-1}$. Values in parentheses are suspected to be contaminated, see text.)

| Depth (m) | Sampler | Copper | | Cadmium | | Zinc | | Nickel | |
|---|---|---|---|---|---|---|---|---|---|
| | | Ext. | Chelex | Ext. | Chelex | Ext. | Chelex | Ext. | Chelex |
| 0 | Raft | 105,106 | 69 | 15.1,16.2 | 15 | 7,10 | <15 | 304,339 | 217 |
| 25 | Go-Flo | 109,102 | 60 | 23.9,23.3 | 22 | 33,29 | 18 | 232,228 | 166 |
| 50 | Go-Flo | 106,97 | 50 | 38.3,36.5 | 35 | (186,202) | (214) | 261,295 | 190 |
| 100 | Go-Flo | 92,98 | 28 | 61.8,60.8 | 61 | 69,82 | 63 | 284,301 | 198 |
| 110 | CIT | 94,93 | 45 | 60.2,62.3 | 64 | 76,74 | 63 | 349,320 | 213 |
| 200 | Go-Flo | 96,94 | 26 | 73.3,77.5 | 70 | 180,175 | 149 | 323,314 | 248 |
| 300 | Go-Flo | 94,100 | — | 80.9,80.3 | — | 186,192 | — | 378,378 | — |
| 400 | Go-Flo | 93,99 | 26 | 85.3,89.6 | 92 | 229,226 | 180 | 364,440 | 371 |
| 410 | CIT | 95,94 | — | 86.7,87.9 | — | 248,244 | — | 434,442 | — |
| 600 | Go-Flo | 112,94 | 33 | 118,— | 109 | 314,— | 310 | 445,— | 407 |
| 630 | CIT | (125,129) | — | (102,104) | — | (322,352) | — | (527,557) | — |
| 800a | Go-Flo | 110,98 | 40 | 110,118 | 109 | 404,378 | 428 | 521,501 | 470 |
| b | | 123,— | — | 116,109 | — | 407,375 | — | 521,536 | — |
| 1020 | CIT | 116,124 | — | 110,108 | — | 419,445 | — | 576,589 | — |
| 1200 | Go-Flo | 151,132 | 26 | 110,98 | 109 | 519,510 | 456 | 693,605 | 576 |
| 1560 | CIT | (220,223) | — | (93,93) | — | (547,567) | — | (2000,1900) | — |
| 1800 | Go-Flo | 173,170 | 81 | 107,102 | 103 | 579,588 | 500 | 556,693 | 579 |
| 2030 | CIT | 209,204 | — | 96,95 | — | 641,576 | — | 569,645 | — |
| 2500 | Go-Flo | 224,222 | 98 | 99,95 | 94 | 628,617 | 654 | 626,568 | 599 |
| 2950 | CIT | 239,240 | — | 78,84 | — | 600,603 | — | 676,627 | — |

the total metal values in open ocean waters. The Chelex results are equivalent to the dissolved metals that chelate to the resin, plus that fraction of particulate metal leached with 2 M nitric acid from any particulates that accumulate on the resin bed.

*Comparison between sampling methods*

A primary objective of this study was the comparison of several different clean sampling methods. Consistency of results among samplers would imply that the samples collected are, in fact, uncontaminated and meaningful in terms of understanding the marine geochemistry of these elements. A direct statistical comparison of the samplers is not possible, because the samples were collected from different depths. However, the samples collected closest together (100, 110 m; 400, 410 m) can be compared to demonstrate the consistency between the Go-Flo and CIT samplers. The copper, cadmium, and zinc results obtained by solvent extraction for the different samplers appear identical. The nickel values are in fair agreement. The samplers can also be compared indirectly by means of the vertical profiles obtained. Figure 1 presents plots of replicate results obtained by solvent extraction for the four metals. Although marked

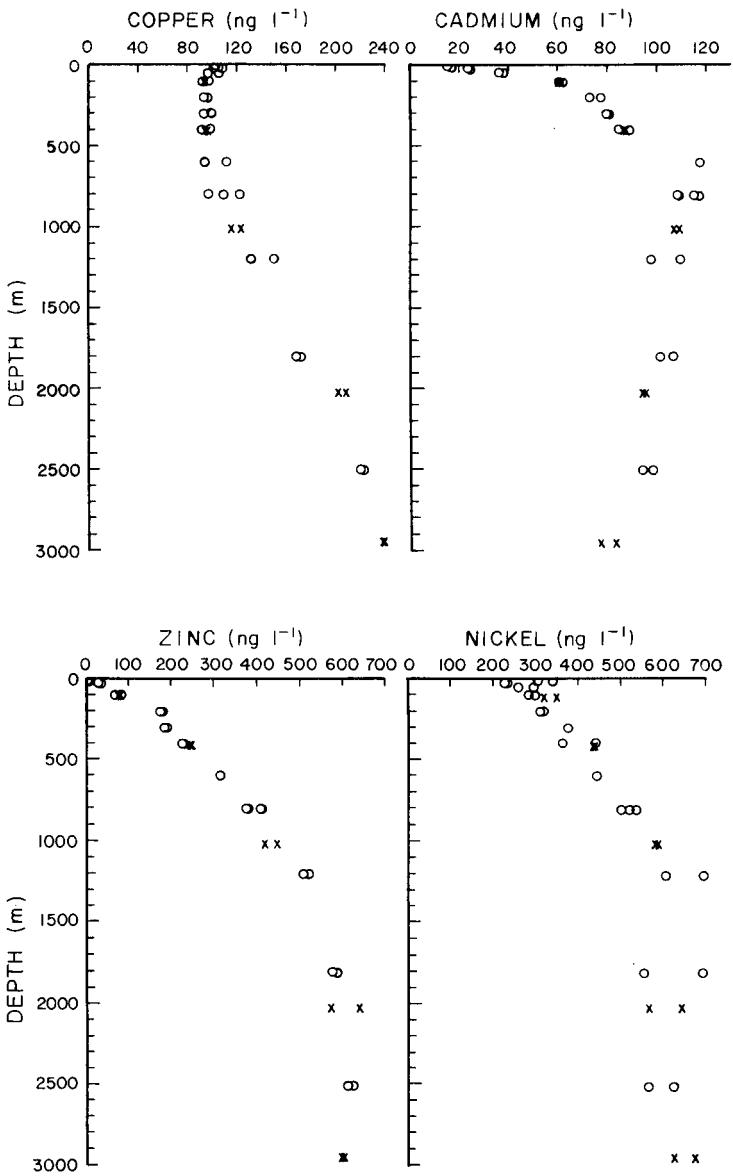


Fig. 1. Comparison of profiles obtained with Go-Flo (O) and CIT (X) samplers. Data points represent replicate extraction values.

vertical gradients exist, it is readily apparent that the samples collected by the various sampling techniques yielded consistent data which fit smoothly into the observed profiles.

Three of the samples from Table 2 have not been included in the plots of Fig. 1. The 630-m and 1560-m CIT samples were contaminated because of a

faulty seal. This allowed leakage of water that had been in contact with the inside of the stainless steel sampler into the polyethylene sample bags. Schaule and Patterson found these two samples to be contaminated for lead (personal communication). On the basis of the present results, the copper and nickel concentrations were increased by 20—60 ng $l^{-1}$ and 100—1500 ng $l^{-1}$, respectively, but, the cadmium and zinc results show no evidence of such contamination. The problem with this seal was subsequently corrected by Schaule, and it appears that these two are the only questionable CIT samples. In addition, the first Go-Flo sample collected on the cruise (50 m) appeared to be contaminated for zinc by approximately 150 ng $l^{-1}$; this was most likely a result of either inadequate flushing of the sampler before collection, or contamination during transfer from sampler to storage bottle. Whatever the cause, this was the only Go-Flo sample that showed a discrepancy from the other samples collected.

*Comparison of concentration techniques*

Another primary objective was to compare the results obtained by solvent extraction concentration with an independent technique (Chelex-100). Figure 2 presents vertical profiles for the mean extraction data along with the Chelex-100 results.

The copper results show a major discrepancy, with a mean difference between extraction and Chelex values of 72 ± 27 ng $l^{-1}$. The Chelex column effluent from the samples at 25 m and 2500 m was collected and analyzed by solvent extraction (Table 3). The mean amounts of copper found, 63 and 135 ng $l^{-1}$, respectively, were approximately equal to the difference between the Chelex and extraction data for the two samples. Thus, it appears that about 60% of the copper in sea water is not removed by the Chelex technique. This result confirms a reassessment of Chelex-100 for trace metal concentration from sea water [20], which showed that quantitative removal of copper required prior acidification and heating, followed by readjustment of the pH to 5.4. Riley and co-workers [20] assumed that a fraction of the copper is associated with colloidal and fine particulate matter and is not affected by the chelating resin. The acidification and storage involved in the present solvent extraction technique should liberate this fraction so that quantitative results for total copper can be obtained.

The cadmium profiles show excellent agreement. The difference between techniques averaged 1.3 ng $l^{-1}$, well within the precision expected, and cadmium could not be detected (< 0.5 ng $l^{-1}$) in the Chelex effluent. The zinc values appear reasonably consistent. The Chelex results are somewhat lower (19 ± 38 ng $l^{-1}$); the large standard deviation is attributable to the lack of precision in analysis of the Chelex samples. The average difference is similar to the amount of zinc found in the Chelex effluent (ca. 8 ng $l^{-1}$). While this comprises only a few percent of deep-water zinc values, it can be an appreciable fraction of the surface-water zinc. Nickel values are also lower when the Chelex method is used. The mean difference of 65 ± 35 ng $l^{-1}$ between the two techniques agrees well with the average value of 57 ng $l^{-1}$ found in the Chelex

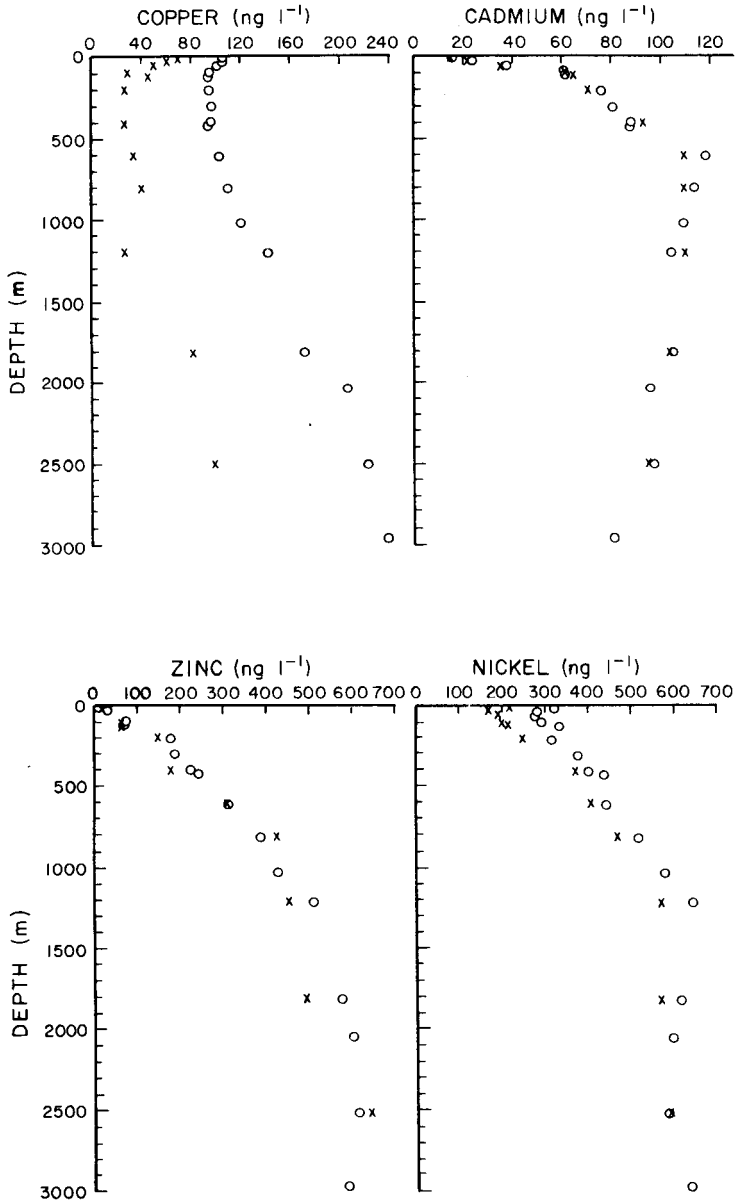


Fig. 2. Comparison of profiles from solvent extraction (O, values expressed as average of two or more replicates) and Chelex-100 (X) techniques.

effluent.

Thus, the Chelex technique yields substantially lower values for copper and nickel than the solvent extraction, and the differences are approximately equal to the amounts found in the effluent from the Chelex column.

TABLE 3

Chelex effluent measured by solvent extraction (ng $l^{-1}$)

| Sample | Copper | Cadmium | Zinc | Nickel |
|---|---|---|---|---|
| 25 m after 1 h | 59 | <0.5,<0.5 | 8 | 70 |
| after 8 h | 66,64 | <0.5,<0.5 | 27,31 | 62,58 |
| 2500 m after 1 h | 152,114 | <0.5,<0.5 | 8,7 | 68 |
| after 8 h | 135,140 | <0.5,<0.5 | 8,6 | 28 |

*Storage and filtering experiments*

Two additional experiments were also undertaken. The first involved taking additional samples from the Go-Flo bottles after they had stood for 2 h on the ship, to check for contamination and/or absorption of the trace metals; significant changes of concentration were not found (Table 4). This indicates that the composition of the samples is not altered during the transit time involved in bringing a deep sample to the surface. The second experiment entailed filtering the sea water through 0.4-$\mu$m Nucleopore filters and collecting the dissolved phase; this was designed to test for possible contamination during filtration. The results are given in Table 5, which also shows upper and lower limits of the particulate metal concentrations in the California current determined in this laboratory. In general, the values for the filtered samples plus the particulate fraction fall within the estimated precision of the unfiltered or total metal concentration. In deep waters, the particulate trace metals are less than 1% of the total metal concentration so that filtration causes insignificant differences. In the 25-m sample, the ranges of particulate values are 1—9, 1.5—4, 3—27, and 0.3—2% of the total copper, cadmium, zinc, and nickel, respectively. Thus, it can be concluded that filtering the sea water did not contaminate the samples to any appreciable extent.

*Comparison of results with other investigations*

The lack of a suitable standard reference sea water precludes a rigorous determination of the accuracy of the solvent extraction technique, hence the

TABLE 4

Comparison of sea water drawn from Go-Flo samplers immediately and after 2 h by the solvent extraction method
(All values in ng $l^{-1}$)

| Sample | Copper | Cadmium | Zinc | Nickel |
|---|---|---|---|---|
| 25 m: initial | 110,109 | 30.9,31.5 | 24,28 | 332,320 |
| after 2 h | 107,107 | 30.5,30.9 | 26,33 | 323,348 |
| 2500 m: initial | 224,222 | 99,95 | 628,617 | 625,568 |
| after 2 h | 222,236 | 95,99 | 646,625 | 661,678 |

TABLE 5

Comparison of filtered and unfiltered Go-Flo samples by the solvent extraction method (All values in ng $l^{-1}$)

| Sample | Copper | Cadmium | Zinc | Nickel |
|---|---|---|---|---|
| 25 m: unfiltered | 110,109 | 30.9,31.5 | 24,28 | 332,320 |
| filtered | 104,111 | 28.8,25.0 | 22,31 | 325,321 |
| particulate | 1—9 | 0.4—1.0 | 1—7 | 1—6 |
| 1800 m: unfiltered | 173,170 | 107,102 | 579,588 | 556,693 |
| filtered | 158,162 | 107,109 | 525,565 | 603,— |
| particulate | 1.5—3 | 0.05 | 1.5—2 | 5—10 |

accuracy is estimated to be similar to the precision. An additional estimate of the reliability of the sampling and analytical techniques can be made by comparing the oceanic profiles determined here with other relevant investigations.

The copper profiles (determined by solvent extraction) presented here and by Bruland et al. [5] are in good agreement with the vertical profile of copper in the California current reported by Boyle et al. [4], and are similar to results reported for the Atlantic Ocean [2, 6, 7]. The cadmium profile shown here exhibits a marked correlation with the labile nutrients, phosphate and nitrate [10]; similar correlation and depth distribution have been reported earlier [2, 8, 9]. The nickel profiles described by Sclater et al. [11] are very similar to the profile determined by the extraction technique in the present study. Zinc data comparable to those presented here and by Bruland et al. [12] are not available, but the consistency obtained and the excellent correlation with silicate [12] provide a degree of confidence.

*Conclusion*

The combination of sampling methods, solvent-extraction concentration, and analysis by f.a.a.s. provides a valuable procedure for obtaining precise and apparently accurate measurements of copper, cadmium, zinc and nickel in sea water. The large concentration factor (200:1), together with low reagent blanks, provides detection limits that are well below those of other published techniques, and are substantially below even the lowest reported natural levels of these trace metals. Studies of the dynamics and biogeochemical processes involved in establishing the oceanic distributions of these metals can therefore be made with greater confidence.

The authors are greatly indebted to B. Schaule and C. Patterson for aliquots of water collected with their sampler, and to the University of Washington for the use of the RV Thomas G. Thompson. They also thank W. Landing for help in the initial development of the extraction technique, J. Bellows for help in the design and construction of the Porta-lab and sampling equipment, and M. Stephenson for help with the Chelex procedure. This work was

supported by National Science Foundation grants OCE 75-13380, OCE 77-23684, OCE 75-13659, and IDO 75-01303, and U.S. Bureau of Land Management grants CT5-52 and CT6-40.

REFERENCES

1 P. Brewer, in J. P. Riley and G. Skirrow (Eds.), Chemical Oceanography, Vol. 1, 2nd edn., Academic Press, London, 1975, Chap. 7.
2 M. L. Bender and C. L. Gagner, J. Mar. Res., 34 (1976) 327.
3 E. Boyle and J. M. Edmond, Nature (London), 253 (1975) 107.
4 E. A. Boyle, F. Sclater and J. M. Edmond, Earth Planet. Sci. Lett., 37 (1977) 38.
5 K. W. Bruland, G. A. Knauer and J. H. Martin, Trans. Am. Geophys. Un., 58 (1977) 1156.
6 R. M. Moore and J. D. Burton, Nature (London), 264 (1976) 241.
7 R. M. Moore, Earth Planet. Sci. Lett., in press.
8 E. A. Boyle, F. Sclater and J. M. Edmond, Nature (London), 263 (1976) 42.
9 J. H. Martin, K. W. Bruland and W. W. Broenkow, in H. L. Windom and R. A. Duce (Eds.), Marine Pollutant Transfer, Heath, Massachusetts, 1976, p. 159.
10 K. W. Bruland, G. A. Knauer and J. H. Martin, Limnol. Oceanogr., 23 (1978) 618.
11 F. R. Sclater, E. Boyle and J. M. Edmond, Earth Planet. Sci. Lett., 31 (1976) 119.
12 K. W. Bruland, G. A. Knauer and J. H. Martin, Nature (London), 271 (1978) 741.
13 B. K. Schaule and C. C. Patterson, in preparation.
14 C. C. Patterson and D. M. Settle, in P. D. LaFleur (Ed.), Accuracy in Trace Analysis: Sampling, Sample Handling, Analysis, U.S. National Bureau of Standards Special Publication 422, 1976, p. 321.
15 J. D. Kinrade and J. C. Van Loon, Anal. Chem., 46 (1974) 1894.
16 L. G. Danielsson, B. Magnusson and S. Westerlund, Anal. Chim. Acta, 98 (1978) 47.
17 J. P. Riley and D. Taylor, Anal. Chim. Acta, 40 (1968) 479.
18 P. Figura and B. McDuffie, Anal. Chem., 49 (1977) 1950.
19 A. Hirose, K. Kobori and D. Ishii, Anal. Chim. Acta, 97 (1978) 303.
20 M. I. Abdullah, O. A. El-Rayis and J. P. Riley, Anal. Chim. Acta, 84 (1976) 363.

*Analytica Chimica Acta*, 105 (1979) 247—253


# ATOMIC-ABSORPTION SPECTROMETRIC DETERMINATION OF COBALT, NICKEL, AND COPPER IN GEOLOGICAL MATERIALS WITH MATRIX MASKING AND CHELATION-EXTRACTION

R. F. SANZOLONE, T. T. CHAO* and G. L. CRENSHAW

*U.S. Geological Survey, Box 25046, Denver Federal Center, Denver, Colorado 80225 (U.S.A.)*

(Received 17th July 1978)

SUMMARY

An atomic-absorption spectrometric method is reported for the determination of cobalt, nickel, and copper in a variety of geological materials including iron- and manganese-rich, and calcareous samples. The sample is decomposed with $HF—HNO_3$ and the residue is dissolved in hydrochloric acid. Ammonium fluoride is added to mask iron and aluminum. After adjustment to pH 6, cobalt, nickel, and copper are chelated with sodium diethyldithiocarbamate and extracted into methyl isobutyl ketone. The sample is set aside for 24 h before analysis to remove interferences from manganese. For a 0.200-g sample, the limits of determination are 5—1000 ppm for Co, Ni, and Cu. As much as 50% Fe, 25% Mn or Ca, 20% Al and 10% Na, K, or Mg in the sample either individually or in various combinations do not interfere. Results obtained on five U.S. Geological Survey rock standards are in general agreement with values reported in the literature.

Errors in the atomic-absorption spectrometric determination of cobalt, nickel, and copper caused by major- and minor-element interferences are well documented [1—6]. With increased awareness of the magnitude of interelement interferences and the need for analyses of secondary weathering products such as iron- and manganese-oxide coatings, ferromanganese nodules or concretions, and caliche or desert varnish in geochemical work, alleviation or elimination of the interferences caused by iron, manganese, calcium, and other elements becomes essential. An appropriate choice of method for partitioning of elements depending on their mode of occurrence or chemical forms in the sample, by sequential fractionation or partial dissolution techniques, can result in conditions where the ratio between the interfering elements and the elements to be determined is much greater than in the original sample. Separation by chelation-extraction, e.g. with sodium diethyldithiocarbamate [7—10], has been used extensively to isolate the elements of interest from possible interferences in sample matrix.

The proposed method makes use of a chelation-extraction system whereby cobalt, nickel, and copper are chelated with sodium diethyldithiocarbamate at pH 6 and extracted into methyl isobutyl ketone before atomic-absorption spectrometry. Ammonium fluoride is used to mask iron and aluminum. The manganese interference is removed by taking advantage of the instability of

manganese chelate in the organic phase. The method is free from interferences by common elements in a variety of sample media and may have wide applications in geochemical exploration.

## EXPERIMENTAL

### *Apparatus*

A Varian AA6 atomic-absorption spectrometer was used for all determinations. The instrument was equipped with a simultaneous background corrector, an automatic gas control unit, a variable nebulizer, and Westinghouse hollow-cathode lamps. The glass bead and variable nebulizer were adjusted for maximum absorbance. The flow-meter reading was set at 4.0 for air and 0.1 for acetylene. All absorbance readings were taken with a burner height of 11.5 divisions. Additional instrument parameters are given in Table 1. With the burner set parallel to the light path and instrument settings as given, a working range of 1—40 $\mu$g Co and Ni, and 1—20 $\mu$g Cu in the organic phase may be determined. With the burner turned at a 90° angle relative to the light path, 20—200 $\mu$g Co, Ni and Cu in the organic phase may be determined.

### *Reagents and standards*

*Sodium diethyldithiocarbamate (NaDDTC; 2% w/v).* Dissolve 2 g of NaDDTC in 100 ml of water. Prepare fresh daily.

*Neutralizing-buffer solution.* Dissolve 32 g of sodium hydroxide in 200 ml of water. Dissolve 68 g of sodium citrate dihydrate and 4 g of citric acid monohydrate in 200 ml of water. Combine the two solutions and mix well.

*Ammonium fluoride solution (12.5% w/v).* Dissolve 62.5 g of ammonium fluoride in 500 ml of water. Transfer the solution to a separatory funnel, add 10 ml of NaDDTC solution, and shake. Add 20 ml of methyl isobutyl ketone (MIBK) and shake again. Allow the MIBK phase to separate completely (usually overnight) and drain the clear fluoride solution to a dry clean bottle. This procedure is necessary to remove Co, Cu, and especially Ni contamination from the reagent to lower the blank readings.

*Cobalt, nickel, and copper stock solutions.* Prepare each individual metal stock solution (1000 $\mu$g ml$^{-1}$ Co, Ni, or Cu) from Specpure metal oxide by dissolving 1.407 g $Co_2O_3$, 1.273 g NiO, or 1.252 g CuO in 50 ml of 6 M HCl

TABLE 1

AA6 settings for determination of Co, Ni, and Cu

| Element | Lamp current (mA) | Wavelength (nm) | Slit (nm) |
|---|---|---|---|
| Co | 5.0 | 240.7 | 0.2 |
| Cu | 5.0 | 232.0 | 0.2 |
| Ni | 2.5 | 324.7 | 0.5 |

with heat, and diluting to 1 l with additional HCl so that the acidity of the final solution is 2 M. Through dilutions with 2 M HCl, combined stock solutions containing 10 and 100 $\mu$g ml$^{-1}$ Co, Ni, and Cu are prepared from individual stock solutions.

*Combined standard solutions.* Two series of combined standard solutions are required. The first series (0, 0.1, 0.2, 0.5, 1, 2, and 4 $\mu$g ml$^{-1}$ Co, Ni, and Cu) is prepared by diluting 0, 1, 2, 5, and 10 ml of the 10 $\mu$g ml$^{-1}$ combined stock solution, and 2 and 4 ml of the 100 $\mu$g ml$^{-1}$ combined stock solution to volume in 100-ml volumetric flasks with 2 M HCl. This series is used when the burner is aligned parallel to the light path. The second series (0, 2, 4, 7.5, 10, 15, and 20 $\mu$g ml$^{-1}$ Co, Ni, and Cu) is prepared by diluting 0, 2, 4, 7.5, 10, 15, and 20 ml of the 100 $\mu$g ml$^{-1}$ combined stock solution to volume in 100-ml volumetric flasks with 2 M HCl, and is used when the burner is turned at a 90° angle to the light path. For calibration curves, pipet 10 ml of each of the combined standard solutions of either series to screw-cap tubes (25 × 150 mm) and treat as sample solutions in the following procedure.

*Procedure*

Weigh 0.200 g of less than 100-mesh soil, rock, or stream sediment into a 100-ml Teflon beaker. Moisten the sample with a few drops of water. Add 5 ml of concentrated nitric acid and place the beaker on an oscillating hot-plate preset at 135—140°C for 10 min. Cool and add 10 ml of 50% HF and evaporate to dryness. Add 5 ml of 11 M HCl and evaporate to dryness again. Remove the beaker from the hot-plate, pipet 5 ml of 4 M HCl on to the residue, and loosen it with a Teflon spatula to aid in dissolution. Transfer the solution and any remaining residue to a screw-cap tube (25 × 150 mm) with 5 ml of water. A reagent blank is carried through the digestion to provide a blank for the acids used.

Add first 10 ml of 12.5% $NH_4F$ and then 10 ml of the neutralizing-buffer solution to the sample solution in the tube, mixing well after each addition with a vortex mixer. The pH of the solution at this point should be around 6. Add 1 ml of NaDDTC solution and mix well. Finally, add 5 ml of MIBK, cap the tube, and shake for 2 min. Centrifuge the tube to help separate the organic phase, and set it aside for 24 h before aspirating the organic phase into the flame for Co, Ni, and Cu determinations. A series of combined standard solutions is treated as above procedure to obtain the calibration curves. The extracted Co, Ni, and Cu complexes are stable in the organic phases for at least 40 h.

## RESULTS AND DISCUSSION

*Sensitivity*

With the instrument settings as outlined and the burner positioned parallel to the light beam, 5—200 ppm of Co and Ni, and 5—100 ppm of Cu in the sample can be determined. With the burner turned perpendicular to the light

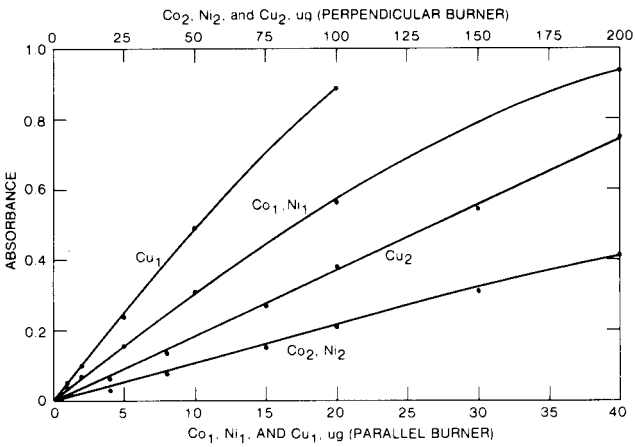


Fig. 1. Calibration curves for Co, Ni, and Cu with the burner either perpendicular (upper abscissa) or parallel (lower abscissa) to the light beam.

beam, 100—1000 ppm of the three metals in the sample can be determined. Calibration curves for both burner positions are given in Fig. 1. For determinations of even higher concentrations of metals, a smaller sample size may be used.

*Interferences*

With the NaDDTC—MIBK system, no interferences were found in the determination of microgram amounts of Co, Ni, and Cu in the presence of 10% Na, K, or Mg, 20% Al, 25% Ca, or 50% Fe in the sample. These metals may be present individually or in various combinations. Iron and aluminum are prevented from precipitation on adjustment of the sample solution to pH 6 with the neutralizing-buffer solution by masking with ammonium fluoride [11—13]. Fluoride forms an insoluble salt with calcium, but this does not interfere with the extraction of Co, Ni, and Cu.

Manganese is extracted under the experimental conditions and causes significant enhancement of values of all three metals when its concentration in the sample exceeds 0.1%. The enhancement levels off when the concentration of manganese in the sample reaches 5%, and remains constant up to 20% Mn. However, the extracted MnDDTC was found to be unstable in the MIBK phase, in agreement with other investigators [8, 9, 14]. A time—stability study with synthetic solutions showed a drastic decrease of manganese in the organic phase in the first 1—2 h (Fig. 2) until its complete disappearance after 24 h. Enhancement of Co, Ni, and Cu values by manganese also exhibited a decreasing trend parallel to the decrease of manganese in MIBK and no enhancement was evident after 24 h (Fig. 3), establishing the cause-effect relationship between manganese and the absorbance enhancement. To eliminate manganese interference, the sample solutions and standards with all required reagents added according to the procedure were set aside for 24 h before analysis. No

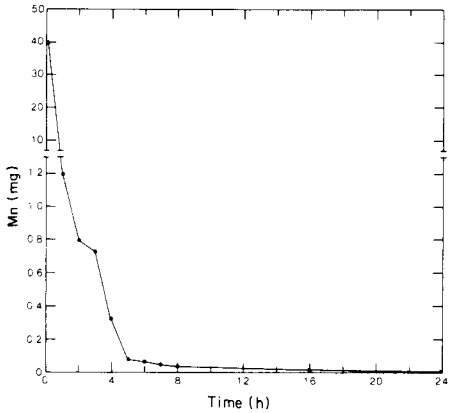


Fig. 2. (left) Time course of the decrease of manganese in the organic phase (at zero time, the total Mn (40 mg) corresponds to 20% Mn in the sample). Experiments with concentrations corresponding to 0.25%, 1%, and 5% Mn in the sample gave similar results.

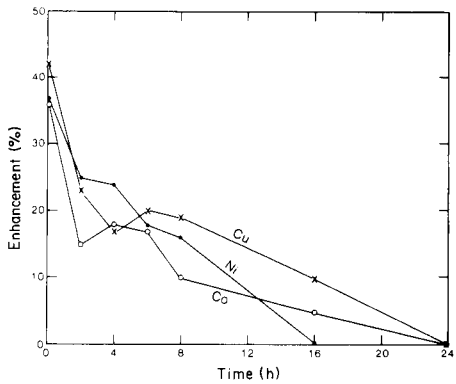


Fig. 3. (right) Time course indicating the enhancement of absorbance of 10 μg Co, Ni, and Cu by 40 mg Mn corresponding to 20% Mn in the sample. Experiments with 20 μg Co, Ni, and Cu and Mn concentrations corresponding to 5% and 10% Mn in the sample gave similar results.

interference was observed with samples containing up to 25% Mn or 38% $MnO_2$.

Thus, the proposed method can be applied to the determination of Co, Ni, and Cu in a wide range of geological materials including iron- and manganese-rich, and calcareous samples.

*Analytical data*

The method was applied to five U.S. Geological Survey rock standards. The results are compared with those reported in the literature in Table 2. The values of Co, Ni, and Cu obtained by this method are in the same general order of magnitude as the reported values.

Replicate analyses of six U.S. Geological Survey geochemical reference samples gave relative standard deviations of less than 5% for all three metals (Table 3). The same six geochemical samples were spiked with two levels of Co, Ni, or Cu before acid digestion. Recoveries ranged from 92 to 108% (Table 4).

TABLE 2

Concentrations of Co, Ni, and Cu (ppm) found in U.S.G.S. standard rock samples compared with literature values

| Sample | Co | | Ni | | Cu | |
|---|---|---|---|---|---|---|
| | Found | Literature | Found | Literature | Found | Literature |
| G-2 | 5.6 | 9.4[a], 3.8[b], 5.0[f] | 3.8 | 6.1[a], 1.8[b], 3.0[c], 1.8[e] | 11.6 | 11.0[a], 9.0[b], 11.0[c], 9.1[e] |
| GSP-1 | 9.1 | 11.8[a], 5.6[b], 7.0[c], 6.9[f] | 10.3 | 11.0[a], 6.0[b], 7.0[c], 8.0[e] | 41.4 | 32.4[a], 29.6[b], 33.0[c], 31.9[e] |
| AGV-1 | 18.9 | 21.1[a], 11.9[b], 16.0[c], 15.3[d], 15.0[f], 16.4[g] | 15.3 | 20.2[a], 10.6[b], 15.0[c], 18.7[d], 15.9[e] | 73.3 | 58.2[a], 53.3[b], 61.0[c], 65.0[d], 57.4[e] |
| BCR-1 | 48.7 | 40.2[a], 30.7[b], 37.0[c], 33.0[d], 36.0[f], 36.4[g] | 12.5 | 15.2[a], 8.0[b], 10.0[c], 18.1[e], 9.9[e] | 21.0 | 17.8[a], 14.3[b], 15.0[c], 22.4[d], 15.8[e] |
| PCC-1 | 123.0 | 105.4[a], 84.0[b], 183.0[d], 115.0[f] | 2343.0 | 2346.0[a], 1870.0[b], 2313.0[d], 2340.0[e] | 10.9 | 10.4[a], 8.4[b], 10.0[d], 9.8[e] |

[a]Flanagan [15], average of atomic-absorption values. [b]Armannsson [16]. [c]Kawabe [17]. [d]Hannaker and Hughes [8]. [e]Uchida et al. [18]. [f]Mountjoy [19]. [g]Kiss [20].

TABLE 3

Five replicate determinations of Co, Cu, and Ni in six geochemical reference samples [21] by the proposed method. All values in ppm

| Sample | Material | Co | | | Ni | | | Cu | | |
|---|---|---|---|---|---|---|---|---|---|---|
| | | Range | Mean | $s_r$ (%) | Range | Mean | $s_r$ (%) | Range | Mean | $s_r$ (%) |
| GXR-1 | Jasperoid | 8.4— 9.2 | 8.8 | 4.7 | 40.1—44.9 | 42.5 | 4.9 | 1092.0—1171.0 | 1129.0 | 3.2 |
| GXR-2 | Soil | 7.8— 8.9 | 8.3 | 4.9 | 13.4—14.9 | 14.4 | 4.3 | 61.5—66.2 | 63.4 | 3.2 |
| GXR-3 | Fe—Mn rich deposit | 57.8—60.4 | 59.2 | 1.7 | 57.8—62.0 | 60.4 | 2.6 | 13.6—14.6 | 14.2 | 3.1 |
| GXR-4 | Cu mill heads | 15.9—17.0 | 16.6 | 4.2 | 42.9—44.0 | 43.5 | 1.0 | 6580.0—7000.0 | 6780.0 | 2.5 |
| GXR-5 | Soil | 22.5—25.4 | 24.1 | 4.7 | 48.6—54.4 | 51.9 | 4.3 | 288.0—324.0 | 308.0 | 4.7 |
| GXR-6 | Soil | 13.0—14.3 | 13.6 | 4.1 | 23.5—25.8 | 24.8 | 3.5 | 63.2—64.9 | 63.9 | 1.2 |

TABLE 4

Recoveries of known amounts of Co, Cu, and Ni added to six geochemical reference samples [21] before acid digestion. (Average of duplicates of 0.2-g samples)

| Sample | Co | | | | Ni | | | | Cu | | | |
|---|---|---|---|---|---|---|---|---|---|---|---|---|
| | Present (μg) | Added (μg) | Found (μg) | Recovery (%) | Present (μg) | Added (μg) | Found (μg) | Recovery (%) | Present (μg) | Added (μg) | Found (μg) | Recover (%) |
| GXR-1 | 1.8 | 1 | 2.9 | 103.6 | 10.7 | 5 | 16.0 | 101.9 | 234.0 | 100 | 344.0 | 103.0 |
| GXR-1 | 1.8 | 2 | 4.1 | 107.9 | 10.7 | 10 | 21.7 | 104.8 | 234.0 | 200 | 428.0 | 98.6 |
| GXR-2 | 1.4 | 1 | 2.3 | 95.8 | 3.2 | 1 | 4.2 | 100.0 | 13.8 | 5 | 18.4 | 97.9 |
| GXR-2 | 1.4 | 2 | 3.2 | 94.1 | 3.2 | 2 | 4.9 | 94.2 | 13.8 | 10 | 23.1 | 97.1 |
| GXR-3 | 11.1 | 5 | 16.1 | 100.0 | 13.5 | 5 | 18.6 | 100.5 | 2.9 | 1 | 4.2 | 107.7 |
| GXR-3 | 11.1 | 10 | 22.2 | 105.2 | 13.5 | 10 | 24.2 | 103.0 | 2.9 | 2 | 5.0 | 102.0 |
| GXR-4 | 2.8 | 5 | 7.2 | 92.3 | 8.1 | 5 | 12.1 | 92.4 | 1320.0 | 300 | 1523.0 | 94.0 |
| GXR-4 | 2.8 | 10 | 12.0 | 93.8 | 8.1 | 10 | 19.0 | 95.3 | 1320.0 | 600 | 1824.0 | 95.0 |
| GXR-5 | 3.9 | 5 | 8.6 | 96.6 | 10.9 | 5 | 16.9 | 106.3 | 65.4 | 30 | 90.0 | 94.3 |
| GXR-5 | 3.9 | 10 | 12.9 | 92.8 | 10.9 | 10 | 20.1 | 96.2 | 65.4 | 60 | 121.1 | 96.6 |
| GXR-6 | 2.0 | 5 | 6.6 | 94.3 | 4.4 | 5 | 8.7 | 92.6 | 10.0 | 5 | 14.1 | 94.0 |
| GXR-6 | 2.0 | 10 | 12.2 | 101.7 | 4.4 | 10 | 13.5 | 93.8 | 10.0 | 10 | 20.6 | 103.0 |

REFERENCES


1 G. J. S. Govett and R. E. Whitehead, J. Geochem. Explor., 2 (1973) 121.
2 K. Fletcher, Econ. Geol., 65 (1970) 588.
3 H. M. Nakagawa, U.S. Geol. Surv. Bull., 1408 (1975) 85.
4 G. K. Billings, At. Absorpt. Newsl., 4 (1965) 357.
5 H. D. Fleming, Anal. Chim. Acta, 59 (1972) 197.
6 L. L. Sundberg, Anal. Chem., 45 (1973) 1460.
7 A. Wyttenbach and S. Bajo, Anal. Chem., 47 (1975) 1813.
8 P. Hannaker and T. C. Hughes, Anal. Chem., 49 (1977) 1485.
9 J. Nix and T. Goodwin, At. Absorpt. Newsl., 9 (1970) 119.
10 K. Kuwata, K. Hisatomi and T. Hasegawa, At. Absorpt. Newsl., 10 (1971) 111.
11 K. L. Cheng, Anal. Chem., 33 (1961) 783.
12 A. G. Fogg, S. Soleymanloo and D. T. Burns, Talanta, 22 (1975) 541.
13 A. Purushottam, P. P. Naidu and S. S. Lal, Talanta, 20 (1973) 631.
14 M. Yamagisawa, M. Suzuki and T. Takeuchi, Anal. Chim. Acta, 43 (1968) 500.
15 F. J. Flanagan, U.S. Geol. Surv. Prof. Paper, 840 (1976) 131.
16 H. Armannsson, Anal. Chim. Acta, 88 (1977) 89.
17 I. Kawabe, J. Earth Sci. Nagoya Univ., 23/24 (1976) 1.
18 T. Uchida, M. Nagase, I. Kojima and C. Iide, Anal. Chim. Acta, 94 (1977) 275.

*Analytica Chimica Acta*, 105 (1979) 255—262


# DETERMINATION OF ALKYL LEAD COMPOUNDS IN AIR BY GAS CHROMATOGRAPHY AND ATOMIC ABSORPTION SPECTROMETRY

B. RADZIUK, Y. THOMASSEN** and J. C. VAN LOON*

*Departments of Geology, Chemistry and the Institute for Environmental Studies, University of Toronto, Toronto M5S 1A1 (Canada)*

Y. K. CHAU

*Canada Center for Inland Waters P.O. Box 5050, Burlington L7R 4A6, Ontario (Canada)*

(Received 4th July 1978)

SUMMARY

Alkyl lead compounds are condensed from a 70-l street air sample in a series of four traps at —72°C, separated by gas chromatography and determined by atomic absorption spectrometry with electrothermal atomization. Total atmospheric alkyl lead averaged 14 ng Pb $m^{-3}$. Vehicular exhaust fumes are an insignificant contributor to this total. Tetraethyllead, the only alkyl lead compound used in southern Ontario gasoline, is unstable in air. Besides decomposing, it reacts to give other alkyl lead compounds, which can be determined by the technique described. Evaporation of gasoline is almost exclusively the source of alkyl lead compounds in street air.

In spite of the advent of lead-free gasoline in some countries, there is still a large quantity of the leaded product sold throughout the world. Depending on location, lead from gasoline is the major source of lead pollution in the environment. Other sources such as mining, smelting and chemical production only become major sources in localized areas. Most research workers [1—3] believe organic lead to be a small percentage, i.e. 0.1—14% depending on location, atmospheric conditions etc., of the total lead in urban air. The potential environmental and health hazard from lead is determined by the chemical species [4]. It is important, therefore, to have a reliable method for the determination of the individual forms of lead.

With the exception of the work of Laveskog [5], the determination of individual alkyl lead compounds in street air does not appear to have been described. Laveskog's method involved gas chromatographic—mass spectrometric (g.c.—m.s.) instrumentation, which is not available to most workers. Several workers have used gas chromatography—atomic absorption spectrometry (g.c.—a.a.s.) for the determination of alkyl lead compounds in gasoline [6—8]. Atomic absorption can respond specifically to lead compounds, thus simplifying the interpretation of chromatograms.

---

**On leave from Institute of Occupational Health, Oslo (Norway).

Harrison et al. [3] trapped organic lead compounds from street air and eluted them directly into the flame of an atomic absorption spectrometer, thus determining total organic lead. In such a study it would be an advantage to employ furnace atomization since organic lead exists in air at very low levels and the furnace can give a detection limit gain of up to 3 orders of magnitude.

A procedure is given below for the determination of individual alkyl lead compounds in street air.

## EXPERIMENTAL

### *Apparatus*

The Perkin-Elmer 603 atomic absorption spectrophotometer used was equipped with a deuterium background corrector, an HGA 2100 graphite furnace and a Perkin-Elmer Model 56 recorder. The radiation source was a Perkin-Elmer electrodeless discharge lamp operated at 10 W. A Pye gas chromatograph (Series 104) was interfaced to the graphite furnace with a tantalum connector (Fig. 1) machined from a 6.4-mm diameter rod (Ventron Corp. U.S.A.). The glass chromatographic column (150-cm long, 0.6-cm o.d.) was packed with 3% OV-101 on Chromosorb W (80—100 mesh). The effluent was transferred to the furnace by Teflon-lined aluminium tubing (3-mm o.d.), heated electrically to 80°C.

The g.c.—m.s. system consisted of a Varian Series 1400 gas chromatograph and a Finnigan quadrupole spectrometer Model 1015-C. The chromatographic column was identical to the above.

Glass bottles (250 and 2500 ml) equipped with silicon septa were used for the stability experiments.

Sample handling was by Hamilton glass syringes of appropriate volumes.

### *Reagents*

Tetramethyllead and tetraethyllead were obtained from Ventron Corp. Trimethylethyl-, dimethyldiethyl- and methyltriethyllead were provided

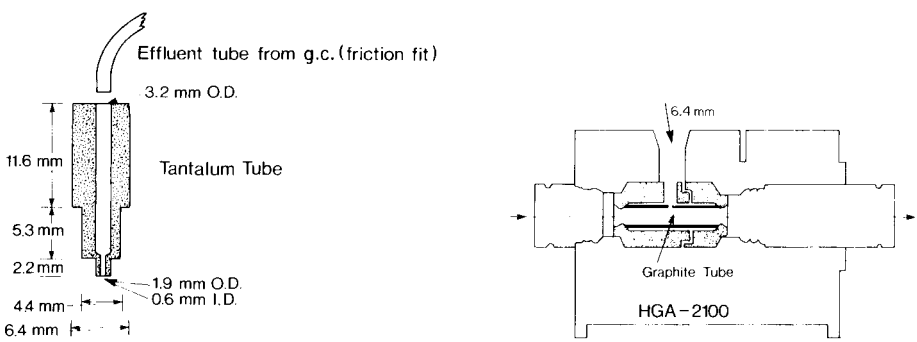


Fig. 1. Tantalum connector positioned in the furnace.

by the Ethyl Corporation (Ferndale, Mich., U.S.A.). Freshly diluted lead standards were prepared daily in analytical-grade methanol or benzene. The carrier gas for gas chromatography was purified dry nitrogen. The graphite furnace was flushed with purified argon. Analytical-grade nitric acid was used for the leaching of lead from the filters.

*Sampling*

The adsorption tubes for air samples were U-shaped Teflon-lined aluminium tubes (30 cm long, 3 mm o.d.) packed with 3% OV-101 on Chromosorb W (80—100 mesh). Moisture was condensed from air by using glass U-tubes at −15°C. The air was sampled with a peristaltic pump, Model LG-100, Little Giant Pump Co. (Oklahoma City, U.S.A.).

Atmospheric particulates were collected on 37-mm diameter Whatman No. 40 ash-free cellulose filter paper. The diameter of the exposed filter area was 20 mm. The air intake was inside a 2-l vessel placed upside down so that only particles smaller than ca. 10 $\mu$m were sampled. The filter holder was connected to a Sargent-Welch Duo-Seal vacuum pump, Model 1400 B, (Skokie, Ill.), calibrated with a flow meter at the start and end of the sampling period. Connections were made using new Tygon or Teflon tubing.

*Procedures*

The atomic absorption spectrometer was operated, with background correction, at the 283.3-nm lead resonance line, with a spectral bandwidth of 0.7 nm. The graphite furnace was heated continuously for 20-min periods at 1500°C by using the charring stage at the longest time setting. For optimal gas flow from the gas chromatograph, the quartz windows were removed from the furnace assemblies. The graphite furnace was operated with an internal flow of 40 ml $min^{-1}$. Because of the high carrier gas flow, the sensitivity was unaffected by the internal gas flow. The above optimal operating conditions were arrived at while using a gas chromatograph oven temperature of 150°C and a carrier gas flow rate of 140 ml $min^{-1}$.

The stability of alkyl lead compounds was studied by injecting 100-$\mu$g amounts into glass bottles. The bottles were stored under various conditions (see below). Samples of the atmosphere inside the bottles were taken with gas-tight syringes. Samples (0.1—5 ml) were injected onto the column and the oven was programmed from 90 to 200°C with a heating rate of 40°C $min^{-1}$.

Air and exhaust were sampled directly for organic lead compounds with four parallel traps maintained at −72°C in a dry ice—methanol bath. Water was precondensed in U-tubes at −15°C (sodium chloride in crushed ice). The flow through the traps averaged 70 ml $min^{-1}$ over periods from 30 min (exhaust) to 18 h. Each trap was kept in dry ice until it was attached to a 4-way valve installed between the carrier gas inlet and the injection port of the gas chromatograph. The trap was immersed in boiling water. After 1 min, the volatilized fraction of the sample was introduced to the g.c. column by diverting the carrier gas through the 4-way valve. The g.c. oven was programmed

from 50 to 200°C with a heating rate of 40°C $min^{-1}$. Mixed alkyl lead standards were added to blank traps which were run under identical conditions for calibration.

Air samples were introduced to the g.c.—m.s. system as described above. The chromatographic conditions were also identical to those used in the g.c.—a.a.s. analysis. Peaks at the appropriate retention times were examined for alkyl lead compounds.

The particulate material was collected for periods from 30 min (exhaust) to 18 h at a flow rate of 1 $m^3$ $h^{-1}$. The exposed areas of the filters were transferred to sealed Teflon 50-ml decomposition vessels and leached at 100°C for 30 min with 2 ml of (1 + 1) nitric acid, the solution being diluted to 10 ml with water. Blanks were prepared by treating unexposed filters in the same way. The samples were analyzed by flame atomization according to the manufacturer's settings, against standards containing the same amount of nitric acid.

## RESULTS AND DISCUSSION

### *Atomization temperature*

Chromatograms of a standard containing the five alkyl lead compounds were recorded at atomization temperatures of 700—2300°C. Peak heights for methyltriethyllead are plotted in Fig. 2 as a function of temperature. A

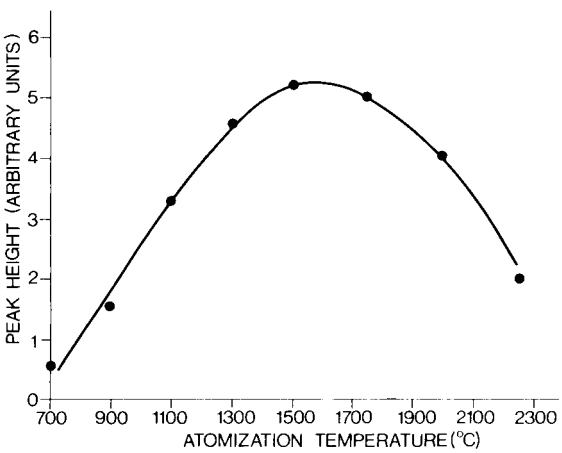


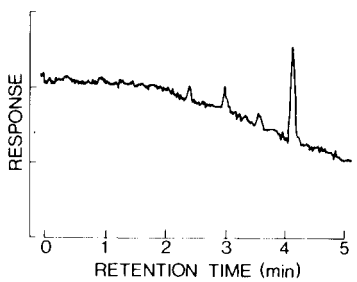


Fig. 2. Peak-height dependence on atomization temperature for methyltriethyllead. Note: Temperatures given are those indicated on the power supply. They are not necessarily true temperatures since the readings may be affected by changes in the furnace resistance due to the transfer tube.

Fig. 3. Lead-response chromatogram from a 70-l air sample, showing the presence of alkyl lead compounds; in order of increasing retention time the four peaks are from trimethylethyl-, dimethyldiethyl-, methyltriethyl- and tetraethyllead. The baseline drift is due to single-beam operation of the spectrometer.

similar relationship was found for the other alkyl lead compounds. Thus, the relative peak heights for the individual compounds are dependent only on chromatographic conditions.

When the tantalum connector is used, the furnace may be heated to 2500°C without damage to the tantalum. Operated at 1500°C the lifetime of the graphite tube ranged between 10 and 15 h.

*Interferences*

Atomic absorption spectrometry is element-specific as long as molecular-absorption and/or light-scattering interferences can be eliminated. In flame atomic absorption these are seldom a problem. However, both phenomena are frequently encountered in electrothermal atomization. The deuterium background corrector will adequately compensate for broad-band light losses of a reasonable magnitude which are relatively constant over the bandpass of the monochromator. Light scattering generally behaves in the latter manner. In contrast, molecular absorption commonly consists of a continuum on which fine structure is superimposed. If a component of the fine structure overlaps the absorption line being employed, then deuterium background correction will compensate only partially.

Carbon-rich compounds such as toluene and cyclohexane gave broad-band absorption which exceeded the capacity of the background corrector. However, the solvents used in this study, methanol and benzene, were easily separated from the lead compounds.

*Collection efficiency, gas sampling and detection limit*

Chau et al. [8] found that the recovery of the five lead compounds from air in a cold trap containing OV-1 at −80°C was 94—105%. This was done without precondensing moisture. Analysis of the water traps used in the present study showed that these contained less than 1% of a known amount of tetraethyllead.

Ten injections of 5-ml air samples containing 4 ng of each of the five lead compounds were made to determine the reproducibility of retention time and peak height in sampling large volumes. Relative standard deviations were found to be less than 3 and 5%, respectively. The baseline stability was not affected by changes in carrier gas flow caused by injection of large volumes.

The detection limit was found to be about 40 pg of lead for each compound, based on peak-height measurements. For a 70-l air sample, 0.5 ng $m^{-3}$ of each compound could be detected.

*Lead in gasoline and motor vehicle exhaust fumes*

Chromatograms were obtained for several gasolines from various local (Southern Ontario) suppliers. In each case tetraethyllead was the only detectable lead compound.

The exhaust gases from each of two vehicles (Dodge Van 1974 and Ford

Torino 1975) were sampled for 30 min after a cold start. In each case the total concentration of lead found by this method was 2.7 mg Pb $m^{-3}$. The concentration of alkyl lead was less than 70 ng $m^{-3}$. Thus, the ratio between total and alkyl lead exceeds 38000:1.

*Identification of alkyl lead compounds in air*

Air was sampled 3 m above the ground, 5 m from a relatively busy urban street (College Street, Toronto). The mean total lead concentration was found to be 650 ng Pb $m^{-3}$. Total alkyl lead concentrations averaged 14 ng Pb $m^{-3}$, so that the ratio between total and alkyl lead was 46:1. A typical chromatogram of an air sample based on lead detection is shown in Fig. 3. Concentrations of individual alkyl lead compounds were calculated from the peak heights in this chromatogram. The concentrations were: trimethylethyllead, 1 ng Pb $m^{-3}$; dimethyldiethyllead, 2 ng Pb $m^{-3}$; methyltriethyllead, 1 ng Pb $m^{-3}$; tetraethyllead, 8 ng Pb $m^{-3}$. The relative standard deviation for the determination of these compounds in air was 30%, principally because of uncertainty in sample volumes. The reproducibility of the retention times of these alkyl lead compounds in air was 7%. These results are much lower than those reported by Robinson et al. [9].

It should also be noted that the very small proportion of lead present as alkyl lead compounds in exhaust fumes suggests that exhaust emission is an insignificant contributor to the presence of alkyl lead compounds in the atmosphere. This is in agreement with the results of Harrison et al. [3].

The presence of other alkyl lead compounds was surprising in that local gasoline contains only tetraethyllead. An alternative method of identification was sought to confirm this observation. Laveskog [4] reported the use of g.c.—m.s. for determination of tetramethyl- and tetraethyllead in air and exhaust. Thus, a 20-l sample of air was analyzed in this way. With the equipment used, it was possible to detect 0.5 $\mu$g of each lead compound in a benzene solution. The chromatogram obtained showed the presence of high-molecular-weight compounds at various retention times, including those which correspond to tetramethyl- and tetraethyllead. Individual mass spectra included fragments with mass numbers which could correspond to alkyl lead compounds. In no case, however, could the presence of lead be confirmed by the characteristic isotope ratio. This indicates that high-molecular-weight compounds which do not contain lead are present in air at much higher concentrations than alkyl lead compounds. Gas chromatography—mass spectrometry was therefore unsatisfactory for the determination of alkyl lead compounds in air under the chromatographic conditions of this study. It seems unlikely that the chromatography employed by Laveskog would separate alkyl lead compounds from other organic compounds with similar molecular weights. This may explain Laveskog's very high results ($> 1$ mg $m^{-3}$) for tetramethyl- and tetraethyllead in exhaust fumes.

*Reaction of tetraethyllead in air*

Shapiro and Frey [10] state "Tetraorganolead compounds react with a wide variety of substances". Tetraalkyllead compounds have been shown to be thermally unstable, and photochemical decomposition will also occur. Harrison et al. [3] therefore concluded "their lifetime in street air is probably relatively short".

In the present study a series of experiments was carried out to measure their lifetime. Tetramethyllead, tetraethyllead and a mixture of the two were introduced into separate glass bottles under various conditions. The composition of the gas mixture was monitored over a period of time. The results showed that tetramethyllead is relatively stable in air, but tetraethyllead reacts appreciably, even over a few hours, to form other alkyl lead compounds. The reaction is accelerated by light. In the binary mixture, a greater yield of the intermediates was observed.

Figure 4 shows a representative chromatogram of the atmosphere in a reaction bottle containing tetraethyllead, after standing in darkness for 24 h. Comparison with Fig. 3 shows that tetramethyl-, dimethyldiethyl- and methyltriethyllead are formed. Figure 5 shows that in an atmosphere saturated with gasoline the rate of formation of other alkyl lead compounds from tetraethyllead is markedly increased. In an atmosphere containing natural gas, similar behaviour is observed. There is little observable effect on reactivity when a mixture of tetramethyllead and tetraethyllead or the pure compounds are stored in vehicle exhaust rather than air. The formation of

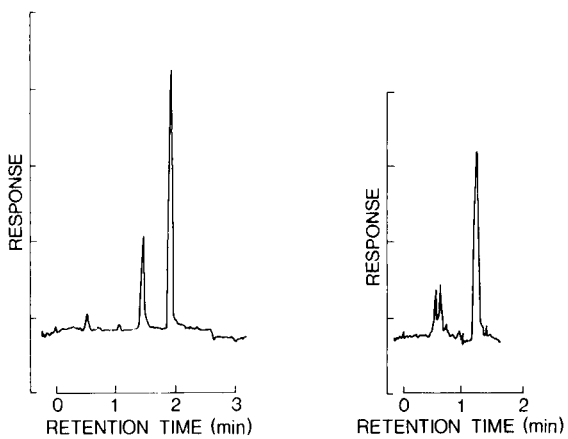


Fig. 4. Chromatogram showing reaction of tetraethyllead after 24 h in air in darkness. The compounds are identified in order of increasing retention time as tetramethyl-, dimethyldiethyl-, methyltriethyl- and tetraethyllead. Column heated from 90 to 200°C at 40°C $min^{-1}$.

Fig. 5. Chromatogram showing reaction of tetraethyllead after 24 h in a gasoline-saturated atmosphere in darkness. All five lead alkyls containing methyl and ethyl are present. The column was held at 150°C, so that faster separation was obtained.

intermediates is only slightly influenced by exposure to light but increases significantly with the surface-to-volume ratio of the container.

*Conclusions*

The proposed procedure can be used for the determination of the individual alkyl lead compounds in air.

Exhaust fumes from engines burning leaded fuel contribute little to the alkyl lead compounds in street air. This result is in agreement with the conclusion of Harrison et al. [3] that the evaporation of gasoline must be the main source of these compounds in air. The presence of alkyl lead compounds other than tetraethyllead in the atmosphere in areas where gasolines contain only tetraethyllead may be explained by gas-phase reactions, but the mechanisms of the reactions are not yet fully understood.

This work was supported by grants from the Ontario Ministry of the Environment under the Research Grants Programme of the Air Resources Branch, the Royal Norwegian Council for Scientific and Industrial Research and the University of Toronto. Perkin-Elmer Corporation, Norwalk, Connecticut, U.S.A., kindly lent the atomic absorption equipment. The authors thank I. Davies for his technical assistance, and H. Huneault of Canada Center for Inland Waters for performing the g.c.—m.s. analyses.

REFERENCES

1 L. J. Snyder, Anal. Chem., 39 (1967) 591.
2 L. J. Purdue, R. E. Enrione, R. J. Thompson and B. A. Bonfield, Anal. Chem., 45 (1973) 527.
3 R. M. Harrison, R. Perry and D. H. Slater, Atmos. Environ., 8 (1974) 1187.
4 P. T. S. Wong, B. A. Silverberg, Y. K. Chau and P. V. Hodson, in J. O. Nriagu (Ed.), Biogeochemistry of Lead in the Environment, Elsevier, Holland, 1978, pp. 279—342.
5 A. Laveskog, Second International Clean Air Congress Proceedings, Washington D.C., December 1970, p. 549.
6 B. Kolb, G. Kemmner, F. H. Schleser and E. Wiedeking, Fresenius Z. Anal. Chem., 221 (1966) 166.
7 D. A. Segar, Anal. Lett., 7 (1974) 89.
8 Y. K. Chau, P. T. S. Wong and H. Saitoh, J. Chromatogr. Sci., 14 (1976) 162.
9 J. W. Robinson, L. Rhodes and D. K. Wolcott, Anal. Chim. Acta, 78 (1975) 78.
10 H. Shapiro and F. W. Frey, The Organic Compounds of Lead, J. Wiley, New York, 1975, pp. 63—97.

*Analytica Chimica Acta*, 105 (1979) 263—270


# ELECTROTHERMAL ATOMIZATION FROM METALLIC SURFACES
## Part 1. Design and Performance of a Tungsten-tube Atomizer†

V. SYCHRA*, D. KOLIHOVÁ. O. VYSKOČILOVÁ and R. HLAVÁČ

*Laboratory of Flame Spectrometry, Institute of Chemical Technology, 166 28 Prague 6 (Czechoslovakia)*

P. PÜSCHEL

*Research Institute for Brown Coal, 43437 Most (Czechoslovakia)*

(Received 20th June 1978)

SUMMARY

A tungsten-tube atomizer has been developed and tested for a number of elements. The atomizer can be accommodated in the support of a commercial Varian carbon rod atomizer (CRA-63 or CRA-90) and operated as an alternative to the graphite tubes and cups. Characteristic concentrations, detection limits, optimum atomization temperatures, reproducibility and profiles of calibration curves obtained for Ag, Al, Ba, Cd, Co, Cu, Mg, Mn, Ni, Pb and V are similar to those obtained with the graphite-tube atomizer. The main advantage of this atomizer is its simple construction, low cost, long lifetime and excellent analytical performance, particularly for elements forming refractory carbides.

Several metal-based electrothermal atomization devices have been used as substitutes for the conventional graphite-based systems during the last few years. These atomizers have been based on heated boats [1—10], rods [11, 12], strips [13—15] and filaments [16—37] made of various metals, such as tantalum [1—10, 12—14, 20, 21, 28, 29], tungsten [11, 16—18, 22, 24—27, 30, 31, 33, 35—38], molybdenum [15, 29, 39, 40], rhenium [19], platinum [16—18, 23, 32], copper [34], etc. Most of these atomizers can be classified as "open systems". A metal tube atomizer has been used as an alternative to a graphite-tube atomizer in a commercial IL 455 electrothermal atomizer (Instrumentation Laboratory Inc., Lexington, Mass.) [38]. A molybdenum micro-tube atomizer has been described and tested in detail by Ohta and Suzuki [39, 40].

Some authors have tried to improve the performance of graphite atomizers for determinations of elements forming refractory carbides by inserting a metal foil into the atomizer. Good results have been reported, for instance, with a tantalum-lined graphite atomizer for the determination of barium [41], arsenic and selenium [42]. However, experience with such atomizers in this Institute has been rather bad. Because of imperfect heat transfer

†Presented to the XX.C.S.I. and 7.I.C.A.S. (Symposium No. 3, Chlum u Třeboně), September, 1977, Czechoslovakia.

between the inner wall of the graphite atomizer and the metal foil, the lifetime of the atomizer and the reproducibility of analytical signals are not satisfactory.

Potential advantages claimed for metallic electrothermal atomizers are as follows: the need for only a relatively low input power, simple manufacture (in most cases), higher heating rate compared to graphite atomizers, no problems with carbide formation, long lifetime (depending on the kind of metal, quality of protective atmosphere and solution analyzed), and lower background emission from a metal surface in the 250—350-nm spectral region than that from a graphite surface at the same temperature.

Metallic atomizers, of course, can also suffer from several important disadvantages, compared to graphite atomizers. Their mechanical resistance may decrease after long extensive heating; there is a danger of formation of intermetallic compounds between the metal surface and the analyte, resulting in severe memory effects and/or drastic drops in sensitivity; and the chemical resistance is lower, leading to corrosion problems. The last disadvantage should be overcome by preparing and maintaining the metal surface in an unreactive state, e.g. as a nitride, but this can be done only when there is experimental evidence that the quality of the metal surface does not play an important role in the formation of free atoms.

It seems reasonable to expect that more attention will be paid to atomization from metal surfaces in the near future. In this paper, a simple metal-tube electrothermal atomizer is described, which can be accommodated in the support of a Varian carbon rod atomizer (CRA-63 or CRA-90) and operated as an alternative to the graphite tubes or cups.

## EXPERIMENTAL

### *Apparatus*

All measurements were carried out with a Varian Model AA6 single-beam atomic absorption spectrometer. A Varian A-25 recorder with a 0.5-s full-scale response was used for recording transient signals. The slit widths, wave-lengths and lamp currents suggested by the manufacturer were used throughout.

*Atomizer.* The atomizer itself consists of two profiled metal strips (0.1-mm thick) that are held in two copper supporting electrodes [43]. The strips form a cylindrical cavity (5 mm long and 3.5 mm i.d.) (Fig. 1). Details of the strip and of the supporting electrode are shown in Fig. 2. It is very important to screw both strips to the supporting electrode to ensure good and reproducible electrical contact. The metal-tube atomizer and supporting electrodes are located in the CRA-63 workhead.

A special silica chamber (Fig. 3) is placed on top of the chimney of the CRA-63 to improve the efficiency of the inert gas sheath, i.e. to minimize diffusion of air to the metal surface. The chamber is adjusted and positioned against the metal-tube atomizer and in the optical axis by means of two stainless steel needles stabbed through the chimney holes. The inert gas sheath

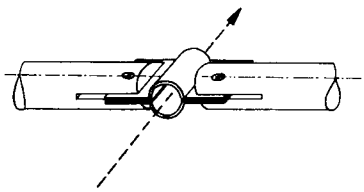

Fig. 1. Metal-tube atomizer and supporting electrodes.

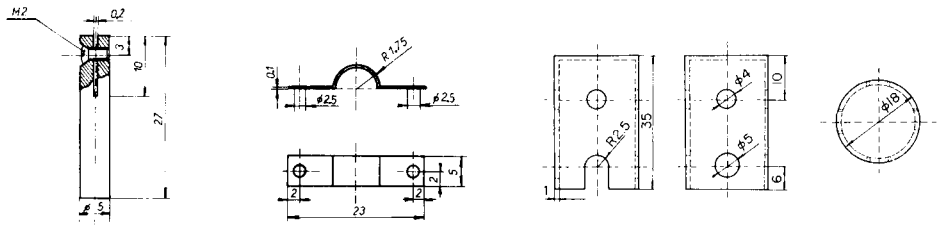


Fig. 2. Profiled metal strip (side view and top view) and supporting electrode (side view).

Fig. 3. Side view and top view of the silica chamber.

is a critical factor for metal-based atomizers. Argon (99.999% purity, flow rate 3 l $min^{-1}$) or an argon—hydrogen mixture (10% v/v hydrogen) were used as the protective atmosphere. Gas flow rates were measured with the CRA-63 gas control unit. The carbon rod unit with the metal-tube atomizer and with the silica chamber is shown in Fig. 4.

The metal-tube atomizer is heated with a modified Varian CRA-63 power supply. Lower input power is generally needed for the metal atomizer (30—45% of the input power for a carbon-tube atomizer depending on the metal used). A Variac 10-A autotransformer was therefore placed in the transformer circuit of the CRA-63 power supply, so that the input power could be changed

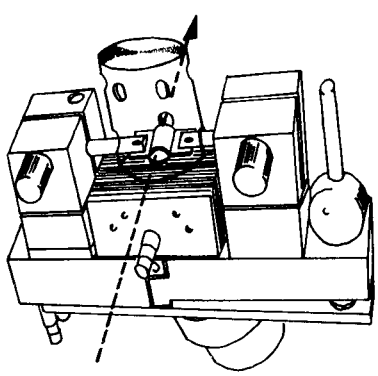

Fig. 4. Carbon rod unit with the metal-tube atomizer and the silica chamber.

continuously from 0 to 100% (see Fig. 5). A simple switch (SW 3) makes it possible to operate either a graphite or a metal-tube atomizer.

Various metals (tungsten, molybdenum, tantalum, platinum, iridium) were tested for the construction of the tube atomizer. All analytical data reported in this paper were obtained with the tungsten atomizer. Results obtained with other metals will be reported separately. The tungsten-tube atomizer was made from 5-mm tungsten strips (99.99% purity; Metallwerke, Plausee, Austria).

*Measurement of the atomizer temperature*

The atomizer surface temperatures were measured with an optical pyrometer and confirmed by measurements with Pt/Pt—Rh and Ir/W miniature thermocouples. All temperature measurements were done in the stepwise mode, i.e. 5—10 s after the atomization cycle started. For the tungsten-tube atomizer and 45% of the original input power of the CRA-63 power supply, the dry, ash and atomize settings 0—10 corresponded to the temperatures 0—120°C, 0—1600°C, and 0—3200°C, respectively.

*Sampling*

A 1—5-$\mu$l aliquot of the sample was placed in the center of the lower metal strip with an adjustable 5-$\mu$l syringe (Scientific Glass Engineering Pty. Ltd., Melbourne) with a disposable Teflon tip. It is extremely important to use a micropipet or a microsyringe with a soft plastic tip and not to press firmly on the strip, which becomes fragile after several atomization cycles. Samples were delivered into the atomizer cavity from either end; a delivery hole made in the center of the upper strip reduces significantly the lifetime of the atomizer.

*Reagents*

Specpure metals (Johnson-Matthey Ltd.) were used for the preparation of stock solutions of the metals (1000 $\mu$g ml$^{-1}$). Solutions of Ag, Pb, Cd, Cu, Ni, Co, Mn, Ba, Al and Mg were prepared as nitrates; vanadium was prepared

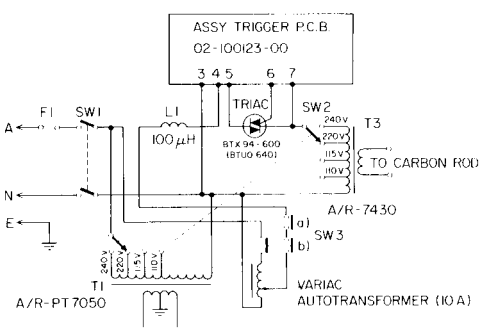


Fig. 5. Modification of the CRA-63 power supply for the metal-tube atomizer. Switch SW3 can be turned to operate a graphite atomizer (position a) or a metallic atomizer (position b

as vanadyl sulphate. All working solutions were prepared immediately before use by dilution with twice-distilled, deionized water and were acidified with an appropriate acid to a final concentration of 1% (v/v). The solutions were stored in polyethylene bottles.

## RESULTS AND DISCUSSION

### *Analytical data*

Table 1 lists the optimum atomization temperatures, characteristic concentrations and detection limits of the elements studied. Characteristic concentrations obtained for the tungsten-tube atomizer are slightly worse (by a factor of 2—8) than those published by the manufacturer for the CRA-90 carbon-tube, except for barium, which is more sensitive with the tungsten-tube atomizer. This small decrease in sensitivity was expected, and is probably mainly due to the short length of the tungsten tube, i.e. the short residence time of the analyte atoms in the tube, particularly when very high heating rates are applied.

The optimum atomization temperatures found for the tungsten-tube atomizer are, for all elements studied, nearly the same as those recommended for the carbon tube. However, dependence of the analytical signal on the temperature is more complex for the tungsten tube. Apparently lower absorption at higher temperatures was observed, for all the elements studied, with the tungsten-tube atomizer. This is probably due to the increased thermal

TABLE 1

Analytical data for tungsten-tube atomizer

| Element[a] | Optimum atomization temperature, (°C) | Characteristic concentration[b] (pg/1%) | Detection limit (pg) |
|---|---|---|---|
| Ag | 1200 | 0.8 (0.2) | 0.2 |
| Al | 2200 | 80[c] (15) | 12 |
| Ba | 2300 | 10[c] (15) | 3 |
| Cd | 1000 | 1 (0.15) | 0.2 |
| Co | 2100 | 15[c] (5) | 2.5 |
| Cu | 1800 | 12 (4) | 2 |
| Mg | 1900 | 0.4[c] (0.06) | 0.1 |
| Mn | 1900 | 5 (0.6) | 1 |
| Ni | 2100 | 16[c] (10) | 4 |
| Pb | 1450 | 25 (4) | 5 |
| V | 2500 | 125[c] (70) | 25 |

[a] All elements were used as their nitrate salts, except vanadium (sulphate).
[b] Values in parentheses are the characteristic concentrations for the Varian CRA-90 itself.
[c] In an argon—hydrogen atmosphere (3 l Ar $min^{-1}$, 0.35 l $H_2$ $min^{-1}$).

expansion of the inert gas in the tube and also to the relatively slow response of the electronic circuitry used. Similar temperature effects have been found with other atomizers [4, 11, 20].

*Effect of protective atmosphere*

For some elements (see Table 1), a significant increase in sensitivity was achieved when hydrogen was added to the inert gas (argon). For aluminium, barium and vanadium, the appearance temperatures as well as the optimum atomizing temperatures are much lower in the argon—hydrogen mixture than in pure argon. This indicates a different mechanism of atom formation in the argon—hydrogen mixture and in argon; a detailed investigation of the effect will be reported later.

*Calibration curves and reproducibility*

Figure 6 shows calibration curves for silver, copper, and vanadium, respectively. These curves have shapes similar to those obtained with the carbon-tube atomizer; better linearity can be achieved when the signals are integrated, i.e. with peak-area measurements.

The reproducibility was determined from 25 measurements of a standard solution of lead, with 2.5-$\mu$l injections. The relative standard deviation was 2.6% for 2 ng of lead. Reproducibilities were similar for other elements.

*Lifetime of the atomizer*

When properly operated, the tungsten-tube atomizer does not exhibit marks of wear or deterioration in performance for a reasonably long time (changes in resistance, oxidation, contact problems between the tube and the supporting electrodes, changes in sensitivity, etc.). The atomizer can be reused at least 350—500 times, depending on the purity of the inert gas, acidity of the solution analyzed and the temperature used. The main limiting factor for the lifetime of the atomizer is its mechanical and chemical resistance.

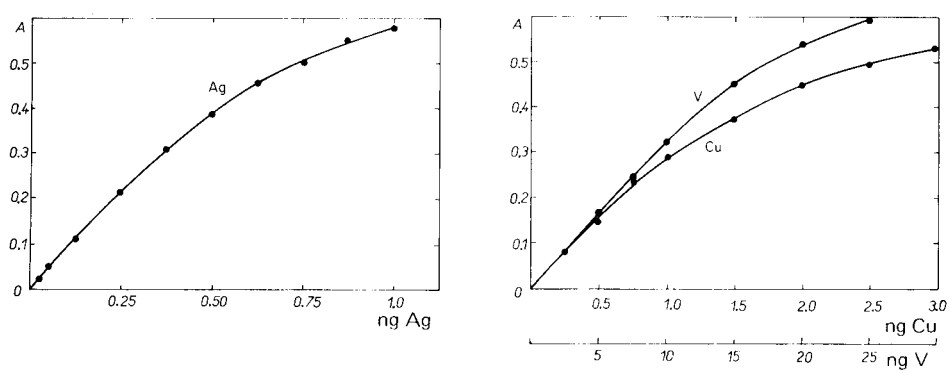


Fig. 6. Calibration curves for silver and copper in an argon atmosphere, and for vanadium in an argon—hydrogen atmosphere.

Until recently, only 5-mm tungsten strips were available; accordingly, all the results presented were obtained with 5-mm tungsten tubes. Very recent experiments with tungsten-tube atomizers 10-mm long and of 3.5-mm inner diameter indicate that the characteristic concentrations and detection limits can be improved 2—3-fold compared to those obtained with the 5-mm tubes, although the optimum atomizing temperatures and linear ranges are very similar.

Practical examples of analytical applications of the tungsten-tube atomizer for the determination of some refractory elements in complex matrices will be reported in later papers.

REFERENCES


1 H. M. Donega and T. E. Burgess, Anal. Chem., 42 (1970) 1521.
2 J. Y. Hwang, P. A. Ullucci, S. B. Smith Jr. and A. L. Malenfant, Anal. Chem., 43 (1971) 1319.
3 J. Y. Hwang, P. A. Ullucci and S. B. Smith Jr., Am. Lab., August 1971.
4 J. Y. Hwang, C. J. Mokeler and P. A. Ullucci, Anal. Chem., 44 (1972) 2018.
5 H. V. Lagesson, Mikrochim. Acta, 1 (1974) 527.
6 L. F. Grushko, N. P. Ivanov and M. S. Chupakhin, Zh. Anal. Khim., 29 (1974) 1842.
7 E. R. Blood and G. C. Grant, Anal. Chem., 47 (1975) 1438.
8 W. G. Schrenk and R. T. Everson, Appl. Spectrosc., 29 (1975) 41.
9 K. Dittrich, E. John and I. Rohde, Anal. Chim. Acta, 94 (1977) 75.
10 K. Dittrich and K. Borzyn, Anal. Chim. Acta, 94 (1977) 83.
11 J. E. Cantle and T. S. West, Talanta, 20 (1973) 459.
12 J. Aggett and A. J. Sprott, Anal. Chim. Acta, 72 (1974) 49.
13 M. R. Sensmeier, W. F. Wagner and G. D. Christian, Fresenius Z. Anal. Chem., 277 (1975) 19.
14 J. A. Goleb and C. R. Midkiff Jr., Appl. Spectrosc., 29 (1975) 44.
15 T. Hasegawa, M. Yanagisawa and T. Takeuchi, Anal. Chim. Acta, 89 (1977) 217.
16 M. P. Bratzel Jr., R. M. Dagnall and J. D. Winefordner, Anal. Chim. Acta, 48 (1969) 197.
17 M. P. Bratzel Jr., R. M. Dagnall and J. D. Winefordner, Appl. Spectrosc., 24 (1970) 518.
18 J. D. Winefordner, Pure Appl. Chem., 23 (1970) 35.
19 B. Hircq, Proceedings of the 3rd International Congress of Atomic Absorption and Atomic Fluorescence Spectrometry, Paris, 1971, Adam Hilger, London.
20 T. Takeuchi, M. Yanagisawa and M. Suzuki, Talanta, 19 (1972) 465.
21 T. Maruta and T. Takeuchi, Anal. Chim. Acta, 62 (1972) 253.
22 M. Williams and E. H. Piepmeier, Anal. Chem., 44 (1972) 1342.
23 S. R. Goode, A. Montaser and S. R. Crouch, Appl. Spectrosc., 27 (1973) 355.
24 J. V. Chauvin, M. P. Newton and D. G. Davis, Anal. Chim. Acta, 65 (1973) 291.
25 M. P. Newton, J. V. Chauvin and D. G. Davis, Anal. Lett., 6 (1973) 89.
26 J. V. Chauvin, M. S. Thesis, University of New Orleans, 1973.
27 M. P. Newton and D. G. Davis, Anal. Lett., 6 (1973) 923.
28 T. Maruta and T. Takeuchi, Bunseki Kagaku, 22 (1973) 602.
29 N. S. McIntyre, M. G. Cook and D. G. Boase, Anal. Chem., 46 (1974) 1983.
30 W. Lund and B. V. Larsen, Anal. Chim. Acta, 70 (1974) 299.
31 W. Lund and B. V. Larsen, Anal. Chim. Acta, 72 (1974) 57.
32 J. M. Mansfield, T. S. West and R. M. Dagnall, Talanta, 21 (1974) 787.
33 M. P. Newton and D. G. Davis, Anal. Chem., 47 (1975) 2003.
34 M. P. Newton and D. G. Davis, Anal. Lett., 8 (1975) 729.
35 W. Lund, B. V. Larsen and N. Gundersen, Anal. Chim. Acta, 81 (1976) 319.

36 R. D. Reid and E. H. Piepmeier, Anal. Chem., 48 (1976) 338.
37 D. D. Siemer and H. Y. Wei, Anal. Chem., 50 (1978) 147.
38 J. Y. Hwang and G. P. Thomas, Am. Lab., November (1974).
39 K. Ohta and M. Suzuki, Talanta, 22 (1975) 465; 23 (1976) 560.
40 K. Ohta and M. Suzuki, Anal. Chim. Acta, 83 (1976) 381; 85 (1976) 338; 96 (1978) 77.
41 G. D. Renshaw, At. Absorpt. Newsl., 12 (1973) 158.
42 R. B. Baird and S. M. Gabrielian, Appl. Spectrosc., 28 (1974) 273.
43 ČSSR Patent No. 174728, 1977.

*Analytica Chimica Acta*, 105 (1979) 271—279


# ELECTROTHERMAL ATOMIZATION FROM METALLIC SURFACES
## Part 2. Atom Formation Processes in the Tungsten-tube Atomizer†

O. VYSKOČILOVÁ, V. SYCHRA* and D. KOLIHOVÁ

*Laboratory of Flame Spectrometry, Institute of Chemical Technology, 166 28 Prague 6 (Czechoslovakia)*

P. PÜSCHEL

*Research Institute for Brown Coal, 43437 Most (Czechoslovakia)*

(Received 20th June 1978)

SUMMARY

A modified carbon rod atomizer (Varian M-63) is used to study the mechanism of atom formation of Al, Ba, Co, Pb, Ni and V in a tungsten-tube atomizer by a combined thermodynamic—kinetic approach. The atomizer is made from two profiled tungsten strips held in two copper supporting electrodes and forming a cylindrical cavity (5 mm long, 4 mm i.d.). Appearance temperatures and atomization energies are compared with those obtained for a graphite-tube atomizer. The major pathways leading to gaseous atoms are thermal dissociation of the metal oxide (or hydroxide) and reduction of the metal oxide followed by the atomization of free metal, depending on the protecting atmosphere (argon or argon—hydrogen mixture) and analyte.

Several papers in recent years have attempted to explain the mechanism of atom formation in graphite-based electrothermal atomizers. Campbell and Ottaway [1] used a purely thermodynamic approach for studying the atomization process; kinetic studies were made by Fuller [2, 3], and further contributions were reported by Torsi and Tessari [4, 5], Johnson et al. [6] and others. A combined thermodynamic—kinetic approach was used in a comprehensive study of the mechanism of atom formation in graphite furnaces by Sturgeon et al. [7].

The emphasis in research on metal-based electrothermal atomizers has so far been laid on their construction and analytical evaluation. Apart from the work of Aggett and Sprott [8], who compared appearance temperatures measured with carbon-filament and tantalum-filament atomizers and postulated that thermal dissociation processes on the metal surface are usually responsible for the formation of atomic vapor, there is practically no information on the mechanism of atom formation on metal-based atomizers. The work reported below was undertaken in an attempt to obtain some understanding of these processes. A simple tungsten-tube electrothermal

†Presented to the XX.C.S.I. and 7.I.C.A.S.(Symposium No. 3, Chlum u Třeboně), September, 1977, Czechoslovakia.

atomizer was used for this purpose; it can be accommodated in the Varian CRA-63 or -90 system and operated as an alternative to graphite tubes or cups.

## EXPERIMENTAL

### *Apparatus*

The tungsten-tube atomizer has already been described in detail [9]. All measurements were carried out with a Varian Model AA6 single-beam atomic absorption spectrometer. The absorbance signal was led to a six-channel storage oscilloscope (Tesla OPD 280 U, Czechoslovakia) directly from the recorder socket of the AA-6 indicating module. To prevent any distortion of the absorbance signal and to shorten the time constant of the detection system, all capacitors in the damping circuit were switched off. Slit widths, wavelengths and lamp currents suggested by the manufacturer were used.

The atomizer surface temperatures were measured with a sensitive photodiode (Tesla PP90, Czechoslovakia) placed over the atomizer. The signal from the photodiode was calibrated with an optical pyrometer and with Pt/Pt—Rh and Ir/W miniature thermocouples. To measure the temperature—time profile, the signal from the photodiode was led directly to the six-channel storage oscilloscope.

### *Reagents*

Specpure metals (Johnson-Matthey Ltd.) were used for preparation of the stock solutions of metal ions (1000 $\mu$g ml$^{-1}$). Solutions of Al, Ba, Co, Ni, and Pb were prepared as nitrates; Al, Ba and Ni were also prepared as chlorides, but vanadium was prepared as vanadyl sulphate. All working solutions were prepared immediately before use by dilution with twice-distilled deionized water and were acidified with the appropriate acid to a final concentration of 1% (v/v). The solutions were stored in polyethylene bottles.

### *Sampling*

Aliquots (1—5 $\mu$l) of the sample were placed in the center of the lower metal strip with an adjustable 5-$\mu$l syringe (Scientific Glass Engineering Pty. Ltd., Melbourne) equipped with a disposable Teflon tip.

### *Measurement of absorbance—time and temperature—time profiles and evaluation of the activation energy of atomization processes*

Absorbance—time and temperature—time profiles were measured simultaneously with a 6-channel storage oscilloscope. The absorbance signal was led to the first channel (sensitivity 0.025 absorbance per cm), the signal from the photodiode to the second channel (sensitivity 0.5—1 mV cm$^{-1}$, i.e. ca. 50—100°C cm$^{-1}$). Fast scan (25 ms cm$^{-1}$) was used. Both profiles were simultaneously photographed. From these traces and from the temperature calibration of the photodiode signal, plots of the logarithm of

the absorbance vs. the reciprocal of the absolute temperature were drawn for a range of 100—200 ms (depending on the element) beyond the appearance time, covering absorbance values less than 0.25. From the slope of such plots, the activation energy, $E_a$, of the atomization process was evaluated as described by Sturgeon et al.[7]. The $E_a$ data reported in this study are the average of at least five separate determinations. For each element, the mass of analyte chosen corresponded to 0.5 absorbance. Absorbance traces were obtained with the following temperature programme: dry, 100°C (10 s); ash, 400°C (20 s); atomize, 1500°C for Pb, 2100°C for Co, Mg, Ni, and 2400°C for Al, Ba, V. The ramp atomization mode (ramp rate of 500—800°C $s^{-1}$ depending on the element) was used in all cases.

## RESULTS AND DISCUSSION

### *Basic assumptions*

Because of the tubular design of the metallic atomizer, the model described by Sturgeon et al. [7] was used to study the mechanism of atom formation. This model assumes that an analyte surface—gas phase equilibrium exists within the tube and that the production of free atoms is characterized by a unimolecular rate constant. With these assumptions, which were satisfactorily confirmed for the graphite furnace, a plot of the logarithm of the absorbance as a function of the reciprocal absolute temperature yields a straight line with a slope of $-(E_a + \Delta H^0)/2.3\,R$, where $E_a$ is the activation energy of the limiting step in the atomization pathway, $\Delta H^0$ is the standard enthalpy change accompanying the phase transition, and $R$ is the gas constant. From the $E_a$ values, with the physicochemical properties, appearance temperature and thermodynamic data for the analyte, a reasonable mechanism for atom formation may be postulated.

Of course, the above assumptions for the graphite furnace may not be strictly valid for the atomizer used here. The rapid rate of the temperature increase and the very fast transient signals generated by the tungsten-tube atomizer, in addition to its relatively small size which gives a short residence time of analyte atoms in the optical path, may not allow adequate time for the physical and chemical processes to reach equilibrium before the atomic species have been lost. Despite this, the model was used in an attempt to obtain at least a rough picture about the atomization processes on the tungsten surface.

Sturgeon et al. [7] postulated three major possible atomization mechanisms for the graphite furnace: (1) carbon reduction of the metal oxide followed by atomization of the free metal, sometimes with the formation of dimeric species as an intermediate; (2) gas-phase or (3) solid-phase thermal dissociation of the metal oxide; (4) gas-phase thermal dissociation of the metal halide. The following equations explain the mechanisms:

$$\begin{array}{l} M_xO_y\ (s,l) + y\,C\ (s) \rightarrow x\,M\ (s,l) + y\,CO\ (g) \\ \qquad\qquad\qquad\qquad\quad \downarrow\uparrow \\ \qquad\qquad\qquad\qquad\quad x/2\ M_2\ (g) \rightarrow x\,M\ (g) \end{array} \qquad (1)$$

$$M_xO_y\ (s,l) \rightleftharpoons M_xO_y\ (g) \rightarrow xM\ (g) + yO\ (g) \quad (2)$$

$$M_xO_y\ (s,l) \rightleftharpoons xM\ (g) + yO\ (g) \quad (3)$$

$$MX_m\ (s,l) \rightleftharpoons MX_m\ (g) \rightarrow M\ (g) + mX\ (g) \quad (4)$$

where M is the analyte and X is a halide.

The main purpose of this study was to establish the validity of these mechanisms for the tungsten-tube atomizer, and particularly to see if the tungsten surface can act as a reducing agent for the analyte oxide. Thermodynamically, tungsten reduction of most analyte oxides at the temperatures employed should be the favored reaction ($\Delta G_r^0 < 0$):

$$3MO\ (s,l) + W\ (s) \rightarrow 3M\ (s,l,g) + WO_3\ (s,l,g) \quad (5)$$

However, it is reasonable to suppose, as did Aggett and Sprott [8] for a tantalum atomizer, that this reduction is not likely to occur or will be very slow, because tungsten trioxide forms a coherent stable film on the surface of the metal: $WO_3\ (s) \rightarrow WO_3\ (l)$ at 1743 K; $WO_3\ (l)$ decomposes at 2100 K. As the growth of the surface oxide ($WO_3$) proceeds by diffusion of the metal through the film to the surface [10], the diffusion rate will determine the rate of reduction. Provided that diffusion is slow in comparison with the atomization time of the analyte, thermal dissociation of the analyte oxide should be preferred.

In some experiments, reduction conditions within the atomizer were improved by introducing hydrogen (10% v/v) into the inert gas sheath. The reduction of the analyte oxide with hydrogen is thermodynamically very favorable for a number of metal oxides:

$$MO\ (s,l) + H_2\ (g) \rightarrow M\ (s,l,g) + H_2O\ (g) \quad (6)$$

It was expected that in some cases the addition of hydrogen to the protecting atmosphere would help to reduce the analyte oxide, and would change the atomization mechanism compared to that observed for the pure inert atmosphere. Atomization energies were therefore measured in pure argon as well as in the argon—hydrogen mixture.

Sturgeon et al. [7], in agreement with the findings of Johnson et al. [6], have shown that when the activation energy barrier to analyte vaporization is small, i.e., for sublimation and vaporization of metals or for small masses of analyte oxides where all the monoxide is transferred to the gas phase, there is a linear relationship between the atomization energy ($E_a$) and the appearance temperature ($T_a$) of the analyte. The slope of such a plot was found to be approximately 0.250 kJ $mol^{-1}$ $K^{-1}$. This relationship was shown to be useful for estimates of atom production. With a knowledge of the experimental appearance temperature of the analyte, a reasonable estimate of $E_a$ may be obtained. The $E_a$ value may then be correlated with that of some possible atomization process. Since it was also found that the correlation between the atomization energy and appearance temperature was

independent of the type of graphite atomizer used, it was considered [7] that this correlation might be quite universal. In order to check this suggestion for the tungsten atomizer, the experimental atomization energies were compared with those derived from the experimental appearance temperatures by using the "universal" $E_a$ vs. $T_a$ plot.

*Mechanisms of atom formation of the elements*

Table 1 presents the appearance temperatures for Al, Ba, Co, Ni, Pb and V measured in argon and argon—hydrogen atmospheres. There are substantial differences between the appearance temperatures measured in the different atmospheres for Al, Ba and V, which could indicate different mechanisms of atom formation. Table 1 also shows the appearance temperatures obtained with the original Varian CRA-63. These appearance temperatures compare well (except for Al) with those published by Sturgeon et al. [7] for a Perkin-Elmer graphite furnace.

Table 2 lists the $E_a$ values obtained experimentally for the elements atomized from aqueous solutions as well as the $E_a$ values derived from the experimental appearance temperatures by using the "universal" $E_a$ vs. $T_a$ plot for both the protecting atmospheres studied. Corresponding literature data for the energies of some possible atomization processes are also listed.

*Aluminium.* Two different experimental atomization energies were obtained for aluminium—794 and 640 kJ $mol^{-1}$ for the argon and argon—hydrogen atmospheres, respectively—regardless of whether the analyte was taken as nitrate or chloride. These energies could not be correlated with those of some possible atomization process. It seems reasonable to suppose that the vapour in equilibrium with $Al_2O_3$ (s,l) is a complex mixture of atomic and molecular species, e.g. Al, AlO, $Al_2O$, $Al_2O_2$, $O_2$, O, and in the case of the argon—hydrogen mixture also AlOH, AlH, $H_2$, H and OH. Thus more than one reaction is involved in the formation of Al (g) and none of them pre-

TABLE 1

Appearance temperatures for the tungsten-tube atomizer in argon and argon—hydrogen atmospheres

| Element[a] | Appearance temperature (K) | | |
|---|---|---|---|
| | Ar | Ar + $H_2$ | Graphite tube[b] |
| Al | 2200 | 1950 | 1850 |
| Ba | 2190 | 1775 | 2170 |
| Co | 1480 | 1530 | 1450 |
| Ni | 1430 | 1550 | 1540 |
| Pb | 1140 | 1165 | 980 |
| V | 2225 | 1850 | 2145 |

[a]Al, Ba and Ni were tested as nitrates and as chlorides, Co and Pb as nitrates, and V as sulphate.
[b]Varian CRA-63 with argon atmosphere.

TABLE 2

Atomization energies measured with tungsten-tube atomizer

| Element[a] | Atomization energy, $E_a$ (kJ mol$^{-1}$) | | |
|---|---|---|---|
| | Ar | Ar + $H_2$ | Literature values [7, 11][b] |
| Al | 794 (556)[c] | 640 (493) | Al (l) = 284; Al—O (de) = 485 |
| Ba | 795 (552) | 416 (447) | Ba (l) = 149; Ba—O (de) = 548<br>Ba—OH (de) = 460 |
| Co | 355 (376) | 399 (410) | Co (s) = 428; Co—O (de) = 368 |
| Ni | 235 (355) | 418 (405) | Ni (s) = 430; Ni—O (de) = 372<br>Ni—Ni = 231 |
| Pb | 393 (297) | 390 (305) | Pb (l) = 178; Pb—O (de) = 380 |
| V | 1091 (595) | 470 (481) | V (s) = 514; V—O (de) = 644 |

[a]See footnote (a), Table 1.
[b](s) denotes the heat of atomization of the element (298 K); (l) denotes the heat of vaporization of the element; (de) denotes the bond dissociation energy.
[c]Values in parentheses are atomization energies calculated from the "universal" plots of appearance temperature vs. $E_a$.

dominates. It can be concluded only qualitatively that in both the atmospheres studied thermal dissociation processes are responsible for the formation of aluminium atoms and that the presence of hydrogen lowers the energy necessary for atomization. The $E_a$ values calculated from the "universal" $E_a$ vs. $T_a$ plot are substantially lower than those found experimentally and give only qualitative evidence for thermal dissociation mechanisms (cf. [7]).

*Barium.* As can be seen from a typical $E_a$ plot in Fig. 1, two experimental atomization energies were found for barium—795 and 416 kJ mol$^{-1}$ for the argon and argon—hydrogen atmospheres, respectively—regardless of whether the nitrate or chloride was used. Oscilloscope traces of the corresponding absorbance—time and temperature—time profiles are shown in Fig. 2. The $E_a$ value of 795 kJ mol$^{-1}$ corresponds quite well to the negative heat of formation (756 kJ mol$^{-1}$) of BaO (s) at the appearance temperature, calculated for BaO (s) → Ba (g) + 1/2 $O_2$ (g) at 2200 K. This should indicate a solid-phase thermal dissociation process for barium in the argon atmosphere. However, the $E_a$ value of 552 kJ mol$^{-1}$ calculated from the "universal" $E_a$ vs. $T_a$ plot is in very good agreement with the bond dissociation energy of BaO (g), i.e. 548 kJ mol$^{-1}$, which indicates oxide dissociation in the gaseous phase. The only reasonable explanation for these observations is that in this case the mass of analyte used (25 ng) was too high for the atomizer and conditions used and all the BaO (s) had not vaporized. Thus the $E_a$ value found experimentally corresponds to the solid-phase dissociation mechanism, while the $E_a$ value obtained from the "universal" $E_a$ vs. $T_a$ plot (the validity of which assumes the activation energy barrier to analyte vaporization to be small, i.e. small analyte masses where all the monoxide is transferred to the

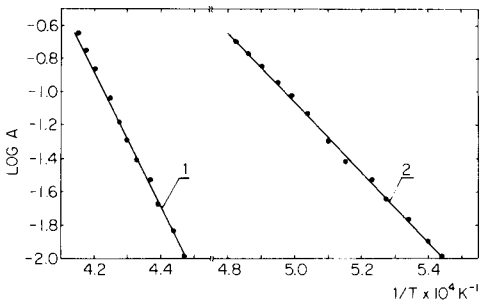


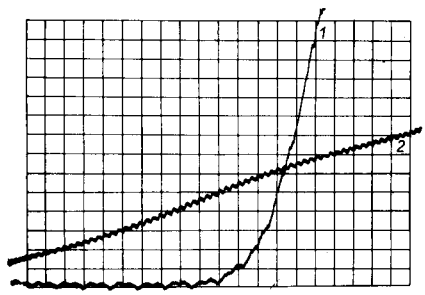


Fig. 1. $E_a$ plots for barium in the argon (1) and argon—hydrogen (2) atmospheres; $E_a$ (1) = 795 kJ mol$^{-1}$; $E_a$ (2) = 416 kJ mol$^{-1}$.

Fig. 2. Oscilloscope trace of absorbance—time (1) and temperature—time (2) profiles for barium in the argon—hydrogen atmosphere. Vertical scale, absorbance (0.025 per scale division) or temperature (100°C per scale division); horizontal scale, sweep speed (25 ms per scale division).

gas phase, and the appearance temperature to be independent of the analyte mass) predicts the oxide dissociation in the vapor phase.

In the argon—hydrogen atmosphere, both $E_a$ values obtained — 416 and 447 kJ mol$^{-1}$ — are, within experimental error, close to the bond dissociation energy of BaOH (460 kJ mol$^{-1}$), which seems to be the major supplier of gaseous atoms in this atmosphere.

*Cobalt.* $E_a$ values of 355 and 399 kJ mol$^{-1}$ were obtained experimentally for cobalt in the argon and argon—hydrogen atmospheres, respectively. These energies can be attributed to the bond dissociation energy of CoO (g) and to the heat of vaporization of solid cobalt, which have values of 368 and 428 kJ mol$^{-1}$, respectively. The experimental $E_a$ values are in good agreement with those predicted from the "universal" $E_a$ vs. $T_a$ plot. The proposed atomization mechanisms for cobalt are therefore vapor-phase thermal dissociation of CoO (g) after sublimation in the argon atmosphere, and reduction of CoO (s) with hydrogen and vaporization of solid cobalt in the argon—hydrogen atmosphere. The reduction of CoO (s) with hydrogen at the appearance temperature is thermodynamically very favourable.

In contrast to the reduction atomization mechanism postulated for the graphite surface [7] in the tungsten-tube atomizer with an argon atmosphere, the cobalt atoms result from thermal dissociation of the oxide.

*Nickel.* The atomization of nickel in the argon—hydrogen atmosphere proceeds in a manner similar to that for cobalt. For both the nitrate and chloride forms of nickel, the $E_a$ value measured was 418 kJ mol$^{-1}$ (predicted value, 405 kJ mol$^{-1}$). This may be rationalized as the heat of atomization of solid nickel (430 kJ mol$^{-1}$) after reduction of NiO (s) with hydrogen ($\Delta\ G_r^0$ at 1550 K $< 0$).

For atomization in the argon atmosphere, the energy of 355 kJ mol$^{-1}$ predicted from the $E_a$ vs. $T_a$ plot is in very good agreement with the bond

dissociation energy of NiO (g). The experimental $E_a$ value of 235 kJ $mol^{-1}$, which was verified several times, can only be interpreted as the Ni—Ni bond energy, the value of which is 231 kJ $mol^{-1}$. However, there is no reasonable explanation for the existence of dimeric species in this case under the conditions used.

*Lead.* Two nearly identical experimental $E_a$ values (393 and 390 kJ $mol^{-1}$) were obtained for lead in the two atmospheres investigated. These values indicate that the gaseous lead atoms arise from thermal dissociation of PbO (g) after its sublimation, and that reduction reactions with tungsten or hydrogen do not play a role in the formation of atoms. The $E_a$ values obtained from the "universal" $E_a$ vs. $T_a$ plot were significantly lower than those obtained experimentally. This may indicate an exception in the validity of this plot.

*Vanadium.* The $E_a$ value of 1091 kJ $mol^{-1}$ found experimentally in the argon atmosphere can be rationalized as the sum of the energies of the negative heat of formation of $V_2O_3$ (s) at 2200 K and the heat of vaporization of V (l), which is approximately 1085 kJ $mol^{-1}$. This excellent agreement suggests a solid-phase dissociation mechanism followed by vaporization of liquid vanadium in the pure inert gas atmosphere. The predicted $E_a$ value corresponds well to the bond dissociation energy of VO (g) and indicates a gas-phase dissociation. This discrepancy between the two $E_a$ values can be explained in the same way as for barium, i.e. that too much analyte was used in the measurement. The measured and predicted $E_a$ values for the argon—hydrogen atmosphere are in good mutual agreement and correspond quite well to the heat of atomization of V (s). A reasonable interpretation of these results involves a reduction mechanism, i.e. reduction of $V_2O_5$ (s) with hydrogen, which is thermodynamically feasible at 1850 K, followed by vaporization of the metal.

*Conclusions*

The results presented, despite their semiquantitative nature, support the expected mechanisms of atom formation in the tungsten-tube electrothermal atomizer, i.e. thermal dissociation of analyte species without intervention of reduction reactions of the analyte oxide with the metal of the atomizer. The addition of hydrogen to the argon protective atmosphere can sometimes change significantly the mechanism of atom formation compared to experiments in pure argon, because of reduction processes.

The "universal" $E_a$ vs. $T_a$ plots proved satisfactory in most cases as a means of predicting the possible atomization pathway at the tungsten surface, but more work is required for generalization of some of the results presented. The behaviour of other elements on other metallic surfaces will be reported later.

REFERENCES

1 W. C. Campbell and J. M. Ottaway, Talanta, 21 (1974) 837.
2 C. W. Fuller, Analyst, 99 (1974) 739.
3 C. W. Fuller, Analyst, 100 (1975) 229.
4 G. Torsi and G. Tessari, Anal. Chem., 47 (1975) 839.
5 G. Tessari and G. Torsi, Anal. Chem., 47 (1975) 842.
6 D. C. Johnson, B. L. Sharp, T. S. West and R. M. Dagnall, Anal. Chem., 47 (1975) 1234.
7 R. E. Sturgeon, C. L. Chakrabarti and C. H. Langford, Anal. Chem., 48 (1976) 1972.
8 J. Aggett and A. J. Sprott, Anal. Chim. Acta, 72 (1974) 49.
9 V. Sychra, D. Kolihová, O. Vyskočilová, R. Hlaváč and P. Püschel, Anal. Chim. Acta, 105 (1979) 263.
10 F. T. Sisco and E. Epremian, Columbium and Tantalum, J. Wiley, New York, 1963, p. 339.
11 R. C. Weast (Ed.), Handbook of Chemistry and Physics, 55th edn., Chemical Rubber Co., Cleveland, Ohio, 1975.

*Analytica Chimica Acta*, 105 (1979) 281—287


# CALCULATION OF THE OPTIMAL EXPERIMENTAL CONDITIONS FOR LIQUID—LIQUID EXTRACTIONS WITH DIETHYLDITHIOCARBAMIC ACID

SIXTO BAJO

*Swiss Federal Institute for Reactor Research, 5303 Würenlingen (Switzerland)*

(Received 17th July 1978)

SUMMARY

A simple mathematical treatment of the liquid—liquid extraction of metals with diethyldithiocarbamic acid is given. The expressions derived can be applied directly in practical work and have been checked against experiments with some metals. The metal extraction constants for the carbon tetrachloride—water and chloroform—water systems are listed.

Liquid—liquid extraction is a well-established separation technique. One of the best-known extraction agents is diethyldithiocarbamic acid (HDDC). Several hundred papers have been published in the last decade describing the experimental aspects of its application to the extraction of various metal ions. As the extraction constants for the chloroform—water and carbon tetrachloride—water systems are well known for a number of metals, it becomes possible to estimate mathematically the optimal conditions which will be required for the quantitative separation of the ions in a mixture.

This paper, which was partly inspired by the work of Ringbom [1], shows the derivation of some simple, mathematical expressions which will make it possible to calculate the experimental parameters required for a specific separation. The derivation is valid only for the extraction of metals, and considers only the influence of the $\alpha$-value (Ringbom—Schwarzenbach coefficient or side-reaction coefficient) and the distribution of diethyldithiocarbamate between the phases.

The HDDC constants and the extraction constants for various different metal ions are given in Tables 1 and 2, respectively. Information concerning the extraction of mixed complexes (i.e. complex of the metal, DDC and another anion) such as PdCl(DDC) [20], HgCl(DDC) [22], $AuCl_2$(DDC) [23], $AuCl(DDC)_2$ [24], $SbI_2$(DDC) and $SbI(DDC)_2$ [25], $AsI_2$(DDC) and $AsI(DDC)_2$ [26] can be found in the references cited.

TABLE 1

Literature values for the acidity constant, $K_a$, and distribution constant, $K_D$, of diethyldithiocarbamic acid

| log $K_a$ [a] | log $K_D$ [b] | |
|---|---|---|
| | $CCl_4/H_2O$ | $CHCl_3/H_2O$ |
| −3.95 [2] | 2.62 [5, 7] | 3.62 [9] |
| −3.39 [3] | 2.39 [8] | 3.37 [8] |
| −3.38 [4] | | |
| −3.6 [5] | | |
| −3.35 [6] | | |

[a]Defined in eqn. (7).
[b]Defined in eqn. (6).

TABLE 2

Literature values of the extraction constant, $K_{ex}$, and the two-phase stability constant, $\beta_{n,o}$, for the diethyldithiocarbamate complexes of different metal ions. For the same organic solvent, $K_{ex}$ and $\beta_{n,o}$ are related by the equation: $\beta_{n,o} = K_{ex}\ (K_D/K_a)^n$

| Ion | log $K_{ex}$ [a] | | log $\beta_{n,o}$ [b] | |
|---|---|---|---|---|
| | $CCl_4/H_2O$ | $CHCl_3/H_2O$ | $CCl_4/H_2O$ | $CHCl_3/H_2O$ |
| Ag(I) | 11.52[10], 11.90[11], 11.9[12] | | 18.11[11] | 19.3[5] |
| Bi(III) | 16.79[11], 16.8[12], 16.48[13] | 15.9[15], 15.7[16] | 35.42[11], 35.20[21] | 36.52[21] |
| Cd(II) | 5.41[11], 5.8[12], 5.13[13] 5.81[14], 5.94[14] | 5.4[15], 5.50[16] 5.6[17], 5.77[18] | 17.83[11], 18.68[21] | 17.8[5], 18 |
| Co(II) | 2.33[11] | | 14.75[11], 18.53[21] | 19.76[21] |
| Cu(II) | 13.70[11], 14.0[12], 14.1[13] | 13.0[15], 12.81[16] | 26.12[11], 26.76[21] | 26.7[5], 27 |
| Fe(II) | 1.24[11] | | 13.46[11] | |
| H(I) | | | 6.21[7], 6.21[11] | 7.0[19] |
| Hg(II) | 32.12[11], 30[12], 29.1[13] | 26.92[16] | 44.56[11] | |
| In(III) | 10.34[11], 12[12], 9.59[13] | 9.9[15], 9.95[16] | 28.97[11] | |
| Mn(II) | −4.42[11] | | 8.00[11], 10.23[21] | 10.48[21] |
| Ni(II) | 11.58[11] | | 24.00[11], 18.30[21] | 19.00[21] |
| Pb(II) | 7.77[11], 8.0[12], 5.74[13], 8.07[14], 8.19[14] | 7.0[15], 5.0[16], 7.94[18] | 20.19[11], 20.80[21] | 20.4[5], 21 |
| Pd(II) | >32[11], >29[13] | | | 69.8[20] |
| Tl(I) | −0.53[11], −1.0[12], 0.03[13] | | 5.68[11] | 6.7[19] |
| Zn(II) | 2.54[10], 2.96[11], 2.8[12], 2.85[14] | 2.2[15], 2.3[16], 2.39[18] | 15.38[11], 15.40[21] | 16.3[5], 15 |

[a]Defined in eqn. (2).
[b]$\beta_{n,o} = [M(DDC)_n]_{wo}/[M][DDC]^n_w$.

EXTRACTION OF A METAL

The liquid—liquid extraction of a metal ion, M (ionic charges are omitted in order to simplify the formulation), from an aqueous solution by diethyldithiocarbamic acid, HDDC, into an organic solvent can be described by the equation

$$M_w + n\{HDDC\}_o \rightleftharpoons \{M(DDC)_n\}_o + n\ H_w \qquad (1)$$

wherein $n$ is a coefficient dependent on the charge of the metal ion and o indicates the organic phase.
The extraction constant, $K_{ex}$, for this reaction is given by:

$$K_{ex} = [M(DDC)_n]_o [H]_w^n / [M]_w [HDDC]_o^n \quad (2)$$

where w denotes the aqueous phase.
The Ringbom—Schwarzenbach coefficient, $\alpha_M$, of the metal is given [1, 27] by $\alpha_M = [M']/[M]_w$, where M′ represents all species, except $M(DDC)_n$, which contain the metal. The distribution ratio, $D_c$, of the metal between the two phases is defined by $D_c = [M(DDC)_n]_o/[M']_w$, and the extracted fraction, $F$, of the metal M is

$$F = [M(DDC)_n]_o V_o / ([M(DDC)_n]_o V_o + [M']_w V_w) \quad (3)$$

where $V_w$ and $V_o$ represent the volumes of the aqueous and the organic phases, respectively.

Thus, eqn. (2) can be transformed to

$$K_{ex} = \frac{F}{(1-F)R} \frac{[H]_w^n}{[HDDC]_o^n} \alpha_M \quad (4)$$

with $R = V_o/V_w$. After normalization of the metal content of the system, $[M(DDC)_n]_o V_o + [M']_w V_w = 1$. If the diethyldithiocarbamate is introduced into the system via the organic phase with an initial molarity, $C_{HDDC}$, then

$$V_o C_{HDDC} = [HDDC]_o V_o + [HDDC]_w V_w + [DDC]_w V_w \quad (5)$$

assuming that $V_o C_{HDDC}$ is very large in comparison with the total amount of M.

The distribution constant of diethyldithiocarbamate between the two phases is given by

$$K_D = [HDDC]_o/[HDDC]_w \quad (6)$$

and

$$K_a = [DDC]_w [H]_w/[HDDC]_w \quad (7)$$

where $K_a$(HDDC) is the acidity constant. Combining eqns. (5—7) yields

$$[HDDC]_o = C_{HDDC} \Big/ \left\{1 + \frac{1}{RK_D}\left(1 + \frac{K_a}{[H]_w}\right)\right\} \quad (8)$$

Substitution of eqn. (8) into eqn. (4) leads to

$$\frac{1}{F} = 1 + J\alpha_M / C_{HDDC}^n K_{ex} \quad (9)$$

wherein

$$J = \left\{1 + \frac{1}{RK_D}\left(1 + \frac{K_a}{[H]_w}\right)\right\}^n \frac{[H]_w^n}{R}$$

Figure 1 shows the values of $J$ as a function of $[H]_w$ (pH = 0, 1, 2, . . . ,12) at different values of $R$ ($R$ = 1, 0.5, 0.3 and 0.1) and $n$ ($n$ = 1, 2, 3 and 4) for the chloroform—water system. The values log $K_a$ = —3.35 and log $K_D$ = 3.37 were taken from Table 1. When the values of $\alpha_M$ and $K_{ex}$ are known, then $F$ is readily found by means of eqn. (9).

*Estimation of* $\alpha_M$

The $\alpha_M$ coefficient takes into account the reactions between M and the other ions in the system (buffer, complexing agents, etc.) as well as any complexes other than $M(DDC)_n$ which are formed between M and DDC. Thus $\alpha_M$ is defined as

$$\alpha_M = \alpha_{M(A)} + \alpha_{M(B)} + \alpha_{M(C)} + \cdots + \alpha_{M(j-1)} \quad (10)$$

where A, B, C, . . . are the $j$ different ligands which react with M. Each coefficient of the type $\alpha_{M(A)}$ can be taken from the list given by Ringbom [1] or calculated by the method of Ringbom and Still [28]:

$$\alpha_{M(A)} = 1 + \sum_{i=1}^{x} [A]^i \beta_i \quad (11)$$

where $\beta_i$ is the cumulative dissociation constant of $MA_i$.

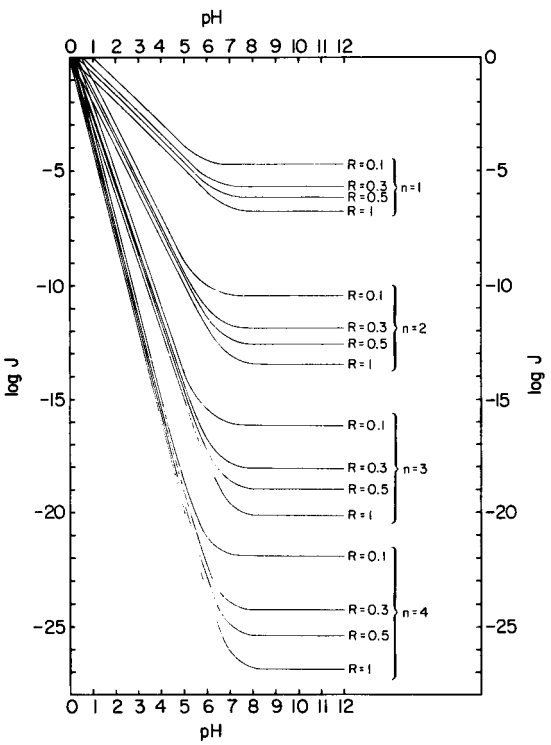


Fig. 1. Values for $J$ as a function of pH at different values of parameters $n$ and $R$ for the $CHCl_3$—$H_2O$ system.

It is particularly interesting to know the $\alpha_M$ value for quantitative extraction of M, i.e. $F \geqslant 0.999$, and for quantitative retention of M in the aqueous phase, i.e. $F \leqslant 0.001$. Applying eqn. (9) gives $\alpha_M \leqslant (K_{ex}C^n_{HDDC}/J) \times 10^{-3}$ with $F \geqslant 0.999$, and $\alpha_M \geqslant (K_{ex}C^n_{HDDC}/J) \times 10^3$ with $F \leqslant 0.001$.

## DISTRIBUTION OF DIETHYLDITHIOCARBAMATE BETWEEN THE PHASES

If the total amount of diethyldithiocarbamate in the system is taken as unity, then

$$[HDDC]_o V_o + [HDDC]_w V_w + [DDC]_w V_w = 1 \quad (12)$$

and from eqns. (6) and (7) it can be seen that the fractions of the species $[HDDC]_o$, $[HDDC]_w$ and $[DDC]_w$ are:

$F_{[HDDC]_o} = RK_D\,[H]_w/E$; $F_{[HDDC]_w} = [H]_w/E$, and $F_{[DDC]_w} = K_a/E$

where $E = (RK_D + 1)\,[H]_w + K_a$ (13)

Equation (13) allows three acidity ranges to be defined:

(a) $[H]_w \geqslant 100 \cdot K_a/(RK_D + 1)$ (14)

for which $F_{[HDDC]_o} = RK_D/(RK_D + 1)$, $F_{[HDDC]_w} = 1/(RK_D + 1)$, and $F_{[DDC]_w} = K_a/(RK_D + 1)[H]_w$. Practically all of the diethyldithiocarbamate is in the organic phase ($F_{[HDDC]_o} \geqslant 0.99$).

(b) $[H]_w \leqslant K_a/100\,(RK_D + 1)$ (15)

for which $F_{[HDDC]_o} = RK_D\,[H]_w/K_a$, $F_{[HDDC]_w} = [H]_w/K_a$, and $F_{[DDC]_w} = 1$. Practically all of the diethyldithiocarbamate is then in the aqueous phase ($F_{DDC} = 1$).

(c) $[H]_w = K_a/(RK_D + 1)$ (16)

for which $F_{[HDDC]_o} = RK_D\,[H]_w/2K_a$, $F_{[HDDC]_w} = [H]_w/2K_a$, and $F_{[DDC]_w} = 1/2$. The diethyldithiocarbamate is thus distributed between the two phases. Table 3 gives the acidity limits for the preferential ($\geqslant 99\%$) concentration of diethyldithiocarbamate in one of the phases as a function of $R$ for the chloroform—water system. The same constants as in Fig. 1 were used.

In eqn. (9), $C_{HDDC}$ is the initial molarity of HDDC in the organic phase. If the diethyldithiocarbamate is originally in the aqueous phase, $C_{HDDC}$ must be calculated from the volume of the organic phase. It is preferable to start with a solution of HDDC in chloroform, especially if the extraction is to be made from an acidic solution. Diethyldithiocarbamate decomposes rapidly in such a medium [3].

The $\alpha_M$ value may be calculated or taken from the literature (see above). If the aqueous solution of the metal which is to be extracted does not contain any complexing agents, e.g. a perchloric acid solution, and if the pH is low enough to avoid the formation of metal—hydroxy complexes, then $\alpha_M = 1$, which simplifies the application of eqn. (9).

TABLE 3

pH Limits for the retention of (HDDC, DDC) in a single phase system ($CHCl_3$—$H_2O$)

| $R$ | $F_{[HDDC]_o} \geq 0.99$[a] | $F_{[DDC]_w} \geq 0.99$[b] |
|---|---|---|
| 1.0 | ≤4.72 | ≥8.72 |
| 0.5 | ≤4.42 | ≥8.42 |
| 0.3 | ≤4.20 | ≥8.20 |
| 0.1 | ≤3.72 | ≥7.72 |

[a]Calculated from eqn. (14).
[b]Calculated from eqn. (15).

## EXPERIMENTAL

### *Preparation of a solution of HDDC in chloroform*

To prepare a solution of HDDC in chloroform, shake equal volumes of $Zn(DDC)_2$ in chloroform and 2M HCl together for 30 s in a separatory funnel. Let the mixture stand for 1 min and then drain the organic phase into another separatory funnel which contains the aqueous phase to be extracted. Perform the extraction immediately.

The molarity of the solution of HDDC is twice that of the $Zn(DDC)_2$ solution which was used to prepare it (see eqn. 1). Solutions of HDDC in chloroform cannot be stored and must therefore be prepared immediately before use [18]. The $Zn(DDC)_2$ can be replaced by $Cd(DDC)_2$ or $Pb(DDC)_2$. Solutions of $Zn(DDC)_2$ and $Cd(DDC)_2$ in chloroform can be stored for at least 40 days with no change in the titer [18]. The same is probably true for solutions of $Pb(DDC)_2$ in chloroform. The method for preparation of $Zn(DDC)_2$, $Cd(DDC)_2$ and $Pb(DDC)_2$ has been described [29].

### *Extraction of metal ions*

The validity of eqn. (9) was checked by extracting ions (100 $\mu$g) labelled with appropriate $\gamma$-emitting isotopes in diluted perchloric acid (100 ml). The organic phase (30 ml) was $3.4 \times 10^{-3}$ M HDDC in chloroform. Extractions were carried out in 250-ml separatory funnels on a shaking machine with an amplitude of 6 cm and a frequency of 6.6 $s^{-1}$. The results are given in Table 4. Shaking time was 2 min (Zn, Cd) or 10 min (In, Mn). The values of log $K_{ex}$ used were 2.39 (Zn), 5.77 (Cd), 9.95 (In) and −3.5 (Mn); the last value has only been estimated [21]. The value of $\alpha_M = 1$ was assumed in all cases. Agreement between calculated and measured results is good.

The author is indebted to Dr. Thomas Campbell (Institute for Analytical Chemistry, University of Vienna, Austria) and Mr. Paul Barroyer (Swiss Federal Institute for Reactor Research, Würenlingen, Switzerland) for helpful discussion.

TABLE 4

Liquid—liquid extraction of some metal ions with HDDC at different pH values of the aqueous phase ($F$ is given in per cent)

| pH | Zn(II) | | Cd(II) | | In(III) | | Mn(II) | |
|---|---|---|---|---|---|---|---|---|
| | $F$ calc. | $F$ found | $F$ calc. | $F$ found | $F$ calc. | $F$ found | $F$ calc. | $F$ found |
| 0.0 | 0.09 | 0.08 | 67.2 | 56.4 | 99.0 | 99.9 | 0.00 | <0.02 |
| 1.0 | 7.9 | 9.2 | 99.5 | 98.9 | >99.9 | 99.9 | 0.00 | <0.02 |
| 2.0 | 89.5 | 92.8 | >99.9 | 99.9 | >99.9 | 99.9 | 0.00 | 0.03 |
| 3.0 | 99.9 | 99.9 | >99.9 | 99.9 | >99.9 | 99.9 | 0.11 | 0.12 |

REFERENCES


1 A. Ringbom, Complexation in Analytical Chemistry, Interscience, New York, 1963, pp. 38, 259, 352 et seq.
2 R. Zahradnik and P. Zuman, Collect. Czech. Chem. Commun., 24 (1959) 1132.
3 S. J. Joris, K. I. Aspila and C. L. Chakrabarti, Anal. Chem., 41 (1969) 1441.
4 K. I. Aspila, C. L. Chakrabarti and V. S. Sastri, Anal. Chem., 45 (1973) 363.
5 E. Still, Suom. Kemistiseuran. Tied., 73 (1964) 90.
6 H. Bode and K. J. Tusche, Fresenius Z. Anal. Chem., 157 (1957) 414.
7 H. Bode, Fresenius Z. Anal. Chem., 142 (1954) 414.
8 H. Bode and F. Neumann, Fresenius Z. Anal. Chem., 169 (1959) 410.
9 K. I. Aspila, C. L. Chakrabarti and V. S. Sastri, Anal. Chem., 47 (1975) 945.
10 J. Růžička and J. Stary, Talanta, 14 (1967) 909.
11 J. Stary and K. Kratzer, Anal. Chim. Acta, 40 (1968) 93.
12 J. Stary and R. Burcl, Radiochem. Radioanal. Lett., 7 (1971) 235.
13 J. Stary and J. Růžička, Talanta, 15 (1968) 505.
14 Yu. A. Zolotov, I. P. Alimarin and B. Ya. Spivakov, Bull. Acad. Sci. USSR, Div. Chem. Sci. (English translation), 3 (1969) 516.
15 P. C. A. Ooms, U. A. Th. Brinkman and H. A. Das, Report ECN-77-018, Stichtung Energieonderzoek Centrum Nederland, Petten (Netherlands), 1976.
16 P. C. A. Ooms, U. A. Th. Brinkman and H. A. Das, Radiochem. Radioanal. Lett., 31 (1977) 317.
17 S. Bajo and A. Wyttenbach, Anal. Chem., 49 (1977) 158.
18 S. Bajo and A. Wyttenbach, Anal. Chem., in press.
19 K. Vadasdi, P. Buxbaum and A. Salamon, Anal. Chem., 43 (1971) 318.
20 G. B. Briscoe and S. Humphries, Talanta, 16 (1969) 1403.
21 Yu. I. Usatenko, V. S. Barkalov and F. M. Tulyupa, Zh. Anal. Khim., 25 (1970) 1458.
22 A. Wyttenbach and S. Bajo, Helv. Chim. Acta, 56 (1973) 1198.
23 H. Chermette, J. F. Colonat and J. Tousset, Anal. Chim. Acta, 80 (1975) 335.
24 H. Chermette, J. F. Colonat and J. Tousset, Anal. Chim. Acta, 88 (1977) 331.
25 T. Bouda and J. Stary, Radiochem. Radioanal. Lett., 22 (1975) 25.
26 J. Stary and J. Prasilova, Radiochem. Radioanal. Lett., 18 (1974) 99.
27 A. Ringbom, J. Chem. Educ., 35 (1958) 282.
28 A. Ringbom and E. Still, Anal. Chim. Acta, 59 (1972) 143.
29 A. Wyttenbach and S. Bajo, Anal. Chem., 47 (1975) 1813.

*Analytica Chimica Acta*, 105 (1979) 289—295


# DUAL-WAVELENGTH SPECTROPHOTOMETRIC DETERMINATION OF TRACES OF MERCURY(II) WITH SOLUBILIZED DITHIZONE: AN APPROACH TO SIMPLIFIED ANALYTICAL PROCEDURES FOR ENVIRONMENTAL POLLUTANTS†

KEIHEI UENO*, KAYOKO SHIRAISHI, TŌRU TŌGŌ, TAIROKU YANO**, ISAO YOSHIDA*** and HIROSHI KOBAYASHI§

*Department of Organic Synthesis, Faculty of Engineering, Kyushu University, Fukuoka 812 (Japan)*

(Received 4th July 1978)

SUMMARY

A simple spectrophotometric procedure is described for the determination of traces of mercury, with solubilized copper(II) dithizonate. Sample water containing 0.05 — 0.25 μg of mercury(II) is mixed with an aqueous solution of copper dithizonate containing Triton X-100 at pH 1 ($H_2SO_4$). After 5 min, dual-wavelength photometry is used to measure the difference in absorbances at 507 and 493 nm, which is proportional to the mercury concentration. The advantages are that no reagent blank is necessary and the equipment is simple. Few cations interfere; silver(I) and iron(III) can be masked by chloride and fluoride, respectively.

Simplified procedures for field analyses of environmental pollutants without sophisticated instruments are in great demand for routine checks on the environment. This paper reports an approach to simplified procedures for the determination of traces of mercury(II) in aquatic samples.

Mercury(II) ion is usually determined by flameless atomic absorption spectrometry with or without preconcentration. Though this procedure is highly sensitive and free from interferences, the instruments are expensive and have to be operated in laboratories by trained technicians. Simplified field analytical procedures require minimum manipulations of samples and reagents, and simple instruments that can be operated by untrained personnel.

As an example of the development of systems to fulfil these requirements, a spectrophotometric determination of mercury(II) with dithizone was investigated with a dual-wavelength spectrophotometer [1]. The main advantages of this instrument are that the reagent blank is compensated automatically

†Contribution No. 499 from the Department of Organic Synthesis, Kyushu University.

**Present Address: Yamaguchi Prefectural Consultants Center for Commerce and Industry, Yugaki, Asada, Yamaguchi 753, Japan.

***Present Address: Department of Industrial Chemistry, Kumamoto Institute of Technology Ikeda-machi, Kumamoto 862, Japan.

§ Present Address: Research Institute for Industrial Sciences, Kyushu University.

without need for blank solutions, and no reference cell is needed. Another simplifying device is to eliminate the solvent extraction process in the dithizone method by solubilizing dithizone and metal dithizonates in water with nonionic surfactants such as Triton X-100 [2].

Although the final goal of this investigation is to construct a filter-type dual-wavelength photometer for the mercury determination, this paper reports the fundamental information needed to construct such an instrument, as well as the recommended analytical procedure based on this principle.

## EXPERIMENTAL

### *Reagents*

*Standard mercury(II) solution (500 ppm).* A weighed amount of mercury(II) nitrate was dissolved in 0.05 M sulfuric acid, and the concentration was determined by EDTA titration (pH 6, xylenol orange). The solution was diluted to the desired concentration just before use.

*Dithizone and metal dithizonates.* Dithizone ($H_2Dz$) was purified as described by Sandell [3]. Zinc and copper dithizonates, $M(HDz)_2$, were prepared by shaking the dithizone solution in chloroform with a slight excess of the metal ion in aqueous solution, followed by treatment with dilute aqueous ammonia (1:100) to remove unreacted dithizone, and then evaporation of solvent to obtain the metal dithizonate.

*Dithizone—Triton X-100 solution.* Purified dithizone (10 mg) was triturated in an agate mortar with a small portion of aqueous 20% (w/v) Triton X-100 solution and diluted to 100 ml with the same solvent.

*Metal dithizonate—Triton X-100 solution.* About 5 mg of zinc or copper dithizonate was treated with 20% Triton X-100 solution in a similar manner as above. The resulting solution was filtered through a membrane filter (Sartorius, pore size 0.45 $\mu$m) to obtain transparent solutions. All other reagents were of analytical grade.

### *Instrument*

A Hitachi Model 556 Dual-wavelength Spectrophotometer equipped with a 10-mm quartz cell was used.

### *Analytical procedure*

Place the sample water containing 0.05—0.25 $\mu$g of mercury(II) in a 25-ml volumetric flask, to which add 5 ml of 0.5 M sulfuric acid and 5 ml of copper dithizonate—Triton X-100 solution. Dilute to volume with water. After 5 min observe the absorbance difference at $\lambda_1$ = 507 nm and $\lambda_2$ = 493 nm, using a 1-cm standard cell.

If interference by silver(I) or iron(III) is expected, add 0.1 ml of 0.1 M HCl or 3 drops of 50% HF, respectively.

## RESULTS AND DISCUSSION

*Dual-wavelength absorption photometry*

As described previously [1], reagent blanks can easily be compensated by this technique, without the use of a reference cell. This advantage is very appropriate for simplified analytical procedures, because only sample and standard solutions and a single cell are needed.

*Selection of the reagent for mercury(II)*

Dithizone is well known as a very selective and sensitive reagent for mercury(II). The only other cations which react with dithizone at pH 1 are copper(II), silver(I) and bismuth(III). It is one of the very few reagents which give highly colored complexes ($\epsilon = 4—5 \times 10^4$ l mol$^{-1}$ cm$^{-1}$) with mercury(II) at pH 1 [3]. It does, however, have several disadvantages. It is very sensitive to air oxidation, deteriorates easily and decolorizes as the solid or in solutions. The absorption spectrum of free dithizone overlaps considerably with those of metal dithizonates, so that laborious photometric procedures are necessary to compensate the reagent blank. Furthermore, as the reagent and the metal complexes are not soluble in water, solvent extraction processes are normally used.

In the present investigation, the instability of the reagent was overcome by stabilizing it as zinc or copper dithizonate. The water insolubility of dithizone and metal dithizonates was overcome by solubilizing them with the aid of the non-ionic surfactant Triton X-100. The hydrophobic dithizone and metal dithizonates are converted to the non-ionic micelle, so that transparent aqueous solutions of dithizone and metal dithizonates are obtained. By these improvements, dithizone can be kept stable in aqueous solutions, and the color reactions of dithizone with metal ions can be observed in the aqueous solution.

*Dual-wavelength photometric approaches for mercury(II)*

Several photometric approaches are possible for the dual-wavelength photometric determination of traces of mercury(II) with the solubilized dithizone or metal dithizonates.

The first approach is the dual-wavelength photometry of mercury(II) dithizonate in the presence of free dithizone. When the stabilized zinc dithizonate solution is mixed with the sample water containing mercury(II) at pH 1, the reactions will proceed as follows:

$$Zn(HDz)_2 + 2H^+ \rightleftharpoons 2H_2Dz + Zn^{2+}$$

$$2H_2Dz + Hg^{2+} \rightleftharpoons Hg(HDz)_2 + 2H^+$$

where $H_2Dz$ represents the free dithizone. In this case, dithizone is freed in situ from the zinc complex at pH 1, eventually reacting with mercury(II). In this pH region, the freed zinc does not interfere with the mercury determina-

tion. Thus, the photometry of mercury dithizonate is conducted in the presence of excess of dithizone, as in the conventional photometry with dithizone. From the absorption spectra of dithizone and mercury dithizonate (Fig. 1), the dual-wavelengths can be chosen at 510 and 663.6 nm to compensate the absorption of the free dithizone. The absorbance difference, $\Delta A$ ($= A_{510} - A_{663.6}$) is proportional to the mercury concentration; an example of a calibration line is also shown in Fig. 1.

However, the absorption spectrum of free dithizone changes rapidly because of oxidative decomposition (Fig. 2). Therefore, it is necessary to choose the $\lambda_2$ value depending on the quality of the dithizone. Although dithizone is stabilized as zinc dithizonate, it is still necessary to choose an optimum $\lambda_2$ value every time because free dithizone is so unstable that the spectral curve may change markedly during the analytical procedure.

The second approach was the dual-wavelength photometry of mercury dithizonate after the complete oxidation of free dithizone. In this procedure, the solubilized dithizone reagent was reacted with mercury(II) at pH 1, and

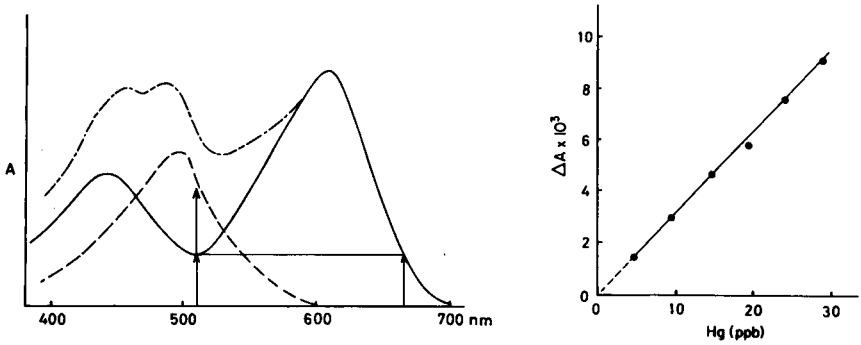


Fig. 1. Absorption spectra of dithizone and mercury(II) dithizonate, $Hg(HDz)_2$, in aqueous Triton X-100 solution at pH 1. (—) Dithizone; (---) mercury dithizonate; (·--) mixture. The calibration line for $\lambda_1$ = 510 nm, $\lambda_2$ = 663.6 nm is also shown.

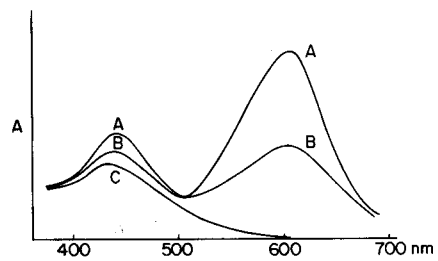


Fig. 2. Spectral change of dithizone during oxidation with $H_2O_2$ at pH 1. (A) Pure dithizone; (B) intermediate oxidation state; (C) final oxidation state.

then the excess of unreacted dithizone was oxidized with 6% hydrogen peroxide at room temperature. Figure 3 shows the change of absorbances of free dithizone at 420 nm and of mercury dithizonate at 495 nm during the oxidation process. The absorbance of mercury dithizonate remained unchanged after about 10 min, whereas that of dithizone decreased and approached a constant value after 90 min. The final absorption spectra of both components after oxidation are shown in Fig. 4, and these did not change over the period 90—150 min. Thus, in this procedure, the mercury dithizonate is determined in the presence of the oxidation product of dithizone, where the dual wavelengths can be chosen at $\lambda_1 = 367 \pm 8$ nm and $\lambda_2 = 467 \pm 8$ nm as indicated in Fig. 4, and be fixed at these values regardless of the quality of the dithizone.

In a typical procedure, the sample water was mixed with the solubilized dithizone reagent at pH 1, to which 30% hydrogen peroxide was added to give a final concentration of 6%; then the mixture was left at room temperature in a dark room for 2 h, and finally subjected to photometry. The sensitivity of this method is almost the same as that of the first one, but it has a major advantage that the dual wavelengths can be fixed. However, the procedure is still inconvenient as a simplified method, because more than one hour is needed for the complete oxidation of free dithizone.

The third approach was to apply dual-wavelength photometry to the mercury dithizonate after the exchange reaction of copper(II) dithizonate with mercury(II) ion at pH 1. When the solubilized copper dithizonate is mixed with mercury(II), the exchange reaction proceeds readily

$$Cu(HDz)_2 + Hg^{2+} \rightleftharpoons Hg(HDz)_2 + Cu^{2+}$$

because the conditional stability constant of the mercury(II) complex seems

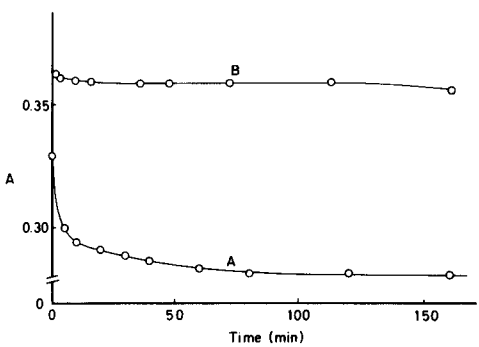


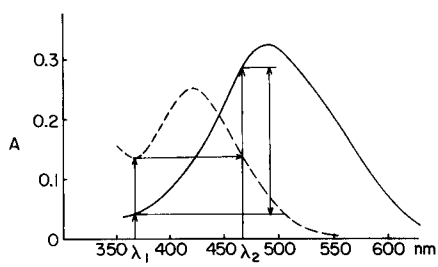


Fig. 3. Change of absorbances of dithizone and mercury dithizonate during oxidation at pH 1. (A) Dithizone (at 420 nm); (B) mercury dithizonate (at 495 nm).

Fig. 4. Selection of dual wavelengths for the determination of mercury dithizonate in the presence of oxidized dithizone. (—) Mercury dithizonate; (---) oxidized dithizone.

to be much higher than that of the copper complex. The reaction was complete within 5 min, and the spectral change caused by the exchange reaction was found to be proportional to the mercury concentration (Fig. 5). Accordingly, in this procedure, dual-wavelength photometry was applied to the mixture of mercury- and copper dithizonates, with $\lambda_1$ and $\lambda_2$ selected as 567 and 493 nm, respectively, as indicated in Fig. 5. A typical calibration line is also shown in Fig. 5.

In this case, the only interfering cations which may be found in environmental water samples are silver(I) and iron(III). The stability constant of silver(I) dithizonate is so high that it is also involved in the exchange reaction, causing a positive error, but it can be masked in amounts up to equimolar with mercury by adding 0.1 M hydrochloric acid. Iron(III) may oxidize copper dithizonate, causing negative errors, but can be masked in molar amounts up to 100-fold mercury by adding a few drops of 50% hydrofluoric acid. Other cations do not interfere; the interference study is summarized in Fig. 6.

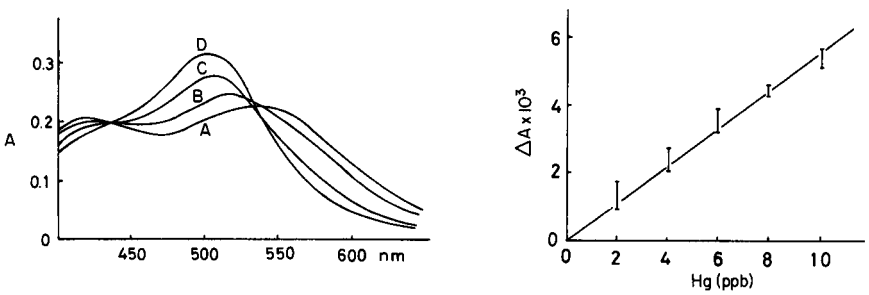


Fig. 5. Spectral change caused by the exchange reaction of copper(II) dithizonate with mercury(II) at pH 1. Hg concentration (ppm): (A) 0; (B) 0.1; (C) 0.4; (D) 1.0. A calibration line for $\lambda_1$ = 567 nm, $\lambda_2$ = 493 nm is also shown.

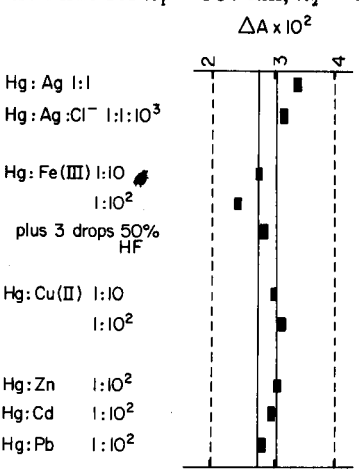


Fig. 6. Effects of diverse cations on the determination of 100 ppb of Hg. Solid horizontal lines indicate ±5% error limits. Molar ratios are indicated.

The analytical procedure described in the Experimental section is very simple. Thus, the final approach is highly recommended as a simplified procedure for the determination of traces of mercury in environmental water samples. As the slit widths of the photometer can be set as wide as 10 nm without lowering the sensitivity for mercury, a simple dual-wavelength photometer equipped with two filters (570 and 490 nm) could be constructed for this purpose.

The authors are grateful for a Grant in Aid for Special Project Research (Detections and Controls of Environmental Pollution, No. 210410) by the Ministry of Education.

REFERENCES

1 S. Shibata, Angew. Chem. Int. Ed. Engl., 15 (1976) 673.
2 H. Watanabe and J. Miura, Bunseki Kagaku, 26 (1977) 196.
3 E. B. Sandell, Colorimetric Determination of Traces of Metals, 3rd edn., Interscience, New York, 1959, p. 170.

*Analytica Chimica Acta*, 105 (1979) 297—310


# SYNCHRONOUS EXCITATION METHOD FOR INCREASING SENSITIVITY IN FLUORIMETRY
## The Limitations caused by Raman and Rayleigh Scatter

J. C. ANDRE*, M. BOUCHY and M. L. VIRIOT

*I.N.P.L. Laboratoire de Chimie Générale, E.R.A. n° 136 du C.N.R.S., 1 rue Grandville, 54042 Nancy Cedex (France)*

(Received 14th June 1978)

SUMMARY

In cases where the fluorescence of a compound is perturbed by Rayleigh scatter and by stray reflections at the exciting wavelength, the method of synchronous excitation, where the wavelengths of excitation ($\lambda_e$) and of analysis ($\lambda_a$) are scanned simultaneously with a constant step, $c = \lambda_a - \lambda_e$, between them, gives a distinct improvement in the measurement. When the measurement is hampered by this type of stray light and by Raman scatter simultaneously, it is shown that the technique of synchronous excitation again allows an improvement of the measurement compared to conventional techniques, if appropriate values of $c$ are selected. The use of this technique is illustrated for the measurement of the concentration of phenol in aqueous solution; a lower limit of determination of the order of 5 ppb can be obtained.

If a compound is fluorescent, its concentration can be determined, after previous standardization, by measuring the intensity of fluorescence emitted at a given wavelength. In principle, it seems possible to extend the limit of detection of a fluorescent compound by increasing, for example, the luminous intensity of the exciting light, or by enlarging the slit width of the analysing and excitation monochromators, or lastly by amplifying the photodetector signal. However, below a certain concentration which depends on the nature of the substance and on the apparatus, many factors intervene and limit the sensitivity of the spectrofluorimeter used. In particular, in many cases, the emission spectrum of a substance present in small concentration can be partially masked by the Rayleigh and Raman scatter of the solvent. Such an effect is shown in Fig. 1.

Synchronous excitation, which has been used for the determination of fluorescent tracers [1] and drugs [2] eliminates the effects of Rayleigh scatter at wavelengths adjacent to those of excitation. This technique of synchronous excitation was introduced by Lloyd [3] for the detection of aromatic compounds, and has been used by other authors in similar fields [4, 5]. The technique [1] is both qualitative and quantitative: the excitation ($\lambda_e$) and emission ($\lambda_a$) wavelengths are simultaneously varied with a constant step $c$ ($c = \lambda_e - \lambda_a$)

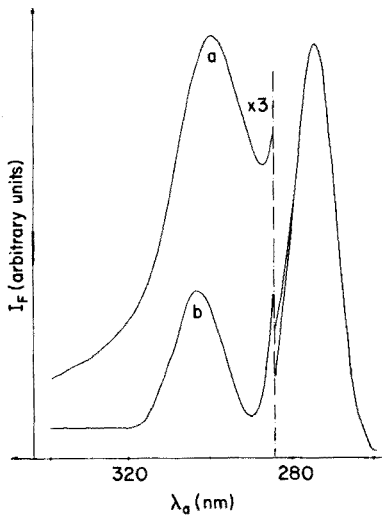


Fig. 1. Fluorescence spectra of phenol. (a) 70 ppb phenol; (b) blank. Excitation, 270 nm; solvent, de-ionized water; excitation and emission slit widths, 10 nm. The peak at 270 nm corresponds to the Rayleigh scatter; the Raman scatter occurs at 303 nm.

between them, and this allows partial elimination of interfering effects caused by stray light entering the analysing monochromator in the region of $\lambda_e$.

However, as shown in Fig. 1, in certain cases the measurement can be affected simultaneously by Rayleigh and Raman scatter. This occurs in analyses for compounds like phenol or benzene (pollution of water [6]) or pharmaceuticals (e.g. epinephrine, podophyllotoxine, amphetamines, etc. [2, 7]). Spectrofluorimetric determinations of drugs such as amphetamines can be improved by using synchronous excitation [2]. However, when these experiments were carried out, it appeared that Raman scatter was only partially eliminated, and this limited the measurements.

A more complete study of the synchronous excitation method for the determination of compounds like phenol, which was chosen as a reference substance, is presented here. The problems of the measurement are discussed, the optimal values for step (c) and for the slit widths are established, and the best general conditions when measurements are affected simultaneously by Rayleigh and Raman scatter are described.

## EXPERIMENTAL

The JY3 spectrofluorimeter used was equipped with an accessory allowing the recording of synchronous excitation spectra. Phenol (Fluka, puriss.) and de-ionized water were used.

The simulations were done with Hewlett-Packard 9830 and CII-Mitra 15 computers.

Figure 2 shows the contour curves representing the intensity, $I(\lambda_e, \lambda_a)$, of Raman scatter and of stray light generated by excitation of a fluorescence cell filled with de-ionized water. This shows clearly that, because the spectra are linear in $\lambda$ rather than in $\lambda^{-1}$, the maximum of the Raman scatter is not separated by a constant increment from $\lambda_e$. The relationship is $1/\lambda_R = 1/\lambda_e - 1/\bar{\lambda}$, i.e. $\lambda_R = \lambda_e\bar{\lambda}/(\bar{\lambda} - \lambda_e)$, where $\bar{\lambda}$ is the wavelength corresponding to the active Raman transition. The symbols used are identified in Table 1.

Under the conditions of synchronous excitation, the curve $\lambda_R(\lambda_e)$ is not parallel to the direction of excitation; this causes the appearance of a large band on the spectrum. These effects are shown also in Fig. 3 where a Raman spectrum at a fixed wavelength of excitation is compared to a Raman spectrum obtained by synchronous excitation.

*The shape of Raman spectra obtained by synchronous excitation*

If the symbols described in Fig. 4 are used, and $c$ is the constant step between the excitation and analysis wavelengths, then when the slit widths of the excitation and analysing monochromators are equal, it is possible to calculate the expression for the luminous intensity which penetrates into the fluorescence cell:

$$I_1(\lambda) \propto I_e(\lambda)T_e(\lambda) * \mathscr{L}_e(\lambda) \qquad (1)$$

The symbol $*$ indicates the convolution of $I_e(\lambda)T_e(\lambda)$ by the band-pass function of the excitation monochromator at the wavelength $\lambda_e$ represented by $\mathscr{L}_e(\lambda)$, or

$$I_1(\lambda) \propto \int_{-\infty}^{+\infty} I_e(\lambda + x)\, T_e(\lambda + x)\, .\, \mathscr{L}_e(\lambda + x)\, dx$$

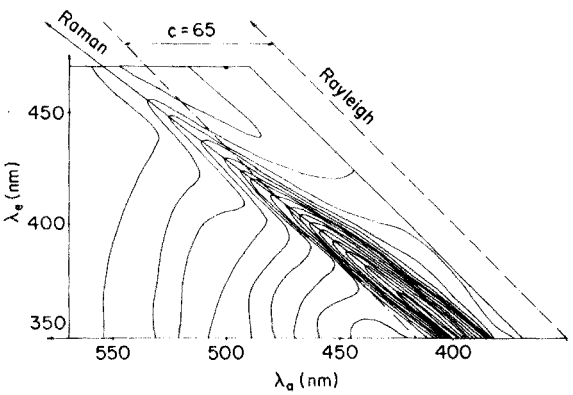


Fig. 2. Contour lines corresponding to the Raman scatter of water showing clearly the gap between $\lambda_e$ and the Raman scatter as a function of $\lambda_e$. Solvent, de-ionized water; excitation and analysing slit widths, 10 nm; (—·—) synchronous excitation with $c$ = 65 nm.

TABLE 1

List of symbols used

| | |
|---|---|
| $a$ | 2.7726 |
| $c$ | Constant step |
| $C_m$ | Limit of detection |
| $l$ | Size of the slits of both monochromators when $l_e = l_a$ |
| $l_a$ | Size of the slits of analysis monochromator |
| $l_e$ | Size of the slits of excitation monochromator |
| $l_{1/2}$ | Width at half-height of the synchronous excitation spectrum |
| $I(\lambda)$ | Sum of all the stray intensities |
| $I_a(\lambda)$ | Luminous intensity absorbed by the sample |
| $I_e(\lambda)$ | Luminous intensity emitted by the light source |
| $I_E$ | Intensity of electronic noise |
| $I_F(\lambda)$ | Fluorescence intensity |
| $I_P(\lambda)$ | Intensity of stray light emitted at all wavelengths |
| $I_R(\lambda)$ | Intensity of Raman scatter |
| $I_S(\lambda)$ | Intensity of scattered light |
| $I_1(\lambda)$ | Intensity which penetrates into the fluorescence cell |
| $I_2(\lambda)$ | Raman scatter intensity |
| $I_3(\lambda)$ | Observed Raman scatter intensity |
| $L$ | Width at half height of $\mathscr{L}_e(\lambda)$ |
| $R(\lambda)$ | Photomultiplier tube response |
| $T_a(\lambda)$ | Transmission of the analysis monochromator |
| $T_e(\lambda)$ | Transmission of the excitation monochromator |
| $\mathscr{D}(\lambda)$ | Function of scattering |
| $\mathscr{L}_a(\lambda)$ | "Band-pass" function of the analysis monochromator |
| $\mathscr{L}_e(\lambda)$ | "Band-pass" function of the excitation monochromator |
| $\mathscr{R}(\lambda)$ | Function of Raman scatter |
| $\epsilon(\lambda)$ | Molar absorptivity at wavelength $\lambda$ |
| $\lambda'$ | Wavelengths of emission of Raman scatter |
| $\lambda_a$ | Analysis wavelength |
| $\lambda_e$ | Excitation wavelength |
| $\lambda_a^\circ$ | Analysis wavelength leading to maximum fluorescence intensity |
| $\lambda_e^\circ$ | Excitation wavelength leading to maximum fluorescence intensity |
| $\lambda_R$ | Maximum of Raman scatter |
| $\bar{\lambda}$ | Wavelength corresponding to the active Raman transition |
| $\eta(\lambda)$ | Fluorescence spectrum of the sample |
| $\phi$ | Quantum fluorescence yield |
| $\Delta\lambda_R$ | $\lambda_e^2/(\bar{\lambda} - \lambda_e)$ |
| $I_F(\lambda_a)/l_{1/2}$ | Characteristic value which indicates both the sensitivity and the selectivity of the measurement |
| S.L. | Stray light |

For a rigorous treatment, these relationships must be subjected to double convolution on $I_e(\lambda)$ by a function of the entrance slit width and the result convoluted by the product of the transmission of the monochromator with a function of the exit slit width of the excitation monochromator.

Raman scatter, proportional to $1/\lambda^4$ [8] corresponds to a luminous emission $I_2(\lambda)$, shifted in wavelength with respect to the excitation. If $\mathscr{R}(\lambda)$ represents the transfer function caused by the Raman effect, then $I_2(\lambda') \propto I_1(\lambda)\,\mathscr{R}(\lambda)$, or

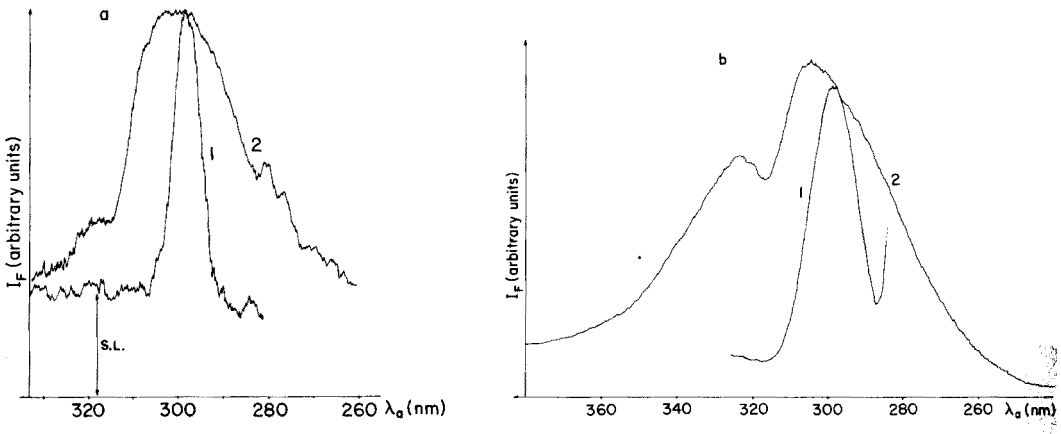


Fig. 3. Comparison of Raman scatter spectra obtained at fixed excitation wavelength and by the synchronous excitation method. Solvent, de-ionized water. (a) Excitation and analysing slit widths, 4 nm; (b) excitation and analysing slit widths, 10 nm. Spectra 1 obtained with excitation at 270 nm; spectra 2 obtained for $c$ = 27.5 nm.

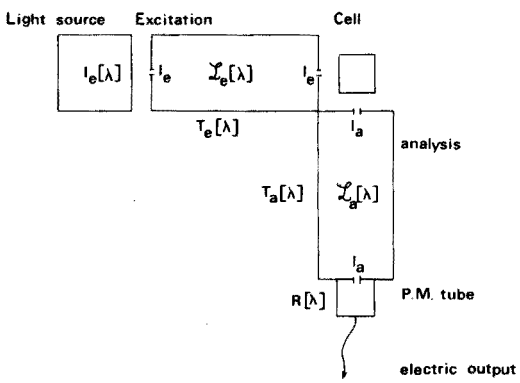


Fig. 4. Symbols and apparatus used.

$$I_2(\lambda') \propto I_1(\lambda) \frac{\lambda_e \bar{\lambda}}{\lambda_e + \bar{\lambda}} \frac{1}{\lambda_e^4} \tag{2}$$

Thus, the electric signal, a function of different parameters of the apparatus, can be expressed by

$$I_3(\lambda) \propto I_2(\lambda') T_a(\lambda') R(\lambda') * \mathscr{L}_a(\lambda) \tag{3}$$

where $\mathscr{L}_a(\lambda)$ represents the band-pass function of the analysing monochromator in the vicinity of wavelength $\lambda_a$.

*Choice of band-passes for the two monochromators.* The bandpass functions $\mathscr{L}_e(\lambda)$ and $\mathscr{L}_a(\lambda)$ can be traced experimentally by changing the size $l$ of the slits (in nm) of the two monochromators. More rigorously, following Parker [8], the function $\mathscr{L}_e(\lambda)$ must be represented by an isosceles triangle with base $2l_e$. However, because of optical and perhaps electronic imperfec-

tions, it can be shown that this is not exactly correct. $\mathscr{L}_e(\lambda)$ can be simulated better by a function close to that of the triangle, i.e. a gaussian function:

$$\mathscr{L}_e(\lambda) = \exp\{-a\,[(\lambda - \lambda_e)/l_e]^2\} \qquad (4)$$

where $a = 2.7726$ and where when $|\lambda - \lambda_e| = l_e/2$, then $\mathscr{L}_e(\lambda_e + l/2) = 1/2$ (cf. Fig. 5).

Note that Fig. 5 makes it possible to calculate the width $L$ at the half-height of $\mathscr{L}_e(\lambda)$. A complete calculation shows that $L = (l_e^2 + l_a^2)^{\frac{1}{2}}$. Thus, the use of slit widths of 2 nm for $l_a$ causes a maximum error of only 2% in the determination of $L$ if $l_e = 10$ nm. The values of the slit widths "10 nm" provided by the manufacturer can be verified experimentally. It was found that $l_e$ was 9.5 nm, a value close to that indicated.

For a given value of $c$, it has already been shown [2] that $l_e$ and $l_a$ must be chosen so that $l_e + l_a \leqslant c$; this eliminates most effectively the effects of scattering in the wavelength region of excitation. Under these conditions, the fluorescence intensity is maximal when $l_e = l_a = l$. Accordingly, equal slit widths were chosen for further calculations and for the experimental work.

*Influence of slit size on the Raman spectra.* With the assumption that $I_e(\lambda)$, $T_e(\lambda)$, $T_a(\lambda)$ and $R(\lambda)$ are constant, simulated Raman spectra obtained by synchronous excitation for different values of $l_e = l_a = l$ were calculated by computer. It is clear from Fig. 6 that an increase in $l$ results in a considerable broadening of the Raman spectrum; the result is verified experimentally in Fig. 3. Under these conditions, the problem posed is to compare this broadening with the broadening of a constant-step fluorescence spectrum of phenol.

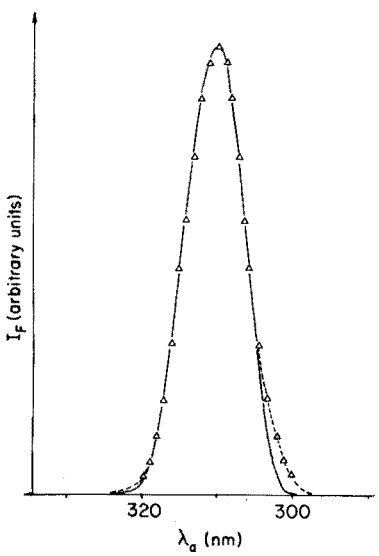


Fig. 5. Simulation of $\mathscr{L}_e(\lambda)$ by a gaussian function. (——) Scatter spectra with excitation at 310 nm, excitation slit width 10 nm and analysing slit width 2 nm. (-----) Best-fitting gaussian curve.

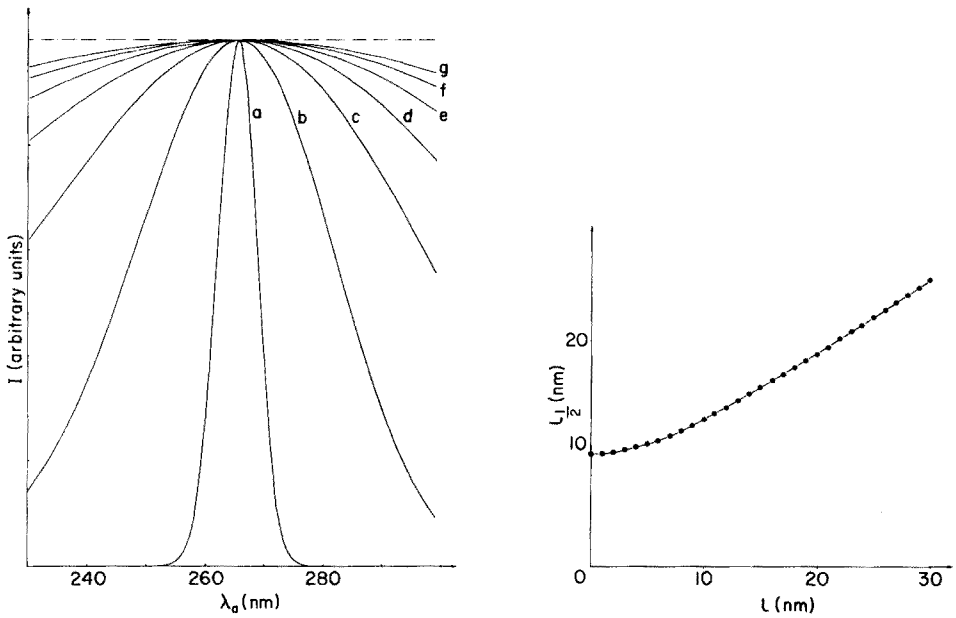


Fig. 6. Simulation of a Raman spectrum of water for different values of $l$ by synchronous excitation. $I_e(\lambda)$, $T_e(\lambda)$ = constant; $T_a(\lambda)$, $R(\lambda)$ = constant; $c$ = 23 nm. The values of $l$ are: (a) 1 nm; (b) 5 nm; (c) 10 nm; (d) 15 nm; (e) 20 nm; (f) 25 nm; (g) 30 nm.

Fig. 7. Simulation of synchronous excitation spectra of phenol for $c$ = 15 nm: variations of $l_{1/2}$ with $l$.

As can be seen from Fig. 7 for a constant step of 15 nm, the width at half height of the spectrum of phenol varies more gradually than $l$. Under these conditions, qualitative analysis of the phenol fluorescence will not be affected by enlarging the slit widths.

*Intensity of the Raman scatter at the analysing wavelength*

The values of $I_e(\lambda)T_e(\lambda)$ and $T_a(\lambda)R(\lambda)$ can be measured experimentally by appropriate techniques [8—10]; thus an expression for $I(\lambda)$ can be calculated from the relationships (1—3) for a given value of $c$. A typical result is presented in Fig. 8.

## OPTIMAL CHOICE OF THE CONSTANT STEP AND THE SLIT WIDTH

When the measurement of fluorescence intensity is affected only by the scattering and the stray light at the excitation wavelength, conditions can be selected so that $c$ corresponds to the gap between the wavelengths of maximal excitation and maximal emission. Thus, a cross-section (for a $c$ value of 23 nm) of the three-dimensional representation of Fig. 2 is presented in Fig. 9; both

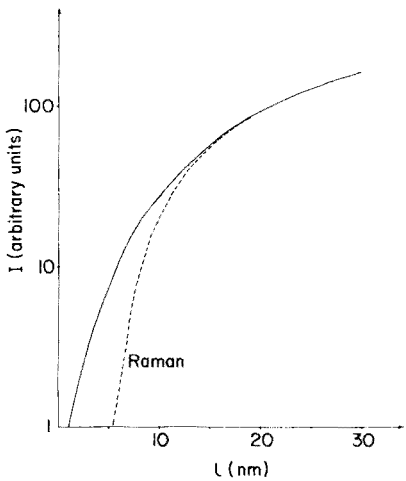


Fig. 8. Influence of $l$ on the intensities of the Raman scatter and of the phenol fluorescence for $c$ = 15 nm.

the phenol fluorescence and the Raman scatter of the solvent are involved. The effect is illustrated in another way in Fig. 10 which shows the constant-step ($c$ = 23 nm) spectra of the solvent and of the fluorescent solution.

*Intensity of fluorescence*

For weak concentrations of phenol (in practice, less than $10^{-5}$ g $g^{-1}$), the fluorescence intensity emitted with a quantum yield $\phi$ is proportional to the concentration, $C$. The luminous intensity absorbed $I_a(\lambda_e)$ is represented by

$$I_a(\lambda_e) \propto \{[I_e(\lambda)T_e(\lambda) * \mathscr{L}_e(\lambda)] * \epsilon(\lambda)\}\ [C] \qquad (5)$$

where $\epsilon(\lambda)$ is the molar absorptivity at wavelength $\lambda$. In the same way, the fluorescence spectrum of phenol, $\eta(\lambda)$, corresponds, except for a multiplier, to the number of photons emitted by the fluorescent substance between $\lambda$ and $\lambda + d\lambda$; the electric intensity leaving the photomultiplier is expressed by the fluorescence intensity:

$$I_F(\lambda_a) = I_a(\lambda_e)\ [\eta(\lambda)T_e(\lambda)R(\lambda) * \mathscr{L}_a(\lambda_a)] \qquad (6)$$

For a given value of $c$, Fig. 8 shows the variations of $I_F(\lambda_a)$ for different values of $l$ ($\lambda_a$ = 270 nm). Figure 11 shows, for $l$ = 1 nm, the variations of the following features: (a) the position of maximum emission $\lambda_a$; (b) the intensity $I_F(\lambda_a)$ of the constant-step spectrum, which can be used quantitatively; (c) the width at half-height $l_{1/2}$ of the constant-step spectrum, which is useful qualitatively; and (d) the quotient $I_F(\lambda_a)/l_{1/2}$ as a function of $c$, which constitutes a characteristic value, without precise theoretical justification, but which gives information simultaneously on the sensitivity ($I_F$) and the selectivity ($l_{1/2}$) of the measurement.

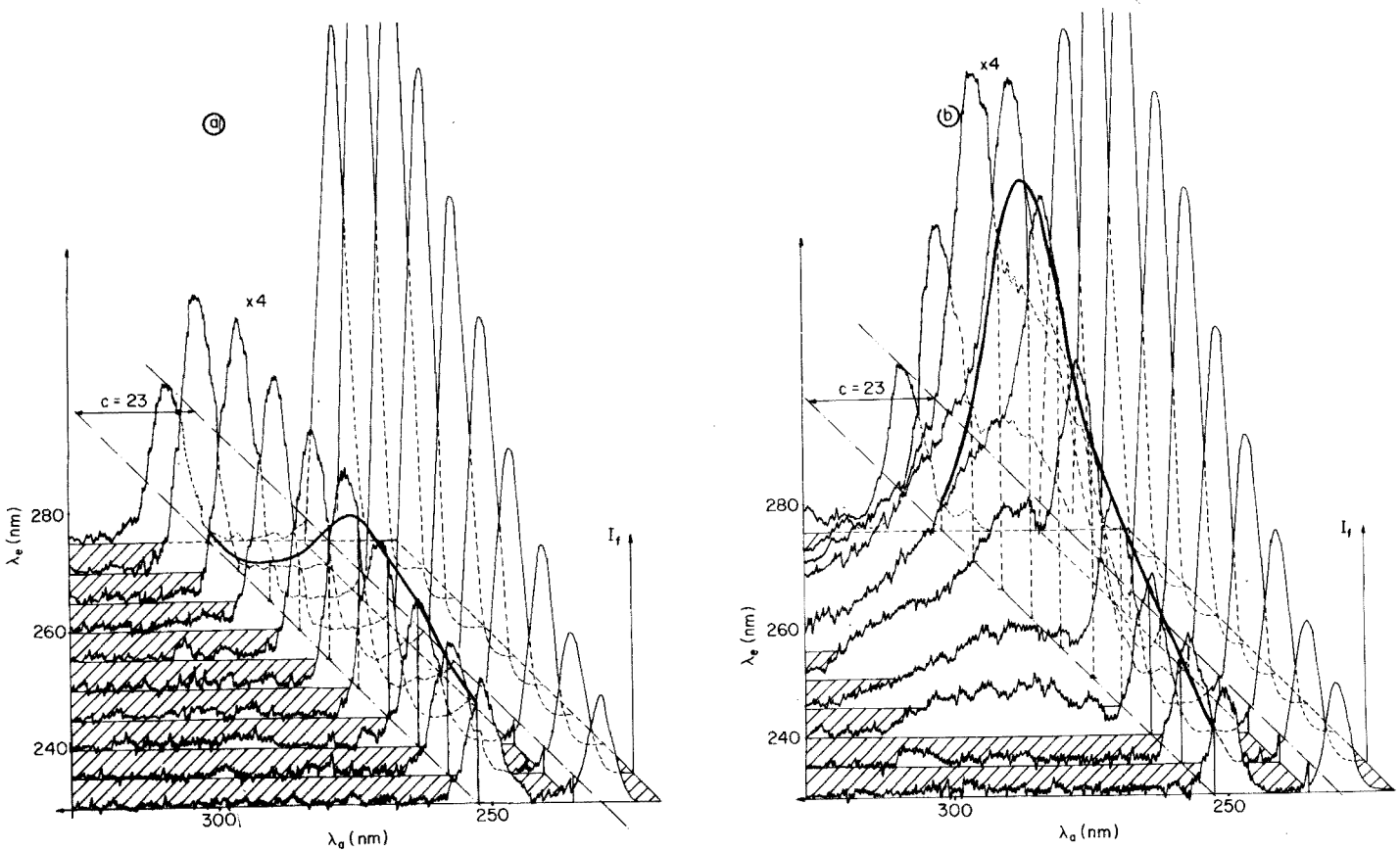


Fig. 9. Visualization of synchronous excitation spectra of (a) the solvent and (b) a solution of 70 ppb phenol. Solvent, de-ionized water; excitation and analysing slit widths, 4 nm. The optical noise corresponding to the stray light emitted at all wavelengths, which is practically constant, has been subtracted for clarity.

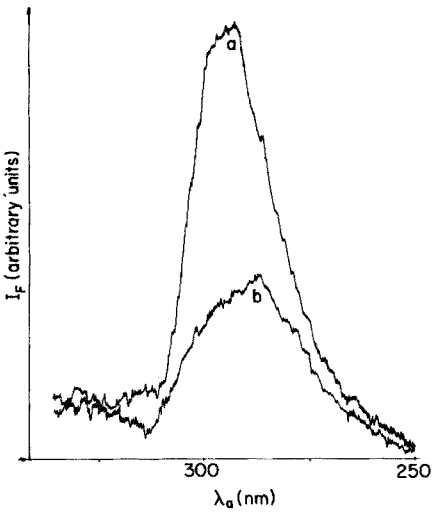


Fig. 10. Synchronous excitation spectra of phenol. (a) 70 ppb phenol; (b) blank. Solvent, de-ionized water; excitation and analysing slit widths, 4 nm.

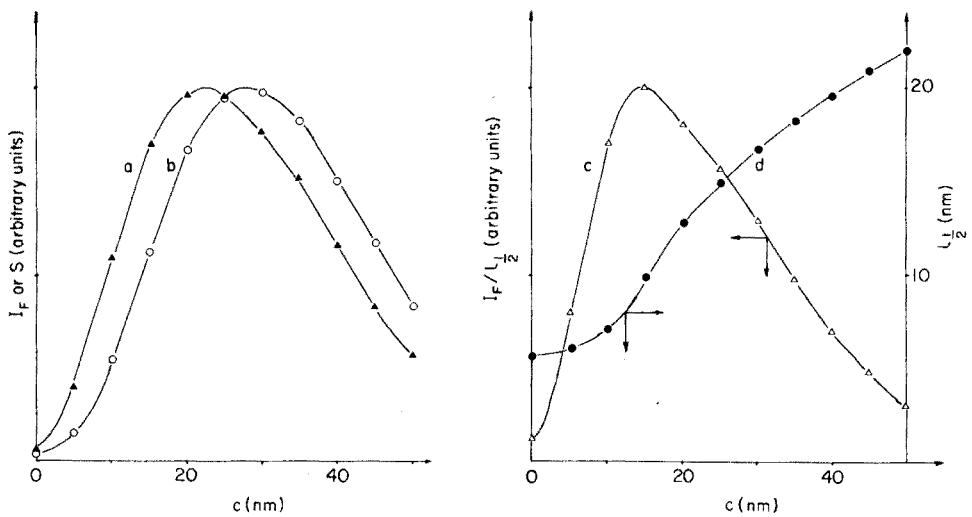


Fig. 11. Influence of $c$ on the fluorescence of phenol, calculated for $l$ = 1 nm. (a) Maximum intensity $I_F$; (b) total fluorescence $S$; (c) $l_{1/2}$ width and half-height of synchronous excitation spectrum; (d) $I_F/l_{1/2}$.

*Limit of detection*

The limit of detection ($C_m$) is defined here as the concentration which gives a fluorescence intensity equal to the sum of all the stray intensities of diverse origin. The stray intensities comprise; (a) electronic noise ($I_E$) which is

independent of $l$, and depends on the electronic components of the apparatus (photomultiplier, amplifier, etc.); (b) scattered light ($I_S$; Rayleigh scatter and stray reflections from the cell wall) near the excitation wavelength; (c) the Raman scatter ($I_R$); and (d) the stray light ($I_p$) emitted at all wavelengths, which depends on the quality of the dispersive systems. $C_m$ is therefore defined when $I_F(\lambda_a) = I_E + I_S + I_R + I_p = I$.

*Expression for* $I_S$. The intensity which enters the cell is represented by $I_1(\lambda)$; if $\mathscr{D}(\lambda)$ is the scattering function, the electric signal corresponding to $I_S(\lambda_a)$ will be represented by

$$I_S(\lambda_a) = [I_1(\lambda)\mathscr{D}(\lambda)T_a(\lambda)R(\lambda) * \mathscr{L}_a(\lambda)] \tag{7}$$

With the cells used classically for spectrofluorimetry, i.e. with four polished faces, the major part of the scattered light consists of light reflected off the faces [10]; $\mathscr{D}(\lambda)$ is practically independent of $\lambda$, whereas the pure Rayleigh scattering is effectively proportional to $1/\lambda^4$ [8].

*Expression for* $I_P$. It is not possible to determine an analytical expression for $I_p$. Accordingly, $I_p$ was measured for different values of $l$ (4, 10 and 35 nm) and interpolation was used to define a qualitative expression as a function of $l$. As the light concerned is emitted at all wavelengths, $I_p$ was initially considered to be effectively independent of $\lambda$. The determination of $I_p$ is illustrated in Fig. 3(a) for $l = 4$ nm. The large Raman "spectrum" with its maximum at about 300 nm can be seen. But for larger values of $\lambda_a$, the signal tends to a constant value because of stray light (S.L.)

*Approximate expressions for* $I_R$ *and* $I_S$. If it is supposed that between $\lambda_e + l$, $\lambda_e - l$ on the one hand, and $\lambda_a + l$, $\lambda_a - l$ on the other hand, $I_e(\lambda)T_e(\lambda)$ and $T_a(\lambda)R(\lambda)$, respectively, vary little, the expressions for $I_R(\lambda)$ and $I_S(\lambda)$ can be considerably simplified:

$$I_S(\lambda_a) \propto I_e(\lambda_e)T_e(\lambda_e)T_a(\lambda_a)R(\lambda_a)l \exp(-ac^2/2l^2) \tag{8}$$

Similarly,

$$I_R(\lambda_a) \propto \{I_e(\lambda_e)T_e(\lambda_e)T_a(\lambda_a)R(\lambda_a)(l/\lambda_e^4)\} \exp(-a(\Delta\lambda_R - c)^2/2l^2) \tag{9}$$

where $\Delta\lambda_R = (\lambda_e \bar{\lambda}/[\bar{\lambda} - \lambda_e]) - \lambda_e = \lambda_e^2/(\bar{\lambda} - \lambda_e)$

The use of these approximate relationships does not modify the calculated values appreciably, and they were therefore used in the calculations.

*Expression for* I. The expressions for $I(\lambda_e)$ have been defined except for a multiplying factor; the factors can be determined from a typical experiment, e.g. with excitation at 270 nm and with $l_a = l_e = l = 4$ nm. Under these conditions, the variations of $1/C_m$ with $l$ and $c$ were calculated, except for the multiplier. The results obtained (Fig. 12) make it possible to define the following features (though only semi-quantitatively, because of the approximate knowledge of $I_p$): (a) the optimal step, c, which lies either between 10 and 15 nm, or between 40 and 45 nm; and (b) the slit widths, $l \approx 6$ nm for $c = 10$—15 nm (effectively $c/2$) and $l \approx 8$ nm for $c = 40$—45 nm.

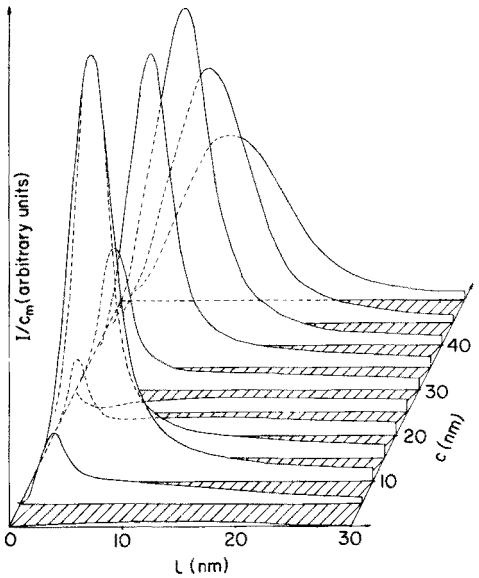


Fig. 12. Results for the simulation of $1/C_m$ with $c$ and $l$.

It is therefore possible to conclude that the step $c$ that would have been chosen a priori, i.e. 20—25 nm, from the excitation and emission spectra of phenol, is not the optimal step. It is convenient to choose step values either small or large enough to be outside the region where Raman scatter is particularly intense. Further, the use of large slit widths is responsible for a decrease of $1/C_m$ mainly because of an increase in $I_P$, but also, less importantly, in $I_S$.

Lloyd [3] and Tyan Vo-Dinh [4] have used the synchronous excitation method for qualitative analyses generally with relatively small values of $c$ ($\leqslant$ 10 nm). The results presented in Fig. 11 show that the smaller the value of $c$, then the greater the reduction in the value of $l_{1/2}$, the width at half height of the constant-step spectrum. Accordingly, the use of smaller steps, i.e. less than 10 nm, improves the selectivity of the measurement. However, as can be observed for phenol in Fig. 12, the value of $1/C_m$ will not be the optimum value.

*Experimental verification*

To verify the results of the above calculations, the variations of $C_m$ with $l$ were measured and a number of synchronous excitation spectra were recorded for different values of $l$ and $c$.

*Experimental variations of* $C_m$ *with* c *for* l = *10 nm.* Figure 13 shows the variations of $C_m$ with $c$ for $l$ = 10 nm, which causes the appearance of two optimal constant steps, 15 nm and 42 nm, very close to the values obtained by calculation. The synchronous excitation spectra recorded for the two values of $c$ and shown in Fig. 14, allow comparison of the measurements. Because of the shape of the spectrum, i.e. the value of $l_{1/2}$, and for reasons connected

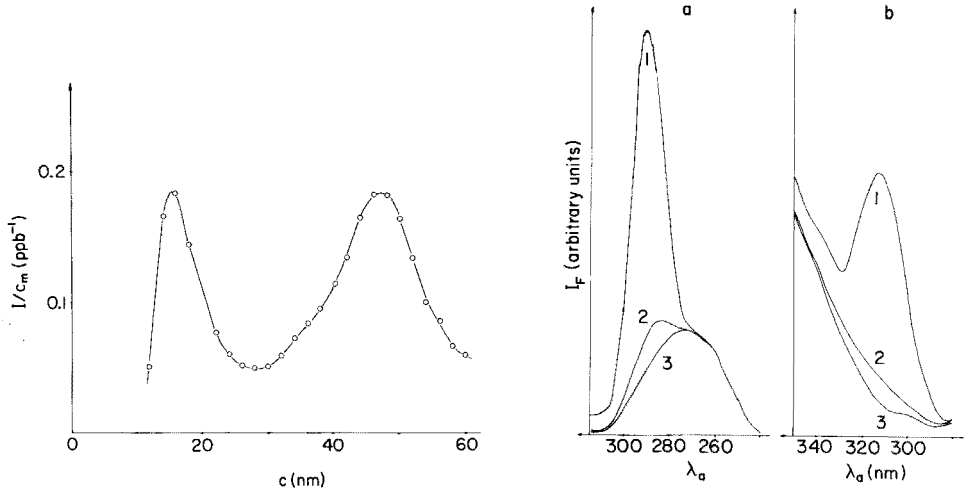


Fig. 13. Experimental variations of $1/C_m$ with $c$ in the case of phenol for $l$ = 10 nm.

Fig. 14. Synchronous excitation spectra of phenol in the range of the smallest measurable concentration, i.e. detection limit, for (a) $c$ = 15 nm, and (b) $c$ = 42 nm. Curves 1—3 correspond to phenol concentrations of 30, 3, and 0 ppb, respectively.

with the shape of the background (the fluorescence spectrum appears as a shoulder on the Raman spectrum for $c$ = 42 nm), a $c$ value of the order of 15 nm is clearly preferable for measurements. In any case, for $l$ = 10 nm, the limit of detection is of the order of $5 \times 10^{-9}$ g g$^{-1}$ (5 ppb).

*Influence of the slits.* The JY3 apparatus available possessed only one discrete set of slit widths, 1, 2, 4 and 10 nm; on removing the slits, the spectral width corresponded to $l \approx 35$ nm. Figure 15 shows the synchronous excitation spectrum for $c$ = 15 nm, $l$ = 4 and $l$ = 10 nm. In contrast to the case of $l$ = 10 nm, when $l$ = 4 nm the background is not affected by the Raman scatter and is consequently almost level. However, the limit then depends on electronic noise (which is no longer negligible although it can be partially eliminated by appropriate damping) and the value obtained for $C_m$ is of the same order as for $l$ = 10 nm. Studies with other values of $l$ would be useful if a larger set of slits were available.

## CONCLUSION

The computer simulation of the use of synchronous excitation in cases where the measurement suffers interference simultaneously from the exciting light and from the Raman scatter, as well as the experimental measurements, prove that the constant step $c$ should be either sufficiently small (12—15 nm) or sufficiently big (40—45 nm), to achieve partial elimination of the stray Raman effect. For the narrow step, the optimal value of the monochromator slit widths is about half the value of the step, as has already been shown when the measurement is limited only by stray light at the excitation wavelength.

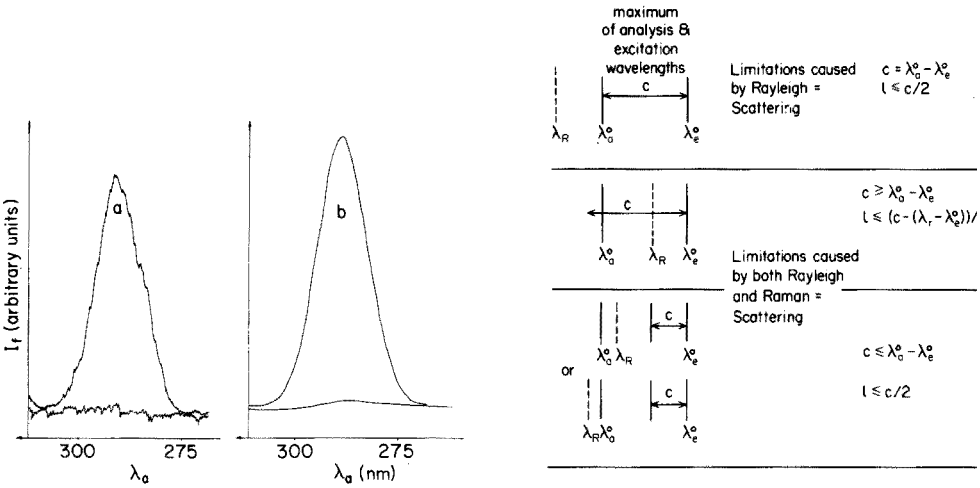


Fig. 15. Influence of $l$ on the synchronous excitation spectra of phenol (70 ppb) for $c$ = 15 nm. (a) $l = l_e = l_a = 4$ nm; (b) $l = l_e = l_a = 10$ nm.

Fig. 16. Generalization of the results.

For the broader step, the optimal value of the slit widths depends simultaneously on the intensity of the scattered light, both Raman and stray light.

Under these conditions, measurements based on synchronous excitation allow a considerable improvement in sensitivity and selectivity even with a conventional spectrofluorimetric apparatus. The selection of optimal values of $c$ and $l$ for a given fluorescent compound can be assisted by using the qualitative generalization shown in Fig. 16.

The authors thank A. Samoun of the society Jobin-Yvon for his technical aid and helpful discussions, and S. Bouchy, M.Sc., for the translation of this paper.

REFERENCES

1 J. C. Andre, M. Bouchy, Ph. Baudot and M. Niclause, Anal. Chim. Acta, 92 (1977) 667.
2 J. C. Andre, Ph. Baudot and M. Niclause, Clin. Chim. Acta, 76 (1977) 55.
3 J. B. F. Lloyd, Nature (Physical Science), 231 (1971) 64.
J. B. F. Lloyd, J. Forensic Sci. Soc., 11 (2) (1971) 83; 11 (3) (1971) 153; 11 (4) (1971) 135
J. B. F. Lloyd and I. W. Evett, Anal. Chem., 49 (1977) 1710.
J. B. F. Lloyd, Industrial Res. (Nov. 15, 1977) 29.
4 Tuan Vo-Dinh, Anal. Chem., 50 (1978) 396.
5 J. U. White, Anal. Chem., 48 (1976) 2089.
6 J. W. Bridges, P. J. Creaven and R. T. Williams, Biochem. J., 96 (1965) 872.
7 S. Udenfriend, Fluorescence Assay in Biology and Medicine, Academic Press, New York, 1962.
8 C. A. Parker, Photoluminescence of solutions, Elsevier, New York, 1968.
9 J. Yguerabide, Rev. Sci. Instrum., 39 (1968) 1048.
10 M. L. Viriot, J. C. Andre and J. Molinari, Etude de synthèse: Spectroscopies des substan fluorescentes en hydrologie, Rapport C.E.A.-C.E.N.G.-SARR/GARTHI/RAP/76-33/ JM/AB, 1976, 94 pp.

*Analytica Chimica Acta*, 105 (1979) 311—317


# FLUORIMETRIC DETERMINATION OF ACIDITY CONSTANTS OF NAPHTHOIC AND ANTHROIC ACIDS

WILLY J. M. UNDERBERG** and STEPHEN G. SCHULMAN*

*College of Pharmacy, University of Florida, Gainesville, Florida 32610 (U.S.A.)*

(Received 24th August 1978)

SUMMARY

A fluorimetric method of determining the acidity constants ($pK_a$ values) of some naphthoic and anthroic acids is presented, based on the changes in fluorescence of solutions of these acids in water on changing the pH. The method is useful in the absence as well as in the presence of excited-state proton transfer. In the latter case, when the excited-state protonation occurs in the same pH region as the ground-state dissociation, resolution of the two processes can be accomplished by addition of a suitable quencher such as iodide. The method permits the accurate determination of the $pK_a$ value of fluorescent compounds, even when they are poorly soluble in water, because of the high sensitivity of the spectrofluorimetry.

The determination of $pK_a$ values of weak acids and bases can be done in several ways. Compounds that are sufficiently soluble in water can be titrated and the pH change followed. For compounds with an appropriate absorption spectrum, the change in absorptivity with pH can be used. Frequently, however, the solubility of a compound is too low or its absorptivity does not change sufficiently with pH to warrant the use of one of the methods mentioned. Some authors have reported the determination of $pK_a$ values of poorly soluble weak acids, using the conductivity of solutions of these acids in water [1—3]. This method, although useful, requires many precautions and corrections to obtain reliable results. Fluorescence spectrometry makes it possible to determine very low concentrations of fluorescent compounds. This technique can be very useful in the determination of equilibrium constants of compounds with low solubility. This possibility has been mentioned in the literature [4, 5] although its range of applicability and limitations has not been well established. It is necessary to take into account the processes that may occur in the excited state, more specifically for present purposes, excited-state proton-transfer processes. These processes can interfere with the simple dependence of the fluorescence spectrum upon ground-state proton exchange and may lead to incorrect $pK_a$ values of the compounds investigated.

In the present paper a fluorimetric method for the determination of $pK_a$ values of some arylcarboxylic acids is described. Adjustments of the method are developed for the cases where excited-state proton transfer occurs.

**Permanent address: Farmaceutisch Laboratorium, Rijksuniversiteit Utrecht, The Netherlands.

## EXPERIMENTAL

### *Chemicals*

1-Naphthoic and 2-naphthoic acid and 2- and 9-anthroic acid (Pfaltz and Bauer, Inc., Stamford, CT.) and 1-anthroic acid, prepared by the method of Carlson [6] were recrystallized several times from 50% ethanol.

The solutions for measurement of the fluorescences were $2.7 \times 10^{-7}$ M in the anthroic acids and $8.0 \times 10^{-6}$ M in the naphthoic acids. The pH of the solutions was adjusted with perchloric acid or hydroxide solution. The use of standard buffers was avoided because of the possible influence of high concentrations of buffer ions on the fluorescence. Sodium iodide was added to a final concentration of $2 \times 10^{-2}$ M, if necessary. The temperature was kept at 25°C throughout.

For the estimations of the solubilities of the neutral acids, a saturated solut of each acid in 1 M perchloric acid was prepared at 25°C. From these solution 1.00 ml of each was transferred to a series of 10-ml volumetric flasks, made alkaline with sodium hydroxide solution, and water was added to the mark. The fluorescences of these solutions were compared with the fluorescences of solutions of the same aromatic acids in 0.1 M sodium hydroxide with concentrations of $6 \times 10^{-7}$ M in the aromatic acid. From the ratios of the fluorescences the solubilities were calculated. In the case of 1-naphthoic acid, wher the anion is very weakly fluorescent, the alkaline solution was acidified to pH 2.5. The fluorescence of this solution was compared with that of the saturated solution, also adjusted to pH 2.5 with sodium hydroxide solution.

### *Apparatus*

Absorption spectra were taken on a Beckman DB-GT spectrophotometer. Fluorescence spectra were recorded on a Perkin-Elmer MPF-2A fluorescence spectrophotometer whose monochromators were calibrated against the xenon line emission spectrum and whose output was corrected for instrumental response by means of a rhodamine-B quantum counter. Excitation was effecte at isosbestic points in the absorption spectra of the neutral acids and their conjugate bases (1-naphthoic acid, 292 nm; 2-naphthoic acid, 278 nm; 1-anthroic acid, 260 nm; 2-anthroic acid, 273 nm; 9-anthroic acid, 256 nm). pH measurements were made on a Markson ElectroMark Analyzer pH meter, with a Markson silver—silver chloride—glass combination electrode.

## RESULTS AND DISCUSSION

The absorption maxima of the naphthoic and anthroic acids shift only slightly as the anions are converted to the neutral molecules with decreasing pH. The absorbances do not change very much with pH. Because the solubilities of the neutral acids in water are rather low (Table 1), $pK_a$ values cannot be determined with great accuracy by potentiometric titration or pH-dependent absorption spectrophotometry, although attempts have been made [7]. The

TABLE 1

Solubilities of some naphthoic and anthroic acids in water

| Compound | Concentration of saturated solution in water at 25°C (M) |
|---|---|
| 1-Naphthoic acid | $3.8 \times 10^{-4}$ |
| 2-Naphthoic acid | $9.3 \times 10^{-5}$ |
| 1-Anthroic acid | $1.2 \times 10^{-5}$ |
| 2-Anthroic acid | $8.2 \times 10^{-6}$ |
| 9-Anthroic acid | $2.5 \times 10^{-5}$ |

conjugate bases of the acids, except 1-naphthoic acid, show an intense fluorescence, while the uncharged naphthoic and anthroic acids show appreciable fluorescence as well. Finally, the cations of the naphthoic acids [8] which are formed by excited-state protonation of the neutral molecules show significant fluorescences, while the anthroic acid cations [9, 10] appear to be weakly fluorescent. The disappearances of the anion fluorescences or the appearances of the fluorescences of the neutral molecules, on lowering the pH, can be used for straightforwardly determining the $pK_a$ values, provided that no excited-state proton-transfer processes occur in the same pH region and, thereby, alter the pH dependences of the fluorescence spectra.

9-Anthroic acid does not undergo excited-state protonation in dilute acid, while 1- and 2-anthroic acid as well as 1- and 2-naphthoic acid do, because of the increased basicity of the carboxylic group in the excited state [11]. These processes overlap the ground-state protonations of the carboxylate ions; this is due to the high protonation rate constants and long lifetimes of the excited neutral molecules. The excited-state protonation of the neutral molecules is reflected in the pH dependences of the fluorescence efficiences of the neutral molecules and their conjugate acids.

The dependence on hydrogen ion concentration of the relative fluorescence efficiency of the neutral acid, BH, is represented by [12]

$$\phi_{BH}/\phi^0_{BH} = (1 + \overleftarrow{k}\,\tau_{BH_2^+})/(1 + \vec{k}\,\tau_{BH}\,[H_3O^+] + \overleftarrow{k}\,\tau_{BH_2^+}) \quad (1)$$

and that of the protonated species, $BH_2^+$, by

$$\phi_{BH_2^+}/\phi^0_{BH_2^+} = (\vec{k}\,\tau_{BH}\,[H_3O^+])/(1 + \vec{k}\,\tau_{BH}\,[H_3O^+] + \overleftarrow{k}\,\tau_{BH_2^+}) \quad (2)$$

where $\vec{k}$ and $\overleftarrow{k}$ are the rate constants for protonation and dissociation, respectively, in the excited state, and $\tau_{BH}$ and $\tau_{BH_2^+}$ are the respective lifetimes of excited BH and $BH_2^+$ in the absence of proton exchange. In every case, the anion as well as the neutral species and the excited cation may be present in the solution and contribute to the fluorescence so that at any point of the curve

$$F = 2.3\,\phi^0_B I_0\,\epsilon_{B^-}[B^-]\,l + 2.3\,\phi_{BH}\,I_0\,\epsilon_{BH}\,[BH]\,l + 2.3\,\phi_{BH_2^+}\,I_0\,\epsilon_{BH}\,[BH]\,l \quad (3)$$

where $F$ is the fluorescence intensity and the first, second and third terms on

the right side of eqn. (3) are the contributions of the anion $B^-$, BH and $BH_2^+$, respectively, to $F$. In these terms $\phi^0_{B^-}$, $\phi_{BH}$ and $\phi_{BH_2^+}$ are the fluorescence efficiencies of $B^-$, BH and $BH_2^+$ (the fluorescence efficiency of $B^-$ is independent of pH), $I_0$ is the intensity of the exciting light, $\epsilon_{B^-}$ and $\epsilon_{BH}$ are the molar absorptivities of $B^-$ and BH at the wavelength of excitation, $[B^-]$ and [BH] represent the equilibrium ground-state concentrations of $B^-$ and BH at the pH of the solution and $l$ is the optical depth of the cell. Considering the ground-state dissociation of BH: $BH + H_2O \overset{K_a}{\rightleftharpoons} B^- + H_3O^+$, where $K_a$ is the dissociation constant of BH. $[B^-]$ and [BH] are related to $K_a$ and the formal concentration of BH, $C_{BH}$, by

$$[B^-] = C_{BH}\, K_a/([H_3O^+] + K_a)$$

and

$$[BH] = C_{BH}\, [H_3O^+]/([H_3O^+] + K_a)$$

At $pH > pK_a + 2$, where $B^-$ is the only absorbing species, $[B^-] = C_{BH}$, [BH] = 0 and $F = F^0_{B^-}$, where $F^0_{B^-} = 2.3\, \phi^0_{B^-} I_0\, \epsilon_{B^-}\, C_{BH}\, l$. At much higher acidities, where $[H_3O^+] \gg K_a$ and excited-state protonation of BH is complete, $[BH] = C_{BH}$, $[B^-] = 0$ and $F = F^0_{BH_2^+}$, where $F_{BH_2^+} = 2.3\, \phi^0_{BH_2^+} I_0\, \epsilon_{BH}\, C_{BH}\, l$. Finally, when $[H_3O^+] \gg K_a$ and no excited-state protonation of BH should occur, BH* should be the only emitting species, $[BH] = C_{BH}$, $[B^-] = 0$ and $F = F^0_{BH}$, where $F^0_{BH} = 2.3\, \phi^0_{BH}\, I_0\, \epsilon_{BH}\, C_{BH}\, l$.

Combination of eqn. (3) with the above expressions for $[B^-]$, [BH], $F^0_{B^-}$, $F_{BH_2^+}$ and $F^0_{BH}$ gives

$$F = F^0_{B^-} \frac{K_a}{[H_3O^+] + K_a} + \left[F^0_{BH}\left(\frac{\phi_{BH}}{\phi^0_{BH}}\right) + F^0_{BH_2^+}\left(\frac{\phi_{BH_2^+}}{\phi^0_{BH_2^+}}\right)\right]\frac{[H_3O^+]}{[H_3O^+] + K_a} \tag{4}$$

If excited-state proton transfer is the only bimolecular process in the excited states of BH and $BH_2^+$, then

$$\phi_{BH}/\phi^0_{BH} + \phi_{BH_2^+}/\phi^0_{BH_2^+} = 1 \tag{5}$$

Combination of eqns. (1) and (2) with (4) and (5) and subsequent rearrangement yields

$$\frac{\phi_{BH}}{\phi^0_{BH}} = \frac{1 + \overleftarrow{k}\,\tau_{BH_2^+}}{1 + \vec{k}\,\tau_{BH}\,[H_3O^+] + \overleftarrow{k}\,\tau_{BH_2^+}} = \frac{F([H_3O^+] + K_a) - F^0_{B^-} K_a - F^0_{BH_2^+}\,[H_3O^+]}{(F^0_{BH} - F^0_{BH_2^+})\,[H_3O^+]} \tag{6}$$

and

$$\frac{\phi_{BH_2^+}}{\phi^0_{BH_2^+}} = \frac{\vec{k}\,\tau_{BH}\,[H_3O^+]}{1 + \vec{k}\,\tau_{BH}\,[H_3O^+] + \overleftarrow{k}\,\tau_{BH_2^+}} = \frac{F^0_{BH}\,[H_3O^+] + F^0_{B^-} K_a - F([H_3O^+] + K_a)}{(F^0_{BH} - F^0_{BH_2^+})\,[H_3O^+]} \tag{7}$$

from which neither a general analytical nor graphical solution for $K_a$ is possible.

In the case of 9-anthroic acid, where the excited-state protonation of the carboxylic group does not overlap the ground-state dissociation process, $\vec{k}$, $\tau_{BH}$

or both are sufficiently small that in the region pH = $pK_a \pm 2$, $\vec{k}\,\tau_{BH}\,[H_3O^+]$ is vanishingly small so that $\phi_{BH}/\phi^0_{BH} = 1$ and $\phi_{BH_2^+}/\phi^0_{BH_2^+} = 0$ during the ground state process and eqns. (6) and (7) reduce to

$$K_a = (F^0_{BH} - F)\,[H_3O^+]/(F - F^0_B) \quad (8)$$

or

$$pK_a = pH - \log\,(F^0_{BH} - F)/(F - F^0_B) \quad (9)$$

which is the Henderson—Hasselbalch equation, with which the $pK_a$ can be calculated from the titration curve.

In the cases of the other acids studied, the two overlapping processes could be separated by adding iodide. Encounters with iodide and other ions of high atomic number promote singlet—triplet intersystem crossing and, thereby, non-radiative deactivation of the excited singlet states of many compounds, resulting in shortening of the lifetimes and quenching of the fluorescence. As $\tau_{BH}$ and $\tau_{BH_2^+}$ are shortened, $\vec{k}\,\tau_{BH}\,[H_3O^+]$ and $\overleftarrow{k}\,\tau_{BH_2^+}$ become smaller, so that higher values of $[H_3O^+]$ are required to cause significant variation of $\phi_{BH}/\phi^0_{BH}$ and $\phi_{BH_2^+}/\phi^0_{BH_2^+}$ with pH. When the concentration of the quencher is high enough, $\vec{k}\,\tau_{BH}\,[H_3O^+]$ and $\overleftarrow{k}\,\tau_{BH_2^+}$ become negligible near pH = $pK_a \pm 2$ and this also reduces eqns. (6) and (7) to eqn. (8), when the two processes become separated. For 1-naphthoic acid this is shown graphically in Fig. 1. After separation of the ground-state and excited-state prototropic processes, the $pK_a$ values of the ground-state dissociation of the anthroic and naphthoic acids can be extracted from the fluorimetric titration curves by monitoring the disappearance of the 1-, 2- and 9-anthroate ions at 432 nm, 405 nm and 408 nm,

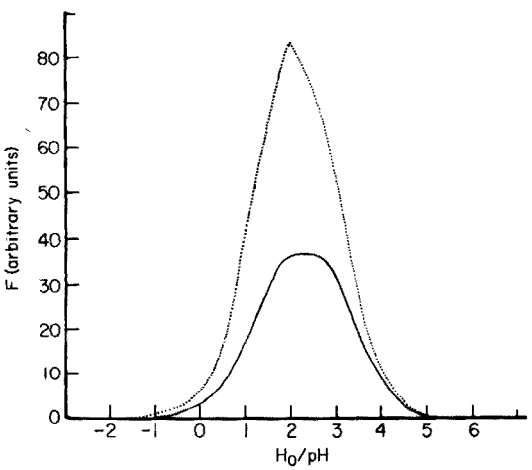


Fig. 1. pH dependence of the fluorescence at 390 nm of 1-naphthoic acid in water. No resolution of the ground-state dissociation and the excited-state protonation is accomplished in the absence of iodide (.....), while the two processes are separated in the presence of $2 \times 10^{-2}$ M iodide (——).

TABLE 2

$pK_a$ values of some naphthoic and anthroic acids, extracted from the fluorimetric titration curves. Comparison of these values with literature data.

| Compound | $pK_a$ | |
|---|---|---|
| | Found[a] | Literature[b] |
| 1-Naphthoic acid | 3.60 ± 0.06 | 3.70 |
| 2-Naphthoic acid | 4.22 ± 0.05 | 4.17 |
| 1-Anthroic acid | 3.71 ± 0.04 | 3.69 |
| 2-Anthroic acid | 4.08 ± 0.05 | 4.18 |
| 9-Anthroic acid | 2.74 ± 0.04 | 3.65, 2.4, 3.0 |

[a] Average of 8 points of the fluorimetric titration curve.
[b] See text for references.

respectively, and the appearance of the neutral acids at 390 nm and 394 nm for 1- and 2-naphthoic acid, respectively. These $pK_a$ values are listed in Table 2. They are corrected for the influence of the ionic strength, because

$$K_a = a_{H_3O^+}\, a_{B^-}/a_{BH} \approx a_{H_3O^+}\, [B^-]\, \gamma_{B^-}/[BH] \qquad (10)$$

where $a_{H_3O^+}$ is the activity of the hydronium ions, obtained by measuring the pH, $\gamma_{B^-}$ is the activity coefficient of the anion, and $[B^-]$ and [BH] are the equilibrium concentrations of the anion and the neutral acid, respectively. $\gamma_{B^-}$ is calculated from the Debye–Hückel equation [13]: $-\log \gamma_{B^-} = 0.51\, \mu^{\frac{1}{2}}/1 + \mu^{\frac{1}{2}}$, where $\mu$ represents the ionic strength of the solution. The data obtained are in good agreement with the literature values, as Table 2 shows. The only exception is 9-anthroic acid, for which compound different $pK_a$ values have been reported by different authors [5, 6, 14]. These differences are probably due to the low solubility of the compound, causing difficulties in the measurement of pH, changes in absorbance and conductivity, etc. Fluorimetry, as a more sensitive technique, permits the accurate determination of much lower concentrations of the acid, which probably makes the present values more reliable.

Attempts have been made to determine $pK_a$ values of the acids at higher temperatures. Iodide as a quencher can be used up to 35°C. Above this temperature the iodide is substantially oxidized, especially at lower pH, and the values thus obtained become unreliable.

REFERENCES

1 J. G. Ives, J. Chem. Soc., (1933) 731.
2 J. F. J. Dippy and F. R. Williams, J. Chem. Soc., (1934) 1888.
3 J. F. J. Dippy, S. R. C. Hughes and J. W. Laxton, J. Chem. Soc., (1954) 1470.
4 T. C. Werner and D. M. Hercules, J. Phys. Chem., 73 (1969) 2005.
5 S. G. Schulman, in Modern Fluorescence Spectroscopy, Plenum Press, New York, 1976, Vol. 2, p. 247.
6 C. A. Carlson, J. Chem. Soc., (1930) 1932.
7 K. Lauer, Ber. Deut. Chem. Ges., 70B (1937) 1288.
8 A. R. Watkins, J. Chem. Soc., Faraday Trans. 1, 68 (1972) 28.

9 S. G. Schulman and I. Pace, J. Phys. Chem., 76 (1972) 1966.
10 S. G. Schulman, A. C. Capomacchia, W. L. Paul, P. J. Kovi and J. F. Young, Z. Phys. Chem., N.F., 87 (1973) 308.
11 A. Weller and W. Urban, Angew. Chem., 66 (1954) 336.
12 S. G. Schulman and R. J. Sturgeon, Anal. Chim. Acta, 93 (1977) 239.
13 R. G. Bates, Determination of pH, Theory and Practice, J. Wiley, New York, Second printing, 1965, p. 11.
14 E. Vander Donckt and G. Porter, Trans. Faraday Soc., 64 (1968) 3218.

*Analytica Chimica Acta*, 105 (1979) 319—325


# SEMI-AUTOMATED FLUORIMETRIC DETERMINATION OF NANOGRAM QUANTITIES OF SELENIUM IN BIOLOGICAL MATERIAL

J. H. WATKINSON

*Ministry of Agriculture and Fisheries, Soil and Field Research Organisation, Ruakura Agricultural Research Centre, Hamilton (New Zealand)*

(Received 6th July 1978)

## SUMMARY

A semi-automated method, based on the solvent extraction and fluorescence of 4,5-benzopiazselenol, is described for the determination of selenium in biological material. Samples, in batches of up to 150, are digested in a mixture of nitric and perchloric acids in temperature-controlled aluminium blocks. Selenate formed in the perchloric acid is reduced to selenite with hydrochloric acid. Metal ion interferences, including hydroxide adsorption of selenite, are prevented by ethylenediaminetetraacetic acid. Sulphate above 50 mM precipitates the 2,3-diaminonaphthalene, so wool digests were diluted accordingly. The digests are analysed from their digestion tubes at the rate of 40 per hour by the semi-automated method. Results for blood and a variety of food samples compare favourably with those obtained by other methods including hydride/atomic absorption and instrumental neutron-activation analysis.

Farm animals in New Zealand, particularly the young, are likely to be deficient in selenium if their blood and/or associated diet contain less than 15 ng Se $ml^{-1}$ and 30 ng Se $g^{-1}$, respectively [1—3]. Research into selenium deficiencies in these animals therefore requires the measurement of selenium at the nanogram level in relatively large numbers of biological samples. The present paper describes the application of a sensitive semi-automated method [4], based on the fluorescence of 4,5-benzopiazselenol, to the determination of selenium in biological material. It has been used, with some modifications [5], over a period of more than three years, for the measurement of selenium in over 15 000 samples.

## EXPERIMENTAL

### *Apparatus*

*Digestion units.* In the development of a suitable digestion procedure, aluminium bars (66 mm × 38 mm × 38 mm) were drilled to hold twenty-one 16 × 100-mm Pyrex digestion tubes, which were selected and cut to fit the standard AutoAnalyzer sample tray. The holes (16.5 mm diameter, 17 mm deep) were spaced at 30 mm along the bars. Four bars were placed together on an aluminium block heated by two 1-kW elements in the base, with the temperature

controlled electronically to within 5°C. The temperatures of the acid digests at different places in the block were also within about 5°C of each other.

For plant and other samples that froth during acid digestion, 25 ml graduated (20 × 150 mm) Pyrex tubes were used. The number and spacing of the holes (22 mm diameter, 25 mm deep) in the bars were as for the smaller tubes.

A block was later designed to hold 110 tubes (10-ml graduated, with ground glass sockets) in five rows of 22 tubes. The spacing was as for the 16 × 100 mm tubes, but the hole was 17.5 mm in diameter and 30 mm deep.

*Digestion tubes.* A 16 × 100 mm size was chosen initially as it fits into a standard Technicon AutoAnalyzer sampler tray, and conveniently holds 10 ml of digest, so that no transfer of solution is necessary. (Dilution to less than 10 ml can cause the ammonium perchlorate to crystallize.) The tube is relatively small so that care is needed to avoid physical loss from frothing or spray.

Graduated 25-ml tubes (20 × 150 mm) were used initially for samples that froth badly, such as dried plant material. Their use does, however, mean an extra transfer of digest to the 3.5-ml AutoAnalyzer plastic cups.

Plant samples can be digested satisfactorily in 10-ml graduated tubes (17 × 125 mm) and placed directly on the AutoAnalyzer by modifying the standard tray. This permits the analysis of most types of biological sample on one block without transfer of digest.

All new glassware was cleaned in a hot mixture of nitric and sulphuric acids before use. Prolonged digestion of perchloric acid in each tube was often necessary to remove residual selenium from their internal walls. Anti-bumping granules were boiled in perchloric acid.

*Digest analysis unit.* This consisted of the sequence: Technicon Sampler IV, Technicon Pump III, Technicon heating bath cartridge, Turner fluorimeter model 111 with Automated Chemistry Adapter, and Rikadenki "Kasset" strip-chart recorder. They were used with the Pyrex glass probe, Technicon T-connector type A2 as phase separator, modified flow cell and optical filters as described previously [4, 5]. The AutoAnalyzer flow scheme was as described by Watkinson and Brown [5].

*Reagents*

All reagents were of analytical or spectroscopic grade, except for ethylenediaminetetraacetic acid (EDTA) which was of technical grade [6], and 2,3-diaminonaphthalene (DAN) in 0.1 M HCl which was prepared as described by Watkinson and Brown [5]. Nitric acid was further purified by distillation.

*Procedures*

*Blood.* Transfer up to 3 ml of blood (with heparin as anti-coagulant) to a Pyrex tube with an automatic diluting machine, the sample being flushed out of the diluter with the minimum amount of water. Add 3.5 ml of a mixture of (5 + 2) $HNO_3$—$HClO_4$, one drop of kerosene, and 2 anti-bumping granules

(approximately 10 mg). Heat from ambient temperature to 150°C in the digestion block, avoiding frothing more than two thirds up the tube. Keep at 150°C until the volume is reduced to less than 3.5 ml, and then gradually raise the temperature to 190°C. When the vigorous reaction at low concentration of nitric acid has ceased, and perchloric acid fumes appear, raise the temperature to 210—215°C. Digest for 30 min after the last trace of nitric acid condensate on the upper part of the tubes is no longer evident. Remove the tubes and allow to cool to ambient temperature while the block cools to 160°C.

Add 0.2 ml of (1 + 1) HCl to each digest with mixing, and place on the block at 140—160°C for at least 5 min. (If nitrogen dioxide is observed, add a further 0.2 ml of (1 + 1) HCl.) Remove, allow to cool, add an anti-bumping granule, and 2 ml of (1 + 1) ammonia solution containing 0.02 M EDTA and 0.001% bromocresol purple. Place on the block previously set at 130°C, increasing the temperature to 135°C after the initial vigorous evolution of gas. Continue to boil off the excess of ammonia until the indicator changes in colour from purple to a distinct yellow. When neutral, mix in 5 ml of 0.1 M HCl as each tube is removed from the block. When cool, dilute to 10 ml with water, and place in the Technicon AutoAnalyzer tray.

*Plant material.* Weigh up to 0.5 g of ground plant material into a 20 × 150 mm Pyrex tube. Add acid, etc., as for blood, but digest less rapidly initially to avoid excessive frothing. (If stood overnight the kerosene may be omitted.) Ensure that all solids on wall of tube are returned to digest. Check for soil contamination, registered as a deeper brown colour, immediately after most solid has dissolved; specks of sand may also be observed. (Soil can erroneously enhance the selenium value). Heat at 150°C to boil off most of the nitric acid, and then increase the temperature gradually to 190°C, interchanging slower and faster boiling tubes where necessary, to avoid charring. If a sample begins to char, add nitric acid (70% w/w) dropwise to decolourize. Continue as for blood samples except that at the end of the step in which ammonia is removed, rinse down the walls of the tube with water to check if all ammonia in the condensate has been removed. After dilution to 10 ml in the tube, transfer to 3.5-ml plastic cups in the AutoAnalyzer sampler tray.

*Other samples.* Solid samples are generally digested as for plant material. Samples high in fat, including milk, are digested a little more slowly. Wool (3.5% S) can give rise to sulphate interference (see later).

*Analysis of digests.* The reagents are pumped according to the flow diagram in Watkinson and Brown [5], except that initially (1) 0.1 M hydrochloric acid is pumped in place of the DAN reagent (to conserve the reagent) and (2) the nipple joint (N18) in the polythene line connecting phase separator to flow cell is disconnected. Any 0.1 M hydrochloric acid passing through the separator during the time for the apparatus to reach a steady state is run directly to waste. At the same time, petroleum ether—ethanol (10% v/v) is passed through the flow cell to ensure it is clean; and this is followed by cyclohexane.

When a steady state is reached, the polythene tubing from the phase

separator is cleared of any aqueous phase with ethanol, and then reconnected to the nipple joint (N18); pumping of the recently shaken DAN reagent is then started.

Normally the system is operated so that 10 ng Se $ml^{-1}$ registers full scale deflection. Digests more concentrated than this are rerun either diluted or at a lower instrumental sensitivity. Samples less than 25% of the preceding sample value are correspondingly enhanced [4], and are also rerun.

At the end of the analysis, the system is cleared of DAN with 0.1 M hydrochloric acid (to avoid deposits of DAN polymer), the polythene solvent line is disconnected at the stainless steel nipple, and the flow cell is flushed with petroleum ether—ethanol (10% v/v).

## RESULTS AND DISCUSSION

### *Recovery of selenium from standards*

Recoveries of selenous acid from 20 consecutive batches taken through to the diluted digest averaged 98.5%, with a standard deviation of 1.5%. The main loss is 1.5% during the digestion in perchloric acid ($^{75}Se$ recoveries).

### *Digestion in nitric—perchloric acid*

Vigorous boiling in the small tubes (16 × 100 mm) at block temperatures above 150°C while the sample contains appreciable amounts of water, e.g. from blood, causes losses in spray up to 11%, and averaging 6% ( from $^{75}Se$ recoveries). For this reason the digest is boiled down to 3.5 ml at 150°C.

The amount of nitric acid in the mixture is critical for several reasons. Most of the organic material is oxidized by nitric acid and therefore it is important not to boil it off so quickly that samples char. Although charring has not been accompanied by loss of selenium [6] under present conditions, even when losses were checked with selenium-75, further nitric acid is required to clear the digest rapidly. An indication of the amount of nitric acid that will remain in the digest at a given temperature is given in Table 1. As the temperature is raised to 150°C from about 125°C, over 90% of the nitric acid is boiled off. The reaction becomes quite vigorous as the amount of nitric acid decreases to about 0.1 ml. Residual nitric acid must then be removed to avoid later incomplete reduction of selenate; for example, 0.1 ml of nitric acid reduces recoveries to only 30—60%. Adding a further 0.2 ml of (1 + 1)

TABLE 1

Approximate boiling point and composition of $HNO_3$—$HClO_4$ mixtures

| B.P. (°C) | 125 | 150 | 165 | 190 | 203 |
|---|---|---|---|---|---|
| $HNO_3$ (ml)[a] | 2.5 | 0.2 | 0.1 | 0.02 | 0 |
| $HClO_4$ (% w/w) | 25 | 60 | 65 | 70 | 72 |

[a]ml of 68% $HNO_3$ remaining in digest.

HCl, or 0.4 ml initially, gives a quantitative recovery; hence if fumes of nitrogen dioxide are observed on adding the (1 + 1) HCl, a second addition should be made. (Residual nitric acid also produces a strong yellow colour on adding the ammoniacal EDTA reagent.) At 190°C only a little nitric acid is left in the digest, and the real problem is to remove the condensate from the cooler upper wall of the tubes. This can be achieved by raising the block temperature to about 10°C above the boiling point of perchloric acid; protecting the tubes from the cool air removing the acid fumes also helps.

The 30-minute digestion with perchloric acid not only ensures complete removal of nitric and nitrous acids, but also complete oxidation of any fluorescent organic compounds, and the conversion of organic forms of selenium to selenous acid, particularly the resistant trimethylselenonium ion [7]. At the same time about half of the selenous acid is oxidized to selenate, although at 190°C the amount of selenate formed is negligible.

The selenate is reduced back to selenite by hydrochloric acid; 0.1—0.6 ml of (1 + 1) HCl gives quantitative reduction. The (1 + 1) HCl also dissolves any iron perchlorate deposited from the concentrated perchloric acid. Above 160°C, solution is lost through vigorous effervescence on addition of the (1 + 1) HCl. Even at a block temperature of 120—160°C, the loss is 2% ($^{75}$Se recoveries), hence digests must be cooled to ambient temperature before the acid is added.

*Complexation, and acidity adjustment*

Because of the varying amount of perchloric acid remaining in each tube after acid digestion, the pH adjustment for the DAN reaction in batch operation was done by neutralizing with ammonia, volatilizing the excess, and adding a constant amount of acid.

The amount of EDTA is sufficient to complex the amounts of the interfering metal ions [4] normally encountered, including iron(III) from blood (about 10 mM Fe). For plants containing more than 1% calcium, some calcium precipitates as the hydroxide and redissolves on acidifying. This does not affect the selenium values (Bowen's standard kale, 4.1% Ca, Table 2). A small amount of calcium phosphate (identified by x-ray fluorescence) also precipitates from most plant digests on adding the ammoniacal EDTA reagent. This carries down about 10—40% of the selenium (labelled with $^{75}$Se), but both the selenium and the precipitate redissolve on acidifying.

*Interference of sulphate in the AutoAnalyzer procedure*

DAN precipitates in the flow stream of the AutoAnalyzer when the sulphate concentration in the digest is of the order of 100 mM, and depresses the recovery of selenium by about 10%. At sulphate concentrations of about 50 mM, a deposit often builds up around the DAN reagent injection point after about 20 consecutive samples, e.g. of wool digests. Further deposition can degrade the mixing of reagent and segmentation by the air bubble, giving unreliable values. The sulphate concentration can be lowered by precipitation as calcium sulphate without error, or by dilution.

TABLE 2

Comparison of methods and laboratories in the determination of selenium in food (ng $g^{-1}$)

| Sample | Proposed semi-automated fluorimetry | Instrumental neutron activation | | Manual fluorimetry | | |
|---|---|---|---|---|---|---|
| | Ruakura ($u^a$) | $r^a$ | $s^a$ | $t^a$ | $w^a$ | $v^a$ |
| IAEA oyster | 1990 | 1830 | 2140 | 2230 | 2220 | 1880 |
| Swordfish | 2830 | 2900 | 3270 | 2950 | 2900 | 2360 |
| Flounder | 1390 | 1430 | 1630 | 1440 | 1470 | 1420 |
| IAEA flour | 280 | 260 | 270 | 295 | 286 | 235 |
| Flour | 805 | 750 | 790 | 860 | 850 | 830 |
| Bowen's kale | 133 | — | — | 125 | 126 | 122 |
| NBS spinach | 37 | — | — | 45 | — | — |
| Skim milk powder | 100 | — | — | 97 | 99 | 85 |
| Slope | N.A. | 1.017 ± 0.052 | 1.173 ± 0.047 | 1.065 ± 0.020 | 1.054 ± 0.025 | 1.241 −0.00014 |
| Intercept | N.A. | −49.5 ± 89.6 | −90.6 ± 81.8 | −1.6 ± 26.4 | 2.9 ± 36.8 | −60.4 |
| Correlation coefficient | N.A. | 0.996 | 0.998 | 0.999 | 0.999 | $R$ = 0.999 |

[a]Laboratories and results from Table 9 of Ihnat and Miller [9].

*Comparison with other methods*

*Blood.* The results for seven blood samples ranging from 10 to 350 ng Se $ml^{-1}$ [8], by the proposed method (F) and the hydride generation—atomic absorption method (H) of Clinton [8], gave the relationship $C_F = -0.45 + 0.991 \times C_H$ with a correlation coefficient ($r$) of 0.9995, where $C_F$ and $C_H$ represent the values for selenium (ng $ml^{-1}$) by the two methods.

*Solid samples.* Nine samples of food, including plant leaves, flour, skim milk powder and fish were analyzed to assist in providing reference values for a collaborative study organized by the Association of Official Analytical Chemists [9]. The values obtained by the proposed method (Table 9, [9]) were within 5% of the mean values estimated as the reference levels (Table 11, [9]), where results were from more than one other laboratory. These included results by instrumental neutron-activation methods.

In a more detailed but rather limited comparison, the results from the five other reference laboratories (Table 9, [9]) were regressed against those from Ruakura, and are given in Table 2. (The results for NBS tuna are omitted because the sample was supplied and analyzed at a different time; the Ruakura results differed slightly from those reported by Ihnat and Miller [9] because of a different weighting in mean values for the analysts involved.) Laboratory $v$ appears to be different from the others in that its regression contains a quadratic term. The others are linearly related to the Ruakura results, with significance at 0.1%. However, the $F$ tests for differences between slopes of the lines are significant at 5%, suggesting that while the methods are consistent within themselves, there is an apparent lack of consistency between methods. This implies that results from the different laboratories cannot be combined readily to yield either statistical information or absolute levels.

In comparing the semi-automated with the manual method for measuring selenium in biological material, the semi-automated method is considerably faster and requires less skilled staff. It is of comparable sensitivity, accuracy and precision, and can handle the same types of samples as the manual method.

The author is grateful to C. J. Clark, Elysia K. Patterson, Gael V. Montgomery-Griffith, and Miriam T. Wingerden for analytical assistance at different times; O. E. Clinton for the hydride/atomic absorption measurements; J. E. Waller for statistical analyses; and M. W. Brown and A. J. Fraser for helpful discussions.

REFERENCES

1 E. D. Andrews, W. J. Hartley and A. B. Grant, N.Z. Vet., J., 16 (1968) 3.
2 H. C. C. Hupkens van der Elst and J. H. Watkinson, Proc. 4th Int. Peat Congr. I—IV (1972) 149.
3 E. D. Andrews, K. G. Hogan and A. D. Sheppard, N.Z. Vet. J., 24 (1976) 119.
4 M. W. Brown and J. H. Watkinson, Anal. Chim. Acta, 89 (1977) 29.
5 J. H. Watkinson and M. W. Brown, Anal. Chim. Acta, 105 (1979) 451.
6 J. H. Watkinson, Anal. Chem., 38 (1966) 92.
7 O. E. Olson, I. S. Palmer and E. E. Cary, J. Assoc. Off. Anal. Chem., 58 (1975) 117.
8 O. E. Clinton, Analyst, 102 (1977) 187.
9 M. Ihnat and H. J. Miller, J. Assoc. Off. Anal. Chem., 60 (1977) 1414.

*Analytica Chimica Acta*, 105 (1979) 327—333


# DIFFERENTIAL KINETIC ANALYSIS AND FLOW INJECTION ANALYSIS

## Part I. The *trans*-1,2-diaminocyclohexanetetraacetate complexes of magnesium and strontium

J. H. DAHL**, D. ESPERSEN and A. JENSEN*

*Department of Chemistry AD, The Royal Danish School of Pharmacy, 2 Universitetsparken, DK-2100 Copenhagen Ø (Denmark)*

(Received 4th September 1978)

SUMMARY

The flow injection principle is used in simultaneous differential kinetic analysis for magnesium and strontium ions in solution. The method is based on the acid dissociation of the *trans*-1,2-diaminocyclohexanetetraacetate complexes of magnesium and strontium ions and on the use of copper(II) ion as a scavenger. A 200-μl sample is used for a two-point kinetic assay; special consideration is given to optimizing the flow parameters. At sampling rates of 60 samples per hour, high reproducibility of measurement and relatively low reagent consumption can be achieved. The limiting factor of the method is that a rather pronounced difference must exist between the rates of reaction of the metal complexes.

The reaction rate constants of dissociation of the alkaline earth complexes of *trans*-1,2-diaminocyclohexane-N,N,N′,N′-tetraacetate (CDTA) are in the ratio of 1:6.5:96:1660 for Mg:Ca:Sr:Ba [1]. Differential kinetic analysis of mixtures of the alkaline earth ions can therefore be achieved by utilizing the differing reaction rates of dissociation of their CDTA complexes. The general reaction mechanism [1] is

$$MCDTA^{2-} + H^+ \underset{k_M^{CDTA}}{\overset{k_H^{MCDTA}}{\rightleftharpoons}} HCDTA^{3-} + M^{2+} \quad (1)$$

$$HCDTA^{3-} + Cu^{2+} \xrightarrow{k_{Cu}^{CDTA}} CuCDTA^{2-} + H^+ \quad (2)$$

where reaction (1) is the rate-determining step with a characteristic rate of dissociation for each metal complex, and reaction (2) is rapid. Copper(II) ion is added as a scavenger so as to force the acid dissociation step in reaction (1) to completion and to permit spectrophotometric observation of the extent to which reactions (1) and (2) have proceeded.

---

**Present address: Novo Industri A/S, Analytical Chemical Department, Novo Allé, DK-2880 Bagsværd, Denmark.

The rate of the exchange reaction, $v_{ex}$, leading to $CuCDTA^{2-}$ is given by $v_{ex} = k_H^{MCDTA}[H^+][MCDTA^{2-}]$, provided that $k_{Cu}^{CDTA}[Cu^{2+}] \gg k_M^{CDTA}[M^{2+}]$ (cf. ref. [1]). It has been shown in previous studies [1, 2] that the rate of dissociation, $k_d$, in the pH range 7—9 can be calculated from $k_d = k^{MCDTA} + k_H^{MCDTA}[H^+]$. The rate expression for an exchange reaction of a mixture of alkaline earth complexes at a fixed hydrogen ion concentration (i.e. under pseudo first-order reaction conditions) can be expressed by

$$d[CuCDTA^{2-}]/dt = k_d^{MgCDTA}[MgCDTA^{2-}] + k_d^{CaCDTA}[CaCDTA^{2-}] + k_d^{SrCDTA}[SrCDTA^{2-}] + k_d^{BaCDTA}[BaCDTA^{2-}] \quad (3)$$

Pausch and Margerum [1] have reported differential kinetic analysis for the alkaline earth—CDTA complexes, using either classical spectrophotometry or stopped-flow spectrophotometry. In practice, only three of the four terms in eqn. (3) contribute significantly to the rate for any given condition, because the ratio of the rate constants $k_d^{BaCDTA}/k_d^{MgCDTA}$ is very large. Pausch and Margerum were, therefore, unable to determine more than three alkaline earth metal ions during one analysis.

Over the last few years flow injection analysis (f.i.a.) [3] has been developed. The purpose of this paper is to show that the flow injection system can be utilized in connection with differential kinetic analysis. The example taken is the determination of magnesium and strontium ions by applying CDTA as the ligand and measuring the colour intensity of a scavenger CDTA complex at two consecutive stations in the flow stream and at suitable time intervals. The method involves a fast and direct injection of the sample into a continuously moving carrier stream without air segmentation. The various parameters that influence the method have recently been examined [4] in order to minimize the consumption of reagents, but at the same time to maintain the high sampling frequency and good precision and accuracy that are characteristic of the flow injection system.

As the f.i.a. method is relatively inexpensive, it has proved useful in practical applications in fields as varied as water and environmental control [5, 6], clinical chemistry [7—9] and agricultural analysis [9—14].

## EXPERIMENTAL

### *Reagents*

All chemicals were of analytical-reagent grade and redistilled water was used throughout. The racemic form of $H_4CDTA$ was recrystallized by dissolution in ammonia followed by addition of dilute nitric acid, filtration and drying at 105°C for 18 h. A standard zinc sulphate solution was used to titrate CDTA (eriochrome black indicator). The metal salts used were all nitrates and were standardized by compleximetric titration with EDTA.

The reagent in the flow system contains $4.00 \times 10^{-2}$ M $Cu(NO_3)_2$ and $2.00 \times 10^{-1}$ M β-alanine, with 2% (v/v) glycerine added, the mixture being adjusted to pH 10.50 with NaOH.

The carrier in the flow system consists of $5.00 \times 10^{-3}$ M β-alanine, with 2% (v/v) glycerine added, the solution being adjusted to pH 10.50 with NaOH.

The standards contain $1.60 \times 10^{-3}$ M CDTA, $5.00 \times 10^{-3}$ M β-alanine and 2% (v/v) glycerine, and are adjusted to pH 10.50 with NaOH; appropriate amounts of magnesium nitrate and strontium nitrate are added to cover a concentration range of $2.00 \times 10^{-4}$—$1.60 \times 10^{-3}$ M $M(NO_3)_2$.

*Apparatus*

Two Beckman DU spectrophotometers modified by means of a d.c. amplifier to a digital display instrument [15], were equipped with a Hellma flow-through cuvette, type 178-QS (volume 80 μl, light path 10 mm). The spectrophotometers were connected to a Servograph REC 61 recorder, furnished with a REA 112 high-sensitivity unit (Radiometer A/S).

An Ismatec Model mp-4 pump (Ismatec S/A) was operated at a speed which corresponded to a flow rate of 2.4 ml $min^{-1}$; the speed was kept constant by means of a servospeed regulator. The tubes (Technicon White/White) had an i.d. of 1.02 mm.

The samples were injected by means of an injection port [16] consisting of a precisely made rotary valve and a loop of a total volume of 200 μl, furnished with a bypass of higher flow resistance. Thus, while the sample was being introduced into the volumetric bore and loop with a syringe, the carrier solution continuously bypassed the injection port. Only when the valve had been turned did the stream in the bypass come to a standstill, and the precise amount of sample solution was injected by the carrier stream from the volumetric bore and loop into the reaction line.

*Manifolds*

The manifolds (Fig. 1) were made from polyethylene tubing (1.0 mm i.d.) and Lego building blocks as described earlier [3]. The different mixing coils

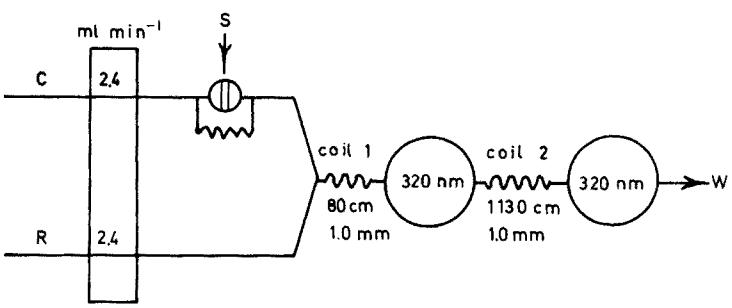


Fig. 1. Flow injection manifold for the spectrophotometric determination of magnesium and strontium ions. S = Point of injection (200-μl samples), W = waste. All tube lengths are given in cm and the internal diameters in mm. Reagent (R) contains $4.00 \times 10^{-2}$ M $Cu(NO_3)_2$, $2.00 \times 10^{-1}$ M β-alanine, 2% (v/v) glycerine; pH 10.50. Carrier (C) contains $5.00 \times 10^{-3}$ M β-alanine, 2% (v/v) glycerine, pH 10.50. $\mu = 0.3$; 22°C.

were made from polyethylene tubing by winding an appropriate length around perspex tubes (13 and 25 mm i.d.). The different connections needed (Y-shape etc.) were made by drilling conical holes in perspex blocks of appropriate size.

*Measuring procedures*

The manifold shown in Fig. 1 was used for the simultaneous determination of magnesium and strontium ions, by measuring spectrophotometrically the formed CuCDTA complex (cf. reactions 1 and 2). Both metal ions can be determined by carrying out two measurements at suitable time intervals by means of the two spectrophotometers.

The system used (Fig. 1) allows the first analysis to be done after the CuCDTA-forming reaction has passed through the 80-cm mixing coil (coil 1). The amount of MgCDTA which has dissociated at this point need not be taken into account, but 2—4% of the amount of SrCDTA (measured experimentally) will inevitably dissociate. This slight dissociation of the strontium complex must occur in the flow system used; a mixing coil shorter than 80 cm (which would be ideal from a dissociation point of view) does not allow complete mixing of the segment to be analyzed and this causes a pronounced instability of the base line. Thus it is possible to obtain an absorbance reading after coil 1 which can be directly related to the total concentration of magnesium and strontium ions. In order to avoid excessive errors in the analysis of solutions containing large concentration ratios of magnesium to strontium ions, the standards were prepared from solutions containing equivalent concentrations of magnesium nitrate and strontium nitrate.

The absorbance reading after coil 2 was carried out after a time interval, during which the dissociation of MgCDTA can still be neglected ($k_d^{MgCDTA} = 2.4 \times 10^{-5}\ s^{-1}$ [17]) whereas approximately 50% of the SrCDTA has dissociated ($k_d^{SrCDTA} = 4.2 \times 10^{-3}\ s^{-1}$ [17]).

## RESULTS AND DISCUSSION

Figures 2a and 2b show a photographic reproduction of a routine run with the manifold from Fig. 1, depicting a series of standards containing $1.60 \times 10^{-3}$ M CDTA and varying concentrations of $M(NO_3)_2$. The rate of analysis was about 30 determinations per hour, but could easily have been increased to about 60 per hour, because it is unnecessary to reach the base line between each determination. Excellent reproducibility of measurement and high base-line stability were obtained.

The calibration graphs constructed from the absorbance readings after coil 1 can be used for a direct determination of the total concentration of magnesium and strontium ions. The absorbance reading after coil 2 corresponds to the original excess of CDTA plus the amount of SrCDTA which has by then undergone dissociation. The absorbances determined after coil 2 must accordingly be corrected for the absorbance corresponding to the

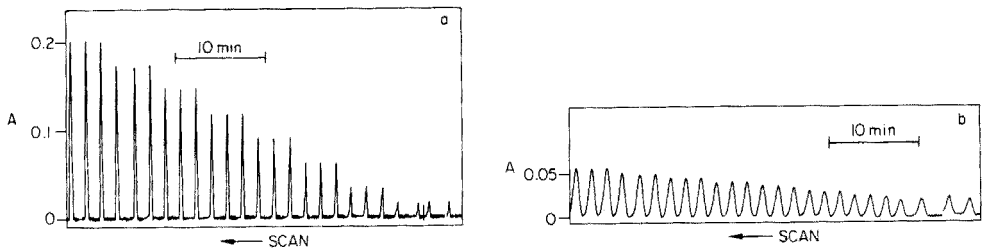


Fig. 2. Routine analysis for magnesium and strontium ions with the flow injection manifold of Fig. 1. From right to left is shown a set of aqueous standards ($7.00 \times 10^{-4}$ M $Mg(NO_3)_2$ + $7.00 \times 10^{-4}$ M $Sr(NO_3)_2$ to $1.00 \times 10^{-4}$ M $Mg(NO_3)_2$ + $1.00 \times 10^{-4}$ M $Sr(NO_3)_2$; $1.60 \times 10^{-3}$ M CDTA). All solutions were analyzed in triplicate. The sampling rate shown in the analysis was approximately 30 determinations per hour. (a) Absorbance readings after coil 1; (b) absorbance readings after coil 2.

original excess of CDTA, and standards containing $2.00 \times 10^{-4}$ to $1.60 \times 10^{-3}$ M CDTA were prepared for this purpose. The calibration graphs were calculated from the absorbances read on the two spectrophotometers by the least-squares method on a Wang 370-2 programmable electronic calculator.

The total concentrations of magnesium nitrate and strontium nitrate, $M(NO_3)_2$, were calculated from

$$[M(NO_3)_2] = (A_I - b_{M(NO_3)_2})/a_{M(NO_3)_2} \quad (4)$$

where $A_I$ is the absorbance reading after coil 1, $a_{M(NO_3)_2}$ is the slope and $b_{M(NO_3)_2}$ is the intercept of the calibration graph for the first measuring station.

The concentration of strontium nitrate was calculated from

$$[Sr(NO_3)_2] = \{A_{II} - ((0.0016 - [M(NO_3)_2])a_{CDTA} + b_{CDTA}) - b_{Sr(NO_3)_2}\}/a_{Sr(NO_3)_2} \quad (5)$$

where $A_{II}$ is the absorbance reading after coil 2; $a_{CDTA}$ is the slope and $b_{CDTA}$ is the intercept of the calibration graph for the standards containing varying amounts of CDTA and obtained from absorbance readings after coil 2; $a_{Sr(NO_3)_2}$ is the slope and $b_{Sr(NO_3)_2}$ is the intercept of the calibration graph also obtained from absorbance readings after coil 2, after correction of these readings for the excess of CDTA. The term 0.0016 in eqn. (5) originates from the constant concentration of CDTA in all solutions, i.e. $1.60 \times 10^{-3}$ M. $[M(NO_3)_2]$ is the total concentration of magnesium and strontium nitrate calculated from eqn. (4).

Table 1 shows the results obtained for the total concentration of magnesium and strontium nitrate and for the individual concentrations of these metal nitrates. The total concentrations of the two metal nitrates were determined with a high degree of accuracy, cf. Table 1. The individual concentrations of magnesium and strontium nitrate, respectively, were, however, determined with relatively large errors especially when the concentration of strontium nitrate was small compared to the concentration of magnesium

TABLE 1

Spectrophotometric determinations of magnesium and strontium ions with the flow injection system as applied to differential kinetic analysis

| Sample | $[M(NO_3)_2$ (total)] ($\times 10^{-4}$ M) | Error (%)[a] | $[Sr(NO_3)_2]$ ($\times 10^{-4}$ M) | Error (%)[a] | $[Mg(NO_3)_2]$ ($\times 10^{-4}$ M) | Error (%) |
|---|---|---|---|---|---|---|
| $2.00 \times 10^{-4}$ M $Sr(NO_3)_2$ + $4.00 \times 10^{-4}$ M $Mg(NO_3)_2$ | 6.29 | +4.8 | 1.93 | −3.5 | 4.36 | +9.0 |
| $4.00 \times 10^{-4}$ M $Sr(NO_3)_2$ + $8.00 \times 10^{-4}$ M $Mg(NO_3)_2$ | 12.12 | +1.0 | 4.73 | +18.3 | 7.39 | −7.6 |
| $8.00 \times 10^{-4}$ M $Sr(NO_3)_2$ + $4.00 \times 10^{-4}$ M $Mg(NO_3)_2$ | 11.86 | −1.2 | 7.82 | −2.3 | 4.04 | +1.0 |
| $3.00 \times 10^{-4}$ M $Sr(NO_3)_2$ + $9.00 \times 10^{-4}$ M $Mg(NO_3)_2$ | 12.10 | +0.8 | 3.53 | +17.7 | 8.57 | −4.8 |
| $9.00 \times 10^{-4}$ M $Sr(NO_3)_2$ + $3.00 \times 10^{-4}$ M $Mg(NO_3)_2$ | 11.69 | −2.6 | 8.68 | −3.6 | 3.01 | +0.3 |
| $2.00 \times 10^{-4}$ M $Sr(NO_3)_2$ + $8.00 \times 10^{-4}$ M $Mg(NO_3)_2$ | 9.86 | −1.4 | 2.13 | +6.5 | 7.73 | −3.4 |
| $8.00 \times 10^{-4}$ M $Sr(NO_3)_2$ + $2.00 \times 10^{-4}$ M $Mg(NO_3)_2$ | 9.67 | −3.3 | 7.51 | −6.1 | 2.16 | +8.0 |
| $2.00 \times 10^{-4}$ M $Sr(NO_3)_2$ + $2.00 \times 10^{-4}$ M $Mg(NO_3)_2$ | 4.04 | +1.0 | 2.18 | +9.0 | 1.86 | −7.0 |
| $4.00 \times 10^{-4}$ M $Sr(NO_3)_2$ + $4.00 \times 10^{-4}$ M $Mg(NO_3)_2$ | 8.02 | +0.3 | 3.96 | −1.0 | 4.06 | +1.5 |
| $6.00 \times 10^{-4}$ M $Sr(NO_3)_2$ + $6.00 \times 10^{-4}$ M $Mg(NO_3)_2$ | 11.96 | −0.3 | 5.61 | −6.5 | 6.35 | +5.8 |

[a]Relative error from the true concentration taken.

nitrate. This analytical drawback of the method can be attributed to the small amount of the strontium complex which has dissociated before the absorbance reading after coil 1. Furthermore, errors must necessarily be larger in the analysis of solutions containing much less strontium nitrate than magnesium nitrate because the calibration graphs were calculated on the basis of solutions containing equivalent concentrations of the two nitrates. Yet the errors observed are much smaller than those obtained when the calibration graphs were constructed on the basis of solutions containing strontium nitrate only.

The flow injection system was also used for analysis of a mixture of magnesium and calcium nitrates, based on the principle described above. The total concentrations of magnesium and calcium ions were determined with a degree of accuracy similar to that shown in Table 1 for magnesium and strontium ions. The individual metal ions (magnesium and calcium) can be estimated but the errors are large. The reason for this inaccuracy is that a finite fraction of the magnesium complex has dissociated before the absorbance reading after coil 2, and as the ratio between $k_d^{MgCDTA}$ and $k_d^{CaCDTA}$ is only 6.5 [1], the dissociation of MgCDTA is not insignificant compared to that of CaCDTA.

## CONCLUSION

The flow injection system has proved to be suitable for simultaneous differential kinetic determinations of magnesium and strontium ions in solution. The analysis is based on acid dissociation of the CDTA complexes of these two ions and on the use of an excess of copper(II) ion as scavenger. Analysis can be done at a rate of 60 samples per hour with very modest reagent consumption. The limiting factor in the combination of flow injection with differential kinetic analysis is that there must be a rather pronounced difference between the rates of reaction of the metal complexes in question. The necessary difference is not found in the rates of dissociation of the magnesium and calcium complexes of CDTA, i.e. magnesium and calcium ions cannot be determined with reasonable accuracy.

The next paper of this series will be devoted to a novel way of combining the flow injection system with differential kinetic analysis of selected alkaline earth ions.

The authors express their appreciation for fruitful and inspiring discussions with Professor J. Růžička and Dr. E. H. Hansen, Chemistry Department A, The Technical University of Denmark.

## REFERENCES

1 J. B. Pausch and D. W. Margerum, Anal. Chem., 41 (1969) 226.
2 D. W. Margerum, P. J. Menardi and D. L. Janes, Inorg. Chem., 6 (1967) 283.
3 J. Růžička and E. H. Hansen, Anal. Chim. Acta, 78 (1975) 145.
4 J. Růžička and E. H. Hansen, Anal. Chim. Acta, 99 (1978) 37.
5 J. Růžička, J. W. B. Stewart and E. A. Zagatto, Anal. Chim. Acta, 81 (1976) 387.
6 E. H. Hansen, A. K. Ghose and J. Růžička, Analyst, 102 (1977) 714.
7 E. H. Hansen and J. Růžička, Anal. Chim. Acta, 87 (1976) 353.
8 E. H. Hansen, J. Růžička and B. Rietz, Anal. Chim. Acta, 89 (1977) 241.
9 J. Růžička, E. H. Hansen and E. A. Zagatto, Anal. Chim. Acta, 88 (1977) 1.
10 J. Růžička and J. W. B. Stewart, Anal. Chim. Acta, 79 (1975) 79.
11 J. W. B. Stewart, J. Růžička, H. Bergamin Filho and E. A. Zagatto, Anal. Chim. Acta, 81 (1976) 371.
12 J. W. B. Stewart and J. Růžička, Anal. Chim. Acta, 82 (1976) 137.
13 F. J. Krug, M. Bergamin Filho, E. A. G. Zagatto and S. S. Jørgensen, Analyst, 102 (1977) 503.
14 E. H. Hansen, F. J. Krug, A. K. Ghose and J. Růžička, Analyst, 102 (1977) 714.
15 B. Nielsen and K. Eberth, Arch. Pharm. Chemi. Sci. Ed., 2 (1974) 130.
16 J. Růžička, E. H. Hansen, M. Mosbæk and F. J. Krug, Anal. Chem., 49 (1977) 1858.
17 N. R. Larsen and A. Jensen, Acta Chem. Scand., A28 (1974) 638.

*Analytica Chimica Acta*, 105 (1979) 335—351


# ORGANIC INTERFERENCES AND THEIR ELIMINATION IN THE 2,4-XYLENOL SPECTROPHOTOMETRIC METHOD FOR NITRATE

GEORGE NORWITZ, JOHN FARINO and PETER N. KELIHER*

*Chemistry Department, Villanova University, Villanova, Pa. 19085 (U.S.A.)*

(Received 18th September 1978)

SUMMARY

The 2,4-xylenol spectrophotometric method for nitrate involves formation of 6-nitro-2,4-xylenol, which is steam-distilled into an ammonia—water—isopropanol mixture. The yellow color of the ammonium salt of 6-nitro-2,4-xylenol is measured at 455 nm. A detailed study of the possible interferences from 123 representative organic compounds is described; 61 compounds interfered (when present in amounts of 0.1 g in the original sample). The interfering compounds can be classified according to their mode of interference: (1) compounds that are readily nitrated or oxidized by nitrate in the sulfuric acid medium used cause low results; (2) compounds containing the $ONO_2$ group that hydrolyze to nitrate cause high results; (3) compounds that steam-distil to produce colored solutions; (4) compounds that steam-distil to produce turbid solutions; (5) compounds that hydrolyze, either in water or sulfuric acid solution, to produce inorganic ions or compounds (e.g. $Cl^-$, $S^{2-}$, and $H_2O_2$) that repress the color development. Three procedures are described for the elimination of the interferences: (1) oxidation of the organic compound with permanganate, reduction of the excess of permanganate with hydrogen peroxide, and destruction of the peroxide by boiling in the presence of Fe(III) catalyst (this is unsuitable for organic compounds containing nitrogen, as there is invariably some oxidation to nitrate); (2) extraction of interfering organic compounds with methyl isobutyl ketone; (3) precipitation—adsorption method involving treatment with zinc sulfate and sufficient sodium hydroxide to precipitate most of the zinc as zinc hydroxide, addition of 3 g of activated carbon, digestion at 55—65°C for 20 min, cooling, dilution, and filtration. Method (3) is applicable to all organic compounds tested except formaldehyde. The amount of organic compound used to test the methods was normally 0.25 g in the solution being treated.

One of the most accurate spectrophotometric methods for the determination of nitrate is the 2,4-xylenol method involving steam distillation [1]. Recently, a comprehensive study of the interferences of inorganic substances with the method and ways of eliminating them were reported [2]. Several investigators [3—7] have pointed out that organic materials interfere with the 2,4-xylenol method for nitrate, but few specific data are available.

Organic materials interfere with practically all methods for the determination of nitrate (spectrophotometric and otherwise). The following ways of eliminating the interferences have been proposed. Oxidation of the organic compound with potassium permanganate [3, 4, 8, 9] or hydrogen peroxide [10—16] has been mainly confined to the determination of nitrate in plants.

Interfering organic compounds have been extracted with solvents, e.g. ethyl ether [17], amyl alcohol [3], and methylene chloride [18]. Various "clean-up" precipitation and/or adsorption procedures have been reported. Thus, many workers have described treatments with mixtures of metal salts, e.g. copper sulfate and sodium hydroxide [19]; copper sulfate and potassium hydroxide [20]; copper sulfate, calcium hydroxide, and magnesium carbonate [21—23]; copper sulfate, calcium hydroxide, magnesium carbonate, and carbon [24]; cadmium chloride, barium chloride, and sodium hydroxide [25, 26]; mercury(II) chloride [27, 28]; lead acetate [10, 29]; zinc sulfate and sodium hydroxide [30—36]; zinc sulfate and barium hydroxide [37]; zinc sulfate and sodium borate [9, 38]; zinc sulfate and potassium hexacyanoferrate(II) [39—42]; zinc sulfate, potassium hexacyanoferrate(II), and carbon [43]; zinc acetate and potassium hexacyanoferrate(II) [9, 44, 45]; zinc acetate, potassium hexacyanoferrate(II) and sodium hydroxide [9, 46]; sodium borate [47]; aluminum cream (prepared by adding ammonium hydroxide to potassium aluminum sulfate solution and decanting) [9, 30, 31, 48, 49]; aluminum cream and carbon [32, 50]; potassium aluminum sulfate (added to a buffered ammoniacal solution of the sample) [9, 51, 52].

Precipitation of proteinaceous matter with acids such as trichloroacetic [53—55], tungstic [23], tungstosilicic [56], or tungstophosphoric [28, 57, 58] has been recommended, as has treatment with activated carbon [59—66].

Chromatographic techniques, including ion-exchange, thin-layer and gel-filtration, have been used. Ion exchange has been applied in the separation of nitrate from organic (and inorganic material) in plants [51, 61, 62, 65, 67—72]; however, the diverse behavior of organic materials in ion-exchange is such that the method has not been useful in general. Thin-layer chromatography has been applied prior to spectrophotometric determination of nitrate [73]. Gel filtration was not successful when applied to nitrate [74]. Dialysis has been used for separating nitrate from particulate or colloidal matter, especially in automatic methods [75—78]; but the method has limited effectiveness in eliminating organic interferences in general.

Correction methods have been applied in visible [64] and u.v. [32, 79—82] spectrophotometric methods when a constant predictable value can be ascribed to a particular type of organic interference.

This paper presents a comprehensive study of the interferences of organic compounds with the 2,4-xylenol method for nitrate and proposes ways of eliminating these interferences.

## EXPERIMENTAL

### *Apparatus and reagents*

A Bausch and Lomb Spectronic 20 colorimeter and a Parnas-Wagner Kjeldahl distillation apparatus were used.

Potassium nitrate (dried at 150°C for 1 h) and other chemicals were of reagent grade.

*Standard nitrate solution* (1 ml = 0.50 mg $NO_3^-$-N). Dissolve 3.6100 g of $KNO_3$ in water and dilute to 1 l in a volumetric flask.

*Silver sulfate solution* (0.44%). Dissolve 4.40 g of $Ag_2SO_4$ in boiling water, cool, and dilute to 1 l.

*Iron(III) solution* (4.4%). Dissolve 22 g of $FeNH_4(SO_4)_2 \cdot 12H_2O$ in water containing a few drops of sulfuric acid and dilute to 500 ml with water.

*2,4-Xylenol solution* (2.5%). Dilute 5 ml of 2,4-xylenol (Eastman-Kodak) to 200 ml with acetone.

Norit A activated carbon (Matheson, Coleman, and Bell).

*Permanganate oxidation procedure (for oxidizable organic compounds, e.g. formaldehyde, phenols, aromatic hydrocarbons, olefinic compounds, and tannic acid, but not organic compounds containing nitrogen)*

Prepare a calibration curve as follows. Transfer 1.00, 2.00, 3.00, and 4.00 ml of the standard nitrate solution to 100-ml volumetric flasks and dilute to the mark. Pipet 10-ml aliquots into 100-ml beakers, cover with watch glasses, and cool in cracked ice for 10 min or more; with the beakers in cracked ice, add 17.0 ml of sulfuric acid slowly, dropwise, from a buret while swirling. Adjust the solutions to room temperature. Add 1.0 ml of the 2,4-xylenol solution, swirl to mix thoroughly, and allow to stand for 15—90 min.

Add 20 ml of water, 35 ml of isopropanol, and 5 ml of ammonia liquor to five 100-ml volumetric flasks. Place one of the flasks under the condenser extension tube of the distillation flask. Introduce the sample through the entry funnel and wash in with 5—10 ml of water. Steam-distil in the usual manner [1] until the volume of liquid in the volumetric flask is ca. 95 ml. Remove the volumetric flask. Dilute the solutions in the volumetric flasks to the mark and mix. Measure the absorbance at 455 nm against distilled water. Deduct a reagent blank carried through the entire procedure and plot absorbance against mg of $NO_3^-$-N (per 10-ml aliquot).

For the analysis of a sample, proceed as follows. If the solution is clear, transfer a portion (up to 50 ml) containing up to 2.0 mg of $NO_3^-$-N to a 250-ml beaker. If the solution is not clear, filter the portion through a fine-texture filter paper and wash with water. Add 5 ml of dilute sulfuric acid (10%) and immediately add an excess of potassium permanganate solution (5%) (25 ml will oxidize up to 0.25 g of most organic compounds). Heat to boiling and boil for 5 min. If the permanganate color disappears, add more permanganate and boil for a further 5 min. Cool to room temperature. Add 7 ml of hydrogen peroxide (30%) slowly, while stirring, to destroy the excess of permanganate (the manganese dioxide will not dissolve unless it is present in small amounts). If any permanganate color remains, add more peroxide. Add 5 ml of Fe(III) solution (4.4%), dilute to about 110 ml, cover with a watch glass, heat to boiling, and boil vigorously for 15 min. Wash down the watch glass and sides of the beaker with water, and boil again vigorously for 15 min. The volume of the solution at this stage should be about 75—90 ml. Cool, filter through a fine-texture filter paper, and wash with water. Add 2 or 3 drops of

silver sulfate solution (0.44%) to test for chloride, bromide, and iodide. If no precipitate is obtained, dilute to 100 ml in a volumetric flask, pipet a 10-ml aliquot into a 100-ml beaker, cool in ice, and proceed as described in the preparation of the calibration curve. If a precipitate is obtained, heat close to boiling and add sufficient silver sulfate solution (0.44%) to precipitate the chloride, bromide, and iodide and provide a moderate excess of silver sulfate (1 mg of $Cl^-$, $Br^-$, and $I^-$ is equivalent to 1.0, 0.44, and 0.28 ml of the silver sulfate solution, respectively). Heat to boiling and boil for 1—2 min. Remove the beaker from the hot plate and test for complete precipitation by adding 1 or 2 drops of silver sulfate solution down the sides. If necessary, add more silver sulfate solution and heat to boiling again. Allow to stand for 15 min or more, filter through a fine-texture filter paper, and wash with water. Dilute to 100 or 200 ml in a volumetric flask, pipet a 10-ml aliquot into a 100-ml beaker, cool in ice, and proceed as described in the preparation of the calibration curve.

*Extraction procedure (for extractable organic compounds, e.g. nitrate esters, phenols, aromatic hydrocarbons, and olefinic compounds)*

Prepare a calibration curve as described in the permanganate oxidation procedure. For the analysis of a sample, proceed as follows. If the solution is clear, transfer a portion (up to 50 ml) containing up to 2.0 mg of $NO_3^-$-N to a 125-ml Squibb-type separatory funnel. If the solution is not clear, filter the portion through a fine-texture filter paper into the separatory funnel and wash with water (this filtration can be omitted if it is known with certainty that the undissolved matter is extractable). Add 3 ml of dilute sulfuric acid (10%). Add 35 ml of methyl isobutyl ketone (MIBK) and shake for 2 min. Allow to settle and drain off the bottom aqueous layer into a clean 250-ml beaker. Add 5 ml of water to the separatory funnel, shake for 2 s (5 shakes), and drain off the bottom aqueous layer into the first aqueous extract. Decant the MIBK (through the top of the separatory funnel), discard it, and wash the separatory funnel with water. Wash the solution from the beaker back into the separatory funnel with a little water, extract with 20 ml of MIBK, and wash with 5 ml of water as before. Make a third extraction with 20 ml of MIBK (unless the amount of organic matter is very small). Test the combined aqueous extracts for chloride, bromide, and iodide by adding 2 or 3 drops of silver sulfate solution (0.44%). If no precipitate is obtained, dilute to 100 ml in a volumetric flask, pipet a 10-ml aliquot into a 100-ml beaker, cool in ice, and proceed as described in the preparation of the calibration curve. If a precipitate is obtained, proceed with the silver halide precipitation as described in the permanganate oxidation procedure.

*Zinc hydroxide and carbon precipitation—adsorption procedure (for all organic compounds except formaldehyde)*

Prepare a calibration curve as follows. Add 2.00, 4.00, 6.00, and 8.00 ml of the standard nitrate solution to 250-ml beakers and dilute to about 100 ml

with water. Add 10 ml of zinc sulfate heptahydrate solution (12.5%) and 10 ml of sodium hydroxide solution (2.4%) and stir for a few seconds. Add 3 g of activated carbon and stir for about 30 s. Heat to 55—65°C and hold at that temperature for 20 min while stirring frequently. Cool to room temperature while stirring occasionally. Wash the solution into a 200-ml volumetric flask, dilute almost to the neck, mix, and adjust to the mark. Shake out any drops of water in the beaker and immediately decant the solution from the volumetric flask into the beaker. Mix, allow to settle for a few min, and filter through a medium-texture filter paper. Discard the first 50 ml of solution and collect ca. 75 ml. Pipet a 10-ml aliquot into a 100-ml beaker, cool in ice, and proceed with the development of the color as described for the calibration of the permanganate oxidation procedure.

For the analysis of a sample, proceed as follows. If the solution is clear, transfer a portion (up to 100 ml) containing up to 4.0 mg $NO_3^-$-N to a 250-ml beaker, and dilute to about 100 ml. If the solution is not clear, filter the portion through a fine-texture filter paper, wash with water, and dilute to about 100 ml. Add the zinc sulfate and carbon, and proceed as in the preparation of the calibration curve up to the point at which the first 50 ml of the solution has been filtered. Pour this solution into a beaker and test for chloride, bromide, and iodide by adding 2 or 3 drops of silver sulfate solution (0.44%). If no precipitate is obtained, filter the 75 ml of the original solution, pipet a 10-ml aliquot into a 100-ml beaker, cool in ice, and proceed as described in the preparation of the calibration curve. If a precipitate is obtained, filter the 75 ml of the original solution, pipet a 50-ml aliquot into a 250-ml beaker, add 3 ml of dilute sulfuric acid (10%), and proceed with the silver halide precipitation as described in the permanganate oxidation procedure.

## DISCUSSION AND RESULTS

### *Study of interference of organic compounds*

The possible interference of 123 representative organic compounds was tested by adding 0.1 g of the compound to a 100-ml beaker containing 8.0 ml of water and 2.0 ml of diluted standard nitrate solution (1 ml = 0.05 mg $NO_3^-$-N). For organic liquids, a volume equivalent to 0.1 g was added by semimicro pipet. The solutions were cooled in ice, 17.0 ml of sulfuric acid was added, and the samples were carried through the procedure. In some instances the experiments were repeated with 0.01 g of the organic compound. Sixty-two compounds did not interfere (0.1 g samples) (Table 1). Sixty-one compounds interfered (Table 2). No attempt was made to ascertain the maximum amount of a compound that could be present without causing interference. However, with certain inert solvents, e.g. pentane, isopropanol, or acetone (but not halogenated hydrocarbons) as much as 1 ml could be present.

The compounds can be classified as follows with respect to their mode of interference:

*1. Compounds that are readily nitrated or oxidized by nitrate in sulfuric acid solution.* Such compounds can frequently be predicted, e.g. olefinic com-

TABLE 1

Organic compounds that did not interfere with the 2,4-xylenol method for nitrate when present in amounts of 0.1 g

| *Hydrocarbons* | *Ketones* | *Saccharides* |
|---|---|---|
| Pentane | Acetone | Sucrose |
| Hexane | Methyl ethyl ketone | *o*-Glucose |
| Anthracene[a] | Methyl isobutyl ketone | Lactose |
| 1-Pentyne | *Esters* | Starch |
| *Alcohols* | Ethyl acetate | Cellulose |
| Methanol | Butyl acetate | *Miscellaneous* |
| Ethanol | Amyl acetate | Ethyl ether |
| Isopropanol | Ethyl phthalate | Diethylamine |
| Butanol | Butyl phthalate | Aniline |
| 2-Propyn-1-diol | *Halogenated hydrocarbons* | Acetonitrile |
| *Acids* | Methylene chloride | Morpholine |
| Formic | Chloroform | Pyridine |
| Acetic | Carbon tetrachloride | L-Aspargine |
| Trichloroacetic | 1-Bromobutane | Benzoyl peroxide |
| Hexanoic | 1-Iodobenzene[a] | D-Camphor |
| Oxalic | *Nitro compounds* | Methyl sulfone |
| Tartaric | Nitromethane | Pentachlorophenol |
| Citric | Nitroethane | Chloral hydrate |
| Sulfamic | Dinitrotoluene | Urea |
| Sulfanilic | *o*-Nitrobenzoic acid | Thiourea |
| Benzoic | Guanidine nitrate | Methyl isothiourea sulfate |
| *m*-Aminobenzoic | Trinitroresorcinol | Cinchonine |
| | | Caffeine |
| | | RDX (cyclotrimethylenetrinitramine)[a] |

[a]Did not completely dissolve in the sulfuric acid.

pounds are usually readily nitrated while alkynes are not. Aromatic compounds with electron-donating groups (e.g. methyl, hydroxyl) are readily nitrated, and those containing deactivating groups (e.g. $NO_2$, COOH) are not. Thus 0.01 g of benzene hardly interferes at all; 0.01 g of toluene and xylene interfere markedly. Some organic compounds that do not interfere (e.g., benzoic acid and aniline) are nitratable, but their nitration requires exceptional conditions.

*2. Compounds that steam-distil to produce interfering colors.* In most instances, these compounds distil without reacting with the nitrate, sulfuric acid, or 2,4-xylenol. The distillate may or may not react with the ammonium hydroxide in the collection flask. With some compounds (e.g. 2,4-dinitrophenol) a large portion of the compound distils; in other cases (e.g. trinitrotoluene, 2,4-dinitroaniline, or *o*-nitroaniline) only a portion distils. Phenol interferes because it is easily nitrated (Table 2). In the experiments with phenol, the color in the collection flask had a peculiar greenish-yellow tint. It was deduced that a nitrated phenol was being distilled, giving a spurious reading; the same greenish-yellow color of practically the same absorbance (about 0.20) was obtained on experimenting with a mixture of phenol (0.01—1.0 g) and 0.10 mg

TABLE 2

Organic compounds that interfered with the 2,4-xylenol method for nitrate (0.1 g of compound and 0.10 mg of $NO_3^-$-N present)

| Compounds readily nitrated or oxidized by nitrate | $NO_3^-$-N found (mg) | Compounds readily nitrated or oxidized by nitrate | $NO_3^-$-N found (mg) |
|---|---|---|---|
| Benzene | 0.082[a] | Sodium oleate | 0.072[e] |
| Toluene | 0.005[b] | Castor oil | 0.062[e] |
| Xylene | 0.009[c] | Naphthenic acid | 0.015[e] |
| Phenol | 0.005[d] | Egg albumin | 0.052 |
| Hydroquinone | 0.022 | Blood albumin | 0.038 |
| Resorcinol | 0.015 | Methyl disulfide | 0.022 |
| 1-Naphthol | 0.075[e] | EDTA | 0.088[a] |
| *p*-Aminophenol | 0.052 | Tyrosine | 0.015 |
| *p*-Chlorophenol | 0.075 | Trypsin | 0.012 |
| *o*-Toluidine | 0.082 | Ascorbic acid | 0.022 |
| Formaldehyde | 0.005[f] | Rennin | 0.035 |
| Acetaldehyde | 0.055 | 2-Butane-1,4-diol | 0.042 |
| Benzaldehyde | 0.032 | 1,4-Naphthenediol | 0.055[e] |
| Tannic acid | 0.019 | Naphthalene | 0.068[e] |
| Pentaerythritol | 0.012 | Diphenylamine | 0.055 |
| Dodecyl sodium sulfate | 0.032 | Chloramine T | 0.082 |
| Cinnamic acid | 0.075 | Dichlorobenzene | 0.029[e] |
| Salicylic acid | 0.049 | Gelatin | 0.075[a] |
| Acetyl salicylate | 0.055 | Detergent (Sparkleen) | 0.082[a] |
| Oleic acid | 0.065[e] | Soap (Ivory) | 0.065[a] |
| **Compounds that steam-distil to produce colored solutions** | | **Compounds containing $ONO_2$ group** | |
| Trinitrotoluene | very high[g] | Nitroglycerin | very high[g] |
| 2,4-Dinitrophenol | very high[g] | Pentaerithritol tetranitrate | very high[g] |
| Nitrosobenzene | very high[g] | Amyl nitrate | very high[g] |
| *o*-Nitroaniline | 0.23 | Nitrocellulose | very high[g] |
| 2,4-Dinitroaniline | 0.150 | | |
| **Compounds that steam-distil to produce turbid solutions** | | **Compounds that hydrolyze to produce interfering ions or compounds** | |
| *o*-Cresol | 0.088[h] | Acetyl chloride | 0.005 |
| Dimethylformamide | 0.124[h] | Benzoyl chloride | 0.022 |
| Cyclohexanol | 0.079[h] | Phenylhydrazine hydrochloride | 0.005 |
| Nitrobenzene | 0.143[h] | Thioacetamide | 0.022[i] |
| Detergent (Fisher FL-70) | 0.105[h] | Peracetic acid[j] | 0.042 |
| 1,4-Dioxane | 0.120[h] | | |
| *o*-Chlorophenol | 0.143[h] | | |

[a]0.01 g did not interfere. [b]Result in the presence of 0.01 g of toluene was 0.015 mg. [c]Result in the presence of 0.01 g of xylene was 0.012 mg. [d]Corrected for absorbance of distilled nitrophenol (see text); result in the presence of 0.01 g of phenol was 0.005 mg. [e]Did not completely dissolve in the sulfuric acid. [f]Result in the presence of 0.01 g of formaldehyde was 0.045 mg. [g]Absorbance greater than 1.5. [h]Solution filtered before making absorbance readings. [i]Strong odor of hydrogen sulfide on adding the sulfuric acid. [j]Prepared by mixing acetic acid and hydrogen peroxide in the presence of a small amount of sulfuric acid as a catalyst [92].

$NO_3^-$-N without the 2,4-xylenol. The compound distilled is probably *o*-nitrophenol as it is much more volatile with steam than *p*-nitrophenol [83]. The dinitro (or trinitro) compound would not be produced in the nitration reaction [83].

*3. Compounds that steam-distil to produce turbid solutions.* In many instances the color seems to develop fully; in others it does not. The results obtained on filtering the turbid solutions were erratic.

*4. Compounds that hydrolyze in water or sulfuric acid solution to produce ions or compounds that repress the color development, e.g. chloride, bromide, iodide, sulfide, or hydrogen peroxide.* The hydrolysis of acetyl chloride takes place in aqueous solution but most of the hydrolysis of benzoyl chloride takes place in sulfuric acid solution. Thioacetamide hydrolyzes to hydrogen sulfide in sulfuric acid solution. Organic disulfides do not interfere by hydrolyzing to hydrogen sulfide. Peracetic acid apparently hydrolyzes to give hydrogen peroxide in aqueous solution (indicated with titanium reagent). Benzoyl peroxide (and presumably other organic peroxides) do not interfere.

There is a type of organic interference from micro-organisms, e.g. bacteria, algae, and fungi (slimes). These micro-organisms, like many other organic materials, may be nitrated or oxidized by the nitrate in the sulfuric acid medium. In addition, there is another aspect of interference, not directly related to the method of analysis, that involves the ability of some micro-organisms to alter the nitrate content of aqueous systems, e.g. some bacteria oxidize ammonia (produced by the decay of proteinaceous matter) to nitrite, or oxidize nitrite to nitrate and others reduce nitrate to nitrite or nitrite to ammonia [84, 85]. Nitrate reductase has been used for the determination of nitrate by incubating the sample in a nutrient medium at 39°C for 5 h [86] or at 45°C for 4 h [87] and determining the nitrite produced. Therefore if the samples cannot be examined without delay, they should be stored in a refrigerator.

As indicated earlier, interferences were studied by adding 17.0 ml of sulfuric acid directly to a mixture of the organic compound, standard nitrate solution and water. Many organic substances that are only slightly soluble in water are dissolved by this means; consequently, the results furnish a more valid indication of possible interferences (anthracene, iodobenzene, RDX, 1-naphthol, oleic acid, sodium oleate, castor oil, naphthenic acid, 1,4-naphthenediol, naphthalene, and dichlorobenzene dissolved only partially in the sulfuric acid). In actual analytical work, material that is insoluble in water should be filtered off prior to the determination; the possibility of undissolved matter going back into solution during the determination is thus avoided.

The extent of interference from organic compounds would be expected to be less for the 2,4-xylenol distillation method than for direct spectrophotometric methods; the distillation separates the colored compound being measured from organic compounds that would interfere by forming colors or turbidities. No error is caused in the 2,4-xylenol method by charring; charring does not occur in sulfuric acid solution of the concentration used.

*Permanganate oxidation procedure for the elimination of interferences*

Potassium permanganate in dilute sulfuric acid medium was the most effective oxidant for eliminating the interference of organic matter; the manganese is usually reduced to $MnO_2$ [88, 89] but, if only small amounts of organic material are present, $MnO_2$ does not precipitate. Formaldehyde and phenolic compounds are oxidized to carbon dioxide and water; olefinic compounds are converted to dihydroxy compounds [88, 89]. The nitrogen in organic compounds containing $NO_2$ or $ONO_2$ groups is converted to inorganic nitrate by permanganate [89]. Chlorine in organic compounds is converted to chloride; bromine and iodine in organic compounds are volatilized as the free halogens.

It was necessary to destroy the excess of permanganate, as it interferes with the spectrophotometric determination of nitrate. This can best be done by treating with hydrogen peroxide and boiling in the presence of iron(III) as a catalyst to destroy the peroxide [2]. There is no loss of nitrate on boiling dilute sulfuric acid containing a few mg of nitrate [2].

The permanganate treatment partially converts organic nitrogen compounds that contain neither $NO_2$ nor $ONO_2$ to inorganic nitrate, but few data are available [3, 4]. This problem was studied by adding 0.1 g of 17 organic nitrogen compounds that did not contain $NO_2$ or $ONO_2$ to about 80 ml of water, treating with 5 ml of dilute sulfuric acid (10%) and 5 ml of potassium permanganate solution (5%), and boiling for 5 min. The solutions were cooled, 5 ml of hydrogen peroxide and 5 ml of iron(III) solution (4.4%) were added, and the peroxide was destroyed by boiling. The solutions were diluted to 100 ml in volumetric flasks and the nitrate was determined on a 10-ml aliquot as usual. The results, expressed as mg of $NO_3^-$-N in 0.01 g of sample (i.e. in the 10-ml aliquot), are shown in Table 3. The results can be converted to percent $NO_3^-$-N in the sample by multiplying by 10. Some oxidation to inorganic nitrate occurs in all the samples tested. Obviously, the permanganate oxidation procedure should not be used for samples containing organic nitrogen com-

TABLE 3

Oxidation of organic compounds containing nitrogen (no $NO_2$ or $ONO_2$) to nitrate by potassium permanganate

| Compound | $NO_3^-$-N (mg) produced from 0.01 g of the compound | Compound | $NO_3^-$-N (mg) produced from 0.1 g of the compound |
|---|---|---|---|
| Acetamide | 0.052 | Trypsin | 0.112 |
| Thioacetamide | 0.038 | L-Aspargine | 0.153 |
| *p*-Aminophenol | 0.28 | Caffeine | 0.055 |
| *m*-Aminobenzoic acid | 0.082 | Egg albumin | 0.035 |
| Diethylamine | 0.038 | Rennin | 0.015 |
| Dimethylformamide | 0.082 | Gelatin | 0.045 |
| Aniline | 0.082 | Urea | 0.015 |
| Morpholine | 0.122 | Thiourea | 0.052 |
| Chloramine T | 0.140 | | |

pounds of any kind. Permanganate does not oxidize ammonium ion to nitrate [89]. Boiling for 30 min did not cause hydrolysis of any of the compounds shown in Table 3 to nitrate. Permanganate quantitatively oxidized nitrite to nitrate [31, 89]; if $NO_2^-$-N is present, a correction should be made by deducting the $NO_2^-$-N from the total $NO_3^-$-N.

*Extraction procedure for the elimination of interferences*

Various solvents were investigated for the extraction technique; benzene and toluene interfere with the method. There are probably many satisfactory solvents but the best results were obtained with methyl isobutyl ketone (MIBK) It is recommended that 3 ml of dilute sulfuric acid (10%) be added before the extraction to ensure the conversion of any interfering salts, e.g. sodium oleate, to the extractable free acid.

The following were incompletely extracted by MIBK (and other solvents), as judged by poor recoveries of added nitrate: formaldehyde, ascorbic acid, tannic acid, peracetic acid, phenylhydrazine hydrochloride (with subsequent silver sulfate treatment), thioacetamide, egg albumin, blood albumin, trypsin, and *p*-aminophenol.

The extraction method was applied to the elimination of interferences from 0.25 g of the organic compounds but it could be used for the removal of larger amounts by modifying the mode of extraction.

Nitrite, if present, should be removed by the addition of sulfamic acid and boiling [2] prior to extraction with MIBK.

*Zinc hydroxide and carbon precipitation—adsorption procedure*

Various precipitation—adsorption techniques that called for the use of metal salts for the elimination of organic interferences were investigated. The most effective method was the zinc sulfate—sodium hydroxide procedure used by the American Association of Official Analytical Chemists in a collaborative method for the determination of nitrate in cheese (the nitrate was determined by reduction to nitrite by cadmium, followed by spectrophotometric determination of the nitrite) [36]. In this precipitation—adsorption method, the equivalent of 1.2 g of $ZnSO_4 \cdot 7H_2O$ and 0.24 g of NaOH is added and the solution is heated to ca. 50°C for 10 min. The pH of the solution (5.5—6.5) after the addition of the alkali is such that most of the zinc precipitates as zinc hydroxide (an excess of sodium hydroxide would cause some zinc to go back into solution as sodium zincate). Also, the pH is close to the isoelectric point of most proteins. Zinc sulfate, unlike aluminum sulfate, gives a precipitate with proteins, e.g. egg albumin, even before the addition of the alkali.

Nitrate was adsorbed by the zinc hydroxide, so that the usual calibration curve was used in work with the zinc sulfate—sodium hydroxide method. Excellent results were obtained for many compounds, including egg albumin, rennin, tannic acid, thioacetamide, pentaerythritol, and dioxane. However, for many compounds (including phenol, nitrated compounds, and formaldehyde) the results were poor.

Since the zinc hydroxide method left something to be desired, experiments were conducted with activated carbon. The results tended to be erratic. The carbon tended to settle quickly and could not be brought into intimate contact with the solution. The amount of nitrate adsorbed by the carbon was insignificant.

It was decided to add 3 g of activated carbon to zinc hydroxide, precipitated as described above; all of the compounds that interfered with the zinc hydroxide method could then be handled, except formaldehyde. However, the method had one drawback. The adsorption by the mixture of zinc hydroxide and activated carbon was so great that ca. 5% of the nitrate was also adsorbed, depending on the carbon used. This necessitated the preparation of the calibration curve by carrying nitrate solution through the entire procedure. The calibration curve was reproducible. It was necessary to use 3 g of carbon: 1 g was ineffective for the removal of phenols and nitrated compounds. The carbon should be added after the zinc sulfate and sodium hydroxide: addition before the sodium hydroxide was not satisfactory as the zinc hydroxide coated the carbon and hindered adsorption. Digestion at 55—65°C was important, especially for elimination of the interference from phenols and nitrated compounds. Shaking at room temperature for 10 min or allowing to stand overnight at room temperature was ineffective.

As is customary in precipitation—adsorption methods, the solution was diluted to volume and a portion filtered; this saves time and eliminates the possibility of the adsorbed impurities being washed out if the entire precipitate were filtered and washed. The slight error arising from the volume of zinc hydroxide and carbon is usually regarded as insignificant. Any such error, however, is cancelled out in the proposed method because the calibration curve is prepared in the same way as the samples. To get an indication of the extent of this error, 3 g of activated carbon was added to a dry 200-ml volumetric flask (previously calibrated over the 200-ml mark), 100.00 ml of water was added with a pipet, and the water was swirled. After a few min, a further 100.00 ml of water was added and the flask was inverted a few times. The carbon was allowed to settle and the meniscus level was read. The apparent volume occupied by the water plus carbon was 101.15 ml; hence, the apparent volume occupied by the 3 g of carbon in contact with water was 1.15 ml. However, from this would have to be deducted the moisture in the carbon (its loss on heating at 120°C for 2 h, which would include other volatile matter besides moisture, was 12.3%). It is difficult to assess the volume occupied by zinc hydroxide as it is essentially a hydrated zinc oxide of indefinite composition.

The solution should be transferred back to the beaker immediately after dilution in the volumetric flask. If it is allowed to stand in the volumetric flask for more than about 2 min, a zinc hydroxide—carbon film, that requires treatment with strong acid, forms.

A clear filtrate was always obtained on filtering the zinc hydroxide and carbon on medium-texture filter paper (Fisher Scientific 9-801C) and filtration was rapid. In experiments with the zinc hydroxide alone, a fine-texture filter paper had to be used.

The blank for the zinc hydroxide—carbon method showed an absorbance of 0.04. Most of this blank seemed to arise from a trace of nitrate in the zinc sulfate.

Organic compounds containing chlorine, bromine, or iodine can hydrolyze to produce chloride, bromide, or iodide, so provision must be made for their elimination by precipitation with silver sulfate; this must be made on a 50-ml aliquot of the filtrate from the zinc hydroxide—carbon treatment. Elimination of the halide by adding the silver sulfate directly to the solution after the addition of the carbon, followed by filtration of the mixture of zinc hydroxide carbon, and silver halide gave erratic results.

The proposed method eliminated the interference of up to 0.25 g of all the compounds tested, except formaldehyde and peracetic acid. The method did not eliminate the interference of even a few mg of formaldehyde but did eliminate that of 0.1 g of peracetic acid (apparently, heating in the presence of carbon causes decomposition of small amounts of hydrogen peroxide). It is probable that other compounds, besides formaldehyde, may not be eliminated by the method. Many polar compounds of low molecular weight, e.g. methanol, which do not interfere with the 2,4-xylenol nitrate method, are probably not adsorbed by the zinc hydroxide and carbon.

In all cases the solutions were filtered prior to the zinc hydroxide—carbon treatment. The solubility of compounds containing $NO_2$ or $ONO_2$ groups is frequently low. The solubility of nitroglycerin in water at 20°C is 0.17% [90]. The experiments on nitroglycerin were performed by extracting the compound from a β-lactose—10% nitroglycerin absorbate (obtained from a pharmaceutical house) with methylene chloride, evaporating off the methylene chloride, adding 100 ml of water and the standard nitrate solution, fitering, washing, and proceeding with the zinc hydroxide—carbon treatment. On carrying nitroglycerin through the procedure without the zinc hydroxide—carbon treatment, a very high result for nitrate was obtained (absorbance of 1.5).

No investigation was made of the amount of a particular organic compound that could be handled by the method. For tannic acid, egg albumin, and phenol, which are soluble to the extent of 2 g per 100 ml, the recoveries for nitrate in the presence of 1 and 2 g, respectively, of these substances were: tannic acid, 95% and 39%; egg albumin, 93% and 45%; phenol, 0.00% and 0.00% (after correcting for the absorbance of the distilled nitrophenol).

A few experiments were conducted on the use of the zinc hydroxide—carbon method for the elimination of inorganic interferences. The method eliminated the interference of up to ca. 50 mg of $Fe^{2+}$ (in the solution from which the 10-ml aliquot is taken) because this amount of $Fe^{2+}$ is quantitatively co-precipitated with zinc hydroxide. Ordinarily, in the absence of a gathering agent, iron(II) hydroxide does not precipitate until ca. pH 7 [91]. The interference of up to ca. 10 mg of sulfide is eliminated by the method, by precipitation as zinc sulfide; precipitation is not quantitative when larger amounts of sulfide are present. The interference of up to ca. 50 mg of hydrogen peroxide is eliminated by decomposing the hydrogen peroxide, previously mentioned in

connection with the interference of peracetic acid. The method eliminated the interference of up to ca. 150 mg of $Mn^{7+}$ and up to ca. 75 mg of $Cr^{6+}$ (by adsorption or reduction). It was of no significant value in eliminating the interference of $S_2O_8^{2-}$, $S_2O_3^{2-}$, $SCN^-$, $ClO_3^-$, $Cl^-$, $Br^-$, and $I^-$.

If a sample containing organics and various interfering inorganic reducing and oxidizing agents is encountered, the interference of these reducing and oxidizing agents should be eliminated after the zinc hydroxide and carbon treatment by the addition of hydrogen peroxide, with boiling to destroy the peroxide in the presence of iron(III) as a catalyst [2]. This treatment could also be used after the solvent extraction technique. In the permanganate oxidation method, the peroxide treatment is in effect already incorporated.

*Effect of order of addition of reagents*

It seemed possible that the interference from organic materials would be less if the 2,4-xylenol were added before the sulfuric acid, rather than after it. In a first series of experiments, solutions containing 0.1 g of the organic compound, 8.0 ml of water, and 2.0 ml of diluted standard nitrate solution (1 ml = 0.05 mg $NO_3^-$-N) were prepared. The 2,4-xylenol solution was added, the solution cooled in ice, 17.0 ml of sulfuric acid added, and the sample distilled as usual. In a second series of experiments, 2.0 ml of the diluted standard nitrate solution was evaporated to dryness and 0.1 g of the organic compound and the 2,4-xylenol reagent were added. Then, 17 ml of sulfuric acid (1.7:1) (at room temperature) was added and the distillation was conducted. In both sets of experiments, it was found that in cases where the interference was marked when the 2,4-xylenol was added last, changing the order of addition of the reagents did not help much. However, if the interference was moderate when the 2,4-xylenol was added last, the interference decreased when the order of addition of the reagents was changed. As changing the order of addition of the reagents did not help in most instances, it was decided to continue to add the 2,4-xylenol last. Also, in the determination of inorganic nitrate there are disadvantages in adding the 2,4-xylenol reagent first. The method described in the first series of experiments has the disadvantage that the 2,4-xylenol precipitates when the 2,4-xylenol solution is added to the water (it then dissolves slowly as the sulfuric acid is added). The method described for the second series of experiments (the evaporation method), has the disadvantage that it cannot readily be applied to samples previously subjected to the silver sulfate treatment for the removal of halide, as nitrate would be lost in evaporating the dilute sulfuric acid solution to dryness. If the solution were made alkaline before the evaporation, this loss would be prevented but insoluble silver salts would form.

In the presence of interfering organic matter, lower results have been reported when solutions were allowed to stand for more than 30 min after the addition of the 2,4-xylenol [3]; however, this was not found to be a problem here, and approximately the same results were obtained whether the solution stood for 15 min or 90 min after the addition of the 2,4-xylenol (the

TABLE 4

Results of procedures for the elimination of interferences
(Unlesss otherwise noted, 0.25 g of the interfering compound was taken with 1.50 mg $NO_3^-$-N for the oxidation or extraction procedure, or 3.00 mg $NO_3^-$-N for the $Zn(OH)_2$-C procedure.

| Interferent | $NO_3^-$-N (mg) in 10-ml aliquot | | | |
|---|---|---|---|---|
| | Present | Found | | |
| | | Oxidation procedure | Extraction procedure | $Zn(OH)_2$-C procedure |
| Phenol | 0.150 | 0.156 | 0.146 | 0.163 |
| Phenol[a] | 0.075 | 0.082 | 0.075 | 0.080 |
| Phenol[b] | 0.000 | 0.005 | 0.000 | 0.005 |
| Resorcinol | 0.150 | 0.146 | 0.150 | 0.157 |
| Hydroquinone | 0.150 | 0.156 | 0.140 | 0.140 |
| *o*-Cresol | 0.150 | 0.146 | 0.163 | 0.163 |
| *p*-Chlorophenol | 0.150[c] | 0.075 | 0.146[d] | 0.145[d] |
| *p*-Chlorophenol | 0.150[e] | 0.160 | — | — |
| Toluene | 0.150 | 0.153 | 0.156 | 0.157 |
| Xylene | 0.150 | 0.153 | 0.143 | 0.163 |
| Acetaldehyde | 0.150 | 0.156 | 0.146 | 0.160 |
| Benzaldehyde | 0.150 | 0.169 | 0.146 | 0.160 |
| Benzaldehyde[b] | 0.000 | 0.019 | 0.005 | 0.005 |
| 1,4-Dioxane | 0.150 | 0.153 | 0.143 | 0.145 |
| Oleic acid | 0.150 | 0.156 | 0.160 | 0.145 |
| Sodium oleate | 0.150 | 0.150 | 0.156 | 0.160 |
| Salicylic acid | 0.150 | 0.146 | 0.150 | 0.163 |
| Dimethyl sulfide | 0.150 | 0.160 | 0.140 | 0 157 |
| Pentaerythritol | 0.150 | 0.156 | 0.140 | 0.152 |
| Lubricating oil | 0.150 | 0.163 | 0.140 | 0.160 |
| Acetyl salicylate | 0.150 | 0.140 | 0.143[f] | 0.145 |
| Naphthalene | 0.150 | 0.153 | 0.150 | 0.163 |
| Detergent (Sparkleen) | 0.150 | 0.156 | 0.146 | 0.157 |
| Detergent (Fisher) | 0.150 | 0.156 | 0.140 | 0.145 |
| Ascorbic acid | 0.150 | 0.153 | X[g] | 0.140 |
| Tannic acid | 0.150 | 0.146 | X | 0.140 |
| Peracetic acid[h] | 0.150 | 0.160 | X | 0.145 |
| Formaldehyde | 0.150 | 0.153 | X | X |
| 2,4-Dinitrophenol | 0.150 | X | 0.150 | 0.163 |
| 2,4-Dinitroaniline | 0.150 | X | 0.146 | 0.140 |
| Nitroglyerin | 0.150 | X | 0.146 | 0.163 |
| Trinitrotoluene | 0.150 | X | 0.150 | 0.155 |
| Dimethylformamide | 0.150 | X | 0.153 | 0.145 |
| EDTA | 0.150 | X | 0.143 | 0.148 |
| Rennin | 0.150 | X | 0.140 | 0.145 |
| 2,4-Diaminophenol dihydrochloride[i] | 0.150[e] | X | 0.153[j] | — |
| 2,4-Diaminophenol dihydrochloride | 0.075[k] | X | — | 0.072 |
| Phenylhydrazine hydrochloride | 0.075[k] | X | X | 0.080 |
| Thioacetamide | 0.150 | X | X | 0.145 |
| Egg albumin | 0.150 | X | X | 0.163 |
| Blood albumin | 0.150 | X | X | 0.145 |
| Trypsin | 0.150 | X | X | 0.157 |
| *p*-Aminophenol | 0.150 | X | X | 0.157 |

[a]Only 0.75 mg (or 1.50 mg) $NO_3^-$-N was taken. [b]In absence of $NO_3^-$-N. [c]0.075 for oxidation procedure (solution diluted to 200 ml after silver chloride precipitation). [d]No chloride ion detected. [e]Solution diluted to 200 ml after silver chloride precipitation; 3.00 mg $NO_3^-$-N tak [f]Solution must be filtered prior to the extraction (or oxidation) procedure. Nitrate recovery was 65% when an attempt was made to extract the undissolved material with MIBK. [g]X = nc usable. [h]Only 0.10 g of peracetic acid was used. [i]0.15 g taken because of large volume of silver sulfate solution needed to precipitate the chloride ion on the entire sample. [j]Solution was purple in color after the extraction but this did not interfere. [k]Solution diluted to 100 r after silver chloride precipitation on a 50-ml aliquot from the zinc hydroxide—carbon filtrat

method used here for developing the color differed somewhat from that used by the earlier investigators). The excess of 2,4-xylenol starts to precipitate from the sulfuric acid after a few minutes, producing a white turbidity that may cause the illusion that the color of the 6-nitro-2,4-xylenol is decreasing.

*Results by the proposed procedures*

The results obtained for 43 synthetic samples with the three methods of eliminating interferences are shown in Table 4. The recoveries are satisfactory. The somewhat high result for benzaldehyde by the oxidation method is apparently due to the presence of a small amount of a nitrogen compound.

The proposed methods should have important applications in the determination of nitrate in pollutants and various organic and biological materials and in the determination of nitrate in production control of nitration processes (with small aliquots).

REFERENCES


1 G. Norwitz and H. Gordon, Anal. Chim. Acta, 89 (1977) 177.
2 G. Norwitz and P. N. Keliher, Anal. Chim. Acta, 98 (1978) 323.
3 J. Blom and C. Treschow, Z. Pflanzenernaehr., Duengung Bodenkd., 13A (1929) 159.
4 C. Treschow and E. K. Gabrielsen, Z. Pflanzenernaehr., Duengung Bodenkd., 32A (1933) 357.
5 F. Alten and G. Weiland, Z. Pflanzenernaehr., Duengung Bodenkd., 32A (1933) 337.
6 F. Alten, B. Wandrowsky and E. Hille, Bodenkd. Pflanzenernaehr., 1 (1936) 340.
7 A. Hamy, Ann. Agron., 15 (1945) 126.
8 E. A. Soboleva, Vop. Pitan., (5) (1969) 63.
9 C. D. Usher and G. M. Telling, J. Sci. Food Agric., 26 (1975) 1793.
10 F. L. Ashton, J. Soc. Chem. Ind., 54 (1935) 389T.
11 E. M. Roller and N. McKaig, Soil Sci., 47 (1939) 397.
12 H. Burstrom, Sven. Kem. Tidskr., 54 (1942) 139.
13 C. M. Johnson and A. Ulrich, Anal. Chem., 22 (1950) 1526.
14 H. L. Golterman, Proc. Koninkl. Ned. Akad. Wetenschap, 58 (1955) 118.
15 M. P. Morris and A. González-Más, J. Agric. Food Chem., 6 (1958) 456.
16 G. Szekely, Talanta, 14 (1967) 941.
17 H. Yagoda, Ind. Eng. Chem., Anal. Ed., 15 (1943) 27.
18 G. Norwitz and H. Gordon, Talanta, 22 (1975) 593.
19 A. L. Clarke and A. C. Jennings, J. Agric. Food Chem., 13 (1965) 174.
20 B. K. Afghan and J. F. Ryan, Environ. Lett., 9 (1975) 59.
21 H. J. Harper, Ind. Eng. Chem., 16 (1924) 180.
22 D. G. Lewis, J. Sci. Food Agric., 12 (1961) 735.
23 T. Greweling, K. L. Davison and C. J. Morris, J. Agric. Food Chem., 12 (1964) 139.
24 G. B. Jones and R. E. Underdown, Anal. Chem., 25 (1953) 806.
25 E. D. Schall and D. W. Hatcher, J. Assoc. Off. Anal. Chem., 51 (1968) 763.
26 M. S. Green, J. Assoc. Publ. Analysts, 8 (1970) 48.
27 R. H. Diven, W. J. Pistor, R. E. Reed, R. J. Trautman and R. E. Watts, Am. J. Vet. Res., 23 (1962) 497.
28 Official Methods of Analysis of Association of Official Agricultural Chemists, 10th edn. Washington, DC, pp. 347, 522.
29 J. H. Dhont, Analyst, 84 (1959) 372.
30 F. D. Snell and C. T. Snell, Colorimetric Methods of Analysis, 3rd edn., Vol. II, Van Nostrand, New York, 1954, pp. 789, 791.

31 D. P. Boltz, Colorimetric Determination of Nonmetals, Interscience, New York, 1958, p. 75.
32 Am. Public Health Assoc., Standard Methods for the Examination of Water and Waste Water, 13th edn., Washington, DC, 1971, pp. 236, 237, 457, 465.
33 P. B. Manning, S. T. Coulter and R. Jenness, J. Dairy Sci., 51 (1968) 1725.
34 H. Schechter, N. Gruener and H. I. Shuval, Anal. Chim. Acta, 60 (1972) 93.
35 A. J. McKay, Aust. J. Dairy Tech., 29 (1974) 34.
36 J. E. Hamilton, J. Assoc. Off. Anal. Chem., 59 (1976) 284.
37 T. N. Wegner, J. Dairy Sci., 55 (1972) 642.
38 R. Grau and A. Mirna, Fresenius Z. Anal. Chem., 158 (1957) 182.
39 M. K. Achtzehn and H. Hawat, Lebensmittel-Ind., 19 (1972) 482.
40 R. Karlsson and L. Torstensson, Talanta, 21 (1974) 945.
41 W. Postel, Brauwissenschaft, 29 (1976) 39.
42 A. Mirna and G. Schuetz, Fleischwirtschaft, 52 (1972) 1337.
43 A. Adriaanse and J. E. Robbers, J. Sci. Food Agric., 20 (1969) 321.
44 C. G. Rammell and M. M. Joerin, J. Dairy Res., 39 (1972) 89.
45 R. Fudge and R. W. Truman, J. Assoc. Publ. Anal., 11 (1973) 19.
46 K. F. Becker, Bundesgesundheitblatt, 17 (1965) 246.
47 C. Selmeci, A. Aczel and S. Peter, Elelmiszervizsgalati. Kozl., 21 (1975) 187.
48 L. Kamm, G. G. McKeown and D. M. Smith, J. Assoc. Off. Agric. Chem., 48 (1965) 892.
49 R. J. Elliott and A. G. Porter, Analyst, 96 (1971) 522.
50 Am. Soc. for Testing and Materials, 1975 Book of ASTM Standards, Part 31, Water, Designation D992-71, 1977.
51 M. J. Follett and P. W. Ratcliff, J. Sci. Food Agric., 14 (1963) 138.
52 F. L. Hart and H. J. Fisher, Modern Food Analysis, Springer-Verlag, New York, 1971, p. 195.
53 S. Klein, Průmysyl Potravin, 9 (1958) 110.
54 H. Hänni, Mikrochem. Ver. Mikrochim. Acta, 36/37 (1951) 912.
55 C. J. Rosene, J. Assoc. Off. Anal. Chem., 52 (1969) 756.
56 E. Davídková and J. Davídek, Průmysl Potravin, 11 (1960) 385.
57 J. Davídek and A. Žáčková, Fresenius Z. Anal. Chem., 18 (1962) 320.
58 J. Davídek, S. Klein and A. Žáčkova, Z. Lebensmitt. Untersuch., 119 (1963) 342.
59 B. Wolfe, Anal. Chem., 15 (1943) 248.
60 L. Procházkova, Fresenius Z. Anal. Chem., 167 (1959) 254.
61 H. G. Wiseman and W. C. Jacobson, J. Agric. Food. Chem., 13 (1965) 36.
62 A. S. Baker, J. Agric. Food Chem., 15 (1967) 802.
63 B. D. McCaslin, T. Franklin and M. A. Dillon, J. Am. Soc. Sugar Beet Tech., 16 (1970) 64.
64 L. D. Sabatka, D. N. Hyder, C. V. Cole and W. R. Houston, Agron. J., 64 (1972) 398.
65 W. W. Eipeson, M. Mahadeviah, R. V. Gowramma and L. V. L. Sastry, J. Food Sci. Tech., 11 (1974) 209.
66 R. Karlsson and L. Torstensson, Talanta, 22 (1975) 27.
67 A. D. Westland and R. R. Langford, Anal. Chem., 28 (1956) 1996.
68 J. L. Paul and R. M. Carslon, J. Agric. Food Chem., 16 (1968) 766.
69 D. B. Johnson, Int. J. Agric. Res., 9 (1970) 271.
70 R. J. Davenport and D. C. Johnson, Anal. Chem., 46 (1974) 1971.
71 B. K. Afghan and J. F. Ryan, Anal. Chem., 47 (1975) 2347.
72 S. L. Pfeiffer and J. Smith, J. Assoc. Off. Anal. Chem., 58 (1975) 915.
73 D. W. Hatcher and E. D. Schall, J. Assoc. Off. Anal. Chem., 48 (1965) 648.
74 D. B. Johnson, Int. J. Agric. Res., 8 (1969) 444.
75 J. E. O'Brien and J. Fiore, Water Eng., 33 (1962) 128.
76 M. H. Lichtfield, Analyst, 92 (1967) 132.
77 R. H. Lowe and J. L. Hamilton, J. Agric. Food Chem., 15 (1967) 359.
78 A. Henriksen and A. R. Selmer-Olsen, Analyst, 95 (1970) 514.

79 E. Goldman and R. Jacobs, J. Am. Water Works Assoc., 53 (1961) 187.
80 R. C. Hosther, Proc. Soc. Water Treat. Exam., 2 (1953) 9.
81 R. C. Hosther and R.-F. Rackham, Analyst, 84 (1959) 548.
82 P. Morries, Proc. Soc. Water Treat. Exam., 20 (1971) 132.
83 L. F. Fieser and M. Fieser, Organic Chemistry, 3rd edn., Reinhold, New York, 1956, p. 628.
84 H. A. Painter, Water Res., 4 (1970) 393.
85 B. Sharma and R. C. Ahlert, Water Res., 11 (1977) 897.
86 G. B. Garner, J. S. Baumstark, M. E. Muhrer and W. H. Pfander, Anal. Chem., 28 (1956) 1589.
87 A. L. McNamara, G. B. Meeker, P. D. Shaw and R. H. Hageman, J. Agric. Food Chem., 19 (1971) 229.
88 R. Stewart, Oxidation Mechanisms, Applications to Organic Chemistry, W. A. Benjamin, New York, 1964, p. 58.
89 I. M. Kolthoff, R. Belcher, V. A. Stenger and G. Matsuyama, Volumetric Analysis, Vol. III, Interscience, New York, 1957, pp. 69, 113.
90 Kirk-Othmer, Encyclopedia of Chemical Technology, 2nd edn., Vol. 8, Interscience, New York, 1965, p. 602.
91 I. M. Kolthoff and E. B. Sandell, Textbook of Quantitative Inorganic Analysis, 3rd edn., Macmillan, New York, 1952. p. 76.
92 F. P. Greenspan, J. Am. Chem. Soc., 68 (1946) 907.

*Analytica Chimica Acta*, 105 (1979) 353—359


# STUDIES IN THE TETRAARYLBORATES
## Part 8. The Synthesis and Reagent Properties of Tetrathienylborates

GILBERT E. PACEY and CARL E. MOORE*

*Department of Chemistry, Loyola University of Chicago, Chicago, Illinois 60626 (U.S.A.)*

(Received 18th July 1978)

SUMMARY

The following cesium tetrathienylborates were synthesized and screened for gravimetric reagent properties: tetrakis(2-thienyl), tetrakis(3-thienyl), tetrakis(5-bromo-2-thienyl), tetrakis(5-chloro-2-thienyl), tetrakis(2,5-dimethyl-3-thienyl), tetrakis(5-ethyl-2-thienyl), tetrakis(5-methyl-2-thienyl), and tetrakis(5-t-butyl-2-thienyl). Of these, the tetrakis(5-alkyl-2-thienyl) borates were not sufficiently stable for complete characterization. The following are possible reagents for cesium and quaternary ammonium cations: sodium tetrakis(2-thienyl), tetrakis(3-thienyl), and tetrakis(2,5-dimethyl-3-thienyl)borates.

In a continuation of studies in tetraarylborates, a series of tetrathienylborates was synthesized. After several studies in the area of substituted phenyl tetraarylborates [1—6], recent efforts have been directed towards the heterocyclic borates, as exemplified by recent work involving tetrakis(1-imidazolyl)-borate [7]. Tetrakis(2-thienyl)borate was reported by Sazanova et al. [8]. It was thought that the thiophene sulfur atoms of the tetrathienylborates might offer interesting possibilities for divalent cation precipitation. Thus, Sazanova's research has been extended and the stability and reagent possibilities of the tetrathienylborates have been extensively investigated.

Three routes were used to synthesize a variety of tetrathienylborates:

Reaction 1

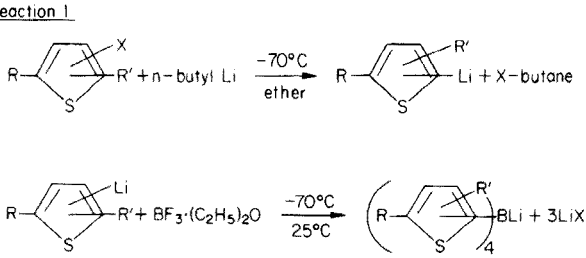





where X = Br or I and R and R′ = H or $CH_3$.

Reaction 2

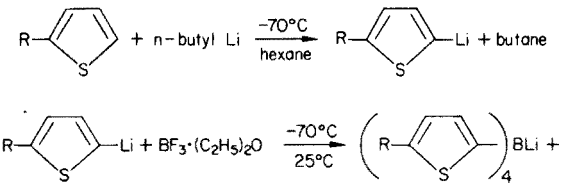


where R = methyl, ethyl or t-butyl

Reaction 3

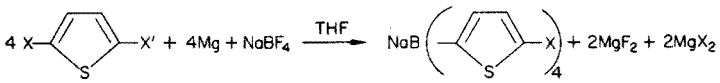


where X and X' = Br or Cl

A temperature of −70°C was maintained in reactions (1) and (2) to prevent interconversion reactions.

## EXPERIMENTAL

*Synthesis of cesium tetrakis(2(or 3)-thienyl)borate*

Reaction sequence (1) was used. Dry ether (200 ml) was brought to −70°C, and 25.0 g (0.1533 mol) of the 2- or 3-bromothiophene was added. While the mixture was vigorously stirred, 96 ml (0.1536 mol) of a 1.6 mol $l^{-1}$ solution of n-butyllithium in hexane was added over a 5-min period. The reaction was instantaneous. Then 5.4 g (0.0380 mol) of boron trifluoride etherate was added. The reaction was allowed to proceed for 1 h at −70°C, and then the mixture was allowed to come to room temperature, which required about 1 h. Lithium fluoride started to appear before the reaction mixture reached room temperature.

The mixture was then poured into 200 ml of ice water and stirred for 10 min. The ether was separated; the aqueous layer was saturated with sodium chloride and extracted three times with 75-ml portions of ether. The ether layers were combined and poured into 200 ml of deionized water. The ether was evaporated on a rotary evaporator and the ether-free solution was filtered through a Celite filter aid mat. The aqueous solution was diluted with 300 ml of deionized water and the borate was precipitated as the cesium salt. Recrystallization of the cesium salt was accomplished by dissolving it in acetone, filtering the solution, and adding water. The cesium salt was filtered and dried under vacuum over calcium chloride at 80°C (yield, 12.1 g).

(Analysis: m.p. > 300°C; 2-thienyl derivative, 40.1%C, 2.4%H; 3-thienyl derivative, 40.1%C, 2.4%H; calculated, 40.35%C, 2.5%H.)

*Synthesis of cesium tetrakis(5-alkyl-2-thienyl)borate*

Reaction sequence (2) was used to synthesize the tetrakis(5-alkyl-2-thienyl)-borates. The solvent employed was ether because hexane retarded these reactions. A sample of 56 ml (0.089 mol) of n-butyllithium in ether was

brought to −70°C. Then, over a 30-min period, 8.7, 10.0 or 12.5 g (0.089 mol) of 2-methyl-, 2-ethyl-, or 2-t-butyl-thiophene, respectively, was added dropwise to the n-butyllithium. After the addition was completed, 2.74 ml (0.0224 mol) of boron trifluoride etherate was added to the reaction mixture. The reaction was allowed to continue for 1 h at −70°C and for an additional hour after the cold bath had been removed.

The reaction mixture was diluted with 100 ml of ether and poured into 100 ml of deionized water. The ether layer was separated; the aqueous layer was saturated with sodium chloride and extracted three times with 75-ml portions of ether. The combined ether layers were poured into 100 ml of deionized water and the ether was evaporated by means of a rotary evaporator. The aqueous solution was filtered through a Celite filter aid mat, and the cesium salt was precipitated, collected, and dried.

The stability of these compounds was poor; therefore, no elemental analysis could be obtained. The only indications of their existence was a cation precipitation pattern of the product that is characteristic of tetra-arylborates. The possible by-products would not be expected to exhibit this activity.

*Synthesis of cesium tetrakis(5-halo-2-thienyl)borates*

Reaction sequence (3) was used to prepare the tetrakis(5-halo-2-thienyl)-borates. A 500-ml 3-necked flask equipped with a magnetic stirrer, water-cooled condenser, and a dropping funnel was flame-dried as nitrogen passed through the assembly. After the assembly had been cooled, 300 and 100 ml of tetrahydrofuran (THF) specially prepared (Aldrich Chemical Co.) for Grignard use were placed in the flask and dropping funnel, respectively. To the dropping funnel was added 25 or 20.4 g (0.1033 mol) of 2,5-dibromo- or 2-bromo-5-chlorothiophene, respectively. To the reaction flask were added 2.48 g (0.1033 mol) of magnesium and 2.81 g (0.0258 mol) of sodium fluoroborate, both previously dried at 110°C for at least 1 h. A 10-ml sample of the THF-thiophene mixture was added to the flask to start the reaction. A slight positive pressure of nitrogen was maintained. Once the reaction had started, the remainder of the THF-thiophene mixture was added dropwise over a 3-h period. The reaction was continued for an additional 5-h period after the addition was complete.

The reaction mixture was poured into 200 ml of ice water and approximately 1 g of sodium carbonate was added. The mixture was stirred for 15 min, and the ether layer separated from the aqueous layer which was then saturated with sodium chloride. The aqueous layer was extracted with three 75-ml portions of ether. The ether layers were combined and poured into 100 ml of deionized water and the ether evaporated by means of a rotary evaporator. The aqueous solution was passed through a Celite filter aid mat, and the borate precipitated by tetramethylammonium bromide. The salt was collected and dried over calcium chloride at 80°C in vacuum. Yields were 33% for the 5-bromo and 25% for the 5-chloro derivatives.

(Analysis: m.p. > 300°C; 5-bromo derivative, 33.2%C, 3.2%H; calculated,

32.8%C, 2.75%H. The 5-chloro derivative could not be purified sufficiently for analysis.)

*Synthesis of cesium tetrakis(2,5-dimethyl-3-thienyl)borate*

Reaction sequence (1) was used to prepare this compound. A sample of 25 g (0.1046 mol) of 2,5-dimethyl-3-iodothiophene was placed in a flask with 200 ml of dry ether. This mixture was brought to −70°C. With stirring, 65.4 ml (0.1046 mol) of n-butyllithium was added. After 15 min 3.20 ml (0.0262 mol) of $BF_3$ etherate was added. The reaction was allowed to proceed for 1 h at −70°C and an additional hour passed as the mixture warmed to room temperature.

The reaction mixture was then poured into 100 ml of deionized water and the ether layer separated. The remaining aqueous layer was saturated with sodium chloride and extracted three times with 75-ml portions of ether. The ether was evaporated under rotary evaporation. The remaining aqueous solution was passed through a Celite filter aid mat and the borate was precipitated as the potassium salt. The salt was dried under vacuum over calcium chloride at 80°C (yield, 30%).

(Analysis after correction for LiI presence: 58.0%C, 5.45%H; calculated, 58.3%C, 5.7%H.)

*Synthesis of soluble salts*

Only three of the tetrathienylborates could be easily obtained as soluble salt solutions. Cesium tetrakis(2-thienyl)borate and cesium tetrakis(3-thienyl)-borate were converted to sodium salts by the use of sodium perchlorate. Equimolar portions of cesium salts and sodium perchlorate were mixed in dry methanol and heated for 2 h. The resulting methanol solutions were filtered to remove the cesium perchlorate and the methanol was evaporated down to give a viscous solution. Water was added and the solution filtered. This solution was used for gravimetric tests.

In the case of tetrakis(2,5-dimethyl-3-thienyl)borate, the trimethylamine salt was reacted with sodium methoxide [3]. An aqueous solution was obtained and used for gravimetric tests. The solid compound was not obtained because of stability problems.

## REAGENT PROPERTIES OF THE TETRATHIENYLBORATES

Qualitative tests were carried out with a 1% solution of a soluble salt. Approximately 1 ml of the reagent was added to 1 ml of 0.1 M solution of the ion to be tested. Table 1 summarizes the results.

Although some divalent cations were precipitated, many of these precipitates underwent decomposition. In the case of the tetrakis(5-alkyl-2-thienyl)borates, decomposition was immediate. Some of the divalent cations were too soluble to be of analytical interest. However, the salts of tetrakis(2-thienyl)borate, tetrakis(3-thienyl)borate and tetrakis(2,5-dimethyl-3-thienyl)borate were of

TABLE 1

Precipitation pattern of tetrathienylborates[a]

| | 2-T | 3-T | 5-ET | 5-ME | DMT | 5-Br | 5-Cl |
|---|---|---|---|---|---|---|---|
| $Li^+$ | | | | | | | |
| $Na^+$ | | | | | | | |
| $K^+$ | | | | | X | | |
| $Rb^+$ | X | | | | X | X | |
| $Cs^+$ | X | X | X | X | X | X | X |
| $Ag^+$ | O | O | O | O | O | O | O |
| $Tl^+$ | O | O | O | O | O | O | O |
| $Hg^{2+}$ | O | O | O | O | O | O | O |
| $Ba^{2+}$ | | | | | | | |
| $Ca^{2+}$ | | | | | | | |
| $Pb^{2+}$ | O | O | O | O | O | O | O |
| $Co^{2+}$ | O | | O | O | O | O | O |
| $Mn^{2+}$ | | | | | X | | |
| $Zn^{2+}$ | | | X | X | X | | |
| $Cd^{2+}$ | | | X | X | X | X | |
| $Cu^{2+}$ | O | O | O | O | O | O | O |
| $Fe^{2+}$ | O | O | O | O | O | O | O |
| $Ni^{2+}$ | | | O | O | O | O | O |
| $NH_4^+$ | O | O | O | O | O | O | O |
| $R_3NH^+$ | O | O | O | O | X | O | O |
| $R_4N^+$ | X | X | X | X | X | X | X |

[a](X) precipitate stable; (o) precipitate unstable.

TABLE 2

Sensitivity of some tetrathienylborates for cesium[a]

| Reagent | Cs taken (mg $ml^{-1}$) | | | | | | |
|---|---|---|---|---|---|---|---|
| | 2 | 0.2 | 0.1 | 0.05 | 0.02 | 0.01 | 0.005 |
| TPB | HI | HI | * | * | SI | SI | TI |
| 2-T | HI | HI | TI | — | — | — | — |
| 3-T | HI | MI | TS | — | — | — | — |
| DMT | HI | HI | MI | MI | MI | SI | SI |

[a]HI = heavy immediately; MI = medium immediately; TI = trace immediately; SI = slight immediately; TS = trace slow; * = no data.

sufficiently low solubility and of sufficiently great stability to show some promise of reagent possibilities. The tetrakis(2-thienyl)borate and tetrakis(3-thienyl)borate anions precipitated protonated basic nitrogen compounds, but only the quaternary ammonium cations produced stable precipitates.

Comparative sensitivity studies for the cesium salts (Table 2) were obtained by mixing 2 ml of a 0.03 M reagent solution with 2 ml of test solution. These data indicate that the tetrakis(2-thienyl)borate and tetrakis(2,5-dimethyl-3-

TABLE 3

Solubilities of tetrakis(2,5-dimethyl-3-thienyl)borates at 20°C

| Cation | pH | Solubilities | |
|---|---|---|---|
| | | ($g\ l^{-1}$) | ($mol\ l^{-1}$) |
| $K^+$ | 8.4 | 0.937 | $1.89 \times 10^{-3}$ |
| $Rb^+$ | 5.1 | 0.316 | $5.85 \times 10^{-4}$ |
| $Cs^+$ | 6.7 | 0.057 | $9.79 \times 10^{-5}$ |

TABLE 4

Gravimetric analysis for cesium with sodium tetrakis(2-thienyl)borate and sodium tetrakis-(2,5-dimethyl-3-thienyl)borate

| Cs taken (mg) | Tetrakis(2-thienyl)borate | | Tetrakis(2,5-dimethyl-3-thienyl)borate | |
|---|---|---|---|---|
| | Cs found (mg) | % Recovery | Cs found (mg) | % Recovery |
| 144.3 | 143.1 | 99.2 | 143.0 | 99.1 |
| | 143.4 | 99.3 | 143.2 | 99.2 |
| | 143.7 | 99.6 | 142.8 | 99.0 |
| 103.1 | 102.4 | 99.3 | 102.0 | 98.9 |
| | 102.6 | 99.5 | 102.2 | 99.1 |
| | 102.3 | 99.2 | 101.7 | 98.6 |
| 61.8 | 61.3 | 99.2 | 61.0 | 98.7 |
| | 61.5 | 99.5 | 61.3 | 99.2 |
| | 61.4 | 99.4 | 61.0 | 98.7 |
| 41.3 | 40.6 | 98.3 | 40.8 | 98.8 |
| | 40.9 | 99.0 | 40.9 | 99.0 |
| | 40.7 | 98.6 | 40.7 | 98.6 |

thienyl)borates have possibilities as gravimetric reagents. The tetrakis(3-thienyl)-borate does not appear to be of sufficiently low solubility for gravimetric analysis.

The solubilities obtained by flame emission photometry for alkali metal salts of tetrakis(2,5-dimethyl-3-thienyl)borate are shown in Table 3. The solubility of the cesium salt is such that gravimetric analysis should be possible. Sazanova et al. [8] reported the solubility of cesium tetrakis(2-thienyl)borate as 100 $ng\ l^{-1}$.

Table 4 contains the results of gravimetric determinations of cesium with the tetrakis(2-thienyl)borate and tetrakis(2,5-dimethyl 3-thienyl)borate anions. The values for cesium were calculated by using the theoretical gravimetric factors of 0.2791 and 0.2259, respectively.

The thermal stability of the compounds in terms of decomposition temperature was determined (Table 5). The tetrakis(2-thienyl)borate and tetrakis(3-thienyl)borate show lower decomposition temperatures than the substituted phenylborates, but in all cases the decomposition curves were similar in shape to those of previously studied tetraarylborates [9].

TABLE 5

Thermal stability of tetrathienylborates

| Compound | Minimum decomposition temp. (°C) |
|---|---|
| Cs tetrakis(2-thienyl)borate | 215 |
| Cs tetrakis(3-thienyl)borate | 235 |
| K tetrakis(2,5-dimethyl-3-thienyl)borate | 250 |
| Cs tetrakis(2,5-dimethyl-3-thienyl)borate | 265 |
| Cs tetrakis(5-bromo-2-thienyl)borate | 250 |

## DISCUSSION

The data indicate that the cesium salts of tetrakis(2-thienyl)borate and tetrakis(2,5-dimethyl-3-thienyl)borate offer possibilities for use in gravimetric analysis, but that neither reagent is selective for cesium.

The decomposition exhibited by these compounds differs from that seen in the substituted tetraphenylborates. Previous work [5] in this laboratory has shown that the acid pathway and the free radical pathway are responsible for the decomposition observed. In the case of tetrathienylborates, the present study indicates that the compounds are stable in dilute acids, and that free radical and electron transfer reactions seem to be involved in the decomposition process. As the apparent order of increasing stability for these compounds is: 5-t-butyl-2-thienyl $\ll$ 5-methyl-2-thienyl $<$ 5-ethyl-2-thienyl $\ll$ 5-bromo-2-thienyl $\leqslant$ 5-chloro-2-thienyl $<$ 3-thienyl $\leqslant$ 2-thienyl $\ll$ 2,5-dimethyl-3-thienyl, it appears that the availability of the 2- and 5-positions to attack is the destabilizing factor.

## REFERENCES

1 F. P. Cassaretto, J. J. McLafferty and C. E. Moore, Anal. Chim. Acta, 32 (1965) 376.
2 C. E. Moore, F. P. Cassaretto, H. Posvic and J. J. McLafferty, Anal. Chim. Acta, 35 (1966) 1.
3 J. T. Vandeberg, C. E. Moore, F. P. Cassaretto and H. Posvic, Anal. Chim. Acta, 44 (1969) 175.
4 M. Meisters, C. E. Moore and F. P. Cassaretto, Anal. Chim. Acta, 44 (1969) 287.
5 M. Meisters, J. T. Vandeberg, F. P. Cassaretto, H. Posvic and C. E. Moore, Anal. Chim. Acta, 47 (1970) 481.
6 F. Jarzembowski, F. P. Cassaretto, H. Posvic and C. E. Moore, Anal. Chim. Acta, 73 (1974) 409.
7 S. Chao and C. E. Moore, Anal. Chim. Acta, 100 (1978) 465.
8 V. Sazanova, E. P. Serebryakov and L. S. Kovaleva, Dokl. Akad. Nauk. SSSR, 113 (1957) 1295.
9 S. Chao, Doctoral Dissertation, Loyola University of Chicago, 1977.

*Analytica Chimica Acta*, 105 (1979) 361—368


# DIRECT TITRATIONS OF ANTIBIOTICS WITH IODATE SOLUTION
## Part 1. Titration of some Selected Penicillins

J. KEITH GRIME*

*Department of Chemistry, University of Denver, University Park, Denver, Colorado 80208 (U.S.A.)*

BARRIE TAN

*Department of Chemistry, University of Otago, P.O. Box 56, Dunedin (New Zealand)*

(Received 16th June 1978)

SUMMARY

The direct titration of penicillins with potassium iodate solution in strongly acidic conditions is feasible. Two end-point techniques are available: the conventional chloroform extraction technique used in iodimetric titrations, is compared with the irreversible indicator, amaranth, which is used in entirely aqueous systems. Results are presented for the determination of penicillin G, ampicillin sodium, and cloxacillin sodium. An oxidation mechanism is proposed.

The most commonly quoted chemical assays for the penicillin group of antibiotics are based on the titration of unconsumed iodine after incubation with the hydrolysed penicillin [1]. The hydrolytic cleavage of the β-lactam ring is usually achieved with a β-lactamase enzyme [2] or with sodium hydroxide. Most intact penicillin molecules do not reduce iodine although those with an unsaturated aliphatic side-chain do so with the β-lactam ring intact [3]. Careful blank estimations must be performed prior to hydrolysis; each mole of penicilloic acid absorbs nine moles of iodine. In practice, however, the method becomes more empirical; the stoichiometry varies between 8:1 and 9:1 depending on experimental conditions [4]. Furthermore, temperature, time, pH, and iodine concentration affect the stoichiometry [5]. In view of this variance, it is usually recommended that a standard sample of the penicillin is titrated under the same conditions and the results calculated on the basis of the calibrated standard [6].

Spectrophotometric methods have been based on the determination of (a) hydroxamic acid, formed by the reaction of the penicillin with hydroxylamine, [7], or (b) the penicillenic acid mercury(II) mercaptides, formed by the reaction of the penicillin with imidazole in the presence of $HgCl_2$ [8]. Alicino [9] has recently proposed an adaptation of his original procedure based on the reaction of penicillins with an excess of *N*-bromosuccinimide. Reproducible results were obtained by titration of the iodine liberated from potassium iodide by the residual *N*-bromosuccinimide after a reaction time of 2 h. Adams et al.

[10] have recently proposed a novel enzymatic penicillin assay based on a pH-stat instrument incorporating coulometric generation of the titrant. An extensive review of chemical methods for the assay of antibiotics has been published [11].

It has been suggested that the variation in stoichiometry of the iodimetric approach can be avoided by the use of iodine monochloride as the oxidant. The iodine produced is subsequently titrated with potassium iodate in strongly acidic conditions to an extraction end-point. The experimentally observed stoichiometry of 1 mol of penicillin to 2 mol of iodate was stated to be consistent with the formation of the appropriate sulphoxide derivative of the penicillin [12] but inspection of the relevant half-reactions indicates that, if the oxidation proceeds only as far as the sulphoxide, 2 mol of penicillin should react with 1 mol of iodate. Thus, for incubation:

$$\text{Penicillin-S} + H_2O = \text{Penicillin-SO} + 2H^+ + 2e$$

$$2ICl_2^- + 2e = I_2 + 4Cl^-$$

$$\text{Penicillin-S} + H_2O + 2ICl_2^- = \text{Penicillin-SO} + 2H^+ + I_2 + 4Cl^-$$

and for titration:

$$(I_2 + 4Cl^- = 2ICl_2^- + 2e) \times 2$$

$$IO_3^- + 2Cl^- + 6H^+ + 4e = ICl_2^- + 3H_2O$$

$$IO_3^- + 10Cl^- + 6H^+ + 2I_2 = 5ICl_2^- + 3H_2O$$

[In the interest of brevity, "Penicillin-S" denotes a typical penicillin molecule with no unsaturated groups in the side-chain, i.e. the sulphur atom is the only relevant oxidizable moiety. For the molecular structure of the individual penicillins examined, see Fig. 1.]

Results obtained with this technique were in overall stoichiometric agreemen with the work of El-Sebai et al. [12]. However, this stoichiometry can only be explained by subsequent oxidation of the penicillin molecule to the sulphonic acid derivative by potassium iodate. Indeed, this would be expected; in strongly acidic conditions, iodate is a more powerful oxidizing agent than iodine monochloride ($E^\circ IO_3^-/ICl_2^- = +1.23$ V; $E^\circ ICl_2^-/\frac{1}{2}I_2 = +1.06$ V [13]). This titration was therefore examined more carefully. Separation of the aqueous and non-aqueous layers after incubation with iodine monochloride and titration of each layer individually with potassium iodate after the addition of the appropriate blank layer elucidated the reactions. The iodate not only oxidized the iodine produced by the reduction of iodine monochloride (non-aqueous layer), but further oxidized the sulphoxide produced in this reaction to a sulphonic acid (aqueous layer). Addition of these two titration results produced the overall experimental stoichiometry, 1 mol of penicillin to 2 mol of iodate (see Discussion).

These preliminary experiments indicated that the direct titration of penicillins with potassium iodate in strongly acidic conditions is feasible. Two end-

point techniques were investigated; the conventional extraction technique was compared with an entirely aqueous system based on the irreversible redox indicator amaranth. Results are presented for the determination of penicillin G, ampicillin sodium, and cloxacillin sodium. An oxidation mechanism is proposed.

## EXPERIMENTAL

### *Reagents*

The following pharmaceutical grade compounds were obtained in sealed vials; penicillin G (benzylpenicillin sodium), ampicillin sodium (sodium 6-[D(-)-α-aminophenylacetamido] penicillinate) and cloxacillin sodium [sodium 6-(3-[2-chlorophenyl]-5-methylisoxazole-4-carboxamido)penicillinate monohydrate]. Elemental analysis showed no significant impurities, and accurate gravimetric studies showed moisture uptake to be insignificant during a typical analysis period. The compounds were used without further purification and solutions were prepared as required.

The buffer solution (pH 6.7) contained 40% (v/v) of $6.67 \times 10^{-2}$ mol $dm^{-3}$ disodium hydrogenphosphate and 60% (v/v) of $6.67 \times 10^{-2}$ mol $dm^{-3}$ potassium dihydrogenphosphate. Chloroform and thioglycollic acid were of laboratory reagent grade. Concentrated hydrochloric acid and potassium iodate were analytical grade chemicals. An aqueous 0.2% (w/v) amaranth solution was used as indicator. Distilled water was used. In a separate series of enthalpimetric experiments with enzymatic procedures, it was observed that, once in solution at pH 6.7, penicillin G undergoes hydrolytic decomposition at a rate of ca. 20% in 10 h. Visual titrations performed up to 24 h after the dissolution of penicillin showed that the analytical results are not affected by this hydrolysis. Storage of penicillin solutions for 24 h is therefore acceptable.

### *Procedure*

*Extraction end-point.* Quantitatively transfer ca. 1 g of penicillin to a 100-$cm^3$ volumetric flask and dilute to the mark with buffer solution; transfer 10.00 $cm^3$ of this solution to a 250-$cm^3$ iodine flask, and add 40 $cm^3$ of 12 mol $dm^{-3}$ hydrochloric acid and 10 $cm^3$ of chloroform. Titrate the mixture with 0.0500 mol $dm^{-3}$ potassium iodate with vigorous shaking. The colour of the chloroform layer changes from colourless to brown or deep red to colourless again. The end-point is taken as the first permanent decolorization of the chloroform layer.

*Amaranth end-point.* Follow the procedure described above, but omit the chloroform. To avoid irreversible decomposition of the indicator caused by transient local concentrations of potassium iodate, add the indicator (1 $cm^3$) about 1 $cm^3$ before the expected end-point. Continue the titration with gentle swirling to a sharp end-point; the colour changes from deep red to pale yellow when the dye is destroyed by an excess of iodate. In order to achieve quantitative oxidation in both titration techniques, cloxacillin was titrated at 40—50°C. Penicillin G and ampicillin sodium were titrated at room temperature.

## RESULTS

Both titration methods produced accurate and precise determinations of the penicillins examined; two moles of potassium iodate were consumed for each mole of penicillin taken. The results obtained by both end-point techniques are shown in Table 1. Both methods have comparable precisions (r.s.d., ca. 1.3%) and recoveries (error, ca. 0.53%). The amaranth method is the more convenient; vigorous shaking during titrant addition is not required and there is a considerable decrease in analysis time.

## DISCUSSION

The stoichiometry of the oxidation of penicillins by iodate in strongly acidic conditions can be rationalized by the mechanism shown in Fig. 1. The acid-catalysed degradation products of penicillin G and ampicillin have been studied [14—16]. The penicillenic acid (I) is formed by a rearrangement which involves the cleavage of the β-lactam ring, formation of an oxazolone ring and the appearance of a free thiol group. Although the rate of formation of (I) depends on hydrogen ion concentration, the rate constant becomes non-linear at a pH less than 3 [17] and finally independent of the hydrogen ion concentration at a pH of ca. 0. This is of critical importance; (I) exhibits a complicated pH dependence as it contains two basic nitrogen atoms, and dissociable protons on the thiol group and carboxylic acid groups. Hence it can exist in a complex equilibrium of several anionic and cationic forms capable of reactions at differing rates via different mechanisms. The high hydrogen ion concentration

TABLE 1

Titration results with extraction and amaranth end-points

| | Penicillin G | Ampicillin sodium | Cloxacillin sodium |
|---|---|---|---|
| *Extraction end-point* | | | |
| Mass taken (mg) | 100.2 | 100.1 | 111.6 |
| Average mass found (mg) | 101.1 | 100.2 | 110.5 |
| Range of mass found (mg) | 100.5—102.5 | 99.26—101.2 | 108.3—115.4 |
| R.s.d. (%)[a] | 0.69 (8) | 0.82 (9) | 2.0 (9) |
| *Amaranth end-point* | | | |
| Mass taken (mg) | 87.52 | 103.7 | 110.1 |
| Average mass found (mg) | 87.26 | 103.0 | 110.3 |
| Range of mass found (mg) | 86.45—89.12 | 102.0—104.8 | 107.5—113.7 |
| R.s.d. (%)[a] | 0.99 (8) | 1.2 (9) | 1.9 (8) |

[a]Number of runs in parentheses.

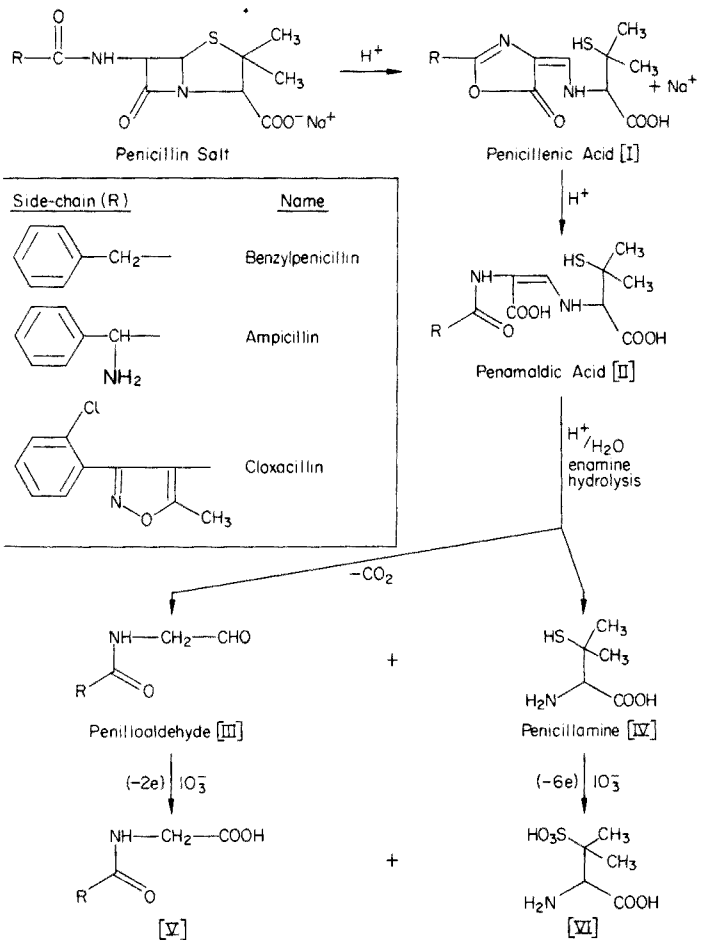


Fig. 1. Oxidation mechanism of penicillins by iodate in strongly acidic conditions.

necessary to make the degradation step independent of pH is compatible with the same requirement to produce the appropriate conditions for the reduction of iodate, i.e. in the presence of a high concentration of acid (3—9 mol $dm^{-3}$), iodate is ultimately reduced to iodine monochloride. In less acidic conditions the reduction occurs only as far as iodine [18]. Accordingly, if the pH of the titration solution is less than 0, the stoichiometry of the overall reaction is independent of small variations of pH.

The formation of penamaldic acid (II) from (I) occurs with relative ease [15, 19]; (II) is an enamine and will undergo hydrolysis. The formation of penicillamine (IV) is well-established and indeed was the first degradation product to be obtained in crystalline form [20]. The other hydrolysis product is a decarboxylated penilloaldehyde (III).

Upon oxidation with iodate the aldehyde (III) is oxidized to the carboxylic acid (V) and the thiol group (IV) is oxidized to the sulphonic acid (VI); these processes occur with electron changes of two and six, respectively. Aliphatic (and aromatic) thiols are oxidized by a variety of reagents to disulphides and higher oxidation products depending on the specific reaction conditions [21]. Possible products from the iodate oxidation of a thiol in strongly acidic conditions are the disulphide [21], sulphone, sulphoxide [22] and sulphonic acid derivatives. In order to establish which oxidation product is formed, thioglycollic acid was titrated with iodate under the experimental conditions described. The stoichiometry observed, 2 mol of $HSCH_2COOH$ with 3 mol of iodate, is consistent with the formation of a sulphonic acid moiety as shown by the following half-reactions:

$$(HSCH_2COOH + 3H_2O = HO_3SCH_2COOH + 6H^+ + 6e) \times 2$$

$$(IO_3^- + 2Cl^- + 6H^+ + 4e = ICl_2^- + 3H_2O) \times 3$$

$$3IO_3^- + 2HSCH_2COOH + 6Cl^- + 6H^+ = 3ICl_2^- + 2HO_3SCH_2COOH + 3H_2O$$

A series of nine such titrations produced results with a precision of 0.28% (r.s.d.) and an error of ca. 0.60% based on this stoichiometry. For a similar half-reaction procedure, the appropriate stoichiometries for the formation of the alternative oxidation products (viz., sulphoxide, sulphone and disulphide) would be represented by the following equations:

$$2HSCH_2COOH + IO_3^- + 2H^+ + 2Cl^- = ICl_2^- + 2H{-}\overset{\overset{O}{\|}}{S}{-}CH_2COOH + H_2O$$

$$HSCH_2COOH + IO_3^- + 2H^+ + 2Cl^- = ICl_2^- + H{-}\overset{\overset{O}{\|}}{\underset{\underset{O}{\|}}{S}}{-}CH_2COOH + H_2O$$

$$4HSCH_2COOH + IO_3^- + 2H^+ + 2Cl^- = ICl_2^- + 2HOOCCH_2{-}SS{-}CH_2COOH + 3H_2($$

Clearly these alternatives do not correlate with the experimental results. The overall stoichiometry for the oxidation of penicillins by iodate in strongly acidic conditions is conveniently described by the following half-reactions:

$$\text{Penicillin} \rightarrow (V) + (VI) + 8e$$

$$(IO_3^- + 6H^+ + 2Cl^- + 4e \rightarrow ICl_2^- + 3H_2O) \times 2$$

$$\text{Penicillin} + 2IO_3^- + 12H^+ + 4Cl^- \rightarrow 2ICl_2^- + 6H_2O + (V) + (VI)$$

In support of this mechanism it has been reported that thiols containing a $\beta$-carboxyl group are particularly susceptible to oxidation, even by iodine. It was suggested [23, 24] that the carboxyl group takes part in an intramolecular attack on the sulphur atom to form an anhydride which may undergo further oxidation to a sulphonic acid.

## CONCLUSIONS

This method is subject to the limitations of any inselective oxidative procedure in that it will be sensitive only to oxidative decomposition and to the presence of non-oxidizable impurities. Clearly, oxidizable excipients will cause interferences in tablet assay.

Indeed preliminary experiments with typical tablet excipients revealed that starch and lactose cause significant interference. The method is therefore restricted to the determination of penicillins in the vial form.

In this respect, penicillin preparations consisting of physical mixtures of drugs, e.g. procaine penicillin, must be treated individually, the approach depending on the nature of the accompanying drug. Procaine interfered with the iodate titration and must be separated prior to the titration of penicillin. A similar procedure to that described in the British Pharmacopoeia may be adopted for this separation [25].

The iodate titration offers several advantages when compared with existing chemical methods for the determination of penicillin compounds. The method described is a one-step, direct titration of the intact penicillin molecule by a primary standard. Incubation or pretreatment steps are therefore unnecessary, resulting in a more convenient and less time-consuming analysis. The stoichiometry of the reaction is known and reproducible, thus avoiding the empirical estimation of reagent uptake inherent in other iodimetric procedures. The end-point is sharp in all cases and reagent blanks were negligible. The technique has been successfully applied to a penicillin with an unsaturated side-chain (cloxacillin); this is a common restriction with iodimetric procedures.

The authors thank R. E. McKeown (Pharmacy Department, University of Otago) for gifts of penicillins and R. T. Weavers and D. J. Hannah (Chemistry Department, University of Otago) for many useful discussions.

## REFERENCES

1 J. F. Alicino, Ind. Chem. Eng., Anal. Ed., 18 (1946) 619.
2 M. R. Pollock, J. Gen. Microbiol., 26 (1961) 239.
3 D. C. Grove and W. A. Randall, Assay Methods of Antibiotics, Medical Encyclopaedia Inc., New York, 1955.
4 J. M. T. Hamilton-Miller, J. T. Smith and R. Knox, J. Pharm. Pharmacol., 15 (1963) 81.
5 K. Ilver, O. I. Johansen and F. Reimers, Acta. Pharm. Intern., 1 (1950) 225.
6 British Pharmacopoeia, H.M.S.O., 1973, p. 88.
7 G. E. Boxer and P. M. Everett, Anal. Chem., 21 (1949) 670.
8 H. Bundgaard and K. Ilver, J. Pharm. Pharmacol., 24 (1972) 790.
9 J. F. Alicino, J. Pharm. Sci., 65 (1976) 300.
10 R. E. Adams, S. R. Betso and P. W. Carr, Anal. Chem., 48 (1976) 1989.
11 J. E. Fairbrother, Pharm. J., 218 (1977) 509.
12 El-Sebai A. Ibrahim, S. M. Rida, Y. A. Beltagy and M. M. Abd El-Khalek, J. Drug. Res. (Egypt), 6 (1974) 13.
13 W. H. Latimer, Oxidation Potentials, 2nd edn., Prentice Hall, New York, 1956.
14 M. A. Schwartz, J. Pharm. Sci., 54 (1965) 472.

15 J. L. Longridge and D. Timms, J. Chem. Soc. B, (1971) 852.
16 J. P. Hou and J. W. Poole, J. Pharm. Sci., 58 (1969) 447.
17 H. Bundgaard, J. Pharm. Sci., 60 (1971) 1273.
18 H. A. Laitinen and W. E. Harris, Chemical Analysis, 2nd edn., McGraw-Hill, New York, 1975, p. 368.
19 B. B. Levine, Arch. Biochem. Biophys., 93 (1961) 50.
20 L. M. Atherden, Bentley and Driver's Textbook of Pharmaceutical Chemistry, 8th edn., Oxford University Press, 1969, pp. 792–794.
21 G. Capozzi and G. Modena in S. Patai (Ed.), The Chemistry of the Thiol Group, Wiley-Interscience, New York, 1974.
22 A. W. Chow, N. M. Hall and J. R. E. Hoover, J. Org. Chem., 27 (1962) 1381.
23 J. P. Danehy and M. Y. Oester, J. Org. Chem., 32 (1967) 1491.
24 J. P. Danehy, B. T. Doherty and C. P. Egan, J. Org. Chem., 36 (1971) 2525.
25 British Pharmacopoeia, H.M.S.O., 1973, p. 386.

*Analytica Chimica Acta*, 105 (1979) 369—374


# DIRECT TITRATIONS OF ANTIBIOTICS WITH IODATE SOLUTIONS
## Part 2. Some Selected Cephalosporins

J. KEITH GRIME*

*Department of Chemistry, University of Denver, University Park, Denver, Colorado 80208 (U.S.A.)*

BARRIE TAN

*Department of Chemistry, University of Otago, P.O. Box 56, Dunedin (New Zealand)*

(Received 31st July 1978)

SUMMARY

A previous method for the determination of penicillins by direct titration with potassium iodate under strongly acidic conditions has been extended to the assay of some selected cephalosporins. Results are presented, including error and precision analyses, for the determination of cephaloridine, cephalothin and cephalexin. The appropriate stoichiometries are 1 mol cephalosporin to 3 mol iodate for cephalothin and cephaloridine; 1 mol to 2 mol iodate for cephalexin. An irreversible aqueous end-point technique has been compared with the chloroform layer method; the latter gives more precise results for the determination of cephaloridine and cephalothin (0.8% and 1.3% r.s.d. respectively). Comparable precision was obtained by either technique for the determination of cephalexin (1.39% r.s.d.).

In order to rationalize the approach towards the chemical determination of cephalosporins it is necessary to consider the structural characteristics of the molecules. Cephalosporins and penicillins differ structurally in their heterocyclic ring systems; the penam moiety of the penicillin molecule contains a 5-membered thiazolidine ring; the 3 cephem moiety of the cephalosporin molecule contains an unsaturated six-membered dihydrothiazine ring. A $\beta$-lactam ring is a common feature of both molecules, and this has resulted in a similar approach to their assay. The methods have in general been based on the iodimetric procedure reported by Alicino [1]. Its universal application to the determination of cephalosporins has been restricted by the difficulties encountered in the hydrolysis of the $\beta$-lactam ring [2]. Furthermore, the cephalosporin ring is resistant to enzymatic hydrolysis [3]. In addition, the side-chains of cephalosporins are generally more complex and this has rendered interpretation of iodine uptake difficult. The original iodimetric procedure [1] was adapted for the determination of cephalosporin C [4], but the iodine consumption per mole of analyte was dependent on the assay conditions [5]. Erratic results were reported when this procedure was applied to cephradine [6]. Alicino more recently reported an indirect procedure for the determination of penicillins and cephalosporins with an excess of *N*-bromosuccinimide

as the primary oxidizing agent [7]; the unconsumed *N*-bromosuccinimide is then titrated iodimetrically. The stoichiometry of the oxidation of penicillins and cephalosporins is time dependent; reproducibility was obtained by standardization of the incubation time at 2 h. The instability of *N*-bromosuccinimide [8] was overcome by refrigerated storage.

Hydrolysis of the cephalosporin lactam ring has been facilitated by the use of a β-lactam enzyme (EC 3.5.2.6) with a high selectivity towards cephradine and related cephalosporins [6]. After enzymatic hydrolysis, the analytical result was obtained by an iodimetric procedure or by differential u.v. spectrophotometry. The latter method was more sensitive but less accurate (r.s.d. = 4.3%). The assay methods applicable to the most frequently encountered cephalosporins, including microbiological, chemical, chromatographic and spectroscopic techniques, have been reviewed elsewhere [9].

Recently, a direct titrimetric method has been proposed for the determination of penicillin compounds based on their oxidation with iodate [10] in strongly acidic solution, which gives the appropriate conditions for the reduction of iodate to iodine monochloride. In less acidic conditions the reduction proceeds only as far as iodine [11].

In this report, the feasibility of extending this technique to the determination of some selected cephalosporins is examined. The relevant stoichiometries and the analytical results from an immiscible layer end-point technique and an aqueous, irreversible indicator end-point method are discussed. The effect of titration temperature on the reaction stoichiometry is also described. Results are presented for the determination of pure cephaloridine, cephalothin injection (containing sodium hydrogencarbonate) and cephalexin capsules (containing magnesium stearate). These compounds were chosen as examples of cephalosporins in common usage. Cephalexin was included to indicate the effect of a non-oxidizable side-chain on the analysis.

## EXPERIMENTAL

### *Reagents*

Cephalexin (7-[D-α-aminophenylacetamido]-3-methyl-3-cephem-4-carboxylic acid, monohydrate) was obtained in capsules from Dunedin Hospital. Cephalothin sodium (7-[2-thienylacetamido]cephalosporanic acid, sodium salt) and cephaloridine (7-[(2-thienyl) acetamido]-3-(1-pyridylmethyl)-3-cephem-4 carboxylic acid betaine, δ-form) were obtained in sealed vials from the same source. Elemental analysis of cephaloridine revealed no significant impurities. The commercial preparations of cephalothin, containing 3% of sodium hydrogencarbonate, and cephalexin, containing 1% of magnesium stearate, were used without purification. Stock solutions of the three cephalosporins were prepared by quantitative dissolution of ca. 1 g of solid in 100 $cm^3$ of buffer solution. The structures of these compounds are shown below.

The buffer solution (pH 6.7) consisted of 40% (v/v) of $6.7 \times 10^{-2}$ mol $dm^{-3}$ disodium hydrogenphosphate and 60% (v/v) of $6.7 \times 10^{-2}$ mol $dm^{-3}$

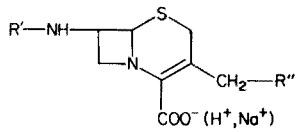


| R' | Name | R" |
|---|---|---|
| 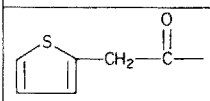 | Cephalothin | 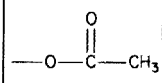 |
| 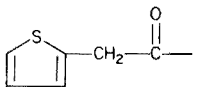 | Cephaloridine | 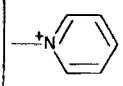 |
| 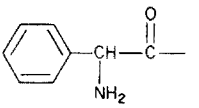 | Cephalexin | —H.$H_2O$ |

potassium dihydrogenphosphate. Chloroform and thiophene were reagent-grade chemicals. The concentrated hydrochloric acid and potassium iodate were analytical reagents. The amaranth indicator was prepared by dissolving 0.2 g of amaranth in 100 $cm^3$ of water. A solution (0.0500 mol $dm^{-3}$ ) of potassium iodate was prepared by dissolving the appropriate amount of analytical-grade potassium iodate in distilled water.

*Procedure*

*Immiscible layer end-point.* Place 10.00 $cm^3$ of the buffered cephalosporin solution, 40 $cm^3$ of concentrated hydrochloric acid, and 5 $cm^3$ of chloroform in a 250-$cm^3$ iodine flask and titrate the mixture (vigorous shaking is required) with standard potassium iodate to the first permanent decolourization of the chloroform layer. In practice, the chloroform layer remained colourless on standing for at least 15 min; during the course of the titration it changed from colourless to brown or deep-red to colourless again. Blank titrations were negligible.

*Amaranth end-point.* A procedure identical to that described above is followed with the exclusion of chloroform from the solution. Add amaranth solution (1 $cm^3$) ca. 2 $cm^3$ before the anticipated end-point, and continue the titration with gentle swirling to the end-point (deep red to orange). The end-point is less well-defined than that (deep-red to yellow) reported for penicillins [10]. Blank titrations are essential here.

## RESULTS

Results for both procedures are presented in Table 1, including error (range) and precision (% r.s.d.) analyses. The sharper end-point of the immiscible

TABLE 1

Results for some cephalosporins

| | Immiscible layer end-point | | | Amaranth end-point | | |
|---|---|---|---|---|---|---|
| | Cephaloridine | Cephalothin sodium | Cephalexin | Cephaloridine | Cephalothin sodium | Cephalexin |
| Mass taken (mg) | 101.2 | 111.2[a] | 105.9[a] | 97.38 | 112.8[a] | 98.62[a] |
| Average mass found (mg) | 100.5 | 115.1 | 106.1 | 97.20 | 116.6 | 100.7 |
| Range of mass found (mg) | 99.4—101.8 | 113.0—117.2 | 103.6—107.8 | 92.8—107.4 | 108.8—122.1 | 98.22—102.3 |
| R.s.d. (%)[b] | 0.79 (9) | 1.3 (8) | 1.3 (8) | 4.5 (9) | 3.6 (9) | 1.2 (8) |

[a]Nominal mass. [b]Number of analyses in parentheses.

layer technique is reflected in the superior precision of this technique, particularly in the determination of cephaloridine and cephalothin. Cephalexin determinations showed comparable precision with both techniques; in this case the amaranth technique is more convenient and less time-consuming.

Preliminary experiments revealed that the excipients present in the cephalothin and cephalexin preparations (sodium hydrogencarbonate and magnesium stearate) do not interfere with the titration. This is reflected in the error analyses which fall within the limits specified for these compounds [12].

The experimental stoichiometry was 1 mol cephalosporin to 3 mol iodate for cephalothin and cephaloridine, and 1 mol cephalosporin to 2 mol iodate for cephalexin (see Discussion).

## DISCUSSION

The poor precision in the determination of cephalothin and cephaloridine by the amaranth technique is undoubtedly related to the difficulty in oxidizing the sulphur moiety in the side-chain. The slower rate of addition of titrant in the immiscible end-point technique is clearly more compatible with the rate of this oxidation. Cephalexin does not have an oxidizable side-chain and shows comparable precision with both end-point techniques; cephalexin shows similar end-point characteristics to those of the penicillins and identical reaction stoichiometry [10].

A definitive mechanistic pathway for the oxidation and hydrolysis of cephalosporins under the conditions of the assay has not, to our knowledge, been reported. However, empirical evidence from titration results suggests that the essential oxidation sequences are similar in essence to those described for the oxidation of penicillins [10]. It is proposed therefore that the stoichiometry of the cephalexin oxidation is consistent with an eight-electron transfer; by analogy with the penicillin mechanism, this could involve the oxidation of a thiol and an aldehyde (formed by hydrolytic cleavage of the dihydrothiazine ring) to sulphonic acid and carboxylic acid moieties respec-

tively. In view of the complex fragmentation patterns possible, a definitive prediction of the reaction products is not feasible. Several degradation and cleavage sequences of the cephalosporins under various conditions have been reported [13].

The stoichiometry of the cephalothin/cephaloridine oxidation is consistent with the additional oxidation of the thiophene side chain to a sulphone, involving a further 4-electron transfer. In order to establish which oxidation product is formed, thiophene (40% alcoholic solution) was titrated with iodate under identical conditions by means of the amaranth end-point technique (a blank titration was necessary). The experimentally observed 1:1 stoichiometry is consistent with the formation of a sulphone as shown by the following half-reactions:

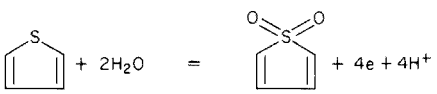

$$IO_3^- + 6H^+ + 4e + 2Cl^- = ICl_2^- + 3H_2O$$

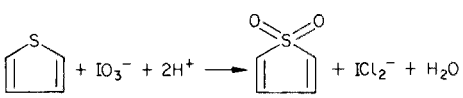

A series of eleven such titrations produced results with a precision of 2.5% r.s.d. and an error of ca. 1.7% based on this stoichiometry. For a similar half-reaction procedure, the appropriate stoichiometry for the formation of sulphoxide (the alternative oxidation product) would be represented by:

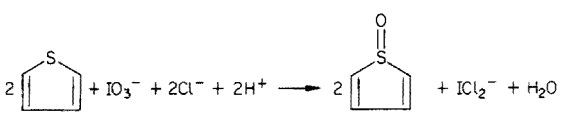

This alternative does not correlate with the experimental results.

Several experiments were performed to ascertain if the thiophene side chain could be further oxidized at elevated temperatures. In a series of titrations of thiophene following incubation at 50°C, the iodate uptake increased with increasing temperature and time of incubation. As expected, cephaloridine and cephalothin behaved similarly, giving an average increase in iodate uptake of ca. 16% following incubation at 50°C for 15—20 min and subsequent titration at this temperature. The end-point at elevated temperatures is, however, vague and the results were analytically unacceptable.

*Conclusions*

The method described offers a one-step, direct procedure for the determination of cephalosporins. The stoichiometry is reproducible. The technique has the same advantages and is subject to the same limitations and interfer-

ences as those described for penicillins [10]. In contrast to the penicillin assay, however, the immiscible layer end-point technique is recommended unless the molecule does not contain an oxidizable side chain (e.g. cephalexin).

One of us (B. T.) thanks the University of Otago for the provision of a Senior Demonstratorship.

REFERENCES

1 J. F. Alicino, Ind. Chem. Eng., Anal. Ed., 18 (1946) 619.
2 R. H. Earle, D. T. Hurst and M. Viney, J. Chem. Soc. C, (1969) 2093.
3 C. H. O'Callaghan and P. W. Muggleton, in E. H. Flynn (Ed.), Cephalosporins and Penicillins: Chemistry and Biology, Academic Press, New York, 1972, p. 452.
4 J. F. Alicino, Anal. Chem., 33 (1961) 648.
5 P. J. Weiss, Antibiot. Chemother., 9 (1959) 660.
6 B. M. Frantz, J. Pharm. Sci., 65 (1976) 887.
7 J. F. Alicino, J. Pharm. Sci., 65 (1976) 300.
8 A. Berka, J. Vulterin and J. Zyka, Newer Redox Titrants, Pergamon Press, London, 1965.
9 L. P. Marrelli, in E. H. Flynn (Ed.), Cephalosporins and Penicillins: Chemistry and Biology, Academic Press, New York, 1972, p. 601.
10 J. K. Grime and B. Tan, Anal. Chim. Acta, 105 (1979) 361.
11 H. A. Laitinen and W. E. Harris, Chemical Analysis, 2nd edn., McGraw-Hill, New York, 1975, p. 368.
12 British Pharmacopoeia, H.M.S.O., 1973.
13 E. H. Flynn (Ed.), Cephalosporins and Penicillins: Chemistry and Biology, Academic Press, New York, 1972.

*Analytica Chimica Acta*, 105 (1979) 375—382


# THE TITRIMETRIC DETERMINATION OF SULPHATE, THIOSULPHATE AND POLYTHIONATES IN MINING EFFLUENTS†

R. MAKHIJA and A. HITCHEN*

*Special Analysis Section, Chemical Laboratory, Mineral Sciences Laboratories, CANMET, Ottawa, K1A 0G1 (Canada)*

(Received 13th June 1978)

SUMMARY

A titrimetric procedure is described for the determination of various forms of sulphur (sulphate, sulphite, thiosulphate, dithionate, tri- and tetrathionates after conversion to sulphate) in mining effluents. Metal ions are removed, after an oxidizing step, by a cation-exchange resin, and the sulphate is precipitated with a known excess of 0.01 M barium chloride at pH 3.5. The excess of barium is back-titrated with standard 0.01 M ethylenediaminetetraacetic acid (EDTA) solution to a *o*-cresolphthalein complexone end-point at pH 11.0. The results obtained are in good agreement with those obtained by lengthy gravimetric procedures. Indirectly, dithionate can be determined, and sulphate and oxidizable thio salts such as thiosulphate and di-, tri-, and tetrathionates can be distinguished.

Thio salts are undesirable in flotation mill effluents because partially oxidized anions (e.g., $SO_3^{2-}$, $S_2O_3^{2-}$ and $S_nO_6^{2-}$) act as a source of belated acidity in tailing ponds and water streams. Recent reviews [1—3] have outlined several analytical procedures for the determination of various individual polythionates. For monitoring purposes, however, it is usually satisfactory to know only the total content of thio salts rather than the individual species. A rapid titration of thio salts in mining effluent has recently been described [4], but the method is not applicable to sulphate, sulphite or dithionate. Other methods for the determination of total sulphate and thio salts have been based on tedious gravimetric methods after conversion of the thio salts to sulphate [5]. Various complexiметric titrations of sulphate have been proposed [6], and interfering cations can be removed on a cation-exchange resin [7].

In this paper, the application of a complexiметric method for sulphate and thio salts based on back-titration of an excess of barium with standard EDTA solution and *o*-cresolphthalein complexone indicator [6] is described. The method consists of determining: (a) the initial sulphate, i.e., the existing sulphate ions plus the sulphate obtained by oxidizing sulphite with iodine; (b) the total sulphate obtained by oxidizing the polythionate anions (including the tetrathionate produced by oxidation of thiosulphate by iodine in (a)) with acidic hydrogen peroxide; and (c) the total sulphate obtained by oxidation of

†Minerals Research Program, Contribution No. 87.

all thio salts including dithionate with a mixture of hydrogen peroxide, potassium chlorate and concentrated nitric acid.

## EXPERIMENTAL

### *Ion-exchange columns*

Prepare columns (1 cm diameter, 20 cm long) using a slurry of Dowex 50W-X8 resin (50—100 mesh) in 1 M hydrochloric acid. Wash the columns with distilled water until the effluent is acid-free.

### *Reagents*

Potassium tri- and tetrathionates were prepared by methods [8] based on those of Stamm et al. [9]. All other chemicals were of analytical grade. Standard solutions (0.01 M) of potassium tetrathionate, sodium sulphate, sodium sulphite and sodium thiosulphate were prepared in distilled water. The thiosulphate solution was standardized iodimetrically. Standard barium chloride solution (0.01 M) in distilled water was standardized against the 0.01 M EDTA solution, which was prepared from the disodium salt and distilled water, and was standardized against a lead solution prepared from high-purity lead. The *o*-cresolphthalein complexone indicator solution was 0.3% (w/v) in distilled water containing enough ammonia liquor for dissolution; it was prepared weekly.

### *Procedures*

*A. Initial sulphate.* (This is defined as the total sulphate resulting from the oxidation of sulphite by iodine and sulphate present in the original solution.). Pipette a suitable aliquot containing 4—70 mg of total initial sulphate into a 150-ml beaker and dilute to 25 ml with distilled water. Acidify the solution with 1—2 drops of 6 M hydrochloric acid and add dropwise 0.004 N iodine solution until a slight yellow colour persists. This oxidizes sulphite to sulphate and thiosulphate to tetrathionate but does not affect dithionate or trithionate. Boil the solution for several minutes to remove the excess of iodine and cool to room temperature. Pass the solution through the ion-exchange column to remove all metal ions. Wash the column with distilled water three or four times (total volume $\simeq$ 60 ml). Adjust the pH of the effluent to 3.5 and bring to the boil. Add a known amount of 0.01 M barium chloride solution in excess (1 ml precipitates about 1 mg of sulphate). Digest the precipitate for 3—4 h on a water-bath to render the precipitate coarsely granular and insoluble. Cool and neutralize the solution with dilute sodium hydroxide solution. Adjust the volume of solution to about 100 ml, add 3—4 drops of indicator and adjust the pH to 11.0 $\pm$ 0.1 with ammonia liquor. Titrate the excess of barium immediately with 0.01 M EDTA solution until the blue colour changes to pale violet. From the amount of 0.01 M barium chloride used for precipitation, calculate the sulphate (plus sulphite) content of the sample.

*B. Sulphate — after hydrogen peroxide oxidation.* Pipette a suitable aliquot containing 4—70 mg of combined sulphate into a 150-ml beaker and dilute to

25 ml with distilled water. Acidify the solution with a few drops of 6 M hydrochloric acid, add 2 ml of 30% hydrogen peroxide solution and heat at 80°C for 15 min; then boil vigorously for several more minutes until all signs of peroxide decomposition cease. Cool to room temperature and pass through the ion-exchange column to remove metal ions. Wash the column with distilled water as in Procedure A. Adjust the pH of the effluent to 3.5 and follow Procedure A to complete the determination, starting at the point of addition of 0.01 M barium chloride solution.

The difference between the values obtained by Procedures B and A is a measure of the thio salts that are oxidized by hydrogen peroxide, i.e., $S_2O_3^{2-}$, $S_3O_6^{2-}$, $S_4O_6^{2-}$.

*C. Sulphate — after potassium chlorate—nitric acid oxidation.* To an aliquot identical to that used in Procedure B, add 2 ml of 30% hydrogen peroxide solution. Heat the solution at 80°C for 15 min, and then add 0.10—0.25 g of solid potassium chlorate and 2—5 ml of concentrated nitric acid. Evaporate the solution to near dryness but do not bake. Cool, and add 25 ml of hot distilled water and sufficient ammonia liquor to turn red litmus just blue. Acidify with 1—2 drops of 6 M hydrochloric acid, boil the solution for several minutes, cool to room temperature, and pass it through the ion-exchange column. Adjust the pH of the effluent to 3.5 and follow Procedure A to complete the determination of total sulphate, starting at the point where the 0.01 M barium chloride is added.

The difference between the values obtained by Procedures C and B is a measure of the dithionate present.

## RESULTS AND DISCUSSION

The results obtained in tests with various synthetic mixtures of the sodium salts of sulphite, sulphate, thiosulphate and dithionate, and potassium tri- and tetrathionates, as well as several mill circuit and mining samples are shown in Tables 1—5.

In the determination of initial sulphate, any sulphite ions are oxidized to sulphate and thiosulphate is oxidized to tetrathionate by the addition of 0.004 N iodine solution. Tetrathionate does not interfere in the determination of initial sulphate. The sulphite concentration can be determined separately [10] if desired and its equivalent sulphate subtracted to yield the concentration of sulphate present in the original solution. Good recoveries of sulphate are obtained (Table 1) and the errors are less than 2%. The "initial sulphate" concentration was determined by gravimetric and titrimetric methods on some typical mining samples and the results were found to be in good agreement (Table 4).

All the thio salts tested, except dithionate, are oxidized to sulphate by hydrogen peroxide in acidic solution, i.e. by Procedure B. The difference in sulphate concentration by this method and by Procedure A gives an estimate of the oxidizable thio salt concentration. The results obtained by the titrimetric

TABLE 1

Determination of initial sulphate in synthetically prepared solutions

| Thio salts taken as $SO_4^{2-}$, (mg) | | | | Equivalent total $SO_4^{2-}$ taken (mg) | Total $SO_4^{2-}$ found (mg) | Difference (mg) |
|---|---|---|---|---|---|---|
| $SO_4^{2-}$ | $SO_3^{2-}$ | $S_2O_3^{2-}$ | $S_3O_6^{2-}$ | | | |
| 4.80 | 0.00 | | | 4.80 | 4.78, 4.82 | −0.02, +0.02 |
| 4.80 | 0.96 | | | 5.76 | 5.79, 5.73 | +0.03, −0.03 |
| 4.80 | 2.40 | | | 7.20 | 7.06, 7.13 | −0.14, −0.07 |
| 4.80 | 4.80 | | | 9.60 | 9.43, 9.59 | −0.17, −0.01 |
| 4.80 | 9.61 | | | 14.41 | 14.32, 14.59 | −0.09, +0.18 |
| 4.80 | 19.22 | | | 24.02 | 23.95, 24.05 | −0.07, +0.03 |
| 4.80 | 28.83 | | | 33.63 | 33.40, 33.55 | −0.23, −0.07 |
| 4.80 | 38.44 | | | 43.24 | 43.35, 43.37 | +0.11, +0.13 |
| 4.80 | 48.05 | | | 52.85 | 52.46, 52.75 | −0.39, −0.10 |
| 4.80 | 0.00 | 0.00 | | 4.80 | 4.82 | +0.02 |
| 4.80 | 0.96 | 1.92 | | 5.76 | 5.75 | −0.01 |
| 4.80 | 2.40 | 4.80 | | 7.20 | 7.18 | −0.02 |
| 4.80 | 4.80 | 9.60 | | 9.60 | 9.75 | +0.15 |
| 4.80 | 9.61 | 19.20 | | 14.41 | 14.47 | +0.06 |
| 4.80 | 19.22 | 38.40 | | 24.02 | 23.90, 24.08 | −0.12, +0.06 |
| 4.80 | 28.83 | 57.60 | | 33.63 | 33.74 | +0.11 |
| 4.80 | 48.05 | 96.00 | | 52.85 | 52.46 | −0.39 |
| 4.80 | 0.00 | 0.00 | 0.00 | 4.80 | 4.80 | 0.00 |
| 4.80 | 0.96 | 1.92 | 0.29 | 5.76 | 5.86 | +0.10 |
| 4.80 | 2.40 | 4.80 | 0.725 | 7.20 | 7.37 | +0.17 |
| 4.80 | 4.80 | 9.61 | 1.45 | 9.60 | 9.84 | +0.24 |
| 4.80 | 9.61 | 19.20 | 2.88 | 14.41 | 14.50 | +0.09 |
| 4.80 | 19.22 | 38.40 | 5.76 | 24.02 | 23.95 | −0.07 |
| 4.80 | 28.83 | 57.60 | 8.64 | 33.63 | 34.70 | +1.07 |

method on synthetic mixtures are shown in Table 2 and are in excellent agreement with the calculated values. The error is less than 2%. Dithionate does not interfere in the determination of total sulphate by Procedure B but is oxidized to sulphate by Procedure C (Tables 2 and 3).

Some mill samples were analyzed by the proposed titrimetric method and by a gravimetric barium sulphate procedure. As shown in Table 5, the results obtained by Procedures B and C of the titrimetric method are in good agreement and confirm the fact that the synthetic samples did not contain dithionat These results are also in good agreement with the gravimetric results determined by the nitric acid—chlorate oxidation method. In contrast, the gravimetric results obtained by the peroxide oxidation method are significantly lower and would lead one to the false conclusion that some dithionate was present. The concentration of dithionate can be calculated by halving the difference between the results obtained by Procedures B and C, i.e., 2 mol $SO_4^{2-} \equiv 1$ mol $S_2O_6^{2-}$. The results in Table 5 obtained on mill circuit solution

TABLE 2

Determination of sulphate and thio salts in synthetically prepared solutions after oxidation with hydrogen peroxide

| Thio salts taken as $SO_4^{2-}$ (mg) | | | | | | Equivalent total $SO_4^{2-}$ taken (mg) | Total $SO_4^{2-}$ found (mg) | Difference (mg) |
|---|---|---|---|---|---|---|---|---|
| $SO_4^{2-}$ | $SO_3^{2-}$ | $S_2O_3^{2-}$ | $S_2O_6^{2-}$ | $S_3O_6^{2-}$ | $S_4O_6^{2-}$ | | | |
| 4.80 | 0.00 | 0.00 | | | | 4.80 | 4.79 | −0.01 |
| 4.80 | 0.96 | 1.92 | | | | 7.68 | 7.62 | −0.06 |
| 4.80 | 2.40 | 4.80 | | | | 12.00 | 11.87 | −0.13 |
| 4.80 | 4.80 | 9.60 | | | | 19.20 | 19.20 | ± 0.00 |
| 4.80 | 9.61 | 19.20 | | | | 33.61 | 32.85 | −0.75 |
| 4.80 | 0.00 | 0.00 | | 0.00 | | 4.80 | 4.78 | −0.02 |
| 4.80 | 0.96 | 1.92 | | 0.29 | | 7.97 | 7.69, 7.54 | −0.28, −0.43 |
| 4.80 | 2.40 | 4.80 | | 0.725 | | 12.72 | 12.44, 12.67 | −0.28, −0.05 |
| 4.80 | 4.80 | 9.60 | | 1.45 | | 20.65 | 20.58 | −0.07 |
| 4.80 | 9.61 | 19.20 | | 2.88 | | 36.49 | 36.83 | +0.35 |
| 4.80 | 19.22 | 38.40 | | 5.76 | | 69.60 | 70.90 | +1.30 |
| 4.80 | 0.00 | 0.00 | | 0.00 | 0.00 | 4.80 | 4.79, 4.80 | −0.01, +0.00 |
| 4.80 | 0.96 | 1.92 | | 0.29 | 0.38 | 8.35 | 8.26 | −0.09 |
| 4.80 | 2.40 | 4.80 | | 0.72 | 0.96 | 13.68 | 13.48 | −0.20 |
| 4.80 | 4.80 | 9.61 | | 1.44 | 1.92 | 22.73 | 22.11 | −0.62 |
| 4.80 | 9.61 | 19.22 | | 2.88 | 3.84 | 40.67 | 39.27 | −1.40 |
| 4.80 | 9.61 | 19.22 | | 5.76 | 3.84 | 43.55 | 43.35 | −0.20 |
| | | 0.96 | 0.96 | 1.44 | 1.92 | 4.32 | 3.84 | −0.48 |
| | | 1.92 | 1.92 | 2.88 | 3.84 | 8.64 | 8.45 | −0.19 |
| | | 3.84 | 3.84 | 5.76 | 7.68 | 17.28 | 17.23 | −0.05 |
| | | 5.76 | 5.76 | 8.64 | 11.52 | 25.92 | 25.78 | −0.14 |
| | | 7.68 | 7.68 | 11.52 | 15.36 | 34.56 | 34.80 | +0.24 |
| | | 9.60 | 9.60 | 14.40 | 19.20 | 43.20 | 43.15 | −0.05 |
| 4.80 | | 1.92 | 1.92 | 2.88 | 3.84 | 13.44 | 13.25 | −0.19 |
| 4.80 | | 3.84 | 3.84 | 5.76 | 7.68 | 22.08 | 21.70 | −0.38 |
| 4.80 | | 7.68 | 7.68 | 11.52 | 15.36 | 39.36 | 39.26 | −0.10 |
| 4.80 | | 9.60 | 9.60 | 14.40 | 19.20 | 48.00 | 46.42 | −1.58 |

no. 1 by the gravimetric method and Procedures B and C of the titrimetric method indicate that a small but significant amount of dithionate is present in the sample; the results on mill circuit sample no. 2 do not indicate any dithionate in excess of analytical error.

*Effect of foreign ions*

Because iodide ions are produced by oxidation of sulphite and thiosulphate by iodine and significant amounts of ammonium chloride are produced during the subsequent treatment of the sample, the effects of these salts were studied. Iodide had no effect on the titration even in large excess, i.e., up to 1.0 g per 50 ml. Ammonium chloride had little effect on the titration provided that

TABLE 3

Determination of sulphate and thio salts in synthetically prepared solutions after potassium chlorate—nitric acid oxidation

| Thio salts taken as $SO_4^{2-}$ (mg) | | | | | | Equivalent total $SO_4^{2-}$ taken (mg) | Total $SO_4^{2-}$ found (mg) | Difference (mg) |
|---|---|---|---|---|---|---|---|---|
| $SO_4^{2-}$ | $SO_3^{2-}$ | $S_2O_3^{2-}$ | $S_2O_6^{2-}$ | $S_3O_6^{2-}$ | $S_4O_6^{2-}$ | | | |
| 4.80 | 0.00 | 0.00 | | 0.00 | 0.00 | 4.80 | 4.82 | +0.02 |
| 4.80 | 0.96 | 1.92 | | 0.29 | 0.38 | 8.35 | 8.77 | +0.42 |
| 4.80 | 2.40 | 4.80 | | 0.72 | 0.96 | 13.68 | 13.62 | —0.06 |
| 4.80 | 4.80 | 9.60 | | 1.44 | 1.92 | 22.56 | 22.19 | —0.37 |
| 4.80 | 9.61 | 19.20 | | 2.88 | 3.84 | 40.33 | 39.82 | —0.51 |
| 4.80 | | 7.68 | 7.68 | 11.52 | 15.36 | 47.04 | 46.75 | —0.29 |
| 4.80 | | 9.60 | 9.60 | 14.40 | 19.20 | 57.60 | 56.74 | —0.86 |
| | | 0.96 | 0.96 | 1.44 | 1.92 | 5.28 | 5.23 | —0.05 |
| | | 1.92 | 1.92 | 2.88 | 3.84 | 10.56 | — | — |
| | | 3.84 | 3.84 | 5.76 | 7.68 | 21.12 | 21.26 | +0.14 |
| | | 5.76 | 5.76 | 8.64 | 11.52 | 31.68 | 31.73 | +0.05 |
| | | 7.68 | 7.68 | 11.52 | 15.36 | 42.24 | 42.14 | —0.10 |
| | | 9.60 | 9.60 | 14.40 | 19.20 | 52.80 | 52.61 | —0.19 |

TABLE 4

Determination of initial sulphate content in mill circuit samples

| Sample No. | Gravimetric ($g\ l^{-1}$) | Titrimetric ($g\ l^{-1}$) | Difference ($g\ l^{-1}$) |
|---|---|---|---|
| 1 | 2.35 | 2.48 | +0.13 |
| 2 | 2.13 | 2.02 | —0.11 |
| 3 | 2.07 | 1.93 | —0.14 |
| 4 | 1.59 | 1.57 | —0.02 |
| 5 | 0.063 | 0.055 | —0.008 |
| 6 | 1.54 | 1.52 | —0.02 |
| 7 | 1.44 | 1.41 | —0.03 |
| 8 | 1.45 | 1.42 | —0.03 |
| 9 | 1.42 | 1.40 | —0.02 |

less than 0.20 g was present but with amounts in excess of this the end-point was not sharp and was often not detectable. Thus it is important to the success of the titration to keep the ammonium chloride concentration (including that arising from the addition of barium chloride) to a minimum.

Sulphide interferes, hence it is oxidized to sulphate by the addition of iodine solution. Any thiosulphate is also oxidized by iodine to tetrathionate in acidic solution but this does not interfere in the initial sulphate determination.

TABLE 5

Determination of sulphate and thio salts in mill circuit and synthetic samples (All results are expressed as sulphate in g $l^{-1}$)

| Sample No. | Oxidation with $H_2O_2$ | | Oxidation with $KClO_3$—$HNO_3$ | | Difference | |
|---|---|---|---|---|---|---|
| | Gravimetric (i) | Titrimetric (ii) | Gravimetric (iii) | Titrimetric (iv) | (iii) − (i) | (iv) − (ii) |
| *Mill circuit samples* | | | | | | |
| 1 | 5.14 | 4.98 | 5.54 | 5.31 | +0.40 | +0.33 |
| 2 | 2.63 | 2.65 | 2.69 | 2.67 | +0.06 | +0.02 |
| *Synthetic samples* | | | | | | |
| 1 | 2.64 | 2.77 | 2.73 | 2.75 | +0.09 | −0.02 |
| 2 | 2.63 | 2.75 | 2.72 | 2.77 | +0.09 | +0.02 |
| 3 | 2.71 | 2.81 | 2.78 | 2.83 | +0.07 | +0.02 |
| 4 | 2.68 | 2.77 | 2.76 | 2.82 | +0.08 | +0.05 |

*Effect of pH*

The pH of the solution during the titration must be kept close to 11, otherwise variable results are obtained. For example, at pH 10.5 the colour change at the end-point is slow and drawn out, and at pH 11.5 about 30% of the original colour intensity persists after the normal end-point is reached [6]. A screened indicator consisting of a mixture of *o*-cresolphthalein complexone and naphthol green was tried but reproducible results were not obtained despite the use of alcohol [6]. The *o*-cresolphthalein complexone gives a very sharp end-point from deep violet to red without alcohol provided that the pH is carefully controlled at 11.0 ± 0.1.

*Conclusions*

The results obtained by the complexiметric titration method for synthetic mixtures and mining effluents compare favourably with those obtained by the tedious gravimetric procedure. The complexiметric method is less time-consuming because there is no need to filter, ignite or weigh the precipitate. The *o*-cresolphthalein complexone indicator is satisfactory if the pH at the end-point is carefully controlled.

With the recommended oxidation procedures, the method can distinguish between non-oxidizable sulphate and the oxidizable thio salts and dithionate. The proposed method is suitable for monitoring mining effluents and retaining pond waters for sulphate and thio salts. Steps can then be taken to ensure the destruction of potential acid-producing thio salts before their discharge to rivers, etc.

REFERENCES

1 L. Szekeres, Talanta, 21 (1974) 1.
2 A. Hitchen and C. W. Smith, Mineral Sciences Laboratories, CANMET, Report MRP/MSL 76-208 (LS), August 1976.

3 C. W. Smith and A. Hitchen, Mineral Sciences Laboratories, CANMET, Report MRP/MSL 76-223 (LS), August 1976.
4 R. Makhija and A. Hitchen, Talanta, 25 (1978) 79.
5 E. Rolia, Mineral Sciences Laboratories, CANMET, Report MRP/MSL 77-21 (TR).
6 G. Schwarzenbach and H. Flaschka, Complexometric Titrations, Translated by H. M. N. H. Irving, 2nd English edn., Methuen, London, 1969.
7 J. S. Fritz and S. S. Yamamura, Anal. Chem., 27 (1955) 1461.
8 A. Hitchen, Mineral Sciences Laboratories, CANMET, Report MRP/MSL 76-279 (TR), December 1976.
9 H. Stamm, M. Goehring and U. Feldman, Z. Anorg. Allg. Chem., 250 (1942) 226.
10 I. M. Kolthoff and R. Belcher, Volumetric Analysis, Vol. 3, Interscience Publishers, New York, 1957.

*Analytica Chimica Acta*, 105 (1979) 383–390


# LIQUID ION-EXCHANGE EXTRACTION STUDY OF HEXACYANOFERRATE(III) WITH TRIOCTYLMETHYLAMMONIUM CHLORIDE (ALIQUAT-336)†

JUN'ICHI ITOH**, HIROSHI KOBAYASHI*** and KEIHEI UENO*

*Department of Organic Synthesis, Faculty of Engineering, Kyushu University, Fukuoka 812 (Japan)*

(Received 4th July 1978)

SUMMARY

Liquid-liquid ion-exchange extraction of various anions including hexacyanoferrate(III) with a chlorobenzene solution of trioctylmethylammonium chloride (TOMA-Cl; Aliquat-336 chloride) is described. The ion-pair extraction constant of TOMA-Cl ($K_{ex}^{Q.Cl} = 10^4$) and the ion-exchange extraction constants of TOMA-Cl for each anion ($K_{ex}^{Cl.X}$) are reported. The order of selectivity of anion extraction is $Fe(CN)_6^{3-}$ (log $K_{ex}^{Q.X} = 22.41$) > $ClO_4^-$ (8.47) > $PAR^-$ (7.80) > $I^-$ (7.32) > $NO_3^-$ (5.81) > $Br^-$ (5.34) > $Cl^-$ (4.00).

Liquid ion-exchange extractions of anions with long-chain tertiary amines and quaternary ammonium salts have been widely used as separation processes in industry as well as in analytical chemistry [1, 2]. Irving and Damodaran [3] were unable to extract hexacyanoferrate(III) and hexacyanoferrate(II) ions in their ion-exchange extraction study on various metal cyanides with tetrahexylammonium salts in MIBK. However, in their later work [4] on the ion-exchange extraction of anionic EDTA complexes with Aliquat-336 in dichloroethane, they successfully extracted multivalent anionic complexes such as $FeY(OH)_2^{3-}$ and $VO_2Y^{3-}$. Qualitatively, the extraction of anions should be favoured by decrease of hydrophilicity, i.e. by increase in size and decrease in charge of the anions, but these results could not be explained on this basis.

The extraction of hexacyanoferrate(III) with Aliquat-336 in chlorobenzene is successful [5], though this would not be expected from the results with the tetrahexylammonium salt—MIBK system. This paper reports on the liquid ion-exchange extraction of anions of various charges with Aliquat-336 chloride (trioctylmethylammonium chloride; TOMA-Cl) in chlorobenzene, and describes an attempt to elucidate the factors governing the selectivity of the anion extraction.

---

†Contribution No. 495 from the Department of Organic Synthesis, Kyushu University.

**Present address: Kitami Institute of Technology, Kitami 090.

***Present address: Research Institute for Industrial Science Kyushu University, Fukuoka 812.

## EXPERIMENTAL

### *Reagents*

TOMA-Cl solution was prepared by dissolving a suitable amount of Aliquat-336 chloride (kindly donated by General Mills Inc.) in chlorobenzene to make a 0.5% (v/v) solution, which was shaken with an equal volume of 0.1 M hydrochloric acid, and then with five successive equal volumes of water. Although about 20% of TOMA-Cl was lost by this treatment, trace impurities and excess of chloride were eliminated, so that the errors in the equilibrium study could be reduced markedly. The concentration of TOMA-Cl was determined by extractive photometric titration (395 nm) at pH 10 with a standard solution of PAR (4-(2-pyridylazo)resorcinol).

PAR solution was prepared from the purified (recrystallized from DMF) commercial product (Dojindo Labs., Kumamoto) and was standardized against a standard nickel(II) solution by photometric titration at pH 9.2.

TOMA-HR (hereafter, a neutral PAR molecule is abbreviated as $H_2R$) solution in chlorobenzene was prepared by shaking equal volumes of solutions of $5 \times 10^{-4}$ M TOMA-Cl in chlorobenzene and $5 \times 10^{-3}$ M PAR in water (pH 10 adjusted with ammonia solution), followed by repeated washing with water (pH 10) until the absorbance of the aqueous phase at 410 nm became less than 0.02. The concentration of the TOMA-HR was determined photometrically by using the molar absorptivity of TOMA-HR in chlorobenzene ($\epsilon$ = $3.00 \times 10^5$ l mol$^{-1}$ cm$^{-1}$ at 395 nm).

All the anions investigated were used as their potassium salts (analytical grade). The twice-distilled water used for the equilibrium study was presaturated with chlorobenzene.

### *Extraction procedure*

Extractions were done in glass-stoppered 50-ml centrifuge tubes. Portions (20-ml each) of TOMA-HR solution in chlorobenzene and of aqueous anion solution (buffered to pH 10), were shaken for 20 min on a mechanical shaker equipped with a constant-temperature (20 ± 0.5°C) water circulation device. The tube was then centrifuged for 15 min at 2000 rpm for phase separation, followed by spectrophotometric measurement of the PAR in the organic and aqueous phases at 395 nm and 410 nm, respectively, to determine the extraction constants.

Similar experiments were done to determine the distribution ratio, D, of TOMA-Cl between chlorobenzene and water; known concentrations of TOMA-Cl in chlorobenzene were used. The total concentration of the TOMA species in the aqueous phase after equilibration, was determined on 5-ml aliquots by ion-pair extraction photometry, after treatment with 5 ml of $1 \times 10^{-3}$ M PAR solution and 5 ml of chlorobenzene at pH 10.

A Hitachi Model 200 recording spectrophotometer equipped with standard 1-cm quartz cells was used.

*Analyses of extraction equilibria*

The ion-exchange extraction constants between TOMA-Cl and various anions, $K_{ex}^{Cl.X}$, were determined indirectly by the method of Irving and Damodaran [3], to avoid undue errors in the complicated analysis for each anion. Thus, the ion-exchange extraction constants between TOMA-HR and anions, and between TOMA-Cl and $HR^-$, were determined separately, and the values of $K_{ex}^{Cl.X}$ were then computed from the two values. This modified method is more convenient than the direct determination, because the concentrations of the distributed species can easily be determined by spectrophotometry. The use of PAR as the indicator anion is advantageous because the dye is readily purified, giving a stable univalent anion with a high molar absorptivity over a wide pH range, and its concentration can be determined accurately by photometric titration with standard metal ion solutions.

The ion-exchange extraction constants between TOMA-HR and various anions can be defined as follows;

$$n\mathrm{QHR}_o + \mathrm{X}^{n-}{}_w = \mathrm{Q}_n\mathrm{X}_o + n\mathrm{HR}^-{}_w$$

$$K_{ex}^{HR.X} = [\mathrm{Q}_n\mathrm{X}]_o\,[\mathrm{HR}^-]^n{}_w/[\mathrm{QHR}]^n{}_o\,[\mathrm{X}^{n-}]_w \qquad (1)$$

where $Q^+$ represents the TOMA cation. It can be assumed that the distributions of the ion pairs, QHR and QX, into the aqueous phase, and the distributions of the anions, $X^-$ and $HR^-$, into the organic phase, are negligible, and so eqn. (1) can be rewritten:

$$K_{ex}^{HR.X} = \frac{(1/n)\,([\mathrm{QHR}]_T - [\mathrm{QHR}]_o)^{n+1}}{[\mathrm{QHR}]^n{}_o\,\{[\mathrm{X}^-]_T - (1/n)\,([\mathrm{QHR}]_T - [\mathrm{QHR}]_o\}} \qquad (2)$$

where $[QHR]_T$ and $[X^-]_T$ represent the initial concentrations of Q-HR in the organic phase and of the anion in the aqueous phase, respectively. Thus $K_{ex}^{HR.X}$ can be obtained from eqn. (2) by determining the concentration of Q-HR in the organic phase photometrically. However, in order to attain the above stoichiometry, clear phase separation is essential, and this can be attained only by adequate centrifugation.

*Distribution of TOMA-Cl between chlorobenzene and water*

The distribution ratio for $Q^+{}_w + Cl^-{}_w = \text{Q-Cl}_o$, can be defined as

$$D = [\mathrm{QCl}]_o/([\mathrm{Q}^+]_w + [\mathrm{QCl}]_w) \qquad (3)$$

and the ion-pair extraction constant of TOMA-Cl can be defined as

$$K_{ex}^{Q.Cl} = \frac{[\mathrm{QCl}]_o}{[\mathrm{Q}^+]_w\,[\mathrm{Cl}^-]_w} \qquad (4)$$

Equation (4) can be rewritten by introducing the distribution coefficient, $P = [QCl]_o/[QCl]_w$, to give

$$D = 1/\left(\frac{1}{K_{ex}^{Q.Cl}\cdot[\mathrm{Cl}^-]_w} + \frac{1}{P}\right) \qquad (5)$$

where $[Cl^-]_w$ can be expressed by $([Cl^-]_T - [QCl]_o - [QCl]_w)$. The value of $[QCl]_w$ is not known, but is very small so that $[Cl^-]_w \approx [Cl^-]_T - [QCl]_o$. The plot of log D vs. log $[Cl^-]_w$ should give a straight line with a slope of 1 over the range where the term $1/P$ can be neglected. The value of $K_{ex}^{Q,Cl}$ can be evaluated from the intercept of this line at log D = 0.

## RESULTS AND DISCUSSION

### *Ion-exchange extraction with TOMA-HR*

Tables 1 and 2 show the results obtained in the ion-exchange extraction study with TOMA-HR and various anions in the water-chlorobenzene system. Equation (2) was used to evaluate $K_{ex}^{HR,X}$, and the values were in good agreement over the concentration range investigated. In the case of hexacyanoferrate(III), analysis of the results indicated the value $n = 3$ in eqn. (2), i.e. a stoichiometry of $TOMA^+$: $Fe(CN)_6^{3-}$ = 3:1 in the complex extracted.

TABLE 1

Equilibrium data for the extraction of chloride, bromide and nitrate ions ($X^-$) by TOMA-PAR in chlorobenzene solution

| $[Q\text{-}HR]_T$ $\times 10^5$ | $[X^-]_T = [X^-]_w$ $\times 10^2$ | $[Q\text{-}HR]_o$ $\times 10^5$ | $[HR^-]_w = [QX]_o$ $\times 10^5$ | $\log K_{ex}^{HR,X}$ |
|---|---|---|---|---|
| *Chloride* | | | | |
| 5 | 99.8 | 0.877 | 4.12 | −3.71 |
| 5 | 49.9 | 1.35 | 3.65 | −3.70 |
| 5 | 20.0 | 2.45 | 2.55 | −3.88 |
| 5 | 9.98 | 3.11 | 1.89 | −3.94 |
| 5 | 4.99 | 3.73 | 1.27 | −4.06 |
| 1 | 9.98 | 0.283 | 0.717 | −3.74 |
| 1 | 4.99 | 0.402 | 0.598 | −3.75 |
| 1 | 2.00 | 0.563 | 0.437 | −3.77 |
| 1 | 0.998 | 0.686 | 0.314 | −3.84 |
| 1 | 0.499 | 0.770 | 0.230 | −3.86 |
| | | | Average | −3.80 |
| *Bromide* | | | | |
| 5 | 2.00 | 1.57 | 3.43 | −2.42 |
| 5 | 0.99 | 2.15 | 2.85 | −2.42 |
| 5 | 0.50 | 2.78 | 2.22 | −2.45 |
| 5 | 0.200 | 3.47 | 1.53 | −2.47 |
| 5 | 0.099 | 3.92 | 1.08 | −2.53 |
| | | | Average | −2.46 |
| *Nitrate* | | | | |
| 5 | 9.98 | 1.20 | 3.80 | −1.92 |
| 5 | 4.99 | 1.91 | 3.09 | −2.00 |
| 5 | 2.00 | 2.59 | 2.41 | −1.95 |
| 5 | 0.998 | 3.24 | 1.76 | −2.02 |
| 5 | 0.499 | 3.73 | 1.27 | −2.06 |
| | | | Average | −1.99 |

TABLE 2

Equilibrium data for the extraction of perchlorate, hexacyanoferrate(III) and iodide ions ($X^-$) by TOMA-PAR in chlorobenzene solution

| $[QHR]_T$ $\times 10^5$ | $[X^-]_T$ $\times 10^5$ | $[X^-]_w$ $\times 10^5$ | $[QHR]_o$ $\times 10^5$ | $[HR^-]_w = [QX]_o$ $\times 10^5$ | $\log K_{ex}^{HR,X}$ |
|---|---|---|---|---|---|
| *Perchlorate at 20°C* | | | | | |
| 5 | 19.9 | 15.2 | 0.32 | 4.68 | 0.66 |
| 5 | 9.95 | 5.66 | 0.71 | 4.29 | 0.66 |
| 5 | 7.46 | 3.42 | 0.96 | 4.04 | 0.70 |
| 5 | 4.98 | 1.56 | 1.58 | 3.42 | 0.68 |
| 5 | 2.49 | 0.36 | 2.87 | 2.13 | 0.64 |
| | | | | | Average 0.67 |
| *Perchlorate at 50°C* | | | | | |
| 5 | 19.9 | 15.2 | 0.30 | 4.70 | 0.68 |
| 5 | 9.95 | 5.63 | 0.68 | 4.32 | 0.68 |
| 5 | 7.46 | 3.38 | 0.92 | 4.08 | 0.72 |
| 5 | 4.98 | 1.51 | 1.53 | 3.47 | 0.72 |
| 5 | 2.49 | 0.30 | 2.81 | 2.19 | 0.74 |
| | | | | | Average 0.71 |
| *Hexacyanoferrate(III)*[a] | | | | | |
| 5 | 20 | 18.82 | 2.18 | 2.82 | −0.97 |
| 5 | 10 | 9.01 | 2.40 | 2.60 | −0.91 |
| 5 | 5.0 | 4.18 | 2.72 | 2.28 | −0.97 |
| 5 | 2.0 | 1.37 | 3.18 | 1.82 | −1.08 |
| 5 | 1.0 | 0.471 | 3.45 | 1.55 | −1.00 |
| | | | | | Average −0.99 |
| *Iodide*[b] | | | | | |
| 5 | 5.00 | 46.0 | 1.01 | 3.99 | −0.47 |
| 5 | 2.00 | 16.8 | 1.80 | 3.20 | −0.47 |
| 5 | 1.00 | 7.51 | 2.51 | 2.49 | −0.48 |
| 5 | 0.50 | 3.19 | 3.19 | 1.81 | −0.49 |
| 5 | 0.20 | 0.93 | 3.93 | 1.07 | −0.50 |
| | | | | | Average −0.48 |

[a] In this case $[HR^-]_w = 3[QX]_o$.
[b] For iodide, $[I^-]_T$ was $10^{-4}$ M instead of $10^{-5}$ M.

The ion pair, $TOMA_3 \cdot Fe(CN)_6$ showed an absorption maximum at 420 nm ($\epsilon \approx 10^3$ l mol$^{-1}$ cm$^{-1}$) in chlorobenzene. However, the photometric error for TOMA · HR caused by this species did not exceed 1% under the experimental conditions shown in Table 2, so that corrections were not made in the analysis of the results.

*Distribution of TOMA-Cl between water and chlorobenzene*

The ion-pair extraction constant of TOMA-Cl, $K_{ex}^{Q,Cl}$, was evaluated as described under Experimental, by plotting $\log D$ vs. $\log [Cl^-]_w$. Though the plots showed some scatter (Fig. 1), a nearly straight line of slope 1 was obtained

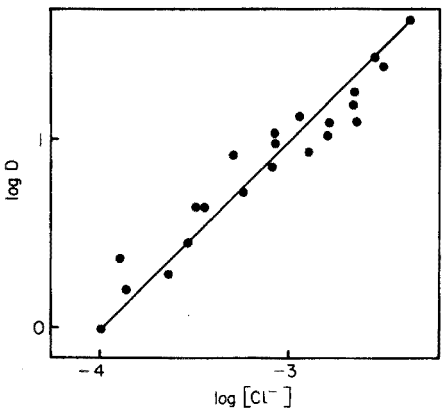


Fig. 1. log $D$ vs. log [$Cl^-$] plots for the distribution of TOMA-Cl.

in the log $[Cl^-]_w$ range −2.3 to −3.8. The plots deviated considerably from the straight line at lower concentrations, probably because the amount of specie concentrated at the liquid—liquid interface cannot be neglected, as $[Q]_T$ is also small at low concentrations. The value of $10^4$ for $K_{ex}^{Q.Cl}$ is slightly lower than that obtained for tetradecyldimethylbenzylammonium chloride (TDBA-Cl) in a water-chloroform system ($K_{ex}^{Q.Cl} = 10^{5.11}$) [6].

*Selectivity for ion-exchange extraction*

Table 3 summarises the results of Tables 1 and 2. The values of $K_{ex}^{Cl.X}$ are the ion-exchange extraction constant of TOMA-Cl for various anions, and were calculated from the equation

$$K_{ex}^{Cl.X} = [QX]_o\,[Cl^-]_w/[QCl]_o\,[X^-]_w = K_{ex}^{HR.X}\,(K_{ex}^{HR.Cl})^{-1} \qquad (6)$$

The values of $K_{ex}^{Q.Cl}$ are the ion-pair extraction constant of $TOMA^+$ and various

TABLE 3

Equilibrium constants for the extraction of anions from aqueous solution by TOMA salts in chlorobenzene at 20°C

| X | log $K_{ex}^{HR.X}$ | log $K_{ex}^{Cl.X}$ | log $K_{ex}^{QX}$ | (TDBA)[a] |
|---|---|---|---|---|
| $Cl^-$ | −3.80 | 0 | 4.00 | (5.11) |
| $Br^-$ | −2.46 | 1.34 | 5.34 | (5.93) |
| $NO_3^-$ | −1.99 | 1.81 | 5.81 | |
| $I^-$ | −0.48 | 3.32 | 7.32 | (7.27) |
| $HR^-$ | 0 | 3.80 | 7.80 | (7.31) |
| $ClO_4^-$ | 0.67 | 4.47 | 8.47 | (7.40) |
| $Fe(CN)_6^{3-}$ | −0.99 | 10.41 | 22.41 | |

[a]Data for TDBA—chloroform system [7].

anions ($X^-$), and were calculated from the following equation with the observed value of $K_{ex}^{Q.Cl} = 10^{4.00}$:

$$K_{ex}^{Q.X} = [QX]_o/[Q^+]_w [X^-]_w = K_{ex}^{Cl.X} K_{ex}^{Q.Cl} \quad (7)$$

The corresponding values for TDBA-Cl in the water—chloroform system [7] are included in Table 3 for comparison.

The order of anion selectivity of TOMA is $ClO_4^- > I^- > NO_3^- > Br^- > Cl^- \gg SO_4^{2-}$ which is similar to that of TDBA. This order, except for the nitrate ion, is also found in ion-pair extraction with tris (1,10-phenanthroline)iron(II) in nitrobenzene [8] or with tris(8-quinolinol)zinc(II) in chloroform [9]. These orders are readily interpreted by the well known working hypothesis that the extraction of anions is favoured by increase in size and decrease in charge.

This hypothesis cannot be extended to the hexacyanoferrate(III) ion, because the selectivity order is $Fe(CN)_6^{3-} > ClO_4^-$ in the TOMA-Cl—chlorobenzene system. However, in a similar experiment with the tetrahexylammonium ($THA^+$) salt in MIBK, Irving and Damodaran [3] found that the order of selectivity was $M(CN)_2^- > ClO_4^- \gg M(CN)_4^{2-} \gg Fe(CN)_6^{3-}$, and were unable to extract $Fe(CN)_6^{3-}$ with Erdman's salt of THA. This order accords well with the above hypothesis. Irving and Damodaran also found, in their experiments on the extraction of EDTA complexes of iron(III) and vanadium(V) with TOMA-Cl in dichloroethane, that the selectivity order was $FeY(OH)_2^{3-} > FeY(OH)^{2-} > FeY^-$ and $VO_2Y^{3-} > VO_2HY^{2-}$. Thus, they were able to extract relatively large and highly charged anions with TOMA-Cl in dichloroethane.

Reviewing these results, it seems likely that anion selectivity in ion-exchange extraction is strongly dependent on the kind of the quaternary ammonium ion and the solvent used.

It is interesting to note that the $K_{ex}^{Q.X}$ value of TOMA-Cl is an order of magnitude smaller than that of TDBA-Cl, whereas $K_{ex}^{Q.X}$ of TOMA-$ClO_4$ is one order larger than that of TDBA-$ClO_4$. This means that the anion selectivity of TOMA is much greater than that of TDBA, indicating that the order of $K_{ex}^{Q.X}$ depends not only on the difference in free energy among anions in the aqueous phase, but also on the structural difference between TOMA and TDBA. Any difference between the free energies of $TOMA^+$ and $TDBA^+$ in the aqueous phase would not affect the selectivity order, because it would contribute equally to the $K_{ex}^{Q.X}$ values for each anion. Accordingly, $K_{ex}^{Q.X}$ should be mainly governed by the relative extent of interaction between the solvent molecules and the respective ion pair in both the aqueous and organic phases.

One of us (J. I.) acknowledges receipt of a Grant-in-Aid for Encouragement of Scientists (275415) from the Ministry of Education. We also thank Prof. T. Yotsuyanagi of Tohoku University for valuable advice on the TDBA—chloroform system.

REFERENCES

1 R. Kunin and A. G. Winger, Angew. Chem. Intern. Ed. Engl., 1 (1962) 149.
2 H. Green, Talanta, 20 (1973) 139.
3 H. M. N. H. Irving and A. D. Damodaran, Anal. Chim. Acta, 53 (1971) 267.
4 H. M. N. H. Irving and R. H. Al-Jarrah, Anal. Chim. Acta, 74 (1975) 321.
5 J. Itoh, T. Yano, H. Kobayashi and K. Ueno, Bunseki Kagaku, 27 (1978) 602.
6 H. Hoshino, T. Yotsuyanagi and K. Aomura, Anal. Chim. Acta, 83 (1976) 743.
7 T. Yotsuyanagi and H. Hoshino, Bunseki, (1976) 743.
8 Y. Yamamoto, Bunseki Kagaku, 21 (1972) 418.
9 E. Sekido, Y. Yoshimura and Y. Masuda, J. Inorg. Nucl. Chem., 38 (1976) 1183, 1187.

*Analytica Chimica Acta*, 105 (1979) 391—396


# DEMASKING REACTIONS OF POTASSIUM HYDROXOTRIFLUOROBORATE WITH LANTHANUM(III) COMPLEXES OF POLYAMINOPOLYCARBOXYLIC ACIDS

## Part 1. Equilibrium Constants for the Reactions with EDTA and NTA Complexes*

YOSHIKI MORIGUCHI

*Department of Chemistry, Fukuoka University of Education, Munakata, Fukuoka 811-41 (Japan)*

(Received 5th June 1978)

SUMMARY

Equilibrium constants for the demasking reactions of potassium hydroxotrifluoroborate ($KBF_3OH$) toward La(III) complexes of EDTA and NTA have been estimated by means of $^1$H-n.m.r. measurement at 35°C. For the constants defined as $K^{BF}_{LaL_m} = [L]^m[La(BF_3OH)_n]/[LaL_m][BF_3OH]^n$, the results were: for EDTA ($m = 1$, $n = 1/3$) $K^{BF}_{LaL} = 10^{2.7}$, and for NTA ($m = 2$, $n = 1/3$) $K^{BF}_{LaL_2} = 10^{26}$. These values are much larger than the equilibrium constants for the well known demasking reaction of fluoride ion toward La(III) complexes of EDTA and NTA, which are —12.43 and —14.92, respectively.

It has been reported [1—3] that the addition of a little potassium hydroxotrifluoroborate ($KBF_3OH$) has a remarkable influence on the visible absorption spectrum of the lanthanum(III) complex of alizarin fluorine blue (3-aminoethylalizarin-*N*,*N*-diacetic acid; alizarin complexan) as well as on the $^1$H-n.m.r. spectra of the lanthanum(III) complexes of EDTA and NTA. Thus, the colorimetric determination of fluorine with lanthanum(III)—alizarin complexan in the presence of borate is affected by the formation of $BF_3OH^-$ in the stepwise replacement of hydroxide by fluoride in the $B(OH)_4^-$ anion [4, 5]. It is considered that the effect of $KBF_3OH$ on the lanthanum(III) complexes is caused by a powerful demasking reaction which can withdraw the metal even from its stable lanthanum(III)—EDTA complex; the effect of $KBF_3OH$ is very much stronger than that of fluoride ion which is a well-known masking or demasking reagent [6—8]. This report compares the demasking effect of $KBF_3OH$ with that of sodium fluoride by determining the equilibrium constants for demasking reagents with lanthanum(III) complexes of EDTA and NTA.

---

*Presented in part at the 26th National Meeting of the Japanese Society for Analytical Chemistry, Yamaguchi, October 1977.

## EXPERIMENTAL

The procedure was similar to that described previously [2, 3]. The $^1$H-n.m.r. spectra were measured at 35°C with a Hitachi R-22 high-resolution spectrometer (90 MHz). The chemical shifts were measured relative to t-butyl alcohol as internal reference ($\tau$ 8.75). The effects of fluoride and fluoroborates on the $^1$H-n.m.r. spectra were observed by the addition of solid NaF, $KBF_3OH$ or $NaBF_4$ to an aqueous solution of 0.2 M lanthanum(III) and EDTA (1:1) or 0.25 M lanthanum(III) and NTA (1:2); these solutions were prepared by adjusting the molar ratio for metal to ligand to 1:1 and 1:2, respectively. EDTA and NTA were analytical-grade disodium salts (Dojin Co., Kumamoto); lanthanum nitrate and sodium fluoride were reagent grade (Katayama Co., Osaka) and were used without further purification. Sodium tetrafluoroborate was purified by recrystallization three times from cold water after filtering a saturated solution of the commercial-grade reagent (Katayama Co., Osaka, purity 90%) together with active carbon. Potassium hydroxotrifluoroborate was prepared by Wamser's method [4]; its purity was confirmed by elemental analyses and by x-ray analysis [4].

## RESULTS AND DISCUSSION

### *$^1$H-n.m.r. spectra*

The $^1$H-n.m.r. spectrum of the aqueous lanthanum(III)—EDTA (1:1) solution shows (Fig. 1) two singlets over a wide pH range, assigned to the ethylene protons ($\rangle NCH_2CH_2N\langle$, peak *A*) and methylene protons ($—CH_2COO—$, peak *B*) in the complex [9]. The spectrum of the aqueous lanthanum—EDTA (1:2) solution at pH values below 6 shows two new singlets at lower field together with *A* and *B*. The new peaks are assigned to the ethylene protons (peak *a*) and the methylene protons (peak *b*) on the free EDTA ligand and may be due to a slow intermolecular exchange between free EDTA and the lanthanum(III)—EDTA complex [9—12].

The spectrum of the aqueous lanthanum(III)—NTA (1:2) solution shows one singlet (peak *B*), which is assigned to the methylene protons on the complex [2, 13].

The addition of NaF has little effect on the spectrum of the lanthanum(III)—EDTA (1:1) solution; peaks *A* and *B* remain unchanged at a lanthanum-to-fluorine ratio of 1:3 (a precipitate formed). In contrast, Fig. 1 shows that the influence of $KBF_3OH$ is much more remarkable; the *a* and *b* peaks become larger and the *A* and *B* peaks decrease as $KBF_3OH$ is added in increasing amounts. Within 30 min of adding the $KBF_3OH$, the spectrum becomes similar to that of the lanthanum—EDTA (1:2) complex in the absence of $KBF_3OH$.

The addition of $KBF_3OH$ has the same effect on the spectrum of the lanthanum—NTA (1:2) solution; a new peak *b*, assigned to the methylene protons of the free NTA ligand, increases in intensity and peak *B* decreases as $KBF_3OH$ is added (Fig. 2).

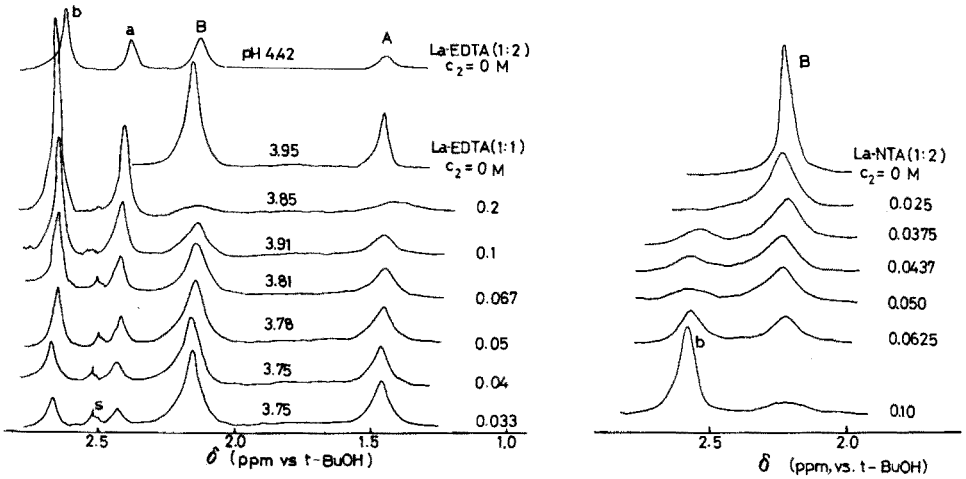


Fig. 1. Dependence of $^1$H-n.m.r. spectral change of the La(III)—EDTA (1:1 and 1:2) solutions (0.2 M solution) on the initial concentration of $KBF_3OH$, $c_2$. *A* indicates the ethylene proton, *B* the methylene proton of La(III)—EDTA, *a* the ethylene proton and *b* the methylene proton of free EDTA. *s* is the side-band signal of water.

Fig. 2. Dependence of $^1$H-n.m.r. spectral change of La(III)—NTA (1:2) complex (0.25 M) on the initial concentration of $KBF_3OH$, $c_2$. *B* indicates the methylene proton signal of La(III)—NTA and *b* the methylene proton signal of free NTA.

The addition of $NaBF_4$ and NaF has little effect on the spectra of these lanthanum complexes unless the solutions are kept standing for a long period. Slight *a* and *b* peaks appear in the spectrum of the lanthanum—EDTA (1:1) complex after standing for 7 days at 35°C after the addition of $NaBF_4$, presumably as a result of the effect of the $BF_3OH^-$ formed by slow hydrolysis of $BF_4^-$.

*Demasking reaction and its equilibrium constant*

The reaction of lanthanum(III) complexes with $BF_3OH^-$, detected by $^1$H-n.m.r. spectrum change, is regarded as a demasking reaction which is much more effective than that of the fluoride ion. This reaction is assumed to be as follows:

$$LaL_m + nBF_3OH \overset{K^{BF}_{LaL_m}}{\rightleftharpoons} mL + La(BF_3OH)_n \quad (1)$$

Charges on the ions in all equations are omitted for simplicity. The product, $La(BF_3OH)_n$ in eqn. (1) is presumed to decompose slowly and to give lanthanum fluorides and borates finally.

The equilibrium constant for eqn. (1) is given by

$$K^{BF}_{LaL_m} = [L]^m[La(BF_3OH)_n]/[LaL_m][BF_3OH]^n = m^m x^{m+1}/(c_1 - x)(c_2 - nx)^n \quad (2)$$

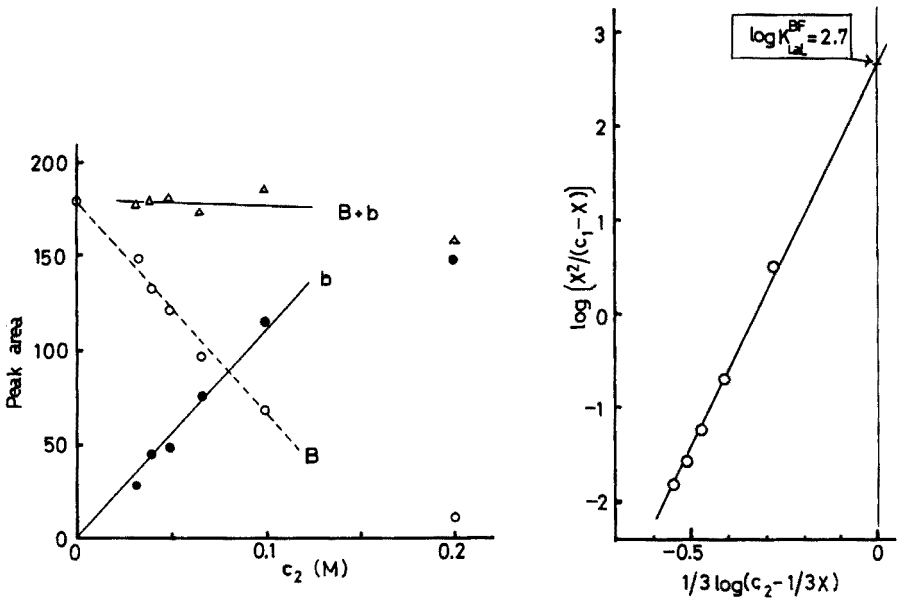


Fig. 3. Dependence of *B*- and *b*-peak areas in Fig. 1 on the initial concentration of $KBF_3OH$, $c_2$. (○) *B*-peak area. (●) *b*-peak area. (△) Sum of *B*- and *b*-peak areas.

Fig. 4. Graphical determination of equilibrium constant, $K^{BF}_{LaL}$ for demasking reaction of $KBF_3OH$ with La(III)—EDTA. See eqn. (3) in text.

where $c_1$ is the initial concentration of the lanthanum(III) complex of EDTA or NTA, and $x$ is the concentration of free EDTA or NTA liberated, estimated by measuring the areas of the *b* and *B* peaks, in the spectra resulting from the initial concentration of $KBF_3OH$ (Fig. 1). These peak areas, obtained as a product of peak height and width at half height, increase and decrease respectively with increasing initial concentration of $KBF_3OH$ (Fig. 3). The sum of the *b*- and *B*-peak areas is constant to within 5%. Equation (2) can be converted to the linear relationship, eqn. (3):

$$\log [m^m x^{m+1}/(c_1 - x)] = n\log (c_2 - nx) + \log K^{BF}_{LaL_m} \quad (3)$$

Thus, the equilibrium constant $K^{BF}_{LaL_m}$ can be obtained from the intercept of a linear plot by adopting a suitable value of $n$ in eqn. (3).As shown in Fig. 4, a good linear relation can be obtained by adopting $n = 0.33$. The equilibrium constant for the lanthanum(III)—EDTA (1:1) complex obtained from the intercept is shown in Table 1 together with the value for the lanthanum—NTA (1:2) complex obtained similarly.

The demasking reaction of the fluoride ion which corresponds to eqn. (1) and its equilibrium constant are given by:

$$LaL_m + nF \overset{K^F_{LaL_m}}{\rightleftharpoons} mL + LaF_n \quad (4)$$

$$K^{F}_{LaL_m} = [LaF_n][L]^m/[LaL_m][F]^n \quad (5)$$

This equilibrium constant cannot be obtained by means of $^1$H-n.m.r. measurement in the same manner as for $KBF_3OH$ because the effect of the fluoride ion on the spectra of the lanthanum(III) complexes of EDTA and NTA is very small under the experimental conditions. However, if the use of potentiometric data is valid in order to compare the demasking reaction of fluoride ion with that of $BF_3OH^-$ the value of $K^{F}_{LaL_m}$ can be estimated by converting eqn. (5) as follows:

$$La + F \rightleftharpoons LaF; K_{LaF} = [LaF]/[La][F]$$

$$La + mL \rightleftharpoons LaL_m; K_{LaL_m} = [LaL_m]/[La][L]^m$$

$$K^{F}_{LaL_m} = \frac{[LaF][L]^m}{[LaL_m][F]} = K_{LaF}/K_{LaL_m} \quad (6)$$

The values of $K^{F}_{LaL_m}$ are obtained by means of $K_{LaF}$, $K_{LaL}$ and $K_{LaL_2}$ which have been measured by potentiometry [14—16] because eqn. (5) becomes equivalent to eqn. (2) in terms of the fluorine atoms when the values of $n$ are 0.33 and 1, respectively. The values shown in Table 1, together with that obtained for $KBF_3OH$, show that the demasking effect of $KBF_3OH$ on lanthanum(III) complexes of EDTA and NTA is much more marked than that of NaF. The effect of $KBF_3OH$ is assumed to be based on a distorted tetrahedron structure containing three fluorines and one hydroxyl group, which has a high affinity for lanthanum; the distortion causes a polarized negative charge on $BF_3OH^-$ and its approach to a lanthanum complex causes a higher local concentration of fluorine about the lanthanum complex than the approach of a fluoride ion. Furthermore, this approach of $BF_3OH^-$ to a La(III)—EDTA complex may preferentially occur at the residual three sites of La(III) which do not bond to the EDTA ligand, if the coordination number of the La(III) remains at nine in aqueous solution [17].

The behaviour of $KBF_3OH$ towards the La(III)—EDTA complex was also detected potentiometrically with a fluoride ion-selective electrode; the $BF_3OH^-$ reacted more strongly with the lanthanum complex than the fluoride

TABLE 1

Equilibrium constants for demasking reactions of NaF and $KBF_3OH$ with La(III)—EDTA and La(III)—NTA complexes

| Ligand | $m$ | $n$ | $LaL_m$ $LaF_n$ | log $K_{LaL_m}$ [a] | log $K_{LaF_n}$ [b] | log $K^{BF}_{LaL_m}$ [c] | log $K^{F}_{LaL_m}$ [d] |
|---|---|---|---|---|---|---|---|
| EDTA | 1 | 1/3 | LaEDTA | 15.13 | | 2.7 | —12.43 |
| NTA | 2 | 1/3 | $La(NTA)_2$ | 17.62 | | 26 | —14.92 |
| F | 1,2 | 1 | LaF | | 2.7 | | |

[a]Potentiometric data at 20°C [15, 16]. [b]Potentiometric data at 25°C [14]. [c]Estimated from eqn. (3). [d]Estimated from eqn. (6).

ion. The demasking effect of $BF_3OH^-$ was also checked by titration with xylenol orange or eriochrome black T as indicator and zinc or lead nitrate solution as the back-titrant because free EDTA is liberated from the lanthanum complex by demasking [18].

REFERENCES


1 Y. Moriguchi, T. Kuwabara and I. Hosokawa, Bull. Chem. Soc. Jpn., 44 (1971) 3496.
2 Y. Moriguchi, Chem. Lett., (1974) 47.
3 Y. Moriguchi, Abstr. No. 1C09, 25th National Meeting of The Japan Society for Analytical Chemistry, Nigata, October 1976.
4 C. A. Wamser, J. Am. Chem. Soc., 70 (1948) 1209.
5 Y. Moriguchi and I. Hosokawa, Nippon Kagaku Zasshi, 92 (1971) 56.
6 R. Pribil, Collection, 19 (1954) 64.
7 R. Pribil and V. Vesely, Chem.-Anal., 12 (1965) 385.
8 I. Sajo, Acta Chim. Sci. Hung., 6 (1955) 251.
9 T. H. Siddall III and W. E. Stewart, Inorg. Nucl. Chem. Lett., 5 (1969) 421.
10 R. J. Kula, D. T. Sawyer, S. I. Chan and C. M. Finley, J. Am. Chem. Soc., 85 (1963) 2930.
11 R. J. Day and C. N. Reilley, Anal. Chem., 36 (1964) 1073.
12 J. L. Sundmeier and C. N. Reilley, Anal. Chem., 36 (1964) 1698.
13 D. Chapman, D. R. Lloyd and R. H. Prince, J. Chem. Soc., (1963) 3645.
14 J. W. Kury, A. D. Paul, L. G. Helper and R. E. Connic, J. Am. Chem. Soc., 81 (1959) 4185.
15 G. Schwarzenbach, G. Gut and G. Anderegg, Helv. Chim. Acta, 37 (1954) 937.
16 T. Moeller and R. Ferrus, Inorg. Chem., 1 (1962) 55.
17 J. L. Hoard, Byungkook Lee and M. D. Lind, J. Am. Chem. Soc., 87 (1965) 1612.
18 Y. Moriguchi and T. Yoshimatsu, Anal. Chim. Acta, 105 (1979) 397.

*Analytica Chimica Acta*, 105 (1979) 397—401


Short Communication

# DEMASKING REACTIONS OF POTASSIUM HYDROXOTRIFLUOROBORATE WITH LANTHANUM(III) COMPLEXES OF POLYAMINOPOLYCARBOXYLIC ACIDS

## Part 2. Application in Selective Demasking of the Lanthanum(III)—EDTA complex†

YOSHIKI MORIGUCHI* and TOSHIO YOSHIMATSU

*Department of Chemistry, Fukuoka University of Education, Munakata, Fukuoka 811-41 (Japan)*

(Received 5th June 1978)

The demasking action of $KBF_3OH$ on the lanthanum(III)—EDTA complex is much more effective than that of NaF [1]. In the present report, this demasking effect is utilized in back-titrations of the EDTA liberated from the lanthanum complex. The selectivity of the demasking was checked in mixtures with heavy metal or lanthanide ions. The effect can be applied to the determination of lanthanum in the presence of some other metals.

*Experimental*

*Reagents.* Sodium fluoride of reagent grade was used. Potassium hydroxotrifluoroborate ($KBF_3OH$) was synthesized by the method of Wamser [2]. EDTA solution (0.01 M) was prepared from the analytical-grade disodium salt (Dojin Co., Kumamoto).

Zinc and lead nitrate solutions (0.01 M) were prepared from the reagent-grade salts and standardized against 0.01 M EDTA with xylenol orange as indicator. Xylenol orange was used as an aqueous 0.2% (w/v) solution, and eriochrome black T as a methanolic (0.1%) (w/v) solution containing hydroxylammonium chloride [3].

*Lanthanum(III)— and lanthanide(III)—EDTA complex solutions.* Solutions (0.01 M) were prepared by dissolving the equivalent amount of disodium-EDTA in a La, Pr, Nd, Sm, Gd, Dy, Ho, Er, or Yb nitrate solution, prepared by dissolving the oxides (Katayama Co., Osaka; purity 99.8%) of these elements in dilute nitric acid. The molar ratios of metal to EDTA in the complexes were checked with xylenol orange indicator after adjusting the solutions to pH 5—5.5 with hexamine.

*Heavy metal—EDTA complex solutions.* Solutions (0.01 M) of the EDTA complexes of Fe(III), Co(II), Ni(II), Cu(II), Zn(II) and Pb(II) were prepared by dissolving the equivalent amount of disodium—EDTA in solutions of their nitrates. The molar ratios of metal to EDTA were checked with xylenol

†Part of this report was presented at the 37th National Meeting of the Chemical Society of of Japan, Yokohama, April 1978.

orange, eriochrome black T or murexide as indicator after the pH had been adjusted to the appropriate value with hexamine or aqueous ammonia.

*Determination of liberated EDTA by back-titration.* To test single EDTA complexes, add 1 ml or 5 ml of 0.01 M disodium-EDTA to 5 ml of 0.01 M metal—EDTA (Fe(III), Co(II), Ni(II), Cu(II), Zn(II), Pb(II), La(III), some lanthanides(III)); dilute the solution to 50 ml with deionized water, and adjust to pH 5—5.5 with hexamine or to pH 10 with ammonia—ammonium chloride buffer solution. Keep standing for 30 min after dissolving sodium fluoride or $KBF_3OH$ in the solution, and determine the EDTA liberated by demasking with 0.01 M zinc nitrate or lead nitrate solution with xylenol orange (pH 5—5.5) or erio T (pH 10) indicator after readjusting the pH, if necessary.

To test ternary mixtures containing lanthanum(III)—EDTA add 2 ml of each of two 0.01 M metal—EDTA complexes (Co(II), Ni(II), Pb(II), Pr(III), Sm(III), Dy(III), Er(III)) to 5 ml of 0.01 M lanthanum(III)—EDTA and 2 ml or 5 ml of 0.01 M disodium-EDTA; dilute the solution to 50 ml with deionized water, adjust the pH of the solution and back-titrate the liberated EDTA, as described above, after the addition of sodium fluoride or $KBF_3OH$.

*Results and discussion*

As shown in Table 1, the effective demasking action of $KBF_3OH$ on the lanthanum(III)—EDTA complex can be determined by titration as well as by $^1$H-n.m.r. [1]. The EDTA liberated from the lanthanum(III)—EDTA complex by the addition of $KBF_3OH$ is clearly more than that liberated by the addition of NaF for equivalent amounts of fluorine as well as equimolar concentrations. The effect is especially noticeable at pH 10 (erio T indicator). The demasking effect on other EDTA complexes of heavy metals (Fe(III), Co(II), Ni(II), Cu(II), Zn(II), Pb(II)) was examined in the same manner as the lanthanum(III)—EDTA complex; the effect of $KBF_3OH$ on these complexes is similar to that of sodium fluoride under the experimental conditions. Thus lanthanum can be determined in mixtures with the EDTA complexes of other metals, because the demasking of $KBF_3OH$ is more effective and more selective toward lanthanum(III)—EDTA (Table 2); even in the presence of other EDTA complexes, the demasking effect of $KBF_3OH$ is more remarkable than that of sodium fluoride, particularly at pH 10.

The demasking effect on the EDTA complex of lanthanides, examined for Pr(III), Nd(III), Sm(III), Gd(III), Dy(III), Ho(III), Er(III), and Yb(III) in the same manner as for La(III), is shown in Table 3. The EDTA complexes of heavy lanthanides, e.g. Ho(III), Er(III) and Yb(III), are not demasked at pH 5—5.5 by $KBF_3OH$ as efficiently as NaF, but the complexes of light lanthanides, e.g. Pr(III), Nd(III) and Sm(III), are more effectively demasked at the same pH by $KBF_3OH$. Neither the light nor the heavy lanthanide complexes are demasked at pH 10 by $KBF_3OH$ as efficiently as by NaF when it is added in a fluorine-to-lanthanide atom ratio of less than 50:1. The praseodymium—EDTA complex, however, is effectively demasked by the addition of $KBF_3OH$ in a fluorine-to-praseodymium atom ratio of 130:1. Thus, sequential analysis for lanthanides is possible by means of $KBF_3OH$ instead

TABLE 1

Back-titration of EDTA liberated from lanthanum(III)—EDTA by demasking with NaF and $KBF_3OH$
(0.01 M La(III)—EDTA (5 ml) + 0.01 M EDTA (1 ml) + water; total volume, 50 ml)

| Reagent | Amount added ($\times 10^{-4}$ mol) | F:La ratio | Back titration 0.01 M $Zn^{2+}$ $V_1$ (ml) | Liberated 0.01 M EDTA[a] $V_2$ (ml) | Demasking of La—EDTA[b] (%) |
|---|---|---|---|---|---|
| NaF[c] | 0 | 0:1 | 0.96 (blank) | 0.00 | |
| | 2.5 | 5:1 | 5.22 | 4.26 | 85 |
| | 5.0 | 10:1 | 5.36 | 4.40 | 88 |
| | 15.0 | 30:1 | 5.38 | 4.42 | 88 |
| | 25.0 | 50:1 | 5.91 | 4.95 | 99 |
| $KBF_3OH$[c] | 0.83 | 5:1 | 5.34 | 4.38 | 88 |
| | 1.66 | 10:1 | 5.56 | 4.60 | 92 |
| | 5.00 | 30:1 | 5.93 | 4.97 | 99 |
| | 8.3 | 50:1 | 5.94 | 4.98 | 100 |
| NaF[d] | 0 | 0:1 | 0.99 (blank) | 0.00 | |
| | 1.5 | 3:1 | 0.98 | −0.01 | 0 |
| | 2.0 | 4:1 | 0.97 | −0.02 | 0 |
| | 2.5 | 5:1 | 0.99 | 0.00 | 0 |
| | 25.0 | 50:1 | 0.99 | 0.00 | 0 |
| | 65.0 | 130:1 | 4.84 | 3.85 | 77 |
| $KBF_3OH$[d] | 0.5 | 3:1 | 1.66 | 0.67 | 13 |
| | 0.66 | 4:1 | 3.78 | 2.79 | 56 |
| | 0.83 | 5:1 | 5.22 | 4.23 | 85 |
| | 8.3 | 50:1 | 5.59 | 4.60 | 92 |
| | 21.6 | 130:1 | 5.99 | 5.00 | 100 |

[a]EDTA liberated from La(III)—EDTA complex by demasking, $V_1$ − blank. [b]$(V_2/5) \times 100$. [c]pH 5—5.5. [d]pH 10.

of $PO_4^{3-}$ as used by Pribil and Vesely [4]. In fact, the light lanthanides, Pr(III), Nd(III) or Sm(III) can be determined in mixtures with some EDTA complexes of heavy lathanides.

The selective demasking action of $KBF_3OH$ towards lanthanum(III)—EDTA mixed with some EDTA complexes of lanthanides was examined. The results (Table 2) at pH 5—5.5 shows that selective demasking is found in mixtures with EDTA complexes of heavy lanthanides, e.g. Dy(III) and Er(III), but the effect is almost the same as that of sodium fluoride. This selective demasking, however, is not found in mixtures with EDTA complexes of light lanthanides, e.g. Pr(III) and Sm(III), because these metal ions are demasked together with the lanthanum(III)—EDTA complex. In contrast, the result at pH 10 shows that the demasking of $KBF_3OH$ is not only selective toward the lanthanum(III) complex but also much more effective than that of sodium fluoride even in the presence of the EDTA complexes of light lanthanides.

Although the stability constants of the EDTA complexes of cobalt(II), nickel(II), lead(II) and light lanthanide are close to that of lanthanum(III)—

TABLE 2

Selective demasking action of $KBF_3OH$ on La—EDTA in ternary mixtures (0.01 M La—EDTA ($x$ ml) + 0.01 M Me—EDTA ($y$ ml) + 0.01 M Me'—EDTA ($z$ ml) + 0.01 M EDTA (2 ml) + water; total volume, 50 ml)

| Reagent | Amount added ($\times 10^{-4}$ mol) | F:Me ratio | La, Me, Me'—EDTA added (ml) $x$ | $y$ | $z$ | Liberated 0.01 M EDTA[a] $V_2$ (ml) | Demasking La—EDTA[b] (%) |
|---|---|---|---|---|---|---|---|
| NaF[c] | 5.0 | 10:1 (Ni) | 0 | 0 | 5 | 0.00 | |
| | 5.0 | 10:1 (Co) | 0 | 5 | 0 | 0.04 | |
| | 5.0 | 10:1 (La) | 5 | 2 | 2 | 4.67 | 93 |
| $KBF_3OH$[c] | 1.66 | 10:1 (Ni) | 0 | 0 | 5 | 0.00 | |
| | 1.66 | 10:1 (Co) | 0 | 5 | 0 | 0.03 | |
| | 1.66 | 10:1 (La) | 5 | 2 | 2 | 4.87 | 97 |
| NaF[d] | 25.0 | 50:1 (Ni) | 0 | 0 | 5 | 0.07 | |
| | 25.0 | 50:1 (Pb) | 0 | 5 | 0 | −0.01 | |
| | 25.0 | 50:1 (La) | 5 | 2 | 2 | 2.00 | 40 |
| $KBF_3OH$[d] | 8.3 | 50:1 (Ni) | 0 | 0 | 5 | 0.05 | |
| | 8.3 | 50:1 (Pb) | 0 | 5 | 0 | 0.05 | |
| | 8.3 | 50:1 (La) | 5 | 2 | 2 | 3.63 | 73 |
| NaF[c] | 2.5 | 5:1 (Dy) | 0 | 5 | 0 | 0.00 | |
| | 2.5 | 5:1 (Er) | 0 | 0 | 5 | 0.00 | |
| | 2.5 | 5:1 (La) | 5 | 2 | 2 | 4.91 | 98 |
| $KBF_3OH$[c] | 0.83 | 5:1 (Dy) | 0 | 5 | 0 | 0.00 | |
| | 0.83 | 5:1 (Er) | 0 | 0 | 5 | 0.00 | |
| | 0.83 | 5:1 (La) | 5 | 2 | 2 | 5.00 | 100 |
| NaF[d] | 25.0 | 50:1 (Pr) | 0 | 5 | 0 | 0.00 | |
| | 25.0 | 50:1 (Sm) | 0 | 0 | 5 | 0.00 | |
| | 25.0 | 50:1 (La) | 5 | 2 | 2 | 0.00 | 0 |
| $KBF_3OH$[d] | 8.3 | 50:1 (Pr) | 0 | 5 | 0 | 0.00 | |
| | 8.3 | 50:1 (Sm) | 0 | 0 | 5 | 0.00 | |
| | 8.3 | 50:1 (La) | 5 | 2 | 2 | 4.98 | 100 |

[a]Liberated EDTA from metal—EDTA complex by demasking, see Table 1. [b]($V_2$/added 0.01 M La (III)—EDTA, ml) × 100. [c]At pH 5—5.5. [d]At pH 10.

EDTA, the difference in stability of their complexes increases at pH 10; the conditional stability constants of the complexes increase with increasing pH: $K_{M'L'} = K_{ML}/\alpha_M \alpha_{L(H)}$, where $K_{M'L'}$ and $K_{ML}$ are the conditional and normal stability constants of the EDTA complexes, respectively, and $\alpha_m$ and $\alpha_{L(H)}$ are the side-reaction coefficients of metal and EDTA ligand, respectively. Both of these coefficients are either greater than or equal to one; the values of $\alpha_{L(H)}$ at pH 5 and at pH 10 are $10^{6.6}$ and $10^{0.5}$ for EDTA, respectively [5].

In addition to the effect of pH on the stability of EDTA complexes, it is

TABLE 3

Demasking action of $KBF_3OH$ on lanthanide—EDTA complexes

| Reagent | Amount added | | Demasking of Me—EDTA (%)[a] | | | | | | | |
|---|---|---|---|---|---|---|---|---|---|---|
| | ($\times 10^{-4}$ mol) | F:Me ratio | Pr | Nd | Sm | Gd | Dy | Ho | Er | Yb |
| NaF[b] | 2.5 | 5:1 | 55 | 38 | 12 | 0 | 0 | 0 | 0 | 0 |
| | 5.0 | 10:1 | 90 | 80 | 80 | 69 | 5 | 0 | 0 | 0 |
| $KBF_3OH$[b] | 0.83 | 5:1 | 73 | 57 | 26 | 2 | 0 | 0 | 0 | 0 |
| | 1.66 | 10:1 | 95 | 90 | 83 | 81 | 29 | 0 | 0 | 0 |
| NaF[c] | 25.0 | 50:1 | 0 | 0 | 0 | | | | | |
| | 65.0 | 130:1 | 0 | 0 | 0 | | | | | |
| $KBF_3OH$[c] | 8.3 | 50:1 | 0 | 0 | 0 | | | | | |
| | 21.6 | 130:1 | 93 | 0 | 0 | | | | | |

[a](Liberated EDTA from lanthanide—EDTA complex/added lanthanide—EDTA complex) $\times$ 100; see Table 1. [b]At pH 5—5.5. [c]At pH 10.

assumed that the demasking effect of $KBF_3OH$ on the lanthanum(III)—EDTA complex occurs because $KBF_3OH$ contains hydroxyl and fluoro functional groups.

REFERENCES

1 Y. Moriguchi, Anal. Chim. Acta, 105 (1979) 391 (Part 1).
2 C. A. Wamser, J. Am. Chem. Soc., 70 (1948) 1209.
3 H. Diehl, C. A. Goetz and C. C. Hach, J. Am. Water Works Assoc., 42 (1950) 40.
4 R. Pribil and V. Vesely, Chemist-Analyst, 54 (1965) 100.
5 A. Ringbom, Complexation in Analytical Chemistry, J. Wiley, New York, 1963.

*Analytica Chimica Acta*, 105 (1979) 403—407


Short Communication

# THE DETERMINATION OF LEVODOPA AND CARBIDOPA IN COMPOUND TABLETS BY HIGH-PERFORMANCE LIQUID CHROMATOGRAPHY AND SPECTROFLUORIMETRY

SHAHIDA T. HAMID[‡] and JOHN WALKER*

*The Department of Pharmacy, Chelsea College, University of London, Manresa Road, London SW3 6LX (Gt. Britain)*

(Received 5th June 1978)

Levodopa or L-dopa [dihydroxyphenylalanine; (—) - (3,4-dihydroxyphenyl)-L-alanine; L(—)-2-amino-2-(3,4-dihydroxyphenyl)propanoic acid; I, R=H, R′=$NH_2$] used in the treatment of Parkinsonism has been formulated with carbidopa [L-2-hydrazino-2-methyl-3-(3,4-dihydroxyphenyl)propanoic acid; I, R=$CH_3$, R′=$NHNH_2$; monohydrate] in Sinemet tablets. The latter substance, an inhibitor of dopa decarboxylase, delays the in vivo destruction of levodopa and prolongs its anti-Parkinsonism effect. The combination is supplied as Sinemet 275 (levodopa 250 mg, carbidopa 25 mg) and Sinemet 110 (levodopa 100 mg, carbidopa 10 mg).

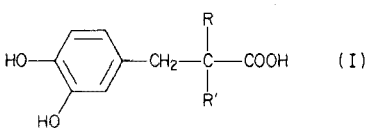

(I)

Methods reported for the assay of levodopa include colorimetry [1], spectrophotometry [2—4], electrochemical oxidation at a tubular carbon electrode [5], polarography [6], gas—liquid chromatography [7, 8], liquid chromatography [9], and non-aqueous titrimetry [3, 10]. Spectrofluorimetry and thin-layer chromatography have been used for the determination of levodopa in the presence of carbidopa [11] and a spectrofluorimetric method for the determination of carbidopa in plasma has been reported [12].

An accurate, precise and rapid method for the simultaneous determination of these two closely related substances is desirable. Of the methods available, high-performance liquid chromatography (h.p.l.c.) appeared promising; a preliminary attempt to separate the trimethylsilyl derivatives of levodopa and carbidopa by g.l.c. had been unsuccessful. A suitable method has been developed and the results are compared with those obtained by spectrofluorimetry.

[‡]Present address: Syntex Pharmaceuticals, The Ridgeway, Iver, Bucks., Gt. Britain.

*H.p.l.c.*

*Materials.* Ethanol, methanol, potassium dihydrogenphosphate, and phosphoric acid were AnalaR grade, and levodopa (B.P), carbidopa monohydrate (reference sample supplied by Merck, Sharp and Dohme, Ltd.,), Sinemet tablets (Merck, Sharp and Dohme, Ltd.,) and guanosine puriss (Koch Light Laboratories Ltd.,) were used.

The mobile phase was potassium dihydrogenphosphate (0.05 M) in 10% (v/v) ethanol in water, previously degassed, and adjusted to pH 2.9 with phosphoric acid.

*Apparatus.* The h.p.l.c. apparatus comprised a constant-flow pump (Waters Associates Ltd., M-6000A); a single-beam variable-wavelength detector (Cecil Instruments Ltd., Model 212) fitted with an 8-$\mu$l flow-cell; a seamless stainless steel tubular column (150 × 6.3 mm o.d., 4.6 mm i.d.) packed from a slurry in methanol (60%, w/v), Spherisorb S5W-SCX form (Phase Separations Ltd.,) introduced through a precolumn and pressurized to 5000 psig as described by Cox et al. [13]. Injections were made with a 10-$\mu$l Hamilton syringe by a stopped-flow technique. Chromatograms were recorded at a chart speed of 5 mm $min^{-1}$ (Perkin-Elmer 56 recorder). All work was done at room temperature with a flow-rate of 0.5 $cm^3$ $min^{-1}$ at pressures between 600 and 1000 psig.

*Method.* The response of the detector at 280 nm, checked over concentration ranges of 1.2—0.075 mg $cm^{-3}$ for levodopa and 0.32—0.02 mg $cm^{-3}$ for carbidopa in 0.05 M hydrochloric acid, was linear.

A reference solution containing levodopa and carbidopa (500 $\mu$g $cm^{-3}$) in 0.05 M hydrochloric acid was used in preliminary experiments to determine the optimum working conditions for the separation; injections of 2 $\mu$l were made. These resulted in the choice of mobile phase stated above. Adequate resolution was obtained ($R$=1.45). Guanosine was chosen as the internal standard, as it showed linearity of detector response at 280 nm over the concentration ranges used. In all instances peaks were very sharp. Peak height ratios were used in calculations.

*Assay of Sinemet tablets*

*Standard solution.* A solution containing levodopa, carbidopa and guanosine (500, 50, and 200 $\mu$g $cm^{-3}$, respectively) in 0.05 M hydrochloric acid was prepared.

*Recovery of levodopa and carbidopa.* A powder containing lactose, starch, magnesium stearate and talc (90, 5, 2 and 1 parts, respectively) was prepared to represent tablet excipient. To 450 mg of this powder was added 1 g of levodopa and 100 mg of carbidopa and the product was mixed thoroughly. Four aliquots (380 mg) were weighed into 100-$cm^3$ graduated flasks and 0.05 M hydrochloric acid (50 $cm^3$) was added. The flasks were shaken mechanically (30 min), and the contents were adjusted to volume and filtered (rejecting the first 10 $cm^3$). Aliquots (10 $cm^3$) of the filtrate were pipetted into 50-$cm^3$ graduated flasks, 10 $cm^3$ of guanosine solution (0.1% (w/v), equivalent to a final concentration of 200 $\mu$g $cm^{-3}$) was added to each, and

the solutions were made up to volume. Injections (2 μl and 8 μl for levodopa and carbidopa respectively) were made by the stopped-flow technique. Sample and standard injections were made alternately. The results were as follows. For levodopa, mean recovery = 98.8% ($n$ = 4, range 98.7—99.4); $v$ = 0.18, $s$ = 0.42, $s_r$ = 0.43. For carbidopa, mean recovery = 101.3% ($n$ = 4, range 100—101.9); $v$ = 0.22, $s$ = 0.47, $s_r$ = 0.46.

*Tablet assay.* Tablets (20) were weighed and powdered; ten aliquots of the powder, each approximately equivalent in weight to one tablet, were transferred to 100-$cm^3$ graduated flasks and 0.05 M hydrochloric acid (50 $cm^3$) was added to each. The contents of each flask were subsequently treated exactly as described in the previous section starting at "The flasks were shaken mechanically .....". The results (Table 1) were calculated as follows: % recovery for levodopa (or carbidopa)/tablet = ($A$ (sample)/$A$(std) × $B/C$ × $D/E$ × 100) where $A$ (sample) = peak height of sample/peak height of internal standard; $A$ (std.) = peak height of standard/peak height of internal standard; $B$ = average tablet weight (mg); $C$ = sample weight (mg); $D$ = standard weight (mg); $E$ = stated dose per tablet (mg).

*Single tablet assays.* One tablet, placed in a 100-$cm^3$ graduated flask with 0.05 M hydrochloric acid (1 $cm^3$) was disintegrated ultrasonically; a further 50 $cm^3$ of 0.05 M hydrochloric acid was added and the procedure described in the previous section was followed. Fifteen tablets were assayed, and the results (Table 1) were calculated as follows: % recovery for levodopa (or carbidopa)/tablet = ($A$ (sample) × $D$ × 100)/($A$ (std.) × $E$).

*Spectrofluorimetry*

In order to obtain a valid comparison of the methods, the spectrofluorimetric assays were made on the same sample of tablet powder as was used for the h.p.l.c. assays; aliquots of the same solution were used for both spectrofluorimetric determinations. Levodopa was assayed by a procedure suggested by Merck, Sharp and Dohme [11]; the results are recorded in Table 1. For carbidopa, the method used was a modification of that described by Vickers and Stuart [12].

*Materials.* 4-Dimethylaminobenzaldehyde, trichloroacetic acid, anhydrous sodium sulphate, and chloroform were AnalaR grade.

TABLE 1

Comparison of assay results

| | H.p.l.c. | | | | Spectrofluorimetry | |
|---|---|---|---|---|---|---|
| | Replicate assays (10) | | Single tablet assays (15) | | Replicate assays (4) | |
| | Levodopa | Carbidopa | Levodopa | Carbidopa | Levodopa | Carbidopa |
| Recovery range (%) | 97.2—99.7 | 100.4—102.1 | 96.3—102.2 | 98.7—109.3 | 98.7—105.5 | 101—105.5 |
| Mean recovery (%) | 98.6 | 101 | 98.5 | 101.9 | 101.35 | 103.7 |
| $v$ | 0.58 | 0.39 | 8.7 | 7.3 | 10.16 | 4.42 |
| $s$ | 0.76 | 0.625 | 2.95 | 2.7 | 3.19 | 2.1 |
| $s_r$ | 0.77 | 0.62 | 2.99 | 2.65 | 3.15 | 2.03 |

*Instrument.* Baird Fluoripoint FP100 spectrofluorimeter.

*Response linearity.* From a standard carbidopa solution (1 $\mu$g cm$^{-3}$), a series of dilutions was made as follows: to 0, 1, 2, 4, 6 and 8 cm$^3$ of the standard were added 16, 15, 14, 12, 10 and 8 cm$^3$ respectively of 0.05 M hydrochloric acid. To each solution was added 5 cm$^3$ of aqueous 10% (w/v) trichloroacetic acid solution and 15 cm$^3$ of ethanolic 0.4% (w/v) 4-dimethylaminobenzaldehyde solution followed by thorough mixing. The resulting solutions, containing 0, 1, 2, 4, 6 and 8 $\mu$g respectively of carbidopa, were then extracted with 3 × 15-cm$^3$ portions of chloroform; the chloroform extracts were combined, filtered through anhydrous sodium sulphate into 50-cm$^3$ graduated flasks, and made up to volume with chloroform. The fluorescence of the resulting solutions was measured in a 1-cm quartz cell (excitation wavelength, 466 nm; emission wavelength, 546 nm). Over the concentration range used, a linear response was obtained for intensity of fluorescence vs. concentration of carbidopa. A solution containing 10 $\mu$g of levodopa, similarly treated, gave no fluorescence at 546 nm.

*Tablet assay.* From the same sample of powdered tablets used for the h.p.l.c. assay, powder equivalent to ca. 12.5 mg of carbidopa was weighed into four 100-cm$^3$ graduated flasks. Hydrochloric acid (50 cm$^3$ of 0.05 M) was added, and the suspension was shaken (25 min), made up to volume with 0.05 M hydrochloric acid, and filtered, rejecting the first few cm$^3$ of filtrate (aliquots of this solution were also used for the spectrofluorimetric assay for levodopa content); 4 cm$^3$ of this solution was diluted to 1 l with 0.05 M hydrochloric acid to give a final solution containing ca. 0.5 $\mu$g cm$^{-3}$ of carbidopa. To 10 cm$^3$ of this solution was added 6 cm$^3$ of 0.05 M hydrochloric acid and 5 cm$^3$ of aqueous 10% (w/v) trichloroacetic acid and the procedure was continued as described for response linearity. The process was repeated three times. The results (Table 1) were calculated as follows: % recovery for carbidopa/tablet = $(25{,}000 \times X \times B \times 100)/(CE)$ where $X$ = weight ($\mu$g) of carbidopa from calibration curve and $B$, $C$ and $E$ are as previously defined.

*Results and discussion*

The h.p.l.c. procedure described offers a suitable method for the simultaneous determination of levodopa and carbidopa in combination. Recovery from a simulated tablet base gave $s_r$ = 0.43 and 0.46% for levodopa and carbidopa, respectively. Table 1 shows the results of replicate tablet assays by the proposed h.p.l.c. method and by spectrofluorimetry. The h.p.l.c. method gave satisfactory values for $s_r$ (0.77 and 0.62% for levodopa and carbidopa, respectively); the differences in precision between the two methods, as measured by the variance ratios, were highly significant [levodopa $F^3_9$ = 17.52; carbidopa $F^3_9$ = 11.33; (upper significance limit 3.86, $P$ = 0.05)]. In addition, the h.p.l.c. method has the advantage of rapidity in comparison with spectrofluorimetry or other methods involving separation stages. A minor disadvantage of the method is that the performance of the column undergoes deterioration during use and this necessitates reassessment of the optimum working

conditions. Dilution of the mobile phase ($<0.025$ M) was found to minimize this effect with the column used. The application of the method to the assay of single tablets is also illustrated by the results shown in Table 1.

The h.p.l.c. method described offers a rapid and accurate assay of levodopa and carbidopa in combination; the precision compares favourably with that of a spectrofluorimetric procedure.

We thank Dr. G. Cox and the Laboratory of the Government Chemist for allowing one of us (S. T. H.) to use their facilities; Mr. G. Drewery (Merck, Sharp and Dohme Ltd.) for information; Merck, Sharp and Dohme Ltd. and Roche Products Ltd. for samples of carbidopa and levodopa, respectively.

REFERENCES

1 N. Maggi and A. Cometti, J. Pharm. Sci., 61 (1972) 924.
2 M. Nedergaard, Pharm. Acta Helv., 45 (1970) 373.
3 United States Pharmacopoeia, XIX (1975) 281.
4 J. Walker, A. Abdulsalam, A. E. Theobald, R. Subrahmanyam and S. K. Verma, J. Pharm. Pharmac., 30 (1978) 401.
5 W. D. Mason, J. Pharm. Sci., 62 (1973) 999.
6 D. Cantin, J. Alary and A. Coeur, Analusis, 3 (1975) 241.
7 C. W. Gehrke, H. Nakamoto and R. W. Zurnwalt, J. Chromatogr., 45 (1969) 24.
8 B. L. Chang, B. F. Grabowski and W. G. Haney, J. Pharm. Sci., 62 (1973) 1337.
9 R. J. Baczuk, G. K. Landram, R. J. Dubois and H. C. Dehm, J. Chromatogr., 60 (1971) 351.
10 British Pharmacopoeia (1973).
11 Merck, Sharp and Dohme Ltd., private communication.
12 S. Vickers and E. K. Stuart, J. Pharm. Sci., 62 (1973) 1550.
13 G. B. Cox, C. R. Loscombe, M. J. Slucutt, K. Sugden and J. A. Upfield, J. Chromatogr., 117 (1976) 269.

*Analytica Chimica Acta*, 105 (1979) 409—412


Short Communication

# A HIGH-PERFORMANCE LIQUID CHROMATOGRAPHIC TECHNIQUE FOR THE DETERMINATION OF 2,5-PIPERAZINEDIONE IN COMPLEX REACTION MIXTURES

BRUCE JON COMPTON and WILLIAM C. PURDY*

*Department of Chemistry, McGill University, 801 Sherbrooke Street West, Montreal, Quebec H3A 2K6 (Canada)*

DAVID J. PHELPS

*Department of Chemistry, St. Mary's University, Halifax, Nova Scotia B3H 3C3 (Canada)*

(Received 24th July 1978)

Numerous polymerization and oligomerization reactions of amino acid esters have been studied [1—4]. In most or all of these reactions, cyclic species derived from dipeptide esters or two moles of an amino acid ester are formed as by-products. In the case of glycine oligomerization, this cyclic compound is known as 2,5-piperazinedione (PDO). Determination of PDO has proven difficult for a number of reasons, including interference from other species in the reaction mixture, particularly oligopeptides; PDO does not react with ninhydrin.

A few methods have been reported for the detection and determination of substantial amounts of PDO: thin-layer chromatography [5], gas-liquid chromatography [6—8], and a sublimation method [9]. For various reasons none of these methods is satisfactory for the determination of PDO in complex mixtures. Full t.l.c. and g.l.c. data have not been reported for this compound. If the t.l.c. method were used, it would be difficult to obtain quantitative data as the spray used detects all NH—CO-containing species. Thus extensive purification and/or derivatization of the reaction mixtures is required. A similar problem is encountered for the g.l.c. procedure, because the peptide material must be derivatized or removed to prevent interference with the proper operation of the column. Many problems could be encountered in a derivatization step; derivatization of dipeptides by classical methods leads to PDO formation [10], clearly an untenable situation in reactions in which ratios of dipeptide to PDO are sought. Finally, the sublimation method [9] is time-consuming, requires relatively large quantities of material, and may not be effective in complex mixtures when other than peptide material is present.

The ideal method for analysis for PDO would be one which is rapid and sensitive, requires a minimum of manipulation and no derivatization, and one in which impurities or other constituents of the reaction mixture do not interfere with the assay. Such an assay for PDO is described here: the method is based on reverse-phase high-performance liquid chromatography (h.p.l.c.) and

involves a single extraction before assay of the reaction mixture. The analytical methodology is described here; the chemistry will be presented in detail elsewhere.

*Experimental*

The reverse-phase h.p.l.c. separations were achieved with the following equipment and conditions: Model 6000A Solvent Delivery Pump (Waters Associates, Milford, Conn.); Model 7120 injection valve with 2-ml sampling loop (Rheodyne Incorp., Berkeley, Calif.); Spectroflow Monitor SF 770 (Schoeffel Instrument Corp., N.J.) at 200 nm in series with a Model 440 Absorbance Detector (Waters Associates) at 254 nm. Two in-series $\mu$-Bondapak C-18 columns (Waters Associates) were used at ambient temperature with a pressure difference of 200 atm. The solvent was 0.45 M phosphate buffer, pH 2.1, and the flow rate 1.5 ml $min^{-1}$. A dual-pen Honeywell Electronik 196 recorder was used to record the two wavelengths monitored (200 and 254 nm), and 80-$\mu$l samples were introduced by microsyringe.

Oligomeric glycine standards (National Biochemical Corporation, Cleveland, Ohio) and reagent-grade PDO (Sigma Chemical Company, St. Louis, Missouri) were used. All other chemicals were reagent grade; the water was double distilled in glass.

Glycine condensation reactions were sampled at times 0, 15, 30, 60, 90 min and 18 h after initiation. The reactions were quenched with the mobile phase at pH 11, extracted with ethyl acetate, acidified and stored in a vacuum desiccator until analyzed. This step was one of convenience to remove volatile interference species which otherwise would elute late in the separation and cause longer analysis times. Total analysis time was approximately 10 min per sample.

*Results and discussion*

PDO is particularly difficult to retain on a reverse-phase system because of the lack of hydrocarbon side-chains. The present method was chosen because it is very suitable for studying amino acids other than glycine, as well as their cyclized products. Other amino acids can be separated easily and quantified with this packing [11, 12].

In the system described, glycine oligomers were slightly retained but not resolved while PDO was well retained (Fig. 1A). No interference was seen for the determination of PDO (Fig. 1B), and linearity between the absorbance at 200 nm and the concentration of PDO injected was observed over the range 0.1—4.0 $\mu$g $ml^{-1}$ with 80-$\mu$l injections (ca. 0.02—0.65 absorbance units). Since PDO does not contain significant chromophoric activity, a wavelength of 200 nm was used to monitor the end absorption of PDO. Observations on glycine and alanine and their oligomers or cyclized products indicated that the amide linkage was primarily responsible for the end absorption monitored for PDO.

The lower limit of detection for PDO in this system was approximately

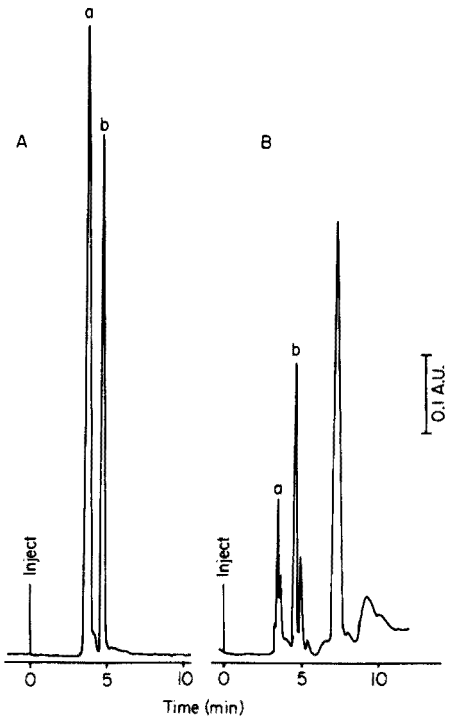


Fig. 1. (A) Separation of glycine (a) from $5.0 \times 10^{-4}$ M PDO (b). (B) Separation of glycine, diglycine, and triglycine (a) from PDO (b) in the extract of the reaction mixture. Conditions as in text.

500 ng per injection or 5 $\mu$g $ml^{-1}$. This was found most appropriate for following the reactions under consideration.

The use of two in-series detectors, one at 200 nm and the other at 254 nm, aided considerably in identifying the more strongly retained compounds and establishing whether spurious results were due to compounds absorbing at 254 nm (i.e. non-peptides). The step involving the vacuum desiccator for removing volatile strongly retained species cut analysis times by 75%. Thus, as illustrated by Fig. 1B, the total analysis time per sample was 10 min but could be reduced further by timing further injections during the middle of the previous separation.

For amino acids and their cyclic products, the requirement of a mobile phase of high ionic strength (0.45 M phosphate buffer, pH 2.1) will not be necessary. Also, the oligomeric peptides will be easily resolved because of their greater hydrocarbon character [11, 12]. Thus a reverse-phase h.p.l.c. system with detection at 200 nm should fulfil all the requirements for following polymerizations and oligomerizations of amino acid esters.

We acknowledge the financial support of the National Research Council of Canada and Dr. B. Belleau for helpful discussions.

REFERENCES

1 H. Brockmann and H. Musso, Chem. Ber., 87 (1954) 581.
2 H.-G. Elias and U. Romer, Makromol. Chem., 102 (1967) 202.
3 T. Iio and S. Takahashi, Bull. Chem. Soc. Jpn., 47 (1974) 2720.
4 Y. Kawabata and M. Kinoshita, Makromol. Chem., 176 (1975) 2807.
5 D. E. Nitecki, B. Halpern and J. W. Westley, J. Org. Chem., 33 (1968) 864.
6 A. B. Mauger, J. Chromatogr., 37 (1968) 315.
7 B. F. Gisin and R. B. Merrifield, J. Am. Chem. Soc., 94 (1972) 3102.
8 R. B. Merrifield, A. R. Mitchell and J. E. Clarke, J. Org. Chem., 39 (1974) 660.
9 H.-G. Elias, U. Romer and H. von Werra, Makromol. Chem., 102 (1967) 183.
10 S. M. Tenneson, unpublished results.
11 I. Molnar and C. Horvath, J. Chromatogr., 142 (1977) 623.
12 W. Monch and W. Dehnen, J. Chromatogr., 140 (1977) 260.

*Analytica Chimica Acta*, 105 (1979) 413—415


Short Communication

# DETECTION OF *N*-ACETYLGLYCINE, *N*-ACETYLGLYCYLGLYCINE, AND *N*-ACETYLGLYCYLGLYCYLGLYCINE BY PAPER CHROMATOGRAPHY

H. A. SOKOL

*Biology and Medicine Division, Lawrence Berkeley Laboratory, University of California, Berkeley, California 94720 (U.S.A.)*

(Received 26th July 1978)

In the radiolysis of diglycine, triglycine, and tetraglycine, *N*-acetylglycine, *N*-acetylglycylglycine, and *N*-acetylglycylglycylglycine, respectively, are often formed. In this laboratory, these compounds are usually separated from the amino acids and peptides by ion-exchange chromatography. After hydrolysis, lyophilization, and concentration in dilute sodium hydroxide solution, the total acetic acid concentration is determined by flame ionization gas chromatography. Generally, recoveries from synthetic target solutions spiked with known amounts of the acetyl derivatives of interest are 80—100%.

Ward et al. [1] similarly determined acetyl groups in proteins and peptides by gas chromatography (g.c.). They hydrolyzed the sample, extracted the liberated acetic acid with t-butyl ethyl ether, and injected this extract into the gas chromatograph. This method poses certain problems for determining acetic acid from very small amounts of *N*-acetylglycine and *N*-acetyl peptides. To obtain adequate g.c. sensitivity, it would be necessary to scale up the procedure considerably and then concentrate the ether extract, which could result in a loss of acetic acid. In addition, the acetic acid peak appears on the shoulder of the very large ether peak, and "ghosting" phenomena may occur [2—4]. Of course, these methods give no indication of the acetyl compound from which the acid is derived.

Some acyl amino acids have been detected by paper chromatography by Kirchenmayer and Kuffner [5], who acetylated amino acids on paper with acetic anhydride and developed the chromatogram with n-butanol—acetic acid—water (8:1:10, v/v). Reio [6] chromatographed *N*-acetylglycine, developed the chromatograms with three different solvent systems, and reported $R_F$ values of 0.54, 0.08, and 0.14; the spots were detected with ninhydrin and bromophenol blue. Whitehead [7] separated *N*-acetyl amino acids (including *N*-acetylglycine) chromatographically in various solvent systems followed by ionophoresis in ethylamine acetate. The separated acids showed up as yellow spots when the paper was dipped in bromocresol green indicator in acetone. Umebayashi [8] chromatographed *N*-acetylglycine in n-butanol—acetic acid—

water (4:1:50, v/v), hydrolyzed the spots on the t.l.c. plates with 6 M HCl, and finally applied the ninhydrin test.

Bergmann [9] determined *N*-acetylglycine as the hydroxamic acid derivative and measured the absorption of the iron(III)-hydroxamic acid complex.

*N*-Acetylglycine and its volatile ester [10, 11] and silyl [12, 13] derivatives have been measured by gas chromatography, and studied by paper and thin-layer chromatography, but *N*-acetylglycylglycine and *N*-acetylglycylglycylglycine were not examined. Gordon et al. [14] examined these two compounds by partition chromatography, but their data indicated that the two could not be satisfactorily separated with their solvent system.

In the work described here, n-butanol—acetic acid—water (8:1:10, v/v) was used as the developing solvent [5]. *N*-Acetylglycine, *N*-acetylglycylglycine, and *N*-acetylglycylglycylglycine could be satisfactorily separated and detected.

*Experimental*

*Chemicals.* All chemicals were reagent grade. n-Butanol, glacial acetic acid, bromocresol green (J. T. Baker), methanol, acetone (Mallinckrodt Chemical Works), morpholine (Eastman Organic), *N*-acetylglycine (NBC) and *N*-acetylglycylglycine (Cyclo Chemical Corporation) were used as received. *N*-Acetylglycylglycylglycine was prepared by the method of Fischer [15].

*Procedure.* After the acetyl compounds of interest had been separated from peptides by ion-exchange chromatography, the effluent fraction was dried and redissolved in absolute methanol. Enough methanol was used to give a spotting solution of 0.001—0.005 M for each compound of interest. A 50-$\mu$l aliquot of this methanolic solution was applied with a micropipet to the base line of Whatman no. 1 paper (35—40 cm long), and the spots were dried in a gentle stream of nitrogen. The spotted paper was equilibrated in a covered chromatographic jar for 1 h and then dipped into the upper phase of the developing solvent. The chromatogram was developed for 18 h at room temperature, withdrawn from the jar, and hung to dry in a hood overnight. The developed chromatogram was then heated at 100°C for 6 h. This heating time was essential in order to see the spots under ultraviolet light without the use of an indicator. At this point the spots can be located, cut out, and processed further as desired.

To see the spots more clearly the paper was dipped into a solution of 0.01% bromocresol green indicator in acetone to which 1 drop of morpholine had been added. After the dipped paper had been dried for 5 min at room temperature, the yellow spots readily showed up against the blue background. The $R_F$ values were 0.59 (*N*-acetylglycine), 0.43 (*N*-acetylglycylglycine), and 0.33 (*N*-acetylglycylglycylglycine).

Although St. Onge et al. [10] found *N*-acetylglycine as a contaminant of analytical-grade acetic acid, evidence for this was not found here. Consequently no effort was made to purify the glacial acetic acid before use in the developing solvent.

This general procedure was used satisfactorily for the detection of these three compounds in aqueous solutions of diglycine, triglycine, and tetraglycine, which were used as $\gamma$-radiolysis targets.

This investigation was supported by the Biomedical and Environmental Research Division of the U.S. Department of Energy.

REFERENCES

1 D. N. Ward, J. Coffey, D. B. Ray and W. M. Lamkin, Anal. Biochem., 14 (1966) 243.
2 C. Van Eenaeme, J. M. Bienfait, O. Lambot and A. Pondant, J. Chromatogr. Sci., 12 (1974) 398.
3 R. C. Dressman, J. Chromatogr. Sci., 8 (1970) 265.
4 R. B. H. Wills, J. Chromatogr. Sci., 10 (1972) 582.
5 T. Kirchenmayer and F. Kuffner, Monatsh. Chem., 93 (1962) 1237.
6 L. Reio, Chromatogr. Rev., 3 (1961) 92.
7 J. K. Whitehead, Biochem. J., 68 (1958) 653.
8 M. Umebayashi, Nippon Dojo-Hiryogaku Zasshi, 39 (1968) 137.
9 F. Bergmann, Anal. Chem., 24 (1952) 1367.
10 L. M. St. Onge, S. L. Kittle and P. B. Hamilton, Anal. Biochem., 71 (1976) 156.
11 D. E. Johnson, S. Scott and A. Meister, Anal. Chem., 33 (1961) 669.
12 B. Rowley and T. Gerritsen, Clin. Chim. Acta, 62 (1975) 13.
13 M. G. Horning, E. A. Boucher and A. M. Moss, J. Gas Chromatogr., 5 (1967) 297.
14 A. H. Gordon, A. J. P. Martin and R. L. M. Synge, Biochem. J., 37 (1943) 79.
15 E. Fischer, Ber., 37 (1904) 2486.

*Analytica Chimica Acta*, 105 (1979) 417—421


Short Communication

# POTENTIOMETRIC TITRATIONS OF HALIDE MIXTURES WITH AN IODIDE-SELECTIVE ELECTRODE

JUNKO MOTONAKA*
*Technical College of Tokushima University, Minamijôsanjima, Tokushima (Japan)*
SANAE IKEDA
*Faculty of Engineering, Tokushima University, Minamijôsanjima, Tokushima (Japan)*
NOBUYUKI TANAKA
*Faculty of Science, Tohoku University, Aramaki, Sendai (Japan)*
(Received 5th June 1978)

There have been several reports on the determination of halide mixtures by potentiometric titration with silver (I) solutions. Co-precipitation is well known to cause errors in the analysis of halide mixtures [1, 2], but there have been few reports [3—5] on ways of avoiding this error. The present communication offers a method of titrating halide mixtures potentiometrically with an iodide-selective membrane electrode. Accurate results can be obtained by adding a coagulating agent, such as aluminum nitrate.

## *Experimental*

*Apparatus.* An automatic potentiometric titrator (Hiranuma Sangyo Co., Ltd., RAT-11S) was used with an Orion Model 94-53A iodide-selective indicator electrode and a saturated calomel reference electrode.

*Reagents.* All reagents were of analytical-reagent grade (Wako Pure Chemical Industries, Ltd.). Commercial potassium iodide, potassium bromide and potassium chloride were recrystallized three times from water. Redistilled water was used. The following stock solutions were diluted appropriately before use: $10^{-2}$ M potassium iodide solution (standardized by the JIS K8913-1961 method); $10^{-2}$ M potassium bromide solution (standardized by the JIS K8506-1961 method); $10^{-2}$ M potassium chloride solution (standardized by the JIS K8121-1961 method); and $10^{-1}$ M silver nitrate solution (standardized by amperometric titration [6]).

*Recommended procedure.* Measure exactly 10 ml each of ca. $10^{-2}$ M potassium iodide, potassium bromide, potassium chloride and aluminum nitrate solutions into a 200-ml titration cell and adjust the volume to 100 ml with redistilled water. Titrate the solution potentiometrically with a $10^{-1}$ M standard silver nitrate solution. The whole procedure requires about 15 min. For titrations of more dilute solutions, use a silver nitrate titrant which is about 100 times more concentrated than the titrand.

*Results and discussion*

*Effect of co-precipitation.* The potentiometric titration curve for a mixture of $10^{-3}$ M concentrations of iodide, bromide and chloride ions is shown in Fig. 1. The titration was not accurate, the curve (dashed line) differing considerably from the theoretical curve (dotted line). The error in the end-point for iodide became smaller when the bromide or chloride ion concentration was increased relative to that of iodide ion (Table 1). The error in the iodide end-point was larger in the presence of bromide than in the presence of chloride ion, because silver bromide naturally tended to co-precipitate more readily. With mixtures of about equal concentrations of all three halides, the errors for all three halides become very large (Table 1). Similar results were obtained when a silver plate electrode was used (Table 1, last line).

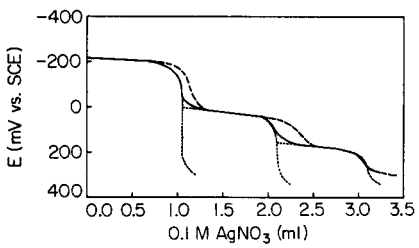


Fig. 1. Potentiometric titration curves for a halide mixture. A mixture of 10 ml each of $10^{-2}$ M potassium iodide, potassium bromide and potassium chloride diluted to 100 ml, without (——) and with (——) aluminum nitrate. (--------) Theoretical titration curve.

TABLE 1

Effect of co-precipitation on the titration of halide mixtures with an iodide-selective electrode

| Sample[a] (M) | | | Relative error[b] (%) | | | Coefficient of variation (%) | | |
|---|---|---|---|---|---|---|---|---|
| KI | KBr | KCl | KI | KBr | KCl | KI | KBr | KCl |
| $10^{-3}$ | $10^{-3}$ | | +15.7 | −14.5 | | 0.2 | 0.2 | |
| $10^{-3}$ | $5 \times 10^{-3}$ | | +14.8 | — | | 0.2 | — | |
| $10^{-3}$ | $10^{-2}$ | | +14.8 | — | | 0.1 | — | |
| $10^{-3}$ | $5 \times 10^{-2}$ | | +3.27 | — | | 0.2 | — | |
| $10^{-3}$ | | $10^{-3}$ | +7.25 | | −8.50 | $0.0_4$ | | 0.1 |
| $10^{-3}$ | | $4 \times 10^{-3}$ | +6.67 | | — | 0.3 | | — |
| $10^{-3}$ | | $10^{-2}$ | +4.69 | | — | 0.3 | | — |
| $10^{-3}$ | | $4 \times 10^{-2}$ | +0.94 | | — | 0.1 | | — |
| | $10^{-3}$ | $10^{-3}$ | | +19.4 | −21.6 | | 0.3 | 0.2 |
| $10^{-3}$ | $10^{-3}$ | $10^{-3}$ | +8.51 | +22.7 | −32.1 | 0.2 | 0.2 | 0.3 |
| $10^{-3}$ | $10^{-3}$ | $10^{-3}$[c] | +8.71 | +23.0 | −32.5[c] | 0.1 | 0.2 | 0.4[c] |

[a]Solution, 100 ml, of potassium iodide, potassium bromide and potassium chloride.
[b]Average of 4 determinations. [c]A silver foil electrode was used for these results.

*Effects of coagulating agents.* Attempts to eliminate the influence of co-precipitation by adding surface-active agents [7] (polyvinyl pyrrolidone and Triton) were unsuccessful, whereas accurate results were obtained on adding coagulating agents (solid curve, Fig. 1). Mixtures of the halides were titrated in the presence of various inorganic salts. When aluminum nitrate was added, the error was less than 0.5% and the relative standard deviation less than 0.2% (Table 2). When aluminum nitrate ($5 \times 10^{-5}$—$10^{-1}$ M) was added to a mixture which was $10^{-3}$ M in each halide, the results were in good agreement with those obtained by the JIS method. Lanthanum nitrate ($10^{-3}$ M), magnesium nitrate, strontium nitrate, calcium nitrate and lead nitrate ($10^{-2}$ M) also had favorable effects. Barium nitrate, aluminum sulfate, and iron(II) sulfate were found not to improve the determinations, although Csakvari and Meszaros [5] reported that barium nitrate had a favorable effect.

All subsequent measurements, therefore, were carried out in the presence of $10^{-3}$ M aluminum nitrate.

*Effect of pH.* Halide mixtures were titrated in solutions of various pH values, the pH being adjusted with sulfuric acid or sodium hydroxide (Fig. 2). Potassium iodide could be determined accurately at pH 1—4, but co-precipitation occurred at pH 4.2—10.5 because of formation of aluminum hydroxide, which did not behave as a coagulating agent. The error in the iodide determina-

TABLE 2

Effects of coagulating agents on the determination of a halide mixture[a]

| Concn. (M) | Coagulating agent | Relative error[b] (%) | | | Coefficient of variation (%) | | |
|---|---|---|---|---|---|---|---|
| | | KI | KBr | KCl | KI | KBr | KCl |
| $10^{-3}$ | $Al(NO_3)_3$ | −0.04 | +0.38 | −0.12 | 0.05 | 0.2 | 0.1 |
| $10^{-2}$ | $Al(NO_3)_3$ | −0.08 | +0.47 | −0.50 | 0.2 | 0.03 | 0.2 |
| $10^{-1}$ | $Al(NO_3)_3$ | −0.12 | +0.21 | −0.33 | 0.1 | 0.2 | 0.2 |
| $10^{-3}$ | $La(NO_3)_3$ | −0.09 | +0.22 | −0.57 | 0.1 | 0.2 | 0.1 |
| $10^{-3}$ | $Al_2(SO_4)_3$ | −0.25 | +1.69 | −1.75 | 0.1 | 0.2 | 0.1 |
| $10^{-2}$ | $Al_2(SO_4)_3$ | −0.50 | +1.10 | −2.19 | 0.1 | 0.3 | 0.3 |
| $10^{-3}$ | $Ba(NO_3)_2$ | +0.63 | +9.80 | −10.8 | 0.1 | 0.2 | 0.2 |
| $10^{-2}$ | $Ba(NO_3)_2$ | −0.59 | +1.93 | −2.00 | 0.2 | 0.3 | 0.2 |
| $10^{-3}$ | $Mg(NO_3)_2$ | +4.82 | +20.8 | −26.1 | — | — | — |
| $10^{-2}$ | $Mg(NO_3)_2$ | +0.19 | +0.81 | −1.01 | 0.1 | 0.1 | 0.2 |
| $10^{-3}$ | $Sr(NO_3)_2$ | +2.58 | +13.8 | −17.1 | — | — | — |
| $10^{-2}$ | $Sr(NO_3)_2$ | +0.10 | +0.54 | −0.76 | 0.2 | 0.3 | 0.2 |
| $10^{-3}$ | $Ca(NO_3)_2$ | +3.66 | +21.5 | −26.1 | 0.1 | 0.3 | 0.2 |
| $10^{-2}$ | $Ca(NO_3)_2$ | −0.02 | +0.54 | −0.76 | 0.2 | 0.2 | 0.2 |
| $10^{-3}$ | $Pb(NO_3)_2$ | −0.15 | +7.73 | −7.54 | — | — | — |
| $10^{-2}$ | $Pb(NO_3)_2$ | −0.40 | +0.60 | −0.25 | 0.03 | 0.1 | 0.2 |
| $10^{-3}$ | $FeSO_4$ | +0.42 | +6.36 | −6.49 | 0.2 | 0.2 | 0.3 |

[a] Solution, 100 ml, of 10 ml each of $10^{-2}$ M potassium iodide, potassium bromide and potassium chloride, and coagulating agent. [b] Average of 4 determinations.

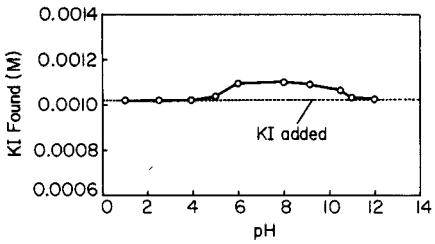


**Fig. 2. Effect of pH on the analysis of a halide mixture. A mixture of 10 ml each of $10^{-2}$ M potassium iodide, potassium bromide, potassium chloride and aluminum nitrate diluted to 100 ml.**

tion decreased above pH 11, because of the amphoteric nature of aluminum hydroxide; the error in the measurement of bromide was then of the order of a few per cent, and chloride was not determined. It may be concluded that pH 1—4 is a suitable range for the determination.

When a mixture of 10 ml each of $10^{-2}$ M potassium iodide, potassium bromide, potassium chloride and aluminum nitrate was diluted to 100 ml, the pH was about 3.9. Accordingly, all subsequent measurements were made with diluted mixtures without adjusting the pH.

*Effect of temperature.* Titrations of halide mixtures were not affected by temperature in the range 1—60° C; for convenience all subsequent measurements were done at room temperature (ca. 20°C).

*Effects of organic solvents.* Titrations of halide mixtures in the presence of various organic solvents showed increased errors as the solvent content increased (Table 3).

*Accuracy and precision.* Table 4 shows the results obtained for halide mixtures at various concentrations. The best results, with relative errors and relative standard deviations of less than 0.4%, were obtained with $10^{-3}$ M halides. It was difficult to determine $10^{-4}$ M chloride [$K_{so}$ (AgCl) = $8.2 \times 10^{-11}$; $K_{so}$ (AgI) = $1.53 \times 10^{-16}$], or to determine bromide at concentrations of $10^{-6}$ M and lower [$K_{so}$ (AgBr) = $2.11 \times 10^{-13}$]. Iodide ion could be determined in the concentration range $10^{-6}$—$10^{-3}$ M, with relative errors of less than ±0.5% and relative standard deviations below 0.9%.

*Conclusions.* Accurate analyses of halide mixtures by potentiometric titration with silver nitrate solution and an iodide-selective electrode are possible if a coagulating agent such as aluminum nitrate is added. When $5 \times 10^{-5}$—$10^{-1}$ M aluminum nitrate media were used, the results for $10^{-3}$ M halides were in good agreement with those obtained by the JIS method. The best results, with relative errors and relative standard deviations of less than 0.4%, were obtained with $10^{-3}$ M halides in $10^{-3}$ M aluminum nitrate. Lanthanu nitrate, magnesium nitrate, strontium nitrate, calcium nitrate and lead nitrate also had favorable effects, but were less satisfactory than aluminum nitrate.

TABLE 3

Effects of organic solvents on the determination of a halide mixture[a]

| Organic solvent | (% v/v) | Relative error (%) | | |
|---|---|---|---|---|
| | | KI | KBr | KCl |
| Methanol | 20 | +0.02 | +0.42 | −0.25 |
| | 40 | −0.15 | +1.02 | −0.75 |
| | 60 | −0.27 | +0.90 | −0.50 |
| | 68 | −0.27 | +1.86 | −1.51 |
| Ethanol | 10 | −0.15 | +0.54 | −0.25 |
| | 20 | −0.02 | +1.14 | −1.01 |
| | 30 | +0.48 | +0.90 | −1.26 |
| | 40 | +0.48 | +1.38 | −1.76 |
| | 60 | +0.38 | +3.18 | −3.63 |
| Acetone | 10 | −0.27 | +0.65 | −0.25 |
| | 20 | −0.02 | +1.14 | −1.01 |
| | 30 | −0.27 | +2.10 | −1.76 |
| | 40 | −0.52 | +2.10 | −1.76 |
| | 60 | −1.40 | +4.14 | −2.52 |

[a]Solution, 100 ml, of 10 ml each of 0.01 M potassium iodide, potassium bromide, potassium chloride and aluminum nitrate, and organic solvent.

TABLE 4

Analysis of halide mixtures

| Sample[a] (M) | | | | Relative error[b] (%) | | | Coefficient of variation (%) | | |
|---|---|---|---|---|---|---|---|---|---|
| $Al(NO_3)_3$ | KI | KBr | KCl | KI | KBr | KCl | KI | KBr | KCl |
| $10^{-3}$ | $10^{-3}$ | $10^{-3}$ | $10^{-3}$ | −0.04 | +0.38 | −0.12 | 0.05 | 0.2 | 0.1 |
| $10^{-3}$ | $10^{-4}$ | $10^{-4}$ | $10^{-4}$ | +0.36 | +1.57 | — | 0.2 | 0.3 | — |
| $10^{-3}$ | $10^{-5}$ | $10^{-5}$ | $10^{-5}$ | +0.36 | −3.38 | — | 0.3 | 1.3 | — |
| $10^{-3}$ | $10^{-6}$ | $10^{-6}$ | $10^{-6}$ | +0.49 | — | — | 0.9 | — | — |

[a]Solution, 100 ml, of potassium iodide, potassium bromide, potassium chloride and aluminum nitrate. [b]Average of 4 determinations.

REFERENCES

1 D. Jaques, J. Chem. Educ., 42 (1965) 429.
2 S. Mesaric and E. A. M. F. Dahmen, Anal. Chim. Acta, 64 (1973) 431.
3 A. J. Martin, Anal. Chem., 30 (1958) 233.
4 E. Pungor, Anal. Chem., 39 (1967) 28A.
5 B. Csakvari and K. Meszaros, Hung. Sci. Instrum., 11 (1968) 9.
6 I. M. Kolthoff and P. K. Kuroda, Anal. Chem., 23 (1951) 1306.
7 V. J. Shiner and M. L. Smith, Anal. Chem., 28 (1956) 1043.

*Analytica Chimica Acta*, 105 (1979) 423—428


Short Communication

# DETERMINATION OF THE PHENOLIC ANALGESICS, CIRAMADOL, MEPTAZINOL, DEZOCINE AND PENTAZOCINE IN PHARMACEUTICAL DOSAGE FORMS BY LINEAR-SWEEP VOLTAMMETRY AT A GLASSY CARBON ELECTRODE

H. K. CHAN*

*Wyeth Laboratories, Huntercombe Lane South, Maidenhead, Berkshire SL6 0PH (Gt. Britain)*

A. G. FOGG

*Department of Chemistry, Loughborough University of Technology, Loughborough, Leicestershire LE11 3TU (Gt. Britain)*

(Received 18th July 1978)

Many methods are available for the determination of drug compounds containing a hydroxyl functional group [1]. In particular, gas chromatography after derivatization [2], u.v. and visible spectrophotometry [3], and high-pressure liquid chromatography [4] have been applied to oxygen-containing drugs. Many of these methods are highly sensitive and selective, and are generally considered to be rapid. Nevertheless, at higher concentration levels a voltammetric procedure can be simpler and less time-consuming, and may be the method of choice if sufficient selectivity can be achieved.

The present work is concerned with the development of voltammetric procedures for the determination of four analgesics: ciramadol [(−)-*cis*-2-(α-dimethylamino-*m*-hydroxybenzyl)cyclohexanol hydrochloride], meptazinol [*m*-(3-ethyl-1-methylhexahydro-1H-azepin-3-yl)phenol hydrochloride], dezocine [(−)-13β-amino-5,6,7,8,9,10,11,12-octahydro-5α-methyl-5,11-methanobenzocyclodecen-3-ol hydrobromide] and pentazocine [1,2,3,4,5,6-hexahydro-8-hydroxy-6,11-dimethyl-3-(3-methylbut-2-enyl)-2,6-methano-3-benzazocine]. These drugs give anodic waves at a glassy carbon electrode when present in a mainly non-aqueous supporting electrolyte.

*Preliminary studies.*

The four analgesics did not give cathodic or anodic voltammetric waves at the glassy carbon electrode in aqueous buffer solutions. Non-aqueous supporting electrolytes, namely 0.1 M sodium acetate—0.1 M acetic acid in 98% methanol, 98% ethanol and 90% isopropanol, and 0.01 M tetraethylammonium perchlorate in 95% ethanol, were studied. Shearer et al. have shown [5] that the methanolic buffer is suitable for the voltammetric determination of paracetamol. In all the non-aqueous supporting electrolytes studied,

an anodic wave was produced for each drug substance, but the ethanolic buffer was the most satisfactory. This electrolyte gave a sufficiently positive potential range to allow the well-shaped anodic waves of the drugs to be observed clearly. The residual current was sufficiently low, reaching a value of 0.25 $\mu$A at +0.9 V. Deaeration of solutions was unnecessary, no difference between the voltammograms obtained with normal and deaerated solutions being observed.

*Experimental*

*Instrumentation.* A PAR 174A polarographic analyzer (Princeton Applied Research Corp.) was used with an Advance XY recorder (model LR 100). The electrode system comprised a working glassy carbon electrode (PAR 9333; nominal surface area 0.28 $cm^2$), a platinum wire counter electrode and a saturated calomel reference electrode held by means of a rubber O-ring in a salt bridge (PAR 9332) containing a saturated aqueous solution of potassium nitrate. The close-fitting O-ring ensured the minimal flow of aqueous electrolyte into the voltammetric cell; this was important in ensuring good results. The voltammetric cell (PAR 9301) had a working volume of 5—50 ml. All potentials are quoted versus the SCE.

The pretreatment of the glassy carbon electrode surface before each scan was important. Preliminary studies of the oxidation of ciramadol showed that irreversible adsorption occurs at the electrode surface during the scan; thus the peak anodic current fell steadily for successive voltammetric scans in a 100 $\mu g\ ml^{-1}$ solution of ciramadol. In order to achieve reproducible peak currents, it was necessary to clean the glassy carbon electrode between scans as follows: the electrode surface was washed first with 95% ethanol and then with chloroform, then cleaned carefully with a non-abrasive paper tissue soaked in chloroform, and finally dried with a dry tissue. When not in use the clean electrode was stored in a boiling tube fitted with a ground-glass joint. When this procedure was followed, excellent precision was obtained.

*Reagents.* Samples of ciramadol, meptazinol and dezocine were available at Wyeth Laboratories: samples of pentazocine were obtained from Winthrop Laboratories Ltd. The purity of all samples was confirmed by thin-layer chromatography. Other reagents were of analytical-reagent grade.

*Supporting electrolyte.* Dissolve 8.2 g of anhydrous sodium acetate in 20 ml of water. Add 5.8 ml of glacial acetic acid and dilute to 1 l with absolute ethanol.

*Standard solutions (1 mg $ml^{-1}$).* Dissolve 100 mg of the drug to be determined in 100 ml of 95% ethanol.

*Calibration.* Dilute aliquots of the standard solution containing less than 7 mg of the drug to 100 ml with the supporting electrolyte in dry volumetric flasks. Transfer a portion of each solution in turn to a clean dry voltammetric cell and obtain the d.c. voltammogram from +0.2 to +1.0 V using a sweep rate of 5 mV $s^{-1}$, low pass filter at 0.3, and sensitivity 10 $\mu$A. Measure the peak heights in the usual way.

*Procedure for solid dosage forms.* Accurately weigh into a 50-ml stoppered centrifuge tube an amount of well ground tablet or capsule content — generally reserved from the average weight determination — containing about 25 mg of the drug. Add by pipette 25 ml of 95% ethanol, stopper the tube and shake vigorously for 30 min to extract the drug. Centrifuge and pipette 5 ml of the supernatant layer into a dry 100-ml volumetric flask. Dilute to 100 ml with the supporting electrolyte and mix well. Transfer a portion of the solution to the voltammetric cell and obtain the voltammogram as before. Compare the peak height with those obtained with standards prepared in the same batch of supporting electrolyte.

*Procedure for liquid dosage forms.* Pipette an aliquot of the liquid dosage form containing about 25 mg of drug into a 25-ml graduated flask and dilute it to 25 ml with absolute ethanol. Pipette 5 ml of this solution into a dry 100-ml volumetric flask, dilute and complete the analysis as described for the solid dosage forms.

*Results and discussion*

Calibration curves for the four drug compounds obtained in the range 10—70 $\mu g\ ml^{-1}$ of the final solution were rectilinear. Typical voltammograms for the four compounds at the 50 $\mu g\ ml^{-1}$ level are shown in Fig. 1: calibration graphs are shown in Fig. 2. The coefficient of variation for the determination of ciramadol (10 determinations) at the 50 $\mu g\ ml^{-1}$ level was 0.8%. The peak potentials for ciramadol, meptazinol, dezocine and pentazocine are 0.87, 0.84, 0.69 and 0.78 V, respectively.

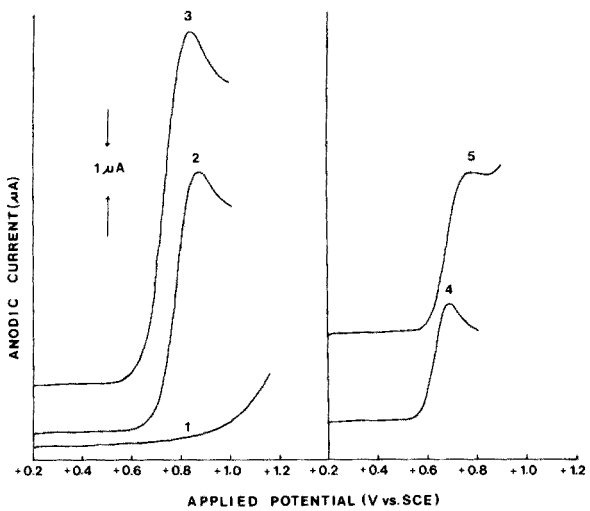


Fig. 1. Typical linear-sweep voltammograms obtained with standards. (1) Blank; (2) ciramadol; (3) meptazinol; (4) dezocine and (5) pentazocine.

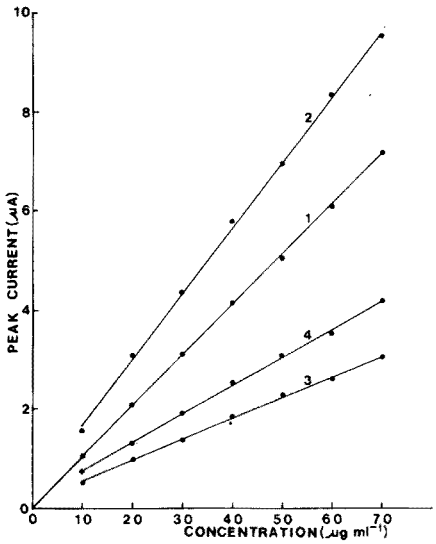


Fig. 2. Calibration graphs for (1) ciramadol, (2) meptazinol, (3) dezocine and (4) pentazocine.

The effect of the water content of the supporting electrolyte on the peak currents and peak potential was investigated (Table 1). The peak current decreases markedly with increasing water content, and it is clearly important that the same batch of supporting electrolyte be used for both samples and standards. The effect of common excipients on the voltammograms obtained was studied in some detail. The excipients studied had no effect on the blank voltammogram at the levels studied, and the recoveries of ciramadol were not affected (see Table 2).

Results obtained for the analysis of solid and liquid dosage forms are given in Table 3. These are in good agreement with results obtained by u.v. spectrophotometry. The coefficients of variation (10 determinations) for tablets (20 mg of ciramadol/tablet) and injections (20 mg of ciramadol/ml) were 1.5% and 1.0%, respectively.

Finally the suitability of the voltammetric method for stability studies was tested on samples of ciramadol that had been photolytically degraded for different periods of time, and other samples that had undergone other

TABLE 1

Effect of water content on $i_p$ and $E_p$ for ciramadol (100 μg ml$^{-1}$) at the glassy carbon electrode

| Water content (%) | 2 | 4 | 8 | 12 | 22 |
|---|---|---|---|---|---|
| $i_p$ (μA) | 4.42 | 4.24 | 3.93 | 3.76 | 3.59 |
| $E_p$ (V) | 0.91 | 0.92 | 0.97 | 1.01 | 1.12 |

TABLE 2

Effect of common formulation excipients on the recovery of 100 μg of ciramadol

| Excipient | Amount of excipient taken | Ciramadol recovered (%) | Excipient | Amount of excipient taken | Ciramadol recovered (%) |
|---|---|---|---|---|---|
| Lactose | 300 mg | 99.0 | Gelatine powder | 300 mg | 101 |
| Microcrystalline cellulose | 500 mg | 100 | Water | 5 ml | 99.8 |
| Amberlite IRP 88 | 13.5 mg | 101 | Saline[a] | 5 ml | 100 |
| Magnesium stearate | 6 mg | 101 | Glycerine BP | 25 mg | 100 |
| Starch | 30 mg | 99.3 | Polyethylene glycol USP 400[b] | 1000 mg | 101 |
| Polyethylene glycol USP 4000 | 50 mg | 99.0 | Tween 80 | 25 mg | 100 |

[a]9 mg of sodium chloride (BP) per ml of water for injection (BP). [b]Carbowax 400.

TABLE 3

Comparison of voltammetric and u.v. spectrophotometric methods for the determination of ciramadol, meptazinol, dezocine and pentazocine in various pharmaceutical dosage forms

| Dosage form | Compound | Amount of drug (mg) | | |
|---|---|---|---|---|
| | | Nominal amount | Voltammetric method | U.v. method |
| Tablet | Ciramadol | 20 | 21.1 | 21.1 |
| | Meptazinol | 200 | 197 | 198 |
| | Pentazocine | 25 | 24.9 | 24.8[a] |
| Capsule | Meptazinol | 75 | 74.3 | 75.2 |
| | Pentazocine | 50 | 50.8 | 50.2[a] |
| Injection | Ciramadol | 20 | 20.8 | 20.6 |
| | Meptazinol | 50 | 49.3 | 50.1 |
| | Dezocine | 20 | 21.2 | 21.2 |
| | Pentazocine | 30 | 30.4 | 30.0[a] |

[a]Assay from NF monograph for pentazocine content.

storage trials (see Table 4). The voltammetric results were compared with results obtained by a quantitative t.l.c.—u.v. method. The ciramadol in the degraded and stored samples was separated from any degradation products on silica-gel plates with toluene—ethanol—ammonia (79:20:1) as eluent; the ciramadol spot was scraped off the plate, and the ciramadol extracted with 95% ethanol and determined by u.v. spectrophotometry. The results obtained by the two techniques (Table 4) are in good agreement and it is concluded that the voltammetric procedure can be used to indicate stability at least with

TABLE 4

Stability of ciramadol under various storage conditions

| Conditions of sample storage | | Ciramadol remaining in sample (%) | |
|---|---|---|---|
| | | Voltammetry | Quantitative t.l.c. |
| 37°C | 3 months | 102 | 100 |
| 37°C H/H[a] | 3 months | 101 | 99.9 |
| 50°C | 3 months | 100 | 101 |
| 105°C | 3 months | 102 | 101 |
| Ultra violet irradiation | 3 days | 88.0 | 86.8 |
| | 7 days | 78.2 | 78.4 |
| | 13 days | 71.6 | 72.0 |

[a]75% relative humidity.

respect to the photolytic decomposition products. Decomposition was not observed in the other stability tests.

The authors thank Wyeth Laboratories for providing facilities and for allowing publication of this paper.

REFERENCES

1 S. Veibel, The Determination of Hydroxyl Groups, Academic Press, London and New York, 1972.
2 J. D. Nicholson, Analyst, 103 (1978) 1, 193.
3 E. G. C. Clarke (Ed.), The Isolation and Identification of Drugs, Pharmaceutical Press, London, Vol. 1, 1969; Vol. 2, 1975.
4 B. B. Wheals and I. Jane, Analyst, 102 (1977) 625.
5 C. M. Shearer, K. Christenson, A. Mukherji and G. J. Papariello, J. Pharm. Sci., 61 (1972) 1627.

*Analytica Chimica Acta*, 105 (1979) 429—432


Short Communication

# IMMOBILIZED WHOLE CELL-BASED FLOW-TYPE SENSOR FOR CEPHALOSPORINS

KUNIO MATSUMOTO, HIDEJI SEIJO and TESUO WATANABE,

*Toyo Jozo Co., Mifuku, Ohito-cho, Shizuoka-ken (Japan)*

and ISAO KARUBE*, IKUO SATOH and S. SUZUKI

*Research Laboratory of Resources Utilization, Tokyo Institute of Technology, Nagatsuta-cho, Midori-ku, Yokohama (Japan)*

(Received 18th July 1978)

For control of an antibiotic fermentation, antibiotics are usually determined by microbioassay based on turbidimetric or titrimetric methods. However, these methods require a long time for cultivation of bacteria [1]. Simple, continuous methods for antibiotic determination are required for fermentation control. The present authors succeeded recently in estimating the biochemical oxygen demand of waste waters [2—4] and determining nicotinic acid [5] by using immobilized whole cells and electrochemical devices.

It was found that *Citrobacter freundii* produced cephalosporinase, which catalyzes the following reaction of cephalosporin, which liberates hydrogen ions:

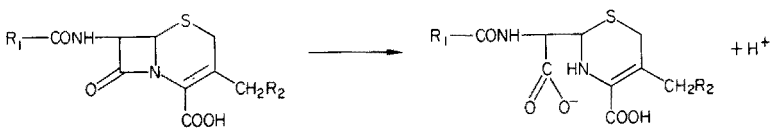


Cephalosporin may therefore be determined from the proton concentration generated in a medium by using immobilized cephalosporinase. Immobilization of cephalosporinase was difficult because the molecular weight of the enzyme is only 30,000 and the enzyme is unstable. Therefore, whole cells of *Citrobacter freundii* were immobilized in a collagen membrane. A microbial sensor composed of a bacteria—collagen membrane reactor and a combined glass electrode can be applied to the determination of cephalosporins in fermentation media as described below.

## *Experimental*

*Materials.* Heart infusion broth (Nisui Pharmaceutical Co., Tokyo) and cephalosporins (Toyo Jozo Co.) were used. Other reagents were of analytical or laboratory grade. Deionized water was used in all procedures.

*Culture of micro-organism. Citrobacter freundii* B-0652 was maintained on peptone-yeast agar. The bacteria were cultured under aerobic conditions at 37°C for 5 h in 1 l of the heart infusion broth (pH 7.0). The cells were centrifuged at 5°C and 8000 G and washed three times with deionized water. About 4.2 g of wet cells were obtained.

*Immobilization of micro-organisms.* Collagen fibril suspension was prepared as described previously [6]. Wet cells (4 g) were added to 60 g of the 0.75% (w/v) suspension. The bacteria—collagen membrane was prepared by casting the suspension on a Teflon plate and drying it at room temperature for 20 h. The bacteria—collagen membranes were treated with a 1% (w/v) glutaraldehyde solution (pH 7.0) for 1 min and dried again at room temperature. The thickness of the membrane was 50—60 $\mu$m.

*Apparatus.* The system used for continuous determination of cephalosporins is illustrated in Fig. 1. The reactor was a biocatalytic type [7] (acrylic plastic, 1.8 cm diam., 5.2 cm long) with a spacer (glass rod, 1.4 cm diam., 5.0 cm long) located in the center. The inner volume of the reactor was 4.1 ml. The bacteria —collagen membrane (10 × 5.5 $cm^2$; 53.276 units) was rolled up with a plastic net (5 × 20 $cm^2$, 20 mesh) and inserted into the reactor. The pH of the sample solution was measured by a combined glass electrode (GC-125 C, TOA Electronics Co. Tokyo) and displayed on a recorder.

*Procedures.* Phosphate buffer ($0.5 \times 10^{-3}$ M, pH 7.2) was transferred continuously to the reactor and sensing chamber. Sample solutions (10 ml) containing various amounts of cephalosporins were transferred to the reactor at 2 ml $min^{-1}$ by a peristaltic pump. The hydrogen ion concentration in the sensing chamber was determined continuously.

The cephalosporinase activity was determined by the method of Perret [8]. The activity yield on immobilization of the cells was 9%.

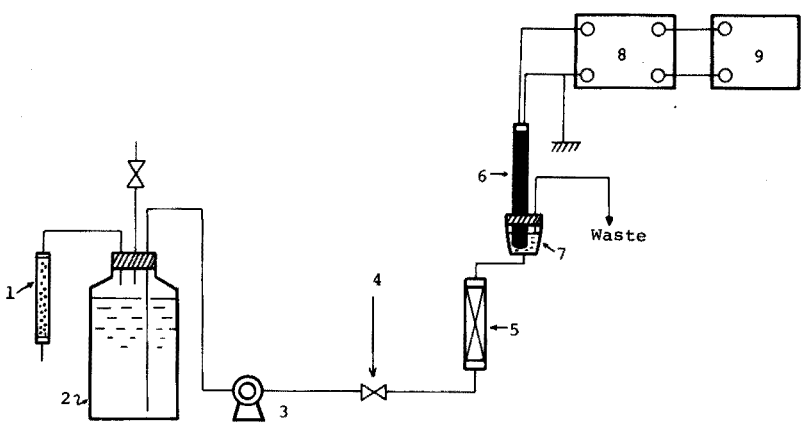


Fig. 1. Immobilized whole cell-based flow-type sensor for cephalosporins. (1) Soda lime; (2) buffer reservoir; (3) peristaltic pump; (4) sample inlet; (5) immobilized whole cell reactor; (6) combined glass electrode; (7) sensing chamber; (8) amplifier; (9) recorder.

*Results*

*Response of the sensor.* Sample solutions (10 ml) containing various amounts of cephalosporins were transferred to the reactor. The electrode potential difference in the sensing chamber increased with time until a maximum was reached. The time required for the maximum to be reached (the response time) depends on the flow rate and activity of the bacteria—collagen membrane. Figure 2 shows the response curves for various concentrations of 7-phenylacetylamidodesacetoxysporanic acid (phenylacetyl-7 ADCA). The maximum potential difference was attained in 10 min at a sample flow rate of 2 ml $min^{-1}$. When $0.5 \times 10^{-3}$ M phosphate buffer was passed into the reactor after a determination, the potential of the glass electrode returned to its initial level within 20 min at 37°C.

*Calibration, re-usability and application.* Figure 3 shows the relationship between the concentrations of various cephalosporins and the potential differences between the initial and maximum states. A linear relationship was obtained between the logarithm of the cephalosporin concentration and the potential difference. As shown in Fig. 3, phenylacetyl-7ADCA, cephaloridine, cephalothin and cephalosporin c were determined by the cephalosporin sensor. Each determination took about 10 min.

The reproducibility was determined with phenylacetyl-7ADCA solution (125 $\mu g\ ml^{-1}$); the relative standard deviation was 10% (2 mV) for 10 experiments. The reactions were not affected by sodium chloride concentrations less than 0.2 M. The immobilized cephalosporinase membranes were active for a month when stored in physiological saline at 5°C.

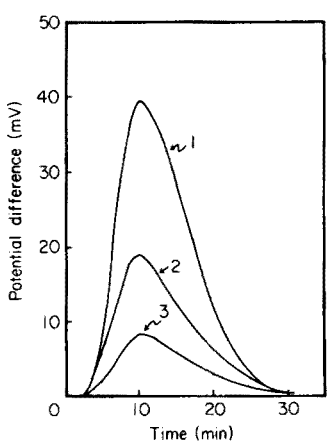


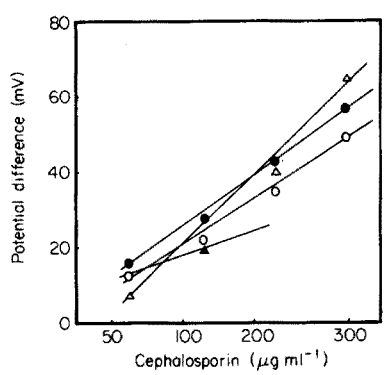


Fig. 2. Response curves for phenylacetyl-7ADCA under the standard conditions: (1) 250 $\mu g\ ml^{-1}$; (2) 125 $\mu g\ ml^{-1}$; (3) 62.5 $\mu g\ ml^{-1}$.

Fig. 3. Calibration curves: (△) Phenylacetyl-7ADCA; (▲) cephalosporin c; (○) CET; (●) CER.

TABLE 1

Determination of cephalosporin c in a fermentation broth

| Method | Broth volume ($\mu$l) | Concentration found (mg ml$^{-1}$) |
|---|---|---|
| Microbial sensor | 100 | 3.5[a] |
| H.p.l.c. | 5 | 3.8 |

[a]Potential difference 7.5 ± 0.7 mV ($n$ = 10).

The re-usability of the microbial sensor was examined with a solution containing 125 $\mu$g ml$^{-1}$ of phenylacetyl-7ADCA. The cephalosporin determination was carried out several times a day, and no change in the potential difference response was observed for a week.

The system was applied to the determination of cephalosporin c in a broth of *Cephalospolium acremonium*, and was compared with a method based on high-pressure liquid chromatography (h.p.l.c.) [9]. The results obtained are shown in Table 1. The relative error of the determination by the microbial system was 8%. Accordingly, the method is suitable for continuous analysis of fermentation broths.

REFERENCES

1 G. D. Darker, H. B. Brown, A. H. Free, B. Biro and J. T. Gooley, J. Am. Pharm. Assoc. Sci. Ed., 37 (1948) 156.
2 I. Karube, T. Matsunaga and S. Suzuki, J. Solid-Phase Biochem., 2 (1977) 97.
3 I. Karube, T. Matsunaga, S. Mitsuda and S. Suzuki, Biotechnol. Bioeng., 19 (1977) 1535.
4 I. Karube, S. Mitsuda, T. Matsunaga and S. Suzuki, J. Ferment. Technol., 55 (1977) 243.
5 T. Matsunaga, I. Karube and S. Suzuki, Anal. Chim. Acta, 99 (1978) 233.
6 I. Karube, S. Suzuki, S. Kinoshita and J. Mizuguchi, Ind. Eng. Chem. Prod. Res. Develop., 10 (1971) 160.
7 I. Satoh, I. Karube and S. Suzuki, J. Solid-Phase Biochem., 2 (1977) 1.
8 C. J. Perret, Nature, 174 (1954) 1012.
9 R. D. Miller and R. Neuss, J. Antibiot., 29 (1976) 902.

*Analytica Chimica Acta*, 105 (1979) 433—438


Short Communication

# MOLECULAR EMISSION CAVITY ANALYSIS
## Part 13. The Indirect Determination of Some Aliphatic Amines and Amino Acids

S. A. AL-TAMRAH, R. BELCHER**, S. L. BOGDANSKI, A. C. CALOKERINOS and ALAN TOWNSHEND*

*Chemistry Department, Birmingham University, P.O. Box 363, Birmingham B15 2TT (Gt. Britain)*

(Received 14th July 1978)

Many methods are used for the determination of amines and amino acids [1, 2]. One that is commonly applied for amines involves reaction with carbon disulphide with formation of a dithiocarbamate. The reaction of primary and secondary amines with carbon disulphide, initially studied by Hofmann [3], offers a means of distinguishing these compounds from tertiary amines, which do not react.

The general reaction for amines and amino acids with carbon disulphide is $R_1R_2NH + CS_2 \rightarrow R_1R_2NH—CSSH$. The reaction of secondary amines is faster than that of primary amines, unless the former are sterically hindered [4]. The mechanism of the reaction with amino acids has been investigated by Zahradnik [5, 6]. Dithiocarbamic acids are weak acids, are often unstable and are usually isolated as their alkali metal or ammonium salts.

In this communication, procedures are described for the determination of aliphatic amines and amino acids based on the formation of their dithiocarbamates, which are measured by the $S_2$ emission formed in a cavity in a hydrogen-based flame [7]. Because of the rapid reaction of secondary amines and some primary amines, the formation of the dithiocarbamates can be accomplished directly in the MECA cavity, thus providing a very rapid analytical procedure. Amino acids react much more slowly, so that the reaction has to be carried out in a separate reaction vessel; the dithiocarbamate produced is then measured by injection of the reaction solution into the cavity.

*Experimental*

*Apparatus.* The MECA instrument used was an adapted flame spectrometer, as described previously [7]. The cavities were those in the heads of stainless steel allen screws [7] pitched 7° downwards from the horizontal and placed

**Present address: Clinical Chemistry, Wolfson Research Laboratories, Birmingham University.

in the centre of the flame, 21 mm above the burner head. The slit width used was 0.91 mm (spectral bandwidth, 3 nm). Emission intensities were measured at 384 nm and recorded as a function of time on a Servoscribe 1S potentiometric recorder. Peak heights were used for quantitative measurements.

*Reagents.* All chemicals, reagents and solvents were of analytical reagent grade; 1000-ppm stock solutions in n-hexane and distilled water for amines and amino acids, respectively, were prepared. Working solutions were prepared daily by dilution with the corresponding solvent in dry glassware.

*Determination of amines.* Inject 5 $\mu$l of 6% (v/v) carbon disulphide in n-hexane into the cavity, immediately followed by 5 $\mu$l of a solution of amine (for concentration, see below) in n-hexane, and allow them to react at room temperature for exactly 1 min. Ignite the flame ($H_2$, 4.1 l $min^{-1}$ ; $N_2$, 6.5 l $min^{-1}$ ) and record the change in emission intensity at 384 nm with time. Switch off the flame after 25 s, and cool the cavity with a cold air blower before injecting the next sample.

*Determination of amino acids.* Mix the appropriate amount of amino acid (see below) dissolved in water with 0.1 ml of aqueous 0.1 M sodium hydroxide solution and 0.2 ml of 10% (v/v) carbon disulphide in acetone in a stoppered 10-ml volumetric flask. Dilute to the mark with water. Allow the solution to stand at room temperature for 3 h. Inject a 5-$\mu$l aliquot into the cavity, ignite the flame ($H_2$, 2.1 l $min^{-1}$; $N_2$, 6.3 l $min^{-1}$ ) after 1 min and proceed as for the determination of amines.

*Results and discussion*

*Amines.* When a 5-$\mu$l aliquot of the 6% carbon disulphide solution in n-hexane is injected into the cavity and the flame is ignited after 1 min, only a very weak $S_2$ emission occurs (Fig. 1d). The solvent and carbon disulphide have evaporated, leaving a slight non-volatile residue from the latter in the cavity. If, however, the same volume of an amine solution (e.g. 100 ppm diethylamine) is injected immediately after the carbon disulphide, ignition of the flame after 1 min gives a much more intense $S_2$ emission (Fig. 1e), owing to the formation of the dithiocarbamic acid. As any excess of carbon disulphide should have evaporated during the 1-min reaction period (apart from the small amount of non-volatile residue) the $S_2$ emission intensity should be an indirect measure of the amount of amine added to the cavity. Injection only of the solvent (Fig. 1b) or amine (Fig. 1c) shows no $S_2$ emission.

Variation of the flame gas flow rates showed that 4.1 l $H_2$ $min^{-1}$ and 6.5 l $N_2$ $min^{-1}$ gave the greatest emission intensity. Introduction of air into the flame greatly reduced the intensity, as noted previously [7], and the reproducibility became very poor. Leaving the cavity in the flame for 25 s ensured that the non-volatile matter deposited in the cavity was evaporated, leaving the cavity clean for the next experiment.

Initially, acetone was used as solvent but n-hexane proved to be better. Acetone appears to react with impurities (mainly sulphide and sulphite) in the carbon disulphide to form less volatile compounds, thus giving rise to a

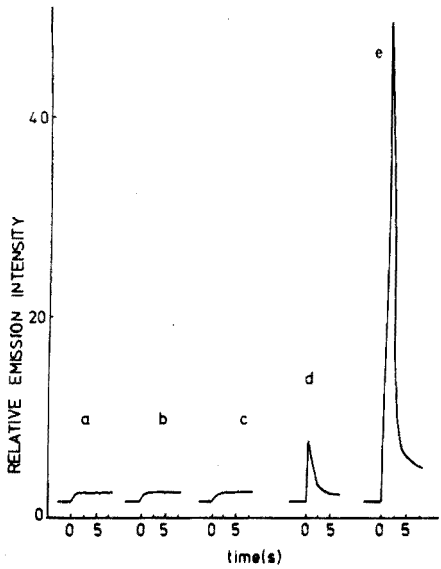


Fig. 1. $S_2$ emission intensities measured at 384 nm over the flame background (a) obtained by igniting the flame (4.1 l $H_2$ $min^{-1}$, 6.5 l $N_2$ $min^{-1}$) 1 min after injection of 5-$\mu$l aliquots of: (b) n-hexane; (c) 100 ppm diethylamine in n-hexane; (d) 6% (v/v) carbon disulphide in n-hexane (i.e. the blank); (e) 6% (v/v) carbon disulphide with 100 ppm of diethylamine, in n-hexane.

high blank. When analytical-grade carbon disulphide was used instead of general-reagent grade, a 90% reduction of the blank was observed. A further 50% reduction was obtained when n-hexane was used.

The time between injection of the two solutions into the cavity and ignition of the flame is the time allowed for the amine and carbon disulphide to react. During that period some of the carbon disulphide reacts with the amine and the remainder evaporates. The carbon disulphide must be in excess to ensure maximum dithiocarbamic acid formation. The effect of various concentrations (1—10%) of carbon disulphide in n-hexane on the emission intensity obtained from 100 ppm of diethylamine is shown in Fig. 2. At the lower carbon disulphide concentrations the emission is weak because there is inadequate carbon disulphide for the reaction to proceed significantly. Increased concentrations, however, cause a sharp rise in intensity, until above ca. 6% (v/v) carbon disulphide maximum intensity is achieved. Thus, a 6% (v/v) solution of carbon disulphide was used for the further studies with all amines.

The effect of evaporation time on the emission produced by the product of the reaction between 100 ppm of diethylamine and 6% (v/v) carbon disulphide was investigated. It was found that no further reaction occurs when more than 1 min has elapsed after injection of reactants. It was also found that evaporation of carbon disulphide is complete at 1 min, leaving only non-volatile impurities in the cavity.

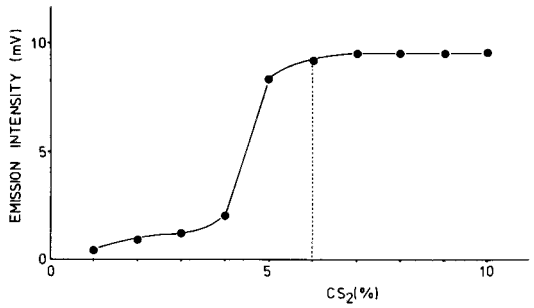


Fig. 2. Effect of carbon disulphide concentration on the $S_2$ emission intensity from the reaction product with 100 ppm of diethylamine.

The typical shape of the calibration curves obtained for amines is shown in Fig. 3 for diethylamine. At high amine concentrations, the curve bends, probably because there is insufficient carbon disulphide for complete reaction. The linear slope, reproducibility and limit of detection for various primary and secondary aliphatic amines are summarized in Table 1. The method described can be applied to various primary and secondary amines, but it is possible to determine significantly smaller amounts of diethylamine than of any other amine tested. The sensitivities (linear slopes) expressed in terms of moles were almost identical for the three secondary amines, however, and were greater than for the primary amines, which react an order of magnitude more slowly [4]. No interference was observed from triethylamine.

*Amino acids.* Unlike amines, amino acids need a long period (ca. 3 h) to react completely with carbon disulphide [8]. Therefore, an approach different from the in situ synthesis in the cavity was required. The amino acid was reacted with carbon disulphide in the presence of excess of sodium hydroxide

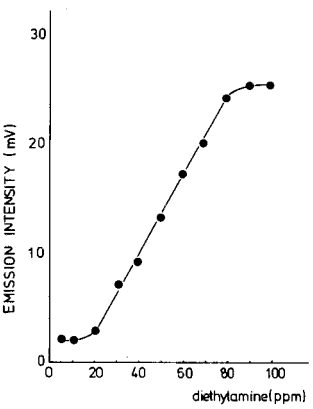


Fig. 3. Calibration curve for diethylamine.

TABLE 1

Determination of amines and amino acids

| Compound | Linear slope | | Linear range ($\mu$g) | Limit of detection[a] ($\mu$g) | Coefficient of variation[b] |
|---|---|---|---|---|---|
| | (mV ng$^{-1}$) | (mV nmol$^{-1}$) | | | |
| Diethylamine | 0.52 | 38 | 0.1—0.4 | 0.025 | 1.7 |
| Di-n-propylamine | 0.35 | 35 | 0.6—2.0 | 0.25 | 2.0 |
| Di-n-butylamine | 0.30 | 38 | 0.6—2.0 | 0.25 | 1.7 |
| n-Propylamine | 0.26 | 15 | 1.0—3.0 | 0.25 | 2.3 |
| n-Butylamine | 0.13 | 9 | 0.6—2.5 | 0.25 | 1.9 |
| Glycine | 0.15 | 11 | 0.01—0.3 | 3 | 2.8 |
| $\alpha$-Alanine | 0.14 | 13 | 0.05—0.5 | 3 | 2.2 |
| Serine | 0.56 | 59 | 0.008—0.024 | 2 | 1.3 |
| Threonine | 1.10 | 131 | 0.005—0.04 | 2 | 1.8 |

[a]Two standard deviations above the blank response.
[b]7 determinations of 1.5 $\mu$g amine except for diethylamine (0.4 $\mu$g); 10 determinations of 0.1 $\mu$g of glycine, 0.4 $\mu$g of $\alpha$-alanine and 0.02 $\mu$g of threonine, and 8 determinations of 0.008 $\mu$g of serine.

in a volumetric flask at room temperature. After completion of the reaction, 5-$\mu$l aliquots of the resulting solutions were injected into the cavity. Ignition of the flame immediately produced an $S_2$ emission profile with two peaks which were not well separated. The first peak ($t_m$ = 1 s) is due to the sulphur-containing impurities in carbon disulphide and the second ($t_m$ = 4 s) is due to the dithiocarbamate, delayed because it is present as the more stable sodium salt. Evaporation for 1 min in the cavity before ignition of the flame removed the first peak.

Glycine was used as a typical amino acid to optimize the flame gas flow rates. The recommended flows are 2.1 l $H_2$ min$^{-1}$ and 6.3 l $N_2$ min$^{-1}$. The effect of different concentrations of carbon disulphide added to a 50-ppm solution of glycine containing 0.1 ml of 0.1 M sodium hydroxide solution was also studied. Addition of $\geqslant$ 0.2 ml of 10% (v/v) carbon disulphide and dilution to 10 ml, thus giving a concentration of $\geqslant$ 0.2% (v/v) in the final reaction solution, is sufficient to give maximum $S_2$ emission intensity. This concentration was used for all subsequent measurements involving amino acids.

Sodium hydroxide must be present during the reaction to produce the sodium dithiocarbamate. The amount of sodium hydroxide for all subsequent studies of amino acids was the same as that used for the optimization of the carbon disulphide concentration, i.e. 0.1 ml of 0.1 M sodium hydroxide solution, to give a final concentration of $1 \times 10^{-3}$ M in the reaction solution.

The effect of reaction time at room temperature (20°C) was investigated for glycine. A reaction time of 3 h is necessary to give maximum emission intensity. This was used for all subsequent measurements with amino acids,

as it agrees with the values given in the literature [8]. The calibration curves, although of a similar general shape to those obtained for amines, were linear over reasonable concentration ranges (Table 1). Table 1 also gives information on sensitivities and detection limits.

*Discussion*

Comparison of the procedures for amines and amino acids shows that the external reaction procedure for amino acids has a sensitivity of the same order of magnitude as for amines. The method is rather more sensitive for serine and threonine than for any of the amines tested, but glycine and alanine show sensitivities very similar to those of the primary amines.

The in situ reaction for amines has the advantage of rapidity of analysis, but also brings disadvantages. The rapid evaporation of carbon disulphide requires its addition in large concentration. Thus the blank signal is much larger for the determination of amines than for amino acids, and the limits of detection and determination are much poorer for the amines. No doubt, application of the amino acid procedure to amines would remove these problems, but this would considerably lengthen the procedure.

A.C.C. and S.A. Al-T. acknowledge the Bodossaki Foundation, Athens, Greece and the University of Riyadh, Saudi Arabia, respectively, for financial support.

REFERENCES

1 S. Siggia (Ed.), Instrumental Methods of Organic Functional Group Analysis, Wiley Interscience, New York, 1972.
2 F. T. Weiss, Determination of Organic Compounds: Methods and Procedures, Wiley Interscience, New York, 1970.
3 A. W. Hofmann, Ber., 1 (1868) 169.
4 B. Phillip and H. Dautzenberg, Faserforschung und Textiltechnik, 19 (1968) 23; Chem. Abs., 68 (1968) 115580k.
5 R. Zahradnik, Chem. Listy, 49 (1955) 1002.
6 R. Zahradnik, Collect. Czech. Chem. Commun., 21 (1956) 447; 23 (1958) 1435, 1443, 1585.
7 R. Belcher, S. L. Bogdanski and A. Townshend, Anal. Chim. Acta, 67 (1973) 1.
8 J. Leonis, Compt-rend. Lab. Carlsberg, Ser. Chim., 26 (1947—9) 316.

*Analytica Chimica Acta*, 105 (1979) 439—443


Short Communication

# EXTRACTION-SPECTROPHOTOMETRIC DETERMINATION OF MICROGRAM QUANTITIES OF URANIUM WITH BENZOYLTRIFLUOROACETONE

S. F. MARSH

*Los Alamos Scientific Laboratory of the University of California, Los Alamos, New Mexico 87545 (U.S.A.)*

(Received 7th July 1978)

An automated spectrophotometer [1] previously developed at the Los Alamos Scientific Laboratory determines uranium or plutonium over the range 1—14 mg at a rate of one sample per 5 min by an extraction-spectrophotometric procedure [2] in which all operations of reagent additions, extraction of uranium or plutonium complexes into an organic phase, and absorbance measurements at the peak and valley are performed in a glass tube without transfers. Many nuclear scrap materials contain sub-milligram amounts of uranium with large amounts of extraneous elements. To determine the low uranium contents, a more sensitive extraction-spectrophotometric method, adaptable to the single-beam, single-tube operation of the instrument, was required.

In many spectrophotometric procedures for determining uranium, the absorbance measurement is made on the extracted uranium complex in the organic phase; however, these procedures often require multiple extractions and discards of specified phases [3—6]. Some [7—9] require a separation of the organic extract, then its incorporation into a buffered, aqueous-miscible single phase. A single extraction of the uranyl—methylene blue complex into methyl isobutyl ketone [10] extracts only 70% of the uranium. Single-extraction methods in which uranium is extracted as a mixed acetylacetone—pyridine complex [11] and as a thiothenoyltrifluoroacetone complex [12] offer molar absorptivities of only 1840 and 900, respectively. An apparently useful procedure [13] uses N-*m*-tolyl-*m*-nitrobenzohydroxamic acid which is not commercially available.

The most promising method, extraction of the uranyl—benzoyltrifluoroacetone (BTFA) complex [14], was selected for evaluation. Modifications have increased the extraction of uranium from <97% to >99%, increased the buffering capacity for acid, and improved greatly the tolerance for extraneous ions by incorporating an effective masking agent. The non-automated version of the method is presented.

## RESULTS AND DISCUSSION

Shigematsu et al. [14] extracted the uranyl—BTFA complex into butyl acetate. With $^{237}U$ tracer, the extraction of uranium was <97%; a level of 99% was desired to provide measurements reliable to within 1%. Various alternative solvents were evaluated, e.g. sec-butyl acetate, benzyl acetate, toluene, butyl propionate, isobutyl propionate, isobutyl isobutyrate, benzyl n-butyrate, pentyl hexanoate, isopentyl benzoate, and isopentyl hexanoate. The highest uranium extraction (99.3%) and the highest molar absorptivity ($1.26 \times 10^4$ l mol$^{-1}$ cm$^{-1}$ at 384 nm, relative to a reagent blank) were obtained with butyl propionate.

Uranium is extracted most efficiently in the pH range 5—6; however, many other metal ions are also extracted under the same conditions. Their interference can be prevented by masking with complexones such as ethylenediaminetetraacetic acid (EDTA), diethylenetriaminepentaacetic acid (DTPA), hydroxyethylethylenediaminetriacetic acid (HEDTA), and cyclohexanediaminetetraacetic acid (CDTA). In agreement with published data [15], CDTA formed very stable complexes with most potentially-interfering multivalent cations, whereas the stability constant of the uranyl complex was at least several orders of magnitude less than the constants for complexes formed with the other reagents. The complex formation of uranyl is further decreased by adding CDTA as its equimolar magnesium complex. Because the stability constant of Mg—CDTA is intermediate between those of uranyl—CDTA and the CDTA complexes of most multivalent cations, magnesium effectively holds CDTA in the presence of uranium while readily releasing it to cations that form stronger complexes.

For pH control, 5 ml of an aqueous buffer-masking solution of 2.15 M hexamethylenetetramine, 0.75 M triethanolamine, and 0.08 M Mg—CDTA provides an optimum pH of 5.6—5.7 for color development with a sample containing 3 meq of acid. To optimize the reliability of this method, the pH of samples is adjusted to this range, if necessary.

The extracted uranyl—BTFA complex in butyl propionate has a broad absorbance spectrum that peaks near 375 nm, as measured on a Heath/McPherson recording spectrophotometer with a reference of BTFA in butyl propionate (Fig. 1). Because the 375-nm peak is not completely separated from the absorbance tail of the BTFA reagent, measurement at 384 nm was selected. Absorbance was also measured at 400 nm as a base-line correction. The difference of the absorbances at these two wavelengths is used as the measure of uranium; this provides higher reproducibility than the conventional technique with a single measurement at or near the peak, relative to a reagent blank.

The recommended procedure (see below) provides an essentially linear relationship between absorbance and uranium content in the range 5—85 $\mu$g. A linear least-squares fit of 36 measurements covering this range gave a correlation coefficient of 0.9998 and a relative standard deviation of the

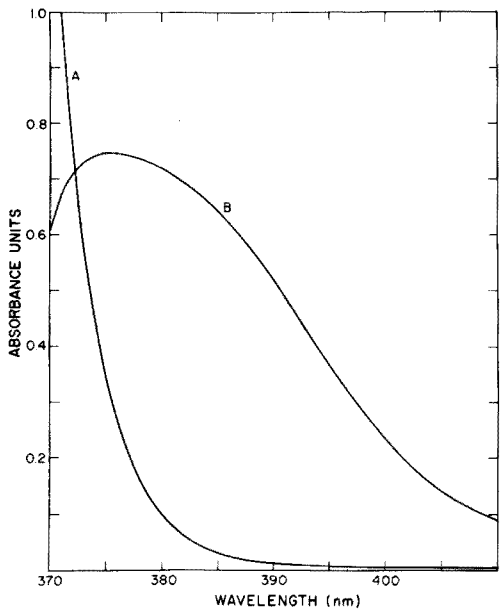


**Fig. 1. Absorbance spectra of (A) BTFA—butyl propionate reagent blank; (B) 48 μg of U as the extracted BTFA complex relative to a reagent blank.**

residual about the regression line of 0.70%. A third-order polynomial fit of 66 measurements covering the range 5–140 μg of uranium gave a correlation coefficient of 0.9998. For most applications, however, the linear range 5–85 μg of uranium is recommended for convenience. The relative standard deviations for a single measurement of uranium (calculated from 6 replicates at each level) were 2.9, 2.0, 1.1, 0.4, 0.3 and 0.2% for 5, 10, 19, 48, 66 and 85 μg of uranium, respectively.

Because many cations form extractable chloride complexes, the aqueous buffering and masking solution is prepared with magnesium nitrate, and the pH is adjusted initially with nitric acid. In the detailed evaluation of tolerances of metal ions (Table 1), nitrate salts were added where feasible. The tolerance for metal ions that form extractable halide complexes, while not evaluated, could be less. The tolerance for non-metal ions is also summarized in Table 1. Each diverse ion was added to 0.20 μmol (48 μg) of uranium, starting at a molar ratio of 1000:1. If a change significant at the 95% confidence level, relative to uranium alone, was obtained, the ion was retested at sequentially lower molar ratios. The tolerance of the method for the metal and nonmetal ions usually present in nuclear fuel cycle materials is excellent.

## *Experimental*

*Aqueous buffering and masking solution.* Dissolve 41.0 g of $Mg(NO_3)_2 \cdot 6H_2O$, 58.3 g of cyclohexanediaminetetraacetic acid, 613 g of hexamethylene-

TABLE 1

Tolerances (mole ratios) of metals and non-metals

| 1000:1 | | 100:1 | | 10:1 | | 1:1 |
|---|---|---|---|---|---|---|
| Ag | K | B | Mn(II) | Al | Mn(VII) | Ce(IV) |
| Cd | La | Ba | Ni | Au | Mo | Pd |
| Cs | Mg | Bi | Pb | Be | Pt | Sn |
| Cu | Na | Ca | Rb | Ce(III) | Ru | Te |
| Ge | Y | Co | Sr | Cr(III) | Sb | Ti |
| Hg | Nitrate | Fe | Sc | Cr(VI) | Se | V |
| Acetate | Perchlorate | Ga | Th | Hf | Zr | Phosphate |
| Bromide | Sulfide | | | Oxalate | | |
| Bromate | Sulfite | In | Tl | | | |
| Chloride | Sulfate | Li | Zn | | | |
| Iodate | Sulfamate | | | | | |
| Nitrite | Thiocyanate | EDTA | | | | |
| | | Fluoride | | | | |
| | | Iodide | | | | |

tetramine, and 200 ml of triethanolamine in distilled water. Dilute to ca. 1.9 l. Adjust to pH 7.50 with 15.7 M $HNO_3$. Allow the solution to cool to room temperature before making the final pH adjustment. Dilute to 2 l with water.

*BTFA—Butyl propionate solution.* Dissolve 3 g of benzoyltrifluoroacetone in butyl propionate. Dilute to a final volume of 1 l with butyl propionate.

*Recommended procedure*

Add not more than 2 ml of sample to 5 ml of buffering and masking solution in a 16 × 125-mm test tube. Adjust, if necessary, to pH 5.6—5.7 with appropriate solutions of $HNO_3$ or NaOH. Add water to a final aqueous volume of 8 ml. Add 3.00 ml of BTFA—butyl propionate solution. Insert a tapered hollow polyethylene stopper firmly and wrap with 1-in. wide masking tape to hold the stopper in place. Transfer the sealed test tube to an inversion mixer; extract for 10 min at about 36—48 rpm. Centrifuge to ensure complete phase separation. Transfer ca. 2.5 ml of the organic (upper) phase to a 10-mm path cuvette with a Teflon cover to prevent evaporation.

Measure the absorbance of the sample at 384 nm and 400 nm. (This makes the use of a reference cell unnecessary; however, BTFA—butyl propionate, used as a reference, will reduce the absolute absorbance value at each wavelength, if desired). Subtract the absorbance at 400 nm from that at 384 nm. Calculate the uranium content from a standard curve prepared with known amounts of uranium extracted and measured in an identical manner.

The assistance of M. R. Ortiz, N. M. Saponara, and F. R. Roensch with measurements, including diverse ion effects, is gratefully acknowledged. D. D. Jackson and R. M. Hollen, who investigated the adaptation of this method to the LASL Automated Spectrophotometer, suggested the two-

wavelength technique. The consultation of J. E. Rein during the course of this investigation is appreciated. This work was sponsored by the U.S. Department of Energy, Division of Safeguards and Security.

REFERENCES

1 D. D. Jackson, D. J. Hodgkins, R. M. Hollen and J. E. Rein, Los Alamos Scientific Laboratory report LA-6091 (February, 1976).
2 W. J. Maeck, M. E. Kussy, G. L. Booman and J. E. Rein, Anal. Chem., 31 (1959) 1130; 33 (1961) 998.
3 E. W. Baumann, Savannah River Laboratory report DP-1458 (May, 1977).
4 W. I. Winters, Atlantic Richfield Hanford ARH-ST-116 (May, 1975), and ARH-SA-250 (June, 1976).
5 S. C. Dubey and T. K. S. Murthy, Bhabha Atomic Research Centre (India) BARC-705 (1973).
6 P. N. Palei, A. A. Nemodruk and A. V. Davydov, Radiokhimiya, 3 (1961) 181 (English translation).
7 T. W. Steele, C. D. Summerson, and H. Stock, National Institute for Metallurgy (South Africa), NIM-906 (January, 1970).
8 K. Sekine, Mikrochim. Acta, (1976) 559.
9 J. Adam and R. Pribil, Collect. Czech. Chem. Commun., 37 (1972) 129.
10 S. C. Dubey, D. V. Jayawant and T. K. S. Murthy, Bhabha Atomic Research Centre (India) BARC-815 (1975).
11 V. M. Shinde, Chem. Anal. (Warsaw), 21 (1976) 813.
12 K. R. Solanke and S. M. Khopkar, Chem. Anal. (Warsaw), 17 (1972) 1175.
13 Y. K. Agrawal, Ann. Chim. (Rome), 66 (1976) 371.
14 T. Shigematsu, M. Tabushi and M. Matsui, Bull. Chem. Soc. Jpn., 37 (1964) 133.
15 A. Ringbom, Complexation in Analytical Chemistry, Interscience-Wiley, New York, 1963, pp. 332—333.

*Analytica Chimica Acta*, 105 (1979) 445—449


Short Communication

# SEMI-AUTOMATIC DIGESTION AND AUTOMATIC ANALYSIS FOR SELENIUM IN ANIMAL FEEDS

F. J. SZYDLOWSKI* and D. L. DUNMIRE

*Raltech Scientific Services, Ralston Purina Company, 900 Checkerboard Square, St. Louis, Missouri 63188 (U.S.A.)*

(Received 17th July 1978)

Large numbers of selenium-fortified feed samples and selenium-containing premix (concentrates) samples, in addition to plant materials and biological tissues containing natural selenium levels, have to be analyzed routinely in this laboratory. The manual AOAC [1] method is lengthy and prone to contamination problems; where the selenium levels are completely unknown, repeats are often required to yield on-curve responses. An automatic method has been sought for some time, and a semi-automatic atomic absorption spectrometric method has been used [2]. With some modifications to suit sample requirements, the method described by Brown and Watkinson [3] has enabled sample analysis time to be reduced considerably.

The digestion of the samples was the lengthiest part of the assay, and a block digestion set-up similar to that used by Chan [4] was considered. The use of a Technicon BD-20 heating unit offered some advantages over the Chan-type block, however, and was preferred. Modifications of the digestor were necessary to handle the perchloric acid fumes safely.

## *Experimental*

*Apparatus.* A Technicon fluoronephelometer equipped with heating bath (II-G, coil 37°C), proportioning pump, sampler IV, strip-chart recorder, 556-nm sharp cutoff filter and 325-nm narrow-pass filter, was used for all automated fluorescence measurements. A Perkin-Elmer Model 203 fluorescence spectrophotometer was used for all manual measurements. The block temperatures of the Technicon BD-20 heating unit (modified) with BD-20/40 control unit used for all sample digestions were monitored with a SI Digital Pyrometer.

Kjeldahl flasks (30 ml) were calibrated and marked at a volume of 35 ml. A Sensorex minimicro-electrode was used for all pH adjustments with a standard pH meter.

*Reagents.* Working standards were prepared from selenium certified atomic absorption standard (1000 $\mu$g Se $ml^{-1}$; Fisher Scientific Co.) fresh with each run by dilution of the concentrate with milli-Q purified water (Millipore Corp).

2,3-Naphthalenediamine (DAN; J. T. Baker) proved suitable, and a 0.5%

(w/v) solution was made up with 0.1 M HCl. Redistilled nitric acid (G. F. Smith and reagent-grade perchloric acid were used for sample digestions. Reagent-grade cyclohexane, hydrochloric acid, disodium ethylenediaminetetraacetate and ammonium hydroxide were used.

*Procedure.* Weigh ca. 0.5 g of sample into an acid-cleaned 30-ml micro Kjeldahl flask (calibrated to 35 ml). Use ca. 1 ml of water to wash down the wall of the flask. Add 10 ml of nitric acid (when excessive foaming is anticipated, e.g. with soy isolates, use 15 ml of (1 + 1) $HNO_3$, reduce the volume to ca. 5 ml by heating, add 5 ml of nitric acid, and then proceed as usual). Place the flasks in the cool digestor. Set the control unit temperature to 70°C, initiate the automatic cycle and set the low temperature timer to 2 h. Set the high temperature timer to 110°C for 4 h (actually 2 h at high temperature). Put the fume ducts in place and turn on the water aspirator. After 4 h, add 2 ml of perchloric acid and revise the temperature settings to 175°C (low) for 4 h and subsequently to 195°C (high) for 6 h (2 h actual) for an overnight digestion. (Note that the hood and water aspirator must be left on.) Take to fumes of perchloric acid at a setting of 230°C, remove and cool. Add 1 ml of water to each flask and fume at 230°C for 1 h. Remove the flasks from the block, cool and add 2 ml of 1 M hydrochloric acid. Place the flasks in a boiling water bath for 15 min. Adjust the pH to ca 1.8 with ammonia solution or 1 M hydrochloric acid as needed and bring to volume with water (35 ml). Place the samples in Technicon sample cups and run on the Technicon fluoronephelometer system (see below) against standards (0—30 ng Se $ml^{-1}$). Adjust the baseline and standard calibration to yield maximum peak height. Measure the peak heights (mm) and calculate concentrations from a standard curve. Dilute samples as needed to yield an on-curve response, making sure that the final dilutions are at about pH 1.8.

*Block digestor modifications.* Since 20 samples were to be digested at a time, each containing perchloric and other concentrated acids, a fume duct was needed to remove the acid fumes and rinse them down the drain, particularly in view of the safety precautions for the handling of perchloric acid [5]. Five fume ducts (4-hole) were made to fit directly over the holes in the aluminum block portion of the digestor. The tapered end connectors then were coupled by means of Tygon tubing to a fume duct collector which in turn was connected to a water aspirator.

Block temperatures were continously monitored and in all cases agreed with the calibration dial on the control unit to within 2°C.

*AutoAnalyzer manifold (Fig. 1).* There were several modifications to the manifold used by Brown and Watkinson [3]. In addition to the different detector, a 30-turn mixing coil was used before the phase separator to increase the percentage extraction, and a 5-turn mixing coil was placed after the phase separator to smooth out baseline fluctuations. As a result, a variable 40-cam was used in which the wash time was increased. A standard Technicon flow cell was used in place of the modified cell and the temperature bath was held at 37°C; these components were conveniently available through the

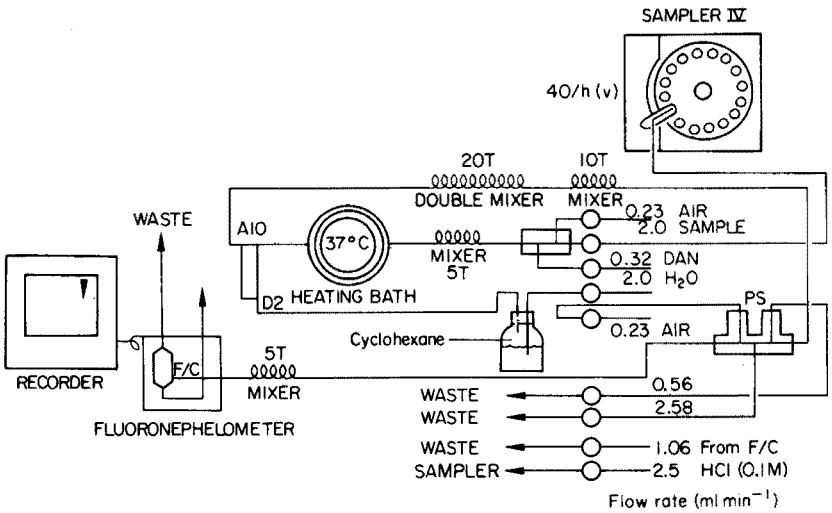


Fig. 1. AutoAnalyzer manifold.

manufacturer. A 1-l water-cyclohexane displacement bottle was used to eliminate cyclohexane attack on the Solvaflex pump tubing. Since water was then being pumped through the pump tubing, SMA type tubing could be used.

A black rubber sleeve was placed over the polyethylene tubing leading to the flow cell, because the baseline noise was increased by exposure to fluores-

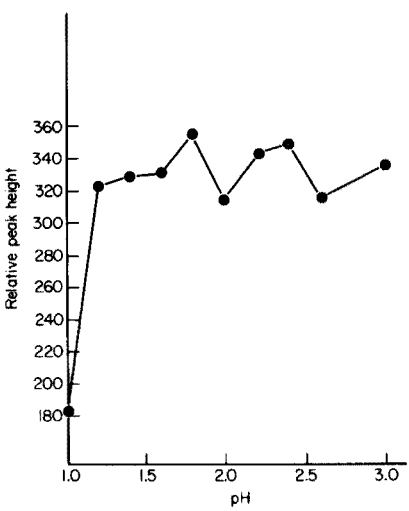


Fig. 2. Plot of Bovine Liver results as a function of pH.

cent lighting. The clear plastic cover of the manifold cartridge had been painted opaque from the start.

*Results and discussion*

The precision and accuracy obtainable with this semi-automatic system were tested by analyzing NBS SRM 1577 Bovine Liver (certified value 1100 ± 100 ng Se $g^{-1}$); 8 analyses gave a mean result of 1053 ng Se $g^{-1}$ (range 963—1100) with $s$ = 51.3 ng $g^{-1}$ and $s_r$ = 4.87%. Better precision was obtained when the same samples and standards were run through the system a second time. This presumably had to do with the stability of the system; the baseline drift was more significant on the first than on the second run, and was further minimized by using a longer wash between samples.

TABLE I

Comparison of automatic vs. manual fluorimetric selenium methods

| | Automatic ($\mu g\ g^{-1}$) | | Manual ($\mu g\ g^{-1}$) | |
|---|---|---|---|---|
| Sample | A | B | A | B |
| Bovine Liver | 1.08 | 1.12 | 1.10 ± 0.10 | (cert.) |
| High moisture corn | 0.03 | 0.04 | 0.06 | 0.03 |
| Haylage A | 0.06 | 0.07 | 0.07 | 0.15 |
| Haylage B | 0.09 | 0.09 | 0.07 | 0.11 |
| Haylage C | 0.06 | 0.06 | 0.07 | — |
| Pet food A | 0.45 | 0.45 | 0.59 | 0.43 |
| Pet food B | 0.46 | 0.45 | 0.38 | — |
| Pet food C | 0.30 | 0.24 | 0.36 | — |
| Pet food D | 0.42 | 0.40 | 0.38 | — |
| Protein product A | 0.17 | 0.15 | 0.19 | — |
| Protein product B | 0.15 | 0.14 | 0.19 | 0.15 |
| Protein product C | 0.60 | 0.57 | 0.68 | — |
| Protein product D | 0.08 | 0.08 | 0.15 | 0.12 |
| Protein product E | 0.15 | 0.13 | 0.20 | 0.18 |
| Fish and shrimp | 0.60 | 0.61 | 0.46 | 0.55 |
| Dog food (dry) | 0.43 | 0.40 | 0.57 | 0.40 |
| Dog food (dry) | 0.37 | 0.37 | 0.38 | 0.57 |
| Dog food (moist) | 0.40 | 0.37 | 0.34 | — |
| Farm Cust. | 0.94 | 1.07 | 1.06 | 1.02 |
| Food spl. | 0.14 | 0.15 | 0.20 | — |
| Rodent diet A | 0.16 | 0.15 | 0.18 | 0.14 |
| Rodent diet B | 0.09 | — | 0.14 | — |
| Rodent diet C | 0.14 | — | 0.15 | — |
| Rodent diet D | 0.32 | — | 0.40 | — |
| Premix A | 88.8 | 90.2 | 89.2 | — |
| Premix B | 81.3 | 84.1 | 83.5 | — |
| Premix C | 183.0 | 180.0 | 158.0 | — |
| Premix D | 201.0 | 200.0 | 189.0 | — |
| Premix E | 74.8 | 75.1 | 91.0 | — |
| Premix F | 150.0 | — | 160.0 | — |

Table 1 shows the results obtained by the proposed method on a wide diversity of matrices. A comparison of the manual versus the proposed automatic method by analysis of variance showed no significant difference ($p$ = 0.10) between the means. With a two-way analysis of variance (method and sample) the correlation coefficients were as follows: automatic run A vs. manual run A, 0.994; automatic run B vs. manual run A, 0.996; automatic run A vs. automatic run B, 0.999. The relative standard deviation of the automatic method was 2.2% for the same samples on two different days. The results listed for the manual method in Table I were obtained by the standard AOAC procedure [1] with modifications as described by Haddad and Smyth [6]; results shown under manual in column B are repeats where a large variance from the automatic result was first obtained. In most cases this rerun brought the mean of the manual values closer to the mean of the automatic values for the same samples.

Michie et al. [7] recently reported a more stable response in the pH range 2.0—3.5. This is contrary to the normally accepted optimum pH range of 1—2 [1—3, 6,8 ] and borders the pH optimum of 2.0 [8] for complex formation with DAN. However, the DAN reagent of Michie et al. was prepared in a more acidic environment (pH ca. 0.30) and a higher sample pH range may therefore have been necessary to obtain the optimum final pH. A strongly acidic (ca. 0.13 M HCl) solution has been reported [9] to yield a more stable DAN reagent and 0.1 M HCl has been listed as yielding maximum fluorescence [10]. A study of the optimum pH range gave the results shown in Fig. 2: from about pH 1.2 to 3.0, there is only a small difference with a maximum value occurring at pH 1.8. The smoothing of the response as a function of pH does not appear above 2.2, as described by Michie [11].

The authors express their gratitude to John Ban for assistance in setting up the automatic method and to Karen Kimball for the manual analyses of the samples.

REFERENCES

1 Official Methods of Analysis of the A.O.A.C. 3.073—3.078, 12 edn., Washington, D.C., 1975, p. 45.
2 F. J. Szydlowski, At. Absorpt. Newsl., 16, (1977) 60.
3 M. W. Brown and J. H. Watkinson, Anal. Chim. Acta, 89 (1977) 29.
4 C. C. Y. Chan, Anal. Chim. Acta, 82 (1976) 213.
5 Guide for Safety in the Chemical Laboratory, 2nd edn., Van Nostrand, N.Y., 1972, p. 194.
6 P. R. Haddad and L. E. Smyth, Talanta, 21 (1974) 859.
7 N. D. Michie, E. J. Dixon and N. G. Bunton, J. Assoc. Off. Anal. Chem., 61 (1978) 48.
8 P. F. Lott, P. Cukor, G. Moriber and J. Solga, Anal. Chem., 35 (1963) 1159.
9 J. B. Wilkie and M. Yound, J. Agric. Food Chem., 18 (1970) 944.
10 C. A. Parker and L. G. Harvey, Analyst, 87 (1962) 558.
11 N. D. Michie, personal communication.

*Analytica Chimica Acta*, 105 (1979) 451—454


Short Communication

# NEW PHASE-SEPARATING DEVICE AND OTHER IMPROVEMENTS IN THE SEMI-AUTOMATED FLUORIMETRIC DETERMINATION OF SELENIUM

J. H. WATKINSON* and M. W. BROWN

*Ministry of Agriculture and Fisheries, Soil and Field Research Organisation, Ruakura Agricultural Research Centre, Hamilton (New Zealand)*

(Received 2nd August 1978)

The earlier method [1] for measuring nanogram quantities of selenium has been improved in several respects. A new and more efficient method of separating the cyclohexane extract of the 4,5-benzopiazselenol from the aqueous phase, prior to measuring its fluorescence, improves the sensitivity and resolution, but more particularly the reliability of phase separation. The phase-separating device can also be used to separate other solvents from water. The most frequent cause of breakdown during the semi-automated analysis of many thousands of samples over about three years has been the occasional passage of aqueous phase through the Technicon 5-point phase separator, resulting in spuriously high fluorescence readings. The improved system breaks down only when the pump tubing deteriorates, which causes marked changes in flow through the separator. The reaction time, and the time to reach the operating temperature have been decreased by replacing two reaction coils at 40°C with one at 50°C, and by substituting a much smaller heating unit for a conventional water bath. In addition, the precision at low concentration (1 ng $ml^{-1}$) has been improved by placing an integrating circuit across the recorder input.

*Apparatus*

The major items of equipment are described previously [1], except that the water bath is replaced with a Technicon heating bath cartridge "L" coil (volume 7 ml), which takes a much shorter time to heat from ambient temperature. The heating unit is fitted into a Technicon analytical module provided with a red perspex cover especially made to screen the glass tubing containing aqueous 2,3-diaminonaphthalene (DAN) from u.v. light.

The Sampler IV probe was modified in two ways: a platinum nipple (Technicon part N13) was sealed into the top part of the Pyrex glass probe to provide a direct connection to the polythene tubing linking it to the pump tube (the previous butt joint occasionally resulted in blockages); this permitted the use of a thicker glass wall for the probe to make it more robust and eliminate whip during probe movement.

An RC integrating circuit having a 4.7-s time constant was placed across the recorder input to smooth out the more rapid variations in the fluorimeter signal, which had a peak-to-trough time of 45 s (40 samples $h^{-1}$). At low concentrations the peak values were easier to read, and at 1 ng Se $ml^{-1}$ the standard error was halved.

*Manifold design*

The flow diagram is detailed in Fig. 1. The main differences from the original method are the method of phase separation and the use of only one 7-ml reaction coil at 50°C.

*Phase separation.* With the standard Technicon 5-point phase separator in the system, a small amount of aqueous phase can readily pass into the cyclohexane stream unless stringent precautions are observed. Imperfect separation can be caused by a variety of circumstances, e.g. a chemically-unclean glass surface in the separator, uneven distribution of cyclohexane and/or air in the stream, and alteration in the relative flow rates from the separator because of differential wear of the respective pump tubes. These factors are far less critical if the standard Technicon T-connector, type A2, is used as a phase separator (Fig. 2). Teflon is used as before to cause the cyclohexane globules to coalesce into a continuous stream, but there are two important differences: the liquids are separated in opposite vertical directions to exploit their difference in density; the existing air bubble for segmentation is retained to maintain segmentation as it passes into the separated cyclohexane stream.

There are two important features associated with the use of the T-connector as a phase separator. First, in the absence of the capillary in the lower arm (Fig. 2), a tongue of cyclohexane builds up in cycles. Since the air bubbles cannot segment the solvent stream in the tongue, there is partial intermixing with corresponding loss of resolution. The accelerated flow of liquid into the throat of the capillary breaks up the lower part of the tongue of cyclo-

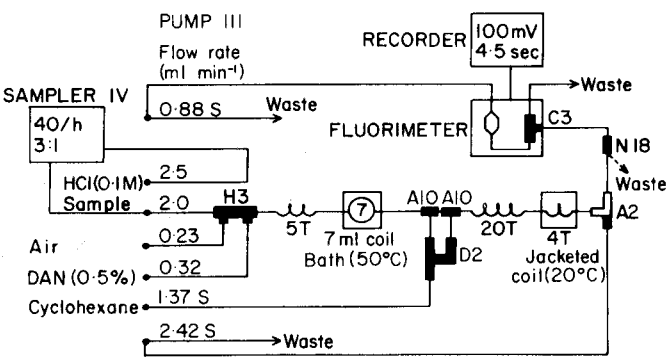


Fig. 1. AutoAnalyzer flow diagram. S after flow rate indicates solvaflex tubing. Transmission lines from sampler probe to pump, and separator to fluorimeter are polythene (i.d. 0.03 in.). All other transmission lines are glass protected from u.v. light.

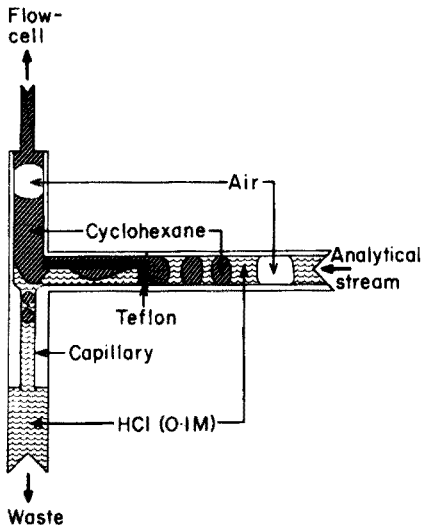


Fig. 2. Phase separation with the Technicon A2 T-connector.

hexane into globules, which are pumped to waste, and so segmentation is maintained (Fig. 2). Secondly, the water vapour in the segmenting air bubble increases on passing through the bath at 50°C and condenses in the 4-turn jacketed cooling coil immediately preceding the phase separator. In the absence of the cooling coil much of the water vapour in the bubbles condenses in the separated cyclohexane stream, and some water is eventually carried into the flow cell.

There are a number of advantages in using the A2 connector as a phase separator: (a) it separates very efficiently without special precautions, so that less cyclohexane is run to waste, a smaller amount of solvent is required, and the greater concentration in the solvent correspondingly increases the sensitivity; (b) the phases separate under more stable conditions in the absence of the sequential removal and injection of bubbles of the standard separator; (c) the wash characteristics are improved, probably because of less intermixing between segments than occurs with the Technicon separator; (d) it is much cheaper than the standard separator. The A2 connector would probably work equally well for all the four combinations of solvent/aqueous phase separations—solvent less or more dense than water, and solvent or aqueous phase required. The standard Technicon methods require, in contrast, four different modes of operation with two glass pieces plus Teflon inserts. Where the heavier solvent is separated a second air bubble would need to be injected. Toluene, which has a density closer to water than that of cyclohexane, and carbon tetrachloride were both separated efficiently from water with the A2 connector as separator. A more polar solvent, amyl acetate, did not separate as cleanly, but n-butanol has been separated successfully in a routine method for alkaline phosphatase [3].

*Reaction temperature.* The preparation of a purer DAN reagent solution, and more stringent exclusion of u.v. light, gave a baseline at 50°C from the 0.5% DAN solution equivalent to 0.1 ng Se $ml^{-1}$ compared with the previous value of 0.5 ng $ml^{-1}$. This permitted the use of only one 7-ml reaction coil, thus almost halving the previous transit time at 40°C.

*2,3-Diaminonaphthalene dihydrochloride in 0.1 M HCl (0.5% w/v).* The reagent is kept in a 2.5-l brown bottle under a layer of 10% n-hexane in cyclohexane, and stored in a refrigerator. It is partly re-purified just before use by mixing the two phases together. There is no deterioration in the reagent (e.g., by deposition of the DAN polymer) after storage for several months at low temperature in the dark. The hydrochloride does not dissolve readily so it is ground as a paste initially.

Recrystallisation of technical-grade DAN is carried out under tungsten light by dissolving it in hot 0.1 M HCl, adding activated charcoal plus a little sulphite [2], and filtering. The filtrate is rapidly cooled and crystals form on adding an equal volume of concentrated hydrochloric acid. Improperly purified DAN can cause unexpected problems; one batch gave normal blank, standard, and serum values, but for whole blood the values were erroneously high. There was some evidence that iron was involved.

The authors are grateful to Miriam T. Wingerden and C. J. Clark for analytical assistance.

REFERENCES

1 M. W. Brown and J. H. Watkinson, Anal. Chim. Acta, 89 (1977) 29.
2 J. H. Watkinson, Anal. Chem., 38 (1966) 92.
3 D. C. Woollard, Auckland Regional Dairy Laboratory, NZ Ministry of Agriculture and Fisheries, private communication, 1978.

*Analytica Chimica Acta*, 105 (1979) 455—464


## Book Reviews

E. L. Wehry (Ed.), *Modern Fluorescence Spectroscopy*, Plenum Press, New York, 1976, Vol. 1: xvi + 238 pp., price $20.40; Vol. 2: xx + 459 pp., price $35.40.

Fluorescence in the u.v.-visible region "after a rather lengthy gestation period", to quote Dr. Wehry, is now widely used in analysis, especially in the medical, biological and environmental areas. Such widespread usage is borne out by the coverage of the two volumes of the present book, ranging from laser-excited fluorescence in air pollution monitoring to fluorescent probing of biological membranes, micelles, and enzyme- and protein-binding sites, and from the study of excited-state molecules and complexes to quantitative analysis of clinical and biological samples. Developments in technology are also well covered, with chapters on computerization of fluorescence measurements, digital and analog measurements, modulation and derivative techniques, dye lasers, internal reflection techniques, and applications involving centrifugal fast analysers. In addition, chemiluminescence measurements in air and water pollution monitoring are dealt with in individual chapters, and many other sections often discuss chemiluminescence.

The editor has succeeded in what is usually a difficult task, in amalgamating the contributions of a number of authors into a coherent account of recent developments in technique and applications. There is occasional overlap in discussion of basic concepts, but this contributes to the smooth progress of the text and would be difficult to avoid. The topics covered are dealt with in a readable, informative manner, and will be of interest to most analytical chemists, irrespective of their specialization. The book itself is well produced and illustrated; very few printing errors were detected. Each volume has an author and subject index.

A. Townshend

Dag T. Gjessing, *Remote Surveillance by Electromagnetic Waves for Air, Water and Land*, Ann Arbor Science, Mich., U.S.A., 1978, viii + 152 pp., price $27.50.

To analyse and monitor situations and events at a distance has long been the prerogative of the astronomer. Only recently has the considerable development in transmitting and monitoring electromagnetic radiation that has occurred in the last 20 years been applied to remote sensing of our own planet. Because of the nature of Earth's atmosphere, the radiation used is restricted to that with wavelengths in the near ultra-violet or longer, but this provides a wide scope of analytical possibilities ranging from the detection of particulate

matter, measurement of waves on the sea, and determination of wind speed, to determinations of individual air pollutants, oil film thickness and rock type.

Information on the techniques used for these measurements and on the determinations which have been carried out, has been difficult to glean from the literature. Thus the present book provides a welcome source of such information, in a very straightforward, clearly-illustrated manner. After a very brief discussion of the origins of the various spectra and spectral ranges that are amenable to remote-sensing applications, a mathematical explanation is given of reflection and scattering effects, and of range limitations. The chapter on the design of optimum systems is particularly interesting, especially with respect to the use of correlation processes for extracting the required signals from complex responses. The book concludes with descriptions of a large number of selected environmental surveillance investigations and techniques in course of development, a valuable adjunct when published work is relatively rare.

The appearance of this book is timely. It provides a fairly clear account of the current status of remote-sensing. In doing so, it emphasises potential rather than achievement, as far as chemical monitoring is concerned. Far more progress seems to have been achieved in aspects of meteorology such as flow and temperature monitoring, which is reflected in the amount of space devoted to such aspects. Nevertheless, the potential exists, and perhaps this small book will inspire its conversion into achievement.

A. Townshend

G. Svehla, *Automatic Potentiometric Titrations*, Pergamon Press, Oxford, 1978, x + 219 pp., price $29.50, £16.50.

Potentiometric titrations done manually are atrociously time-consuming and wearisome. Thus academic rather than applied chemists have bemoaned the fact that Kolthoff and Furman's classic text on these titrations went out of print many years ago. Since automatic titrators removed the slave labour involved in the manual method and the range of potentiometric titrations was extended by ion-selective electrodes, the interest of both applied and academic chemists in potentiometric titrations has revived increasingly over the past 10—15 years. Yet, despite numerous original papers, reviews and textbook chapters, there has been no specific text to which seekers of detailed information could be directed. Accordingly, this book, which is the 60th volume of the Belcher—Freiser series of monographs, fills a definite gap in the analytical literature. In writing about automatic potentiometric titrations, Dr. Svehla could have selected to concentrate on instrumentation; instead, the emphasis of this book is wisely placed on general and theoretical aspects. Starting from the e.m.f. of galvanic cells and the Nernst equation, the reader is led quite firmly through the formalities of the different kinds of

electrode; here the reviewer must take issue with the author — the suggestion of ion-*specific* electrodes is reminiscent of Lundell's idea of the analyst's heaven; one reagent (or electrode) specific for each element. Thereafter, Butler's concept of sharpness index, and acid—base, precipitation, compleximetric and redox titrations are discussed theoretically. The measurement of electrode potentials and the components of automatic titrimeters are then described.

Possibly the most interesting chapter is that on the evaluation of results, where the various methods that have been suggested can be compared; as Dr. Svehla suggests, consultation of the original literature can indeed be amusing. Amusement apart, a proper general understanding of the basics of potentiometric titrations becomes of essential importance as microprocessors take over the wearisome aspects of plotting and interpretation. And here is a text which can be confidently recommended to seekers of detailed information on potentiometric titrations, whether manual or automatic.

A. M. G. Macdonald

D. Midgley and K. Torrance, *Potentiometric Water Analysis*, Wiley-Interscience, Chichester, 1978, xi + 409 pp., price £16.50, $36.50.

The aim of this book is not stated explicitly but it is essentially a practical handbook. In the first part of the text, enough theoretical and technical background material is described for practical analysts. Thus, the first 80 pages are basically a sharp trot through the conventional material on electrodes, meters, monitors, flow cells, autotitrators, essential statistics, and calibration plots. The following 20 pages cover potentiometric titrations including standard addition and subtraction methods; then about 30 pages are devoted to general practical aspects of potentiometry. There are some duplications, some contradictions, and too many printing errors, but overall Part I is a sensible exposition of the essentials for practical work. Part II, the bulk of the book, contains all working details for about thirty procedures from pH measurements through water hardness to aluminium, cyanide and perchlorate. Gas sensors are included; enzyme electrodes are not. Despite the encouraging cover blurb, much too little actually appears in the text about continuous monitoring and how it performs in practice. This is rather disappointing, for the authors work in the English Central Electricity Research Laboratories where a considerable body of expertise on the topic must exist. It is arguable whether work sheets should be printed in all their finicky detail in books such as this; too much space and therefore money is wasted. It is also doubtful if all of these analyses are quite as straightforward as they appear, though the authors do their best to indicate likely interferences and means of ensuring precision and accuracy. Apart from these reservations, this is a good useful book for those who wish

to use potentiometric methods in routine work rather than become involved in the theoretical intricacies of electroanalysis.

J. Kragten, (M. Masson, Trans. Ed.), *Atlas of Metal—Ligand Equilibria in Aqueous Solution*, Ellis Horwood—Wiley, Chichester, England, 1978, 781 pp., price £35.00.

The importance of a proper understanding of the chemistry of equilibria in aqueous solutions can scarcely be over-emphasized. Since Ringbom's book *Complexation in Analytical Chemistry* introduced the subject to wider classes of readers, a great deal of interest has been shown not only by chemists but by environmental, biological and biochemical workers. There is a mass of published information, but the steps required for conversion of the original equilibrium data to some easily assimilable form directly relevant to a problem are lengthy and tedious. Dr. Kragten's book is designed to overcome this barrier to wider understanding and usage, by presenting all the relevant information in graphical form. The reactions of 45 metals with 29 ligands have been studied, the physical constants have been selected critically, and an enormous amount of labour has been done on the preparation of log $\alpha$—pH and pM—pH plots for each system. After a short introductory chapter, the book consists almost entirely of these diagrams, with the selected stability constants and other necessary information given beside each plot. The conditions under which different complexes can exist are quite readily comprehended, which is no mean feat for mixtures of metal ions and ligands complicated by hydrolysis reactions. This then is an excellent reference book which should be available in every library; it is a pity that its price excludes more general distribution.

J. Stary and H. Freiser, *Equilibrium Constants of Liquid—Liquid Distribution Reactions, Part IV: Chelating Extractants (IUPAC Chemical Data Series No. 18)*, Pergamon Press, Oxford, 1978, xii + 228 pp., price $37.00, £20.50.

This book is an extension of Sillén and Martell's Stability Constants of Metal-Ion Complexes, and is another in the series of useful volumes produced by the Commission on Equilibrium Data of the Analytical Chemistry Division of IUPAC. The data here pertain to dialkyldithiocarbamic acids, tropolones, *N*-acylhydroxylamines, cupferrons, $\alpha$-dioximes, diarylthiocarbazones, 8-hydroxyquinolines, 8-mercaptoquinolines, dimercaptobenzenes, $\beta$-diketones, 4-acylpyrazol-5-ones and *o*-nitrosophenols. The compilation is not critical but comprehensive. Production is direct from the typescript, but the layout of the tabulated data is clear, following the same system as in the earlier compilations. This is an essential book for any laboratory engaged in research on extraction systems.

G. Milazzo and S. Caroli, *Tables of Standard Electrode Potentials*, Wiley-Interscience, Chichester, England, 1978, xvi + 421 pp., price $35.00, £17.50.

This compilation is a project of the Electrochemistry Commission of IUPAC. Professor Milazzo's introduction outlines the problems involved in data compilation, and the reasons for his decision to make this one comprehensive rather than critical — *quis custodiet ipsos custodes*? Who indeed could assess critically and accurately the 10,000 papers which have been scanned during the collection of these data over many years? The Tables themselves cover the Periodic Table and contain some weird and wonderful systems, theoretical as well as practical. But it is all there, clearly laid out, and it is for the reader to make his own critical selection. As so often happens with such compilations, the buyer pays for a lot of empty paper. Perhaps some international organization should concern itself not with compilation but with the presentation of compilations in a cheap form suitable for laboratory use rather than the back stacks of libraries.

K. D. Mielenz, R. A. Velapoldi and R. Mavrodineanu (Eds.), *Standardization in Spectrophotometry and Luminescence Measurements, Proceedings of a Workshop Seminar, NBS, Gaithersburg, 1975*, NBS Special publication 466, U.S. Government Printing Office, Washington, 1977, 150 pp., price $5.25 (hardback).

The 1975 Workshop Seminar — a sequel to the 1972 meeting on accuracy in spectrophotometry and luminescence (NBS special publication 378) — covered the topics of luminescence quantum yields, diffuse reflectance spectroscopy and ultraviolet absorption spectrometry. There were five invited papers in each session. The emphasis of the meeting was laid on accuracy. Given the sophistications of the best currently available instrumentation, precision is easily, if expensively, attainable. Accuracy is an entirely different matter, requiring not only reliable standards but a good understanding of how the methods actually work. These fifteen papers are concerned with standards and methods of standardization for the three techniques, and each is well worth reading. The cheapness of reading is altogether exceptional; admittedly this is a reprint of two issues of the NBS Journal of Research, but few such give-aways are now available. It is pleasant indeed to recommend a book which not only should be read but can very realistically be bought by anyone.

K. Cammann, *Das Arbeiten mit ionenselektiven Elektroden*, 2. Auflage, Springer-Verlag, Berlin-Heidelberg, 1977, S.xii + 227, price DM 76.00, $33.50.

The first edition of this book was published in 1973, and the intervening years have seen a consolidation of the use of ion-selective electrodes rather

than any spectacular advances such as those of the 1960's. This second edition is an extensive revision which reflects that consolidation; and the text now follows IUPAC terminology, which simplifies interpretation. The book is very thorough, and there is a good balance between theory and application. The format is larger and this explains how so much additional information has been introduced into about the same number of pages as the first edition. The second edition is certainly by far the better book, and an English translation would be welcome.

F. Vydra, K. Stulik and E. Julakova, (J. Tyson, Trans. Ed.), *Electrochemical Stripping Analysis*, Ellis Horwood, Chichester—Wiley, Chichester, England, 1977, 283 pp., price $33.25, £17.50.

The importance of anodic stripping voltammetry (a.s.v.) requires no emphasis for any student of the recent analytical literature. This book deals quite comprehensively with the subject. The first chapters are devoted to deposition and stripping processes and monitoring methods. Apparatus, experimental techniques and practical applications are described in later chapters. With so many developments in this area taking place almost daily, any text must be out of date before it has had a chance to be translated, edited and printed. Thus the reader would be well advised not to take any given procedure as the last word on the subject. Equally, however, a proper study of this text would help to avoid a good deal of preliminary investigation for any proposed application to the many situations where a.s.v. can provide unrivalled sensitivity and selectivity for multi-element determinations on an economic basis.

A. S. Kertes, *Critical Evaluation of some Equilibrium Constants involving Alkylammonium Extractants*, Pergamon Press, Oxford, 1977, v + 30 pp., price $6.00, £3.30.

This pamphlet reprints a report to the IUPAC Commission on Equilibrium Data. The data covered are the formation constants of salts of tri-n-octylammonium and tri-n-dodecylammonium ions, and the aggregation constants of tri-n-dodecylammonium salts. The author's typescript is reproduced for speed of publication and economy. The full rationale for the recommended values is provided, which makes the pamphlet more interesting reading than the normal data compilation.

G. Anderegg, *Critical Survey of Stability Constants of EDTA Complexes (IUPAC Chemical Data Series No. 14)*, Pergamon Press, Oxford, 1977, v + 42 pp., price $7.00.

In this report to the IUPAC Commission on Equilibrium Data, all published values for the protonation constants and stability constants of EDTA complexes up to 1976 are discussed critically and recommended values are given; rejected values are also noted. For each entry, the method of determination is noted as well as the calculation. The critical surveys are useful in providing a guide to the often confusing multiplicity of values in the literature and in data collections; the snag is that the literature now carries two sets of critically selected data for EDTA complexes and they do not agree, though the field has certainly been considerably narrowed.

J. R. DeVoe (Ed.), *Validation of the Measurement Process, ACS Symposium Series 63*, American Chemical Society, Washington, 1977, vii + 207 pp., price $20.00.

This book is concerned with the use of computational techniques in the validation of measurement processes. The text comprises the six papers presented at a symposium which was part of the ACS April 1976 meeting in New York. The first paper deals with the necessity of statistical control in routine analysis; Grant Wernimont draws on his vast fund of industrial and statistical experience to outline the essentials of analytical measurements and to discuss the fundamentals of control chart analysis, simple and complex statistical control, and the ruggedness of analytical methods. The following three papers are by members of the National Bureau of Standards:
J. J. Filliben deals with the testing of basic assumptions in measurement processes, introducing the reader quite gently to the computerized graphical techniques involved in probability plots; L. A. Currie and J. R. DeVoe discuss systematic error in chemical analysis; G. A. Uriano and J. Paul Cali describe the roles of reference materials and reference methods. The final two papers are quite short: S. N. Deming deals with optimization of experimental parameters, and R. C. Rhodes with sources of variability in chemical analysis. The papers are of a high standard and are blessedly free from jargon.

Dr. Wernimont complains, quite rightly, that most academic courses neglect the importance of statistical control of measurement processes which is so vital to the applied analytical chemist. Here is a book which will help to adjust the balance. It is very strongly recommended not only to applied analysts whose knowledge may be refreshed and extended, but to teachers and their students who will find it a splendid introduction to the vital features of ensuring reliability in routine analysis of any sort.

M. Zief and J. W. Mitchell, *Contamination Control in Trace Element Analysis*, Wiley-Interscience, New York, 1977, xiv + 262 pp., price $28.00, £17.35.

Control of sources of contamination is an aspect of trace analysis which sometimes does not receive the attention that it should. Nevertheless, much trace analysis has been done with increasing reliability since 1955 when it was apparently reported that "inaccuracy by current techniques of analysis has produced a nearly useless body of data"; the quotation (p. 9) thus seems a trifle inept. This book, which is Volume 47 in the Kolthoff—Elving Chemical Analysis series, is written by two members of a team formed between the J. T. Baker Chemical Company and Bell Telephone Laboratories for the production of ultrapure chemicals, and is based on the experience gained in that project.

The basic aspects of ultratrace analysis are discussed first, particularly blanks, standards, and measurement of small volumes. The main chapters are concerned with the construction of clean laboratories, choice of materials for apparatus, purification of reagents, and contamination during routine analysis. A wealth of hard-won and very valuable experience is placed at the disposal of the reader in these central chapters. The final chapter covers selected methods of ultratrace analysis with emphasis on activation analysis, isotope dilution and x-ray fluorescence; other techniques are mentioned, but the brief information given is scarcely worth having. The referencing tends to be erratic and there are very few post-1973 references except to work from the authors' own laboratories. The most serious defect in this book is with regard to sampling, and what happens between the point of sampling and the clean laboratory. Within the confines of a single expert team, these problems probably did not assume importance, but to deal with these matters in a couple of pages with references from ten years or more ago verges on the nonsensical, given the wealth of material in the recent literature. However, despite its lacunae, this is certainly a very useful book, and should be compulsory reading for all engaged in ultratrace analysis.

J. Mitchell, Jr. and D. M. Smith, *Aquametry (2nd edn.) Part I*, Wiley-Interscience, New York, 1977, xi + 632 pp., price $38.00, £22.45.

Mitchell's *Aquametry*, the first edition of this text published in 1948, is one of the minor classics of analytical chemistry. In the intervening thirty years, a great variety of methods has been introduced to cope with demands for the determination of water at concentrations from parts per billion to 100%. The subject has grown to such an extent that *Aquametry* will now appear in three volumes. This first volume covers chemical methods other than the Karl Fischer titration which will be discussed in Volume III, and procedures based on gravimetry, thermogravimetry, thermal conductivity, visible, ultraviolet and infrared spectrometry, nuclear magnetic resonance

and other types of spectrometry, radiochemical methods, and assorted physical methods based on turbidity, vapor pressure, hygrometry, etc. Volume II will deal with electroanalytical procedures.

As would be expected, the contents are excellently organized and well written. Obviously by the time the three volumes have been completed, just about everything one might conceivably need to know about analysis for water will be available in convenient form. It is a massive task, and the contents of this first volume augur well that the finished second edition will become a classic like its predecessor.

C. E. H. Knapman (Ed.), *Developments in Chromatography — 1*, Applied Science Publishers, London, 1978, ix + 245 pp., price $30.00.

Chromatographic methods of separation find applications in very many different areas of science. The original literature is, of course, still increasing at great pace, and so is the number of reviews and books covering recent developments. This first volume of a new series contains six reviews. The topics are the characterization of solute—solvent interactions in gas chromatography (g.c.) by F. Vernon, developments in continuous chromatographic refining by P. E. Barker, g.c. separation of isomers by W. E. Sharples, g.c. detectors by D. W. Grant, molecular-weight distribution by gel permeation chromatography by B. W. Hatt, and chromatography in forensic science by R. N. Smith. All the authors are English, and the book draws heavily on the experience accumulated at the Universities of Aston and Salford. The reviews are quite thorough and workmanlike, covering the literature into 1976. However, it is difficult to give an unreserved welcome to yet another series of chromatographic review articles.

H. M. N. H. Irving, *Dithizone*, The Chemical Society, London, 1977, iv + 106 pp., price £7.25, $14.50.

Dithizone is one of the more useful and sensitive organic reagents available to the analytical chemist. Yet its very sensitivity makes it one of the most infuriating in actual practice. Professor Irving's contributions to the chemistry of dithizone, its complexes and its derivatives require no introduction, and this monograph is a distillation of his unrivalled experience of disentangling the theoretical and practical intricacies of these substances.

The material is discussed in nine main sections: properties, metal—dithizone complexes, photochemistry, extraction, less familiar dithizone complexes, organometallic dithizonates, practical considerations, additional applications, and unresolved problems. This is not a practical manual, but an elegantly written monograph which should be studied, as carefully as it has been written, by anyone who is interested not only in dithizone but in the general development of organic reagents.

G. Wünsch, *Wolfram (W. Fresenius, Ed., Handbuch der analytischen Chemie, Teil 3, Band 6bγ)*, Springer-Verlag, Berlin-Heidelberg, 1978, xiii + 286 S., price DM 146.00, $73.00.

There are few really satisfactory methods of analysis for tungsten, as this monograph with its multitudes of alternative procedures bears witness. The volumes of the Handbuch tend to be comprehensive rather than critical, and this one is no exception. After a brief introduction, the material is organized under the headings: sample preparation, separation methods, gravimetry, titrimetry, photometry, spectral analysis, atomic absorption spectrometry, fluorimetry, polarimetry, catalytic—electrometric methods, thermal analysis, activation analysis, x-ray fluorescence, other methods (x-ray and mass spectrometry and gas chromatography) and finally methods for the investigation of particular tungsten compounds. The literature is covered exhaustively from 1942 to the beginning of 1976 with suitable reference to standard texts for earlier work. Practical details are given as well as explanatory information. The book is written in German; it is certainly an essential text for all who require methods of analysis for tungsten and tungsten-bearing materials.

J. W. Price and R. Smith, *Tin (W. Fresenius, Ed., Handbuch der analytischen Chemie, Teil 3, Band 4aγ;)*, Springer-Verlag, Berlin-Heidelberg, 1978, xi + 262 pp., price DM 146.00, $73.00.

The cover of this volume of the Handbuch bears an uncompromising Zinn. The English-speaking reader therefore receives a pleasant surprise on opening the book to find that the whole thing is in English. The material is organized according to the normal pattern: chapters are devoted to detection, gravimetry, titrimetry, photometry, electroanalysis, extraction, atomic absorption spectrometry, emission spectrometry, x-ray fluorescence, and activation and Mössbauer methods; the subsequent ten chapters deal with analytical methods for tin-bearing materials, from ores to organotin compounds. Unlike most other volumes in the Handbuch, this text makes no claim to be comprehensive. It is, however, written with authority, the authors having drawn widely from their own industrial experience. The literature coverage is quite good, with occasional references to 1974-75, but the 1979 reference (p. 172) is a printing error. Though it is different in nature, this volume is well worthy to stand beside the others in this excellent Handbuch. Some readers will miss the detailed yet concise information on perhaps rather obscure methods which allows a personal opinion to be reached on the viability of a method without recourse to the original literature; others will welcome the fact that the initial selection process has already been done. Whichever way one looks at it, this volume remains essential reading for analytical chemists concerned with tin. The German readers' loss is undoubtedly the English readers' gain, and it is to be hoped that this venture into English will encourage new readers to delve further into the many useful volumes of the Fresenius—Jander Handbuch.

*Analytica Chimica Acta*, 105 (1979) 465—466


## Announcement

---

**Vorschau auf Veranstaltungen der Gesellschaft Deutscher Chemiker und ihrer Fachgruppen im Jahr 1979 und soweit bereits bekannt im Jahr 1980**

| | |
|---|---|
| 1979 | |
| 25—27 April<br>Mainz | *Vortragstagung "Waschmittel und Hygiene"* der GDCh-Fachgruppe Waschmittelchemie. |
| 30 April—3 Mai<br>Endorf b. Rosenheim | *EUCHEM-Konferenz:* Solid State Chemistry and Electrochemistry especially with respect to its Application in Battery Research. |
| 3—4 Mai<br>Berlin | *Vortragstagung Lebensmittelqualität und Zusatzstoffe* gemeinsam veranstaltet von der GDCh-Fachgruppe Lebensmittelchemie und gerichtliche Chemie und der Deutschen Gesellschaft für Ernährung. |
| 21—23 Mai<br>Bad Pyrmont | *Jahrestagung* der GDCh-Fachgruppe Wasserchemie. |
| 20 Juni<br>Frankfurt/M | *GDCh-Vortragsveranstaltung im Rahmen der ACHEMA.* |
| 20—23 August<br>Köln | *ESOC I — 1st European Symposium on Organic Chemistry* unter der Schirmherrschaft der Föderation Europäischer Chemischer Gesellschaften (FECS) organisiert von der GDCh. |
| 3—7 September<br>Frankfurt/M | *EUCMOS XIVth European Congress on Molecular Spectroscopy* über Modern Trends in Spectroscopy |
| 10—14 September<br>Berlin | *18. GDCh-Hauptversammlung* mit folgenden Sektionen: Anorganische Chemie, Organische Chemie, Physikalische Chemie, Technische Chemie, Analytische Chemie, Angewandte Elektrochemie, Anstrichstoffe und Pigmente, Chemieunterricht, Festkörperchemie, Freiberufliche Chemiker, Geschichte der Chemie, Gewerblicher Rechtsschutz, Kristallographie, Lebensmittelchemie und gerichtl. Chemie, Makromolekulare Chemie, Medizinische Chemie, Nuklearchemie, Photochemie, Waschmittelchemie, und Wasserchemie. |
| 17—21 September<br>Mainz | *MAKRO MAINZ 1979*, IUPAC 26th International Symposium on Macromolecules. |
| 4—5 Oktober<br>Frankfurt/M.-Höchste | *Vortragstagung "Elektrolysen (Chlor)"* der GDCh-Fachgruppe Angewandte Elektrochemie. |
| 21—23 November<br>Göttingen | *Vortragstagung der GDCh-Fachgruppe Photochemie.* |

**1980**

| | |
|---|---|
| 29—30 April | *Vortragsveranstaltung der GDCh-Fachgruppe Makromolekulare Chemie.* |
| 28—30 Mai Dortmund | *10th Annual Symposium on the Analytical Chemistry of Pollutants* unter Mitwirkung der GDCh-Fachgruppe Analytische Chemie. |
| 10—13 Juni Berlin | *Vortragsveranstaltung "Non-metals in metals"* gemeinsam durchgeführt von GDCh-Fachgruppe Analytische Chemie, Commission of the European Communities', Commission Bureau of Reference, Verein Deutscher Eisenhüttenleute, und Gesellschaft Deutscher Metallhütten- und Bergleute. |
| 22—25 Juli Dortmund | *3rd International Conference on Organometallic and Coordination Chemistry of Germanium, Tin and Lead.* |
| September Stuttgart | *Vortragstagung "Struktur und Eigenschaften von festen Stoffen"* der GDCh-Fachgruppe Festkörperchemie. |
| September Stuttgart | *Deutscher Lebensmittelchemikertag 1980* der GDCh-Fachgruppe Lebensmittelchemie und gerichtliche Chemie. |
| September Regensburg | *Vortragstagung der GDCh-Fachgruppe Chemieunterricht.* |
| September Jülich | *Vortragstagung der GDCh-Fachgruppe Nuklearchemie.* |
| 21—25 September Hamburg | *111. Versammlung der Gesellschaft Deutscher Naturforscher und Arzte mit CHEMIETAG der Gesellschaft Deutscher Chemiker.* |
| 9—11 Oktober Bad Nauheim | *Vortragsveranstaltung der Arbeitsgemeinschaft Organische Chemie in der Gesellschaft Deutscher Chemiker.* |

Further information from GDCh-Geschäftsstelle, Postfach 90 04 40, D-6000 Frankfurt/M 90.

ANALYTICA CHIMICA ACTA, Vol. 105 (1979)

# AUTHOR INDEX

*(continued from page overleaf)*

*(continued from page opposite)*



*Short Communications*



*(continued on page overleaf)*

# NEW JOURNAL OF ANALYTICAL AND APPLIED PYROLYSIS

**Editors:** H. L. C. Meuzelaar
Flammability Research Center
University of Utah
391 South Chipeta Way,
Research Park,
Salt Lake City, UT 84108, U.S.A.

H.-R. Schulten
Institut für Physikalische Chemie
der Universität Bonn
5300 BONN
Wegelerstrasse 12
G.F.R.

**Associate Editor:** C. E. R. Jones, 36 Green Lane, Redhill, Surrey RH1 2DF, U.K.

This new international journal brings together, in one source, qualitative and quantitative results relating to:

- Controlled thermal degradation and pyrolysis of technical and biological macromolecules
- Environmental, geochemical, biological and medical applications of analytical pyrolysis;
- Basic studies in high temperature chemistry, reaction kinetics and pyrolysis mechanisms,
- Pyrolysis investigations of energy related problems, fingerprinting of fossil and synthetic fuels coal extraction and liquefaction products.

The scope will include items such as the following:

1. Fundamental investigations of pyrolysis processes by chemical, physical and physico-chemical methods.
2. Structural analysis and fingerprinting of synthetic and natural polymers or products of high molecular weight.
3. Technical developments and new instrumentation for pyrolysis techniques in combination with chromatographic or spectrometric methods, with special attention to automation, optimization and standardization.
4. Computer handling and processing of pyrolysis data.

*Pyrolysis is applied in a wide range of disciplines. This journal will therefore be of value to scientists in such diverse fields as: polymer science, forensic science, soil science, geochemistry, environmental analysis, energy production, biochemistry, biology and medicine.*

Contributions will be in the form of: original papers, technical reviews, short communications, letters, book reviews and reports of meetings and committees. The language of the journal is English. Prospective authors should contact one of the editors.

**Publication Schedule and Subscription Information:**

The journal will be published quarterly. The first issue is scheduled to appear in Spring 1979. 1979: Volume 1 (in 4 issues), US $70.75/Dfl. 145.00 including postage

***A free sample copy will be sent on request.***

ELSEVIER

P.O. Box 211,
1000 AE Amsterdam
The Netherlands

52 Vanderbilt Ave
New York, N.Y. 10017

*The Dutch guilder price is definitive. US $ prices are subject to exchange rate fluctuations*

7123

# Evaluation and Optimization of Laboratory Methods and Analytical Procedures

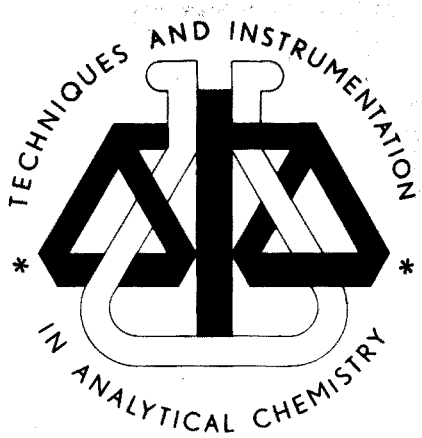


## A Survey of Statistical and Mathematical Techniques

D.L. MASSART, A. DIJKSTRA *and* L. KAUFMAN.

*with contributions by* S. Wold, B. Vandeginste *and* Y. Michotte

**Techniques and Instrumentation in Analytical Chemistry - Volume 1**

This book provides detailed treatment, in a single volume, of formal methods for optimization in analytical chemistry. It is a comprehensive and practical handbook which no analytical laboratory will want to be without.

All aspects of optimization are discussed, from the simple evaluation of procedures to the organization of laboratories or the selection of optimal complex analytical programmes. Quantitative discrete analysis as well as qualitative and continuous measurement techniques are evaluated.

The book consists of 30 chapters divided into 5 main parts.The main sections are: Evaluation of the Performance of Analytical Procedures, Experimental Optimization, Combinatorial Problems, Requirements for Analytical Procedures, and Systems Approach in Analytical Chemistry.

This work will be of practical value not only to those involved with optimization problems in analytical chemistry, but also to those in related fields such as clinical chemistry or specialized fields such as chromatography. Because it discusses the application of many mathematical techniques in analytical chemistry, this book will also serve as a general introduction to the new field of Chemometrics.

**Oct. 1978 xvi + 596 pages US $57.75/Dfl. 130.00 ISBN 0-444-41743-5**

ELSEVIER

P.O. Box 211,
1000 AE Amsterdam
The Netherlands

52 Vanderbilt Ave
New York, N.Y. 10017

*The Dutch guilder price is definitive. US $ prices are subject to exchange rate fluctuations.*

7113

# Phosphine, Arsine and Stibine Complexes of the Transition Elements

**C. A. McAULIFFE,**
*University of Manchester Institute of Science and Technology, U. K.,*

**W. LEVASON,**
*University of Southampton, U. K.*

**Studies in Inorganic Chemistry 1**

This work provides detailed coverage of recent developments (from 1973 to 1977 inclusive) in heavy Group 5 donor chemistry. It deals with the synthesis, structure, and reactivity of transition metal complexes (and also those of copper, silver and gold) of monodentate, bidentate and multidentate ligands containing phosphorus, arsenic, antimony (and bismuth) donors.

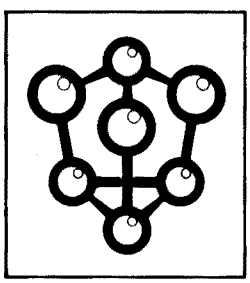

More than a catalogue of publication synopses, this work includes thorough discussions of the syntheses, properties, uses, and the spectral methods of investigation of these complexes. Topics of current interest, such as the internal metallation reactions, are dealt with at some length. New developments, for example polymer-supported reagents, are also treated in detail.

CONTENTS: Chapters: I. Ligand Syntheses. II. Transition Metal Compexes-Preparations and Properties. III. Complexes of Monodentate Ligands. IV. Complexes of Bidentate Ligands. V. Complexes of Multidentate Ligands. VI. Phosphite, Phosphonite, Phosphinite and Amine-Phosphine Complexes. VII. Reactions of Coordinated Group VB Ligands. *Appendix I.* Phosphine Complexes and Catalysis. *Appendix II.* Reviews. *Appendix III.* Abbreviations. References. Subject Index.

**Nov. 1978 xiv + 564 pages US $84.50/Dfl. 190.00 ISBN 0-444-41794-4**

**Further information on this and other chemistry publications will be gladly provided. Please write to our Promotion Department at one of the addresses below.**

ELSEVIER

P.O. Box 211,
1000 AE Amsterdam
The Netherlands

52 Vanderbilt Ave
New York, N.Y. 10017

*The Dutch guilder price is definitive. US $ prices are subject to exchange rate fluctuations.*

7117

*(continued from outside of cover)*



*(continued on page opposite)*

## CONTENTS



*(continued on inside page of cover)*

---



Printed in The Netherlands